ADAPTIVE DIGITAL DISTANCE PROTECTION FOR SERIES COMPENSATED TRANSMISSION LINES

By

FOROOZAN GHASSEMI

Thesis Submitted To The City University

For The Degree Of Doctor Of Philosophy

SEPTEMBER 1989

Power System Protection Laboratory
Department Of Electrical, Electronic
And Information Engineering
City University
Northampton Square
London EC1V OHB

I dedicate this thesis to my wife
whose patience, encouragement and support
inspires me in every aspect of my life.
To my daughter and son with love.
Also to the memory of our daughter Maryam,
who came and passed away during the course of
this study.

LIST OF CONTENTS

Published Papers

SYNOPSIS

Series capacitors offer considerable technical and economical advantages in long distance a.c. transmission. In particular, their excellent reliability and minimal maintenance requirements make series compensation the most cost effective method of enhancing the power transfer capability of an existing or proposed interconnection.

E.H.V. lines employing series capacitors however, pose difficult problems for the line protection relays, not encountered with plain feeders. One important cause of these problems is the resonance between the series capacitor and the line series inductance, which in turn imposes a sub-synchronous oscillation on the system signals. Also, the rapid changes in the circuit parameters, resulting from the operation of the capacitor protection equipment, namely the spark gaps, introduce some difficulties for the line protection schemes, especially an impedance measuring relay. These spark gaps are installed in parallel with the series capacitors to prevent the development of very high voltages across the capacitor which could cause excessive damage to the equipment.

The work presented herein describes a new digital distance relay suitable for series compensated line applications.

The errors in the impedance measurement for a phase to earth fault when the spark gaps do not flash over, are discussed and new methods are proposed to compensate for these errors. The new concept of a complex residual compensation factor, as opposed to a real one, is also discussed.

A new adaptive filtering is incorporated in the relay in order to minimise the detrimental effect of the sub-synchronous oscillation on the relay decision logic.

Finally, the relay is thoroughly tested for many different system configurations, to fully evaluate the relay response.

ACKNOWLEDGEMENTS

The author wishes to express his sincere thanks to professor A.T. Johns, D.Sc., Ph.D. B.Sc., C.Eng., FIEE, SMIEEE, FRSA, for his guidance, invaluable advice and encouragement throughout the course of study.

He would like to thank everyone at the power systems research laboratory for their support and friendship, especially Mr S.H. Lewis and Mr M. Gasparo for their extremely helpful contributions to the preparation of the thesis, and Dr P.J. Moore for friendly discussions throughout the time he spent working on the project.

He is grateful to City University, London, and GEC Measurement, Stafford, for providing the funding for the project and would like to thank the engineers at GECM, especially Mr E.P. Walker, Dr P.A. Crossley, Mr J. Weller and R. Warren for very useful technical discussions.

Finally, he wishes to thank the staff of the school of Electrical and Electronic Engineering, City University, particularly Mrs L. Wilkinson, who have been extremely helpful and encouraging during the studies.

COPYRIGHT DECLARATION

I grant powers of discretion to the University Librarian to allow this thesis (ADAPTIVE DIGITAL DISTANCE PROTECTION FOR SERIES COMPENSATED TRANSMISSION LINES) to be copied in whole or in part without further reference to me. This covers only single copies made for study purposes, subject to normal conditions of acknowledgement.

LIST OF PRINCIPAL SYMBOLS

E.H.V	extra high voltage.
V_S, V_R	line voltage at sending and receiving end of a line respectively.
δ	load angle (phase angle between the sending and receiving end voltages).
P	power transferred along a line.
$v_{(t)}$, $i_{(t)}$	time domain voltage and current.
$v_{(k)}$, $i_{(k)}$	discrete time voltage and current.
f_s	sampling frequency.
T_s	sampling interval $1/f_s$.
$h_{(t)}$	impulse response.
T_w	data window.
$v_{(t)}$, $i_{(t)}$	voltage and current derivatives.
ϕ	phase angle between voltage and current.
Θ	angle between two points on voltage and current signals.
w_o	fundamental angular frequency
w_{su}	sub-synchronous frequency component.
V_{su}, I_{su}	magnitude of voltage and current of sub-synchronous component.
β	phase angle between the fundamental and sub-synchronous components.
C.V.T	capacitor voltage transformer.
C.T	current transformer.
V.T	voltage transformer.
ΔT	sampling time step.
τ	dummy time variable.
A/D	analogue to digital converter.

U.H.S	ultra high speed.
ζ	damping coefficient.
w_n	natural frequency.
TL	relay trip level.
TC	relay trip counter.
CRL1	relay control counter initiated by fault detection.
CRL2	relay control counter initiated by first up-count.
AVLL, AVLU	lower and upper limit on reactance axis to control the Recursive Averager.
R	transmission line resistance.
L	transmission line inductance.
C	capacitance of the series capacitor.
L'	equivalent inductance of transmission line.
Z_{LS}, Z_{LM}	self and mutual impedance of transmission line.
Y_{LS}, Y_{LM}	self and mutual admittance of transmission line.
pps	positive phase sequence.
zps	zero phase sequence.
Z_{L1}, Z_{L0}	positive and zero phase sequence impedance of transmission line.
Y_{L1}, Y_{L0}	positive and zero phase sequence admittance of transmission line.
R_{L1}, R_{L0}	positive and zero phase sequence resistance of transmission line.
X_{L1}, X_{L0}	positive and zero phase sequence reactance of transmission line.
α	proportional fault position.

Z	measured impedance by the relay.
V_{sae}	phase "a" to earth voltage.
I_{sa}	phase "a" current.
I_{res}	residual current.
K_C	conventional residual current compensation factor, CRCF.
K_S	conventional sound phase current compensation factor.
$K_{(\alpha)}$	modified residual compensation factor.
$K_{(\alpha r)}$	new residual current compensation factor, NRCF.
αr	fault position for a fault at the relay zone-1 reach point.

CHAPTER 1

INTRODUCTION AND LITERATURE SURVEY

1.1-Literature Survey

A transmission system comprising of short lines is fairly stiff at the generator ends (bus-bars) because there are a number of infeeding lines from other sources connected to the bus-bar. As the line is short, both the line reactance and line capacitance are relatively small, and in fact the latter can be neglected. This means that a generator can operate at a reasonably low load angle in order to transmit an appreciable amount of power over the line, so that the problem of generator instability due to disturbances is reduced. Because of the stiffness of bus-bars and the interconnection of the system even when a line does go out due to a fault, the majority of faults being transitory in nature anyway, a 3-phase autoreclosure scheme is successfully employed without loss of stability or any serious disruption. Moreover, the presence of a second circuit helps to maintain stability during the autoreclosure sequences of the faulted circuit.

On long lines, however, where the source of generation is often remote from the load points, especially in countries which employ hydro-power schemes, the system at the generator end is relatively weak.

In such cases, the problem of maintaining stability of the system becomes much greater. Double circuit lines are often uneconomical to use because of the very long distances involved.

Because the line is long, both the line inductance and

capacitance are large. The increase in line inductance has the following main effects:

i-The power transfer capability of the line is reduced.

ii-Both the transient and steady-state stability margins of the system for a given power transfer are lowered.

iii-The voltage drop along the line becomes excessive.

The power transfer capability, P, of a transmission line is approximately given by Equation 1.1:

$$P=\frac{V_S \cdot V_R}{X} \sin \delta \qquad 1.1$$

V_S and V_R are the sending and receiving end voltages respectively and X is the inductive reactance of the transmission circuit between the terminals, and δ is the phase angle between V_S and V_R. The power transfer capability can be increased by either increasing V_S, V_R or δ, or decreasing X. The maximum value by which V_S and V_R can be increased to are normally fixed by the steady-state and transient insulation limitations of the transmission system itself. This includes the line and terminal equipment. The value of X is determined by the transmission line and terminal equipment (transformers, generators, etc.) reactances, the minimum value of which is limited by the physical size of equipment and economic consideration.

The inclusion of series capacitors in a.c. transmission systems, particularly where long line sections are involved, is an effective and economic means of improving the power transfer capability and stability of a system. Over the years, a series capacitor employed

in H.V. networks has evolved into a reliable element in transmission systems, achieving an excellent performance and reliability standard [1, 2].

By electrically reducing the effective transmission line lengths brought about by the cancellation of part of the inductive reactance, series compensation offers the following major technical advantages over uncompensated system:

i-The steady-state power transfer capability of the network becomes proportional to the degree of series compensation. That is to say that for the maximum level of series compensation encounterd in practice, (typically 70%) the gain in power transfer capability is around 233%. This implies that the same level of power transfer can be achieved for a reduced load angle between the generation voltages at the line ends, thereby offering some improvement in terms of systems stability [3].

ii-The voltage profile along the line is more evenly distributed under normal load conditions. This leads to a reduction in the reactive volt-drops along the line, which for radially configured systems, dramatically improves the voltage regulation and hence the magnitude of the line voltages at the receiving or load ends.

iii-Greater flexibility is introduced into the system. Power losses depend upon the line cross sectional areas and current distribution, and adjustment in the level of series compensation helps to improve the X/R ratio of the line such that transmission losses are

then minimised.

iv-The possibility of attaining more favourable load distributions between different lines functioning in parallel.

v-The series capacitor is the only static device with true automatic regulation of the voltage and power.

vi-Extremely small losses and good reliability.

vii-providing a cheaper substitute [5, 6] as an alternative to construction of new lines.

In short, series capacitor compensation improves the steady-state transmission characteristic of a power network and reduces transmission losses and costs.

Since the cost of any power capacitor is roughly proportional to the square of the voltage that it must withstand, the series capacitor becomes extremely expensive and uneconomical if it is required to tolerate the large voltage which is developed across them during system disturbances. In general when a capacitor is subjected to any disturbances, abnormal changes take place in the dielectric which result in breakdown or at least produce fatique phenomena which causes ageing and shorten its life.

To protect the capacitor bank in the presence of severe over-voltages which may be developed across the capacitors, particularly under fault conditions, three main type of independent schemes are commonly applied worldwide. These schemes can be classified as:

i-Single Gap Scheme (SGS).

ii-Dual Gap Scheme (DGS).

iii-Dual Gap with Non-linear resistor Scheme (DGNS).

These protection schemes remove or partially remove the capacitor from the line, by diverting the line (or some of the line) current from flowing through the capacitor. This is carried out by connecting some form of by-passes known as spark-gaps in parallel with the capacitor unit. The gaps are set to breakdown and hence to conduct when the voltage across the capacitor exceeds a pre-set threshold, typically 2 to 3 times the nominal or steady-state value which is developed across the capacitor when maximum permitted load current flows through the line.

Capacitor protection schemes are often provided with a circuit breaker in parallel with the spark-gap and the capacitor [5], to deionize the gap after flashing-over and reinsert the capacitor back to the network immediately after the capacitor voltage has reduced below the critical value in order to improve the transient stability of the system as a whole.

In the past decade, great technological advantages have been made in the development of capacitor protection equipments [6, 7, 8]. It seems likely that the DGNS will become commonplace in future applications since many publications highlight their stability boosting effect, both from a by-passing and reinsertion standpoint [6, 7].

In this scheme the capacitor is shunted in such a way as to only partially remove the compensating reactance, whilst retaining full protection against over-voltages. This is achieved by inserting a non-linear resistor in series with the dual gap branch to form the dual gap with non-linear resistor scheme, DSNS. The impedance in the

shunt path varies with the voltage developed across the capacitor/resistor combination, producing a self-regulative action, holding the capacitor voltage to an acceptable level, while merely reducing the compensation as opposed to losing it altogether with the other schemes.

When a series capacitor is (partially) by-passed as a result of operation of its spark-gaps, rapid changes occur in the effective system impedances. Furthermore, it is impossible to predict both the exact number and the precise instant in time at which the various capacitor gaps flash-over; the reason being the fact that under fault conditions there are a vast number of variations which affect the magnitude of over-voltages. These include fault loop resistance, pre-fault loading, source phase sequence ratios as well as capacities, point on wave at which fault occurs, type of fault, etc [9].

The fundamental question of the location of the capacitor in the system is another main problem which must be dealt with. Series capacitor can be placed either at the line ends or at intermediate substation along the line.

If the series capacitor is placed at the line ends where there already exists a switching substation, the need for extra station to install the capacitors is obviated. Hence, the maintenance and operating cost is reduced. However, it has the disadvantage of increasing the short circuit level at the substation which implies that more expensive intrupting equipments must be employed. On the other hand, the advantages attributed to the location along the line are easier protection [10].

However, location along the line means higher installation and operating costs because special intermediate capacitor stations have to be built at a distance from the switching stations.

Differences of view of where the capacitors should be located, either mid-point or at the lines ends, have existed for many years.

In practice, the amount of compensation and the location depends on various factors, including economy, ease of protection, power transfer capability, etc [10]. The mid-point installation for about 50% (or less) compensation tends to be Scandinavian practice, while the USA manufacturers and utilities prefer to place the capacitors in the vicinity of the line ends for a 70% compensation (usually split up into two halves) [11].

The other factor which needs consideration is the position of the voltage and current transducers which supply the line protection gear. When the capacitors are located at the line ends the user has a choice of taking the voltage supply for the relay from either the bus side or the line side of the capacitor bank [12].

The technique favoured in the USA has been to position the current transformers on the bus side, and the voltage transformers on the line side of the capacitor. With this arrangement, the local capacitor effectively forms part of the source impedance. Thus, the impedance seen by a impedance measuring relay, i.e. distance relay, involve only the inductive line impedance and therefore no distortion due to the capacitor [13]. This is a notable advantage of employing line-side voltage measurements.

However, maintaining the directionality of distance relays becomes a major problem, and distance relays, depending on methods of polarization being employed, become prone, to different degrees, to reverse faults.

On the other hand, when voltage measuring equipment (V.T.s) are installed on the source side of the capacitor, the capacitor become part of the transmission line and may be included in the protected zone of distance relays. Also maintaining the directionality of the protective equipments may not be as great as situations where the V.T.s are connected to line side.

In general not all series compensated lines are identical. The major variable for protection are the degree of compensation, the capacitor position and whether it is split into two parts, the type of over-voltage protection and its operating level, and the location of the relay measuring transformers.

Because of all these uncertainties and unsimilarities among series compensated lines,these lines pose difficult protection problems for line relays. Any mode of independent tripping, without the use of communication channels, linking the protection at the two end, is often unsatisfactory. For example, distance relays can, depending on their settings, either over-reach or under-reach as a direct consequence of the operation of the series capacitor protection equipments [14].

A method which is commonly used in practice is to use a distance relay in which the setting is determined assuming that the capacitor is always in the circuit under fault conditions [12, 15]. This method may not be

satisfactory due to the random nature in which a capacitor flashes over under various fault conditions.

The other method is to set the relay assuming that the capacitors have flashed over. Again, there will be a tendency for the relay to over-reach if the capacitor's protective gap does not flash-over under certain fault conditions.

A method of protecting series compensated lines involves the use of distance relays operating in a directional comparison mode in conjunction with either carrier or microwave signalling -channels. For systems with less than 50% series compensation and a capacitor located at the mid-point of the line, such a protection scheme can offer secure and reliable operation [15]. However, when the capacitors are located at the line ends, directional comparison schemes using distance relays are not very satisfactory [16]. For example, a low level fault failing to cause capacitor by-passing, can result in a loss of directionality arising as a result of voltage reversal at the relay location. In the case of double circuit applications, both voltage and current reversals are quite common [11]. A distance relay employing an expanded characteristic of the fully cross polarised mho type (fcpm), goes some way to solving the inversion problem, but the degree of expansion is very dependant upon the type of fault and the impedance ratio of the local source to the capacitive reactance [15].

Hinman and Gonnam [17] proposed a phase comparison technique which compares the phase position of current in each phase wire (and ground) separately. The comparisons

are based on square waves derived directly from the raw (i.e. unfiltered) power system current. This is in contrast to conventional phase comparison schemes which compare a single square wave derived from a network of sequence filters and a mixing transformer. The conventional phase comparison technique incorporates positive sequence and/or negative sequence network and therefore has been vulnerable mainly to the problem of phase impedance imbalance caused primarily by series capacitor protective gaps flashing and re-inserting unsymmetrically. The disadvantage of this approach is the requirement for four separate pilot signal per terminal [18].

Directional voltage blocking schemes have been successfully implemented in conjunction with distance relays to block any maloperation of the relay in the presence of voltage inversion alone.

El-kateb and Cheetham [19] described a new technique utilising the super-imposed voltages and currents, which might over-come the problems of unwanted blockings of distance relays due to operation of directional voltage relays or the apparent capacitive source impedance, utilising the fully cross-polarised mho relay.

Another method is a directional comparison protection suitable for compensated and plain feeder systems which utilises positive and negative sequence relays to detect all types of fault [12], the former is a distance relay with Mho characteristic which provides protection for three phase faults and latter is a negative sequence directional relay which protects the line against all

unbalanced faults. Each relay has a trip and block element. It is designed such that for an internal fault, the trip relay operates before the block relay and by-passes any action taken by the latter. The opposite procedure occurs for external faults. There is a polarising quantity correction factor which is introduced to neutralize the effect of polarising voltage inversion at the relaying point. But this factor is dimensioned by specific ratio of the source reactance to the series capacitive reactance. This type of protection scheme may not perform satisfactorily in a practical series compensated system, since an effective value of source impedance (impedance behind the relay) is not always known and depends upon the infeeding lines and the number of generators connected to the relaying terminal.

In recent years schemes utilising travelling wave techniques, suitable for series compensated lines, have been developed [20], which are based on the work initially carried out by Johns [21]. The basic relay operating principle relies upon deriving two composite superimposed signals using modal voltages and currents at each end of a feeder. The use of modal quantities eliminates the mutual coupling between the phases of a transmission line. The criteria for determining the direction to fault is based on the fact that for an internal fault (fault on protected line) the superimposed modal voltage and current components are of opposite polarities at each end of the feeder. A forward fault indication is thus given by both relay which is sent to the other end via a communication link. Conversely, for an out of zone fault, although the

relay at one end gives a forward fault indication, however, the modal voltage and current components at the other end are of like polarity resulting in a reverse fault indication by that relay which in turn sends a block signal. Limited field experience is available on this topic at present. Also the scheme relies heavily, as any other directional comparison scheme, on the communication link between the two ends of the line.

A commonly encountered problem in series compensated line protection arises due to the presence of so called sub-synchronous resonance that is introduced into the system when capacitor protective gaps do not flash-over [5, 18].

If the sum of the electrical resonant frequency, determined by the inductance and capacitance of the system, and the mechanical resonant frequency given by the masses of the turbine generator set and the torsional properties of the shaft, is equal to the system frequency, an unstable condition exists for which a small disturbance can cause complex electrical and mechanical oscillation [5]. Disasterous effects are possible with weak steam turbine shafts since the high torsional stresses associated with the sub-synchronous resonance are of sufficient magnitude as to cause permanent shaft damage.

From the protection point of view, the interaction between the total fault loop inductance (source and line) and series capacitor can have a frequency bandwidth which may exceed the power frequency, depending upon the fault position [10]. These extraneous frequencies, which are usually underdamped [22] can cause considerable error in

small window calculations, and improper relay operation if not catered for in the relay design.

Faults on any E.H.V. transmission systems have to be cleared as soon as possible to avoid excessive damage. Furthermore, fast fault clearance is essential to maintain system stability and prevent the escalation of single phase to earth fault to multi phase to earth faults. For these reasons many studies have focused on Ultra-High-Speed distance protection utilising digital technology. When Ultra-High-Speed measurements are considered, the waveforms from which measurements must be made can include very significant travelling wave components, which are due to the voltage step change on fault occurrence, in both faulted and healthy phases. The amplitude and frequency of these disturbances depend mainly on the line length, fault inception angle and source termination [23].

The technique described by Gilcrest, et al [24] uses the first and second differentiation of voltage and current to calculate the transmission line impedance. This has been done to minimize errors from the sub-normal frequencies associated with the series capacitors [18]. However, this method is not favourable since higher frequency transients caused primarily by travelling waves are now accentuated.

The desirable features of any line protection scheme for series compensated systems may be summarized as follows:

i-High speed operation.

ii-Application independent

iii-Can detect the changes in the circuit as a result of

capacitor by-passing and adjust itself to the new system condition.

iv-Can cope with the effect of resonance interaction between the series capacitor and the loop inductances.

v-Can maintain its integrity when a voltage or current reversal occurs.

As previously mentioned, in order to achieve fast operating times, the majority of protection schemes which are applied to series compensated systems are heavily dependent upon the communication links between the line ends.

Distance relays which have been successfully employed in plain feeder applications for many years, do not provide a generally satisfactory response when applied to series compensated lines. This is due to the fact that in such lines the estimation of distance to fault from measured impedance is very difficult, because of the negative reactance of the capacitor and changes in the system impedance as a result of capacitor protection gear operation.

However, with the present day state of the art digital technology, it will be possible to design an impedance measuring device which can detect any changes in the system states and adjusts its parameters according to the new state of the system.

One of the advantages of distance schemes is the fact that they can be employed in an independent mode, where the relay trips irrespective of the information from the other end of the line, as well as the unit protection schemes where the tripping relies on the information from

the relay at the other end. Furthermore, since distance relays, somehow compare the measured impedance with a pre-determined boundary, it would be easy to change the relay characteristic once the capacitor gap flash-over is detected.

The new generation digital distance relays have a distinct advantage over the older type of analogue and hybrid analogue/digital relays in that the impedance is calculated at any instant of time and the locus of the impedance is available. Hence, any change in the measured impedance may be detected, if a suitable filtering is employed, and therefore appropriate steps may be taken by the relay.

Since series compensated lines are usually long, the long line transient effect caused by travelling waves may be particularly troublesome, because the frequency of the travelling waves, when considering a long line and depending on sources at the line ends, may be as low as 250 Hz. Special attention must thus be given to this phenomena when designing the filtering process of a digital distance relay.

Distance protection algorithms have evolved over the years. Algorithms based on conventional Fourier Transform techniques [25, 26, 27] are effective in extracting the fundamental components from highly distorted fault waveforms, but their response to a fault is slow. The response of the Fourier Transform method can be improved by using a smaller data window, but small data windows produce problems in current offset conditions and are influenced by travelling wave components. However, the

Finite Fourier Transform can be satisfactorily implemented if used with appropriate filtering [28].

The main disadvantage of the latter methed is that the magnitude response of the orthogonal filters are not the same. Hence, they must be equalized at the power frequency which means that any drift by the system frequency from nominal frequency causes errors in the impedance measurement. Furthermore, low order harmonics in the relaying signals have a detrimental effect on the performance [29].

A modified method uses two direct samples on the relaying signals to solve for the resistive and reactive components of the line impedance. This method has the advantage of being immune to power frequency changes and system harmonics [29].

1.2-Summary Of The Thesis

The problems associated with protection of series compensated lines have already been mentioned. With regard to distance protection, these problems can be classified into two main areas:

i-When capacitors do NOT flash-over i.e. they remain in the circuit. This situation arises from a low level fault or high fault resistance [16, 30]. Also, with the new generation of Ultra-High-Speed protection, the fault may be cleared in considerably less than one cycle which can in turn be much shorter than capacitor gap flash-over times [31]. In such situations significant sub-synchronous resonance components are often present. These components can be close to power frequency and they can cause a significant slowing of

the protection and/or cause transient measuring errors. Furthermore, in some system situations, the presence of the capacitor affects the measuring accuracy of distance schemes. Also, in applications where the capacitors are located at the line ends, the first independent zone of distance protection usually has to be set to less than 80% in order to avoid possible indiscrimination for remote end faults that do not cause remote capacitor flash-over [13, 32].

ii-When capacitors do flash-over, a relay may under-reach significantly in applications where the voltage transducer is located on the bus-bar (source) side of the series capacitor.

The solutions to the foregoing problems are distinct. Problem 1 may be solved by employing specially designed signal processing filters applied to the basic measurands and impedance estimates produced. A solution to problem 2 requires a dynamic adjustment to the relay characteristic following the detection of gap flash-over.

In this thesis proposed solutions related to the problems mentioned in group (i) are presented. Especial attention is given to the situation where the capacitors are located at line ends and the voltage transformers are connected to the source side of the capacitor. A summary of the thesis is now given.

A brief revision of digital distance relaying techniques and algorithms is given in Chapter 2. The discussion will mainly focus on the algorithms which are related to the differential equation line model. A short comparison between different methods is outlined.

Chapter 3 deals with the algorithm chosen for implementation in the proposed digital distance relay. The behaviour of the algorithm when applied to a series compensated line is examined. In particular, the method of differentiating the current signal and its effect in reducing the high frequency oscillation caused principally by the travelling wave is examined.

The digital distance relay structure and computer simulation, together with a brief discussion on primary system simulation is given in Chapter 4. The current and voltage transducer simulations are also included in this chapter. A detailed discussion on capacitor voltage transformers (C.V.T.s) are presented and their effects on distance relays are discussed. Different sections of the simulated digital distance relay are explained in great details. Particular attention is given to the filtering process employed in the relay. In the analogue part of the relay, the anti-aliasing filter and in the digital section the digital pre-fault are thoroughly discussed. The design and performance of a new recursive averager implemented to cater for the sub-synchronous oscillation on the final output of the algorithm is included in this chapter, and finally the relay count regime and trip decision logic is presented.

Chapter 5 is concerned with the accuracy in the measurement of the distance relays when a phase to earth fault occurs. It will be explained that if the conventional methods of current compensation are used in series compensated systems, the measurement will not be accurate. A new method is proposed and implemented in the

relay. It will be shown that the accuracy of the relay is greatly improved when the new method is employed in the relay. The new concept of complex residual compensation factor as opposed to the conventional real compensating factor is also discussed.

The relay response for 70% series compensation, where the capacitor is split into two halves and installed at each end of the line is presented in Chapter 6. The relay characteristic for source side and line side C.V.T. will be shown and relay operating time for the fault inception angle of 0 and 90 degrees are illustrated.

Chapter 7 includes the relay response for the situations where the series capacitor is installed at the mid-point of the line. In order to improve the relay operating time response of the relay, a new relay Quadrilateral characteristic is proposed and implemented in the relay. The relay count regime and trip decision logic suitable for such applications is presented in this chapter.

The thesis will conclude in Chapter 8 and some proposals are given for future work.

CHAPTER 2

DIGITAL DISTANCE RELAY TECHNIQUES

During the past two decades, several algorithms for distance protection have been proposed based on real time impedance measurement. These techniques can be classified into five main groups as follows:

1-Sample-and-derivative calculations.

2-Sinusoidal curve-fitting.

3-Fourier analysis of the relaying signals.

4-Least-squares curve fitting.

5-Solution of differential equation of the protected system model.

The differential equation algorithms (group 5) represent a major theme in line relaying. The algorithms in groups 1 to 4 are mainly based on a description of the waveforms. These algorithms attempt to estimate the fundamental frequency components of currents and voltages in order to compute the impedance to the fault [33]. The differential equation algorithms, on the other hand, are based on a model of the system rather than on a model of the signal.

Consider the single-phase model of the faulted line shown in Fig 2.1. The differential equation relating the voltage and current seen by the relay is:

$$v_{(t)}=R\ i_{(t)}+L\ \frac{d}{dt}\ i_{(t)} \qquad 2.1$$

Since both $v_{(t)}$ and $i_{(t)}$ are measured, it is possible that the parameters R and L and hence the distance to the fault can be estimated.

McInnes and Morrison [25] proposed a solution to Equation 2.1 by integrating over two consecutive intervals:

$$\int_{t_0}^{t_1} v_{(t)}dt = R \int_{t_0}^{t_1} i_{(t)}dt + L\,[i_{(t1)} - i_{(t0)}] \qquad 2.2$$

$$\int_{t_1}^{t_2} v_{(t)}dt = R \int_{t_1}^{t_2} i_{(t)}dt + L\,[i_{(t2)} - i_{(t1)}] \qquad 2.3$$

The intervals in Equations 2.2 and 2.3 must be approximated from the sample values. If the samples are equally spaced at an interval $T=1/f_s$ (where f_s is sampling frequency), and the trapezoidal rule is used for the integrals, viz:

$$\int_{t_0}^{t_1} v_{(t)}dt = \frac{T}{2}\,[V_{(t1)}+v_{(t0)}] = \frac{T}{2}\,[v_1 + v_0] \qquad 2.4$$

Then Equations 2.2 and 2.3 can be written for samples at k, k+1, and k+2 as:

$$\begin{bmatrix} \frac{T}{2}\,(i_{k+1}+i_k) & (i_{k+1}-i_k) \\ \\ \frac{T}{2}\,(i_{k+2}+i_{k+1}) & (i_{k+2}-i_{k+1}) \end{bmatrix} \begin{bmatrix} R \\ \\ L \end{bmatrix} = \begin{bmatrix} \frac{T}{2}\,(v_{k+1}+v_k) \\ \\ \frac{T}{2}\,(v_{k+2}+v_{k+1}) \end{bmatrix} \qquad 2.5$$

Then three samples of current and voltage are sufficient to compute estimates of R and L as follows:

$$R_k = \left[\frac{(v_{k+1}+v_k)(i_{k+2}-i_{k+1}) - (v_{k+2}+v_{k+1})(i_{k+1}-i_k)}{(i_{k+1}+i_k)(i_{k+2}-i_{k+1}) - (i_{k+2}+i_{k+1})(i_{k+1}-i_k)} \right] \quad 2.6$$

$$L_k = \frac{T}{2} \left[\frac{(v_{k+2}+v_{k+1})(i_{k+1}+i_k) - (v_{k+1}+v_k)(i_{k+2}+i_{k+1})}{(i_{k+1}+i_k)(i_{k+2}-i_{k+1}) - (i_{k+2}+i_{k+1})(i_{k+1}-i_k)} \right] \quad 2.7$$

Ranjbar and Cory [34] have proposed a related algorithm in which the limits of integration have been selected to introduce nulls at particular harmonic frequencies. The method is very effective in this regard, but does have a generally longer data window. Also, it tends to ring on fault inception so that the results oscillate severely until the window is completely filled with fault data [35].

Sanderson et al [36] proposed a solution of Equation 2.1 in the form:

$$v_{(t)} = R\, i_{(t)} + L\, i'_{(t)} \quad 2.8$$

$$v'_{(t)} = R\, i'_{(t)} + L\, i''_{(t)} \quad 2.9$$

Where v' is the first derivative of voltage and $i'_{(t)}$ and $i''_{(t)}$ are the first and second derivatives of current signal respectively. The use of the first and second differentiations accentuates noise in the measured parameters. In order to improve the system noise immunity a digital smoothing process has been suggested by fitting a second order polynomial to a data window of seven samples as proposed by Savitzky et al [37].

Johns and Martin showd that the Fourier Transform techniques can be used to solve Equation 2.1 and hence calculate the line parameters [28].

Consider two filters having impulse responses $h_{1(\tau)}$

and $h_{2(\tau)}$, defined over the same window width T_W. The output of the filters are in the following forms:

$$v_{1(t)} = \int_0^{T_W} v_{(t-\tau)} h_{1(\tau)} \, dt \qquad 2.10$$

$$v_{2(t)} = \int_0^{T_W} v_{(t-\tau)} h_{2(\tau)} \, dt \qquad 2.11$$

Defining the filter impulse responses $h_{1(\tau)}$ and $h_{2(\tau)}$ as $\cos(w\tau)$ and $\sin(w\tau)$ respectively, Equations 2.10 and 2.11 can be written in the following form:

$$v_{(t)} = v_{1(t)} + jv_{2(t)} \qquad 2.12$$

and

$$v_{(t)} = \int_0^{T_W} v_{(t-\tau)} \mathrm{EXP}(-jw\tau) d\tau \qquad 2.13$$

Figure 2.2 illustrates in schematic form the formation of two orthogonal components from each input signal. Thus $v_{1(t)}$ and $v_{2(t)}$ are orthogonal components derived from the vector $v_{(t)}$, and similarly for $i_{1(t)}$, $i_{2(t)}$ and $i_{(t)}$. Application of Equations 2.10 and 2.11 to Equation 2.1 gives:

$$v_{1(t)} = R\, i_{1(t)} + L\, i'_{1(t)} \qquad 2.14$$

$$v_{2(t)} = R\, i_{2(t)} + L\, i'_{2(t)} \qquad 2.15$$

Which may be written in the matrix form of Equation 4.16:

$$\begin{bmatrix} v_{1(t)} \\ v_{2(t)} \end{bmatrix} = \begin{bmatrix} i_{1(t)} & i'_{1(t)} \\ i_{2(t)} & i'_{2(t)} \end{bmatrix} \begin{bmatrix} R \\ L \end{bmatrix} \qquad 2.16$$

Inverting the matrix 2.16 to solve for R and L gives:

$$\begin{bmatrix} R \\ L \end{bmatrix} = \frac{1}{D} \begin{bmatrix} i'_{2(t)} & -i'_{1(t)} \\ -i_{2(t)} & i_{1(t)} \end{bmatrix} \begin{bmatrix} v_{1(t)} \\ v_{2(t)} \end{bmatrix} \qquad 2.17$$

where the determinant term is given by:

$$D = i_{1(t)}\, i'_{2(t)} - i'_{1(t)}\, i_{2(t)} \qquad 2.18$$

The line parameters R and L from the relaying to fault point are then given by:

$$R = \frac{v_{1(t)}\, i'_{2(t)} - v_{2(t)}\, i'_{1(t)}}{D} \qquad 2.19$$

$$L = \frac{v_{2(t)}\, i_{1(t)} - v_{1(t)}\, i_{2(t)}}{D} \qquad 2.20$$

In order to obtain two linearly independent equations from system signals similar to those given in Equations 2.14 and 2.15, two direct sample values from each input measurand, which are spaced apart in time by n samples, can be used [38]. This method, when compared to the previous method, has the advantages of immunity to harmonics or system frequency changes [29].

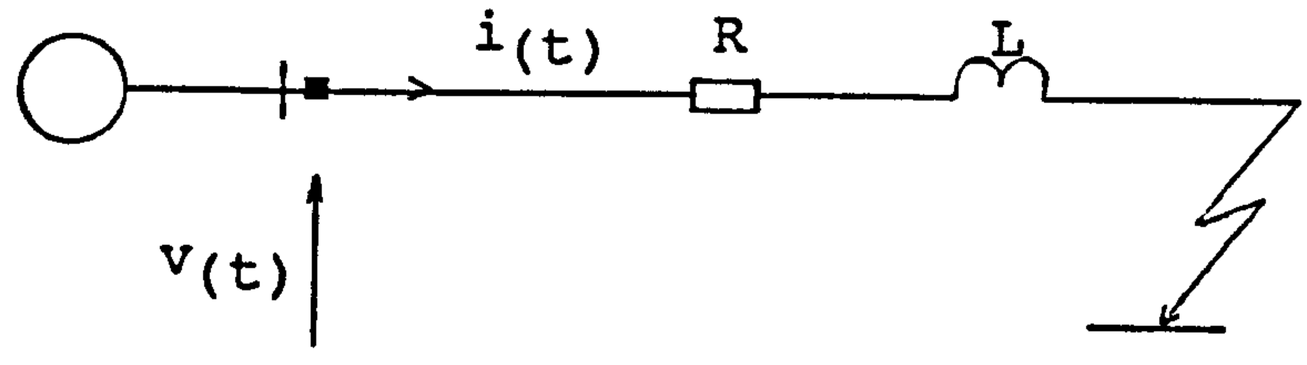

FIG 2.1- Relay Model Of Transmission Line

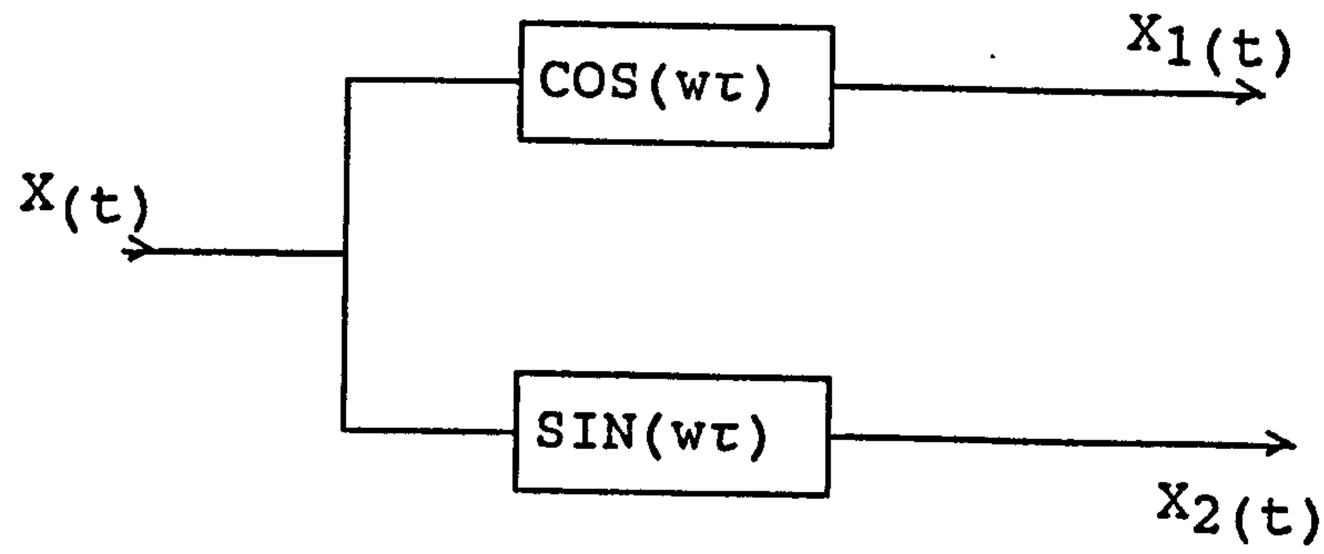

FIG 2.2- Orthogonal Components Formation

CHAPTER 3

TIME SPACED SOLUTION DISTANCE PROTECTION ALGORITHM

In this chapter, first the application of the basic distance protection algorithm to a plain feeder model is discussed and then a series capacitor compensated line is considered.

3.1-The Distance Protection Scheme Algorithm

The new distance protection scheme is based on a modification of the method which was discussed in the preceding chapter [25, 34]. Consider the transmission line model shown in Fig 3.1. The relationship between the relaying voltage, $v_{(t)}$, and current, $i_{(t)}$, is given by the expression,

$$v_{(t)} = Ri_{(t)} + L \frac{d}{dt} i_{(t)} \qquad 3.1$$

If the relay produces two linearly independent equations from each relaying signal ($v_{(t)}$ and $i_{(t)}$), then it is possible to calculate the line parameters, R and L [25, 34, 35]. This can be achieved by considering the solution at two points on the relaying measurands which are apart in time by Θ degrees thus avoiding the process of integration (see Chapter 2). The two simultaneous equations can then be written as:

$$v_{1(t)} = R\, i_{1(t)} + L\, i'_{1(t)} \qquad 3.2$$

$$v_{2(t)} = R\, i_{2(t)} + L\, i'_{2(t)} \qquad 3.3$$

where:

$i'_{1(t)} = \frac{d}{dt} i_{1(t)}$ and $i'_{2(t)} = \frac{d}{dt} i_{2(t)}$

Which may be written in the matrix form of Equation 3.4:

$$\begin{bmatrix} v_{1(t)} \\ v_{2(t)} \end{bmatrix} = \begin{bmatrix} i_{1(t)} & i'_{1(t)} \\ i_{2(t)} & i'_{2(t)} \end{bmatrix} \begin{bmatrix} R \\ L \end{bmatrix} \qquad 3.4$$

Inverting the matrix 3.4 to solve for R and L gives:

$$\begin{bmatrix} R \\ L \end{bmatrix} = \frac{1}{D} \begin{bmatrix} i'_{2(t)} & -i'_{1(t)} \\ -i_{2(t)} & i_{1(t)} \end{bmatrix} \begin{bmatrix} v_{1(t)} \\ v_{2(t)} \end{bmatrix} \qquad 3.5$$

where the determinant term is given by:

$$D = i_{1(t)}\, i'_{2(t)} - i'_{1(t)}\, i_{2(t)} \qquad 3.6$$

The line parameters R and L from the relaying to fault point are then given by:

$$R = \frac{v_{1(t)}\, i'_{2(t)} - v_{2(t)}\, i'_{1(t)}}{D} \qquad 3.7$$

$$L = \frac{v_{2(t)}\, i_{1(t)} - v_{1(t)}\, i_{2(t)}}{D} \qquad 3.8$$

3.2-Steady State Single Frequency Analysis

Let the voltage and current signals be expressed as pure sinusoidal waveforms:

$$v_{(t)} = V \cdot \sin(w_o t) \qquad 3.9$$

$$i_{(t)} = I \cdot \sin(w_o t - \phi) \qquad 3.10$$

Where w_o is the power system frequency and ϕ is the angle between the voltage and current at that frequency. The relaying components $v_{1(t)}$, $i_{1(t)}$, $v_{2(t)}$, and $i_{2(t)}$ of Equations 3.2 and 3.3 can be written as:

$$v_{1(t)}=V\cdot\sin(w_o t) \qquad 3.11$$

$$i_{1(t)}=V\cdot\sin(w_o t-\phi) \qquad 3.12$$

$$v_{2(t)}=V\cdot\sin(w_o t-\Theta) \qquad 3.13$$

$$i_{2(t)}=V\cdot\sin(w_o t-\phi-\Theta) \qquad 3.14$$

Where Θ is the delay angle which is used to produce the second equation (see Fig 3.2).

Appendix 3A shows that R, L, and D are given by:

$$R=\frac{V}{I}\cdot\cos(\phi) \qquad 3.15$$

$$L=\frac{V}{I\cdot w_o}\cdot\sin(\phi) \qquad 3.16$$

$$D=I^2\cdot w_o\cdot\sin(\Theta) \qquad 3.17$$

It is clear from equation 3.17 that if Θ assumes a value corresponding to $k\pi$, where k=0, 1, 2, ..., then the matrix 3.5 becomes singular and therefore no solution for R and L can be expected.

3.3-Application Of The Algorithm To Series Capacitor Compensated Lines

In series capacitor compensated lines a three phase capacitor is inserted into each phase of the transmission system. Thus the capacitor is in series with the line resistance and reactance model as shown in Fig 3.3. This model is valid for lines that are not extremely long, permitting shunt capacitance of the line to be neglected. In the case of series compensated lines, that are infact normally relatively long, shunt admittance effects introduce some errors but do not, in general, corrupt the results exessively [35] (for line length<400 km no errors were observed in steady state calculations).

Considering the effect of the series capacitor, Equation 3.1 can be written as:

$$v_{(t)}=Ri_{(t)} + L\frac{d}{dt}i_{(t)} + \frac{1}{C}\int i_{(t)}\,dt \qquad 3.18$$

Where C is the series capacitor capacitance.

Under steady state conditions, where there is only power frequency present, Equation 3.18 can be expressed as:

$$v_{(t)}=R\cdot I\cdot\sin(w_o t) + L\frac{d}{dt}I\cdot\sin(w_o t) + \frac{1}{C}\int I\cdot\sin(w_o t)\,dt \qquad 3.19$$

or

$$v_{(t)}=R\cdot I\cdot\sin(w_o t) + I\cdot w_o\cdot L\cdot\cos(w_o t) - \frac{1}{w_o\cdot C}I\cdot\cos(w_o t) \qquad 3.20$$

Equation 3.20 can be rearranged in the following form:

$$v_{(t)}=R\cdot I\cdot\sin(w_o t) + (w_o\cdot L - \frac{1}{w_o\cdot C})\cdot I\cdot\cos(w_o t) \qquad 3.21$$

or

$$v_{(t)}=R\cdot I\cdot\sin(w_o t) + (L - \frac{1}{w_o^2\cdot C})\frac{d}{dt}I\cdot\sin(w_o t) \qquad 3.22$$

During a fault however, the above condition is no longer valid and other frequencies, such as sub-synchronous frequency and long line transient effects are likely to result in significant frequencies close to power frequency being present. Hence there is a need for an effective filtering of the system signals, which will be discussed in the following chapter. By band-limiting the voltage and current signals around power frequency, the differential equation which is solved by the algorithm

returns to an equivalent form of Equation 3.23, where $v_{(t)}$ and $i_{(t)}$ are band-limited versions of the signals.

$$v_{(t)}=Ri_{(t)} + L' \frac{d}{dt} i_{(t)} \qquad 3.23$$

where: $$L'=L - \frac{1}{w_o^2 \cdot C}$$

3.4-Effect Of Sub-Synchronous Frequencies

The series capacitors, in series compensated lines, form resonance circuits with the reactance of the transmission line and the source system. This resonance phenomenon, which is usually poorly damped [22], has frequencies which are often lower than the fundamental power frequency. In the next chapter this effect will be discussed in more detail. Consider input signals of the form:

$$v_{(t)}=V_o \cdot \sin(w_o t) + V_{su} \cdot \sin(w_{su} t+\beta) \qquad 3.24$$

and

$$i_{(t)}=I_o \cdot \sin(w_o t-\phi_o) + I_{su} \cdot \sin(w_{su} t+\beta-\phi_{su}) \qquad 3.25$$

where:

w_o, w_{su} =power system and sub-synchronous frequency respectively.

V_o, I_o =voltage and current magnitude of the fundamental components respectively.

V_{su}, I_{su} =voltage and current magnitude of the sub-synchronous components respectively.

β =phase angle between the fundamental & sub-synchronus components.

ϕ_o =phase angle between the power system fundamental voltage and current.

ϕ_{su} =phase angle between the sub-synchronous voltage and current.

It must be noted that in order to simplify the analysis the decaying factor of the sub-synchronous component has been ignored.

The relaying components $v_{1(t)}$, $v2_{(t)}$, $i_{1(t)}$ and $i_{2(t)}$ can thus be written as:

$$v_{1(t)}=V_o \cdot \sin(w_o t) + V_{su} \cdot \sin(w_{su} t+\beta) \quad 3.26$$

$$i_{1(t)}=I_o \cdot \sin(w_o t-\phi_o) + I_{su} \cdot \sin(w_{su} t+\beta-\phi_{su}) \quad 3.27$$

$$v_{2(t)}=V_o \cdot \sin(w_o t-\Theta) + V_{su} \cdot \sin(w_{su} t+\beta-\Theta) \quad 3.28$$

$$i_{2(t)}=I_o \cdot \sin(w_o t-\phi_o) + I_{su} \cdot \sin(w_{su} t+\beta-\phi_{su}-\Theta) \quad 3.29$$

Appendix 3B shows that the line parameters are given by:

$$D=\sin(\Theta) \cdot \{w_o \cdot I_o^2+w_{su} \cdot I_{su}^2 + I_o \cdot I_{su} \cdot (w_o+w_{su}) \cdot \cos[(w_o-w_{su})t-\beta-(\phi_o-\phi_{su})]\} \quad 3.30$$

$$D \cdot R=\sin(\Theta) \cdot \{w_o \cdot V_o \cdot I_o \cdot \cos(\phi_o)+w_{su} \cdot V_{su} \cdot I_{su} \cdot \cos(\phi_{su}) +(A_R^2+B_R^2)^{\frac{1}{2}} \cdot \sin[(w_o-w_{su})t-\beta+\tan^{-1}(A_R/B_R)]\} \quad 3.31$$

where:

$$A_R=w_{su} \cdot V_o \cdot I_{su} \cdot \cos(\phi_{su}) + w_o \cdot V_{su} \cdot I_o \cdot \cos(\phi_o)$$

$$B_R=w_o \cdot V_{su} \cdot I_o \cdot \cos(\phi_o) + w_{su} \cdot V_o \cdot I_{su} \cdot \cos(\phi_{su})$$

and

$$D \cdot L'=\sin(\Theta) \cdot \{V_o \cdot I_o \cdot \sin(\phi_o)+V_{su} \cdot I_{su} \cdot \sin(\phi_{su}) + (A_X^2+B_X^2)^{\frac{1}{2}} \cdot \sin[(w_o-w_{su})t-\beta+\tan^{-1}(A_X/B_X)]\} \quad 3.32$$

where:

$$A_X=V_o \cdot I_{su} \cdot \sin(\phi_{su}) + V_{su} \cdot I_o \cdot \sin(\phi_o)$$

$$B_X=V_o \cdot I_{su} \cdot \cos(\phi_{su}) - V_{su} \cdot I_o \cdot \cos(\phi_o)$$

The above analysis illustrates that when there are two frequencies (power system and sub-synchronous) in the

relaying signal, the resultant measured values contain dc and oscillatory terms which oscillate with a frequency corresponding to the difference between the fundamental and sub-synchronous frequencies. Also it is revealed that the magnitude and phase angle of the ac components are not the same and are independent of Θ. It should be noted that the fault inception angle (point on wave when fault occurs) has been ignored in the preceding analysis. This, if included, may change the phase angle of the ac component of the measured parameters but the frequency of the oscillation will not be affected.

It has already been mentioned that the sub-synchronous oscillation, caused by series capacitors in series compensated systems, are usually under-damped [22] which in turn causes errors in measurement during the time when the Ultra-High-Speed digital distance relay must reach a trip decision. Therefore there is a need for a special filtering of signals and appropriate design for the trip regime. It is also worth mentioning that during a fault high frequency components, caused principally by travelling waves, are also superimposed on the measuring signals and the above analysis with three frequency components (power frequency, sub-synchronous frequency and the dominant travelling wave) on the relaying signals can be applied to investigate the resulting effects on the measured parameters. However, these components have higher damping coefficients and diminish much faster than the sub-synchronous oscillations. Nevertheless they also make the relay decision making process more difficult during the initial period after a fault and consequently

must be filtered from the relaying signals. The relay filtering process will be discussed in more detail in the next chapter.

3.5-Discrete Processing Solution

The need for faster and consistent tripping times has promted an interest in discrete processing techniques. In this technique, samples are fed to the process for individual impedance estimates. The filtered voltage and current can be made available as samples (using the discrete variable k), at intervals T_s in time given by the relay sampling frequency f_s ($T_s=1/f_s$).

In order to produce two simultanous equations, the relay uses direct sample values from each input measurand which are time spaced by n samples as shown in Fig 3.4. Also since a given sample value contains no information about the derivative at the sampling instant, the current derivative can be approximated by computing the difference between two consecutive samples. In the next section it will be explained that a better result can be obtained if the current derivative is computed over m number of samples on each side of the point where a solution is considered. In this method, since the relay has no information about the future samples, the point of solution is delayed so that the current derivative may be calculated. Hence the two simultanous equations from the line model can be expressed as:

$$v_{k-m}=R\cdot i_{k-m} + L'\cdot i'_{k-m} \qquad 3.33$$

$$v_{k-n-m}=R\cdot i_{k-n-m} + L'\cdot i'_{k-n-m} \qquad 3.34$$

where:

$$i'_{k-m}=\frac{i_k - i_{k-2m}}{2 \cdot m \cdot T_s}$$

$$i'_{k-n-m}=\frac{i_{k-n} - i_{k-n-2m}}{2 \cdot m \cdot T_s}$$

Factors which determine the value of n are mainly as follows:

1-'n' must not correspond to an angular displacement of $k\pi$ (k=0, 1, 2, ...) of the fundamental component of the relaying signals (see section 3.2).

2-In order to reduce the window width of the algorithm, which in turn avoids long operating times by the relay, 'n' must be close to unity

3-To avoid ill conditioning of the algorithm under all operating conditions (to preserve independance of the solutions), when executed on a fixed word length processor, 'n' must be greater than unity.

A value of 6 has been suggested for n [29] which proved to be adequate for practical purposes and is used in the digital distance relay.

In section 3.6 the method of differentiating the current signals is explained and a value of 4 is suggested for m. Therefore Equation 3.33 and 3.34 can be expressed in matrix form:

$$\begin{bmatrix} v_{k-4} \\ v_{k-10} \end{bmatrix} = \begin{bmatrix} i_{k-4} & i'_{k-4} \\ i_{k-10} & i'_{k-10} \end{bmatrix} \begin{bmatrix} R \\ L' \end{bmatrix} \qquad 3.35$$

where: $$i'_{k-4}=\frac{i_k - i_{k-8}}{8 \cdot T_s}$$

$$i'_{k-10}=\frac{i_{k-6} - i_{k-14}}{8 \cdot T_s}$$

Inverting the matrix 3.35 to solve for R and L' yields:

$$\begin{bmatrix} R \\ L' \end{bmatrix} = \frac{1}{D_{k-4}} \begin{bmatrix} i'_{k-10} & -i'_{k-4} \\ -i_{k-10} & i_{k-4} \end{bmatrix} \begin{bmatrix} v_{k-4} \\ v_{k-10} \end{bmatrix} \qquad 3.36$$

where:

$$D=i_{k-4} \cdot i'_{k-10} - i'_{k-4} \cdot i_{k-10}$$

R and L' can therefore be expressed as:

$$R=\frac{1}{D_{k-4}}[v_{k-4} \cdot i'_{k-10} - v_{k-10} \cdot i'_{k-4}] \qquad 3.37$$

$$L'=\frac{1}{D_{k-4}}[v_{k-10} \cdot i_{k-4} - v_{k-4} \cdot i_{k-10}] \qquad 3.38$$

Note that the algorithm has a window of 15 samples, which corresponds to 3.75 msec at a sampling rate of 4 kHz.

The reactance is calculated by multiplying the measured L' by the fundamental frequency of the power system. Hence:

$$X=w_o \cdot L'$$

To avoid digital division in the relay, which is considered to be undesirable in a real time calculation by

a microprocessor, the current derivatives can be calculated without dividing by the term $2 \cdot m \cdot T_s$, but instead multiplying X by the same term. Note that the term is eliminated from the calculated D and R. Thus:

$$X = 2 \cdot m \cdot T_s \cdot w_o \cdot L'$$

3.6-Computation Of Current Derivative

In order to compute the current derivative, different methods have been proposed [24, 27, 29]. The method initially adopted in this work was based on the difference between one point on each side of the point of interest (the sample at which R and L' is calculated).

Fig 3.5 shows the frequency response of the difference equation:

$$i'_{k-1} = \frac{i_k - i_{k-2}}{2 \cdot T_s} \qquad 3.39$$

where T_s is the sampling period.

Examination of frequency response of different methods has revealed that in order to suppress the high frequency oscillations in the measured resistance and reactance, caused by travelling waves, the current must be differentiated using more points. Fig 3.6 illustrates the frequency response of the current derivative when nine points are used. The corresponding difference equation being:

$$i'_{k-4} = \frac{i_k - i_{k-8}}{2 \cdot T_s} \qquad 3.40$$

Fig 3.7.a shows i', using one point on each side, for

a fault at 160 km (line length=300 km) and inception angle of 90° where the travelling waves have the maximum effect on the relay measurands. Fig 3.7.b shows the corresponding measured X and R.

Fig 3.8.a illustrates the current derivative for the same fault but for four points on each side of the point where the solution is considered. Fig 3.8.b shows the corresponding measured X and R.

Appendix 3C shows the error involved in taking more points. By comparing Figures 3.7.b and 3.8.b it is revealed that the high frequency oscillation has been greatly reduced, whereas the actual dc values have not been significantly affected. This is important, especially for series capacitor compensated systems where the lines are usually long.

For the foregoing reasons, it is decided to differentiate the current over nine points, i.e., four points on each side of the point in interest.

It must be said that for the results shown, the relaying signals were filtered before the algorithm stage. The filters used will be discussed in the next chapter.

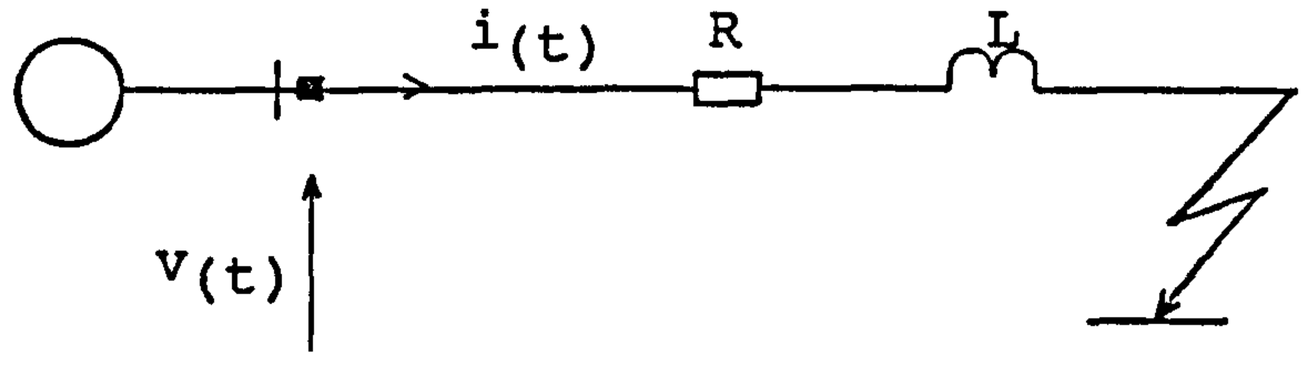

FIG 3.1- Relay Model Of Transmission Line

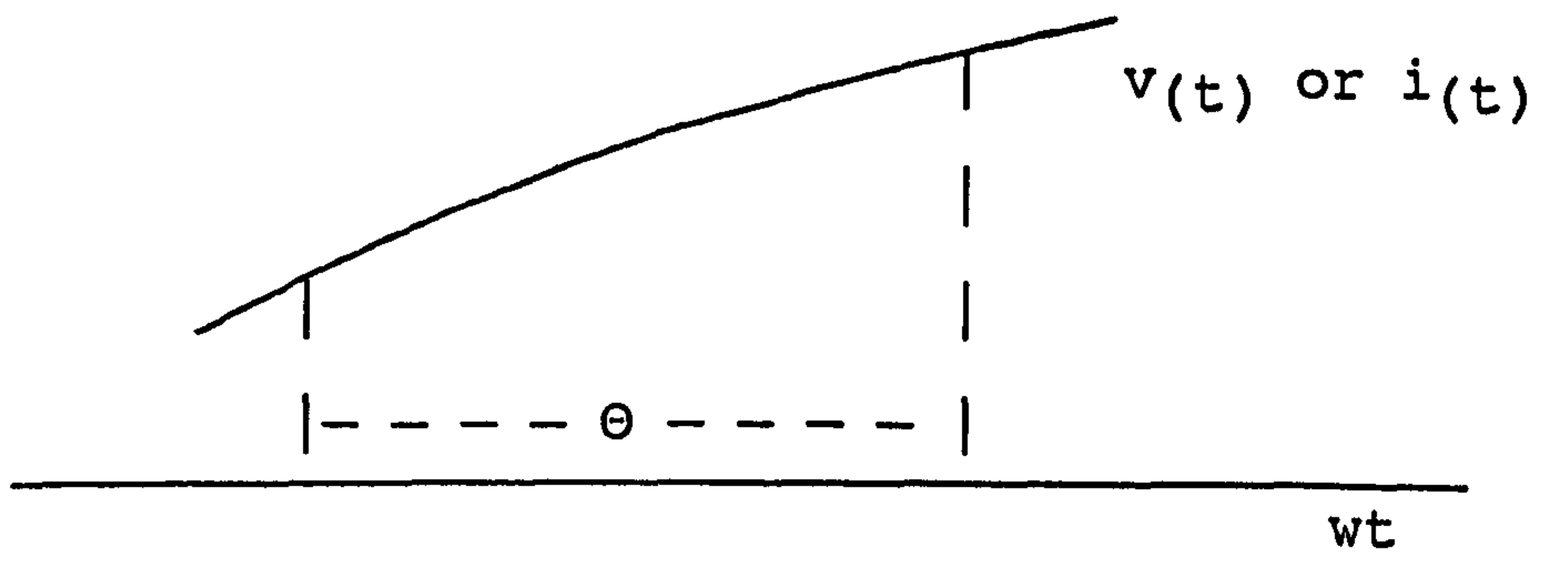

FIG 3.2-Solution Formation Using Time Spacing

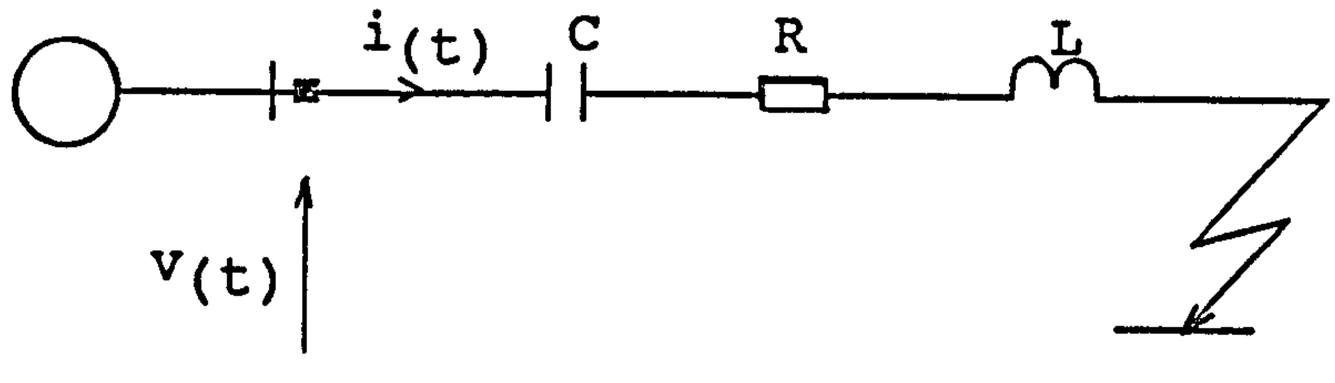

FIG 3.3-Transmission Line Model With Series Capacitor

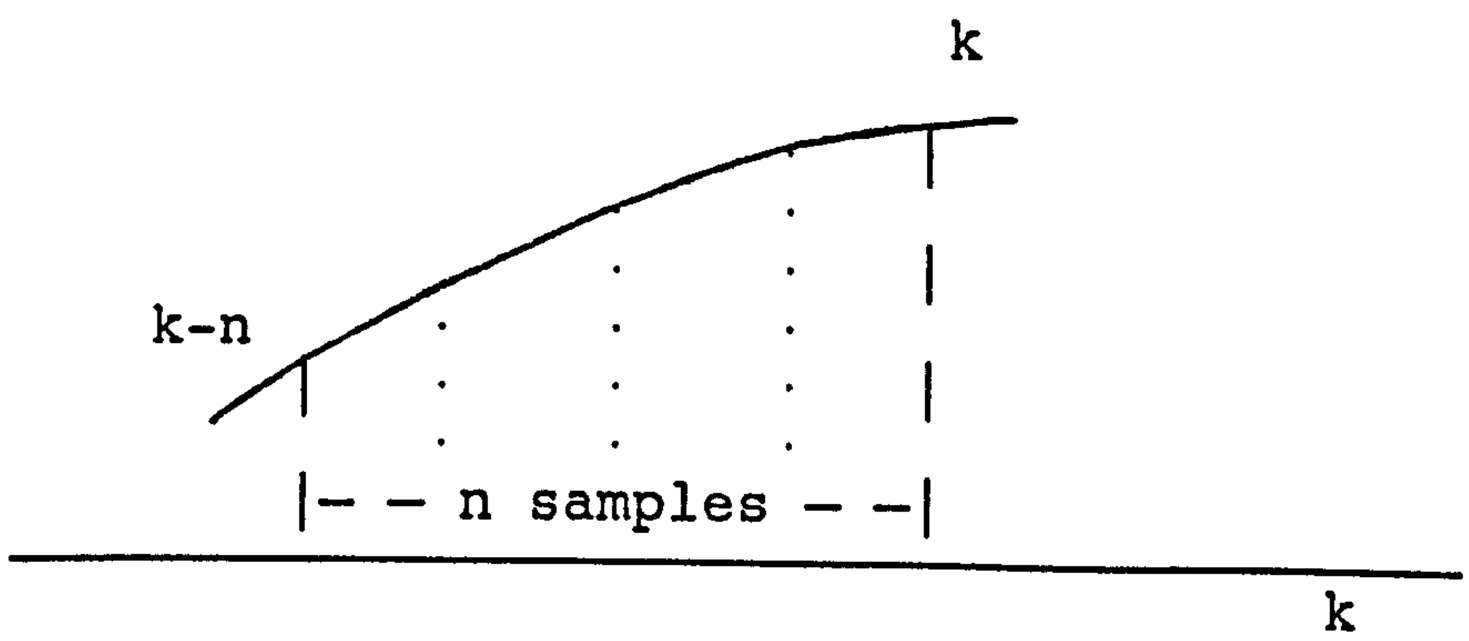

FIG 3.4-Solution Formation Using Discrete k Variable

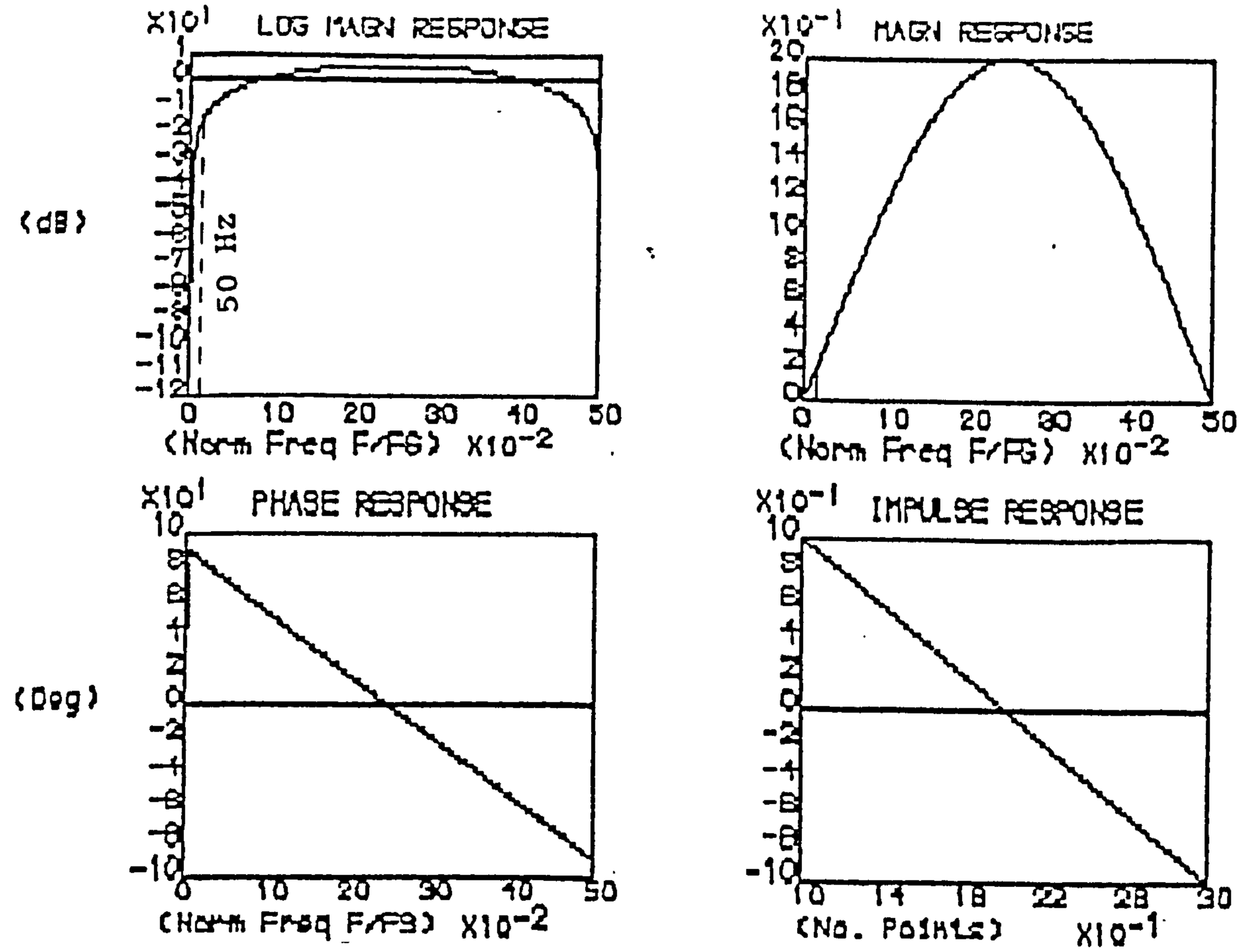

Fig 3.5-Frequency Response Of Equation 3.39

Note that the sampling frequency (fs) is 4 kHz

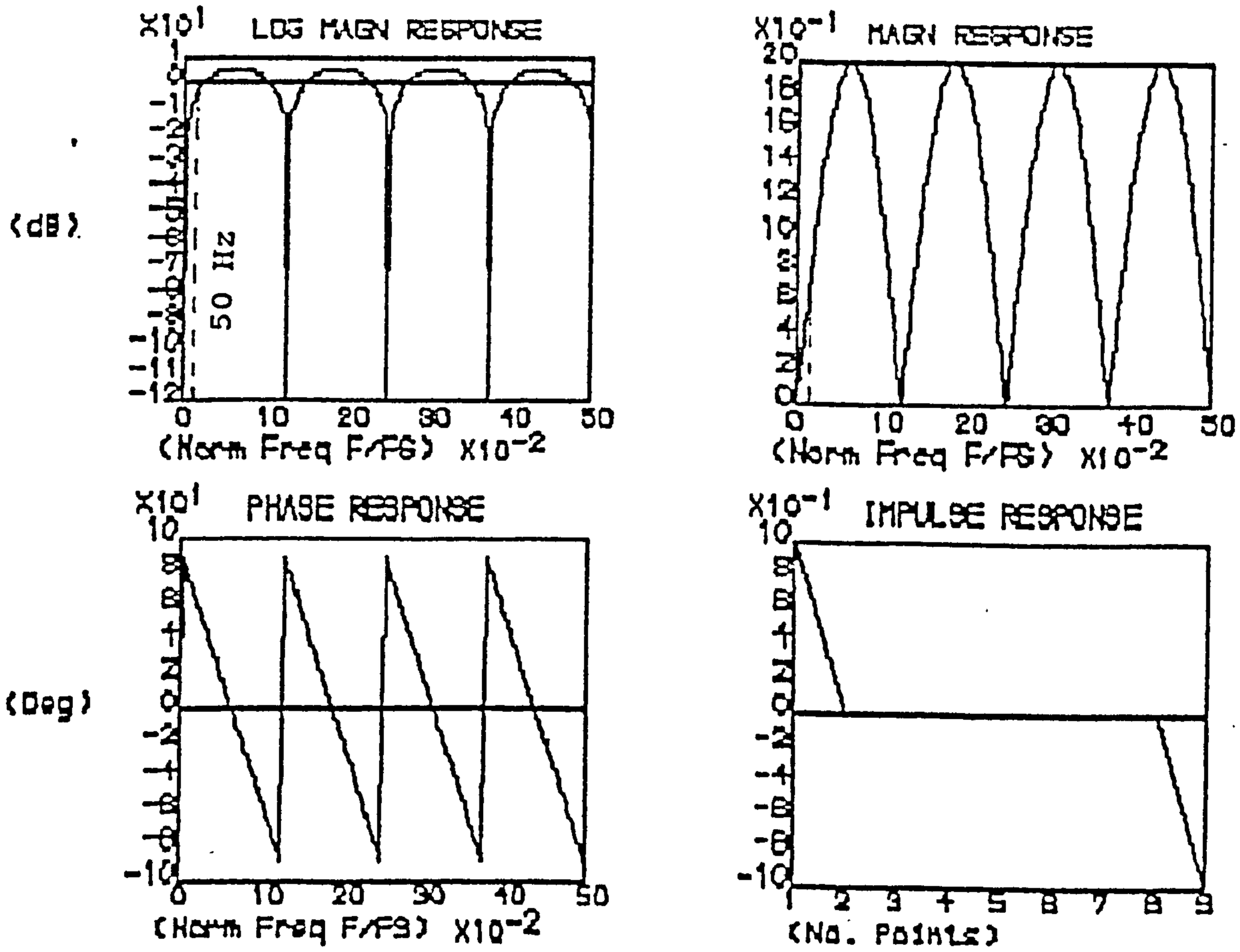

Fig 3.6-Frequency Response Of Equation 3.40

Note that the sampling frequency (f_s) is 4 kHz

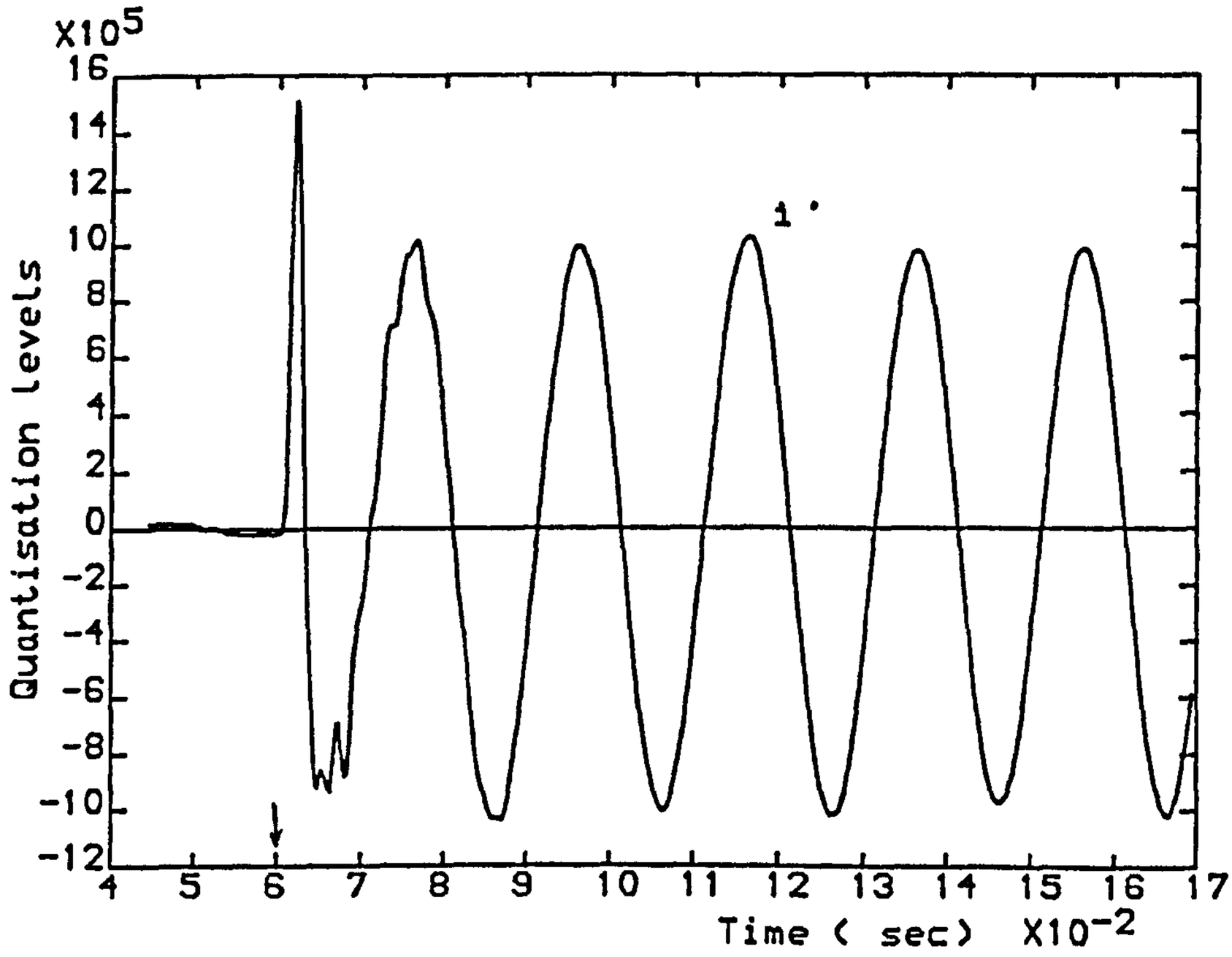

Fig 3.7.a-Current Derivative Using One Point On Each Side

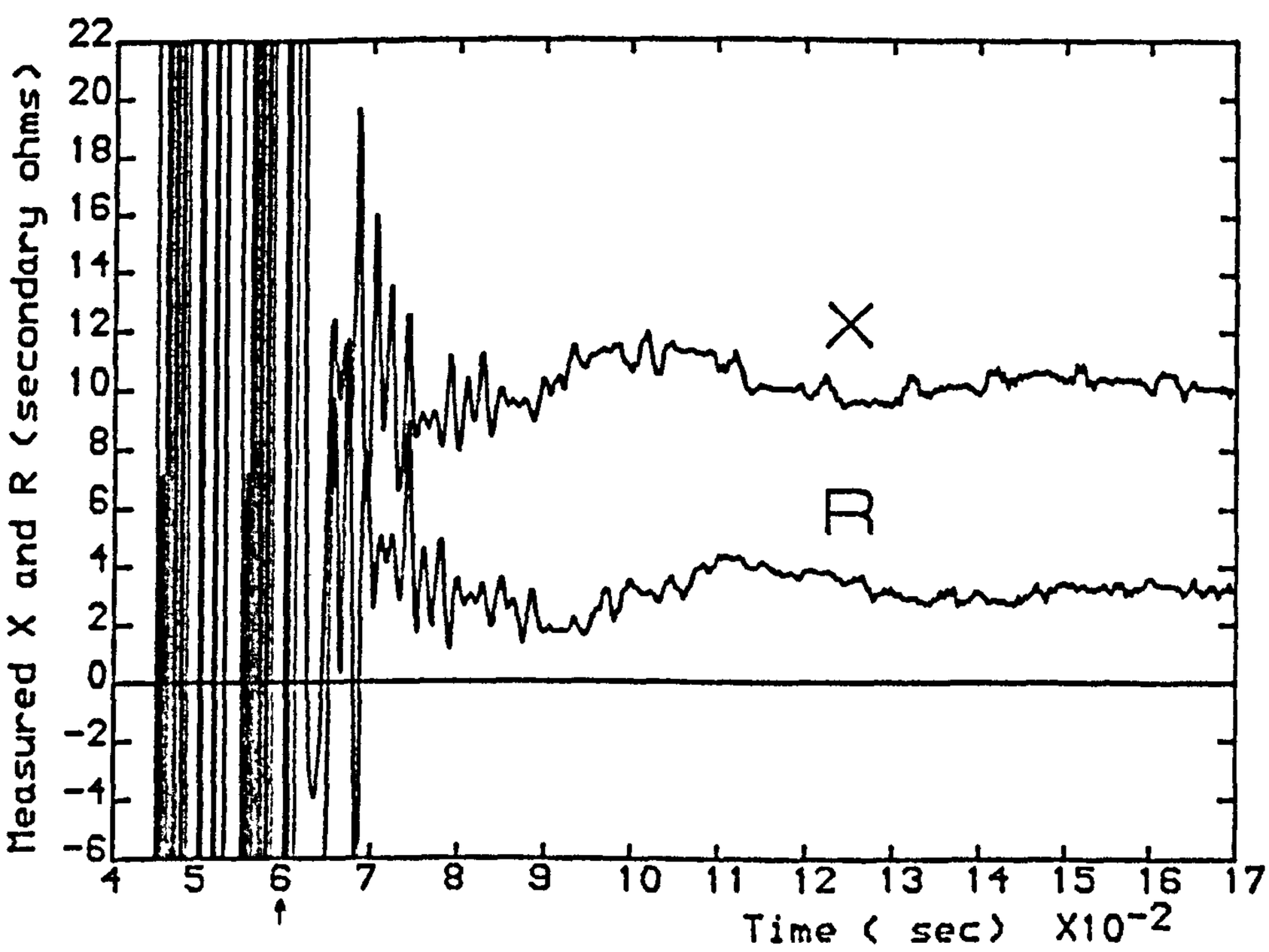

Fig 3.7.b-Measured X and R Using One Point On Each Side

SE SCL-5 GVA, RE SCL-35 GVA, No Load

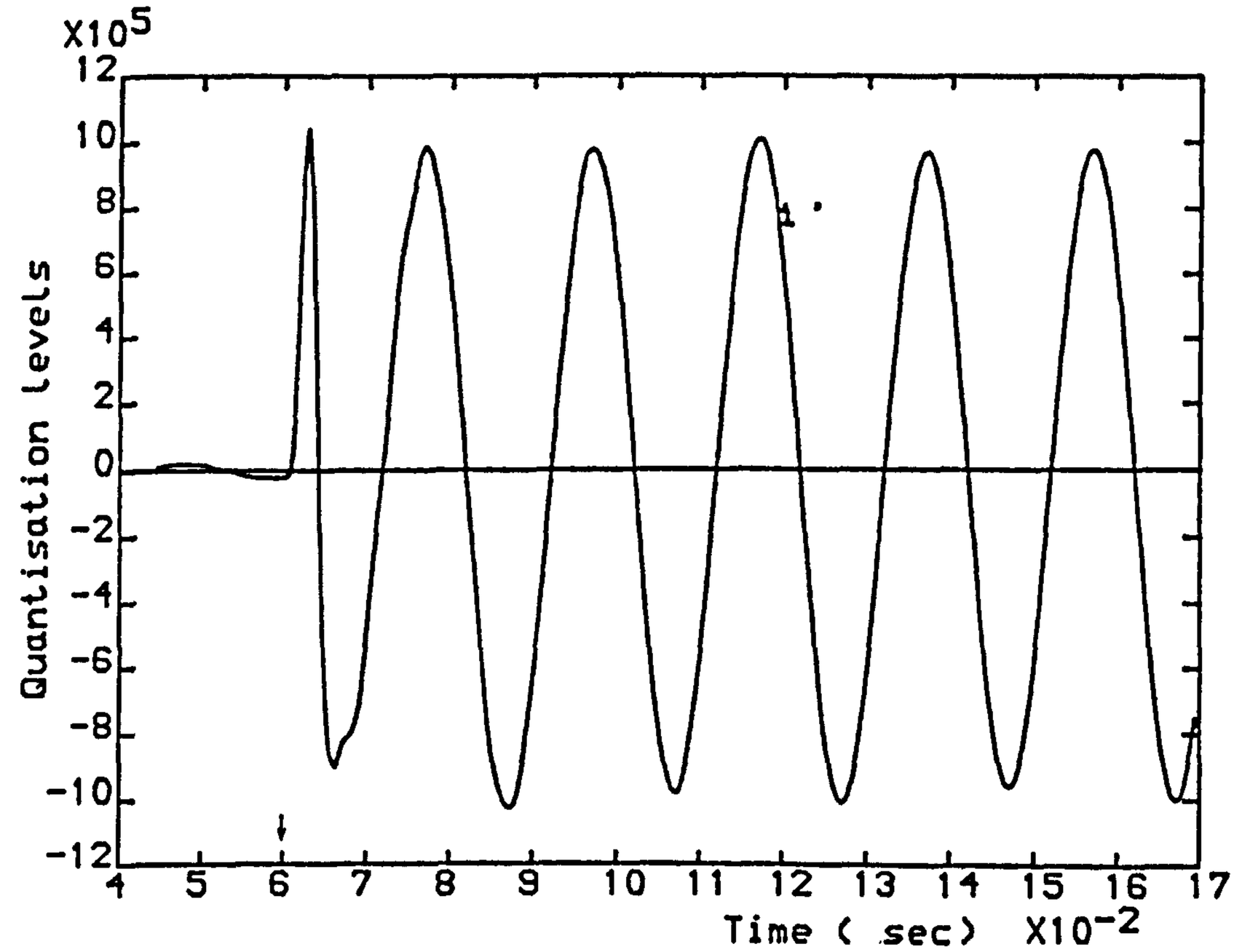

Fig 3.8.a-Current Derivative Using Four Points On Each Side

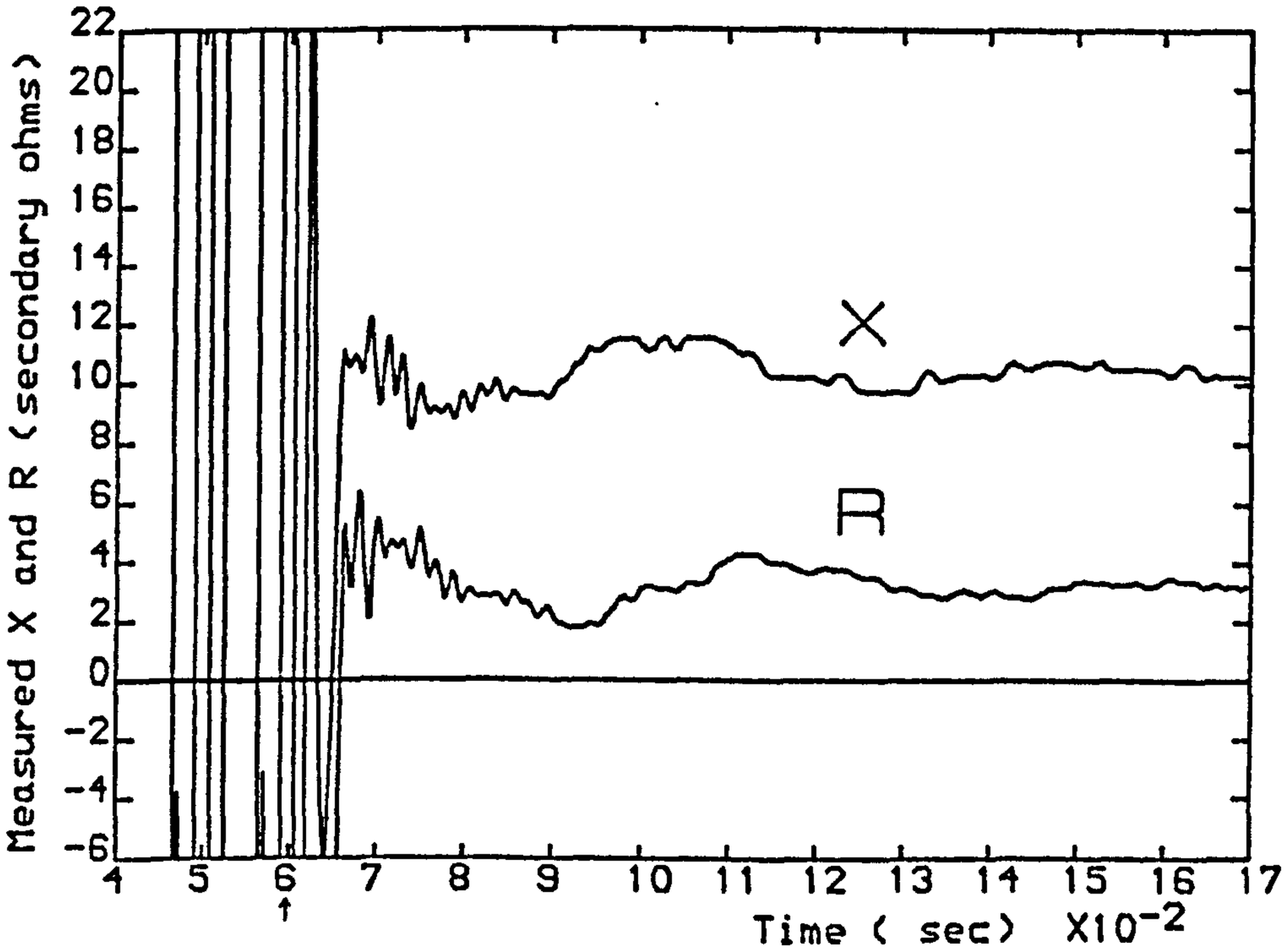

Fig 3.8.b-Measured X and R Using Four Points On Each Side

SE SCL=5 GVA, RE SCL=35 GVA, No Load

CHAPTER 4

DIGITAL DISTANCE RELAY

Digital computers nowadays are very powerful tools in engineering fields. They can be used to accurately simulate and test a system or component before they are actually built or manufactured.

The importance of digital computers in design and test stages of the components of power systems is well known. Advanced methods are now available for modelling and testing complex power systems, such as series compensated lines, on a digital computer [9, 11, 23, 39]. These simulation programes provide not only the steady state, but also the transient response. They are of great values to protective relays designers, for new designs can be tested in laboratories before they are actually installed on the system. In particular when considering Very and/or Ultra-High-Speed protection schemes, when the measurement is carried out in a very short time after fault inception, the waveforms from which measurements are made must contain all transient phenomena which occur in a real system after a short circuit fault. These simulation programs provide, in numerical forms, the voltage and current waveforms at the relaying points.

The primary system simulation program which is used in this study, employs the frequency domain analysis of transmission lines. Full description of the technique and the program is given in references 9 and 40.

The digital simulation of the primary system is run at 8 kHz sampling rate, which therefore yields accurate

information of up to 4 kHz. It is pointless extending this bandwidth since the C.V.T.s which are used without exception on EHV systems, have a very low cut off frequency of typically 600 Hz. Most C.T.s however have a very wide bandwidth, up to 10 kHZ, but an interface is used in the current channel to convert the current to a proportional voltage over a specified frequency range, much less than 10 kHz. Moreover, an analogue low pass filter (discussed later) is employed to pre-filter the signals, with a cut off frequency well below 4 kHz. Hence the requirement to provide very high frequency primary system information, above 4 kHz, is obviated.

The primary system configuration which is simulated thoughout this work is shown in Figure 4.1. Like the most series compensated line constructions, a horizontally constructed transmission line is considered. The complete data of the line is given in Appendix 4A.

4.1-Primary System Interfaces

The primary system interfaces comprise the C.V.T. and C.T. transducers.

4.1.1-capacitor voltage transformer C.V.T.

It is now common practice to seek protective relay operating times of about half a cycle from fault inception. The high speed capability is conditional on the quality of the input voltage signals. Although electromagnetic voltage transformers (V.T.s) have a performance which meets modern protection requirements, the normal practice at transmission system voltages of 100 kV and above is to use capacitor voltage transformers

(C.V.T.s) for protection and measuring functions, these being used in preference to electromagnetic V.T.s for reasons of economy. Unfortunately, errors generated by C.V.T.s during rapidly changing conditions can have detrimental effects on the operation of protective relays [18, 41]. These C.V.T. errors result from energy storage in the C.V.T. circuit, which causes a distorted output for several cycles [18] of the system frequency when the primary voltage changes suddenly, particularly when the primary voltage falls to a small fraction of its rated voltage.

While it is difficult , if not impossible, to make any general statements about the effect of C.V.T. errors on relay performance, one possible relay problem that has been identified is the over-reach of first zone distance relays.

Several solutions have been devised to overcome the C.V.T. transient error problem as far as over-reach is concerned [18]. The mechanism of the digital distance relay trip decision logic, which will be discussed later, is such that the relay operation is delayed for a few millisecond after the fault detection. This method, although not primarily designed for this purpose, overcomes, to some extent, the measuring errors due to the C.V.T. transients.

From the modelling point of view, the C.V.T.s have well defined transfer functions derived from their circuit elements and structures, from which corresponding time domain impulse responses are obtained via inverse Fourier methods.

The effect of any modifying function h(t), upon a time domain variation x(t), may be determined using convolution theorem, such that:

$$y(t) = h(t) * x(t) = \int_{-\infty}^{+\infty} h(\tau) \cdot x(t-\tau) \cdot d\tau \qquad 4.1$$

Where y(t) is the modified version of x(t), and τ is the dummy variable of integration.

If the time scale is divided into 'n' discrete samples of width ΔT, Equation 4.1 can be evaluated via simple numerical integration, which gives:

$$y(n) = \sum_{k=0}^{n} h(k) \cdot x(n-k) \cdot \Delta T \qquad 4.2$$

Hence, the primary voltages at any sample 'n', are found using a past history of the relevant impulse response h(k), together with the profile of the input signal. Figure 4.2.a and b illustrate the impulse and frequency responses of the C.V.T. which was used in the present study.

The three phase voltages are applied to the C.V.T. at their pre-fault peak, to ensure that, at the fault instance no transients are present except those generated by the faults.

The C.V.T. ratio in the simulation is taken as $500x10^3/110$ for the 500 kV system.

4.1.2-current tranformer C.T.

It is assumed that the C.T. has an ideal response over the range of frequencies expected, and therefore is simulated as a step down factor. The saturation of the

C.T. core is also neglected. The ratio is 2000/1.

4.2-The Digital Distance Relay Structure

The digital distance relay was simulated using a standard Fortran program. The outputs from C.V.T. and C.T. are fed to the relay program and the relay calculates the impedance of the line from the relaying to fault point.

The relay can be divided into two main parts:

(i) An analogue part which is mainly instrumentation and signal filtering.

(ii) A digital part, which includes signal filtering, the impedance measurement process and decision logic.

The relay must be capable of meeting conventional distance protection accuracy, nominally 5% of the relay reach, and go further in achieving the advantage of speed and consistency of operation required for ultra fast fault clearance. Tests on the discrete process simulation showed that a sampling rate of 4 kHz is required for U.H.S. performance [42, 28]. Therefore, it was decided to drive the relay at 4 kHz sampling rate. Figure 4.3 shows the structure of the simulated relay. A description of the relay is given below:

(i) Secondary voltage transformer: this is an instrument voltage transformer used for the purpose of signal level adjustment according to the Analogue to Digital A/D converter requirements. The frequency response of such a transformer is taken to be ideal over the operating range of interest.

(ii) Current interface (NOT simulated): this is to convert the current into a proportional voltage. There are different devices, such as the Hall effect device or a transformer with an air gap followed by an integrator, which can be employed. This device is not simulated in the relay simulation. Instead a simple scaling factor was considered for signal level adjustment. The scaling factor is introduced to limit the voltage equivalents of the phase current inputs to ± 10 volts. The choice of the factor depends entirely upon the setting philosophy adopted for the relay. The range of current levels encountered in integrated networks is extremely large and it is necessary to limit or clip the input current if the latter is very high. This permits larger a gain for low current level faults, but introduces some degree of non-linearity into the process. Also the analogue filter used in the relay (discussed later) can suffer from saturation in case the signal exceeds the power supply level available. Therefore, it is essential, at this stage , to adjust the signal level such that saturation or clipping is predicted under the worst possible external fault conditions. Initial adjustments are done so that clipping or saturation does not occur for faults just outside the protected zone.

The residual current is formed, at this stage, by adding the three phase currents.

(iii) Analogue filter: for a sampling frequency of f_s the Nyquist frequency is thus $f_s/2$. All components above $f_s/2$, if unfiltered, will be mapped or translated down into the dc to $f_s/2$ Hz spectrum by the digital process. This is known as aliasing. The anti-aliasing analogue filter is used to filter the frequencies above the Nyquist frequency. A second order low-pass Butterwoth filter is suggested, the transfer function of which takes the standard form of:

$$G_{(s)}=\frac{w_n^2}{s^2 + 2\delta w_n S + w_n^2}$$

The choice of the cut-off frequency and required attenuation largely depends upon the digital stages of the relay. Figure 4.4.a shows the circuit diagram for the proposed analogue filter and Figure 4.4.b illustrates the corresponding frequency response. By cascading two such filters the desired frequency response can be achieved. Figure 4.4.c shows the total frequency response of the filter. From modelling point of view the method explained in Section 4.1.1 was used to obtain the equivalent impulse response of the filter.

(iv) Change in data sampling rate: although the relay operates at 4 kHz sampling frequency, the primary system simulation is derived at 8 kHz, allowing for an accurate simulation of the anti-aliasing filter. The sampling frequency of the relaying signals is reduced in time to 4 kHz at this stage by taking every other samples.

(v) Current clip detector: any current clipping is detected at this stage. If the fault current is very high (i.e. close up faults) and causes saturation of the analogue electronic component of the relay, the clip detector will indicate. This may be used by the relay to initiate the trip directly, irrespective of impedance measurement.

(vi) The Analogue to Digital converter: this is taken to be of 14 bit (13+sign) structure. The eight available signals, three phase voltages, three phase currents and two neutral currents (one from the main line and one from the parallel circuit) are sampled simultaneously by eight sample and holds and then scanned by a multiplexer to a single A/D converter. This stage represents the link between the analogue and digital parts of the process. It must be said that, in computer simulation terms, the difference in analogue and digital quantities is only that the former is perforemed with floating point arithmetic, and the latter with integers. When using a fixed-point representation of a binary number, truncation or rounding errors exist in arithmetic multiplication but not in arithmetic addition. In contrast, these errors are present for multiplication or addition of floating-point binary numbers. In fixed-point format the dynamic range of the number is fixed, and arithmetic addition and multiplication can produce over-flow, thereby producing a result that exceeds the valid dynamic number range. In

floating-point format however the dynamic number range is relatively large and therefore overflow is unlikely to occur.

13 bit converter (13 bit + sign) corresponds to 8192 quantisation levels representing the 10 v input. The conversion gain of the A/D converter is then simply 8192/10=819.2. The range from -10 to +10 volt is thus represented by 16389 quantum levels.

(vii) The residual current compensation process: a great deal of work was carried out on the topic of the residual compensation. This will be discussed in the following chapters. The process which, involves adding a scaled neutral current signals from the main and parallel (if any) circuit to each phase current, is performed digitally rather than analogue wise. In this way a higher resolution is obtained from 13 bit A/D converter for phase current signals.

(viii) The digital pre-filter: it will be explained in Section 4.3 that during the initial post-fault period, the incoming power frequency signal is contaminated by unwanted signals at other frequencies which, in turn distort the impedance measurements. In order to obtain a smooth and accurate measurement it is essential to perform a filtering process and possibly filter out all the unwanted frequencies from the system frequency. The filter and its response will be discussed in Section 4.3.1.

(ix) Production of two relaying components: it was explained in Section 3.5 of Chapter 3 that in order to measure the line parameters from the relaying point, two samples on each relaying signals, $v_{(k)}$ and $i_{(k)}$, are considered. This is done by:

1-storing the incoming signal in a buffer. At the instant of each system clock (relay sampling clock) the samples in the buffer are shifted by one location. In this way, the sample value in the last location of the buffer is discarded and the new sample is placed in the first location. The length of the buffer depends on the delay required by the algorithm (see Chapter 3).

2-to produce two signals from each signal, the samples in the first and last location of the buffer are considered. In this way, two waveforms are produced which are identical but separated in time by a specific delay. Figure 4.5.a and b illustrate the two relaying components of the voltage and current signals respectively.

(x) The relay algorithm and decision logic: it is well known that the protection of series compensated lines require special and delicate design considerations. The method by which the relay calculates the line parameters was explained in Chapter 3. The relay tripping characteristic and trip decision logic will be discussed later.

4.3-Digital Distance Relay Filtering Process

When a fault occurs on an overhead plain uncompensated transmission line, the system voltages and currents are distorted for a period after the fault. Transient phenomena are super-imposed on the system frequency signals. These transient effects can be classified into two main groups:

(i) When a fault occurs on a transmission line the voltage at the fault position is affected. As a result, travelling waves of voltage and accompanying current are initiated. The initial values of these waves are dependent, amoung other factors, on the voltage at the fault position at the instant of fault occurrence. The change in voltage at the fault point travels away from the fault towards the line ends. At the point of discontinuity on the transmission system, part of the wave is transmitted to the next section and part of it is reflected. The method known as lattice diagram and proposed originally by Bewley [43] best analyses the effect of this travelling phenomenon. Figure 4.6 shows a simple Bewley lattice diagram for a fault on a simple transmission line. Walker et al [44] reported results in which it was shown that the frequency of high frequency components were roughly inversely proportional to the distance to fault. Swift [45] explained that how the dominant travelling wave frequency may be affected by the source impedances at the line ends. Reference 46 shows the change in dominant travelling wave for extreme cases of very

low and very high source capacities and different line length.

(ii) A decaying exponential component may appear mainly on the current after a fault occurs. This effect is due to the fact that transmission systems contain inductances and therefore the current state cannot be changed instantly after the fault occurrence.

In series compensated systems however, in addition to the well known fault generated travelling waves and dc offset, the interaction between the total fault loop inductance and the series capacitor create a resonance circuit which causes an oscillation to be super-imposed on the system frequency. In E.H.V systems, the resistance of the lines are small and can be neglected. The resonance frequency is thus given by:

$$f_{su} = \frac{1}{2\pi} \sqrt{\frac{1}{L \cdot C}} \qquad 4.3$$

where:
L=total inductance of the fault loop
C=total capacitance of the fault loop

Figure 4.7 shows the equivalent circuit for a single phase to ground fault, assuming the typical 70% compensation, 35% at each end. Similar circuit with capacitor location in the middle of the line can be used for 50% compensation at the mid-point. The total inductive reactance of the faulted path depends on the fault position which in turn changes the resonance frequency. Referring to Equation 4.3, it is clear that the frequency of the resonance oscillation reduces as the fault position moves away from the source. It must also be noted that for sources with zps/pps impedance ratio of

less than unity the neutral impedance of the source, Z_{SN}, exhibits a negative and therefore capacitive reactance. Also the frequency of resonance oscillation is higher than the power frequency, if the total fault loop reactance is capacitive at power frequency [10].

Figures 4.8 and 4.9 illustrate approximately, the expected resonance (usually called sub-synchronous) frequency for different system source and series compensation. It is clear from Figures 4.8 and 4.9 that the change in resonance frequency tends to be small when the source symmetrical short circuit level becomes very high.

It must be said that, the source termination considered above are representative of a simple machine providing all of the infeed at the busbar. This is a reasonable assumption if the system behind the busbar contains no series compensation.

4.3.1-digital pre-filter

The main pre-filtering process is performed by the FIR (Finite Impulse Response) filters which have well defined transient responses and steady state frequency rejection characteristics. The filtering of the signals is carried out digitally since the following advantages are offered as opposed to analogue equivalent:

(i) Versatility: the weighting constants governing the response of the filter are simply altered by software re-programming.

(ii) Accuracy: background noise introduced by the quantisation of analogue signals can be reduced to well defined, acceptable levels by suitable

conversion gain in the A/D converter stage. Noise in analogue circuits is difficult to quantify since it largely depends upon component tolerances.

(iii) Freedom from drift: digital filters exhibit precisely the same characteristics, no matter how many times they are used. Analogue filters suffer from component ageing and in many circumstances from changes in temperature.

Ideally, the duty of the filtering process is to filter out the dc component and all the frequencies discussed earlier other than the system frequency. However with Ultra-High-Speed operation in mind, the filtering of all unwanted frequencies is very difficult to achieve, since a long filtering process delays the transition of signals from pre-fault to post-fault [46, 47].

It is decided to design a filter with the following characteristics:

(i) The filter length must be as short as possible which in turn makes the post-fault information available for processing in a short time and therefore post-fault impedance can be estimated in a short time after the fault. The time allowed for filtering depends upon the required minimum operating time by the relay.

(ii) To have a zero at dc. This rejects any dc off-set. Although the differential equation obtained from transmission line model (see Chapter 3) recognises the dc exponential component as a valid component, but due to the fact that voltage and current

interfaces introduce some transients which are not related to the line equation, the final impedance measurement may be corrupted. It can be shown that if the dc component in the signals is not true reflection of dc transient in the line model, the final impedance estimates oscillate at a frequency equal to the power frequency. Moreover the exponential component in current affects the Determinant (D) term of matrix 3.36 (see Chapter 3) which may, in turn, cause ill conditioning of the solution [28]. Therefore it is essential to reject any dc component from voltage and current.

(iii) To filter any travelling wave frequency. The main pass-band must be as narrow as possible with the second zero as close as possible to the system frequency. The side lobes must also be small.

(iv) Possibly, it gives some attenuation at resonance frequencies. It was shown earlier that the band width of resonance (sub-synchronous) frequencies is between approximately dc to 80 Hz for a typical system. It is impractical to design a single filter which, at 4 kHz sampling frequency and allowed time for filtering, band limits the signals to around system frequency. Therefore it is decided to impose the filtering of the sub-synchronous components on another filter which will be discussed in the next section.

The required filter is constructed by combining two filters. One with 9 points in impulse response which gives dc rejection and also has four zeros at 0.5, 1, 1.5

and 2 kHz and has equal peaks at 0.25, 0.75, 1.25 and 1.75 kHz. Equation 4.4 gives the filter transfer function in digital form. The other filter is a low-pass filter with 6 points in impulse response whose transfer function is given in Equation 4.5.

$$\frac{Y(Z)}{X(Z)} = a_0Z^0+a_8Z^{-8} \qquad 4.4$$

$$\frac{Y(Z)}{X(Z)} = b_0Z^0+b_1Z^{-1}+b_2Z^{-2} +b_3Z^{-3}+b_4Z^{-4}+b_5Z^{-5} \qquad 4.5$$

where:

$a_0=1.428$ and $a_8=-1.428$

and

$b_0=0.1626$, $b_1=0.1432$, $b_2=0.2015$

$b_3=b_2$, $b_4=b_1$, $b_5=b_0$

Using the convolution theorem the overall impulse response of the filter can be obtained by convolving the two impulse responses as given below:

$$h(t)=h1(t)*h2(t) = \int_{-\infty}^{+\infty} h1(\tau)\cdot h2(t-\tau)\, d\tau \qquad 4.6$$

in discrete form equation 4.6 can be written as:

$$h(k) = \sum_{k=0}^{n} h1(k)\cdot h2(n-k) \qquad 4.7$$

It must be noted that, as one of the convolution properties of linear time-invariant system states, since h1(k) and h2(k) are finite the resulting h(k) will be of finite duration. Equation 4.8 gives the transfer function of the overall filter in digital form. It can be deduced

that the filter has 14 points on its impulse response which corresponds to 3.5 msec at sampling frequency of 4 kHz.

$$\frac{Y(Z)}{X(Z)} = a_0Z^0+a_1Z^{-1}+a_2Z^{-2}+a_3Z^{-3}+a_4Z^{-4}+a_5Z^{-5}+a_6+a_7 +a_8Z^{-8}+a_9Z^{-9}+a_{10}Z^{-10}+a_{11}Z^{-11}+a_{12}Z^{-12}+a_{13}Z^{-13} \quad 4.8$$

where:

$a_0=0.2322$, $a_1=0.2045$, $a_2=0.2877$, $a_3=a_2$, $a_4=a_1$, $a_5=a_0$

$a_6=0.0$, $a_7=0.0$

$a_8=-a_0$, $a_9=-a_1$, $a_{10}=-a_2$, $a_{11}=a_{10}$, $a_{12}=a_9$, $a_{13}=a_8$

Figure 4.10 shows the response of the 9 point filter and Figure 4.11 the low-pass filter. Note that the zero's of the low-pass filter have been arranged to, approximately coincide with the peaks of the 9 point filter. Figure 4.12 illustrates the impulse and frequency response of the overall filter.

It can be seen, from frequency response, that the side-lobes at high frequencies are not low enough compared to the gain at the power frequency. However if the effect of the anti-aliasing filter is considered it can be seen that the overall frequency response is modified and higher attenuation is observed at high frequencies. Fig 4.13 shows the overall frequency response of the pre-filter and analogue anti-aliasing filter. Also, the frequency components higher than the system frequency and lower than approximately 0.4 kHz are amplified by the filter. These components are usually associated with fault positions which are far from the relay points [44, 45, 46].

Since these components are not filtered from the

system signals, the resulting measured reactance and resistance are affected. The attenuation of these frequencies is left to an averaging filter which will be described in the next section.

The digital pre-filter described above is assumed to be most suitable for the application and is employed in the relay simulation.

4.3.2-the Recursive Averager

As explained earlier, when a fault occurs on a series compensated line the interaction between the series capacitor and the total fault loop inductance produce a resonance oscillation which can have a frequency between 5 to 80 Hz depending on the degree of series compensation, position of the series capacitor, system sources and fault position [13, 48, 49].

If the protective gap of the series capacitor does not operate after the occurrence of a fault (capacitors remain in circuit), the relay performance may be greatly affected by the resonance phenomenon especially for faults close to zone boundaries. In such cases, the relay logic may experience difficulty in deciding whether a fault is more likely to be inside or outside the protected zone (and thus maloperates) [11, 18, 49].

It was explained earlier that, it is very difficult to design a short impulse response, very narrow band filter to pass the power system frequency only. Therefore, it is decided to attenuate sub-synchronous oscillation on the output of the relay, i.e. the values DX, DR and D (see Section 4.4) by applying a suitable filter which ideally must have the following characteristics:

(i) It must attenuate or possibly reject any frequency other than the dc, i.e. very sharp low-pass filter.

(ii) It must have the shortest possible impulse response. It must be noted that although the filter is applied to the output, a long impulse response may delay the measurands to reach the steady state values and as a result the relay may maloperate.

It has been proved to be very difficult to devise a filter which perfectly meets both conditions simultaneously. In this respect a lengthy study showed that (i) can be satisfied by employing a recursive filter, which is on contrary to (ii), since a very sharp low-pass recursive filter with a very low cut-off frequency has a relatively long impulse response. An extensive study of various filters has revealed that a specially designed Recursive Averaging filter described by Equation 4.9 is best suited to this application.

$$Y_{(k)}=\frac{1}{M}\left[X_{(k)}+\sum_{n=1}^{n=M-1}Y_{(k-n)}\right] \qquad 4.9$$

where:

$X_{(k)}$=present input sample

$Y_{(k)}$=present output sample

$Y_{(k-n)}$=previous k-n output sample

M=number of elements in the filter

The schematic diagram of this filter is shown in Figure 4.14 The impulse and frequency response of the filter for M=4, 8, 12 and 16 are shown in Figure 4.15.a, b, c and d respectively. It is clearly evident from Figures 4.15.a, b, c and d that as M increases the cut-off frequency decreases and that the impulse response is

inversely proportional to M.

A compromise must be made in choosing a suitable filter for the relay. With regard to frequency response, the ac components, whose frequencies may be very low, is best attenuated by a filter with larger M but the impulse response become extermely long.

A lengthy test has shown that a filter with M=12 is most suitable for this application. The Recursive Averager with 12 locations has a relatively long impulse response. Therefore it is not wise to apply the filter to the measurands continuously, since the advantages of applying the filter to the output is lost.

Figure 4.16 shows the measured reactance when the Recursive Averager is not employed and Figure 4.17 illustrates the measured reactance when the averager is applied continuously. It is clear that the output takes relatively long time to reach its steady state value.

In order to reduce the effect of this problem, it is necessary to apply the averaging filter after the transition period of the measured X and R from pre-fault to post-fault has expired. This requires that the occurrence of the fault is detected by the relay as described in Section 4.4.

To clearly understand how this very versatile filter works, an array or buffer can be considered where the present to last M-1 values of input samples are stored as shown in schematic form in Figure 4.18. The switches SM and S are analogous to the digital logics which are controlled by the relay decision logic.

Under normal system conditions, i.e. pre-fault, the

switch SM is in the SMO position and S in SN position. In this position gates SM0 and SM2 are open and SM1 close, which implies that the input samples are directly passed to the output without any process being carried out on them. The input samples are at the same time stored in the buffer.

When it is required to apply the filter, i.e. after fault, it can be set either to perform as a Recursive or Non-recursive Averager. At the time it is applied switch SM changes position from SMO to SMC, which makes gates SM0, SM1, and SM2 close, open and close respectively. The averaging process is thus started. When switch S is on position SN, the averaging process is non-recusive, since the output is the averaged value of M number of inputs stored in the buffer. Figure 4.19 illustrates the frequency response for a 12 point non-recursive averager. On the other hand, if it is required to change the non-recursive nature of the filter to recursive, switch S changes position from SN to SR, which in turn places the present output sample, $Y_{(k)}$, into the buffer. The next averaging has M-1 inputs and one output. This process, if continued, fills the buffer with output samples. The present output will be based upon M-1 outputs and one input. Thereafter the filter follows Equation 4.9.

The advantages of this Recursive filter are:

(i) It can be changed a to Recursive filter from Non-recursive or vise-versa by changing the position of switch S.

(ii) At the instant it is applied all inputs are averaged , and if the filter is required to perform as a

recursive averager the starting value for recursive action may be close to the actual steady state value. This characteristic of the Recursive-Averager may affect the overall performance of the filter in terms of impulse response.

(iii) There is no weighting of samples involved. The filter action is performed by simple addition of the samples present in the filter buffer.

More details about implementation of the filter is given in the next section.

4.4-Relay Characteristic and Decision Logic

4.4.1-production of quadrilateral characteristic

A conventional distance relay characteristic defines the region where the fault loop impedance converges after fault inception on a transmission line. It is usually plotted on an impedance diagram with R and jX axis. Figure 4.20 shows a typical quadrilateral characteristic for plain uncompensated feeders. The resistive reach is expanded to cover high fault resistance.

A trip is initiated if:

$$X_O < w_O L < X_r \qquad 4.10$$

$$R_O < R < R_r + w_O L \cdot \cot\phi_{L1} \qquad 4.11$$

where ϕ_{L1} is the angle of the line's positive phase sequense impedance. The directional stability is achieved by satisfying the following condition:

$$XMA < w_O LM \qquad 4.12$$

where LM is the directional inductance. More details

about the directional element are given in Section 4.4.2. Multiplying Equation 4.10 by D term and dividing by $w_o T_s$ gives:

$$\frac{X_o}{8 \cdot T_s \cdot w_o} \cdot D < \left(\frac{DL}{8T_s}\right) < \frac{X_r}{8 \cdot T_s \cdot w_o} \cdot D \qquad 4.13$$

multiplying Equation 4.11 by D gives:

$$R_o \cdot D < (DR) < R_r \cdot D + 8 \cdot T_s \cdot w_o \cdot \left(\frac{DL}{8T_s}\right) \cdot \cot\phi_{L1} \qquad 4.14$$

To solve relationship 4.13 and 4.14 the term D, $DL/8T_s$ and DR are obtained directly from expressions (see Chapter 3)

$$D = i_{k-4} \cdot i'_{k-10} - i'_{k-4} \cdot i_{k-10} \qquad 4.15$$

$$DR = v_{k-4} \cdot i'_{k-10} - v_{k-10} \cdot i_{k-4} \qquad 4.16$$

$$DL = v_{k-10} \cdot i_{k-4} - v_{k-4} \cdot i_{k-10} \qquad 4.17$$

where:

$$i'_{k-4} = i_k - i_{k-8} \qquad 4.18$$

$$i'_{k-10} = i_{k-6} - i_{k-14} \qquad 4.19$$

It is apparent from above analysis that the digital division process which is uneconomical and time consuming has been eliminated from the relay boundary comparison. Relationships 4.13 and 4.14 can be simplified in the form of Equations 4.20 and 4.21.

$$K_{Xo} \cdot D < \left(\frac{DL}{8T_s}\right) < K_{Xr} \cdot D \qquad 4.20$$

$$R_o \cdot D < (DR) < R_r \cdot D + K_{Rr} \cdot \left(\frac{DL}{8T_s}\right) \qquad 4.21$$

where the constants K_{Xo}, K_{Xr} and K_{Ro} are given by:

$$K_{XO}=\frac{X_O}{8\cdot T_S\cdot w_O} \qquad 4.22$$

$$K_{Xr}=\frac{X_r}{8\cdot T_S\cdot w_O} \qquad 4.23$$

$$K_{Rr}=8\cdot T_S\cdot w_O\cdot \cot\phi_{L1} \qquad 4.24$$

4.4.2-directional reactance XM

A distance protection relay must maintain consistency of performance for faults within the protected zone. However, the constraints of Equations 4.20 and 4.21 cause unwanted operaton for reverse faults (faults behind the relay). This is more important when the line is compensated by series capacitors and the capacitor is situated adjacent to the relay location (at each end). In order to make the relay truly directional, the principle of directional reactance XM must be implemented.

The relay designer is faced with 3 main options for polarising signals:

(i) self (faulted voltage) polarising

(ii) memory voltage polarising

(iii) sound phase voltage polarising

Within a distance relay the function of the polarising signal is to act as the phase reference signal. The optimum polarising signal is one that maintains its vectorial position regardless of what system parameters, type of fault, fault location or fault resistance occurs [50]. A thorough investigation is needed for choosing the suitable polarising signal in XM calculations for series capacitor compensated lines.

However, experience has shown that the use of memory to store pre-fault voltage signal is normally adequate in maintaining the directional stability of the relay.

The directional reactance measurement uses the delayed samples of the voltage in conjunction with the undelayed samples of the current component. This can be implemented by using a voltage memory bank, to hold the pre-fault samples of the voltage signals. Within the simulation a memory of 5 power frequency cycles is used in the directional reactance calculation.

The directional reactance XM is compared with the directional reactance value XMA, and hence an additional constraint is added to that of Equations 4.20 and 4.21 as follows:

$$XMA < w_O LM \tag{4.12}$$

or

$$\frac{XM}{8 \cdot T_S \cdot w_O} \cdot D < \frac{LMD}{8T_S} \tag{4.25}$$

Equation 4.25 can be written as:

$$K_M \cdot D < \frac{LMD}{8T_S} \tag{4.26}$$

where:

$$K_M = \frac{XMA}{8 \cdot T_S \cdot w_O} \tag{4.27}$$

LMD is directly obtained from expression:

$$LMD = v_{k-6-N} \cdot i_{k-4} - v_{k-N} \cdot i_{k-10} \tag{4.28}$$

N corresponds to the delayed samples which in this case is equal to 400 at 80 samples per cycle (50 Hz system

frequency). Figures 4.21 and 4.22 illustrate the measured XM and X for reverse (at sending end busbar) and forward (30% of the line length) faults respectively.

4.4.3-relay characteristic

In general, the shape of the quadrilateral characteristics of the relay for protecting series compensated lines are similar to the conventional characteristic shown in Figure 4.20. However, there are some practical considerations regarding the boundary settings of the relay when applied to series capacitor compensated lines [13, 49] which will be discussed in the appropriate chapters. Also, a new boundary characteristic will be proposed for a system with the series capacitor location in the middle of the line which will be explained later.

4.4.4-decision logic

The measured impedance is compared with the pre-determined characteristic of impedance which specifies a zone in the impedance plane. The tripping criterion, which is based on single impedance estimate can lead to the degeradation in protection integrity because, in practice, a significant fluctuation in impedance estimates occurs after fault inception. Algorithm simulation shows that a fault just beyond the relay reach can cause impedance estimates falling within the relay characteristic boundary [51]. The impedance transients can be illustrated for voltage maximum faults, where the relaying voltage signals are severly contaminated by travelling wave harmonics, and voltage minimum faults

where the impedance estimates show a downward transient droop.

The relay decision making process must be able to cope with:

(i) long line transient effects: those travelling wave components which are not sufficiently attenuated by the pre-filters, cause a high frequency oscillations on the final measured reactance and resistance.

(ii) the sub-synchronous oscillation which causes the measurands to oscillate at a low frequency about the dc values.

These phenomena are most critical when the faults are around the boundary of the relay. For close up faults (faults well inside the relay characteristic) the relay is required to be fast because the damages caused by high fault current are severe, and also the stability of the integrated power system may be jeopardized. On the other hand, for boundary faults (faults near the forward reach of the relay) the relay must be accurate in deciding whether the fault is inside or outside of the protected zone. The speed of operation for such faults is the second priority.

The foregoing principles are the main philosophy behind the design of the decision logic for the digital distance relay.

The relay trip mechanism comprises a main trip counter, TC, which up-counts when any calculated impedance sample falls within the characteristic and down-counts if a sample is outside the relay boundary, and a trip level, TL, which if the TC reaches that value the trip is

initiated [46, 51].

The relay characteristic is divided into fast and slow counting regions which in turn allows more time for the relay to reach a trip decision for faults near the boundary and at the same time produce fast operation for close up faults. A typical characteristic with divided counting zones is shown in Figure 4.23.

The trip decision making process starts by detecting the disturbance. The fault detection is performed by monitoring the measured DX and DR and determining when they traverse a preset boundary that is larger than the relay characteristic. The constraints applied for these purposes are:

$$1.2 \cdot K_{Xo} \cdot D < \left(\frac{DL}{8T_o}\right) < 1.2 \cdot K_{Xr} \cdot D \qquad 4.29$$

&

$$1.5 \cdot R_o \cdot D < DR < 1.2 \cdot \left(R_r \cdot D + K_{Rr}\left(\frac{DL}{8T_s}\right)\right) \qquad 4.30$$

When the relay detects a disturbance, the process of decision making is started. The process can be generally summarized as follows:

The Trip Level, TL, is set at 256. This means that when the Trip-Counter, TC, reaches this value a trip is initiated. The incremental values for top of the characteristic are initially set at pre-set values. When a fault is detected, a control counter CRL1 is continuously incremented by 1. The Trip-Counter is kept at zero for 4 msec (16 samples at f_s=4 kHz) after the fault detection (CRL1=16) even if the measured impedance moves inside the boundary. This precaution is taken due

to uncertainty during the group delay of the pre-filters.

At the first up-count by the Trip-Counter the second Control-Counter, CRL2, starts which is responsible for resetting the counter and changing the incremental values of the relay characteristic.

When CRL2 reaches a preset value and no trip has occurred the counter will be reset to zero and the incremental values of the top of the characteristic are changed to a lower value. This ensures that for a close up fault, where the measured impedance falls within the fast counting region of the characteristic, the relay response is very fast, whereas by resetting TC and changing the incremental values at the top of characteristic, more time is allowed for the relay to reach a decision.

If CRL2 reaches the second preset value and still no trip is initiated, the relay considers the fault as very close to the boundary. Therefore it slows the counter by changing the incremental values to even smaller values.

If a trip does not occur and CRL2 is greater than 10 and the Trip-Counter becomes zero for one msec(4 samples) the relay considers this as an out of zone fault and resets both Control-Counters, CRL1 and CRL2. The incremental values are also reset to their initial values.

4.4.5-invoking the Recursive Averager

The Recursive Averager is applied when CRL1=16 (4 msec after fault detection). This means that from the fault instant to this time all filtering is done by the pre-filters. However, because the main duty of the Recursive Averager is to attenuate the sub-synchronous frequency on

the measurands, especially when it most affects the trip decision process, i.e. around the reach point, it is decided to introduce a mechanism so as to enable it to change the averager nature to recursive when it is most needed (for faults around the boundary). This is performed by:

(i) when the filter is invoked (CRL1=16), it acts as an ordinary non-recursive averaging filter with 12 points in the impulse response.

(ii) at the same time, the relay checks whether the reactance samples in the averager buffer (memory) are within two boundaries around the forward reactance reach of the relay, specified by AVLL and AVLU.

(iii) if at least 8 reactance samples are not within these limits, then the averager continues to act as a non-recursive averaging filter, attenuating high frequency components on the dc values (see Figure 4.19 for frequency response), i.e. the filter output is not placed in the filter buffer (switch S remains in SN position. see Figure 4.18).

On the other hand, each time at least 8 samples in the buffer are within the specified boundary then switch S changes position from SN to SR and hence averager output is placed into the buffer. Hence the filter acts as a recursive averager.

Values of $0.7 \cdot X_r$ and $2.0 \cdot X_r$ (X_r is the forward reactance reach of the relay) are recommended for AVLL and AVLU respectively.

The mechanism explained above, ensures that, if the

measurands are badly affected by the high frequency oscillations caused by the travelling waves, the filter acts as a non-recursive averager with a finite and short impulse response (3 msec at f_s=4 kHz). In such situations the sub-synchronous oscillation may not be a problem. The relay count regime will cope with the high frequency oscillation on the measurands.

On the other hand, if the dominant oscillation on the measured values are the sub-synchronous oscillation, then the filter is changed to the Recursive Averaging filter.

By setting the lower limit (AVLL) closer to the boundary than the upper limit (AVLU), it is ensured that when the filter is changed to a recursive averager, the initial averaged samples are in the slow-counting/negative-counting region of the characteristic. Hence relatively long transition of the measured reactance (due to bad initial averaged values and relatively long impulse response of the Recursive Averager) inside the boundary is avoided. Figure 4.24 shows the flow chart for the averager logic.

Figure 4.25.a shows the measured reactance for a fault at 60% of the line length and assumed forward reach of 60% of the line length and inception angle of 90°, without averaging filter and Figure 4.25.b illustrates the measured reactance when the filter is applied. It is clearly evident that without the Recursive Averager, the relay may maloperate due to long incursion of the measured reactance into the boundary. On the other hand, when the filter is applied the incursion is reduced and confined to the slow counting region of the characteristic.

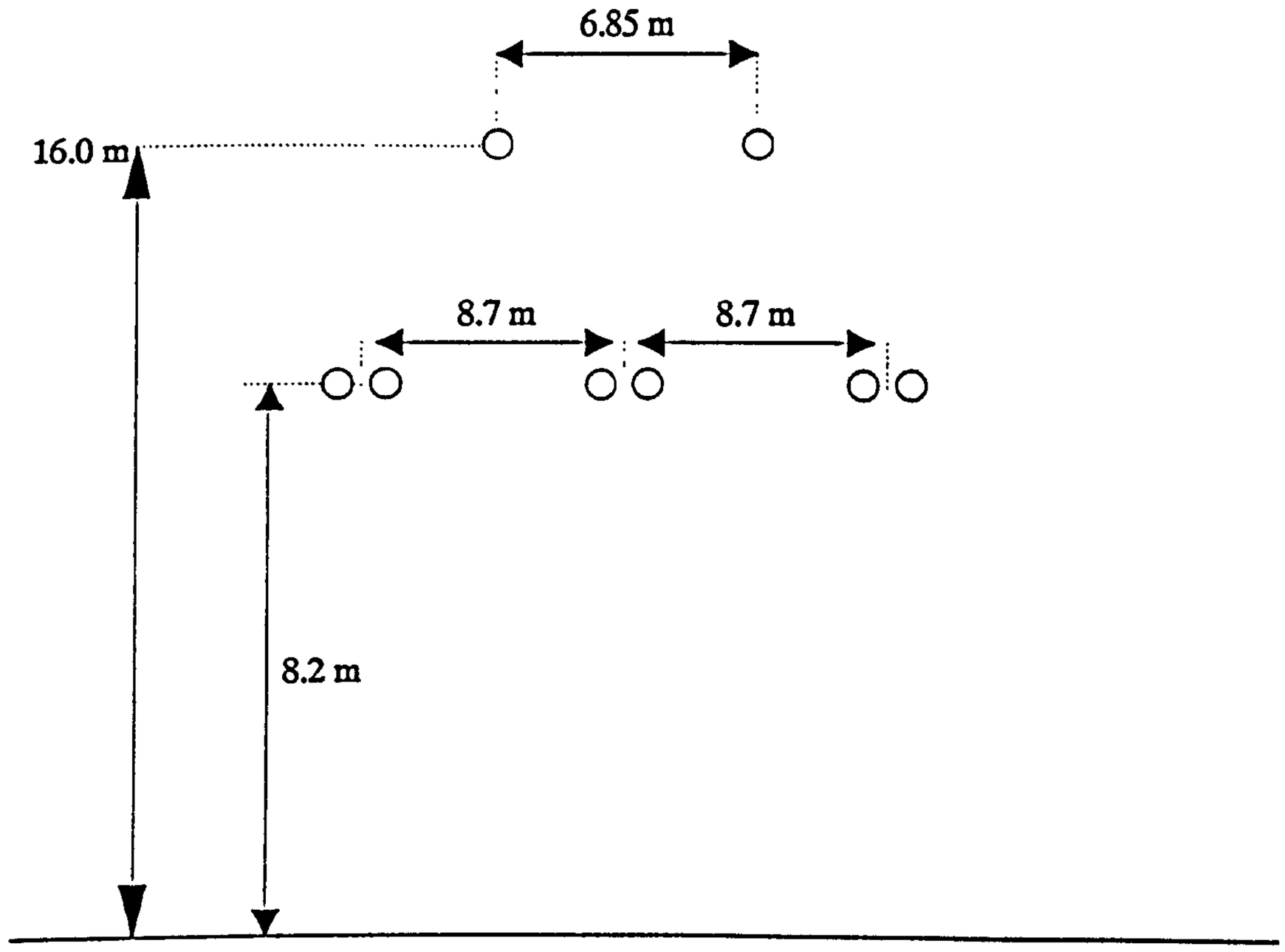

Fig. 4.1 - Line construction

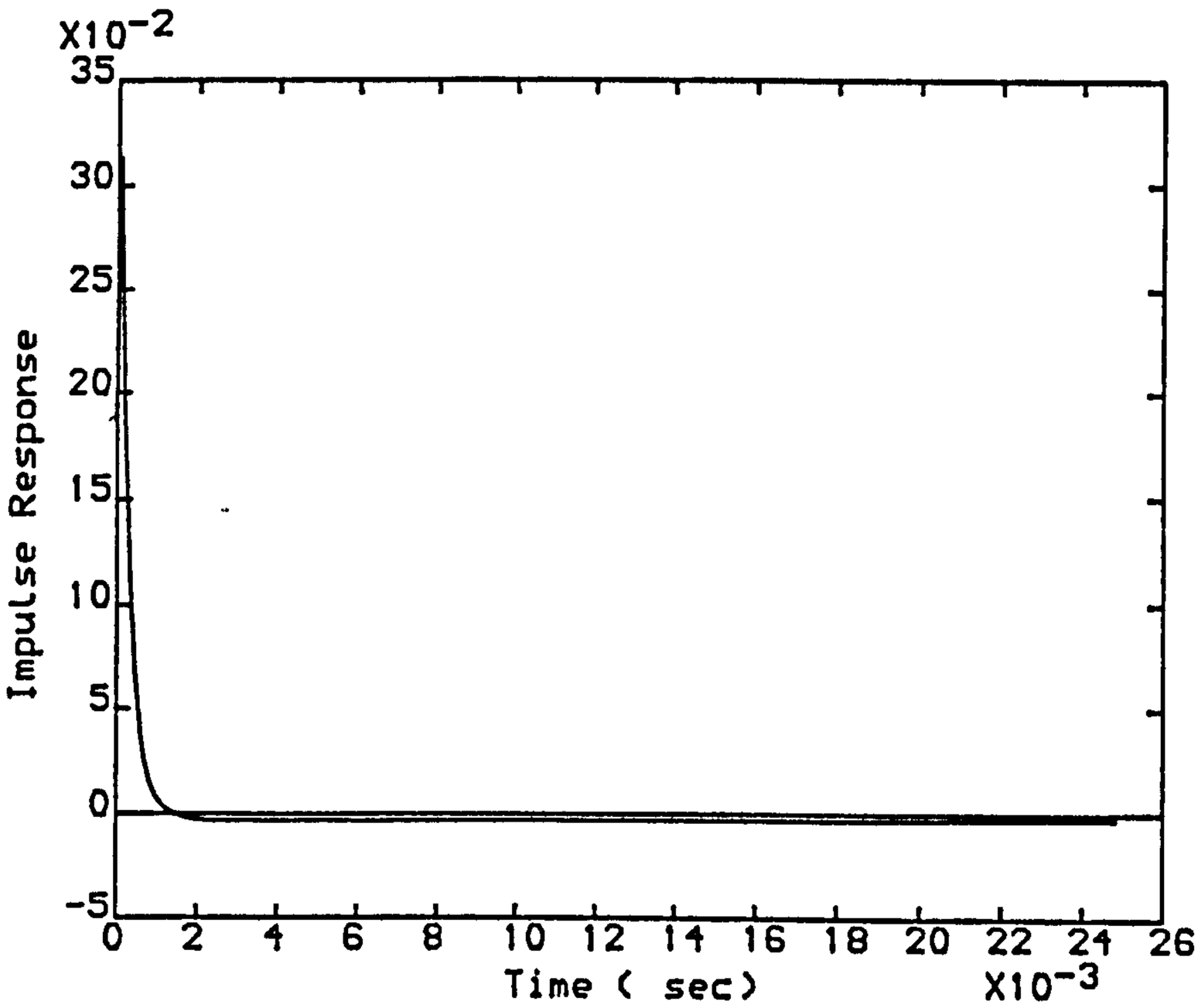

Fig 4.2.a-Impulse Response of the C.V.T. Used in the Simulation.

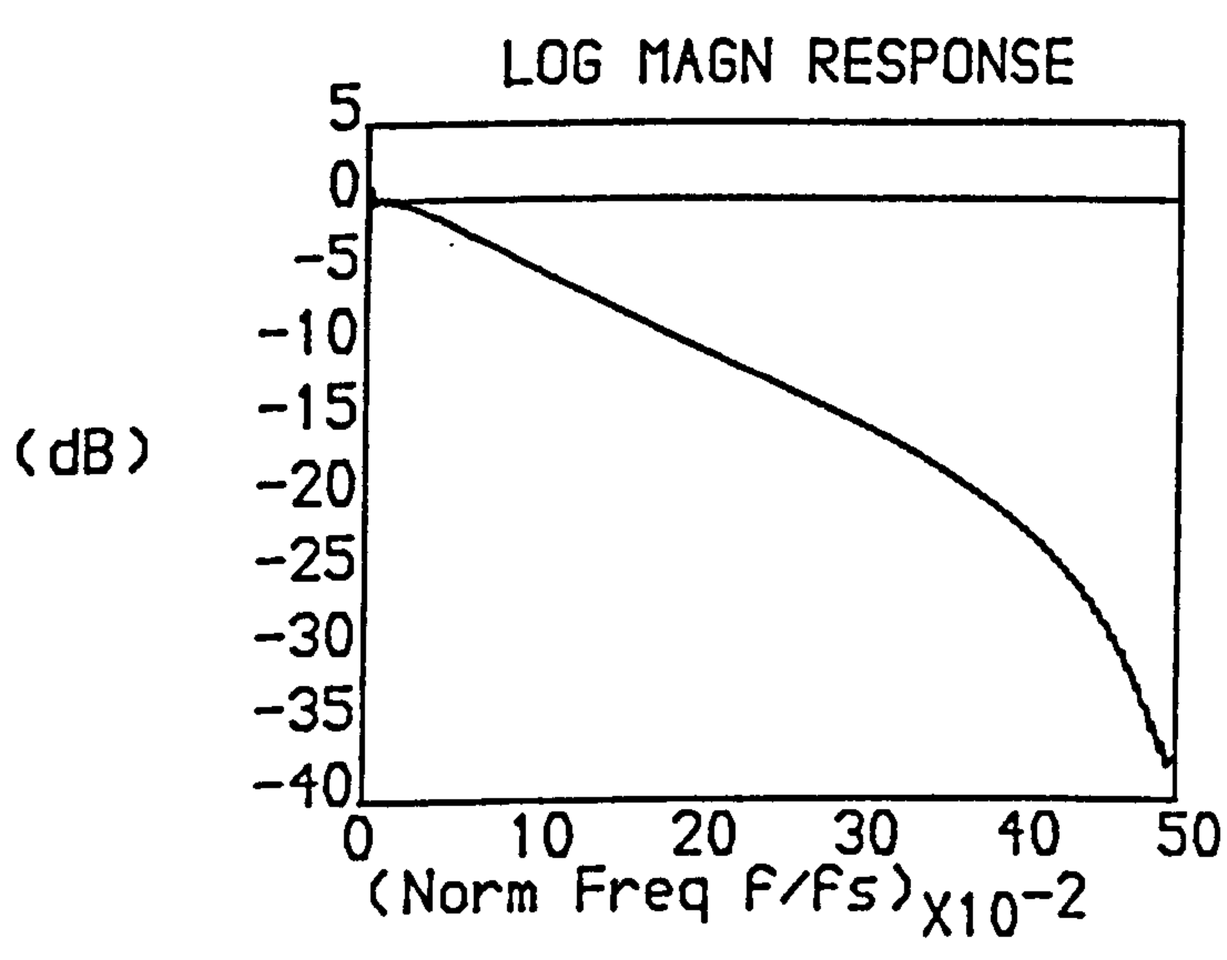

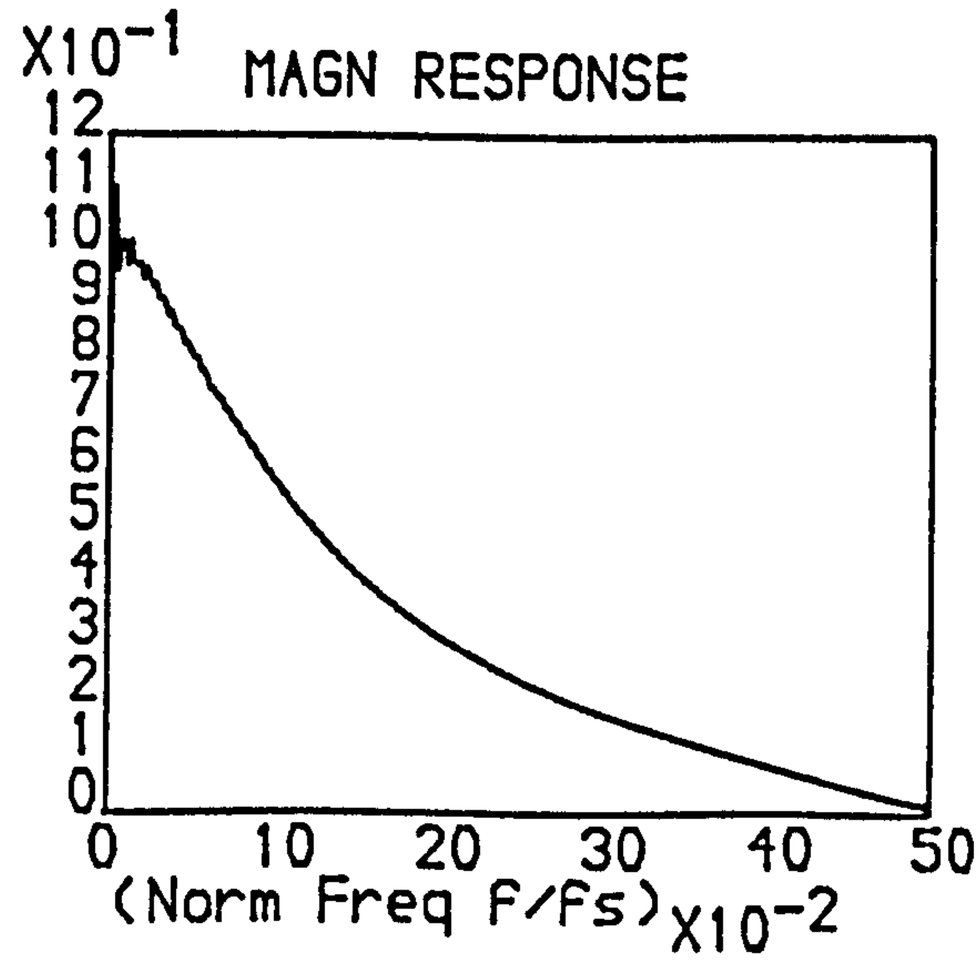

Fig 4.2.b-Frequency Response of the C.V.T. Used in the Simulation.

Note that f_S=8 kHz.

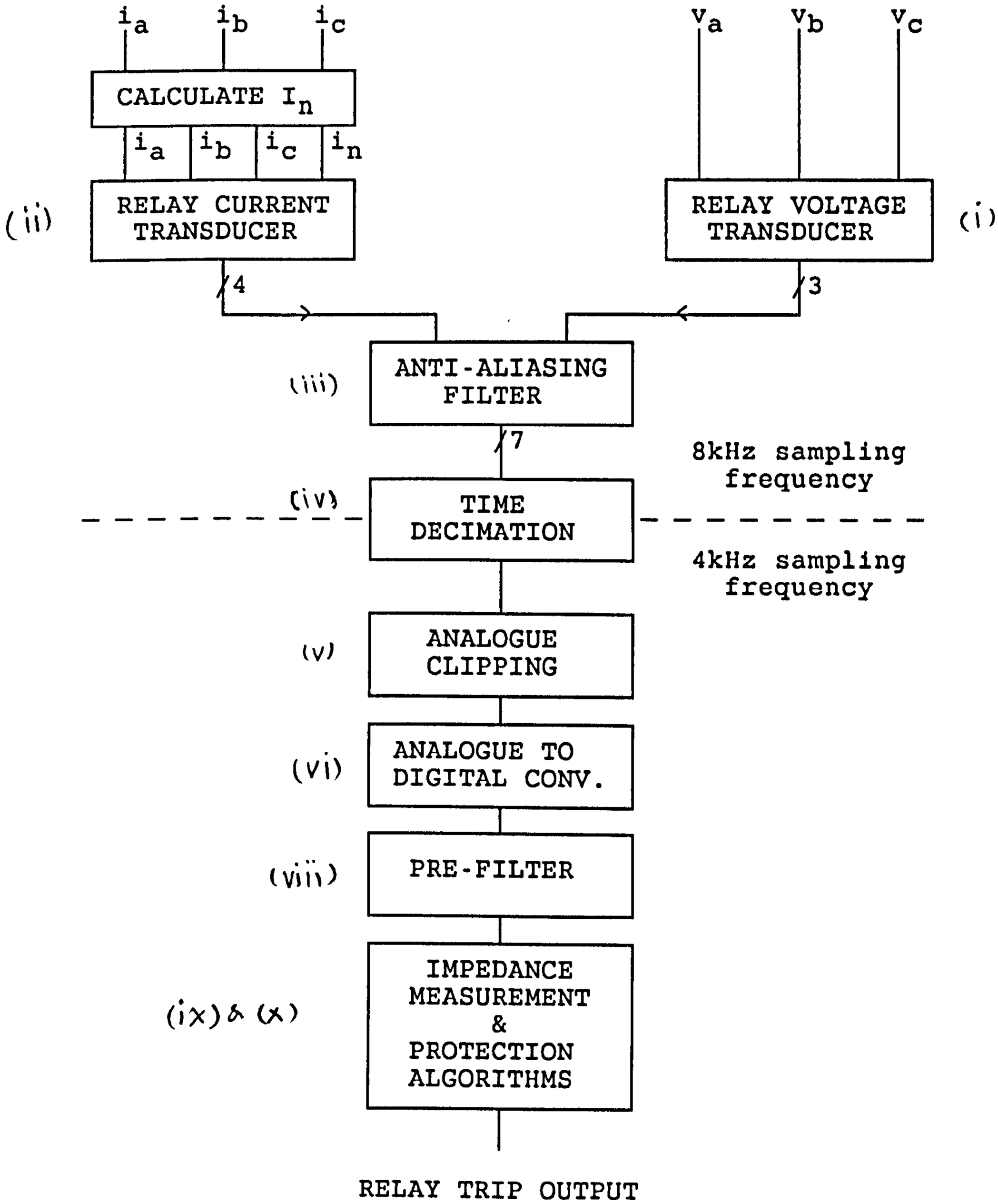

Figure 4.3 Schematic Diagram of relay simulation

Note that the relaying signals (voltages & currents) are supplied to the relay after voltage and current transducers.

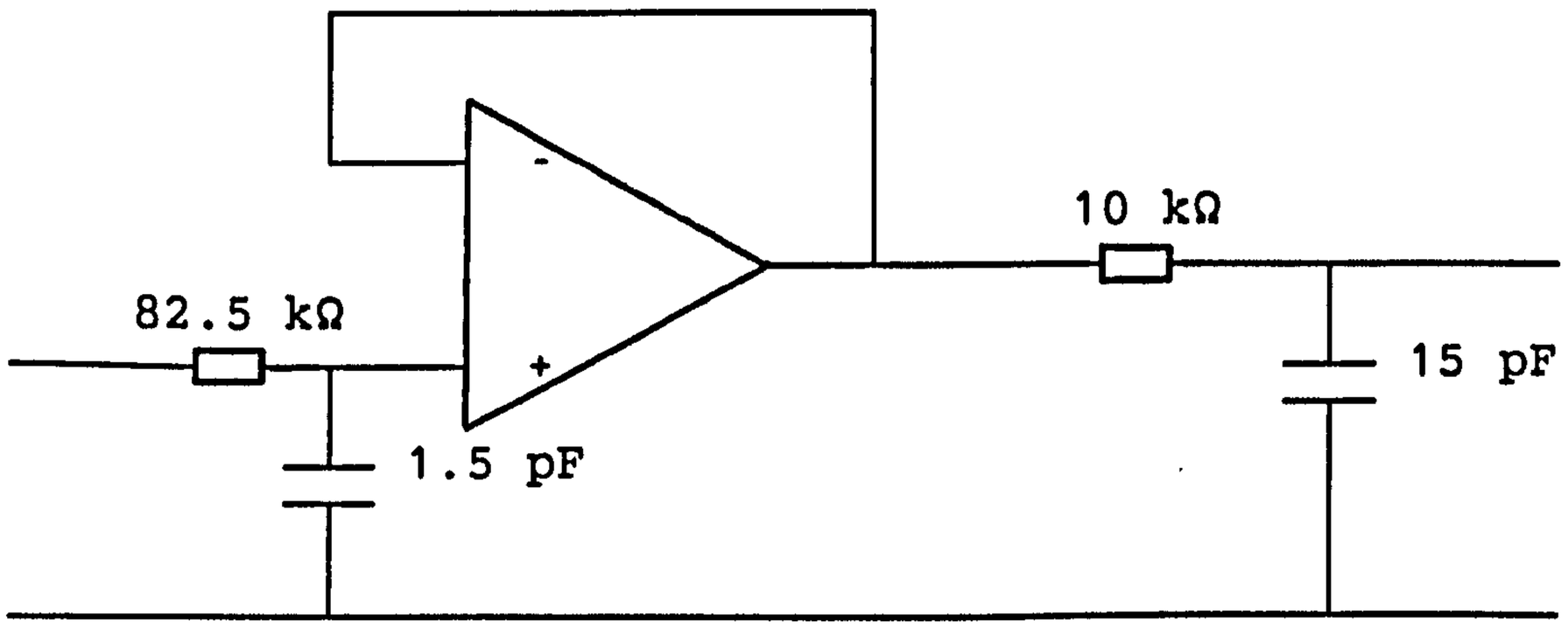

FIG 4.4.a-Analogue filter circuit

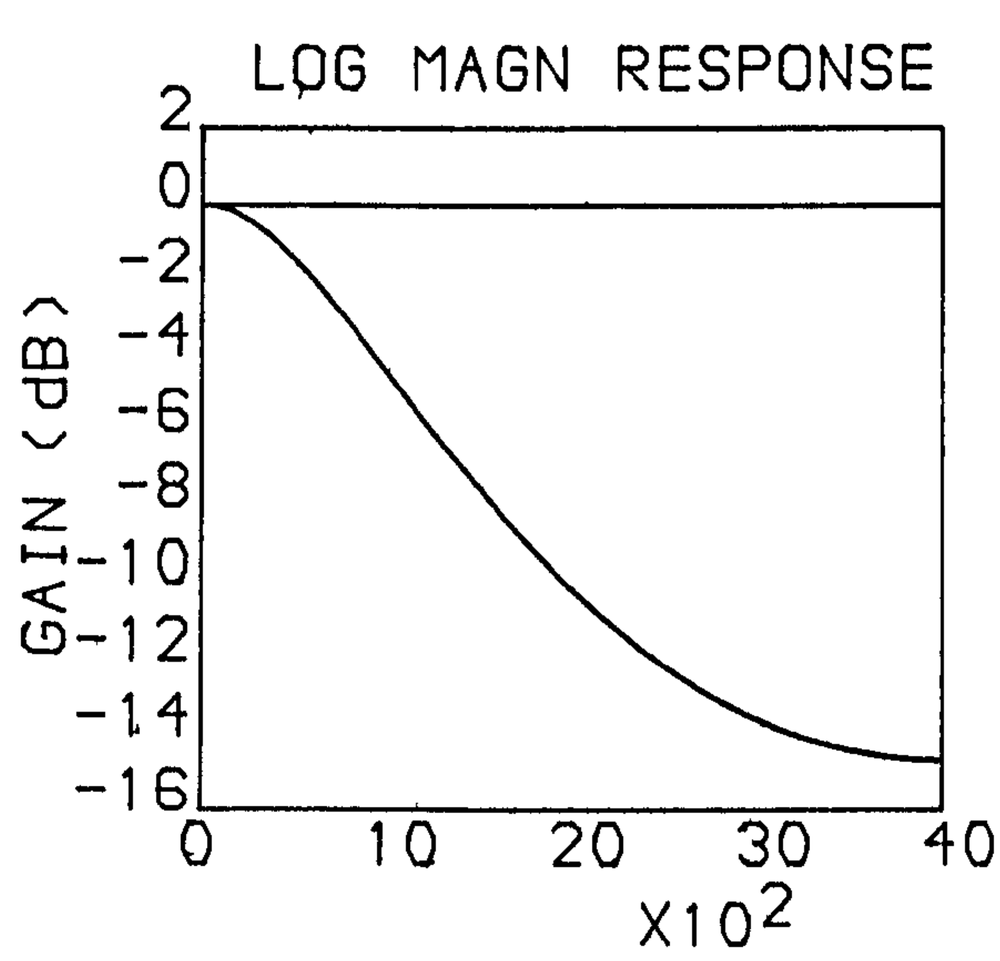

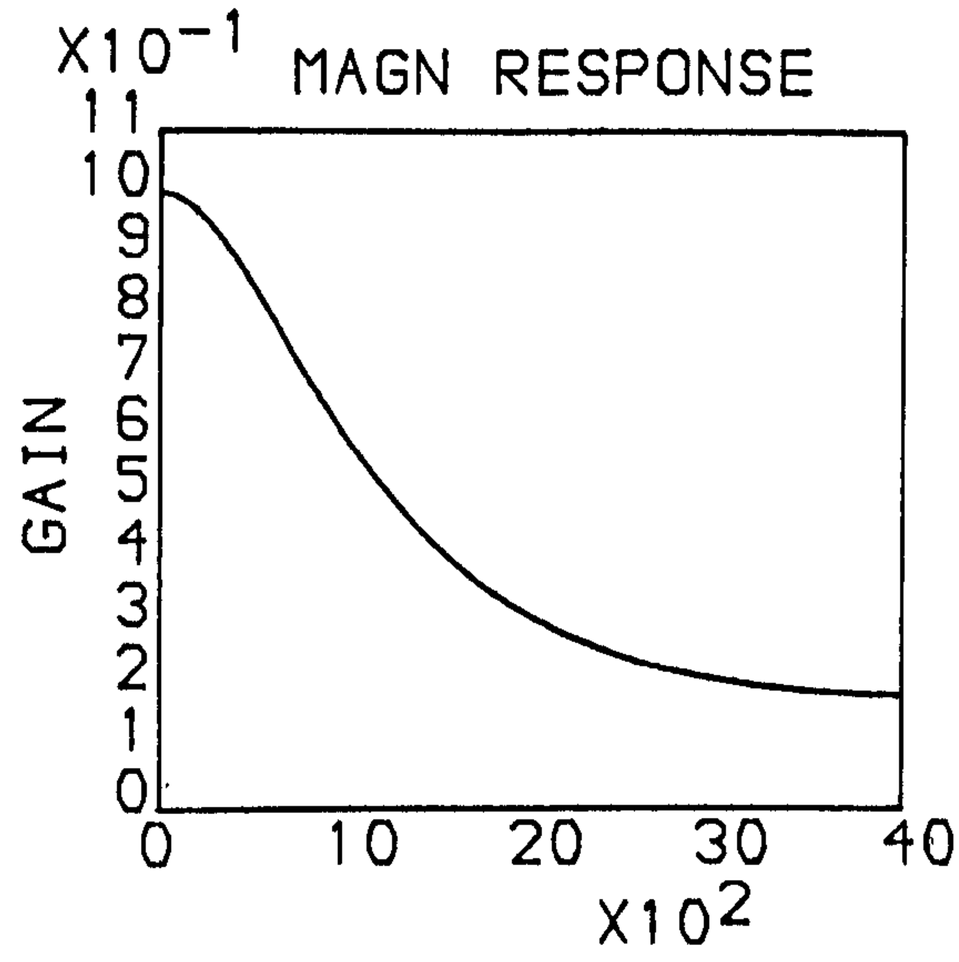

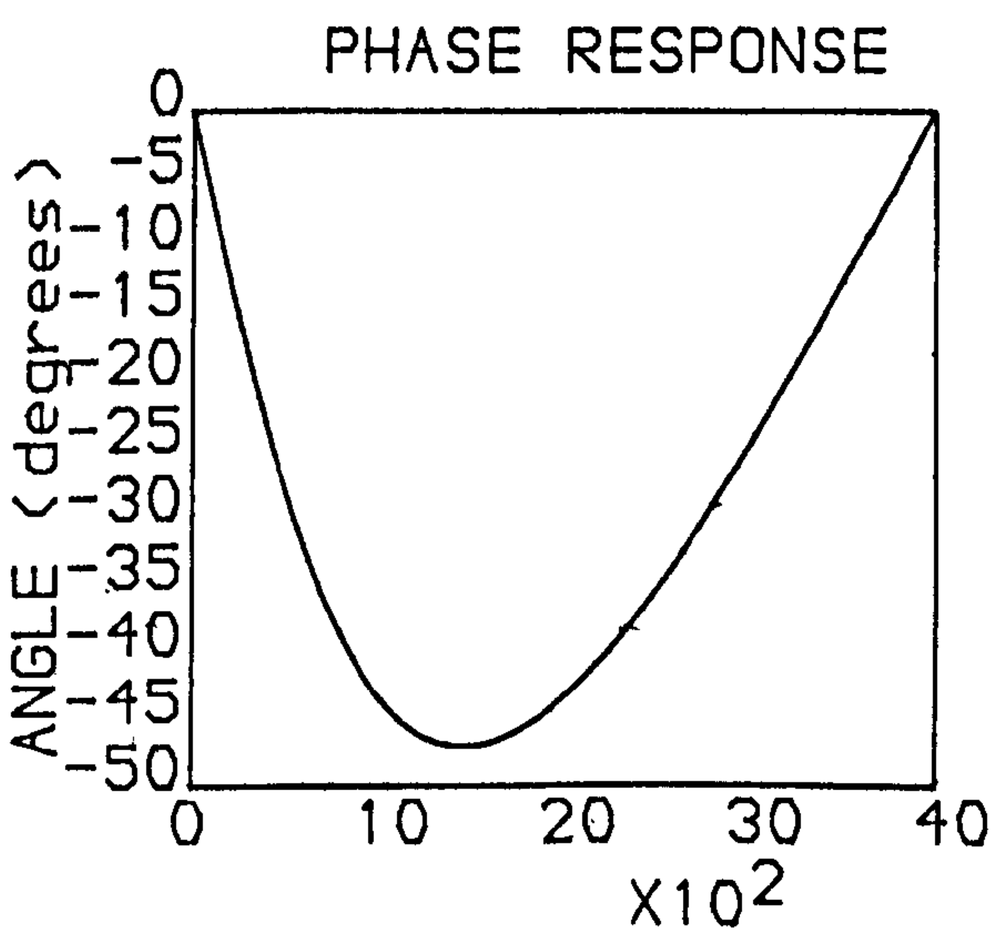

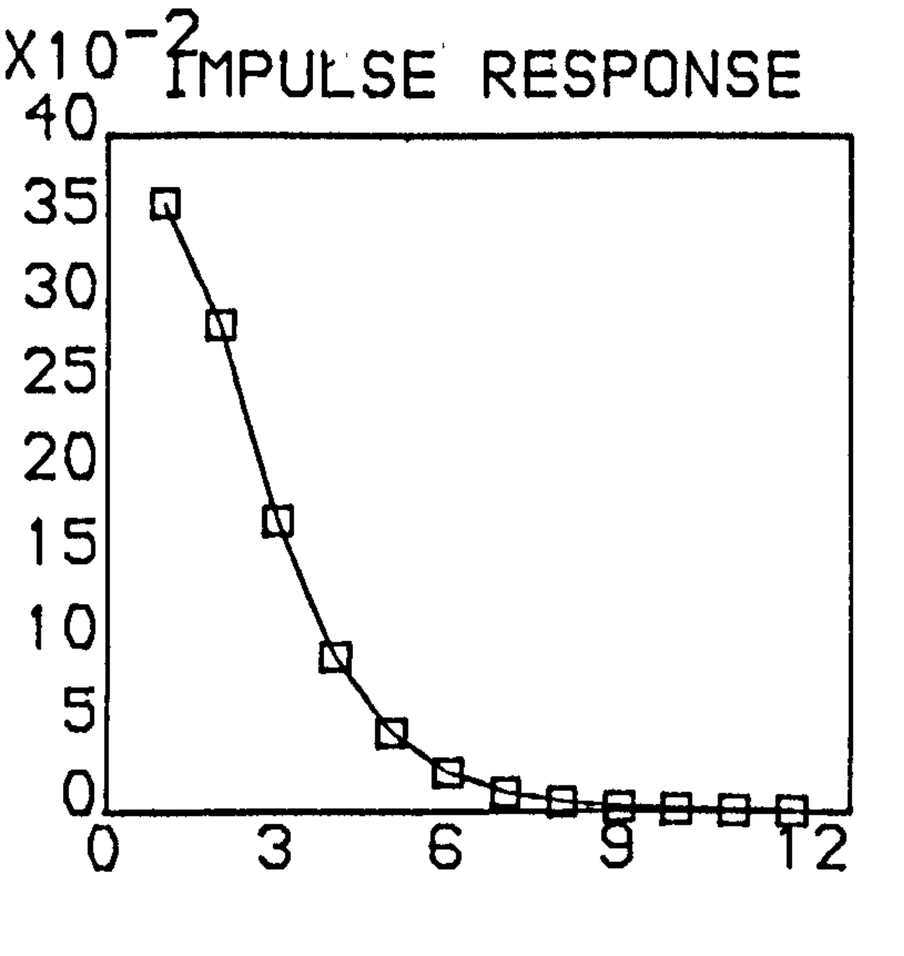

Fig 4.4.b-Response of the Analogue Filter.

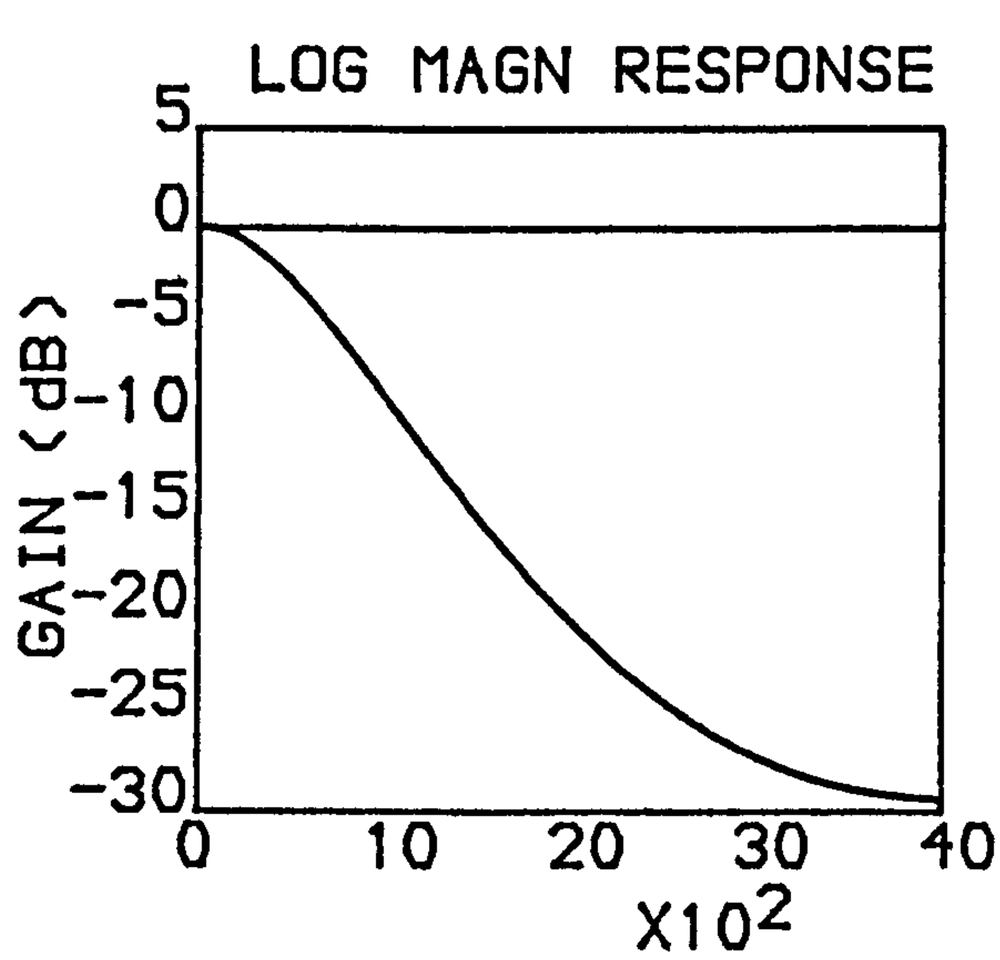

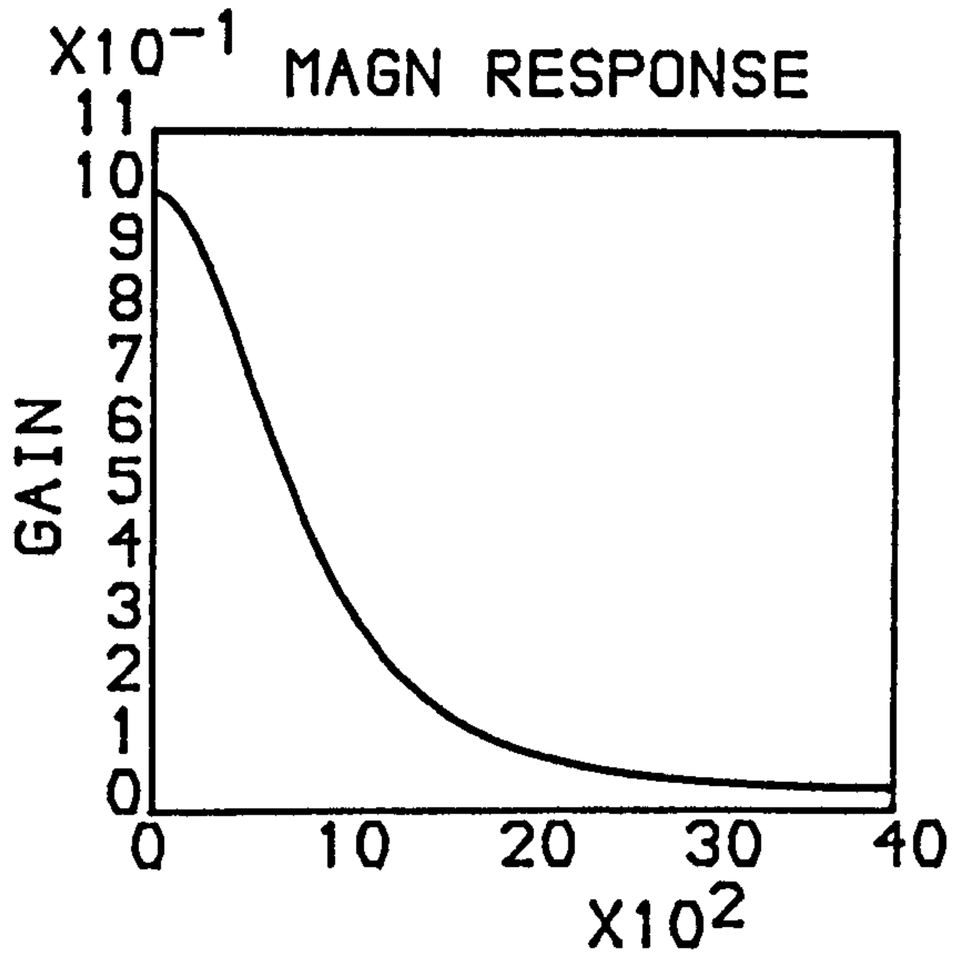

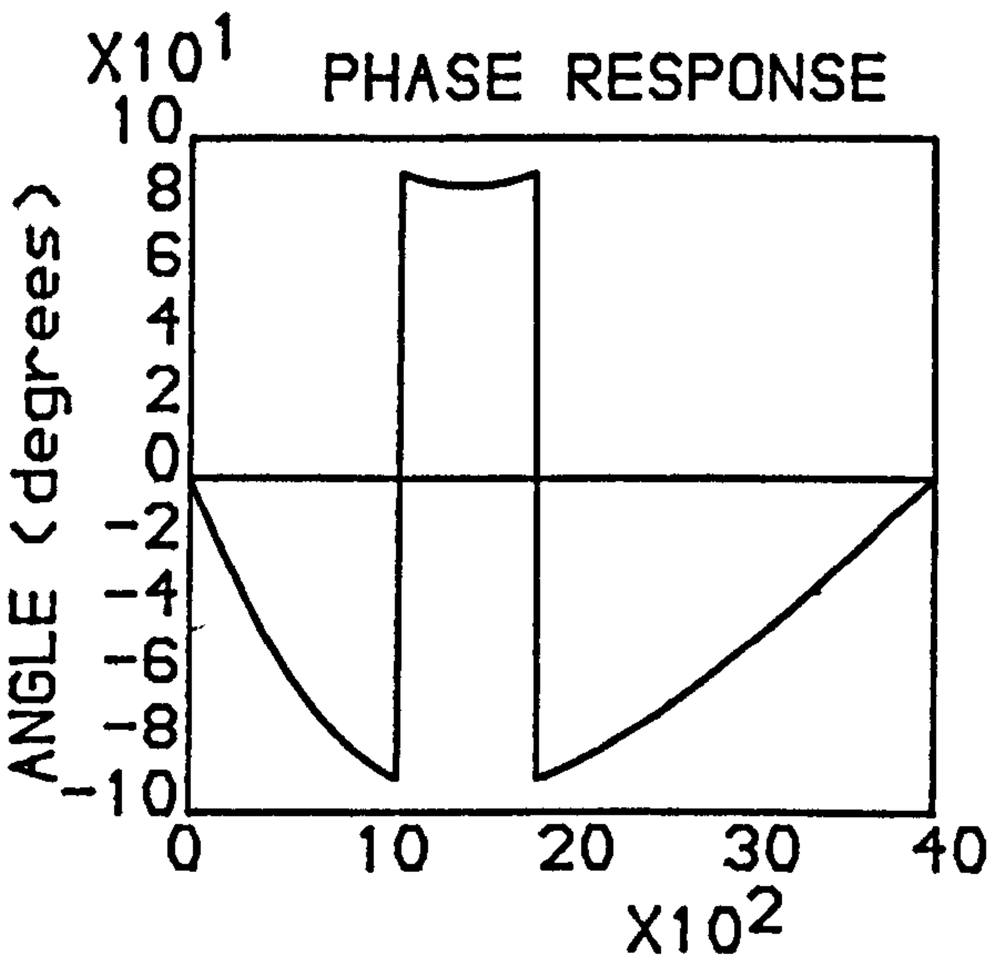

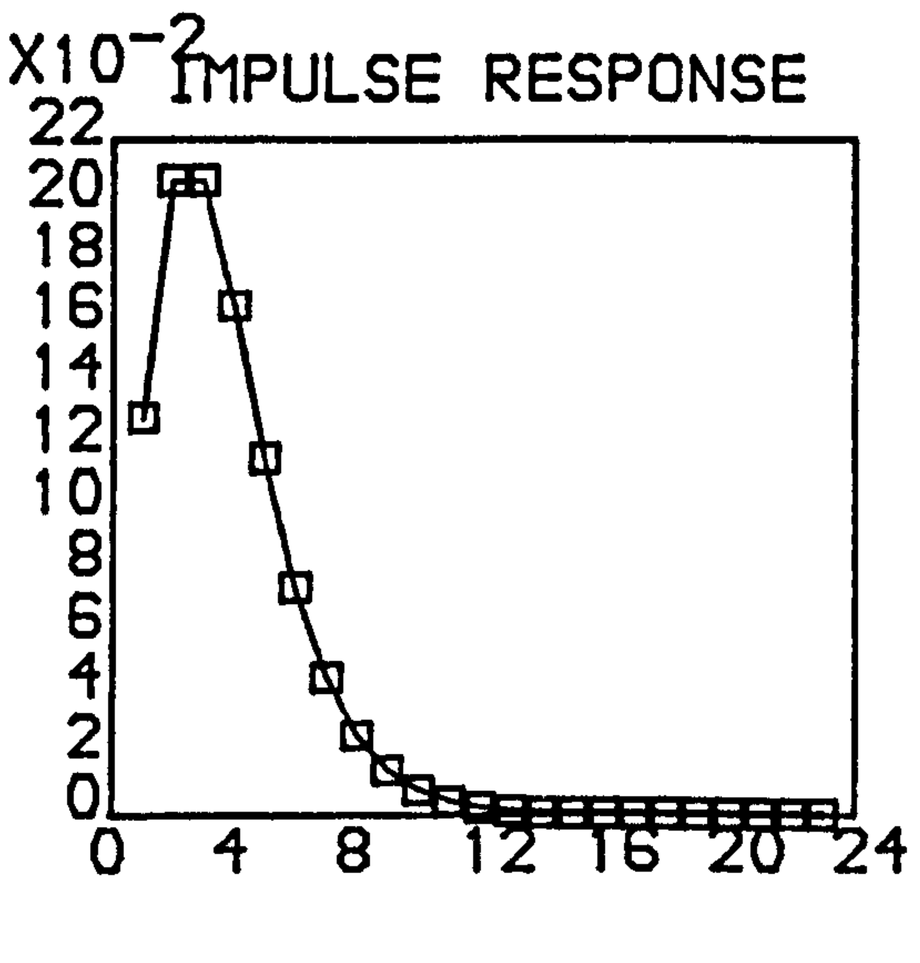

Fig 4.4.c-Total Response of Two Analogue Filters in Cascade.

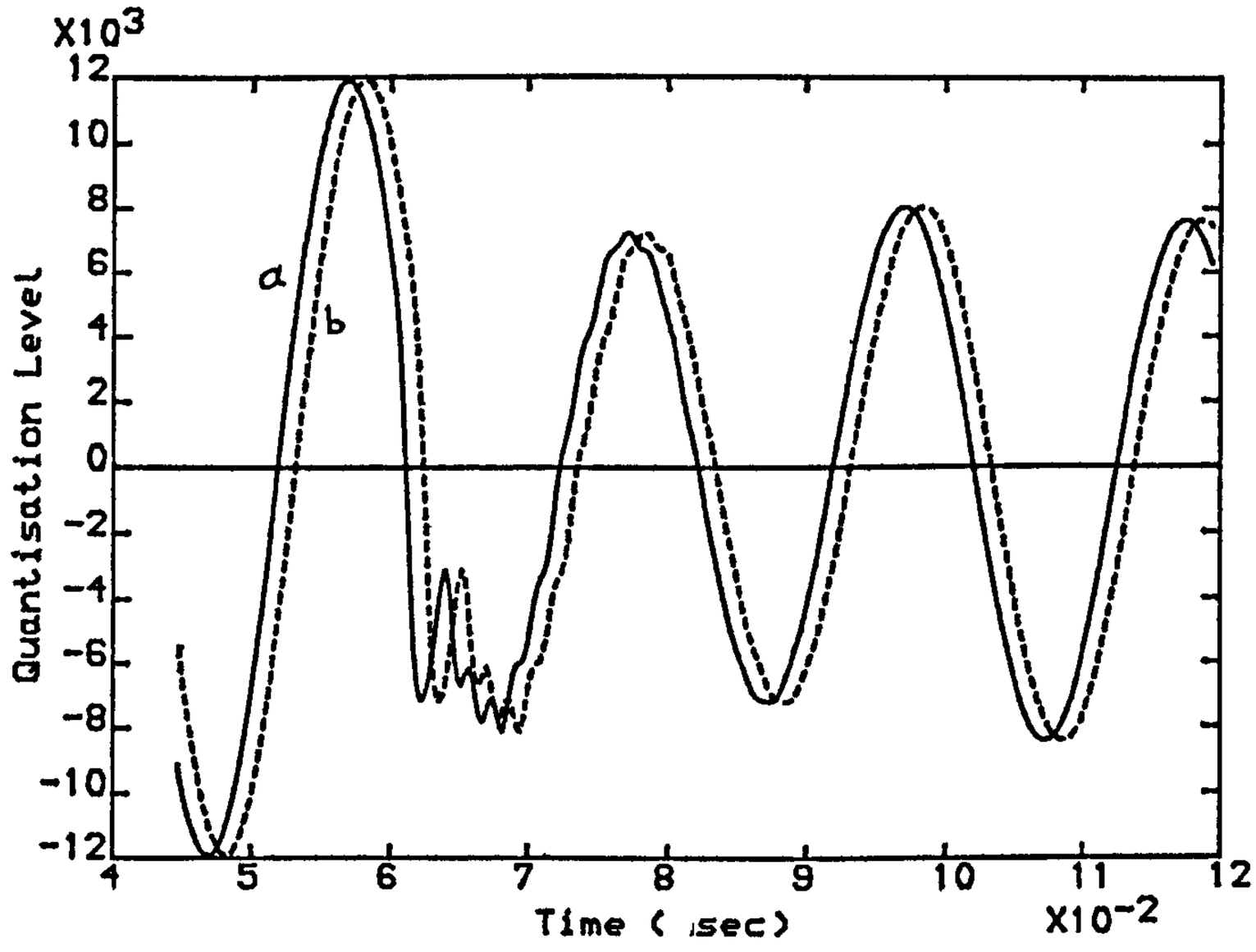

Fig 4.5.a-The Relaying Components of Voltage.
a: the original signal
b: delayed signal

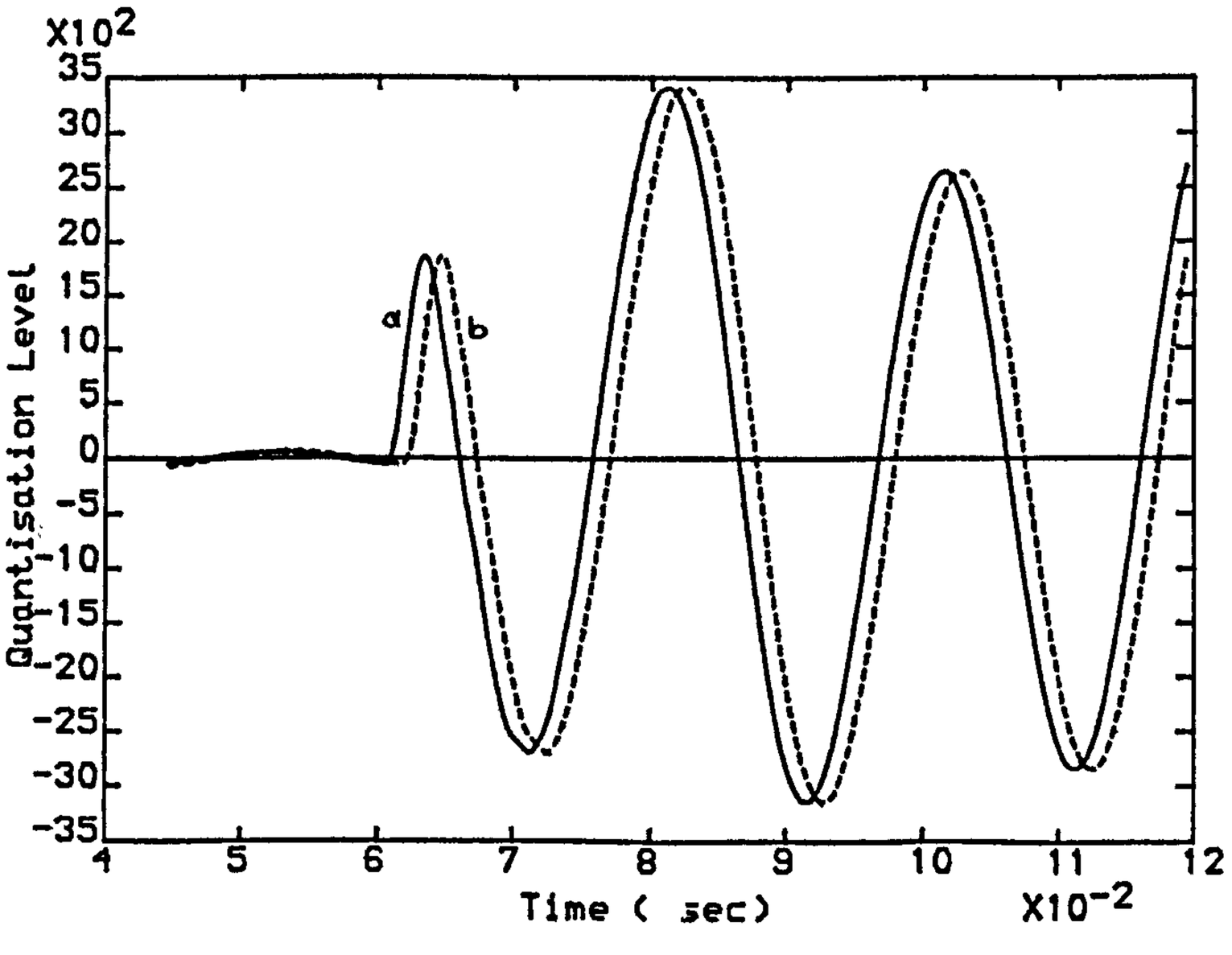

Fig 4.5.b-The Relaying Components of Currents.
a: the original signal
b: delayed signal

SE SCL=5 GVA, RE SCL=35 GVA, NO LOAD, FAULT INCEPTION ANGLE=90°, LINE LENGTH=300 km, 70% SERIES COMPENSATION.

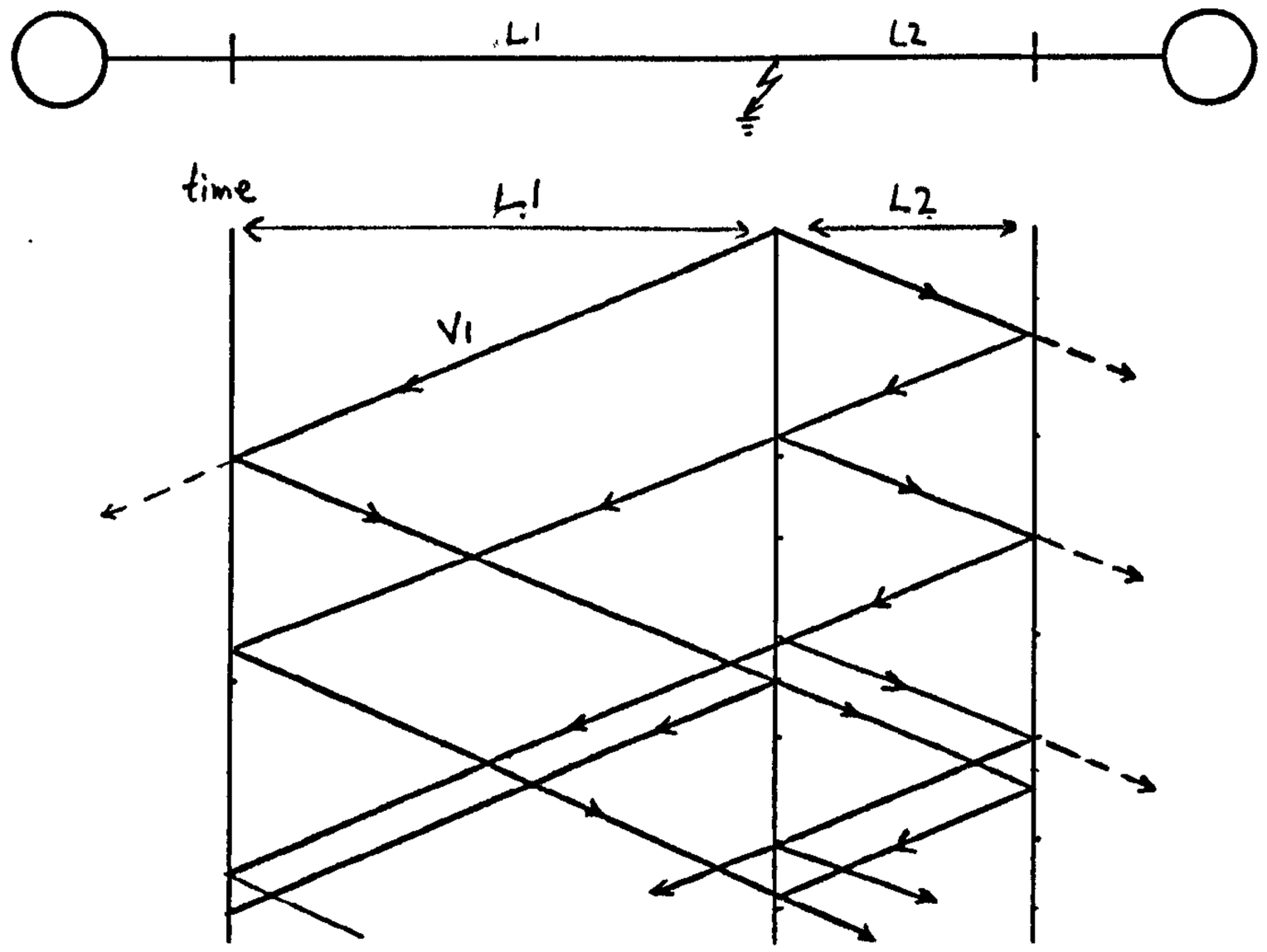

FIG 4.6- Bewley lattice diagram for a simple system

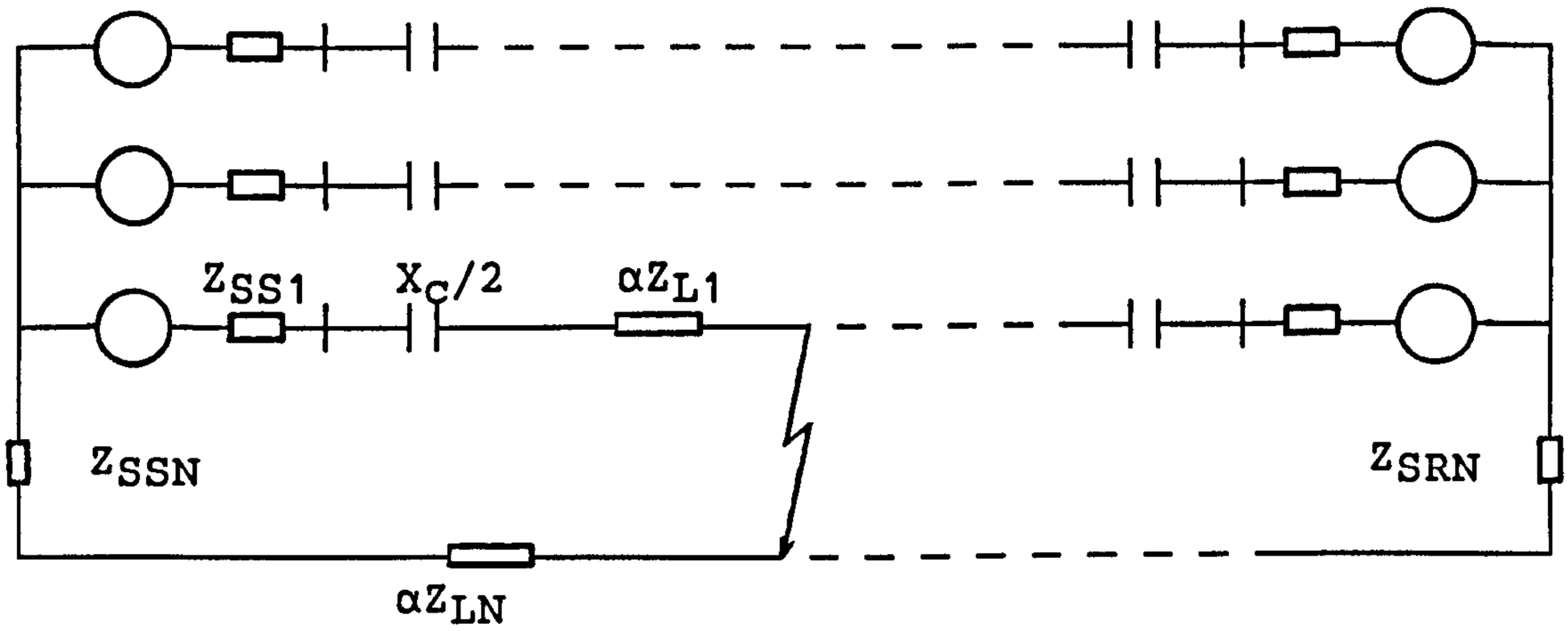

FIG 4.7-Equivalent circuit for an "a" phase-earth fault.

where:

$$Z_{SSN}=1/3(Z_{SS0}-Z_{SS1})$$

$$Z_{LN}=1/3(Z_{L0}-Z_{L1})$$

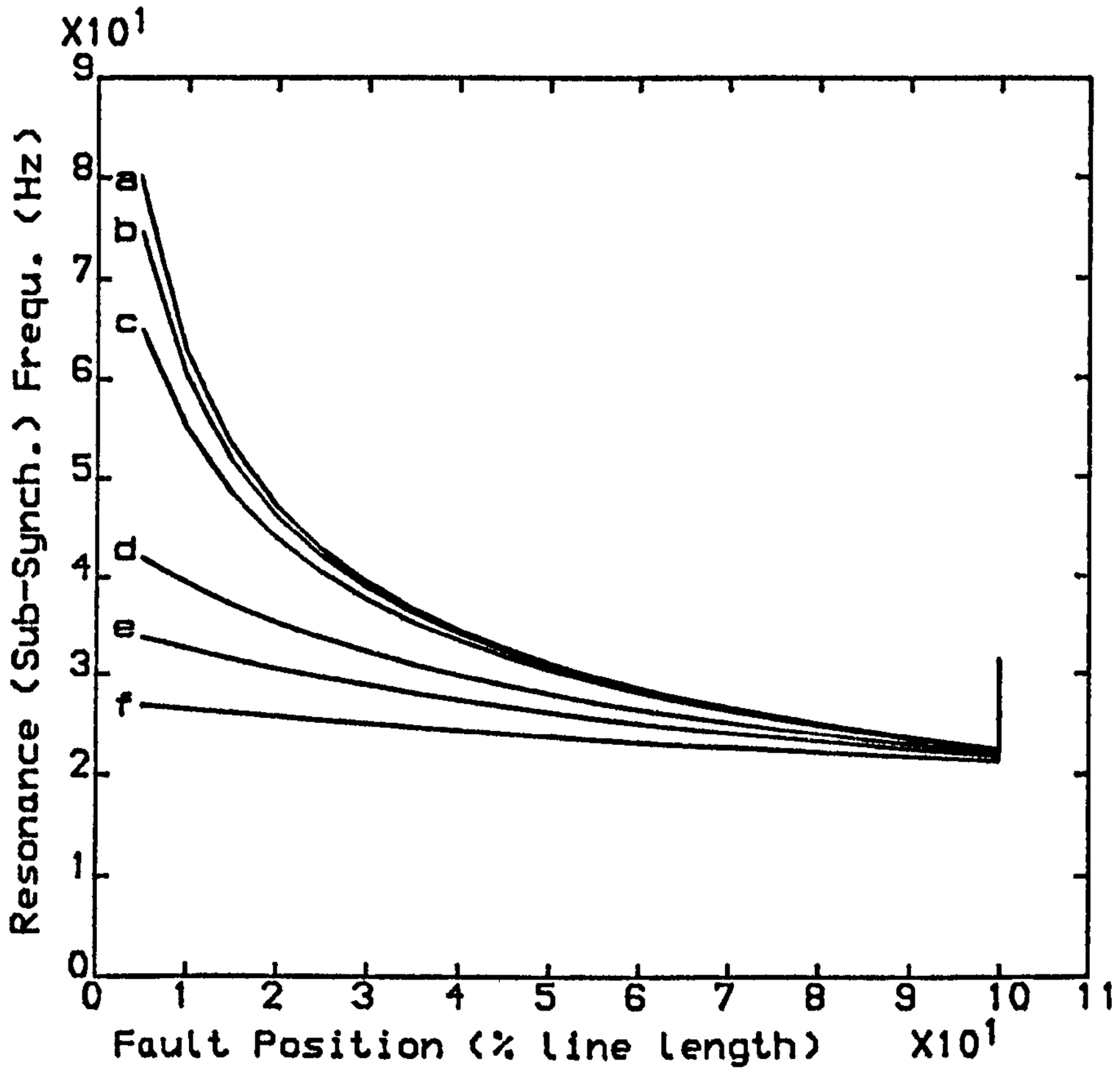

Fig 4.8-Expected Sub-Synchronous Frequency VS Fault Position for 70% Series Compensation (35% at each end).

LINE LENGTH=300 km
SE SCL (GVA)
a=50, b=35, c=20, d=5, e=2.5, f=1.0

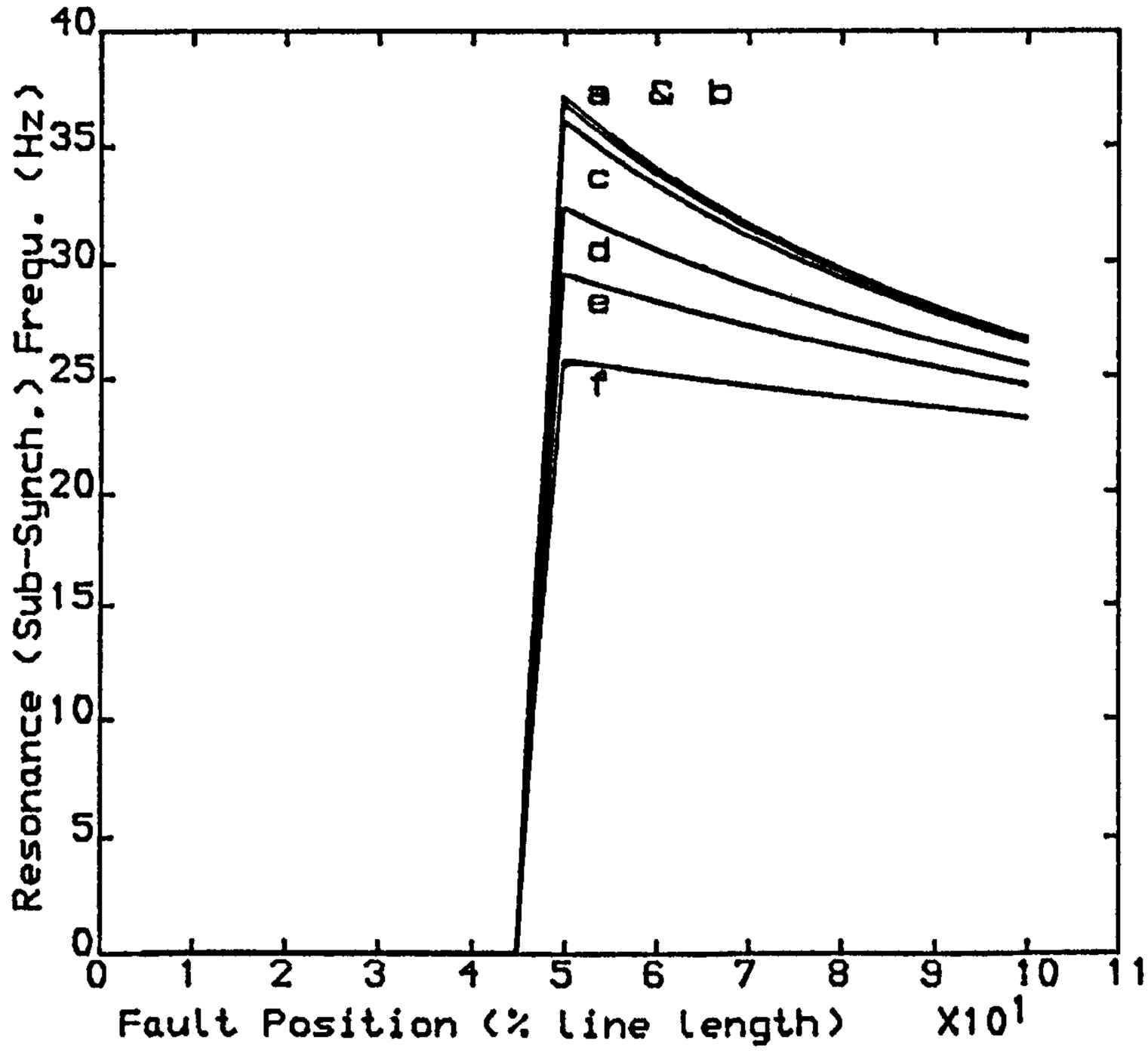

Fig 4.9-Expected Sub-Synchronous Frequency VS Fault Position for 50% Series Compensation at Mid-Point of the Line.

LINE LENGTH=300 km
SE SCL (GVA)
a=50, b=35, c=20, d=5, e=2.5, f=1.0

Note that before the capacitor location, the capacitance present in the circuit is assumed to be infinite which results in zero Sub-Synchronous frequency.

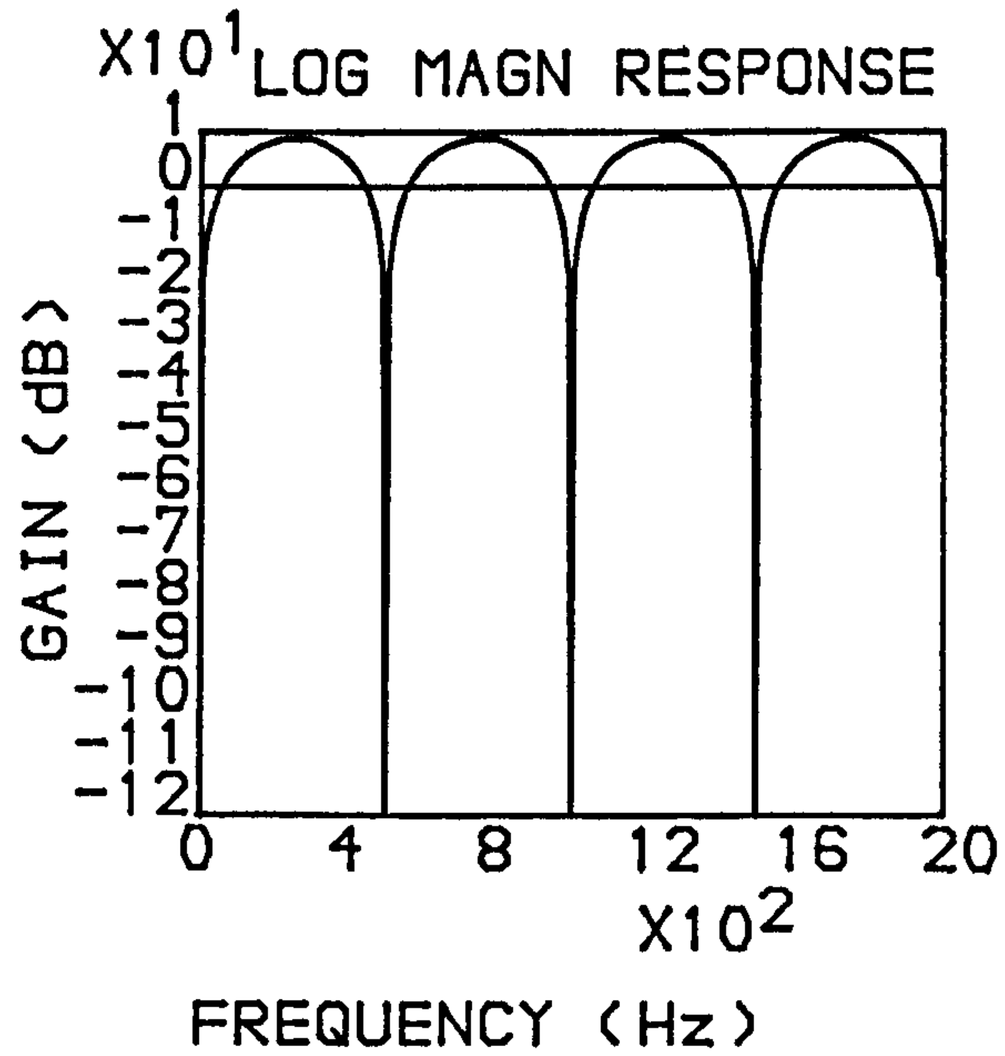

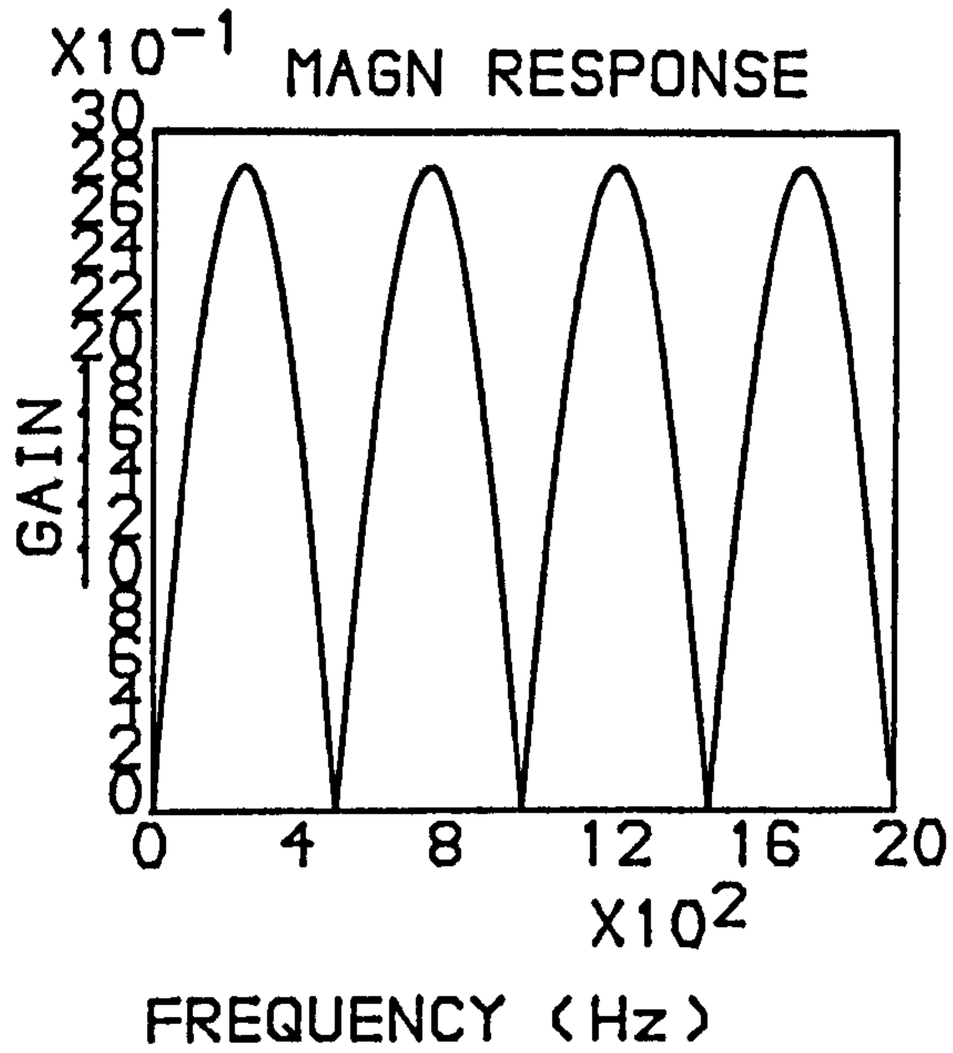

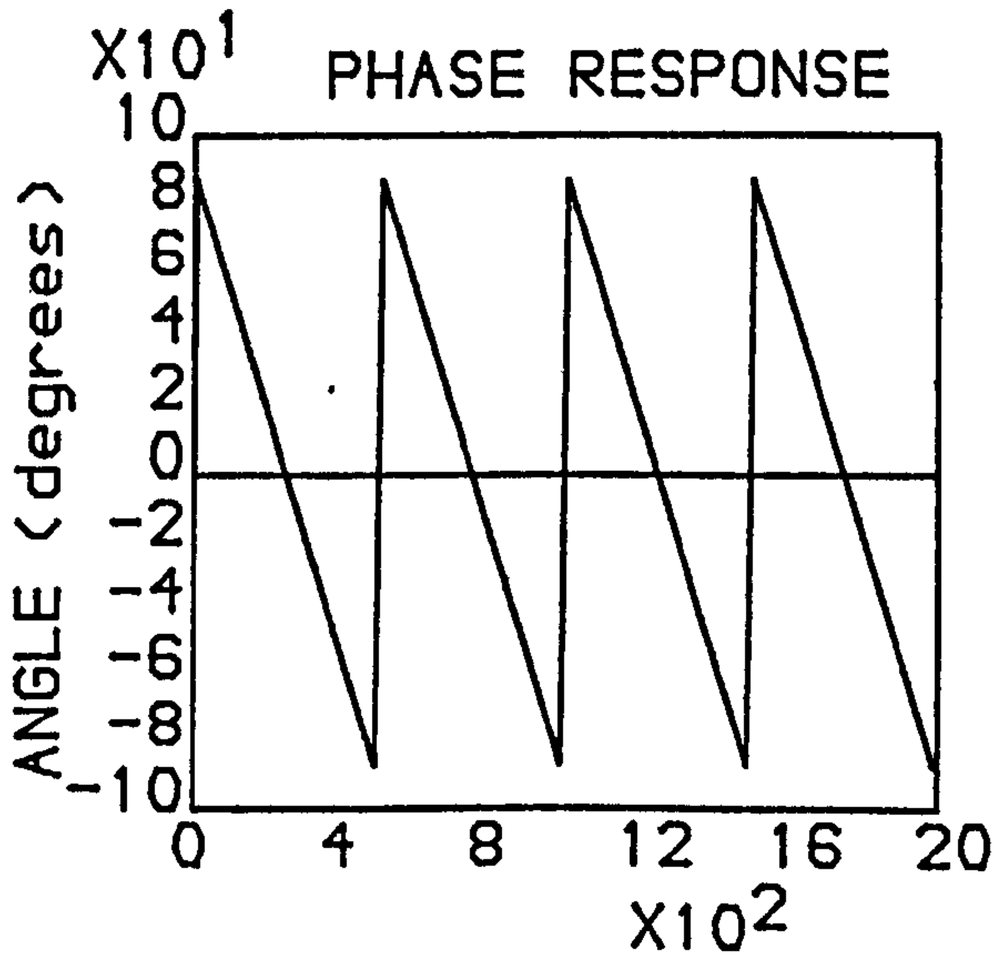

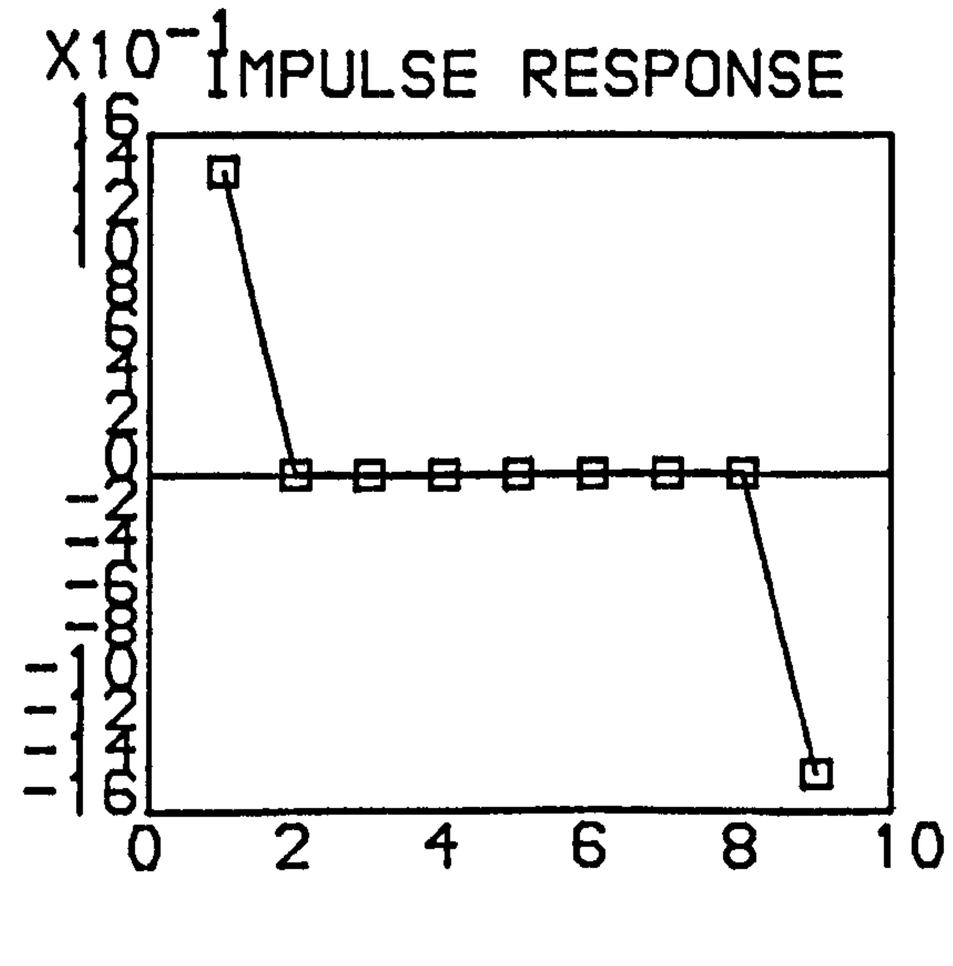

Fig 4.10-The Response of 9 Point Filter (differentiator).

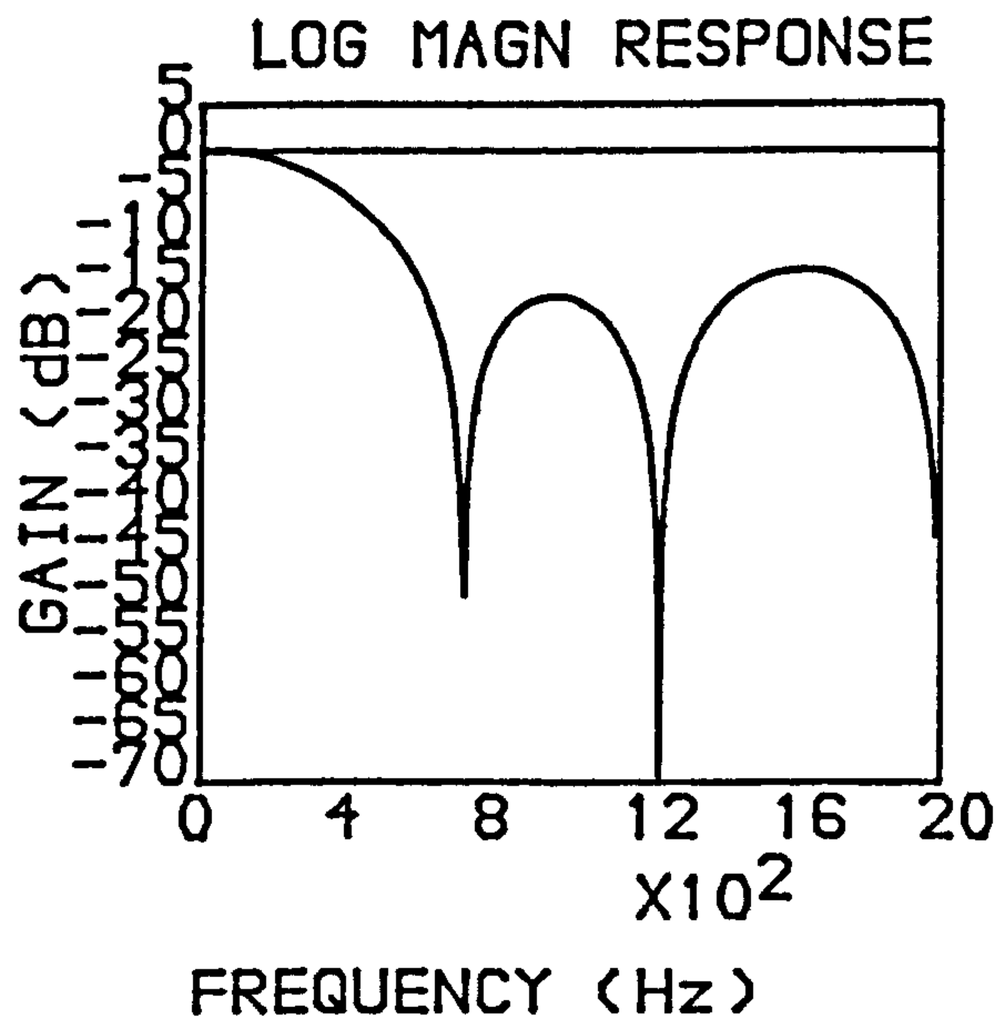

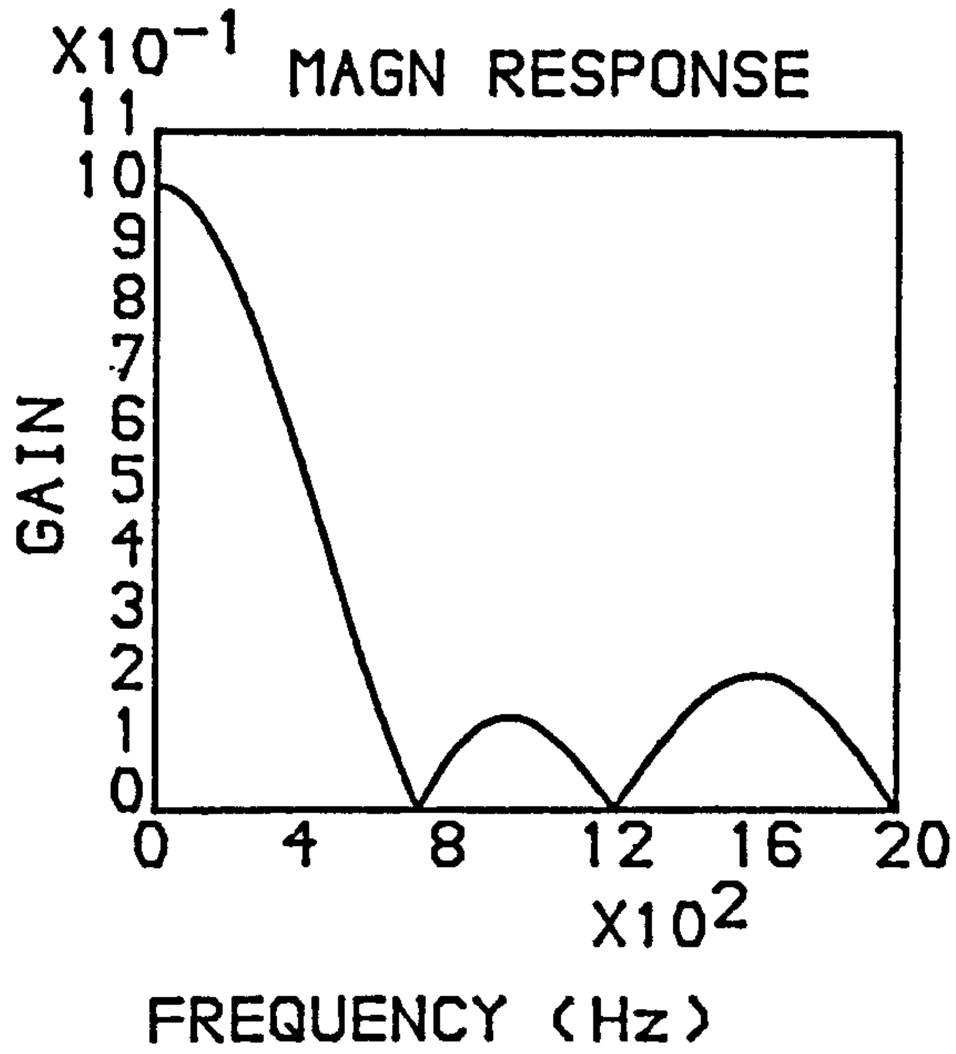

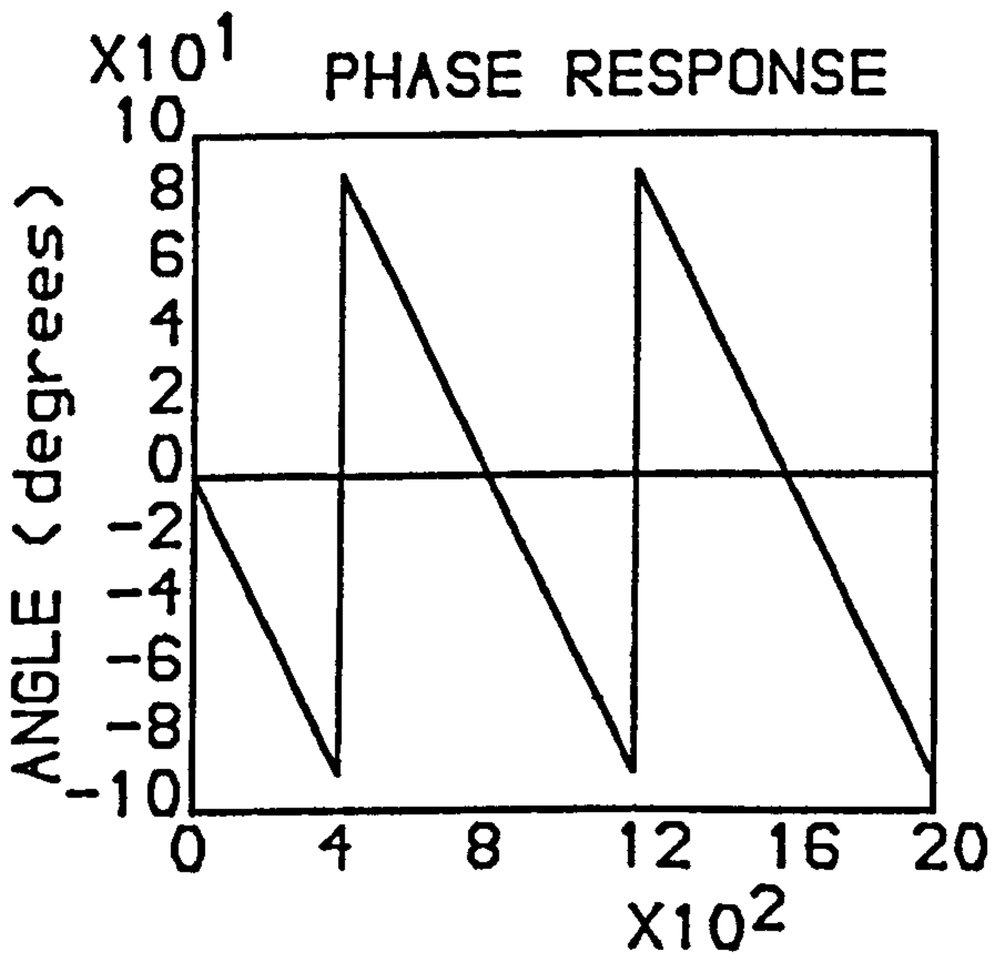

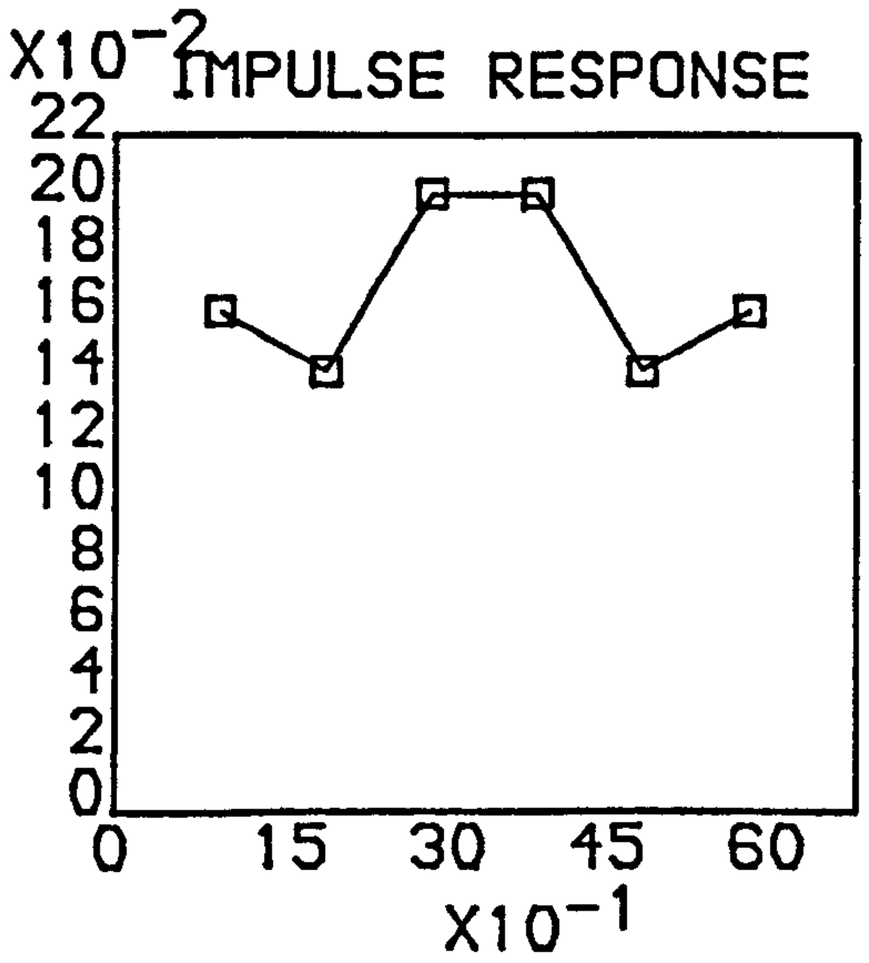

Fig 4.11-The Response of 6 Point Low-Pass Filter.

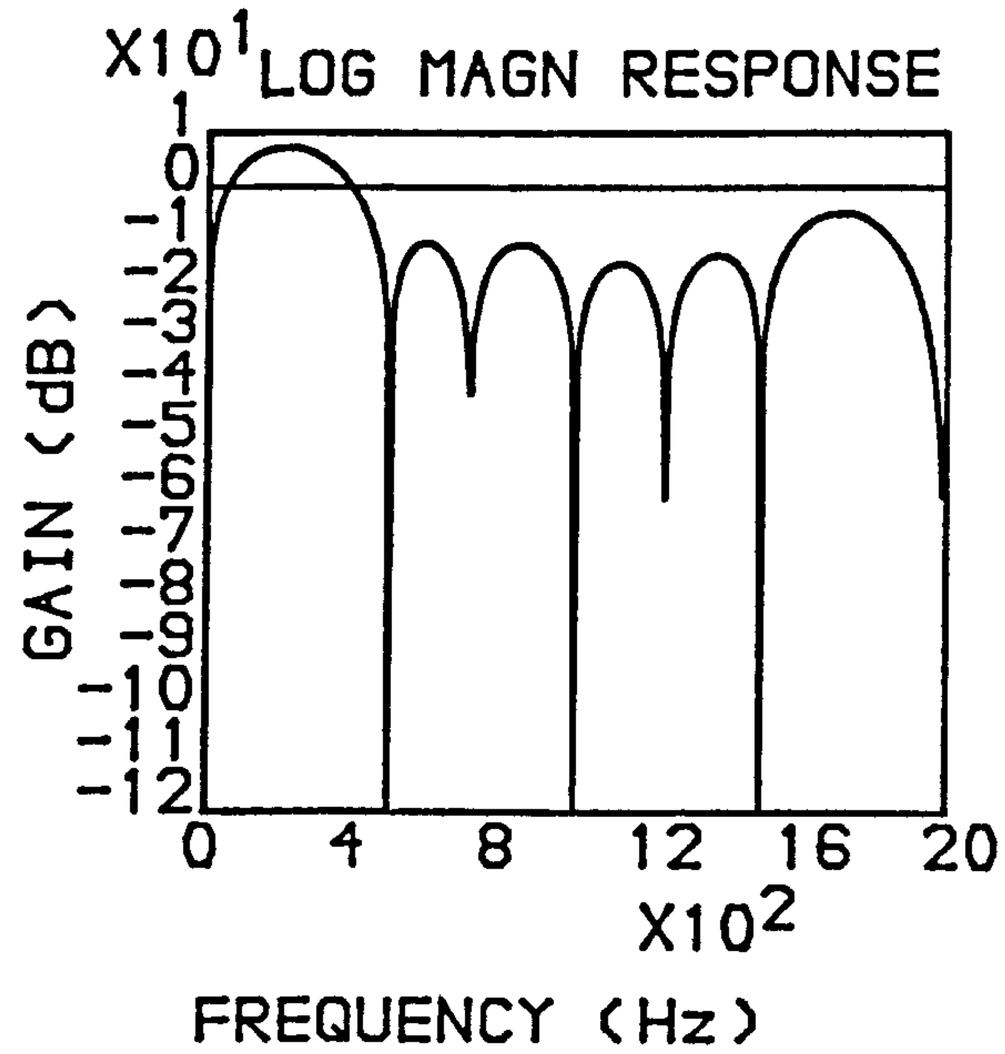

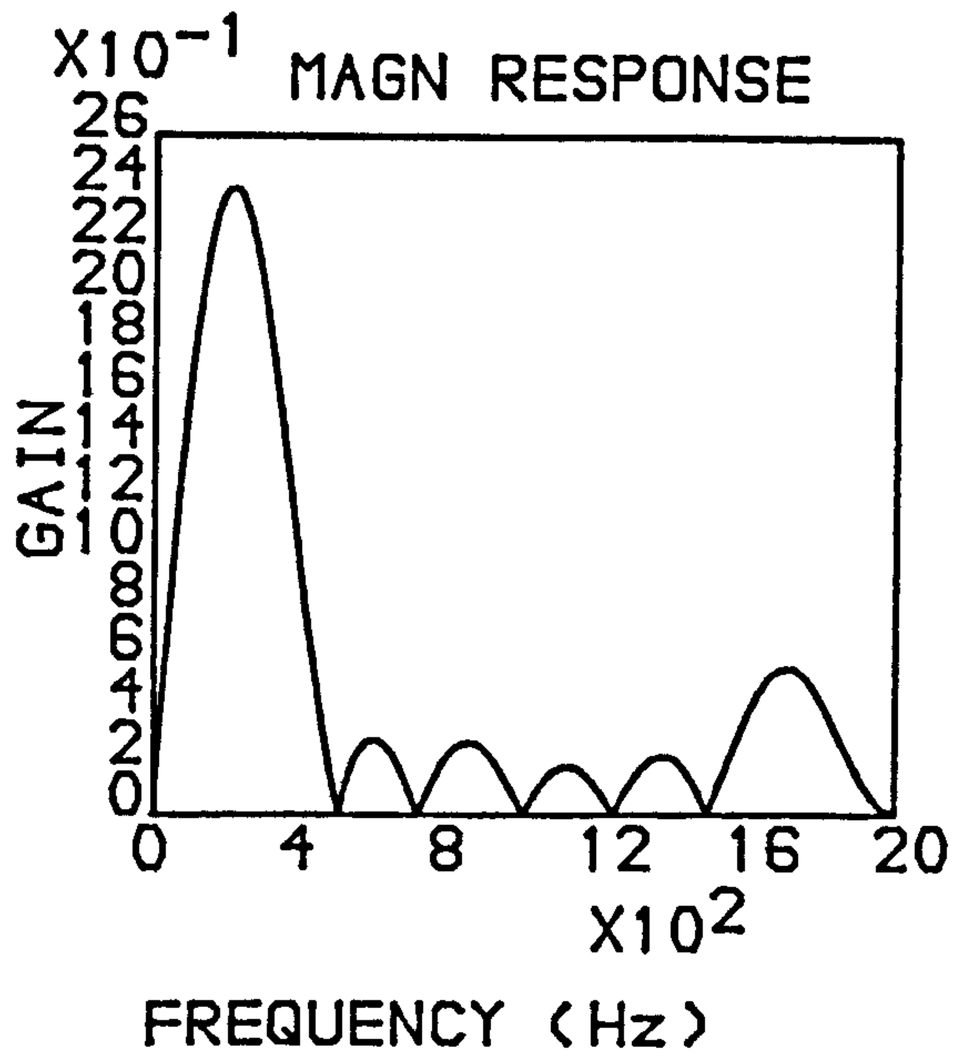

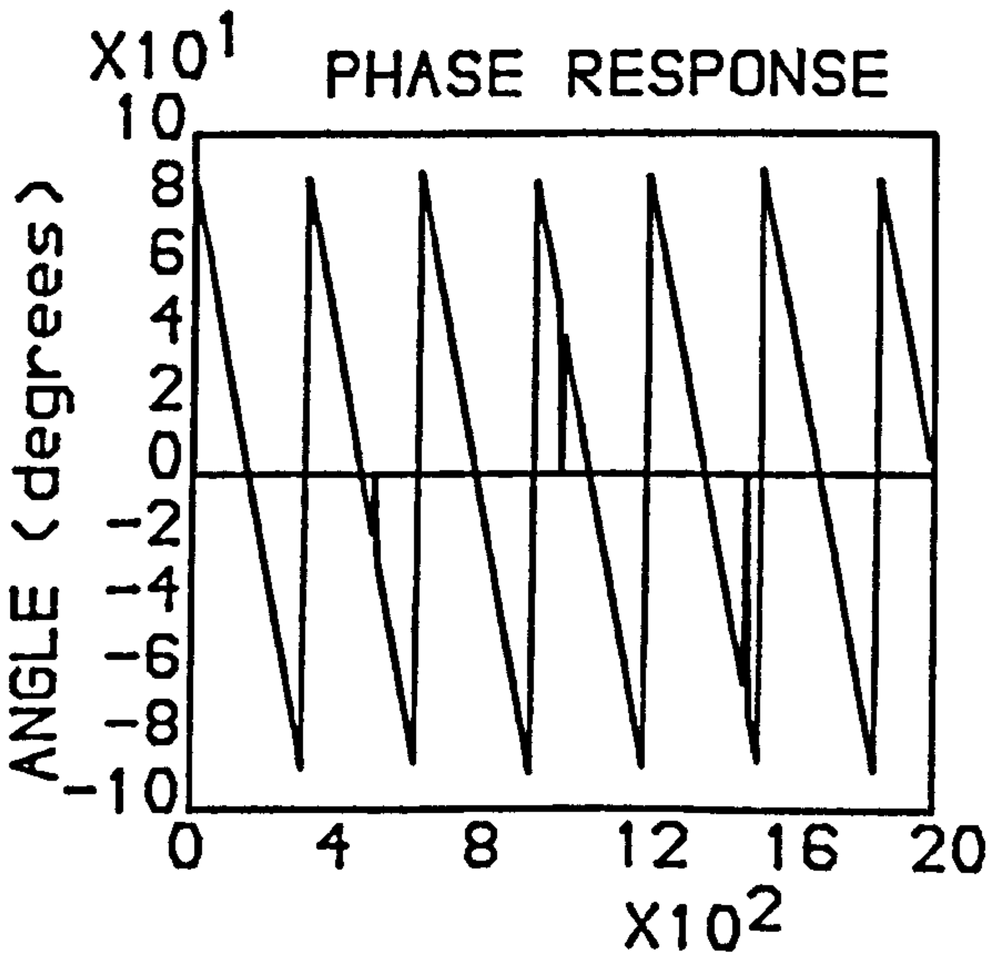

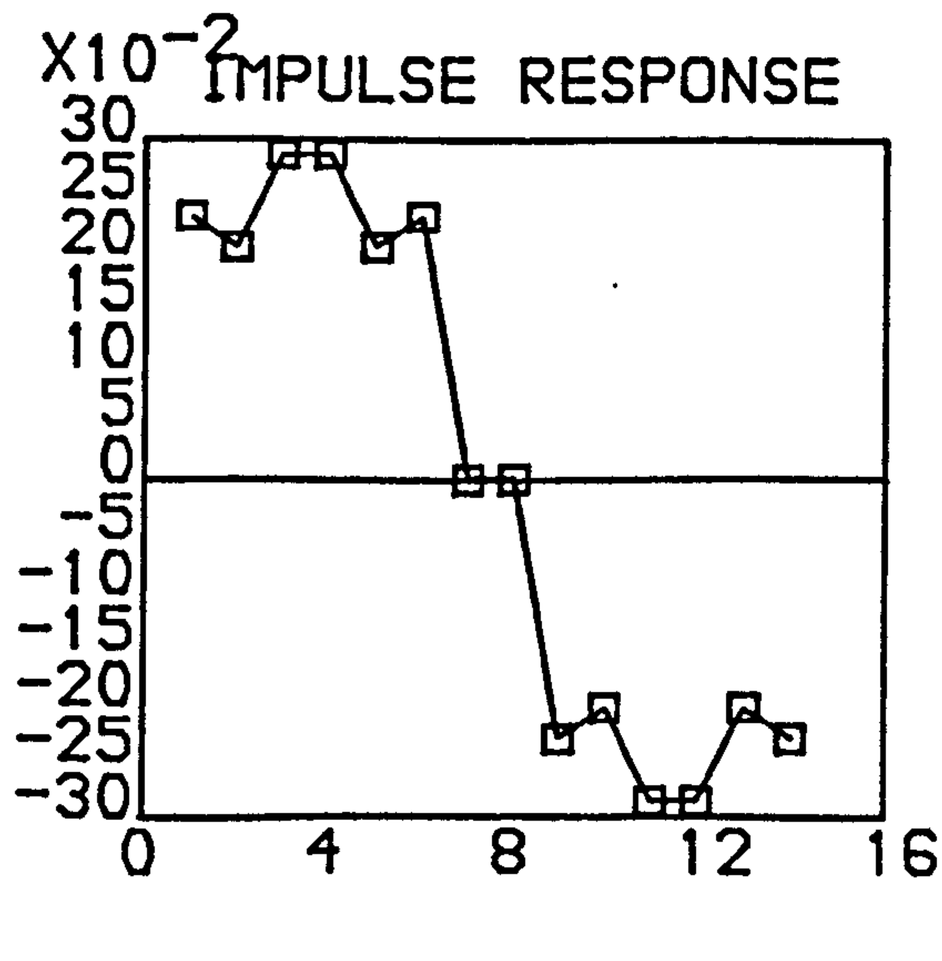

Fig 4.12-The Response of the Digital Pre-Filter.

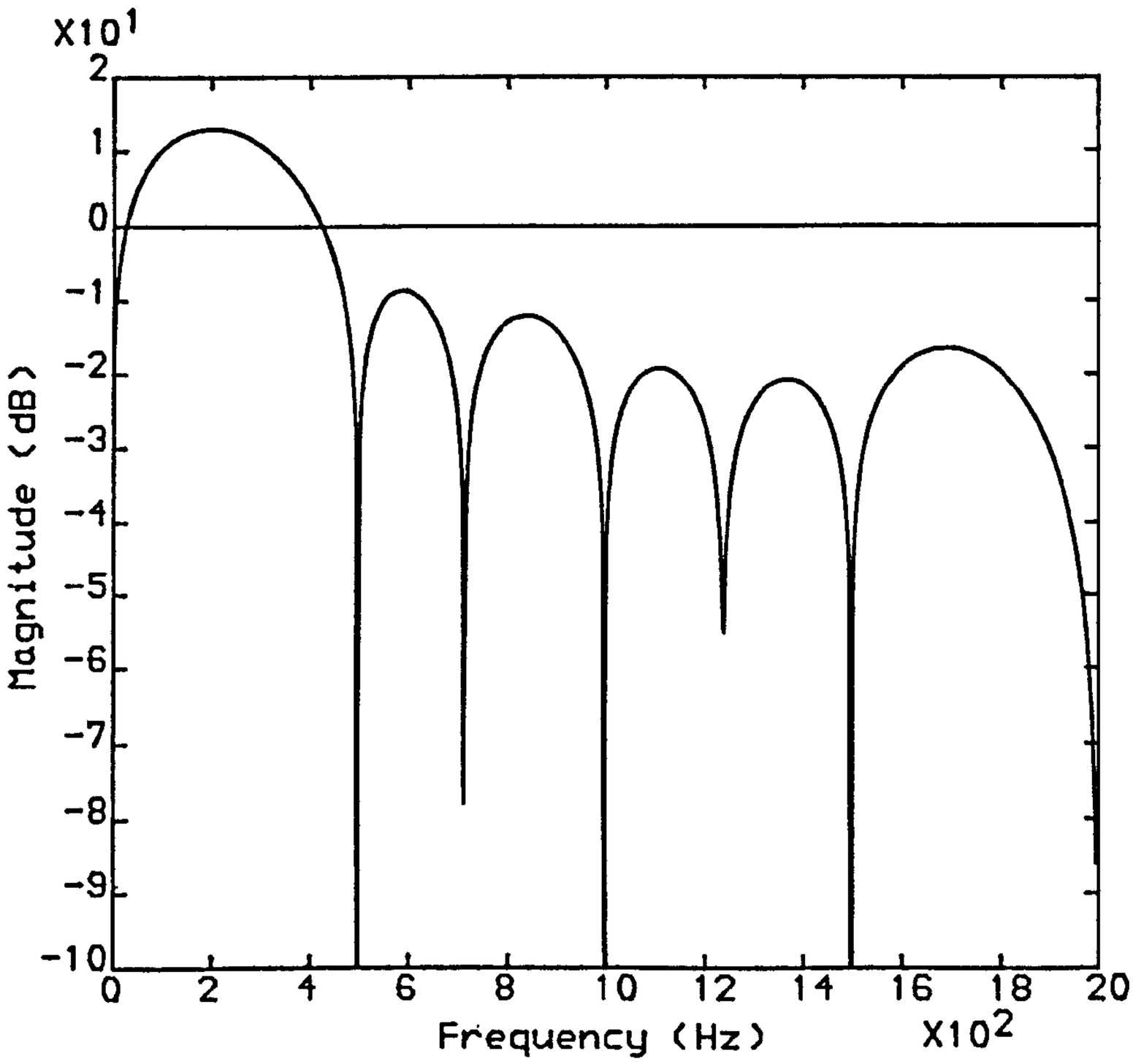

Fig 4.13-Overall Response of the Digital and Analogue Pre-Filter.

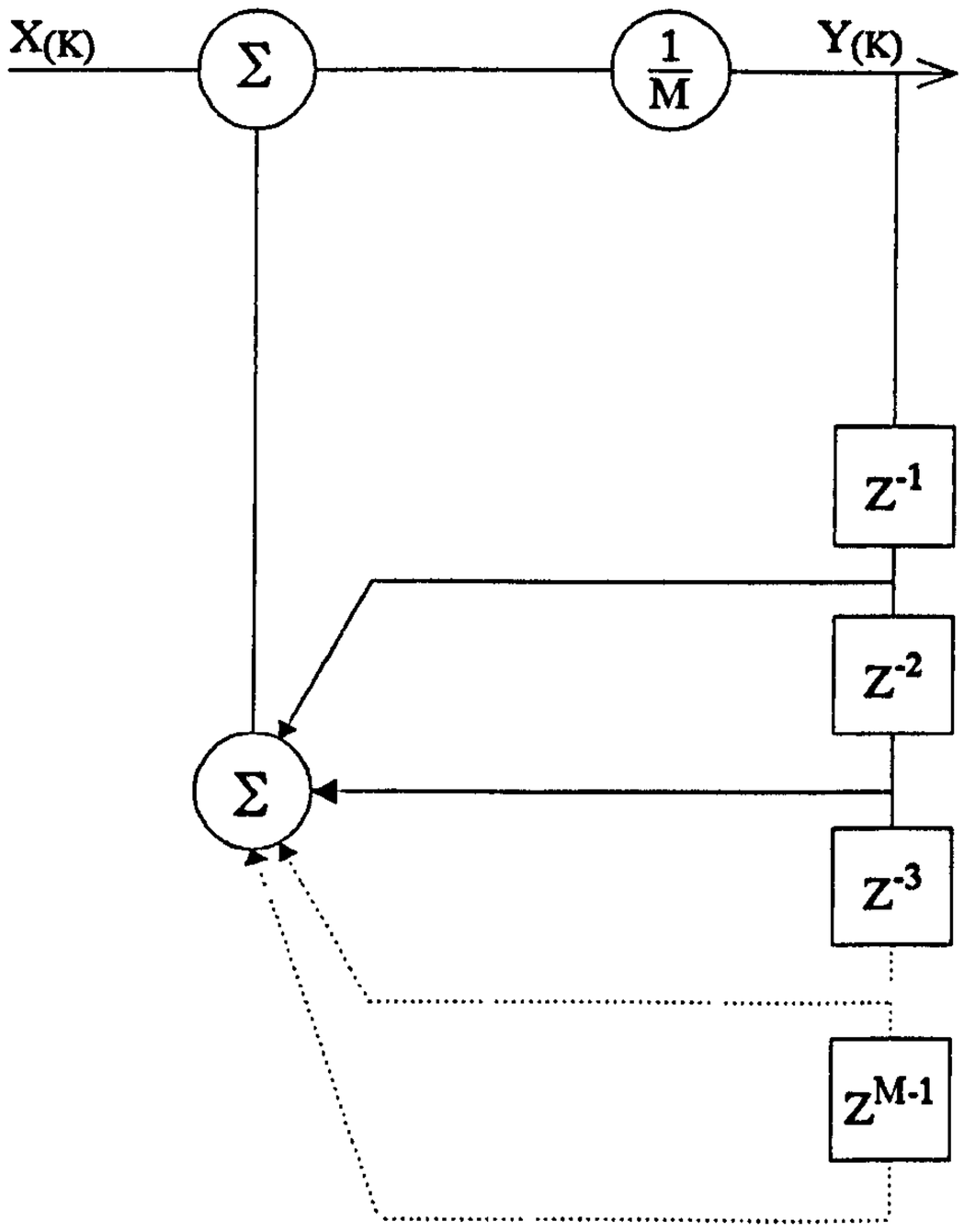

Fig 4.14-Schematic Diagram for Recursive Averager (Equation 4.9).

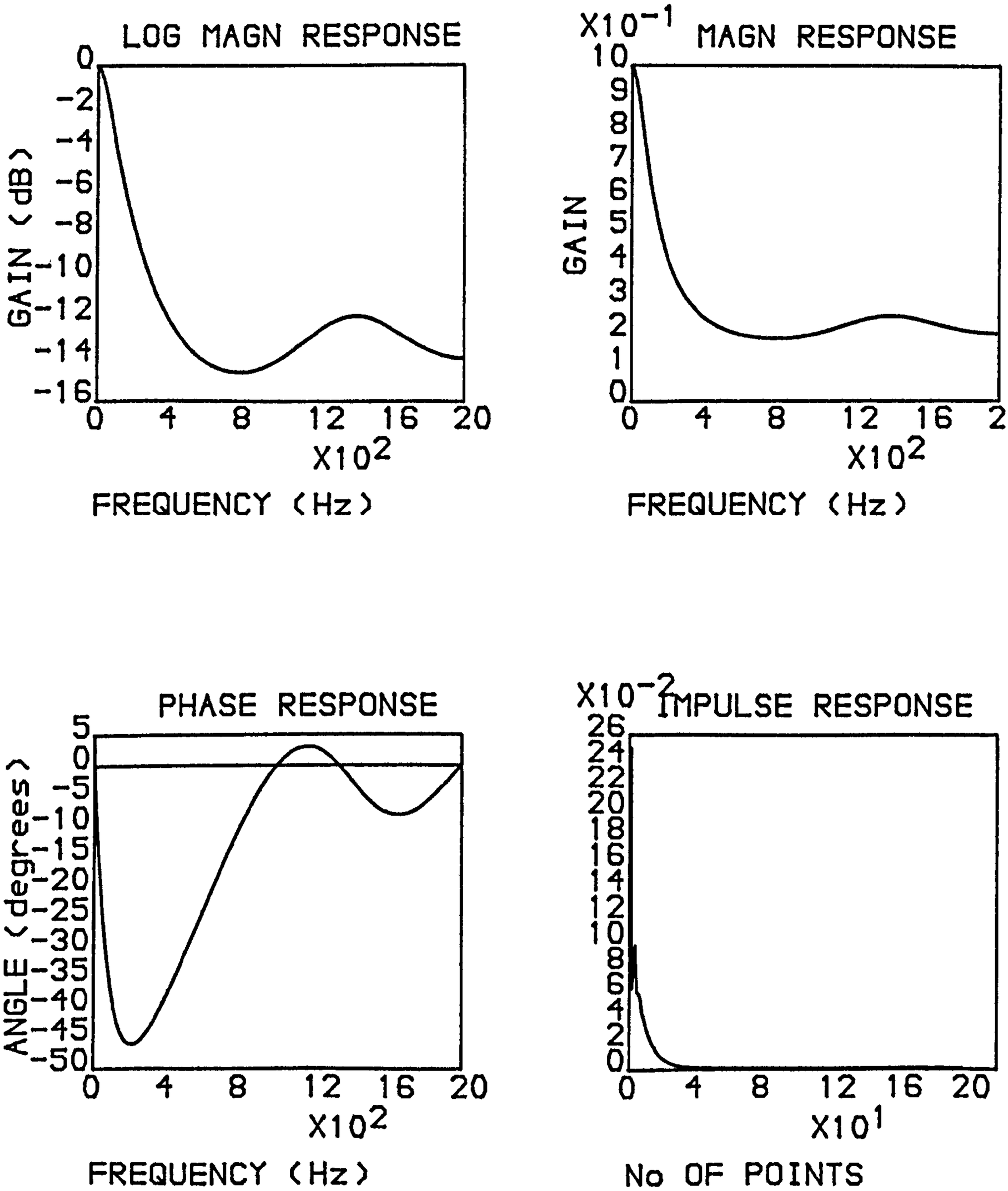

Fig 4.15.a-Response of the Recursive Averager for M=4.

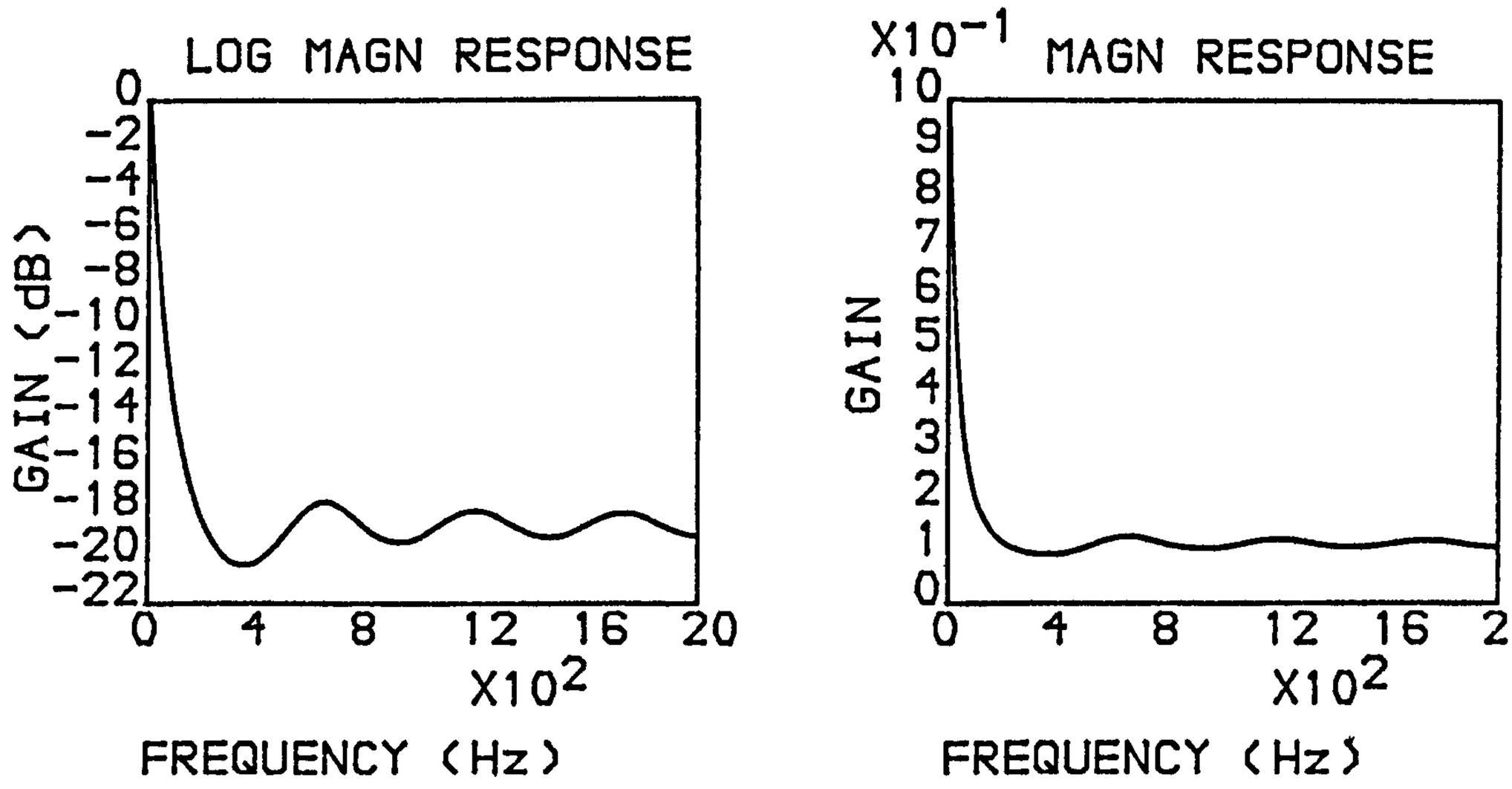

Fig 4.15.b-Response of the Recursive Averager for M=8.

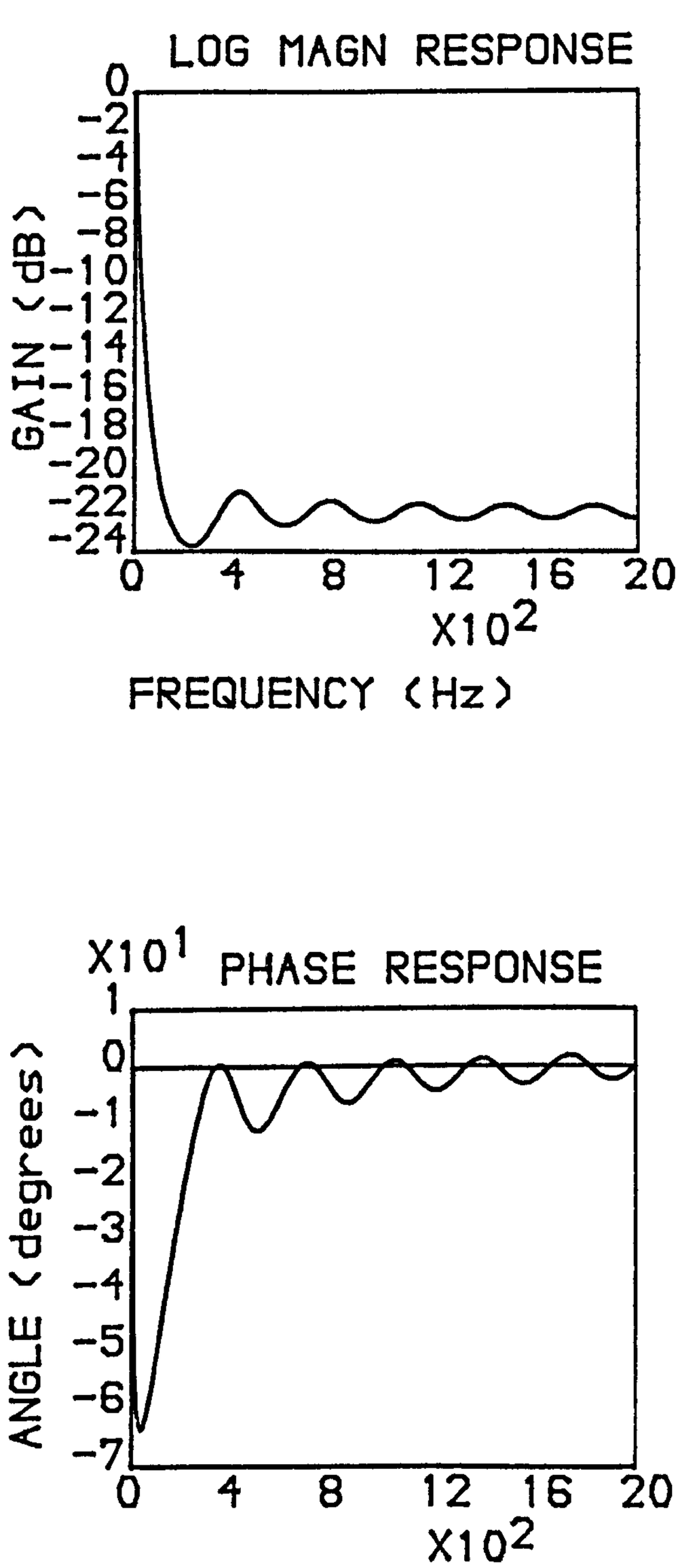

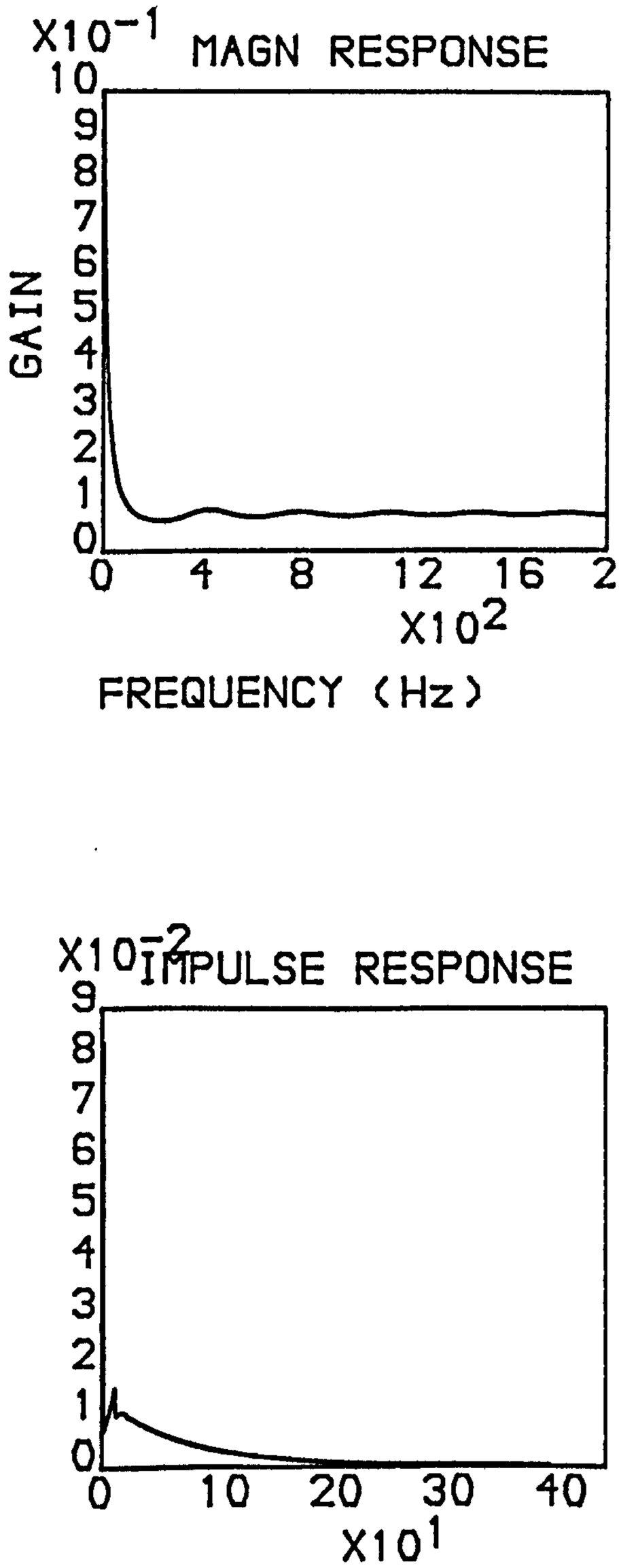

Fig 4.15.c-Response of the Recursive Averager for M=12.

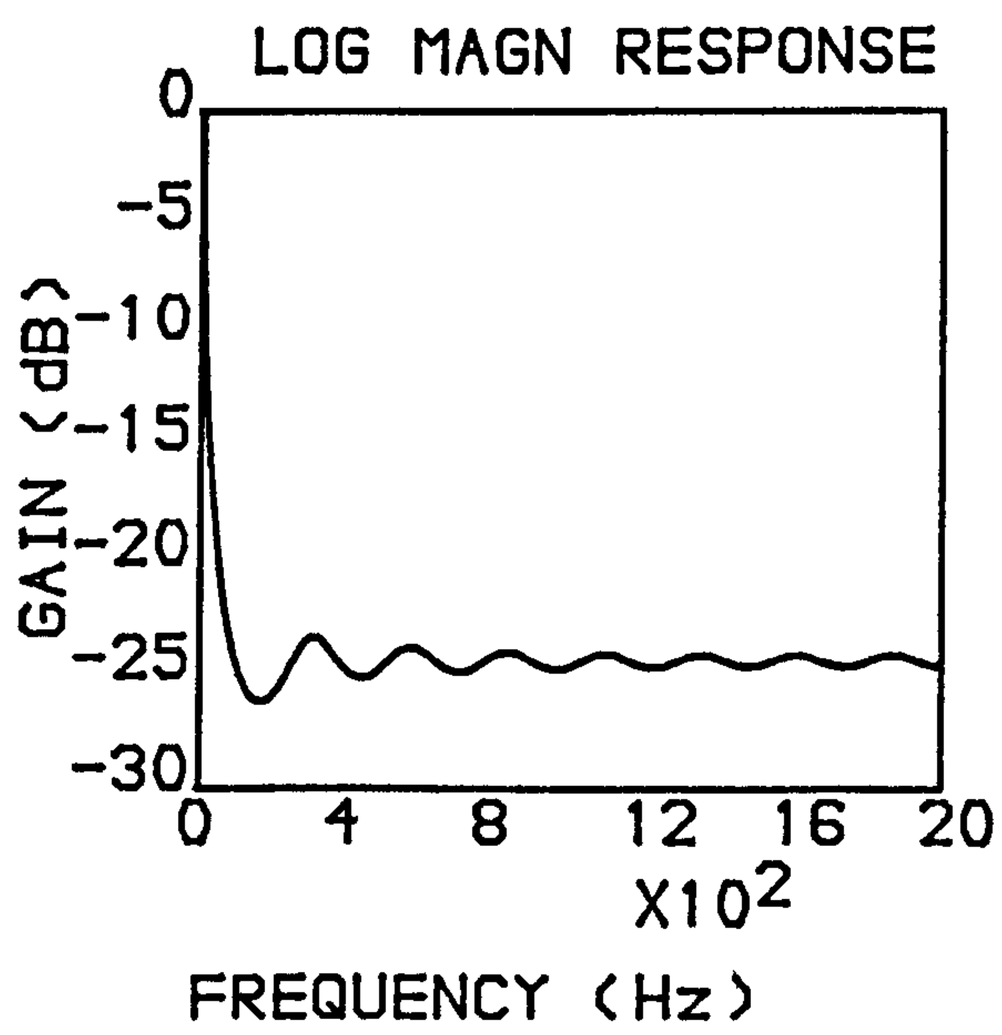

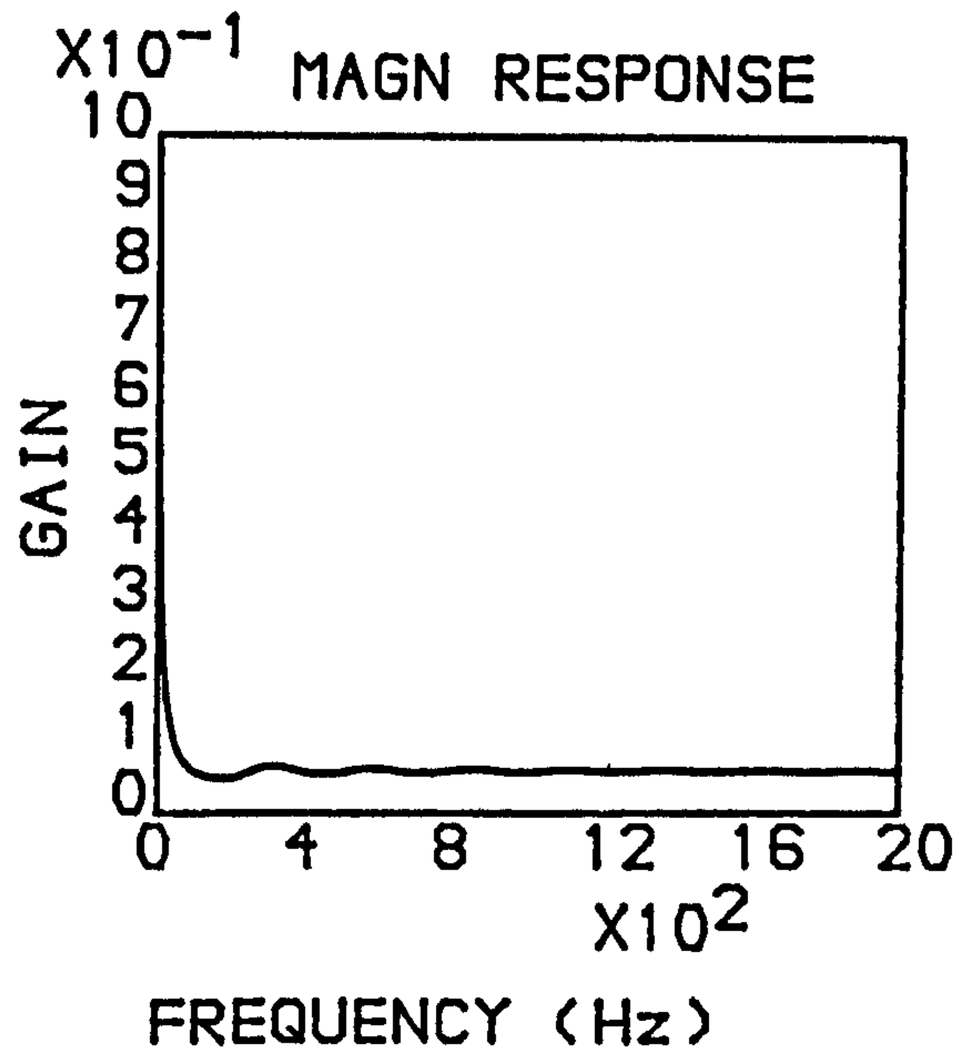

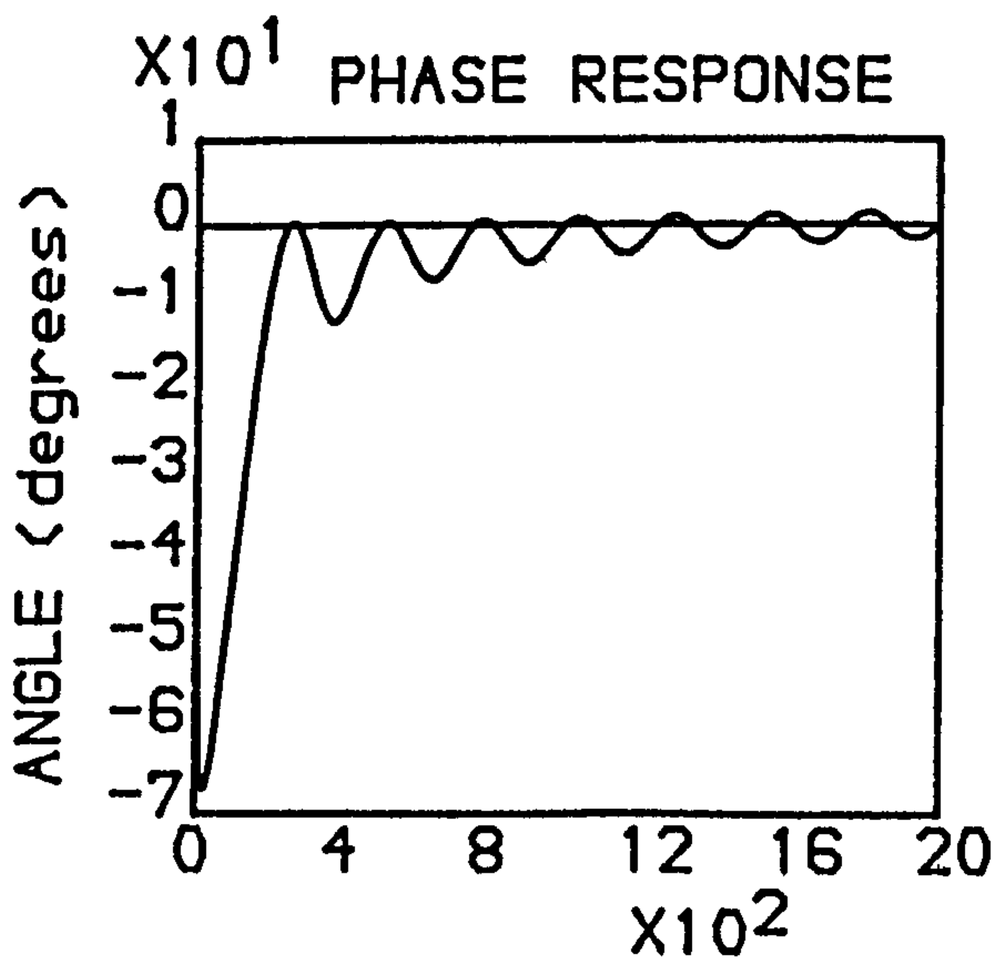

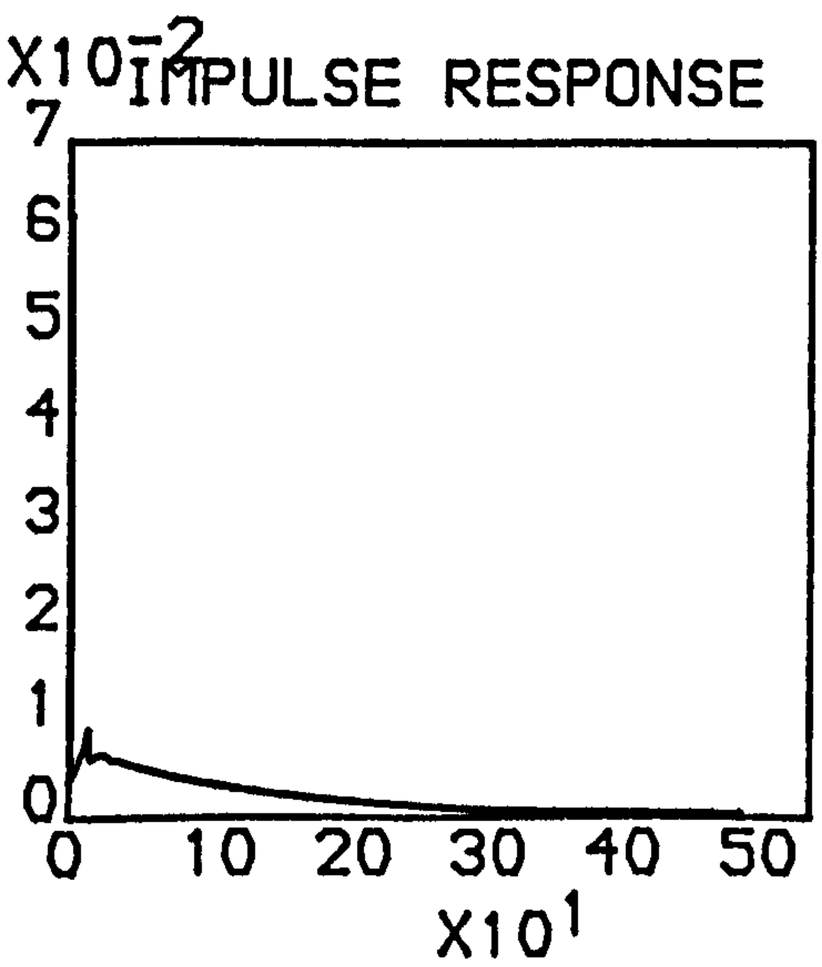

Fig 4.15.d-Response of the Recursive Averager for M=16.

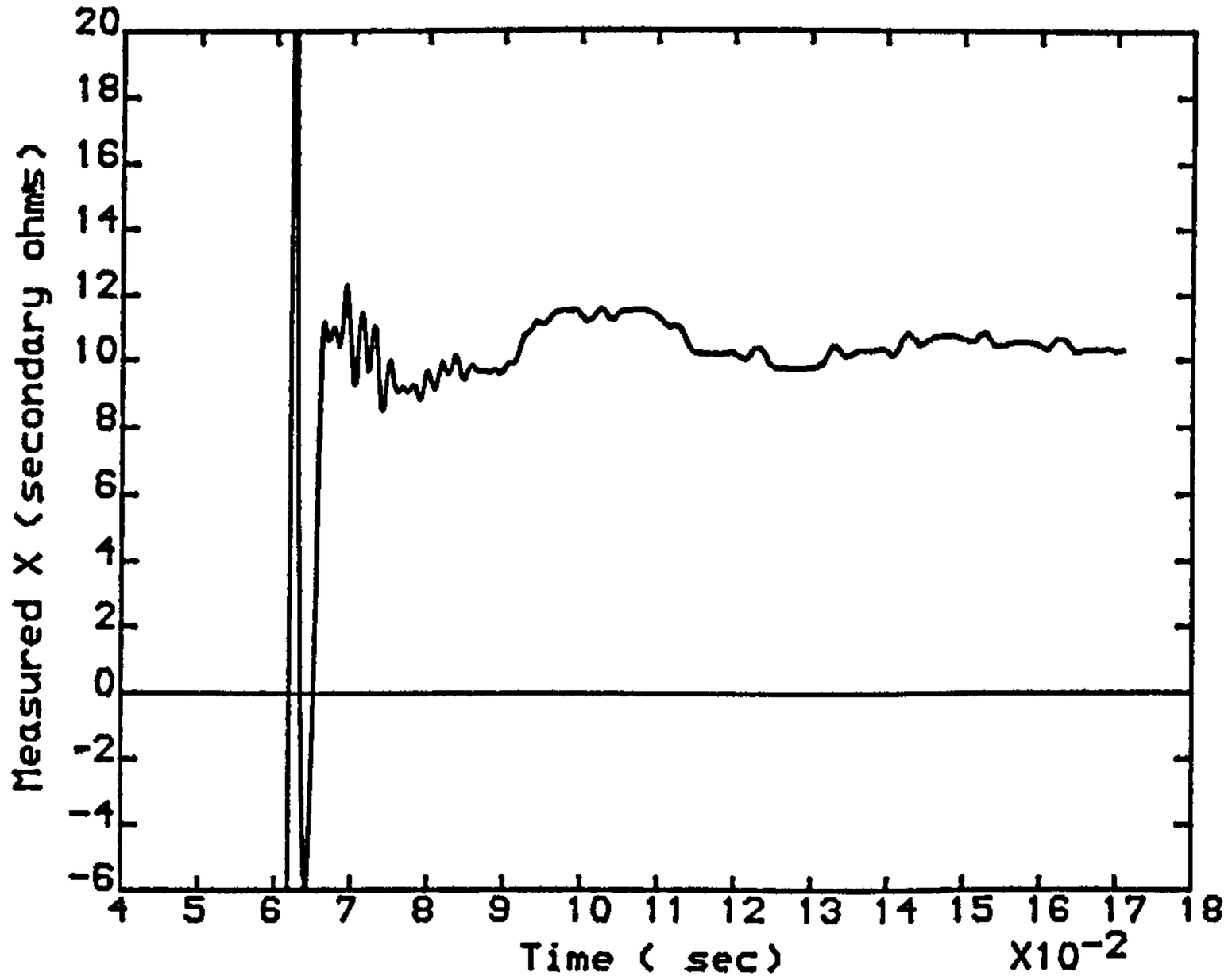

Fig 4.16-Measured Reactance without the Recursive Averager.

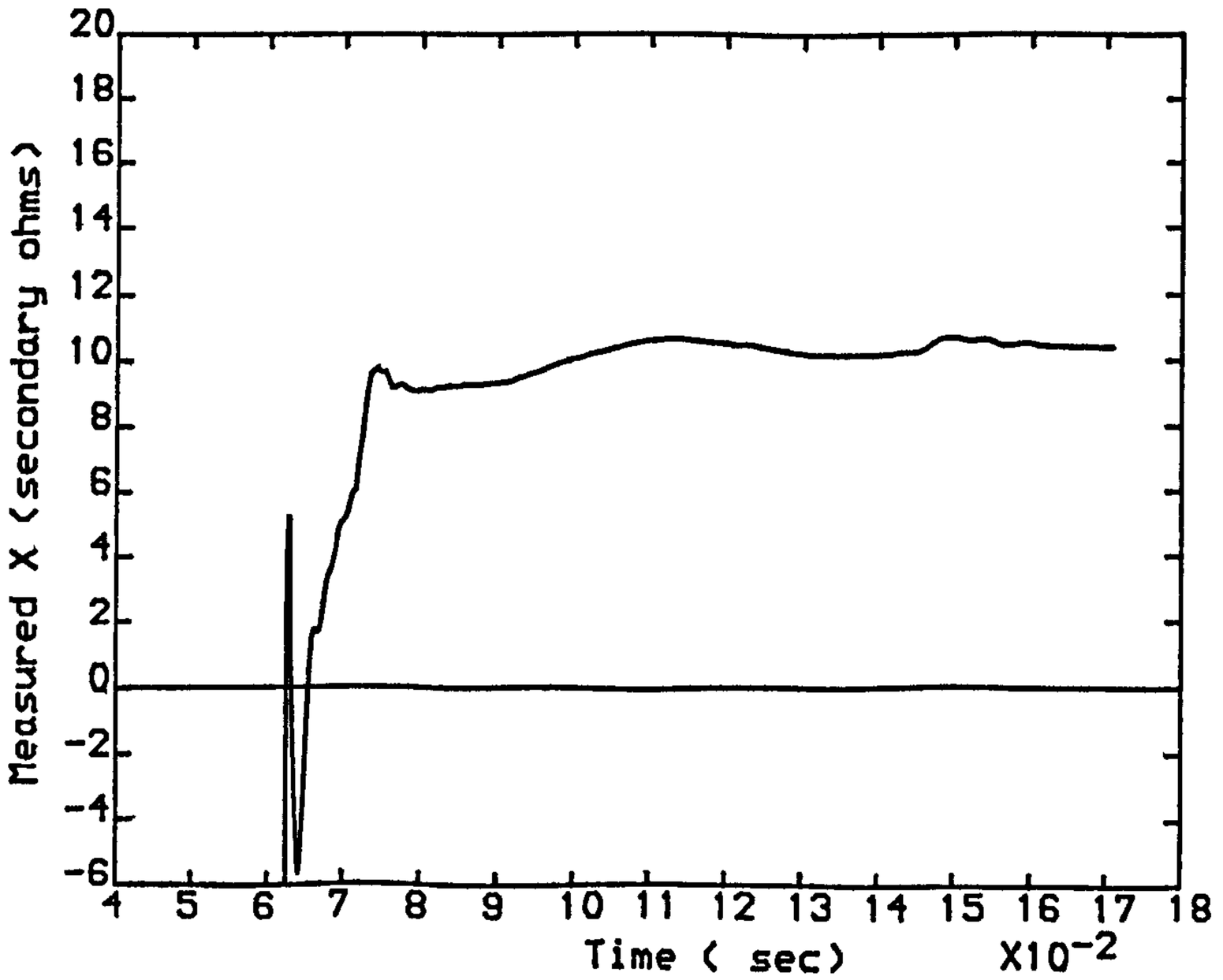

Fig 4.17-Measured Reactance with the Recursive Averager (M=12) when Applied Continuously.

SE SCL=5GVA, RE SCL=35 GVA, LINE LENGTH=300 km.

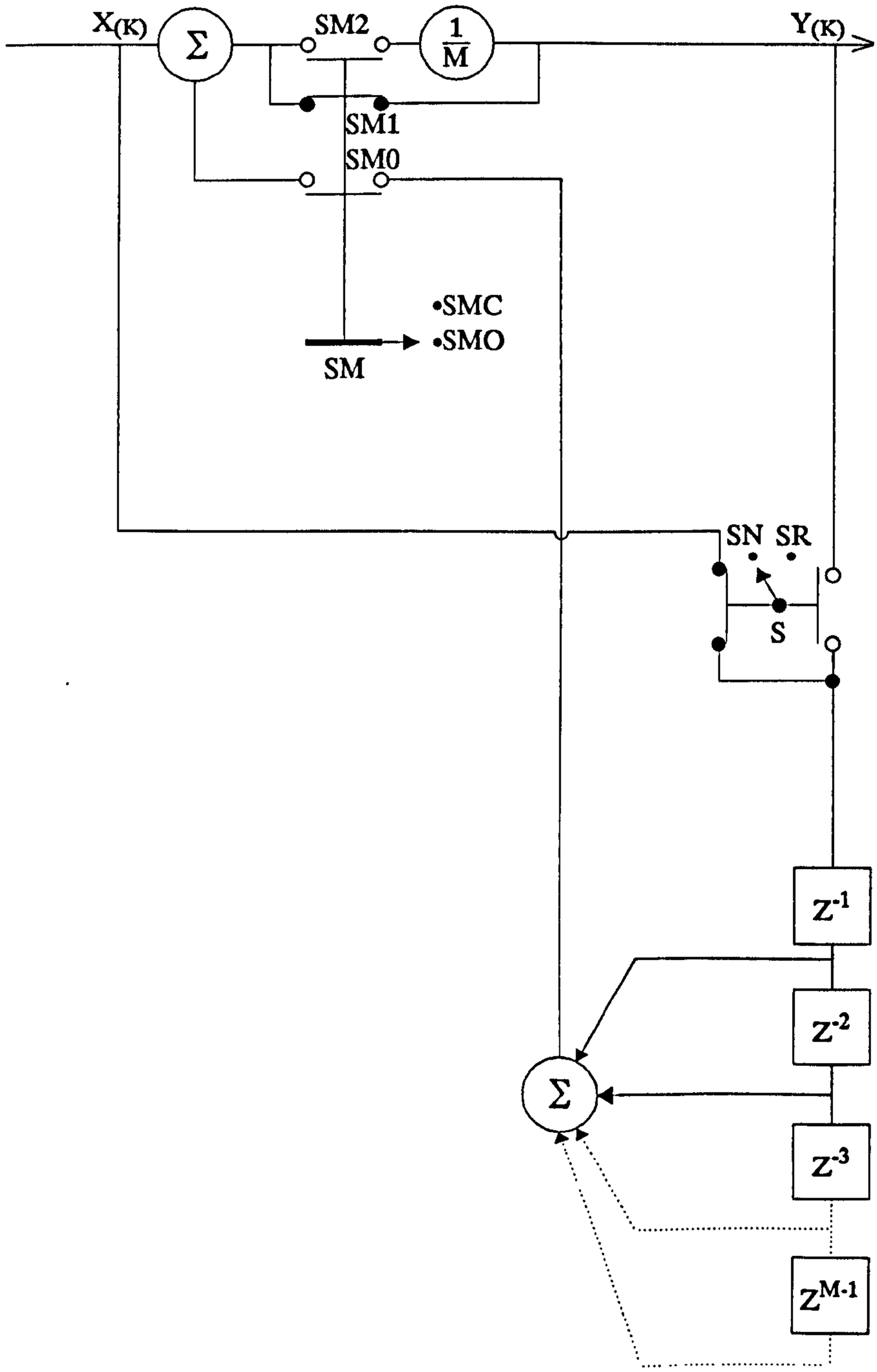

Fig 4.18-Schematic Diagram for switched Recursive Averager.

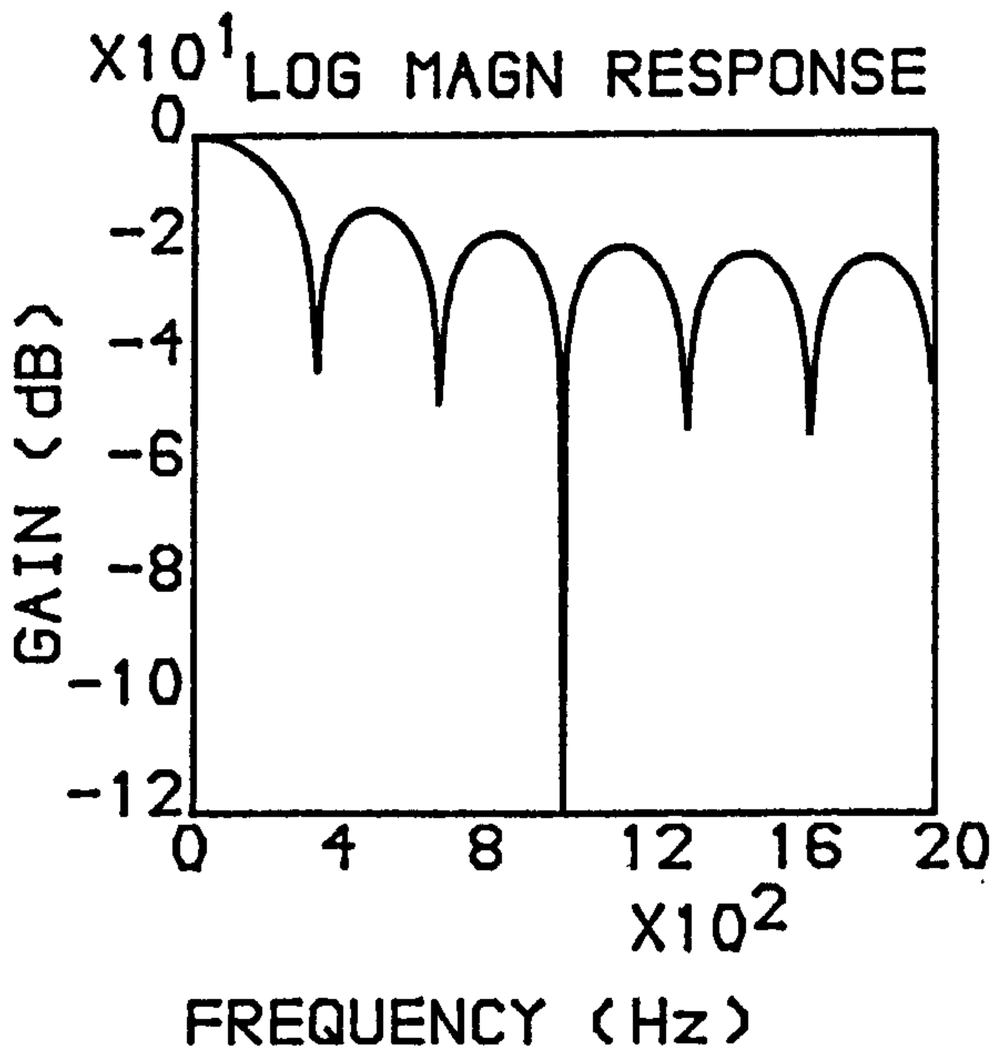

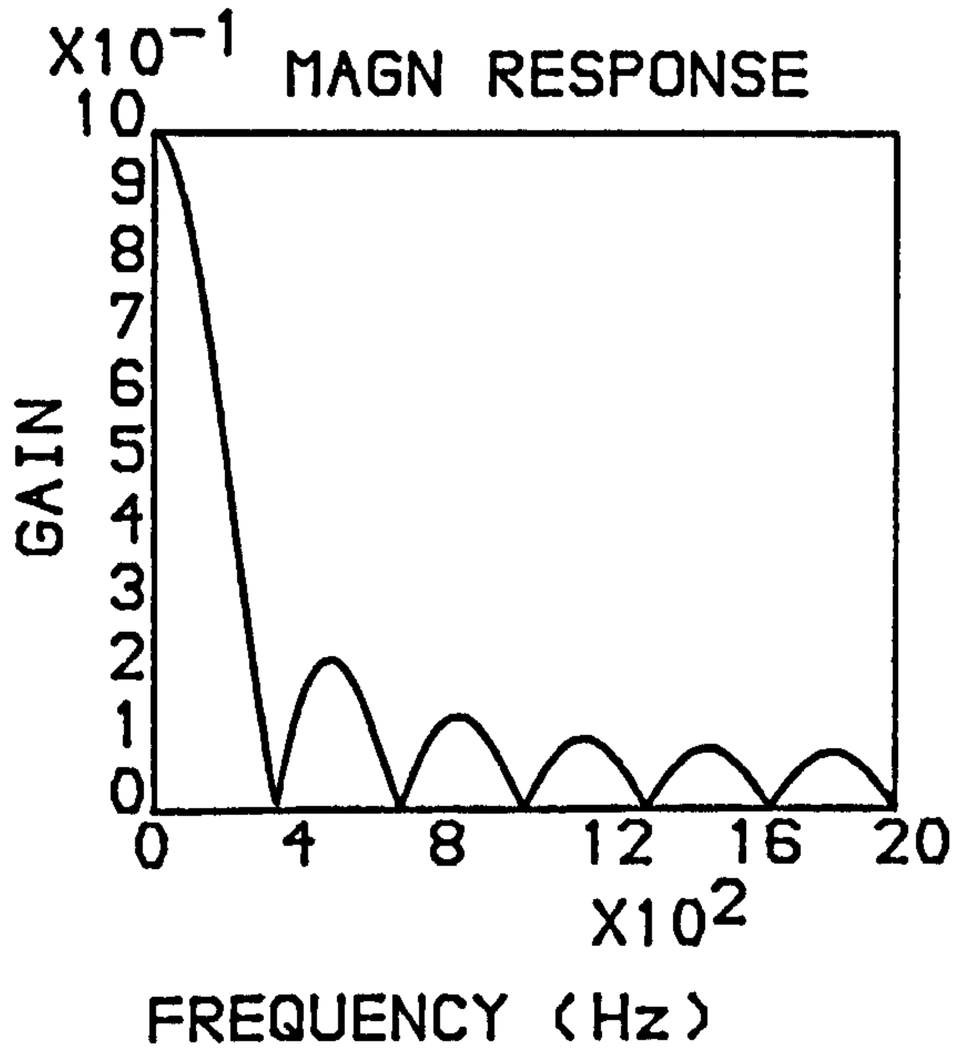

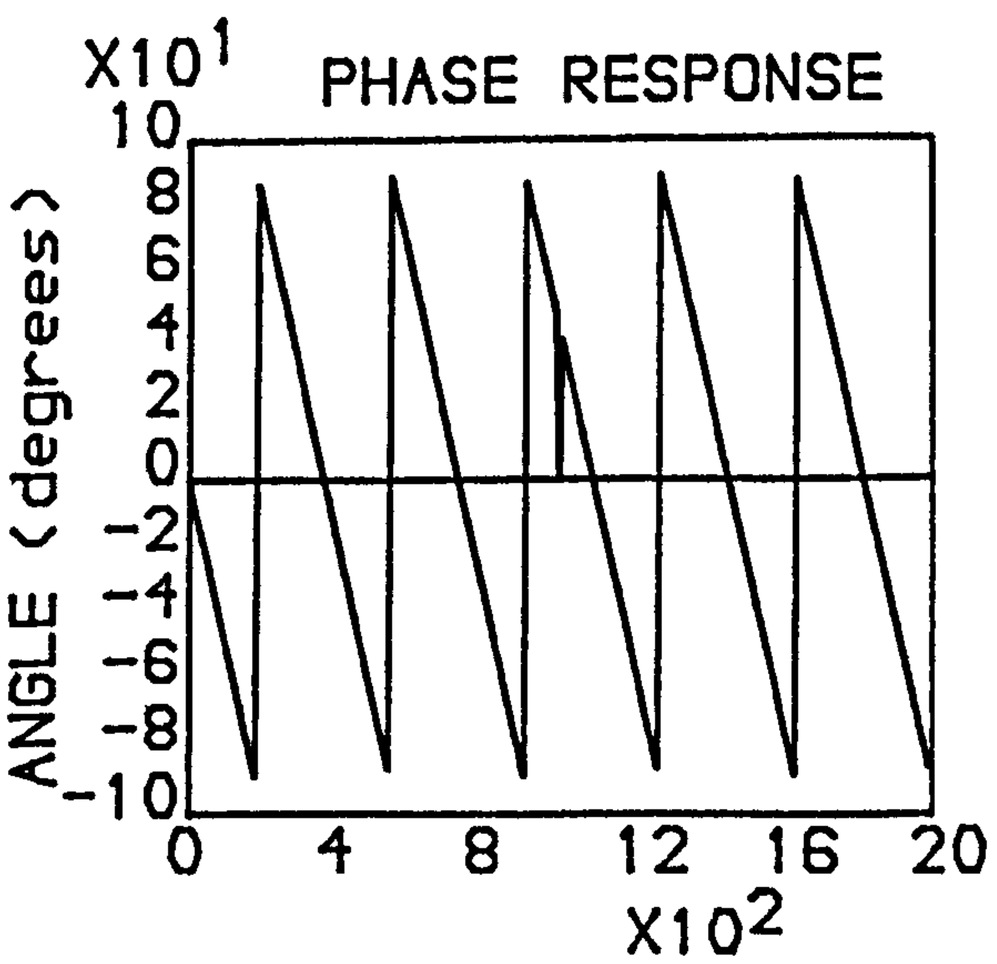

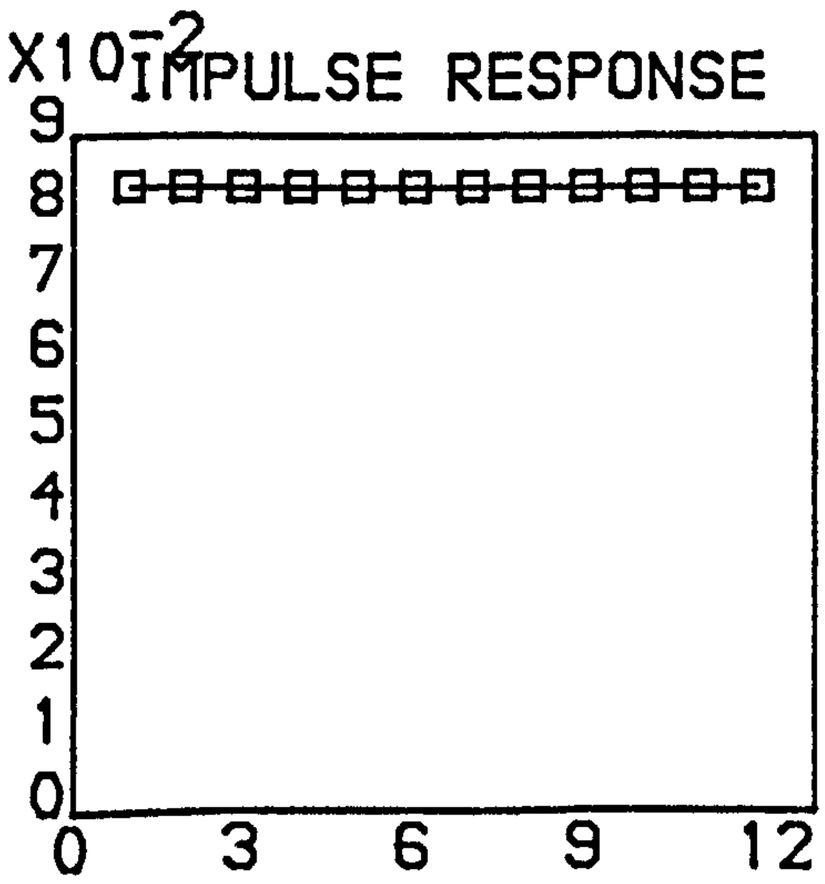

Fig 4.19-The Response of the 12 point Non-Recursive Averager.

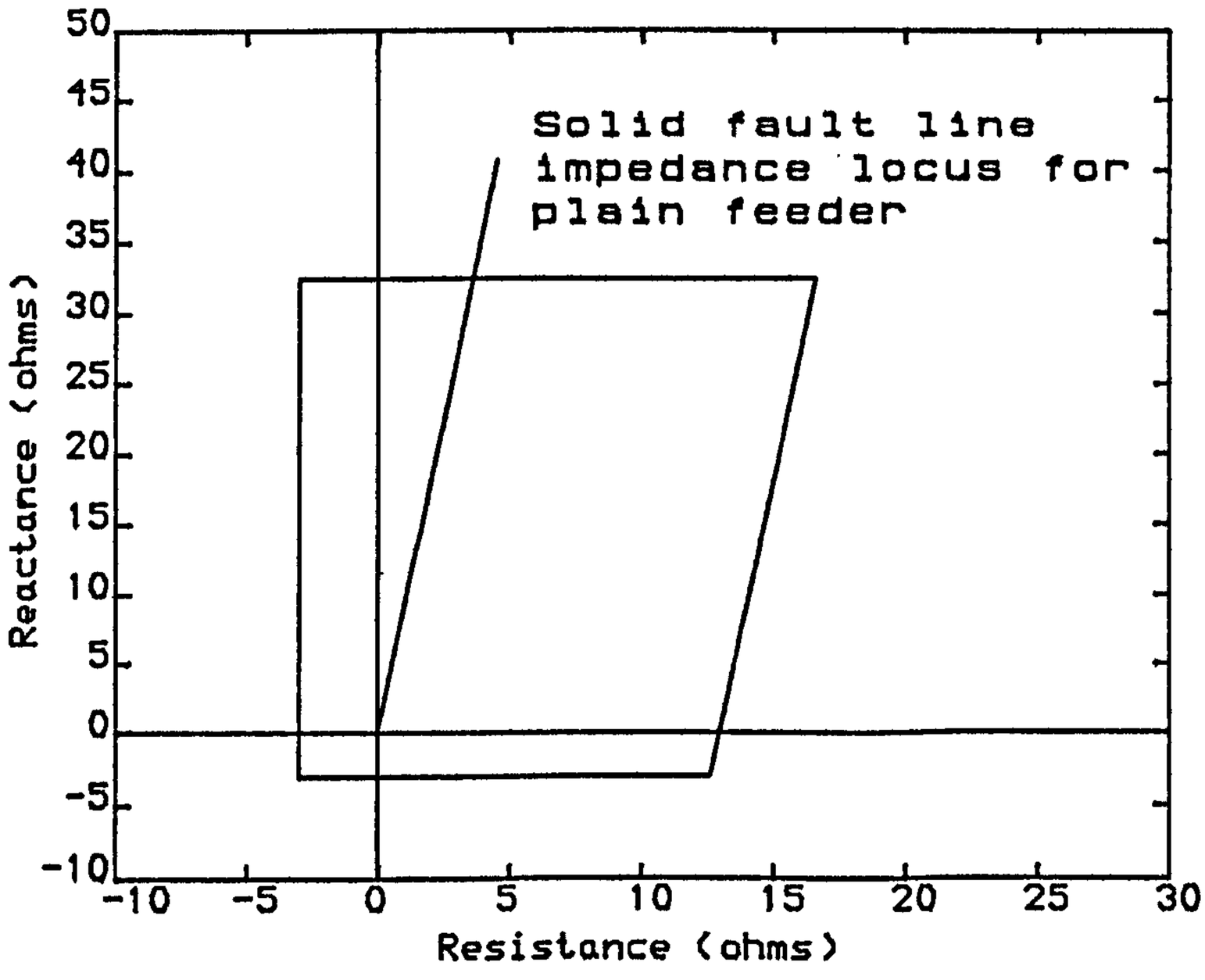

Fig 4.20-Quadrilateral Characteristic for Plain Feeder.

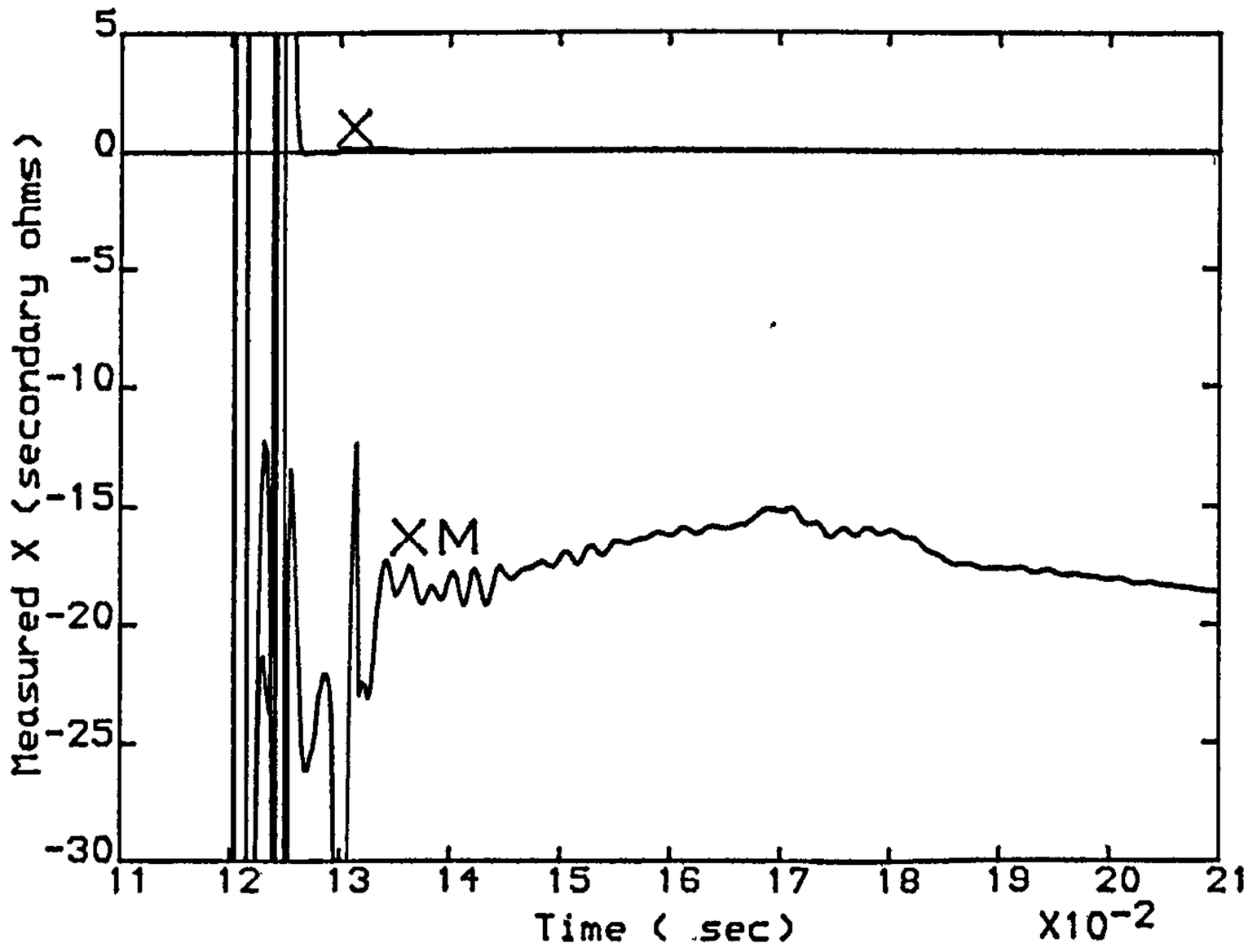

Fig 4.21-Measured XM and X for a Reverse Fault at Bus-Bar

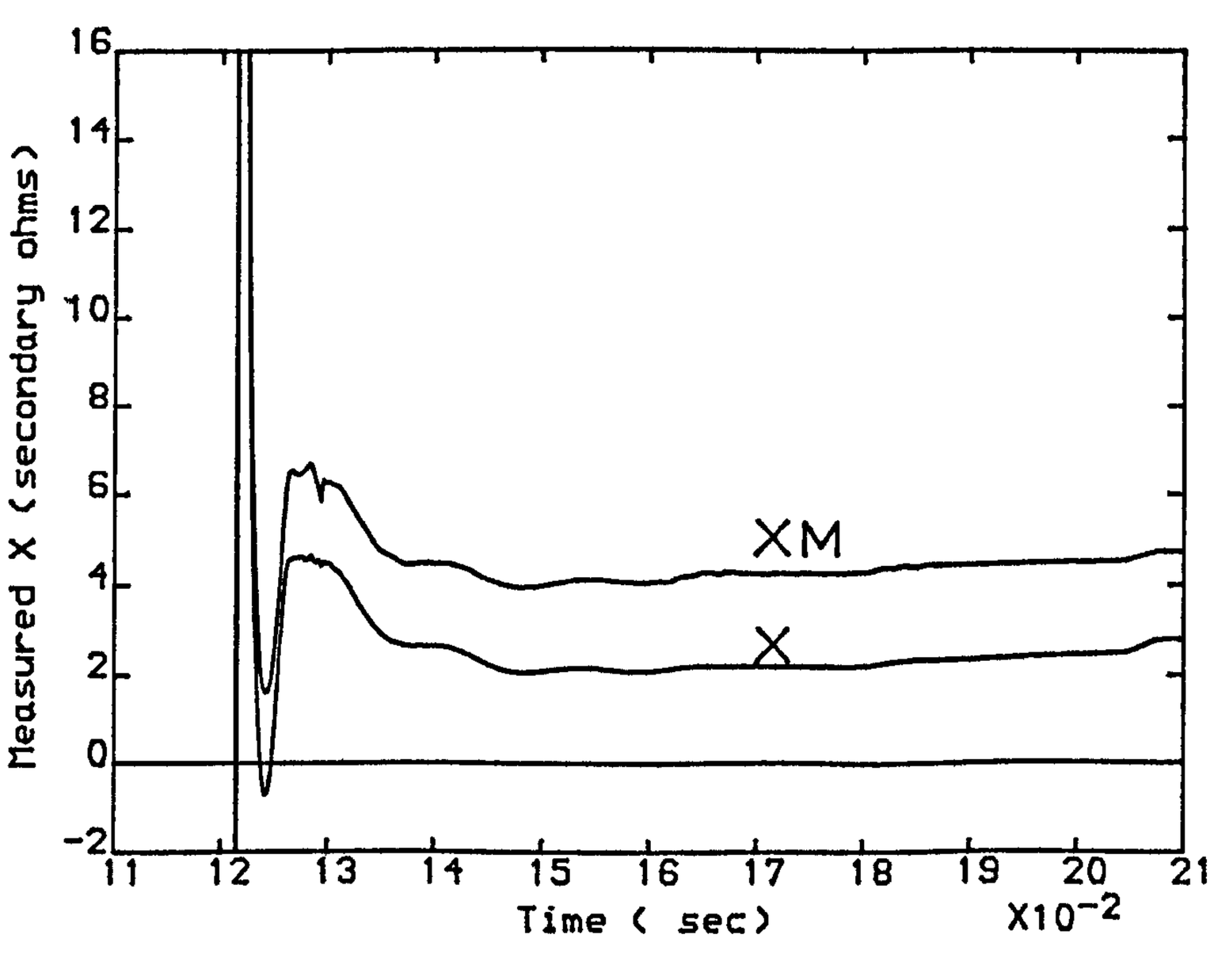

Fig 4.22-Measured XM and X for a Forward Fault at 30% of Line Length.

SE SCL=12GVA, RE SCL=27 GVA, LINE LENGTH=300 km, 70% Series Compensation.

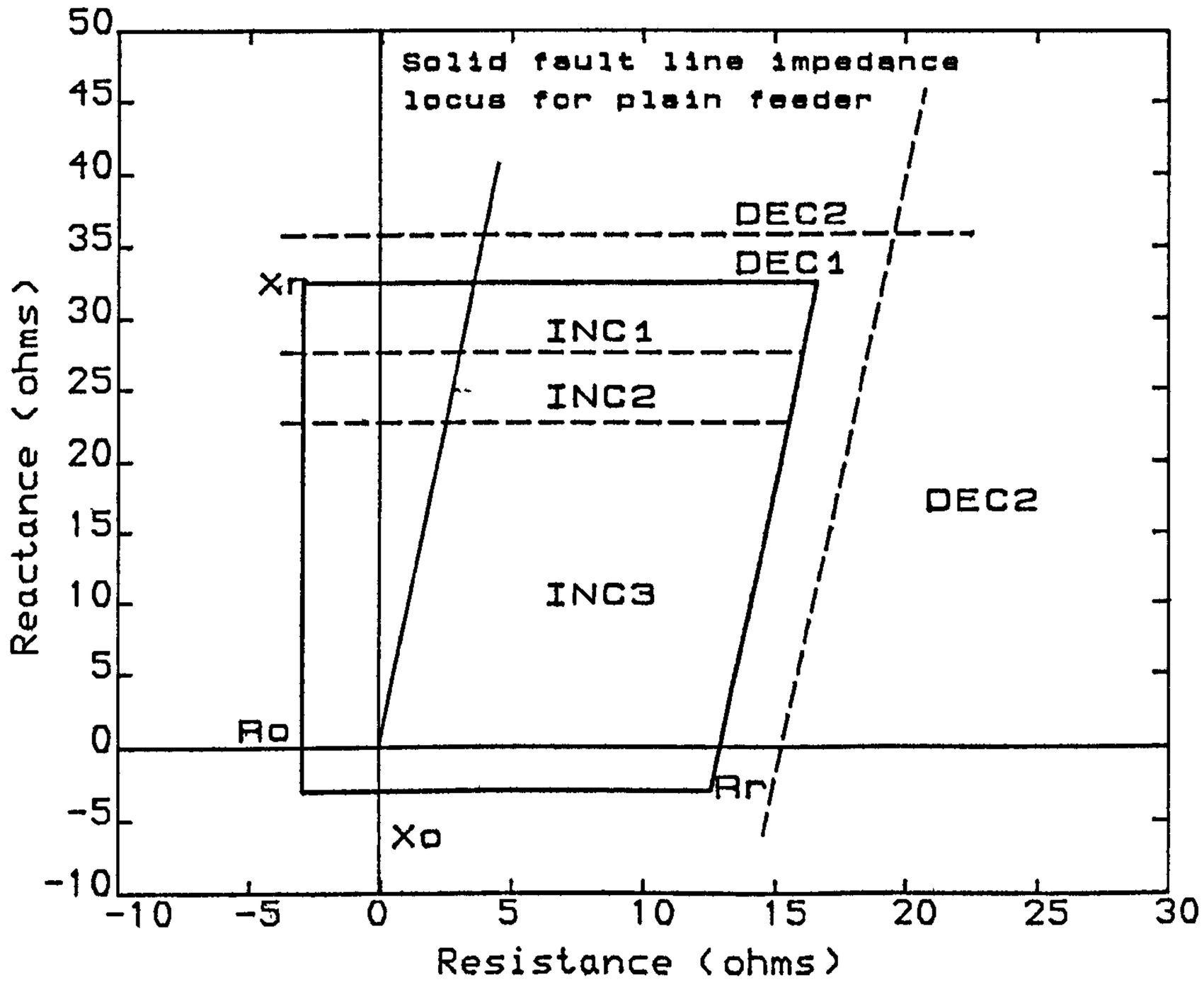

Fig 4.23-Typical Relay Boundary with Different Counting Regions.

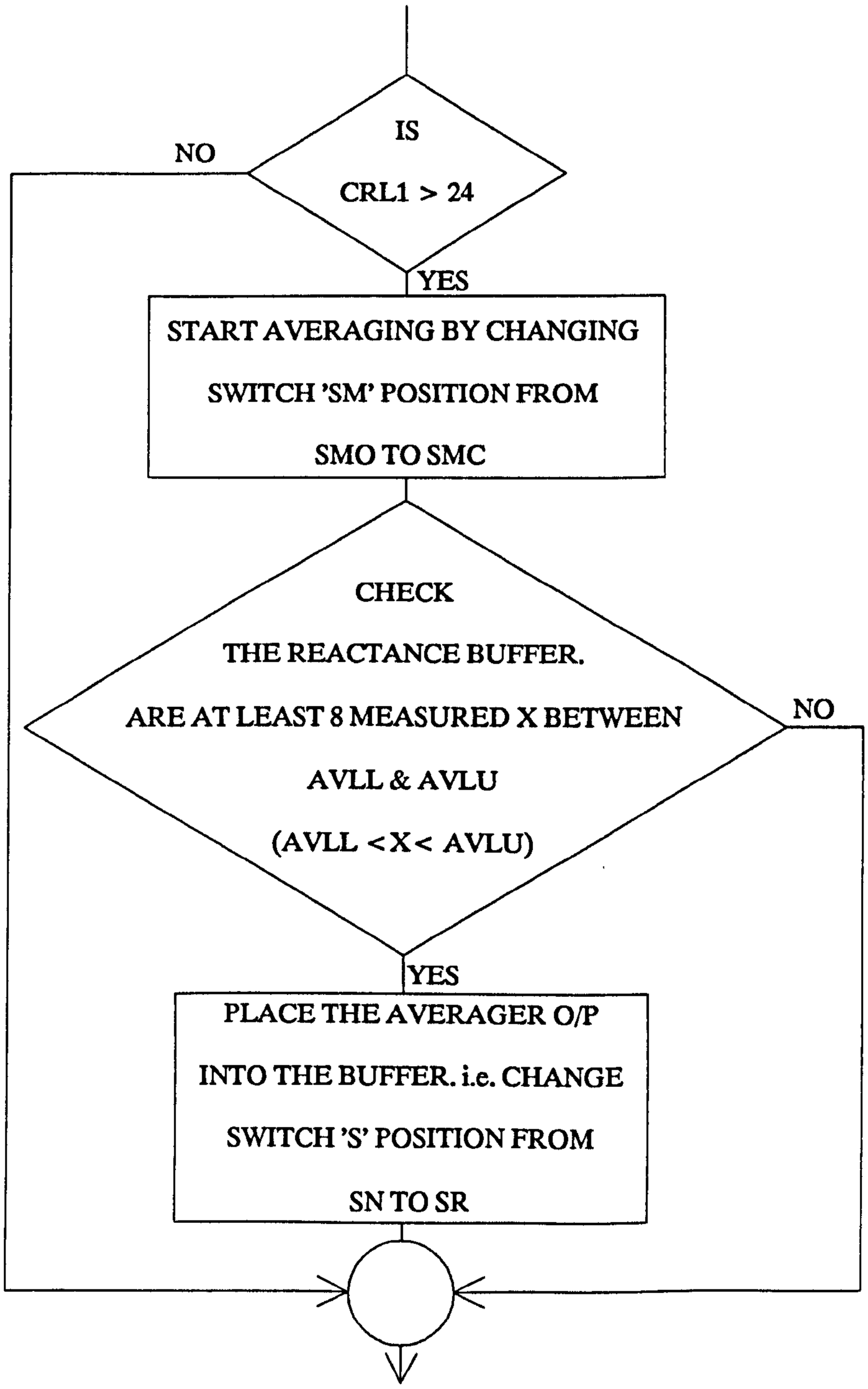

Fig 4.24-Flow Chart for Applying the Recursive Averager.

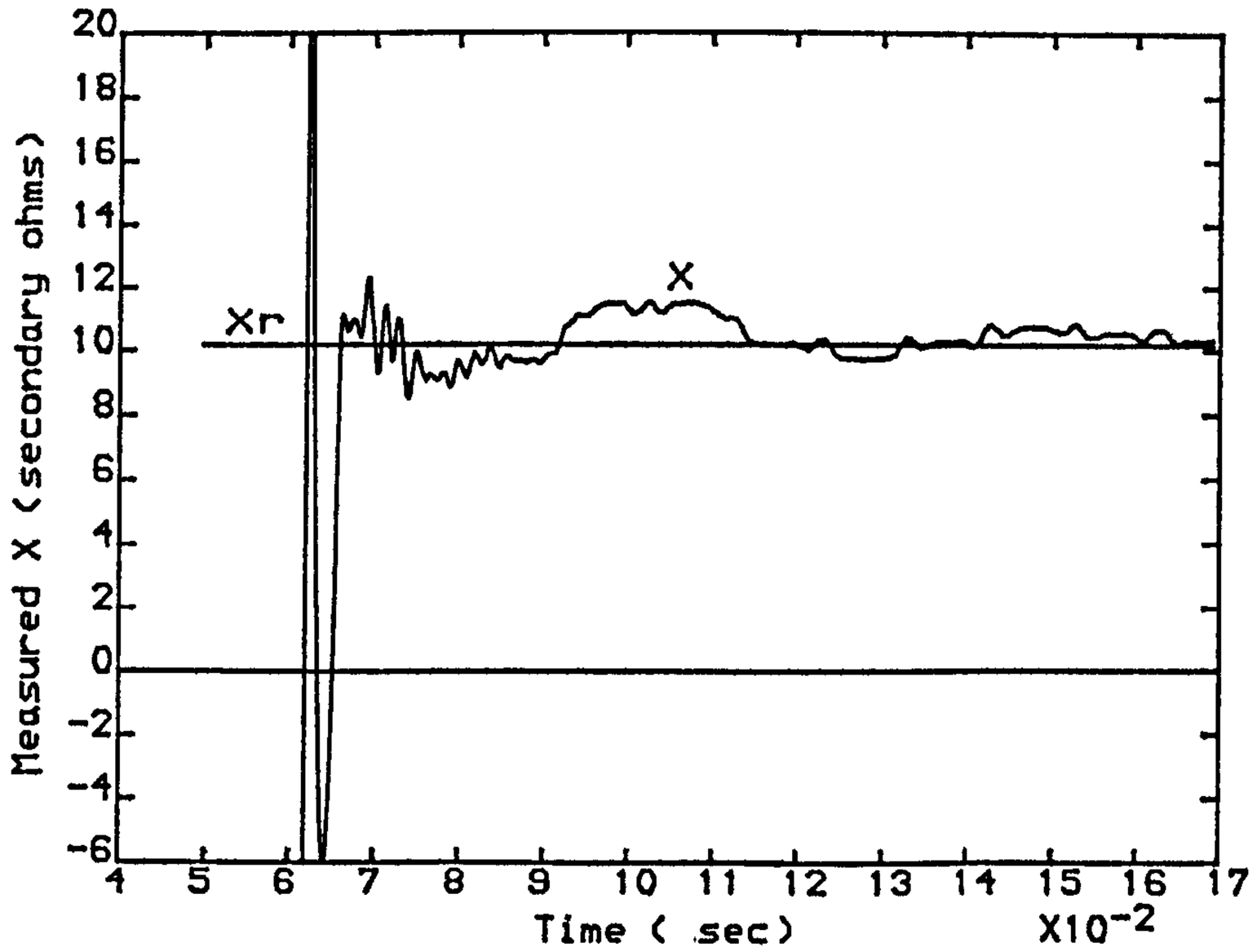

Fig 4.25.a-Measured Reactance for a Boundary Fault (Fault at Forward Reach) without Invoking the Averager.

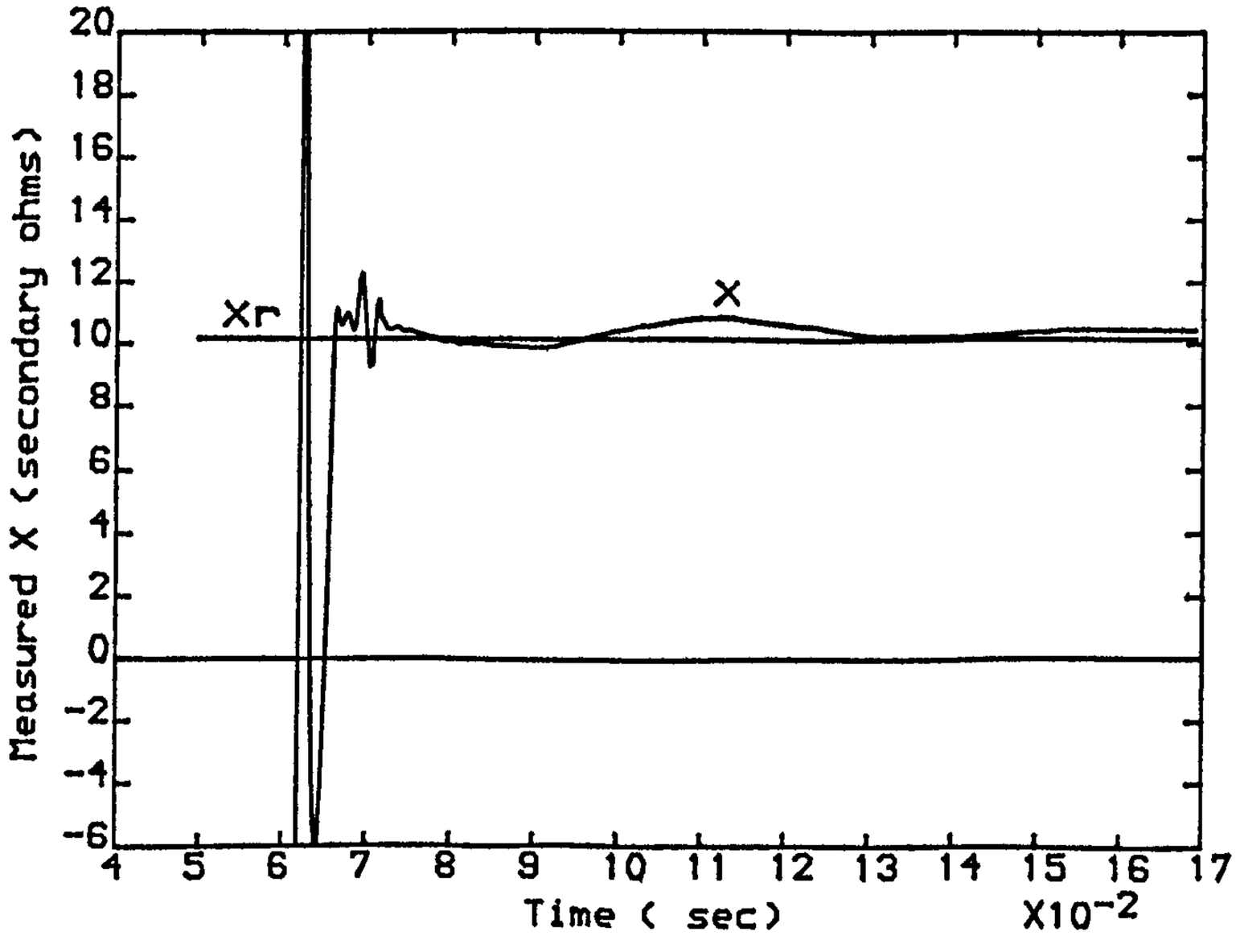

Fig 4.25.b-Measured Reactance for a Boundary Fault (Fault at Forward Reach) with Invoked Averager.

SE SCL=5GVA, RE SCL=35 GVA, LINE LENGTH=300 km.

CHAPTER 5

EARTH FAULT COMPENSATION OF THE DIGITAL DISTANCE RELAY

The principle on which all distance relaying schemes are based is that the impedance of the circuit between the relaying point and the fault is proportional to the distance between them (the impedance per unit length of line is constant, hence the line impedance is proportional to its length).

The distance relays are arranged to measure distance in terms of the positive-sequence quantities for all types of faults, assuming a fully transposed and balanced system [52].

When an "a" phase to ground fault occurs on a transmission system the phase-sequence components of currents in the fault are equal ($I_1=I_2=I_0$). This relationship will also hold for the phase-sequence components of currents in the line, when this constitutes the sole path to the fault.

If, however, there are a number of paths to the fault, as can occur when the system interconnects a number of sources or when the system is multiple earthed, or when both these conditions exist, the relationship $I_1=I_2=I_0$ no longer holds for the line currents although it, of course, still holds for the current in the fault.

Compensation methods are employed to make the relay measure the positive phase sequence impedance of the fault loop, which in turn makes it possible to specify a pre-determined characteristic for the relay. An un-compensated relay no longer measures a unique impedance

for any given fault position, the impedance seen by the relay depending on the number of sources and the number of earth neutrals available at the time. On the other hand however, a compensated relay will, when applied to a plain feeder, measure a unique impedance for any given fault position regardless of source and neutral current return paths [52].

The compensated methods which are used for earth fault distance relays are [52, 53, 54]:

(i) Residual current compensation.

(ii) Sound phase current compensation.

Method (i) involves the addition of a fraction of the residual (neutral) current to the phase currents and method (ii) makes the use of, as the name implies, the sound phase currents and addition to the faulted phase current in order to make the relay measure a unique impedance for any given fault position irrespective of the system condition. The voltage signal used in both methods is the phase to ground voltage.

In a plain uncompensated system the measured impedances by the relay, when methods (i) and (ii) are used, are given by:

(i)

$$Z=\frac{V_{sae}}{I_{sa}+K_c I_{res}}=\alpha Z_{L1} \qquad 5.1$$

where:

Z=measured impedance

V_{sae}=phase voltage at relay point

I_{sa}=faulted phase current at relay point

I_{res}=residual current

Z_{L1}=total pps impedance of line

Z_{L0}=total zps impedance of line

α=proportional fault position

K_C=conventional residual compensation factor

$$= \frac{1}{3}\left(\left|\frac{Z_{L0}}{Z_{L1}}\right| - 1\right) \qquad 5.2$$

and (ii):

$$Z=\frac{V_{sae}}{I_{sa}+K_s(I_{sb}+I_{sc})}= \alpha Z_{LS} \qquad 5.3$$

where:

I_{sb}, I_{sc}=sound phase currents (phase b and c)

K_s=the sound phase compensation factor

$$=\left|\frac{Z_{LM}}{Z_{LS}}\right| \qquad 5.4$$

Z_{LM}=mutual impedance of the line

$=1/3(Z_{L0}-Z_{L1})$

Z_{LS}=self impedance of the line

$=1/3(Z_{L0}+2Z_{L1})$

Note that the compensation factors are assumed to be real.

Errors in distance relay measurement when the above compensation methods are used have been reported by several authors [55, 56]. It will be shown in this chapter that, if any of the above methods, as they stand, are used in distance protection of the series compensated lines, there will be errors in the relay measurements of the fault loop impedance, as long as the capacitors remain in the circuit.

In order to analyse the errors associated with conventional current compensation, three general series compensated line configurations are considered.

(i) 70% total series compensation where %35 is installed at each end, with the voltage transducer located on the bus-bar side of the series capacitor.

(ii) 70% total series compensation with 35% at each end and the voltage transducer on the line side of the series capacitor.

(iii) capacitor location at the mid-point of the line with 50% compensation.

5.1-System with 70% Compensation and the C.V.T. on the Bus-Bar Side of the Relay

Consider Figure 5.1 which shows a typical series compensated line with 70% compensation (35% at each end). The voltage signal for the relay is assumed to be taken from the bus-bar side of the capacitor and sources are represented by a simple generator.

5.1.1-residual current compensation

Appendix 5A shows that when an "a" phase-earth fault occurs on a series capacitor compensated transmission line and the conventional residual compensation factor is used, the impedance measured by the relay is given by:

$$Z=\frac{V_{sae}}{I_{sa}+K_C I_{res}}=\alpha Z_{L1}-j\left(\frac{I_{sa}}{I_{sa}+K_C I_{res}}\right)X_C/2 \qquad 5.5$$

where:

X_C=total capacitor reactance/phase

K_C=conventional residual compensation factor

$$=\frac{1}{3}\left(\left|\frac{Z_{L0}}{Z_{L1}}\right|-1\right) \qquad 5.2$$

=0.774 (for the line under study)

Equation 5.5 shows that if the conventional residual compensation factor, **CRCF**, is used the impedance measured by the relay depends on the expression $I_{sa}/(I_{sa}+K_cI_{res})$. The response of the relay can be analysed by studying the behaviour of the expression $I_{sa}/(I_{sa}+K_cI_{res})$ for different system conditions.

Figures 5.2, 5.3 and 5.4 illustrate the behaviour of the expression $I_{sa}/(I_{sa}+K_cI_{res})$ with respect to the fault position along the line and the receiving end bus-bar, for pre-fault system load angles of -10°, 0° and +10° respectively. It must be noted that the load angles represent the pre-fault phase angle between the sending and receiving end voltages, the latter being the reference voltage vector. Hence a negative phase angle represents power being imported to the bus-bar and a positive load angle implies an exporting power from the relaying terminals.

It is clear from the Figures that the ratio varies with the system source and pre-fault load situations. Thus the measured impedance is affected.

Considering different system short circuit levels, Figures 5.5.a, 5.5.b and 5.5.c show the measured resistance versus pre-fault load angle for different fault position. Figures 5.6.a, 5.6.b and 5.6.c illustrate the corresponding measured reactance. It is clearly evident that the measured impedance is affected by the system pre-fault load. The source impedance affects the residual current distribution which in turn affects the relay

measurement. The resistance measurement in particular is affected more by the load current than is the reactance.

Figures 5.7.a, 5.7.b and 5.7.c illustrate the variation in measured resistance with fault position, for different load angles. Figures 5.8.a, 5.8.b and 5.8.c show the corresponding measured reactance. Note that, if the conventional residual compensation factor is used, a distance relay may significantly under-reach if the reactance reach is set at a value corresponding to the equivalent fault loop reactance.

5.1.2-complex residual compensation factor

When calculating the residual compensation factor it is common to assume that the zero and positive phase sequence impedances of the protected line have the same phase angle ($\angle Z_{L0}=\angle Z_{L1}$). Therefore, the residual compensation factor will be a real number.

However digital distance relays are particularly suited to the implementation of a complex, rather than real, residual compensation factor. Since samples of the residual current are available at discrete instants of time $T=1/f_s$ (where f_s is the digital sampling frequency) it is possible to effectively implement the phase shift associated with the residual compensating factor $\angle K_C$ ($\angle Z_{L0}\neq\angle Z_{L1}$) by taking a sample n samples previous to any measuring sample instant and multiplying it by the magnitude of the compensation factor. For example, K_C is calculated to be equal to approximately $0.782\angle -14.82^{\circ}$. Thus, in a digital relay operating at a sampling frequency of 4 kHz, on a power system having a nominal frequency of 50 Hz, one sample interval corresponds to a phase shift of

4.5°. A constraint is thus imposed on choosing the value of n which, for the assumed sampling frequency (4 kHz) and application illustrated, is equal to 3 which in turn corresponds to -13.5°. For any particular relay and application, the value of n that gives the closest equivalent phase shift to the ideal value is used.

Figures 5.9.a, 5.9.b and 5.9.c show the measured resistance versus fault position for different pre-fault load. Figures 5.10.a, 5.10.b and 5.10.c illustrate the corresponding measured reactance. It can be seen that the variation in measured resistance and reactance with respect to the system pre-fault load and source has been reduced, but the relay still under-reaches.

The foregoing analysis illustrates that if conventional residual compensation is used, the relay measurement will not be accurate and the relay may maloperate .

5.1.3-sound phase current compensation

Appendix 5B shows that if conventional sound phase current compensation is used, the impedance measured by the relay is given by:

$$Z=\frac{V_{sae}}{I_{sa}+K_s(I_{sb}+I_{sc})}=\alpha Z_{LS}-j\left(\frac{I_{sa}}{I_{sa}+K_s(I_{sb}+I_{sc})}\right)X_C/2 \qquad 5.6$$

where: $K_s=\frac{Z_{LM}}{Z_{LS}}$

$=0.442\angle -8.32^\circ$ (for the line under study)

It is clear, from Equation 5.6 that, if conventional sound phase current compensation is used the impedance

measured is affected by the expression $I_{sa}/(I_{sa}+K_s(I_{sb}+I_{sc}))$.

Figures 5.11 and 5.12 show the measured resistance and reactance respectively, when conventional sound phase compensation is used. It can be seen that both measurands are affected by the expression $I_{sa}/(I_{sa}+K_s(I_{sb}+I_{sc}))$. The relay may significantly over-reach or under-reach due to errors in reactance measurement which are caused mainly by system source impedances. Pre-fault load current does not, to any significant, affect the measurement. It must be noted that for faults at the receiving end bus-bar (beyond the remote end capacitor), the relay measures a smaller reactance than the actual line reactance which implies that the setting of the forward reactance reach is even more restricted (see the next chapter).

The method which is commonly used in distance protection schemes is residual compensation, and since neither method has any advantage over the other when used in series compensated lines, it was decided to use the modified version of the residual current compensation. This is described in the next section.

5.1.4-compensation of errors due to the residual current compensation factor

It was shown in Section 5.1.1 that if the conventional residual compensation factor **(CRCF)** is used, the measured impedance by the relay will not be accurate.

In order to ensure that the relay does not maloperate and discriminates correctly between internal and external faults, three methods may be considered:

(i) one may assume that the currents in the healthy phases are much smaller than the faulted phase

current so that, for faults on phase "a", the following relationships may be considered:

$I_{sa} >> I_{sb}$ and I_{sc}

therefore: $I_{sa} \approx I_{res}$

thus Equation 5.5 can be written as:

$$Z = \frac{V_{sae}}{I_{sa}+K_c I_{res}} = \alpha Z_{L1} - j \left(\frac{1}{1+K_c}\right) X_c/2 \qquad 5.7$$

Hence the zone-1 forward reactance reach can be set at:

$$\alpha r X_{L1} - \left(\frac{1}{1+K_c}\right) X_c/2 \qquad 5.8$$

where: X_{L1}=total pps reactance of the line

αr=fault position for a fault at the zone-1 relay reach.

However it has been shown in Section 5.1.1 that the expression $I_{sa}/(I_{sa}+K_c I_{res})$ cannot be considered as a constant and varies with the system condition, and that the measured impedance is not unique for a given fault position.

(ii) to modify the residual compensation factor so that the relay measures the equivalent fault loop impedance, $\alpha Z_{L1} - j\, X_c/2$.

(iii) to modify the relaying signal so that the relay measures the fault loop line impedance, αZ_{L1}.

5.1.5-modified residual compensation factor

Appendix 5C shows that in order to ensure that the relay measures the equivalent pps impedance of the line from the relay to fault point (for relay setting

purposes), the residual compensation factor must be set according to the proportional fault position, α. The measured impedance for a fault on the line is then given by:

$$Z=\frac{V_{sae}}{I_{sa}+K_{(\alpha)}I_{res}}=\alpha Z_{L1}-j\ X_C/2 \qquad 5.9$$

$$\text{where:}\quad K_{(\alpha)}=\frac{1}{3}\left(\frac{\alpha Z_{L0}-j\ X_C/2}{\alpha Z_{L1}-j\ X_C/2}-1\right) \qquad 5.10$$

and for a fault on the receiving end bus-bar:

$$Z=\frac{V_{sae}}{I_{sa}+K_{(\alpha)}I_{res}}=\alpha Z_{L1}-j\ X_C \qquad 5.11$$

$$\text{where:}\quad K_{(\alpha)}=\frac{1}{3}\left(\frac{\alpha Z_{L0}-j\ X_C}{\alpha Z_{L1}-j\ X_C}-1\right) \qquad 5.12$$

This means that only if the fault position is known to the relay will the measured value of impedance be independant of source and pre-fault load current.

Figures 5.13.a and 5.13.b show the variation in magnitude and argument of $K_{(\alpha)}$ versus fault location for the line under study. It must be noted that for a given fault location and degree of series compensation, the residual compensation factor is the same as that shown in Figure 5.13.a and 5.13.b irrespective of the line length. Also, it can be shown that the magnitude of $K_{(\alpha)}$ has a peak which always occurs at 35% of the line length.

It is clear that with the present generation of digital equipment and Ultra-High-Speed operation in mind, it is not possible to set the residual compensation factor

according to the fault position, since the location of the fault is unknown to the relay.

Therefore it is proposed that the residual compensation factor is set at a fixed value $K_{\alpha r}$, assuming the fault position to be at the relay zone-1 reach boundary, where the relay is required to be most accurate.

The procedure of calculating the residual compensation factor is as follows:

1-decide about the relay zone-1 reach. Say it is set at 60% of line length.

2-look on graph of $K_{(\alpha)}$ vs fault location, Figures 5.13.a and 5.13.b, to find corresponding magnitude and argument of $K_{(\alpha)}$ for α=0.6.

Appendix 5D shows that the impedance seen by the distance relay for faults on the line is then given by:

$$Z=\frac{V_{sae}}{I_{sa}+K_{\alpha r}I_{res}}=\frac{I_{sa}+K_{(\alpha)}I_{res}}{I_{sa}+K_{\alpha r}I_{res}}\ (\alpha Z_{L1}-j\ X_C) \qquad 5.13$$

where:

$K_{\alpha r}$=the residual compensation factor for fault at the zone-1

$$K_{\alpha r}=\frac{1}{3}\left(\frac{\alpha r Z_{L0}-jX_C/2}{\alpha r Z_{L1}-jX_C/2}-1\right) \qquad 5.14$$

αr=proportional fault position for fault at the relay zone-1 reach point.

Figures 5.14.a and 5.14.b illustrate the variation in the magnitude and argument of the expression $(I_{sa}+K_{(\alpha)}I_{res})/(I_{sa}+K_{\alpha r}I_{res})$ with fault position for pre-fault load angle of -10 degrees, for the relay zone-1

setting of 60% (αr=0.6). Figures 5.15.a, b and 5.16.a, b show the corresponding graphs for pre-fault load angle of 0 and +10 degrees respectively.

It is clear that for a fault at the relay zone-1 boundary the expression has a magnitude of unity and argument of zero $(I_{sa}+K_{(\alpha)}I_{res})=(I_{sa}+K_{\alpha r}I_{res})$, which implies that the relay measurement is accurate at this point only. It has been shown in Section 5.1.2 that a complex residual compensation factor can be implemented in a digital distance relay. It can be seen from Figure 5.13.a and b that, for a relay set with a forward reach of 60%, which in turn eliminates the possibility of indiscrimination for faults beyond the remote capacitor (see the next chapter), the new residual compensation factor $K_{\alpha r}$ is equal to approximately $1.82\angle-6.2^{\circ}$. A phase shift of -4.5° (f_s=4 kHz) is obtained by taking the first previous sample of the residual current. Hence the residual compensation factor which is used in the relay is $K_{\alpha r}=1.82\angle-4.5^{\circ}$.

Figure 5.17.a, b and c illustrate the variation in measured resistance vs system pre-fault load for different source configurations. Figures 5.18.a, b and c show the corresponding reactance measurement. It is clear that the measurement at the boundary (60%) are unaffected by the pre-fault load. Furthermore variations in reactance measurements with load for other fault positions, especially those near the boundary, are minimal. This in turn enables measuring accuracy to be maximised and avoids both relay overreaching or underreaching.

Figures 19 and 20 show the measured resistance and

reactance vs fault position for different source short circuit levels. The pps resistance and reactance of the fault loop are also shown. Again the effect of the new residual compensation factor **NRCF** on the measurement is clear. In particular, note the constant and load invariant measurement at the boundary (60%) for different load currents. Note also that, the measured reactance for faults at the receiving end bus-bar is larger than the actual line reactance. This is due to the fact that the relay is under-compensated (less current is given to the relay, $1.82\angle -4.5^{\circ}$ instead of $2.45\angle 0.0^{\circ}$), hence measuring a larger value. This effect is one of the advantages of the NRCF method since a bigger margin exists between the measured reactance for receiving end faults and faults at the relay forward reactance reach.

The modified residual compensation factor NRCF provides a better representation of the primary system. Figure 5.21.a shows the measured reactance when the conventional residual compensation factor is used and Figure 5.21.b when the NRCF is employed. It is clear that the travelling wave effect and the sub-synchronous oscillation have been greatly reduced.

5.1.6-modification of the relaying signal

It was shown in Section 5.1.1 that if the conventional residual compensation factor is used, the measured impedance is given by:

$$Z=\frac{V_{sae}}{I_{sa}+K_c I_{res}}=\alpha Z_{L1} -j \left(\frac{I_{sa}}{I_{sa}+K_c I_{res}}\right) X_C/2 \qquad 5.5$$

It is possible to modify the relaying voltage signal

so that the relay measures the fault loop line impedance, αZ_{L1}.

If it is assumed that the capacitor's protective gaps do not operate and they remain in the circuit, the relaying voltage V_{sae} can be compensated by adding a component $jI_{sa}X_C/2$ to it, which in turn eliminates the term $-j(\frac{I_{sa}}{I_{sa}+K_CI_{res}})X_C/2$ from the measured impedance.

This method involves phase shifting the phase current by 90° (represented by j) and multiplying it by the local capacitor reactance which is known. The measured impedance is then given by:

$$Z=\frac{V_{sae}+jI_{sa}X_C/2}{I_{sa}+K_CI_{res}}=\frac{V_{sae}}{I_{sa}+K_CI_{res}} + j(\frac{I_{sa}}{I_{sa}+K_CI_{res}})X_C/2= \alpha Z_{L1} \qquad 5.15$$

Thus, the relay zone-1 forward reach can be set according to the pps impedance of the line only, ignoring the effect of the series capacitor.

It must be noted that the compensation signal $jI_{sa}X_C/2$ is obtained assuming the capacitor reactance at the system frequency.

Figure 5.22.a, b and c illustrate the steady state measurement of the resistance vs fault position for different system pre-fault loading, when a complex K_C is used. Figure 5.23.a, b and c show the corresponding reactance measurement. It can be seen that the relay measurenment, in particular the measured reactance is very accurate for faults on the line.

However, the measurement for a fault at the receiving end bus-bar is not accurate. This is due to the fact that

for such a fault two capacitors are in the circuit (provided neither are by-passed by the gap flash over).

The measured impedance by the relay for this situation is given by:

$$Z=\frac{V_{sae}+jI_{sa}X_C/2}{I_{sa}+K_cI_{res}}=\alpha Z_{L1}-j\left(\frac{I_{sa}}{I_{sa}+K_cI_{res}}\right)X_C/2 \qquad 5.16$$

5.1.7-comments on the compensation methods explained in Section 5.1.5 and 5.1.6

The two methods explained earlier are meant to enhance the accuracy of the digital distance relay measurement. It has been shown that in the latter method the measurement is accurate for all faults on the line up to the remote end bus-bar, whereas the former method makes the relay measurement accurate at only one point, the zone-1 forward reach; for other faults the measurement may be smaller or larger than the actual line impedance.

Figure 5.24.a shows the measured R and X when the NRCF is used for a fault at 50% of the line length and fault inception angle of 90°. Figure 5.24.b illustrates the corresponding measurements when CRCF (complex) and voltage compensation is used.

Figur 5.25 and 5.26 illustrate the corresponding measurement for a fault position of 60% (assumed forward reach) and fault inception angle of 90 and 0 degree.

It can be seen from these typical relay measurements that the NRCF gives a better transient response and has an inherent ability to reduce the travelling wave and sub-synchronous oscillation for faults near the forward reach, hence imposing less pressure on the relay decision logic

and the Recursive Averager (see Chapter 4).

Furthermore, as previously mentioned, in the voltage compensation method the faulted phase current must be phase shifted (displaced) by 90°. The method adopted in this study is to differentiate the current which in turn introduces a 90° phase displacement. Due to the reasons previously explained in Chapter 3, the differentiation is carried out over 9 samples which introduces an extra delay into the impedance measurement process. This is clearly evident from Figures 5.24, 5.25 and 5.26, where the relay reaches the post-fault measurement faster, when the NRCF is used.

5.2-System with 70% Compensation and the C.V.T. on the Line Side of the Relay

Consider Figure 5.27 when the voltage transformer is situated on the line side of the relay and the current transformer on the bus-bar side of the relay. This is a typical arrangment which effectively makes the local capacitor part of the source.

Appendix 5E shows that the conventional residual compensation factor, CRCF, must be used in the relay. The measured impedance for faults on the line is given by:

$$Z=\frac{V_{sae}}{I_{sa}+K_c I_{res}}=\alpha Z_{L1} \qquad 5.17$$

If the fault position is on the receiving end bus-bar, it is clear that the measurement is not accurate. The measured impedance by the relay for a fault at the receiving end bus-bar is given by Equation 5.5, $X_C/2$ being the remote end capacitor reactance.

Figures 5.28.a, b and c illustrate the measured reactance versus fault position for different system source and pre-fault load when a real residual compensation factor is used (K_C=0.774). It is clearly evident that the measurement varies with both the pre-fault load and source, which affects the residual current distribution in the system. The relay may, in this situation, over-reach or under-reach.

Figures 5.29.a, b and c show the corresponding measurement when a complex residual compensation factor is used (K_C=0.78$\angle$-13.5°). The measured reactance is more accurate and unaffected by the system condition.

5.3-System with 50% Compensation at the Mid-Point of the Line

Consider the system shown in Figure 5.30 with the series capacitor situated at the mid-point. The compensation at the mid-point may be less than 50% which is considered to be less troublesome to the protection gear. The mid-point compensation of more than 50% is extremely rare.

Using a similar analysis as that given in Appendices 5E and 5A, for faults before and beyond the series capacitor, it can be shown that, if the conventional residual compensation factor is used, the impedance measured by the relay for an "a" phase-ground fault, before and after the series capacitor are given by:

$$Z=\frac{V_{sae}}{I_{sa}+K_C I_{res}} = \alpha Z_{L1} \qquad \text{for } \alpha<0.5 \qquad 5.18$$

$$Z=\frac{V_{sae}}{I_{sa}+K_C I_{res}} = \alpha Z_{L1} - j\left(\frac{I_{sa}}{I_{sa}+K_C I_{res}}\right)X_C \quad \text{for } \alpha>0.5 \qquad 5.19$$

where:

K_C=conventional residual compensation factor

$$= \frac{1}{3}\left(\frac{Z_{L0}}{Z_{L1}} - 1\right) \qquad 5.2$$

It is clear, from Equation 5.18 that for faults before the mid-point of the line, the relay measurement is accurate, whereas the relay measurement depends on and varies with the expression $I_{sa}/(I_{sa}+K_C I_{res})$ when the fault position is beyond the series capacitor. Figures 5.31, 5.32 and 5.33 illustrate the variation in magnitude and argument of the expression $I_{sa}/(I_{sa}+K_C I_{res})$ versus fault position for system pre-fault load angles of -10°, 0° and +10° respectively. Note that for a fault position of less than 50%, the expression has no effect on the measured impedance (see Equation 5.18). However, it is clearly evident that the current ratio varies with system pre-fault load and source, thus affecting the measured impedance for faults beyond the series capacitor.

Figures 5.34.a, 5.34.b and 5.34.c illustrate the variation with fault position of the resistance, measured for different load angles. Figures 5.35.a, 5.35.b and 5.35.c show the corresponding measured reactance. Note that, if the conventional residual compensation factor is used the relay measurement is accurate for faults before the capacitor location. In particular, note the accurate reactance measurement which does not vary with the system source and pre-fault load. The d crepancy between the measured resistance and the line locus for faults before

the capacitor location is due to the fact that the angle of the residual compensation factor cannot be accurately implemented in the relay (-13.5 instead of -14.82). However, note that the impedance measurement, for a given fault position beyond the capacitor location, varies with the system source and pre-fault load.

In order to ensure that the relay measures the correct value of pps impedance of the line from the relay to fault point (for relay setting purposes) it has been shown that in series compensated lines, the residual compensation factor must be set according to the fault position α (see Section 5.1.5). Considering a series compensated line with 50% compensation at the middle of the line, it can be shown that the impedance measured by the relay is given by:

$$Z=\frac{V_{sae}}{I_{sa}+K_{(\alpha)}I_{res}} = \alpha Z_{L1}-jX_{ce} \qquad 5.20$$

where:

$$K_{(\alpha)}=\frac{1}{3}\left(\frac{\alpha Z_{L0}-jX_{ce}}{\alpha Z_{L1}-jX_{ce}} - 1\right) \qquad 5.21$$

$X_{ce}=0$ for $\alpha<0.5$

$X_{ce}=X_c$ for $\alpha>0.5$

Figures 5.36.a and 5.36.b show the magnitude and argument of $K_{(\alpha)}$ versus fault position. It is evident that $K_{(\alpha)}$ stays at a constant value for fault positions of less than 50% of the line length (capacitor location). However note the variation in magnitude and argument of $K_{(\alpha)}$ with fault position, α, for faults beyond the series

capacitor.

It has been suggested in Section 5.1.5, that, since the relay is required to be the most accurate at and around the boundary, the residual compensation factor is set at a fixed value $K_{\alpha r}$, assuming the fault position to be at the relay zone-1 reach boundary. The measured impedance by the relay is then given by (see Section 5.1.5):

$$Z=\frac{V_{sae}}{I_{sa}+K_{\alpha r}I_{res}}=\frac{I_{sa}+K_{(\alpha)}I_{res}}{I_{sa}+K_{\alpha r}I_{res}}(\alpha Z_{L1}-jX_{ce}) \qquad 5.22$$

where:

$K_{\alpha r}$=the residual compensation factor for fault at the zone-1

$$K_{\alpha r}=\frac{1}{3}\left(\frac{\alpha r Z_{L0}-jX_{ce}}{\alpha r Z_{L1}-jX_{ce}}-1\right) \qquad 5.23$$

$X_{ce}=0$ for $\alpha<0.5$

$X_{ce}=X_C$ for $\alpha>0.5$

If the relay independant zone-1 reach is considered to be before the series capacitor, say at 45% of the line length ($\alpha r=0.45$) and a complex residual compensation factor (assuming $\angle Z_{L0}\neq\angle Z_{L1}$) is considered in the relay, the relay measures accurate impedances for all faults before the mid-point of the line. But for faults beyond the capacitor, the relay measurement will not be accurate.

If it is required to set the relay reach at a value higher than 50%, then the relay measurement is accurate only at the reach point. In this work it is decided to set the relay zone-1 reach at 80% of the line length, which is the common practice in plain uncompensated feeder

distance protection schemes. The required residual compensation factor, for a boundary setting of 80% (αr=0.8) is, from Fig 5.36.a and b, found to be approximately equal to $2.015\angle -4.6°$.

It is evident, from Equation 5.22 that the measured impedance depends on and varies with the expression $(I_{sa}+K_{(\alpha)}I_{res})/(I_{sa}+K_{\alpha r}I_{res})$. Figures 5.37, 5.38 and 5.39 illustrate the variation in the current ratio with fault position for pre-fault load angle of -10°, 0° and +10° respectively. It can be seen that the expression $(I_{sa}+K_{(\alpha)}I_{res})/(I_{sa}+K_{\alpha r}I_{res})$ has a magnitude of about 0.5 to 0.6 and an argument of between 0 to -10 degrees, depending upon the system pre-fault load and source, for faults before the capacitor location. If the current ratio is considered in the form of a+jb, then the real and imaginary part of the measured impedance for faults before the capacitor is given by:

$$Z=(a\alpha R_{L1}-b\alpha X_{L1}) + j(a\alpha X_{L1}+b\alpha R_{L1}) \qquad 5.24$$

It can be seen that the dominant term in the reactive component is $a\alpha X_{L1}$. For the system considered, a is very close to the magnitude of the current ratio, i.e. approximately 0.5 (since the argument is small), which implies that the measured reactance is approximately half the actual line reactance, for faults before the mid-point of the line.

The expression $(I_{sa}+K_{(\alpha)}I_{res})/(I_{sa}+K_{\alpha r}I_{res})$ has a magnitude of unity and an argument of zero for a fault at the relay zone-1 reach; which implies that the relay measures the equivalent fault loop impedance, $\alpha r Z_{L1}-jX_C$.

Figure 5.40.a, b and c illustrate the variation in measured resistance versus fault position for different source configration and pre-fault load. Figures 5.41.a, b and c show the corresponding reactance measurement. It is clear that the measurements at the boundary (80%) are unaffected by the pre-fault load.

Note that due to over-compensation of the relay ($2.015\angle -4.5^{\circ}$ instead of $0.78\angle -14.82^{\circ}$) the measured reactance is smaller than the actual line reactance for faults before the capacitor location. This is one of the advantages of the new modified residual compensation factor: when the the relay zone-1 reach is set at 80% of the line length then faults before the capacitor are far more likely to fall within the relay trip characteristic.

More will be said about this effect in the following Chapters.

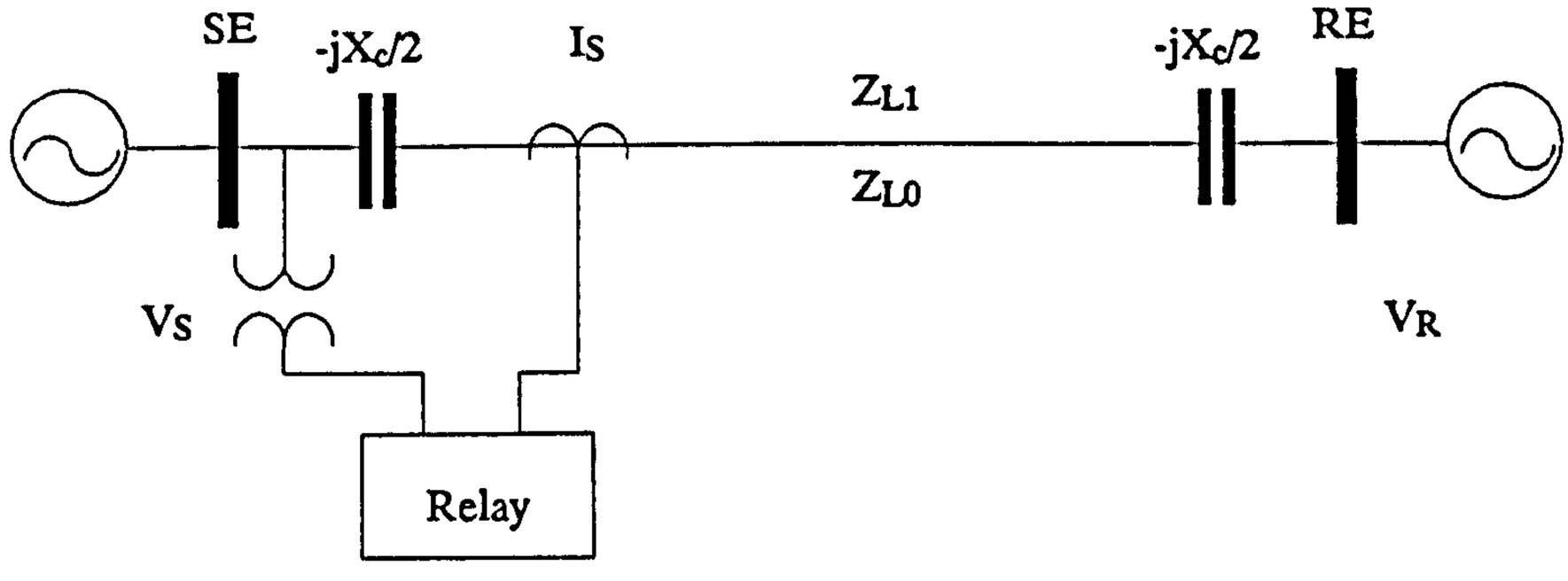

Fig 5.1-System Configuration with Source Side V.T.

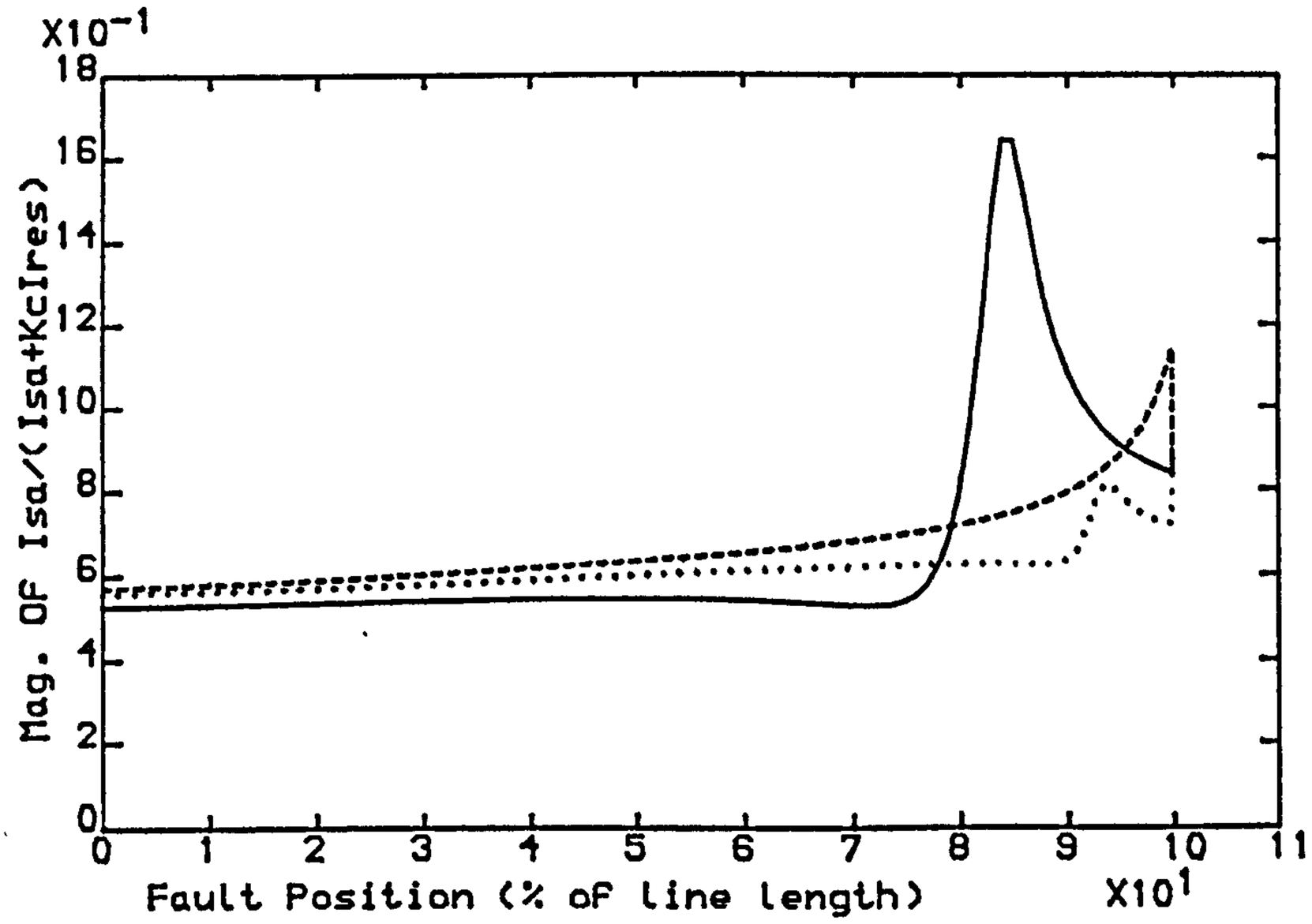

Fig 5.2.a-Variation in Mag. Of Isa/(Isa+KcIres) VS Fault Position For Pre-Fault Load Angle Of -10 Degrees

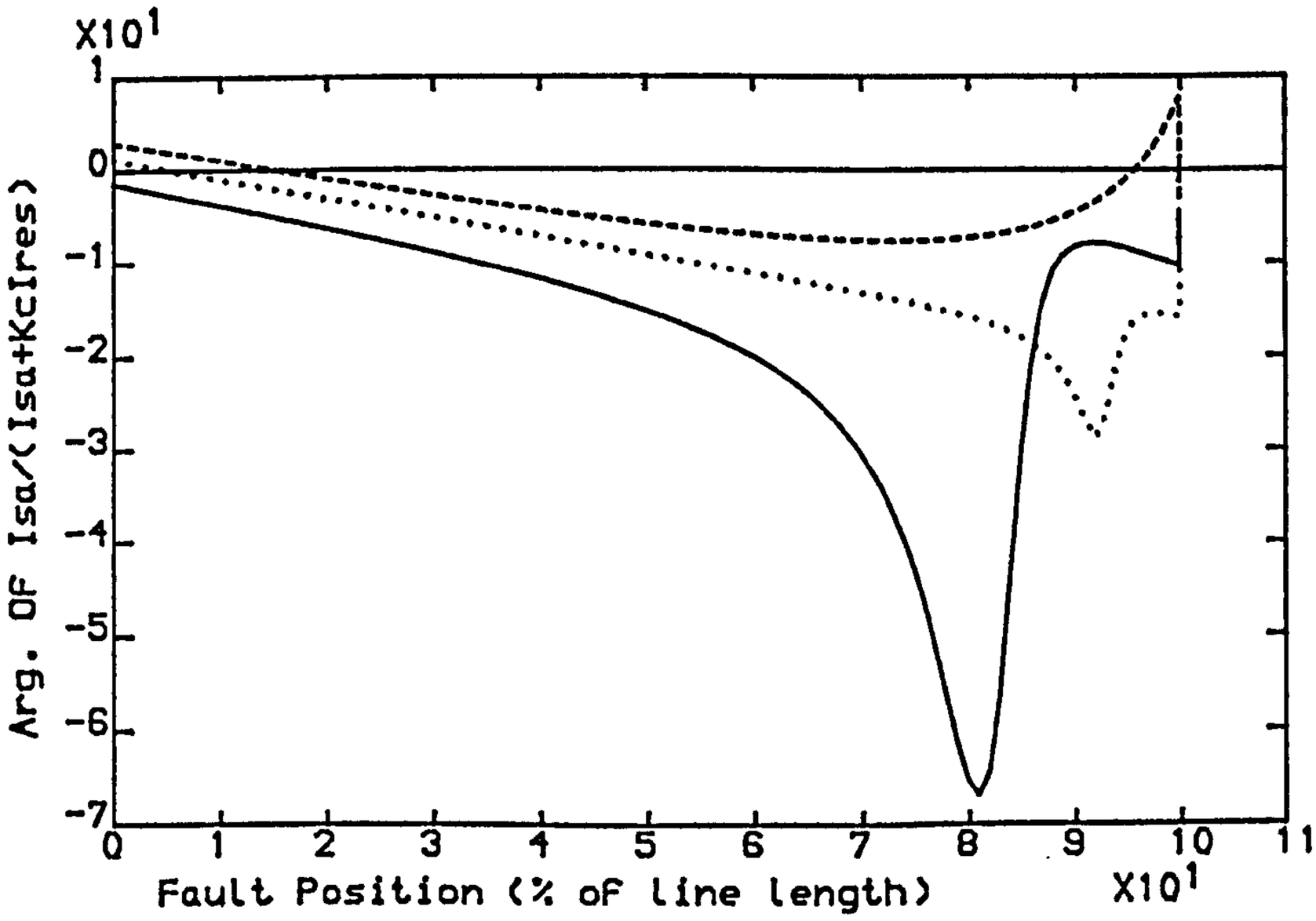

Fig 5.2.b-Variation in Arg. Of Isa/(Isa+KcIres) VS Fault Position For Pre-Fault Load Angle Of -10 Degrees

——— SE SCL-5 GVA, RE SCL-35 GVA
- - - - SE SCL-35 GVA, RE SCL-5 GVA
.... SE SCL-10 GVA, RE SCL-10 GVA
Line Length -300 km

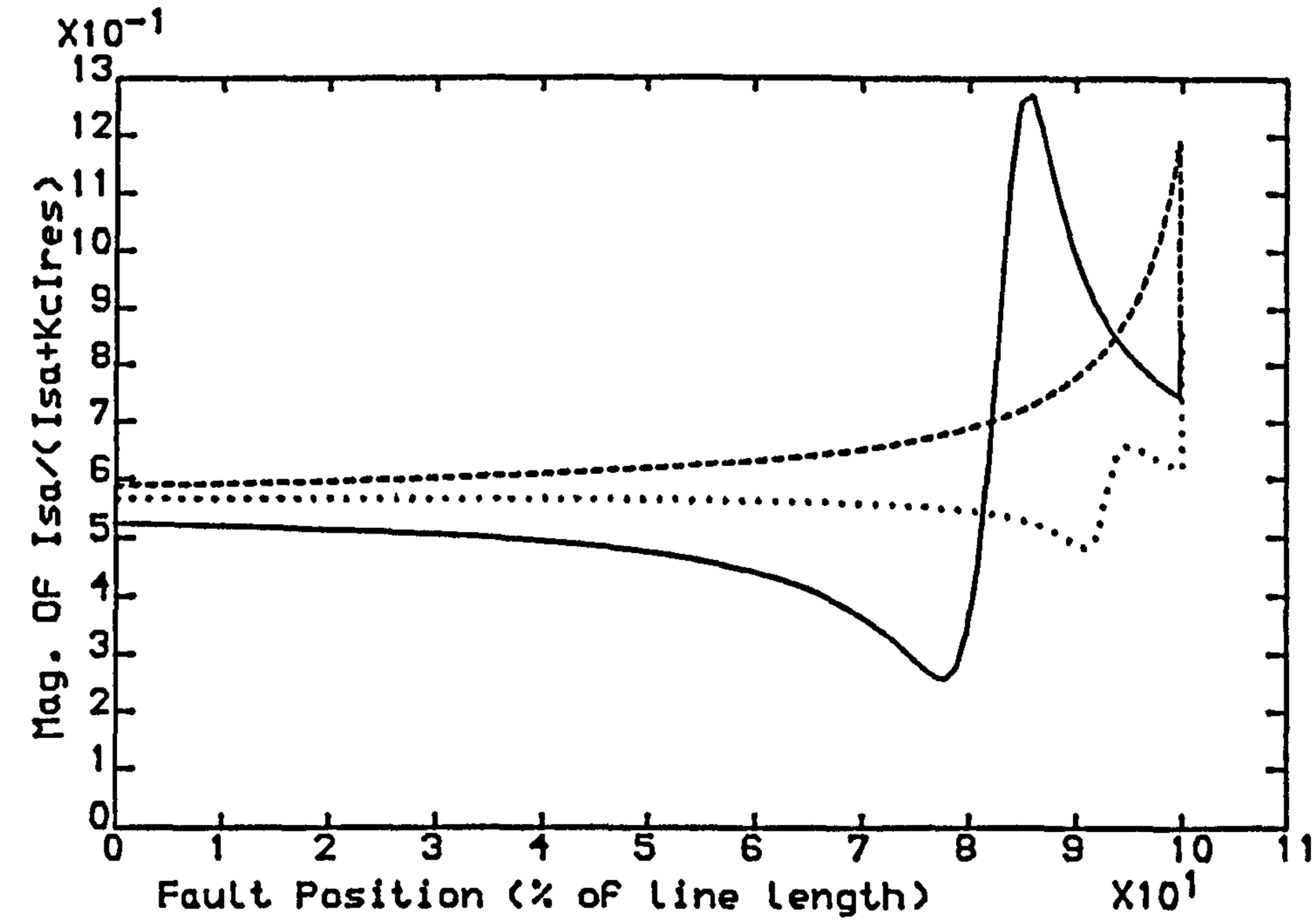

Fig 5.3.a-Variation in Mag. Of Isa/(Isa+KcIres) VS Fault Position For Pre-Fault Load Angle Of 0 Degrees

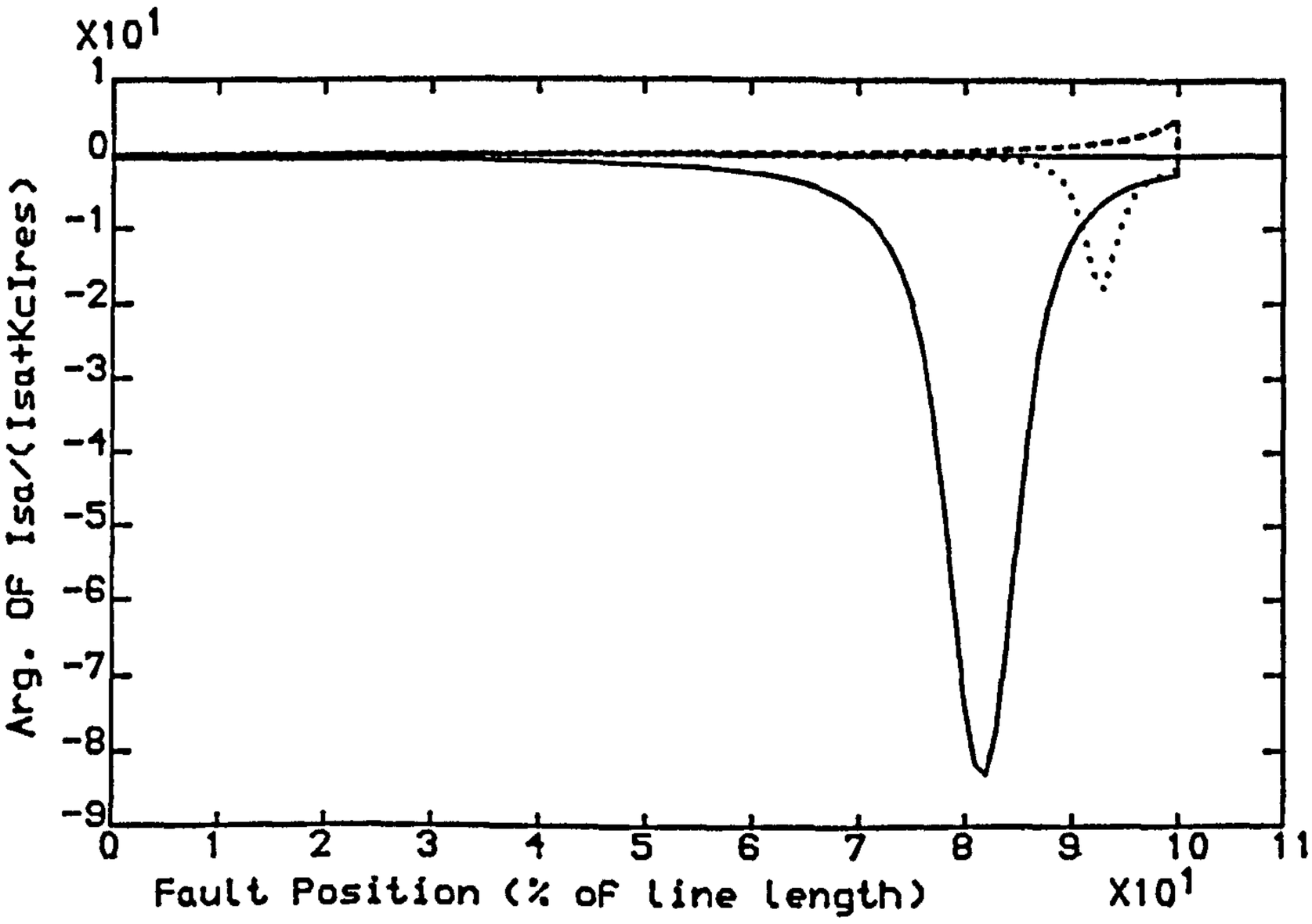

Fig 5.3.b-Variation in Arg. Of Isa/(Isa+KcIres) VS Fault Position For Pre-Fault Load Angle Of 0 Degrees

——— SE SCL=5 GVA, RE SCL=35 GVA
---- SE SCL=35 GVA, RE SCL=5 GVA
.... SE SCL=10 GVA, RE SCL=10 GVA
Line Length =300 km

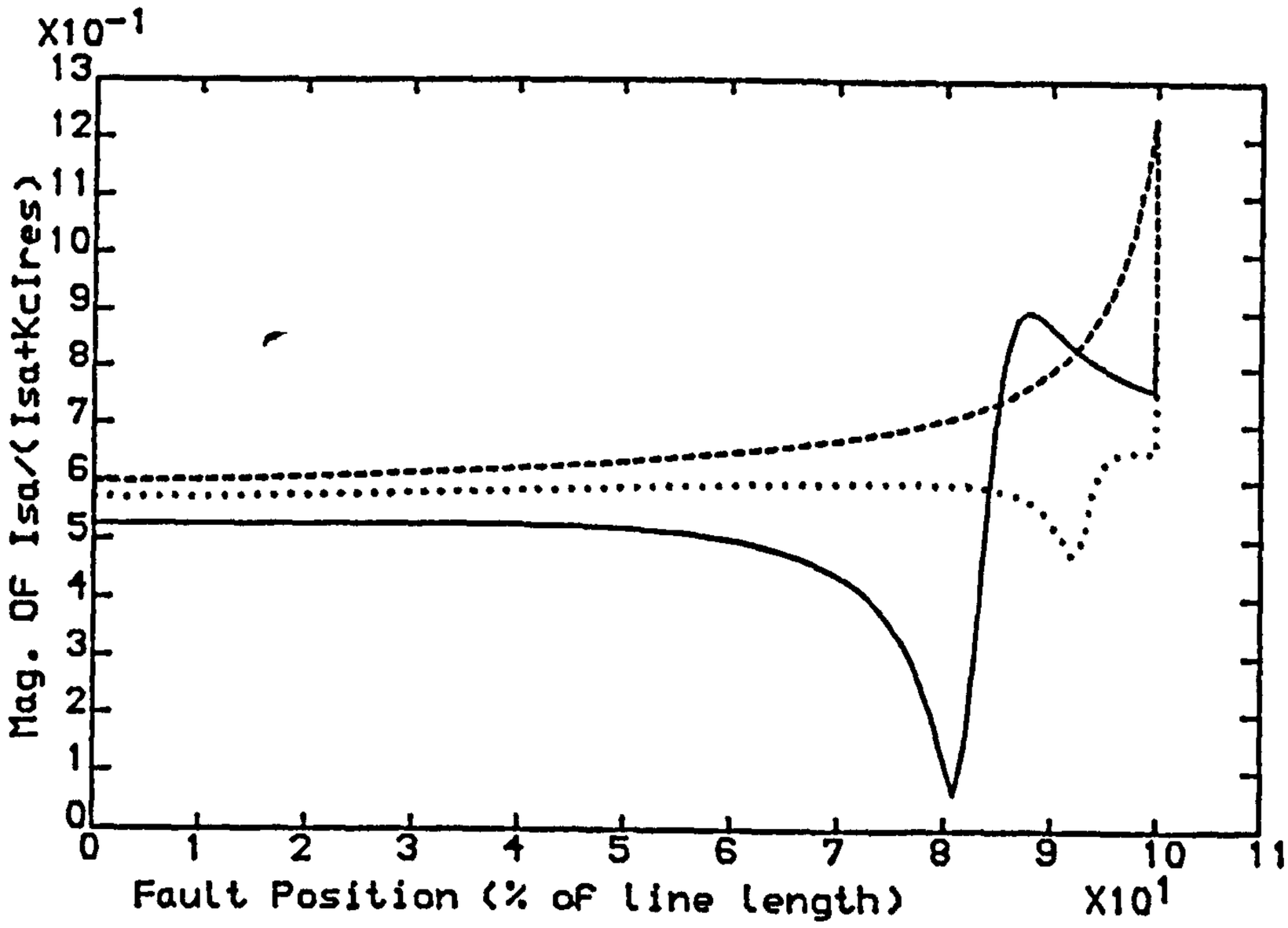

Fig 5.4.a—Variation in Mag. Of Isa/(Isa+KcIres) VS Fault Position For Pre-Fault Load Angle Of +10 Degrees

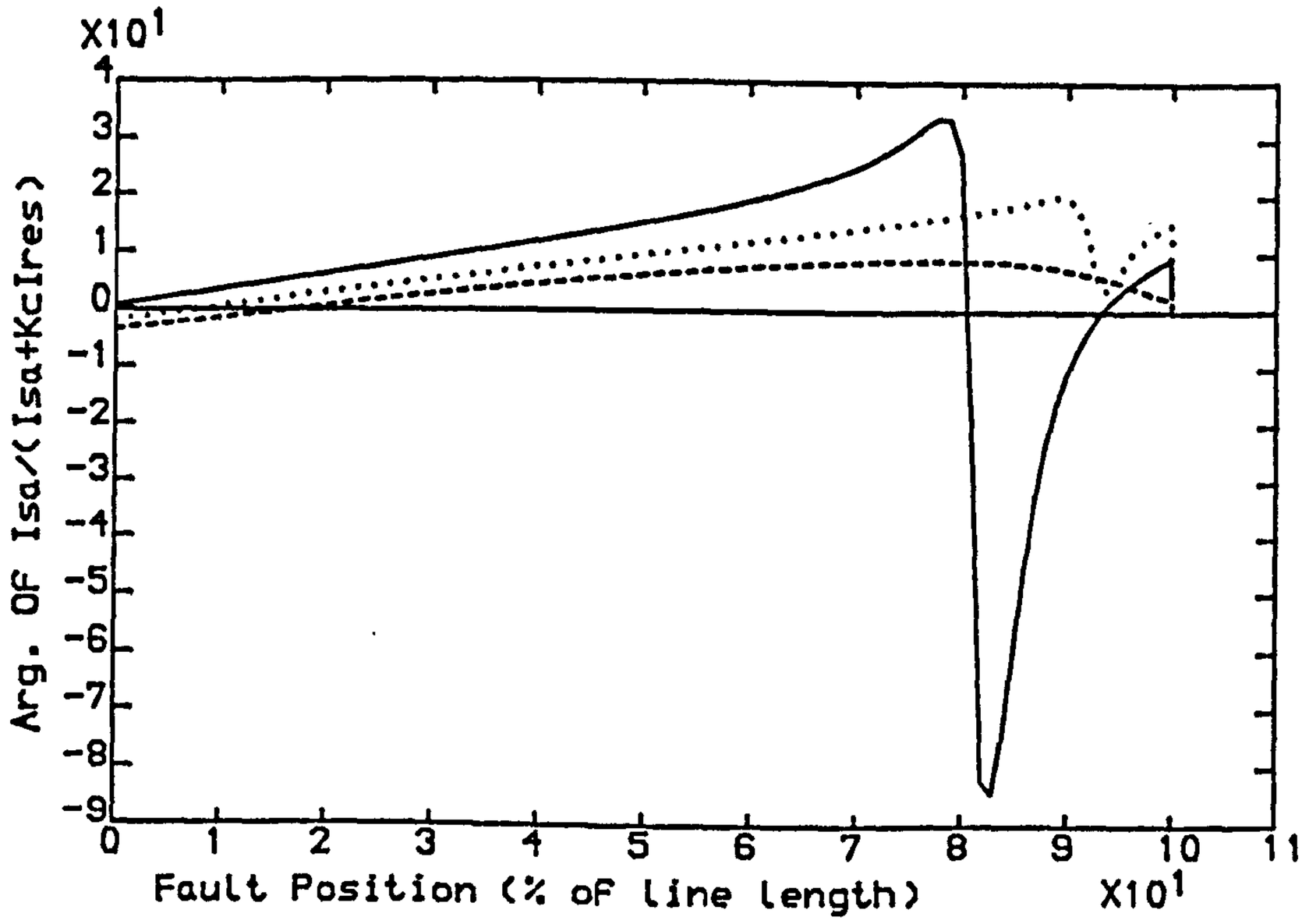

Fig 5.4.b—Variation in Arg. Of Isa/(Isa+KcIres) VS Fault Position For Pre-Fault Load Angle Of +10 Degrees

——— SE SCL=5 GVA, RE SCL=35 GVA
---- SE SCL=35 GVA, RE SCL=5 GVA
.... SE SCL=10 GVA, RE SCL=10 GVA
Line Length =300 km

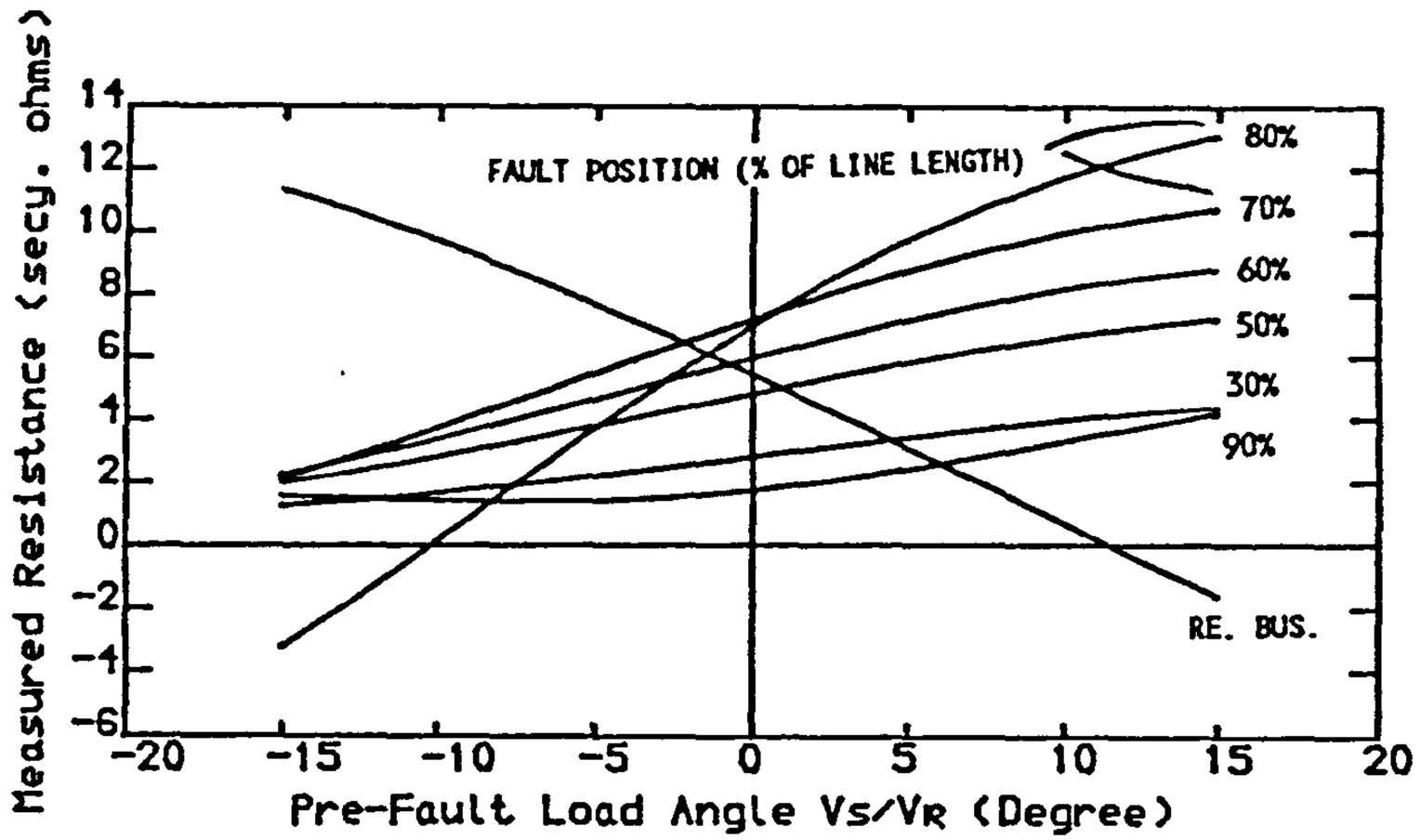

Fig 5.5.a- SE SCL=5 GVA, RE SCL=35 GVA

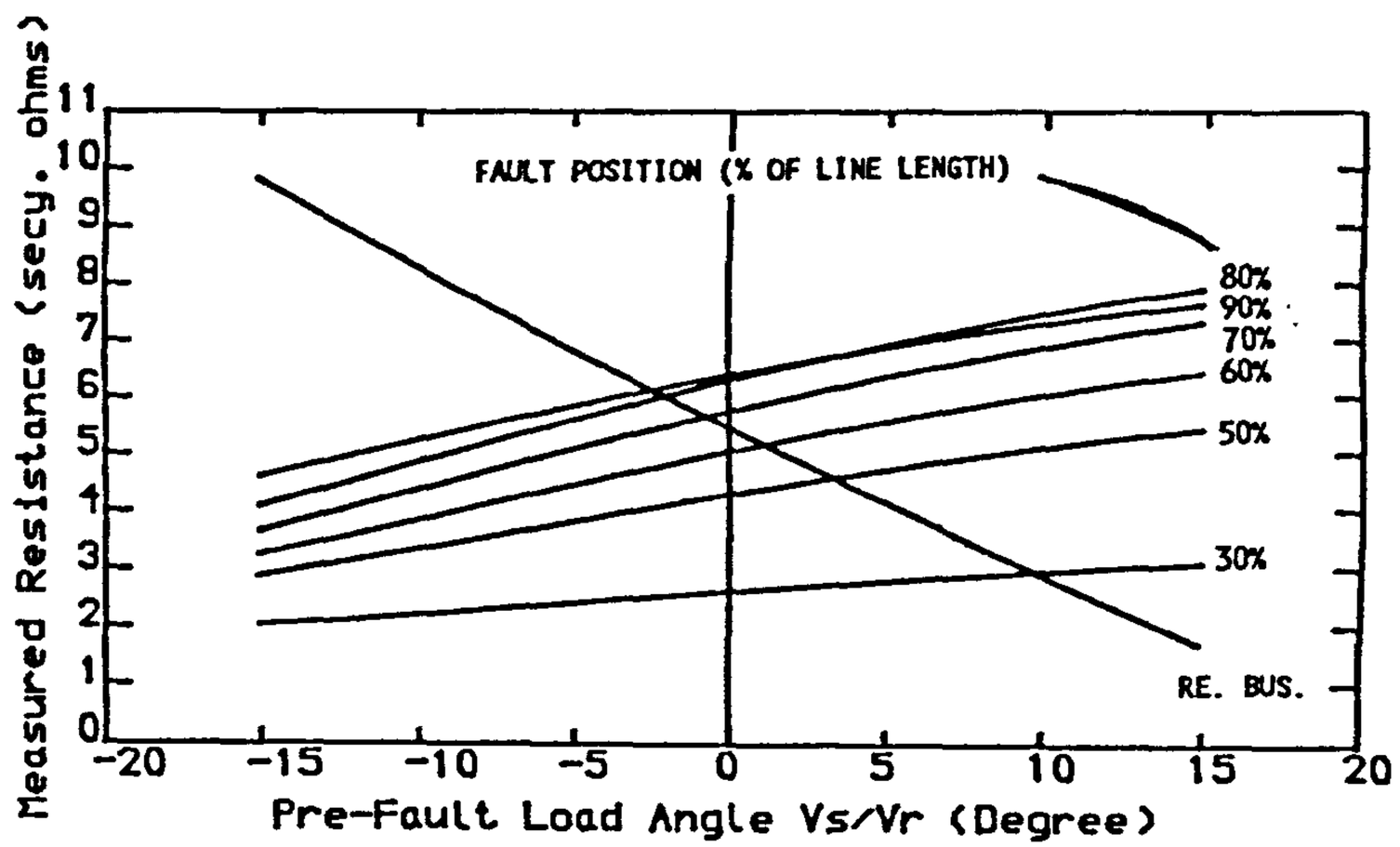

Fig 5.5.b- SE SCL=35 GVA, RE SCL=5 GVA

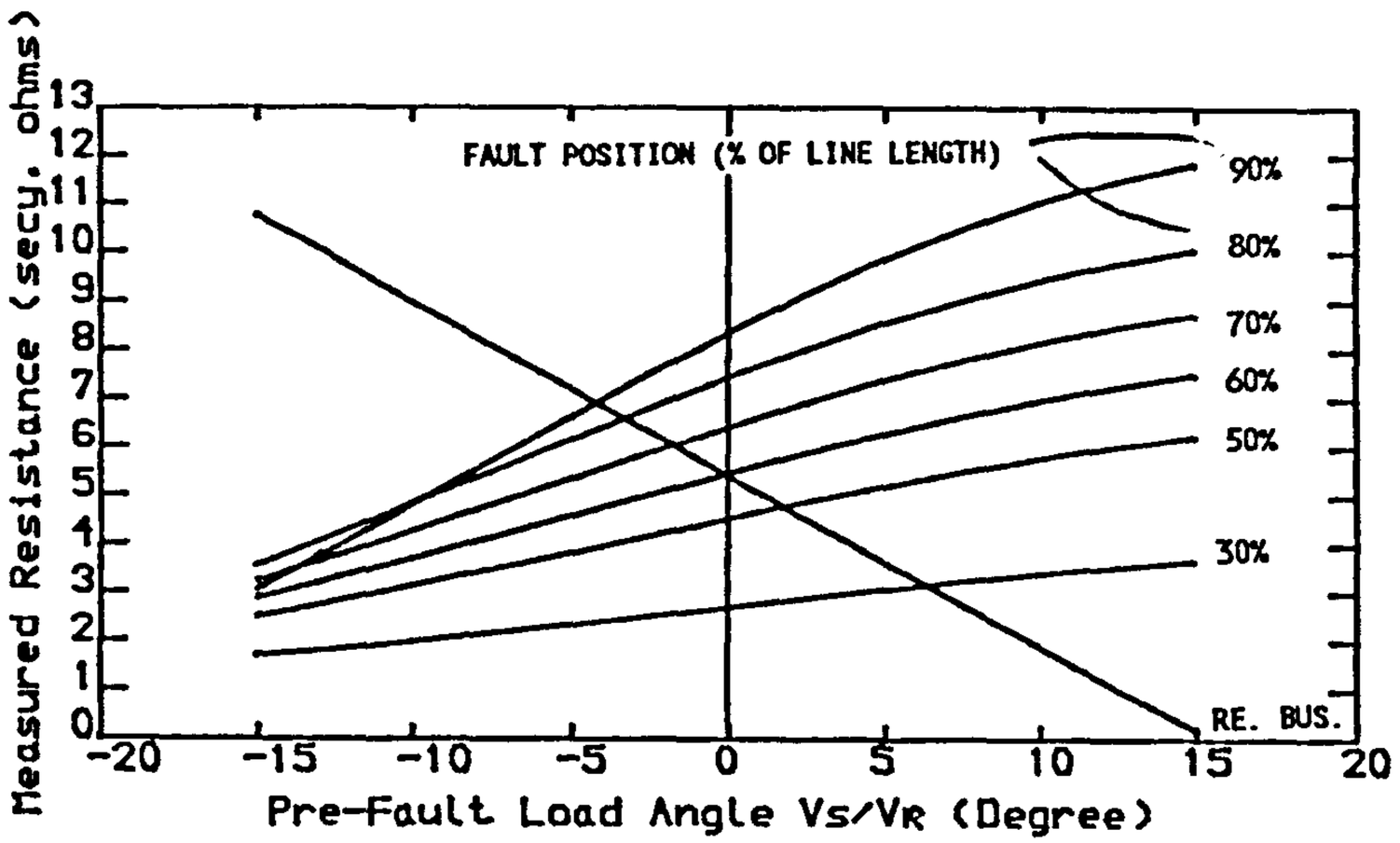

Fig 5.5.c- SE SCL=10 GVA, RE SCL=10 GVA

Fig 5.5-Measured Resistance VS Pre-fault Load, with the Conventional Residual Compensation Factor, K_C=0.774

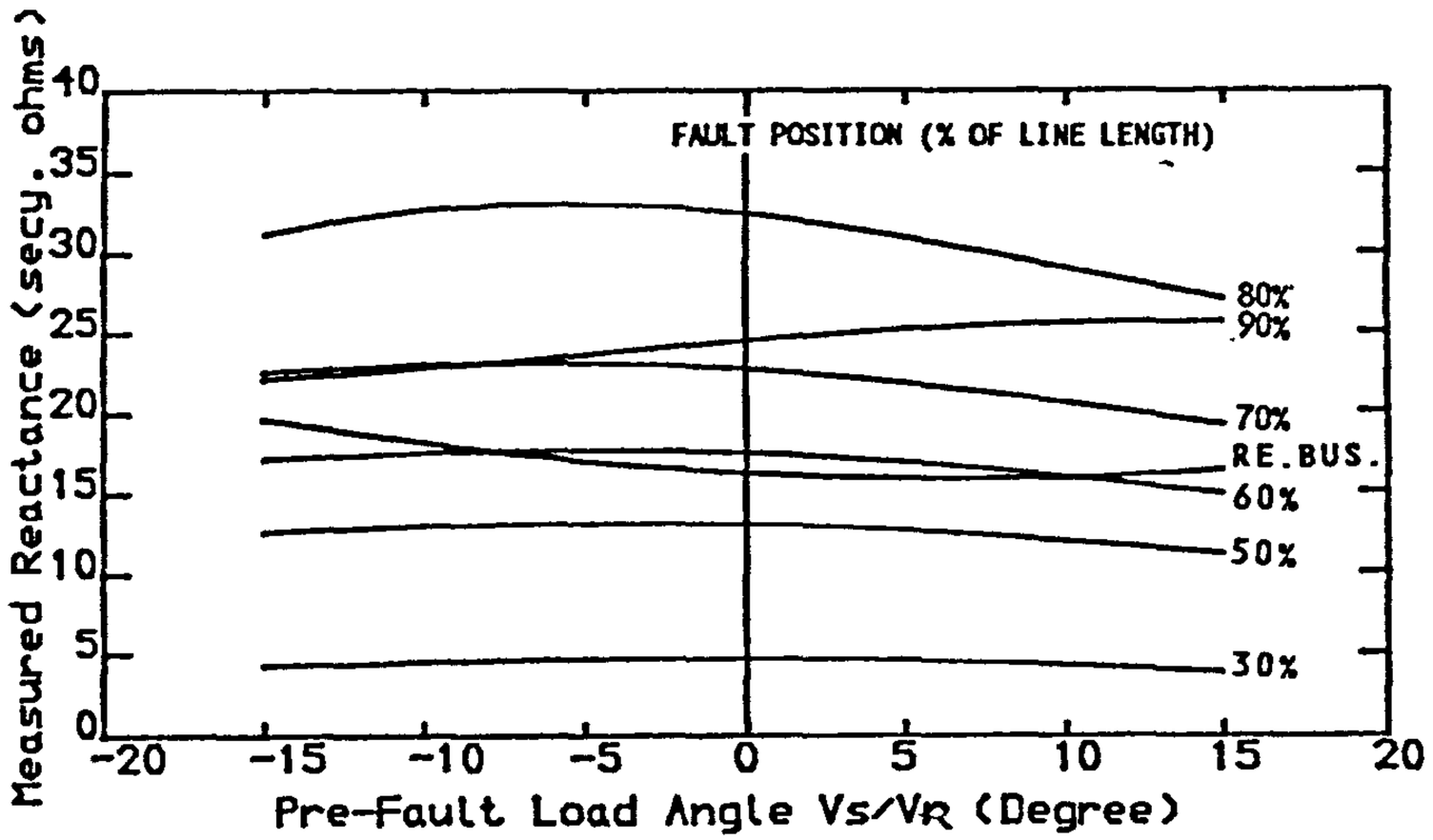

Fig 5.6.a- SE SCL=5 GVA, RE SCL=35 GVA

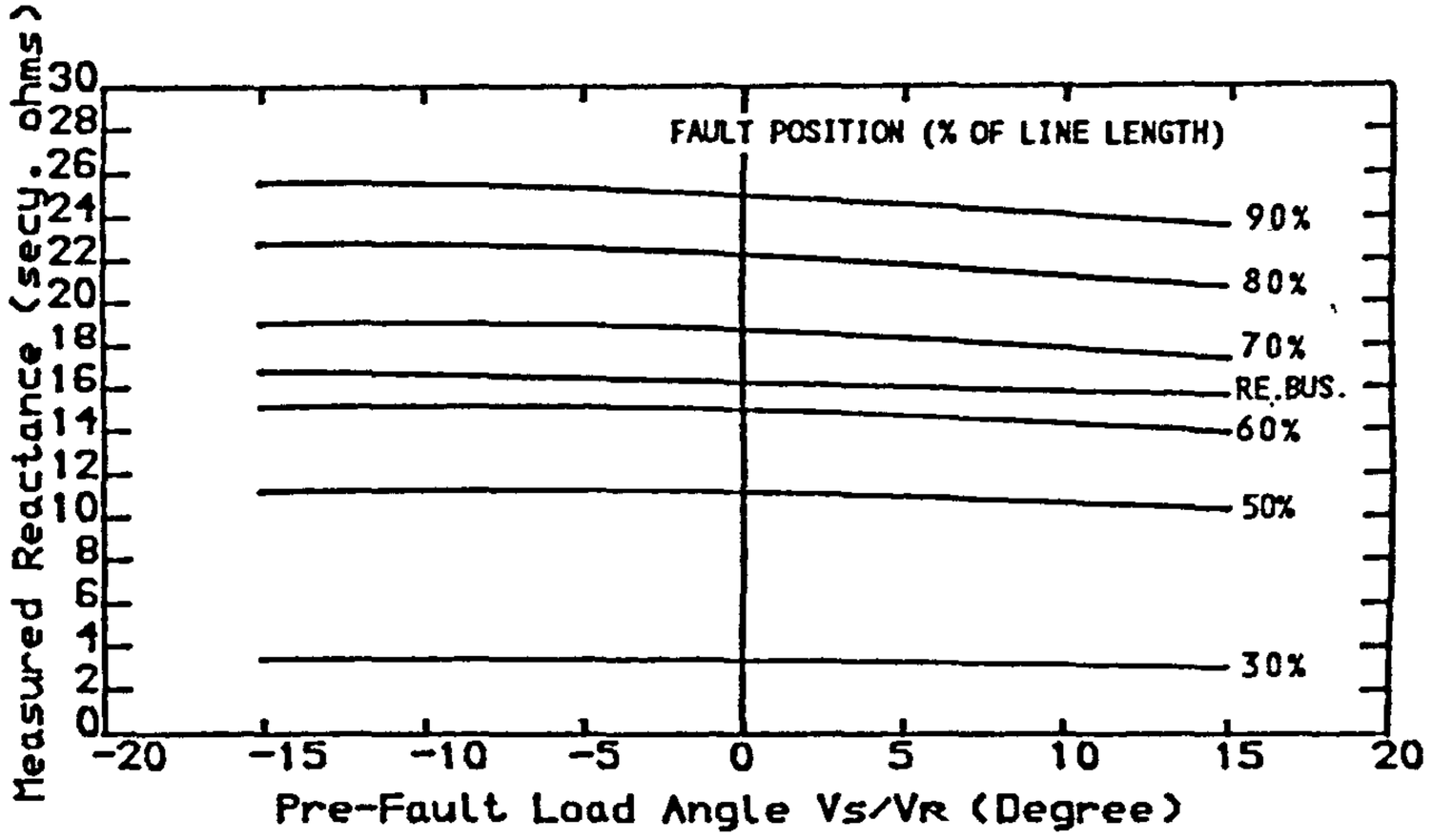

Fig 5.6.b- SE SCL=35 GVA, RE SCL=5 GVA

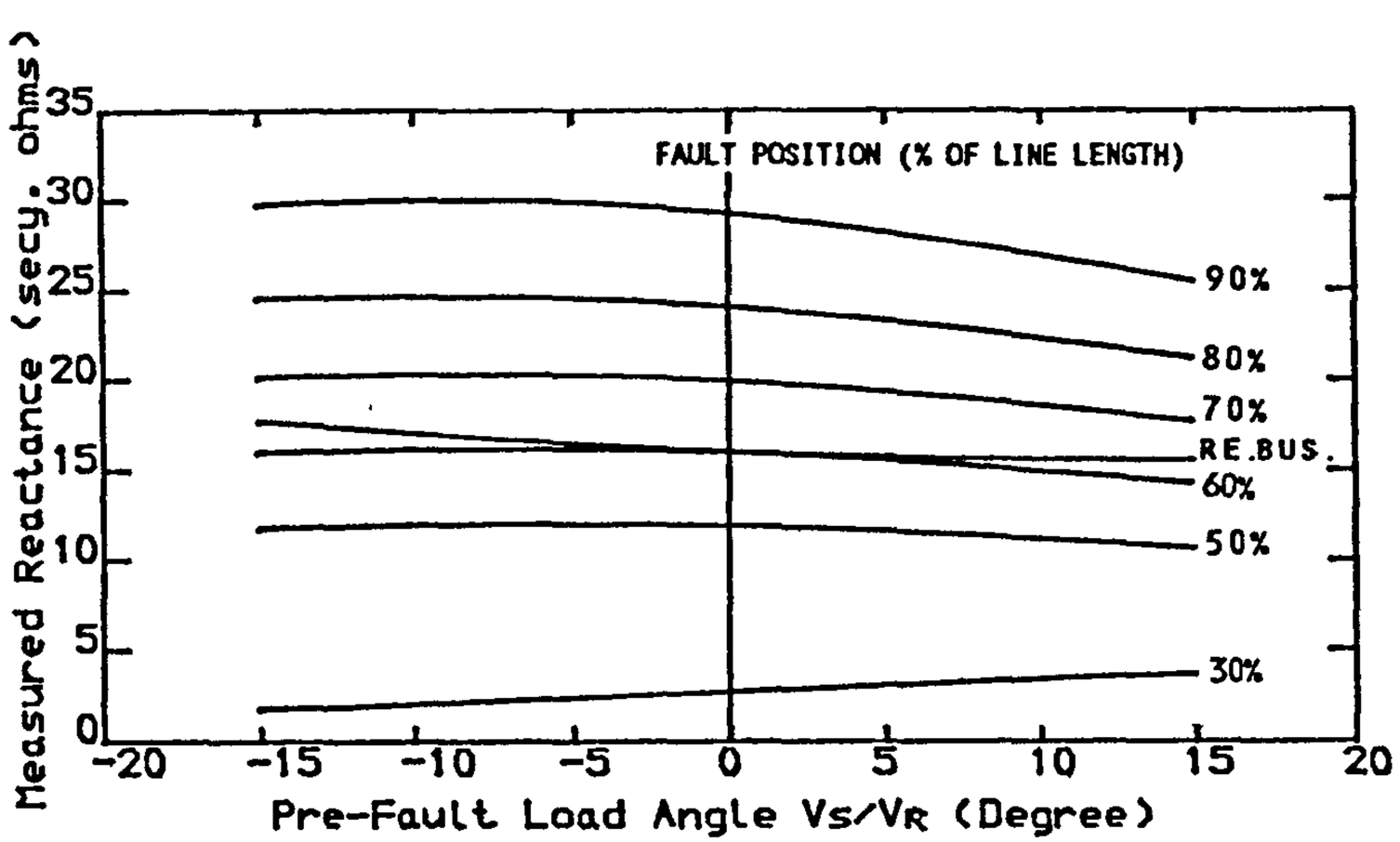

Fig 5.6.c- SE SCL=10 GVA, RE SCL=10 GVA

Fig 5.6-Measured Reactance VS Pre-fault Load, with the Conventional Residual Compensation Factor, K_C=0.774

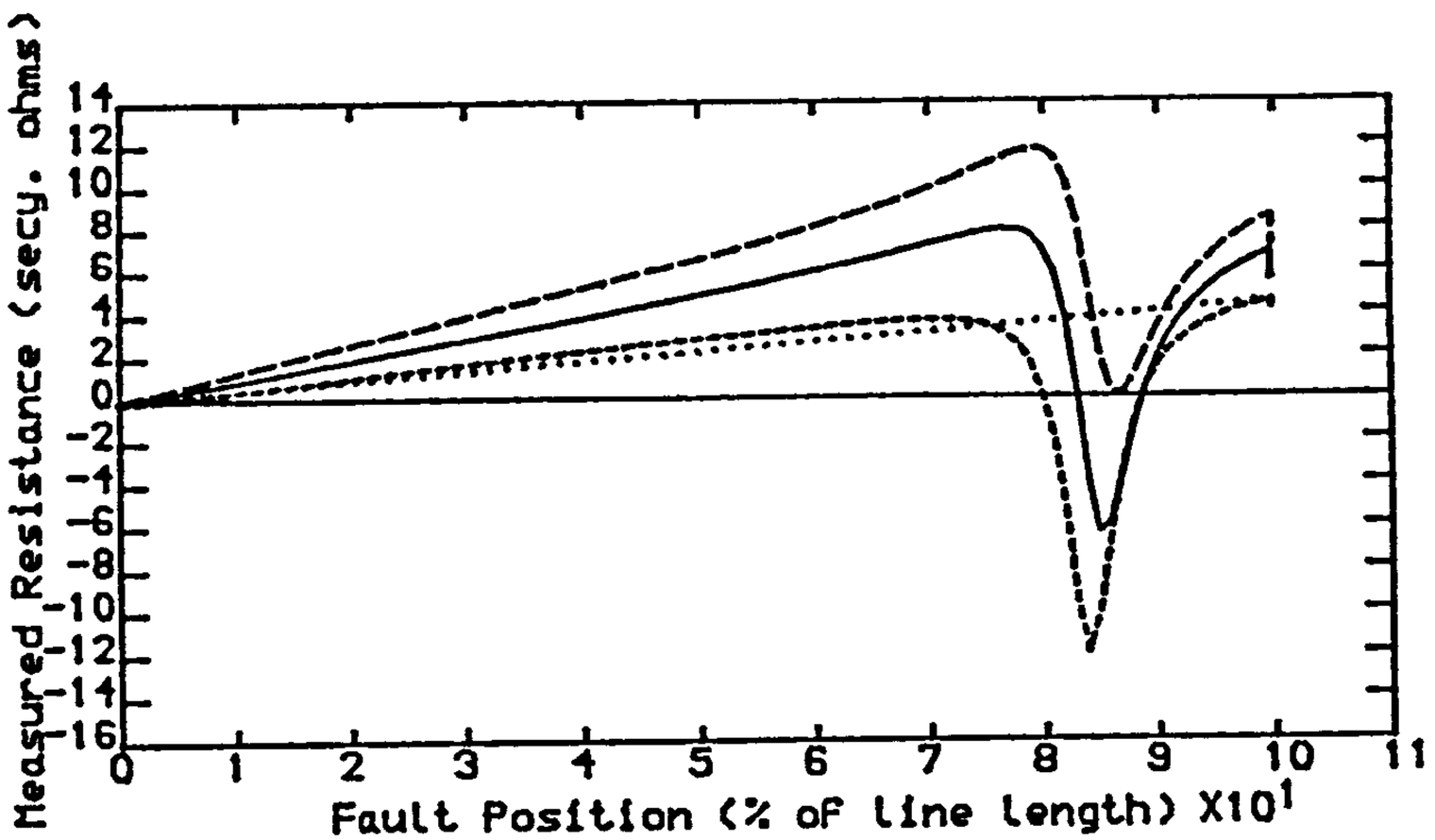

Fig 5.7.a- SE SCL=5 GVA. RE SCL=35 GVA

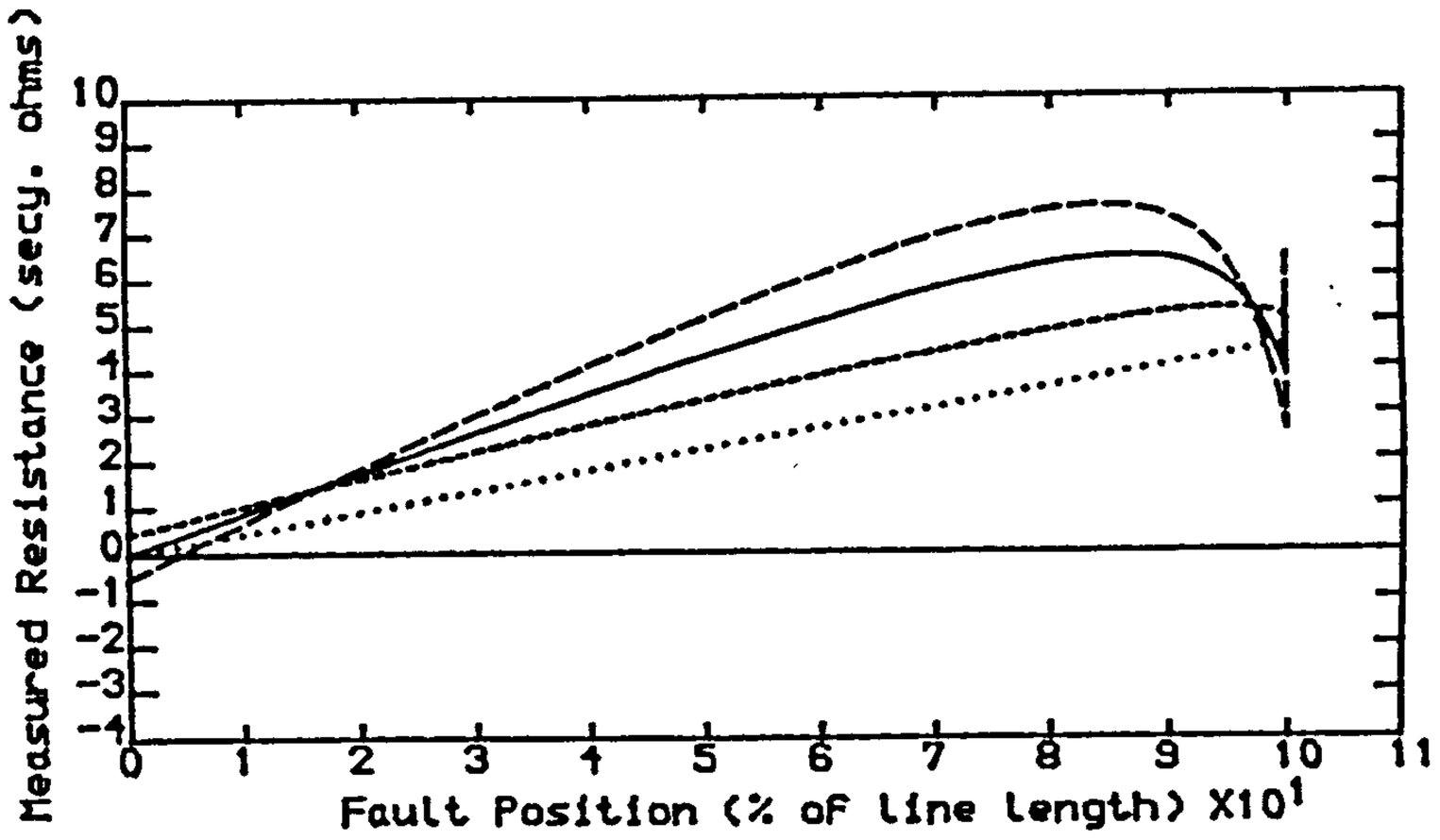

Fig 5.7.b- SE SCL=35 GVA. RE SCL=5 GVA

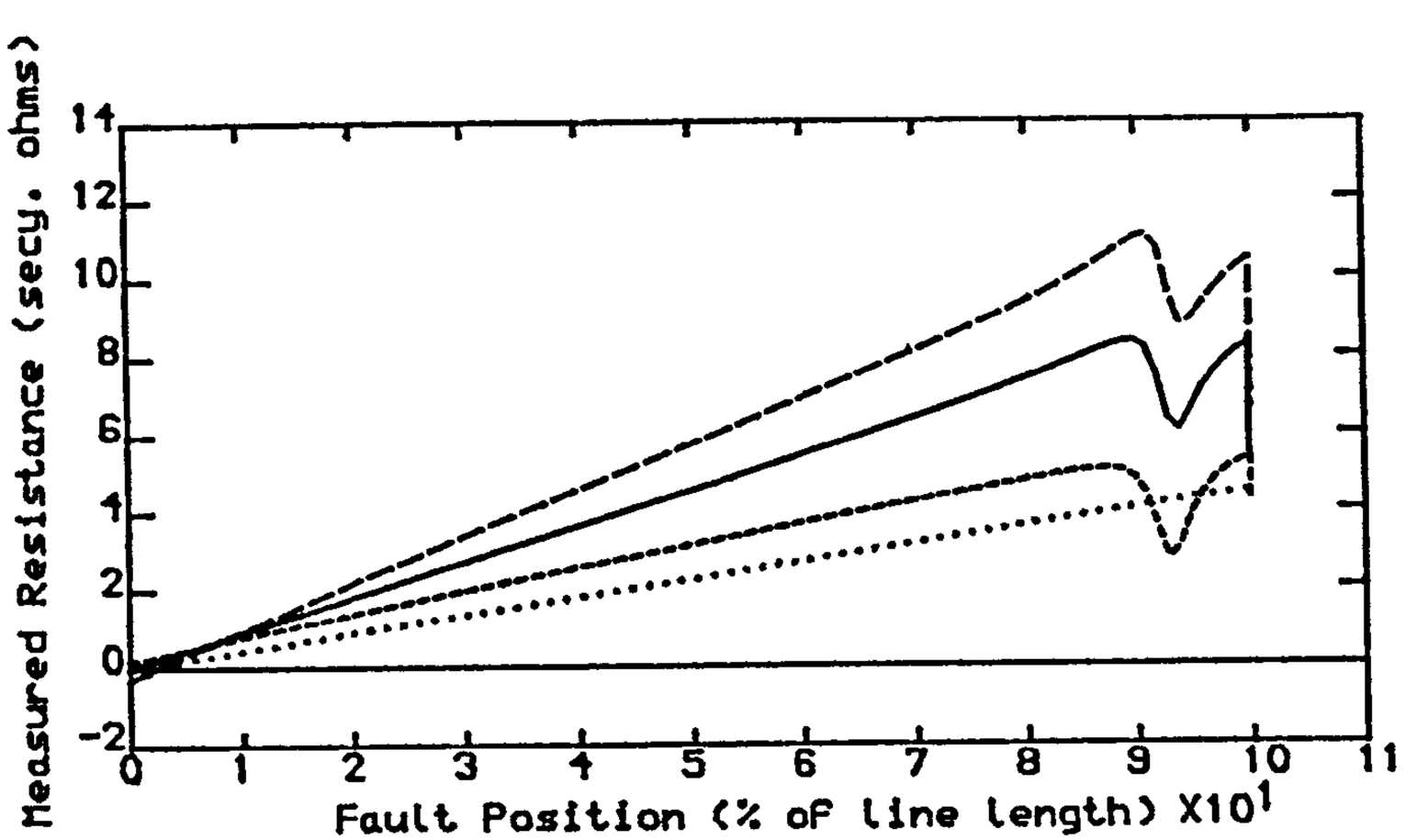

Fig 5.7.c- SE SCL=10 GVA. RE SCL=10 GVA

Fig 5.7-Measured Resistance VS Fault Position with the Conventional Residual Compensation Factor, K_C=0.774

.... Line Locus
---- Pre-Fault Load Angle=-10 deg.
——— Pre-Fault Load Angle=0 deg.
——— Pre-Fault Load Angle=+10 deg.
Line Length=300 km

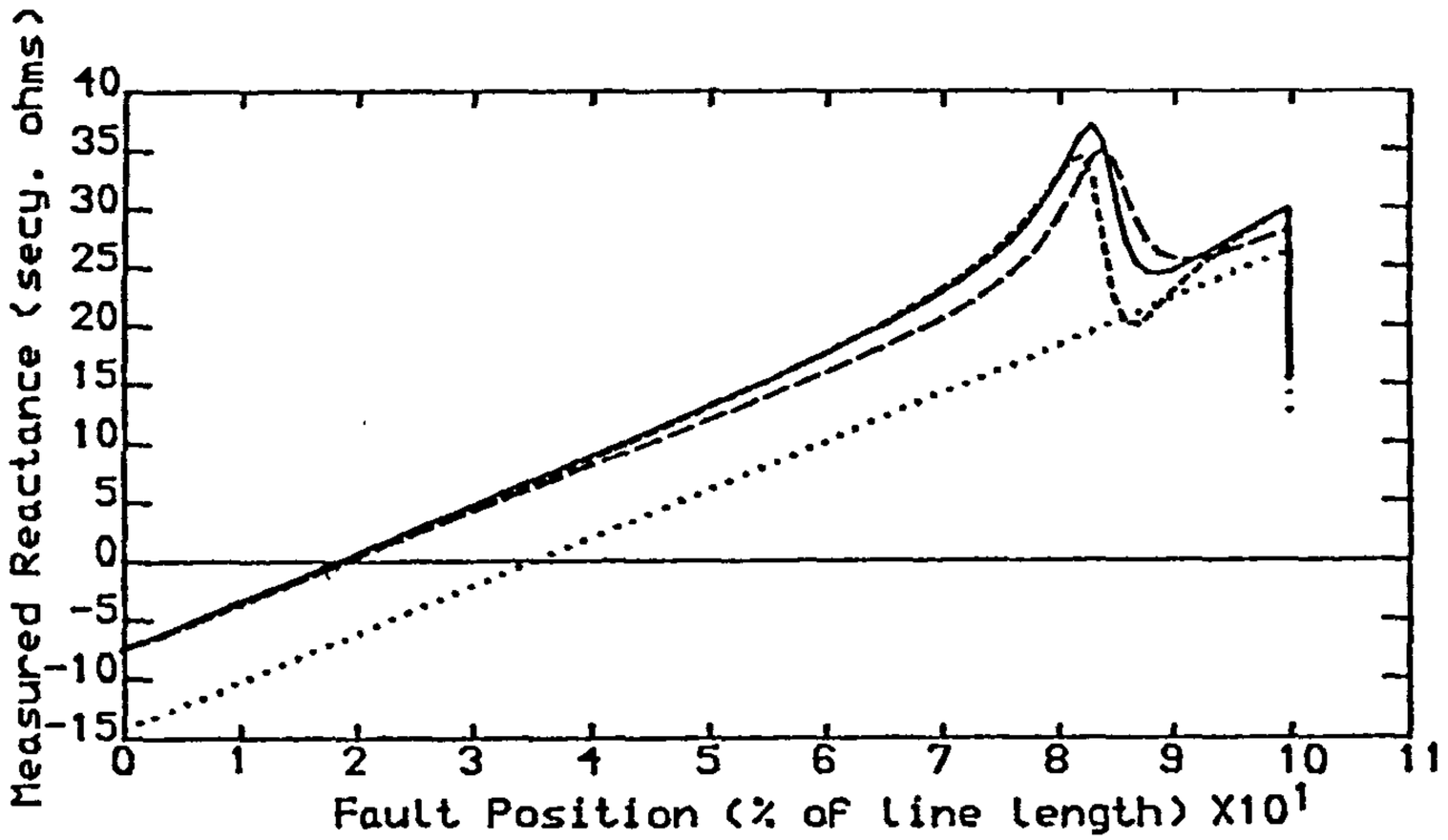

Fig 5.8.a- SE SCL=5 GVA, RE SCL=35 GVA

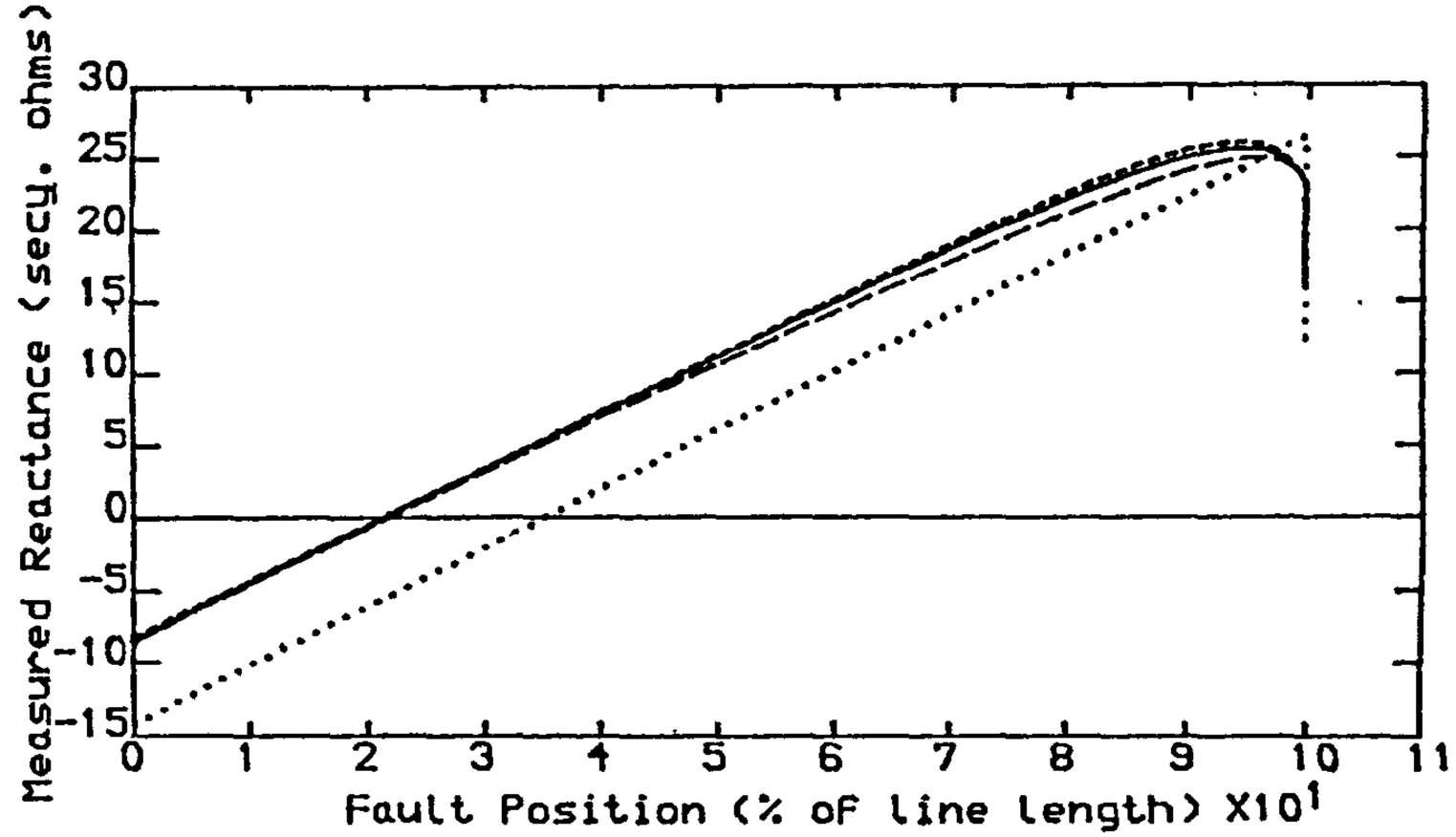

Fig 5.8.b- SE SCL=35 GVA, RE SCL=5 GVA

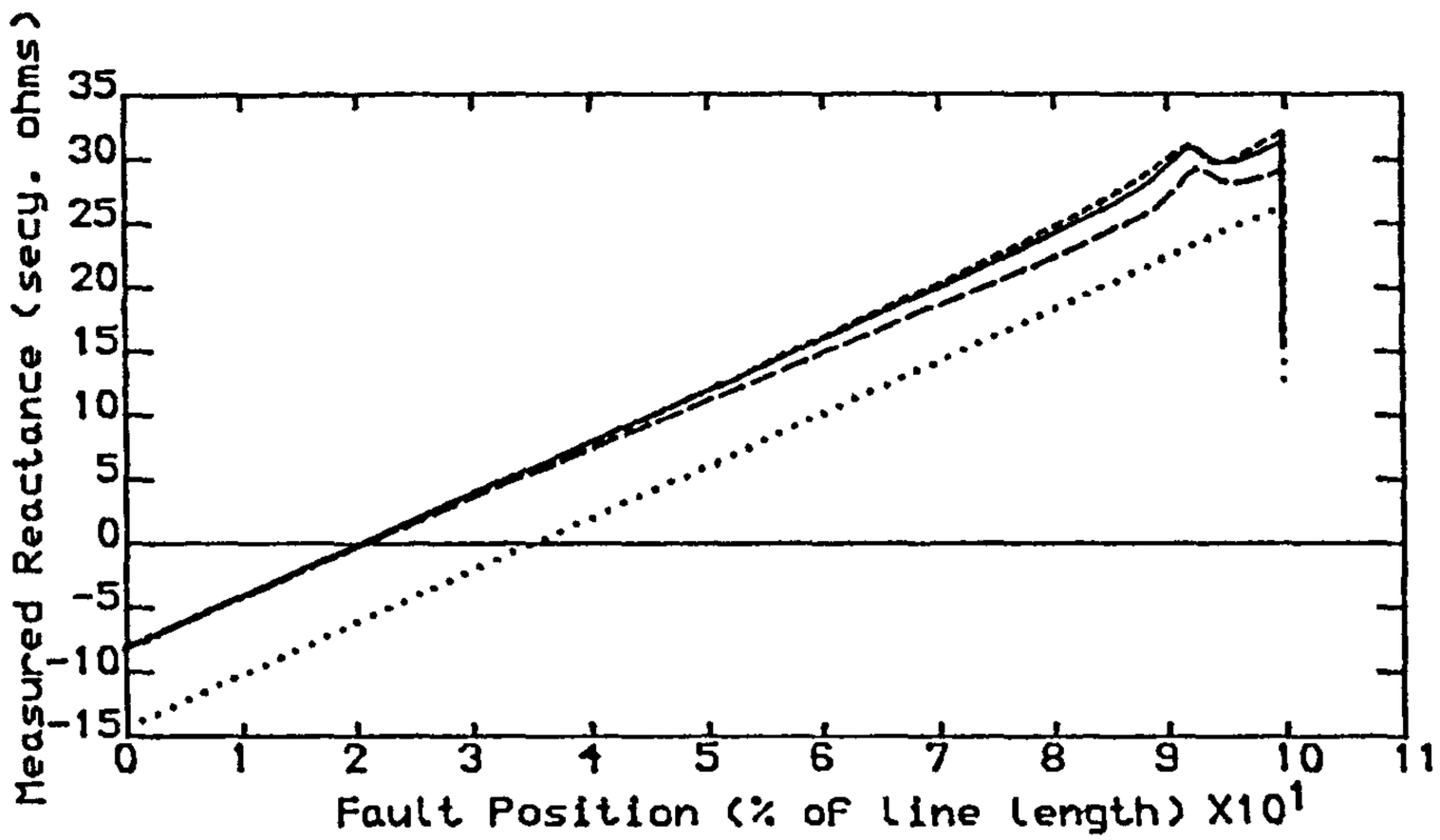

Fig 5.8.c- SE SCL=10 GVA, RE SCL=10 GVA

Fig 5.8-Measured Reactance VS Fault Position with the Conventional Residual Compensation Factor, K_C=0.774

.... Line Locus
---- Pre-Fault Load Angle=-10 deg.
——— Pre-Fault Load Angle=0 deg.
—— Pre-Fault Load Angle=+10 deg.
Line Length=300 km

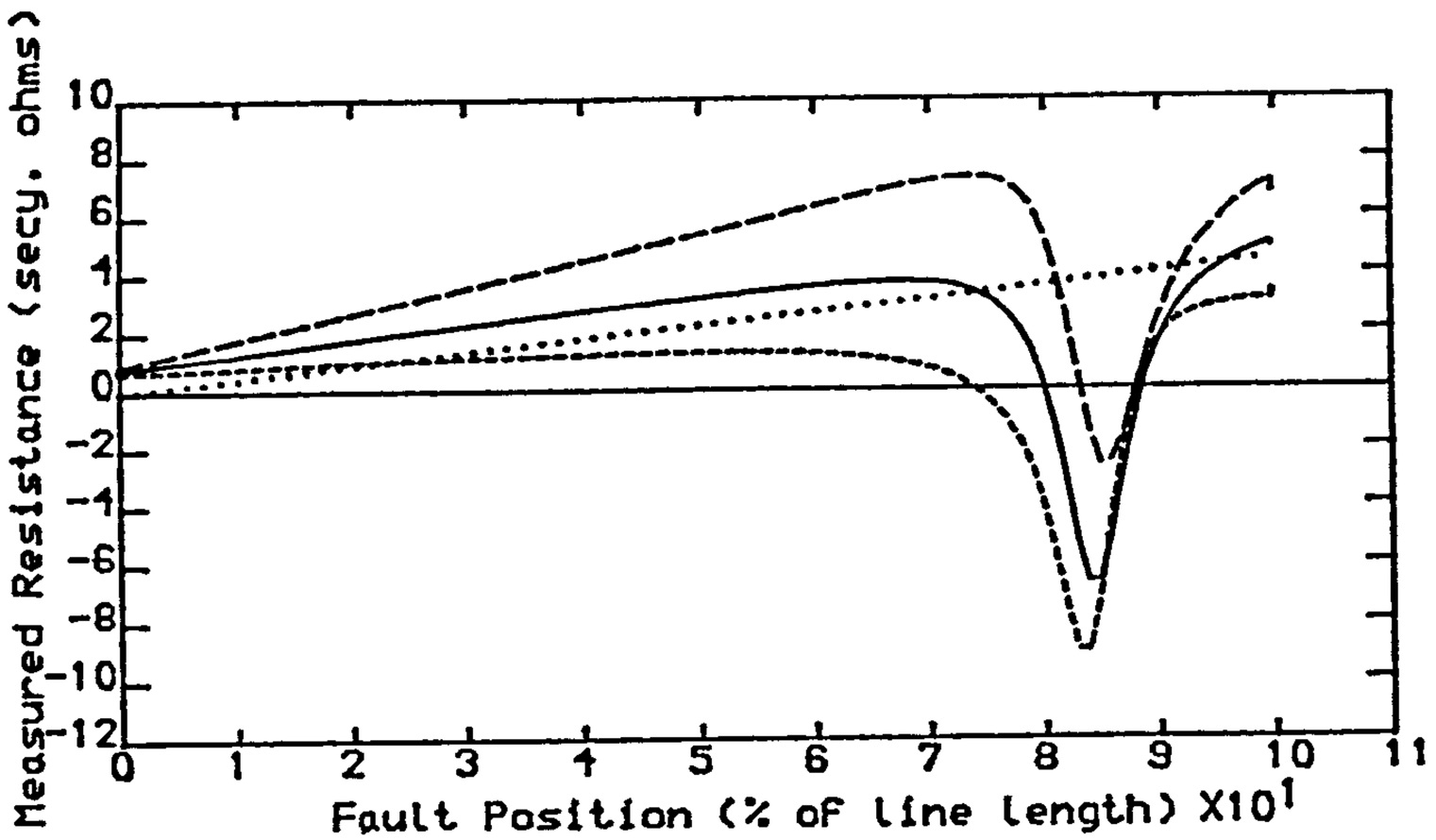

Fig 5.9.a- SE SCL=5 GVA, RE SCL=35 GVA

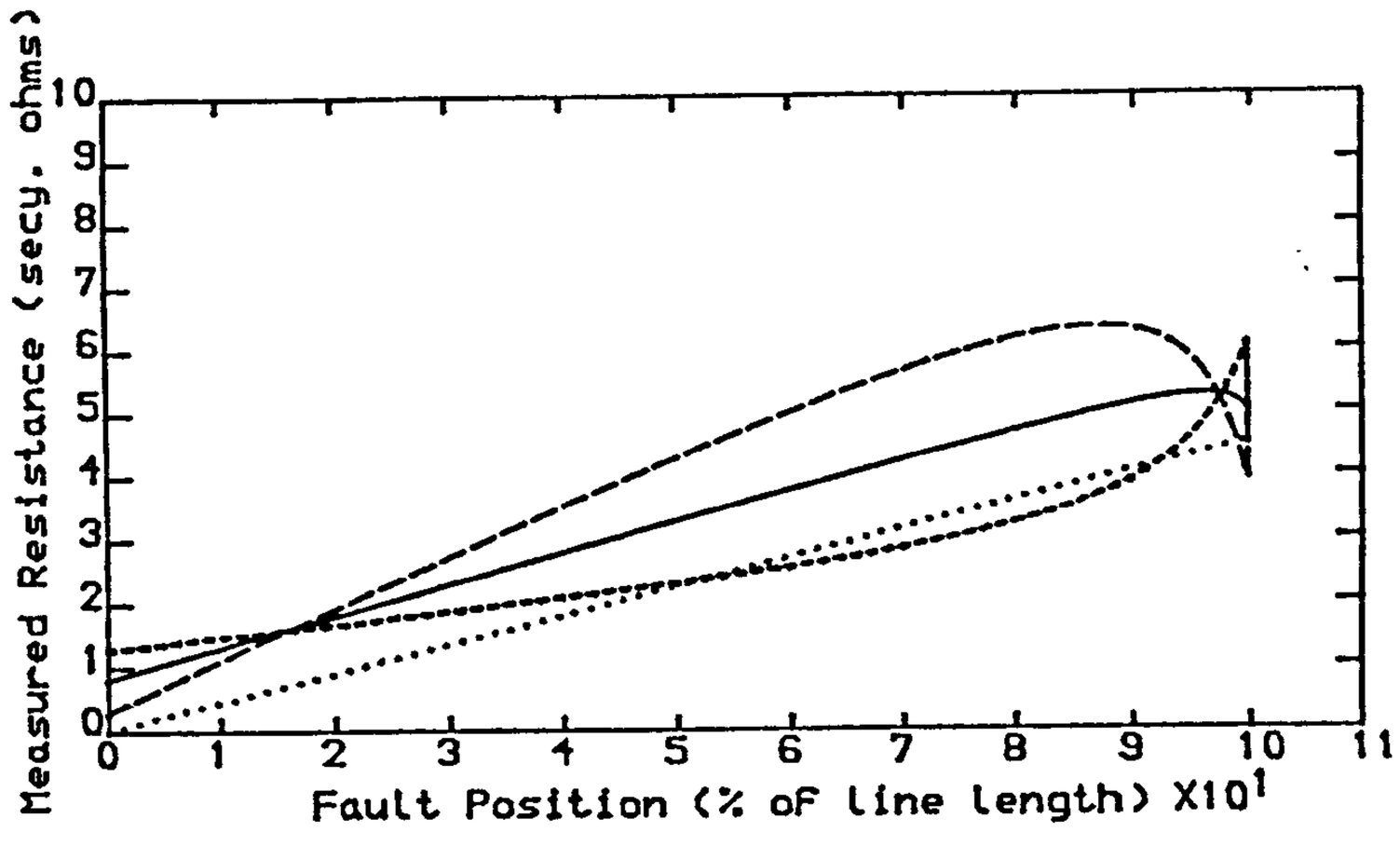

Fig 5.9.b- SE SCL=35 GVA, RE SCL=5 GVA

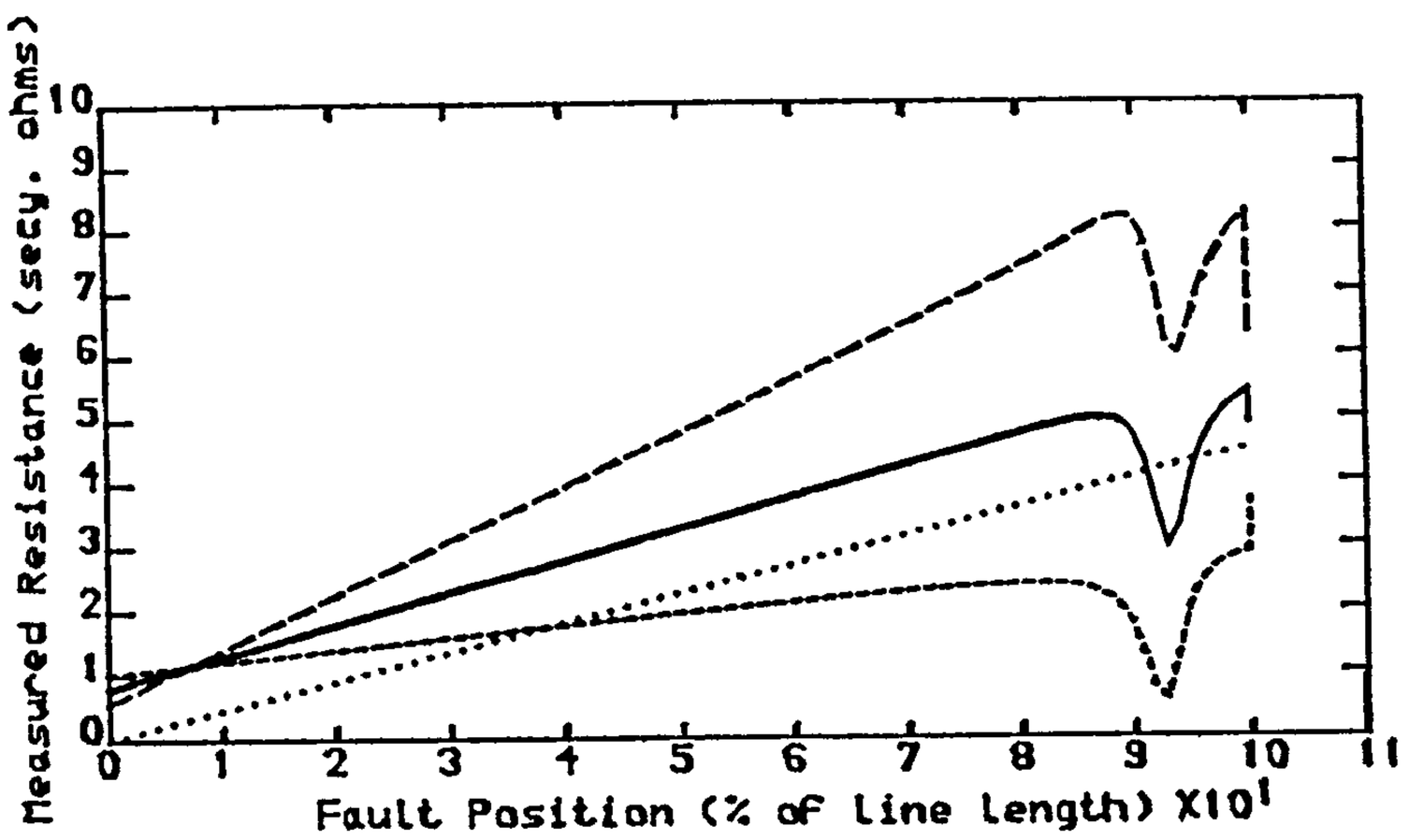

Fig 5.9.c- SE SCL=10 GVA, RE SCL=10 GVA

Fig 5.9-Measured Resistance VS Fault Position with the Complex Conventional Residual Compensation Factor, $K_C=0.78\angle -13.5°$

.... Line Locus
---- Pre-Fault Load Angle=-10 deg.
——— Pre-Fault Load Angle=0 deg.
—— Pre-Fault Load Angle=+10 deg.
Line Length=300 km

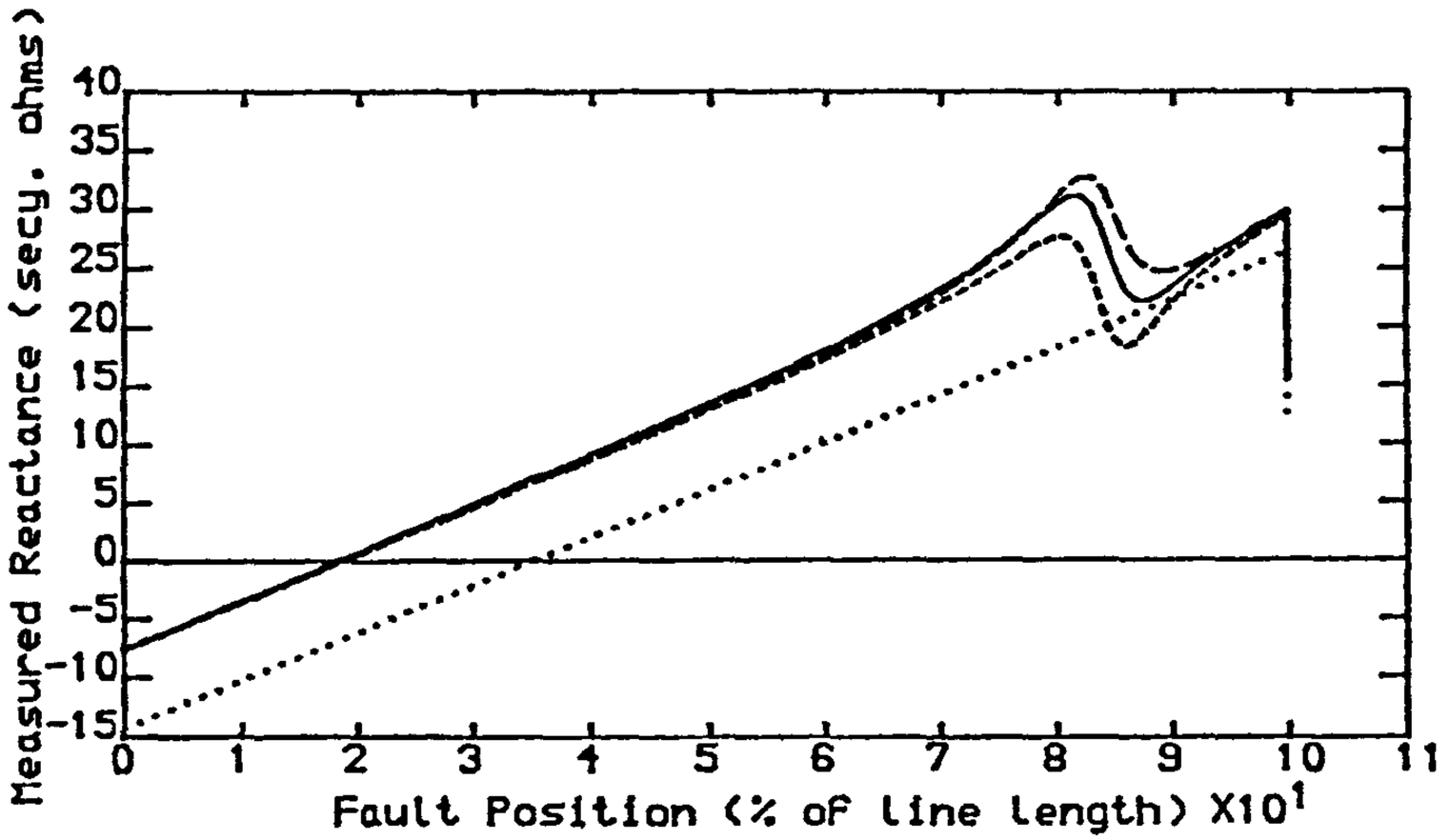

Fig 5.10.a- SE SCL=5 GVA, RE SCL=35 GVA

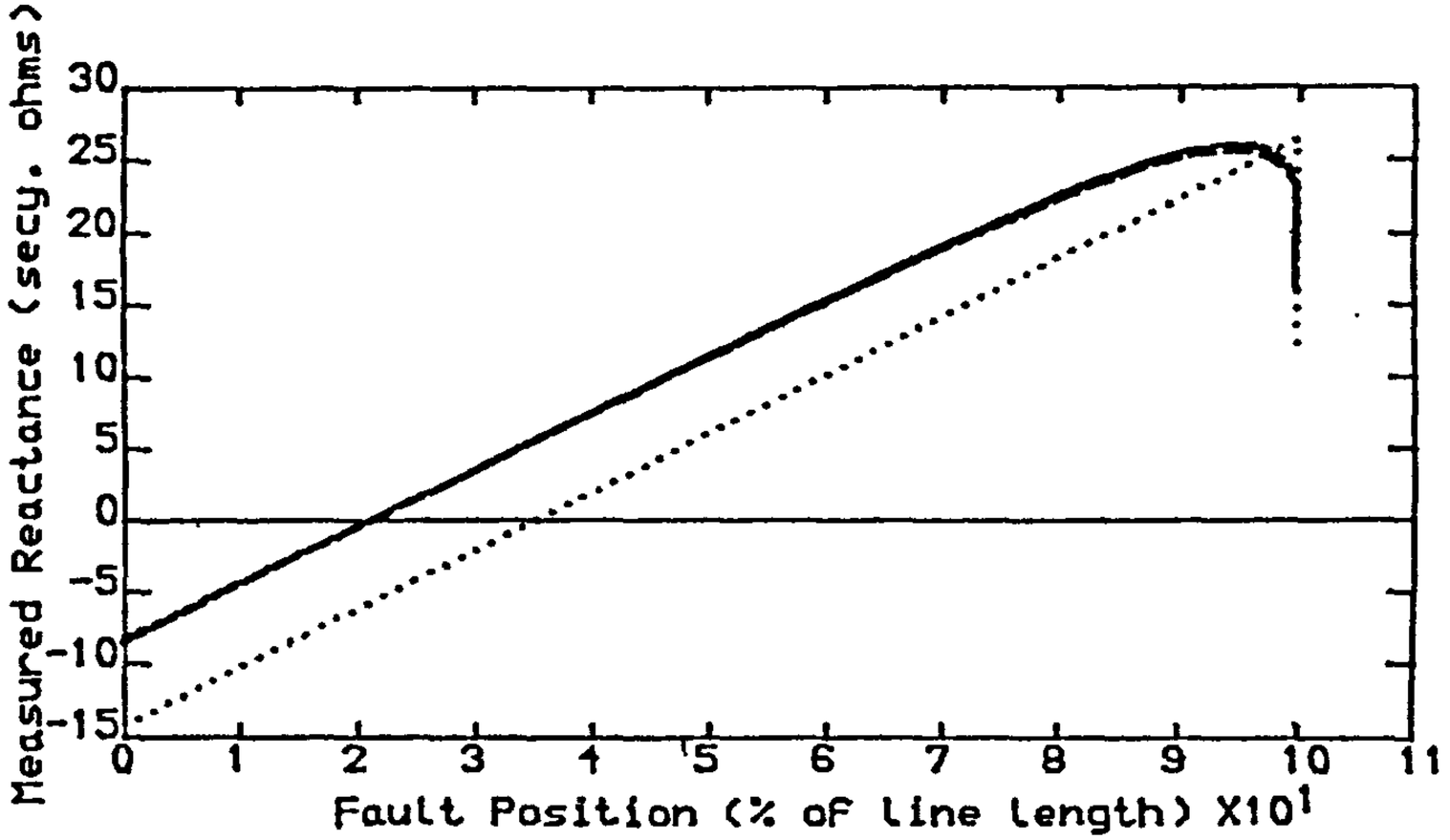

Fig 5.10.b- SE SCL=35 GVA, RE SCL=5 GVA

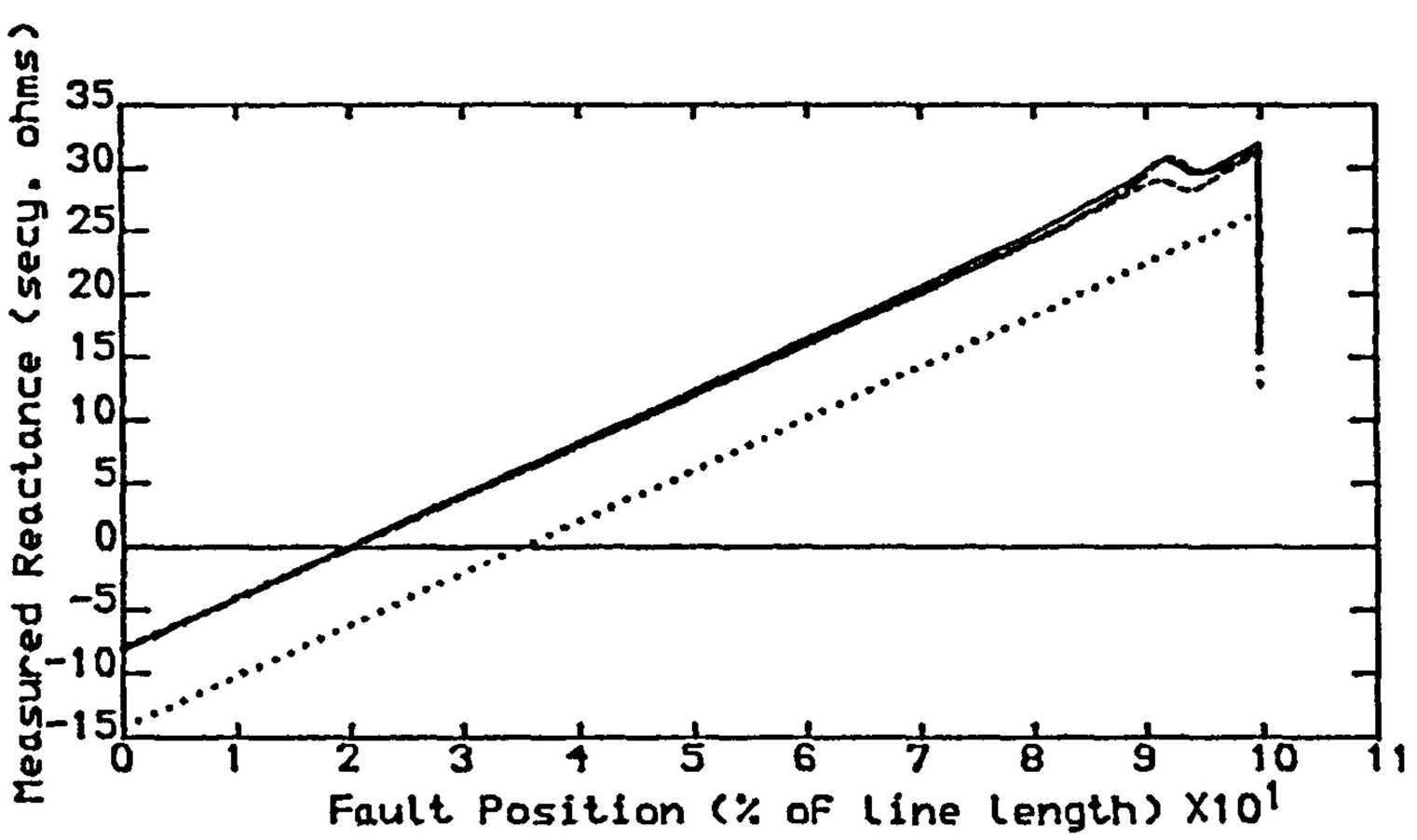

Fig 5.10.c- SE SCL=10 GVA, RE SCL=10 GVA

Fig 5.10-Measured Reactance VS Fault Position with the Complex Conventional Residual Compensation Factor, $K_c=0.78\angle -13.5°$

.... Line Locus
---- Pre-Fault Load Angle=-10
——— Pre-Fault Load Angle=0
——— Pre-Fault Load Angle=+10
Line Length=300 km

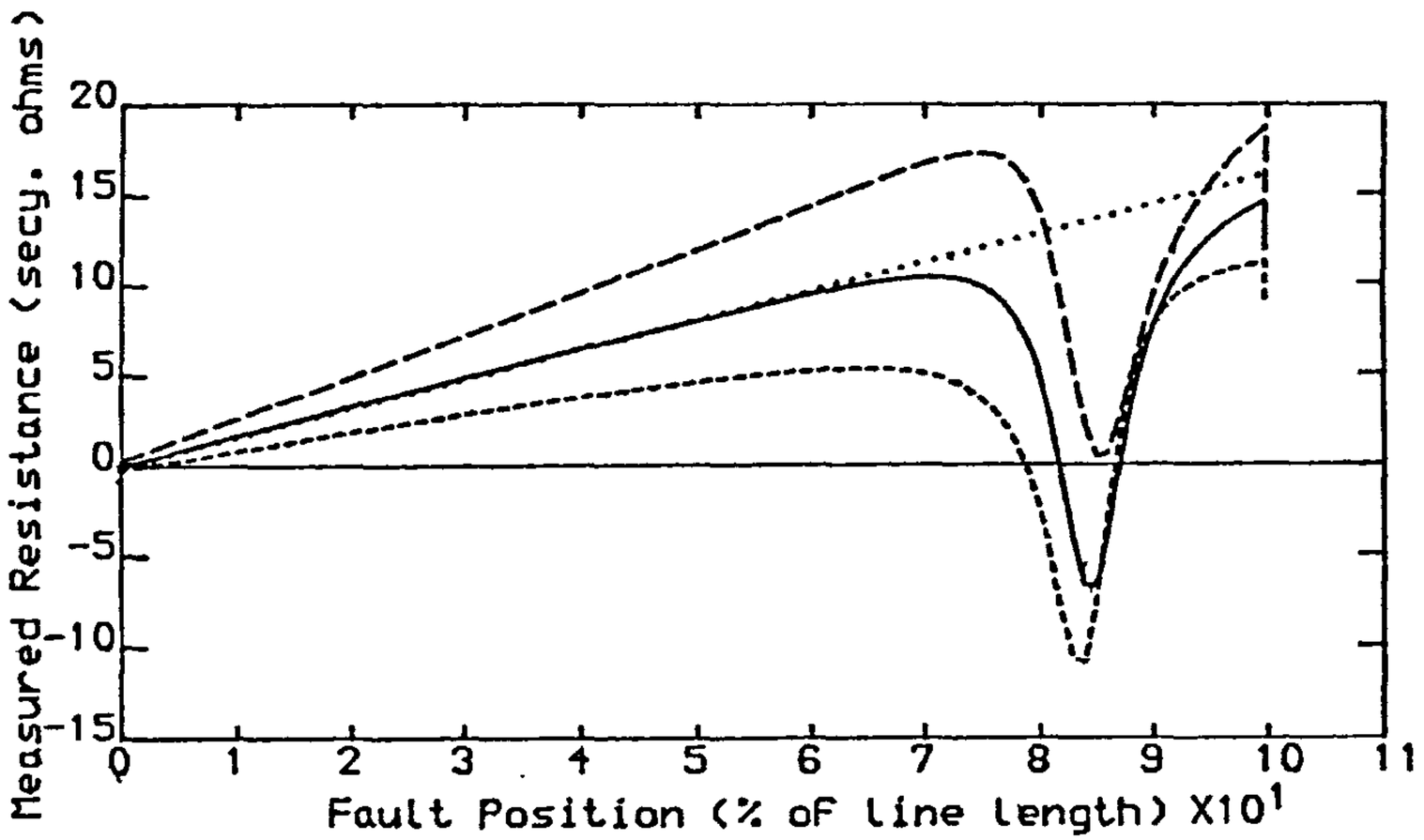

Fig 5.11.a- SE SCL=5 GVA, RE SCL=35 GVA

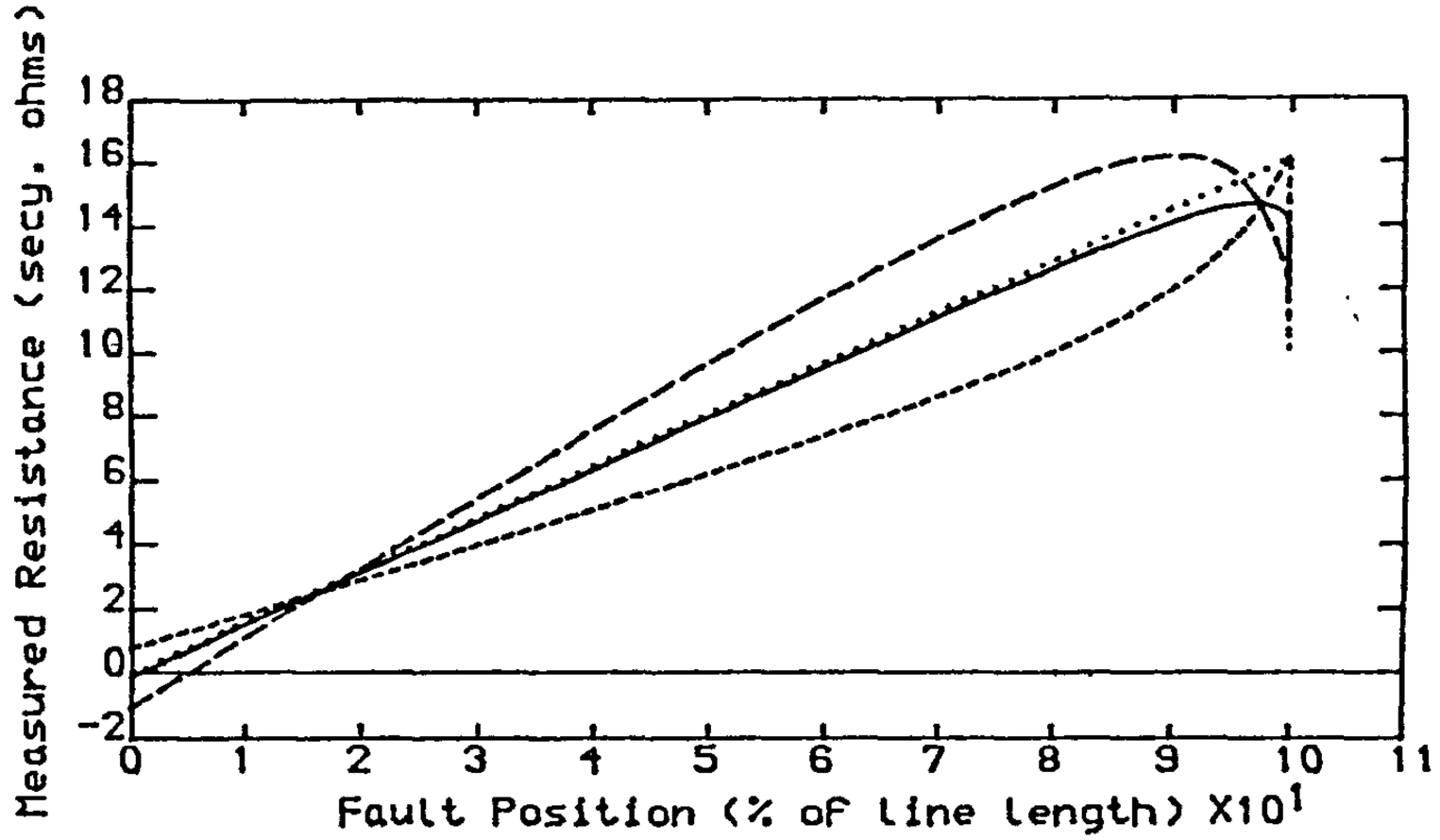

Fig 5.11.b- SE SCL=35 GVA, RE SCL=5 GVA

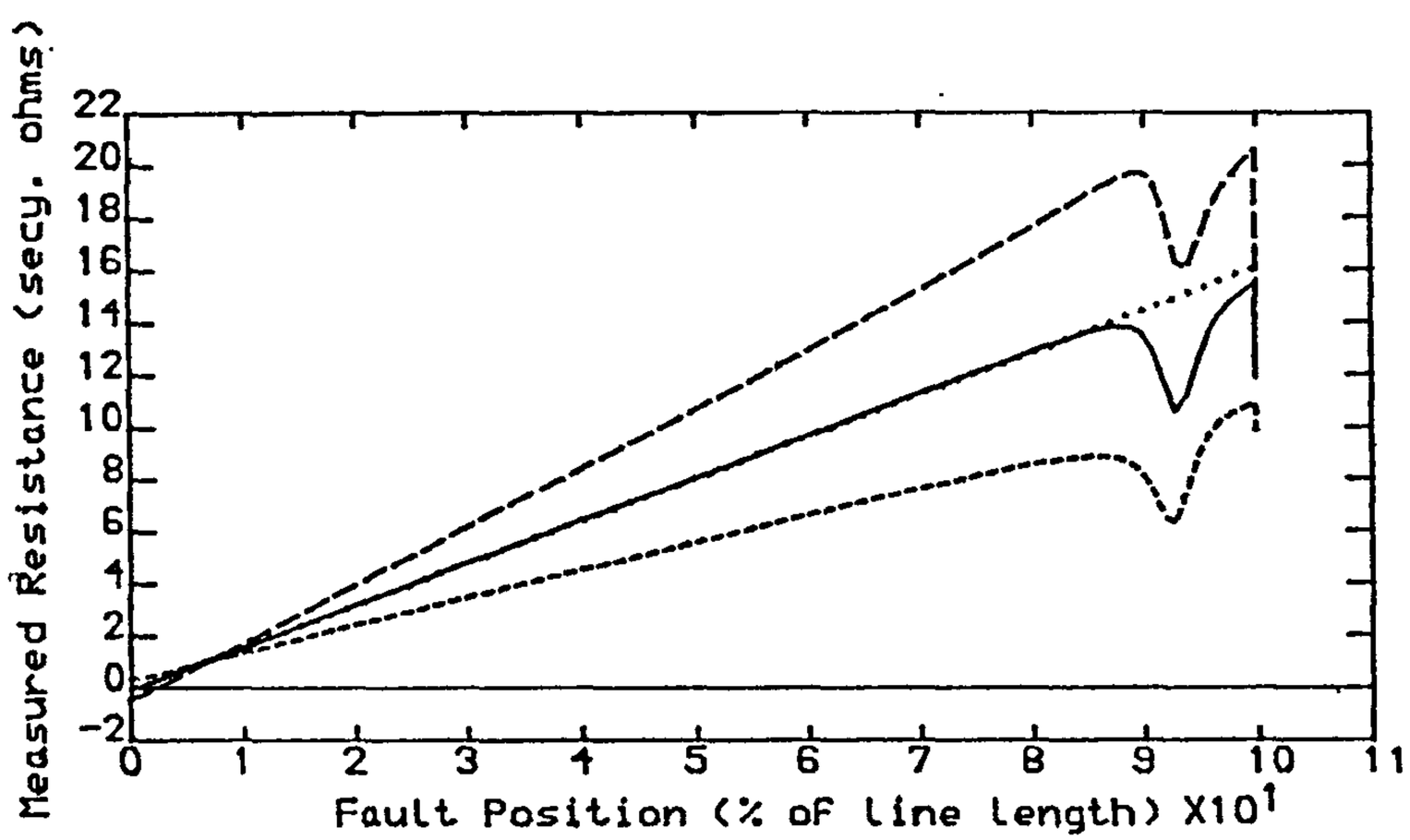

Fig 5.11.c- SE SCL=10 GVA, RE SCL=10 GVA

Fig 5.11-Measured Resistance VS Fault Position with the Complex Sound Phase Compensation Factor, $K_S=0.442\angle-9.0°$

.... Line Locus
---- Pre-Fault Load Angle=-10 deg.
——— Pre-Fault Load Angle=0 deg.
——— Pre-Fault Load Angle=+10 deg.
Line Length=300 km

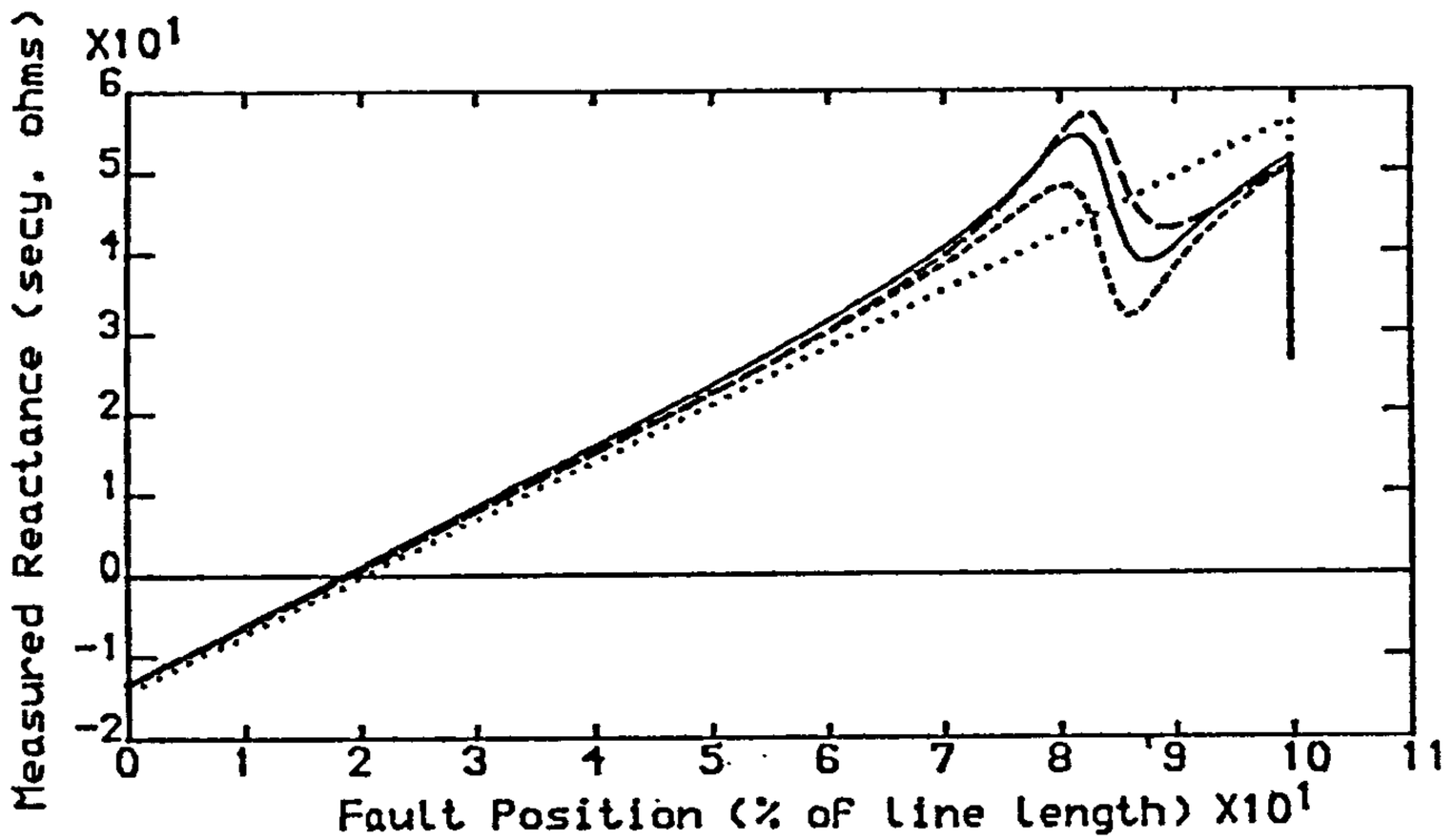

Fig 5.12.a- SE SCL=5 GVA. RE SCL=35 GVA

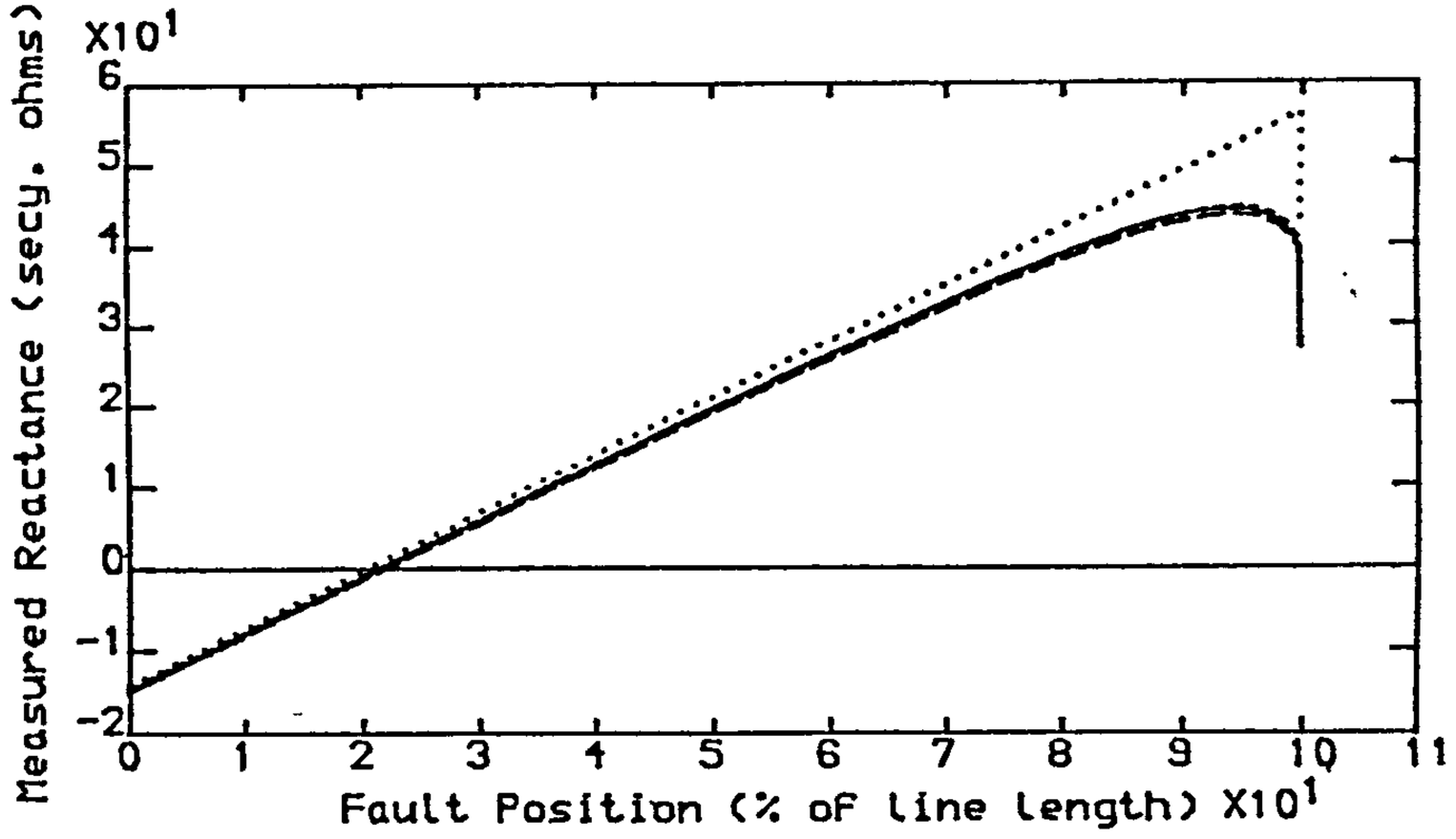

Fig 5.12.b- SE SCL=35 GVA. RE SCL=5 GVA

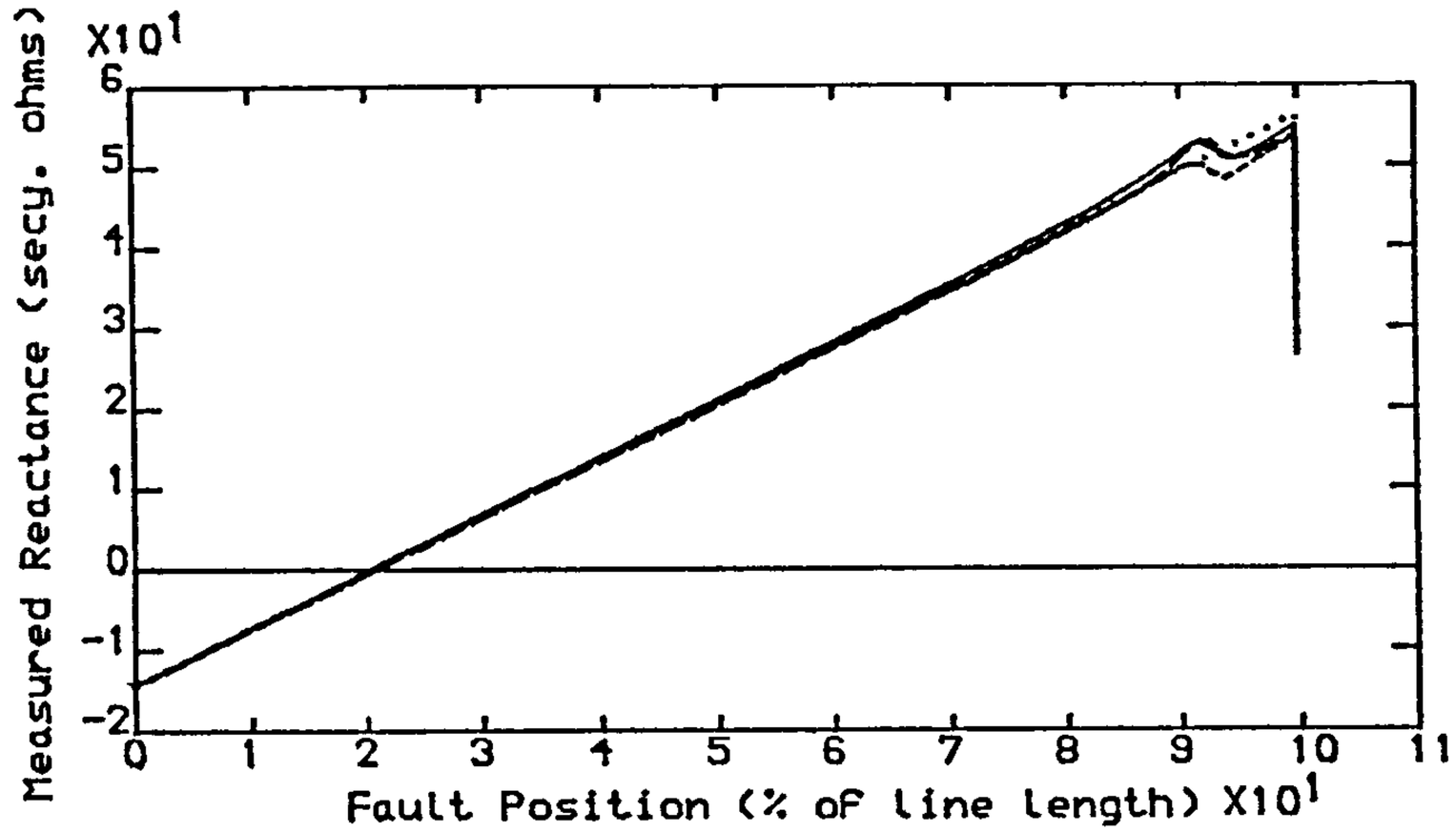

Fig 5.12.c- SE SCL=10 GVA. RE SCL=10 GVA

Fig 5.12-Measured Reactance VS Fault Position with the Complex Sound Phase Compensation Factor, $K_C=0.442\angle -9.0°$

.... Line Locus
---- Pre-Fault Load Angle=-10
——— Pre-Fault Load Angle=0
——— Pre-Fault Load Angle=+10
Line Length=300 km

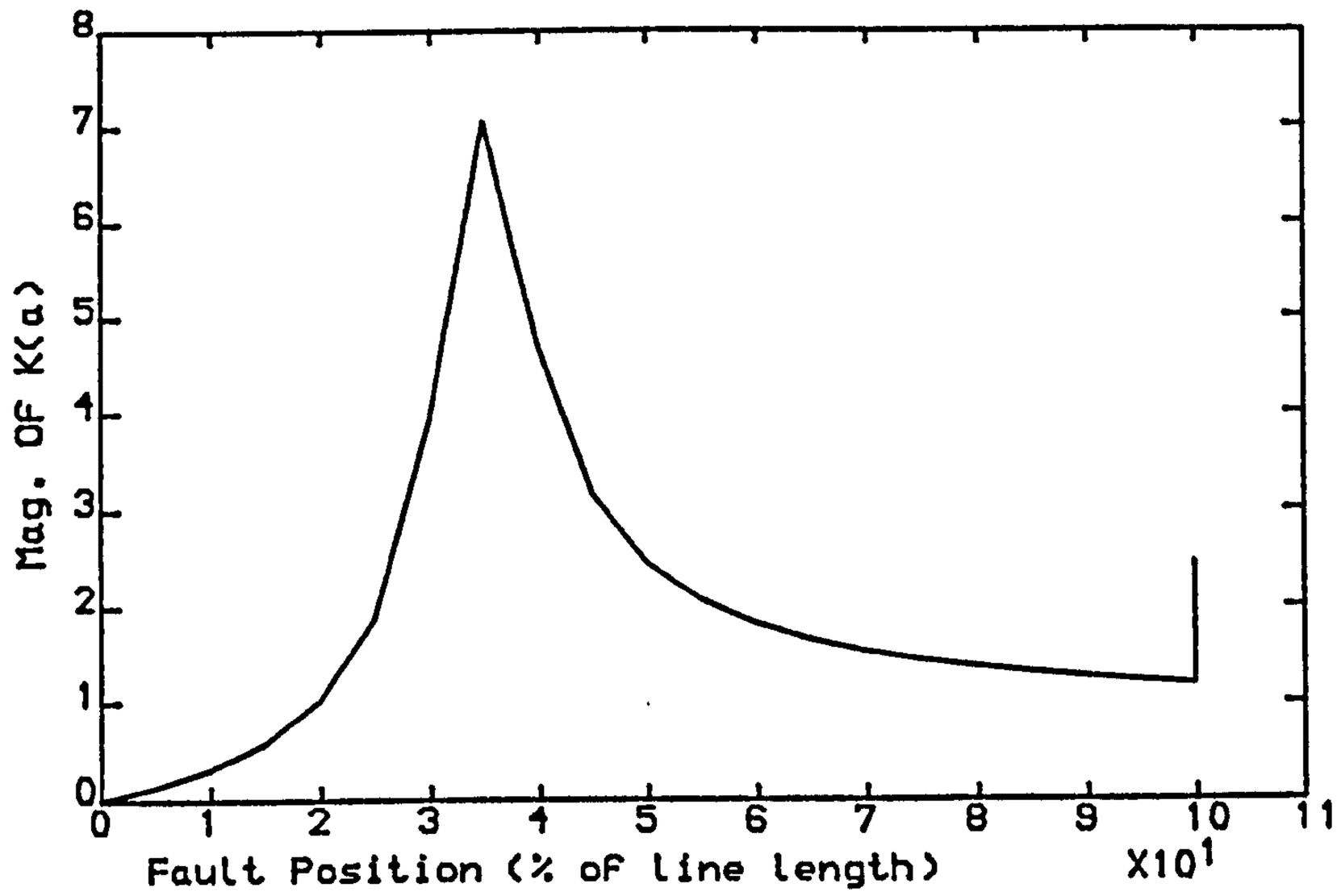

Fig 5.13.a-Variation in Mag. Of K(a) with Fault Position

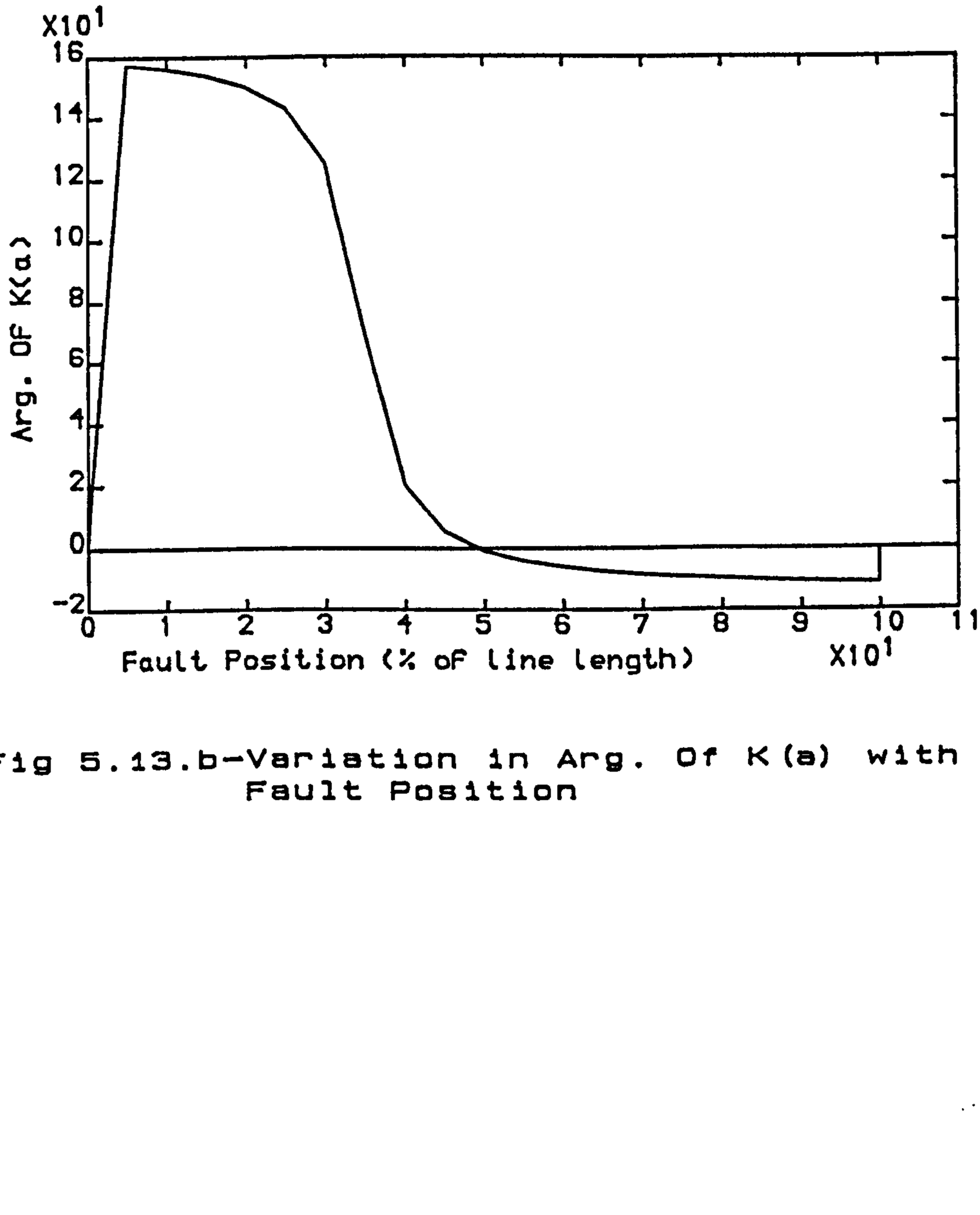

Fig 5.13.b-Variation in Arg. Of K(a) with Fault Position

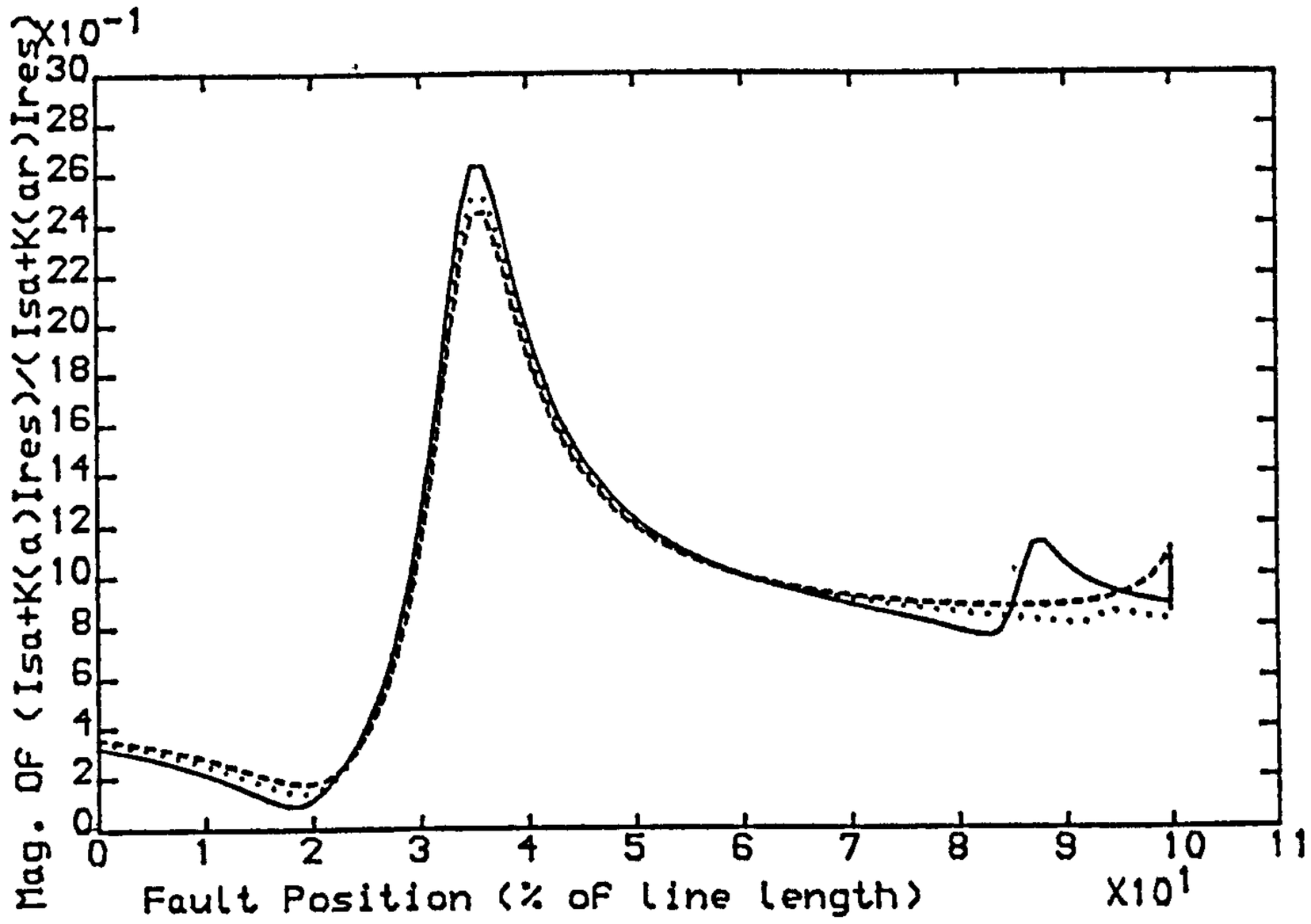

Fig 5.14.a-Variation in Mag. Of (Isa+K(a)Ires)/(Isa+K(ar)Ires) with Fault Position For Pre-Fault Load Angle Of -10 Degrees

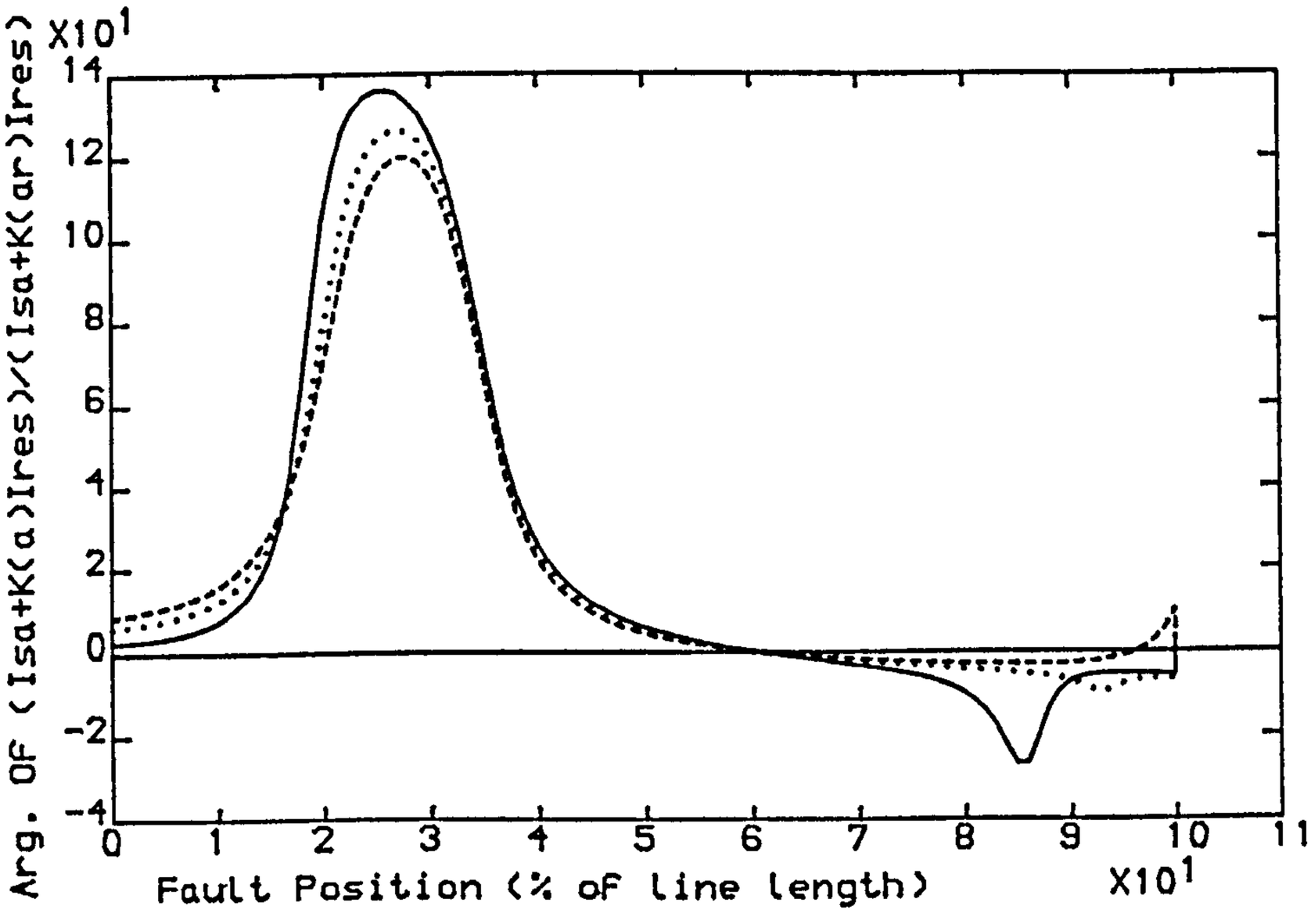

Fig 5.14.b-Variation in Arg. Of (Isa+K(a)Ires)/(Isa+K(ar)Ires) with Fault Position For Pre-Fault Load Angle Of -10 Degrees

——— SE SCL=5 GVA, RE SCL=35 GVA
---- SE SCL=35 GVA, RE SCL=5 GVA
.... SE SCL=10 GVA, RE SCL=10 GVA
Line Length =300 km

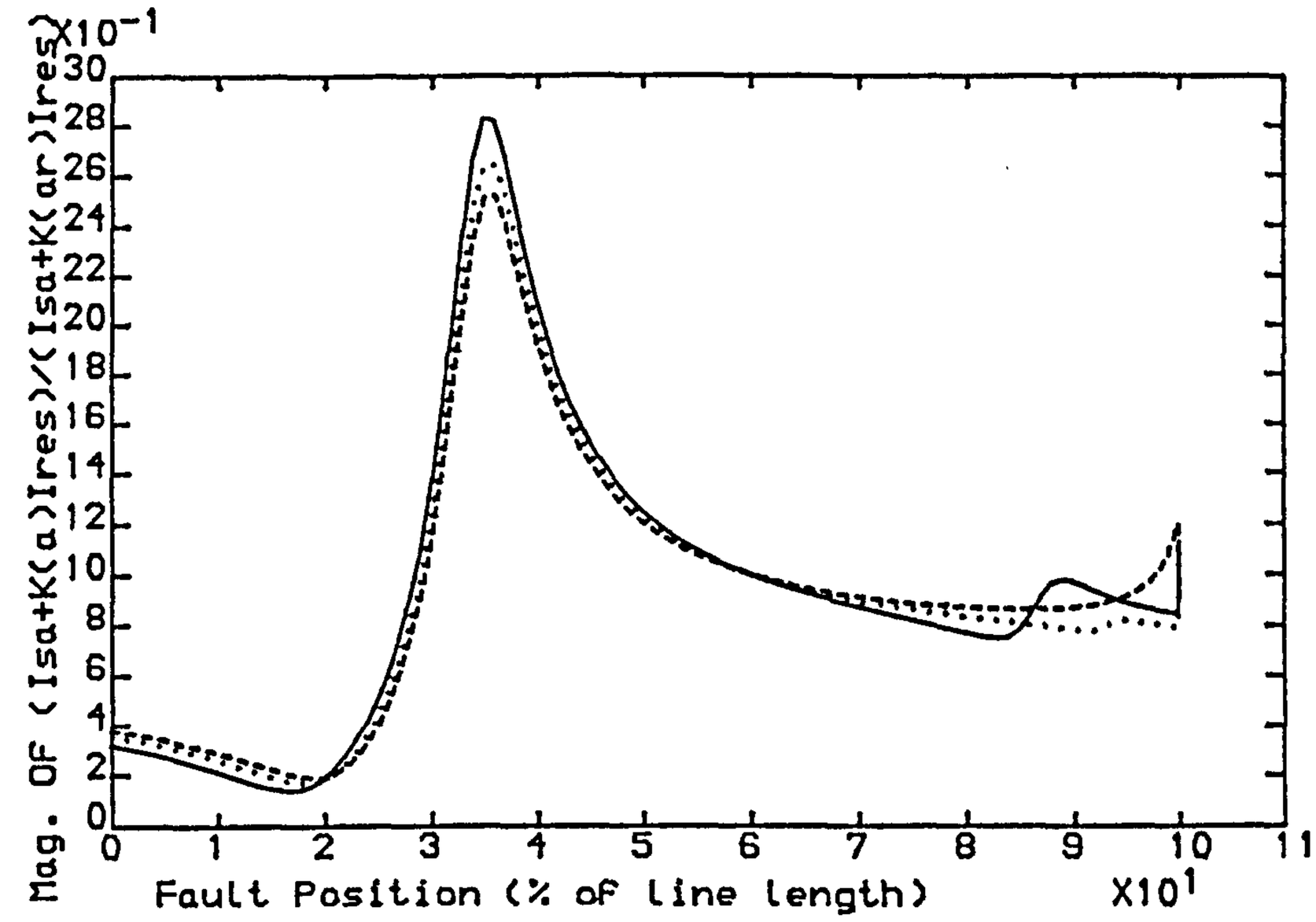

Fig 5.15.a-Variation in Mag. Of
(Isa+K(a) Ires) / (Isa+K(ar) Ires) with
Fault Position For Pre-Fault
Load Angle Of 0 Degrees

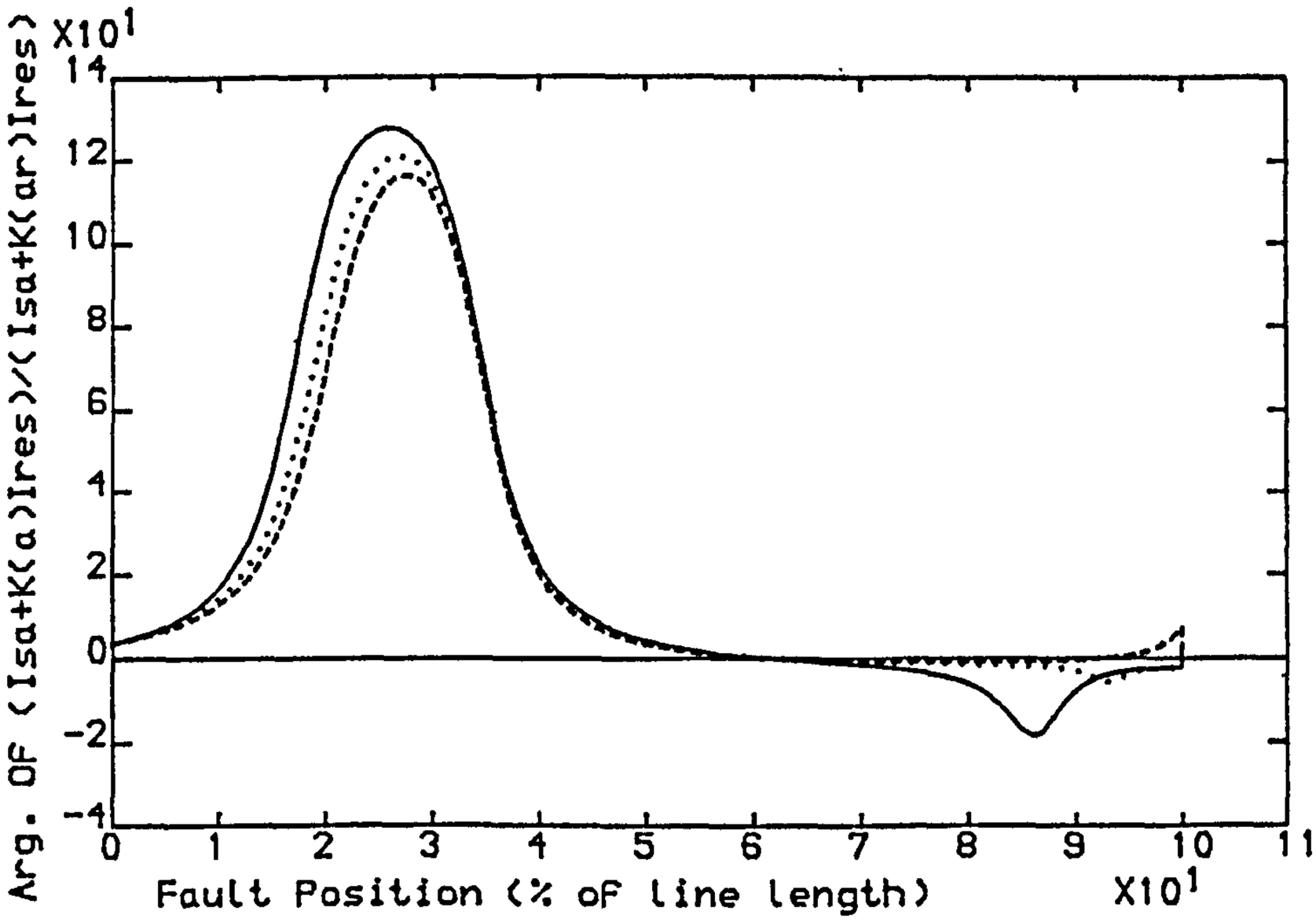

Fig 5.15.b-Variation in Arg. Of
(Isa+K(a) Ires) / (Isa+K(ar) Ires) with
Fault Position For Pre-Fault
Load Angle Of 0 Degrees

——— SE SCL=5 GVA, RE SCL=35 GVA
----- SE SCL=35 GVA, RE SCL=5 GVA
.... SE SCL=10 GVA, RE SCL=10 GVA
Line Length =300 km

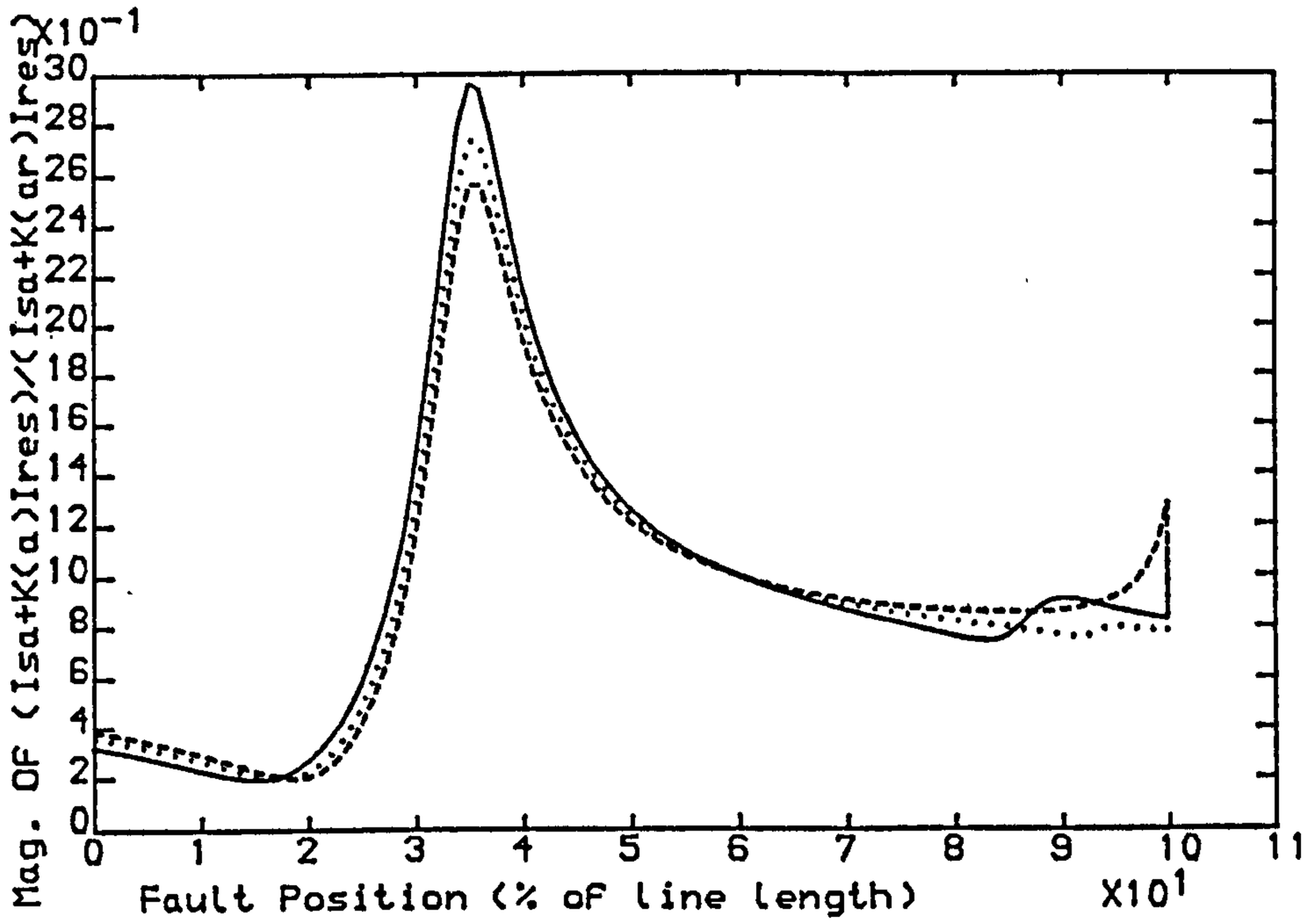

Fig 5.16.a-Variation in Mag. Of (Isa+K(a) Ires) / (Isa+K(ar) Ires) with Fault Position For Pre-Fault Load Angle Of +10 Degrees

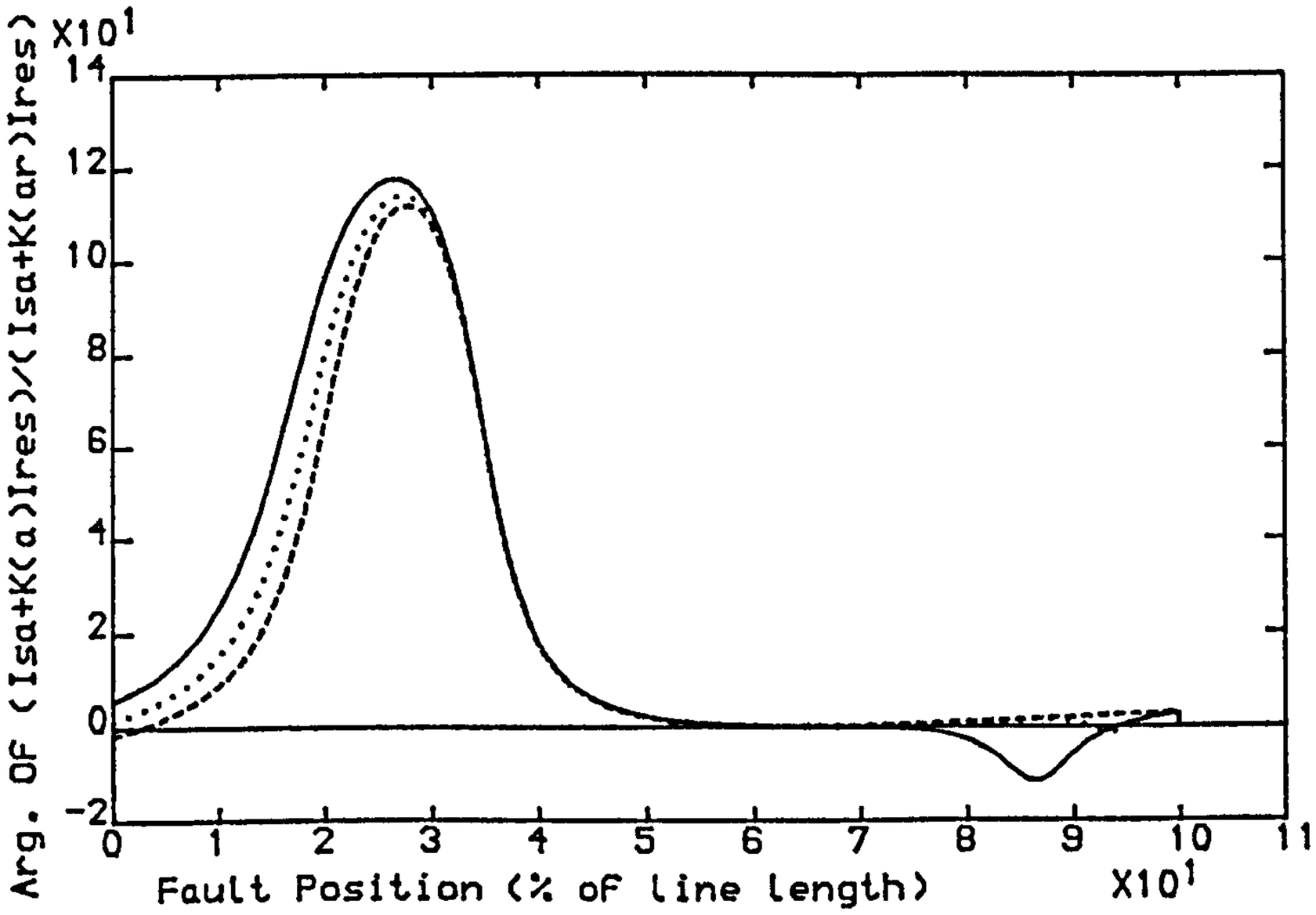

Fig 5.16.b-Variation in Arg. Of (Isa+K(a) Ires) / (Isa+K(ar) Ires) with Fault Position For Pre-Fault Load Angle Of +10 Degrees

——— SE SCL=5 GVA, RE SCL=35 GVA
---- SE SCL=35 GVA, RE SCL=5 GVA
.... SE SCL=10 GVA, RE SCL=10 GVA
Line Length =300 km

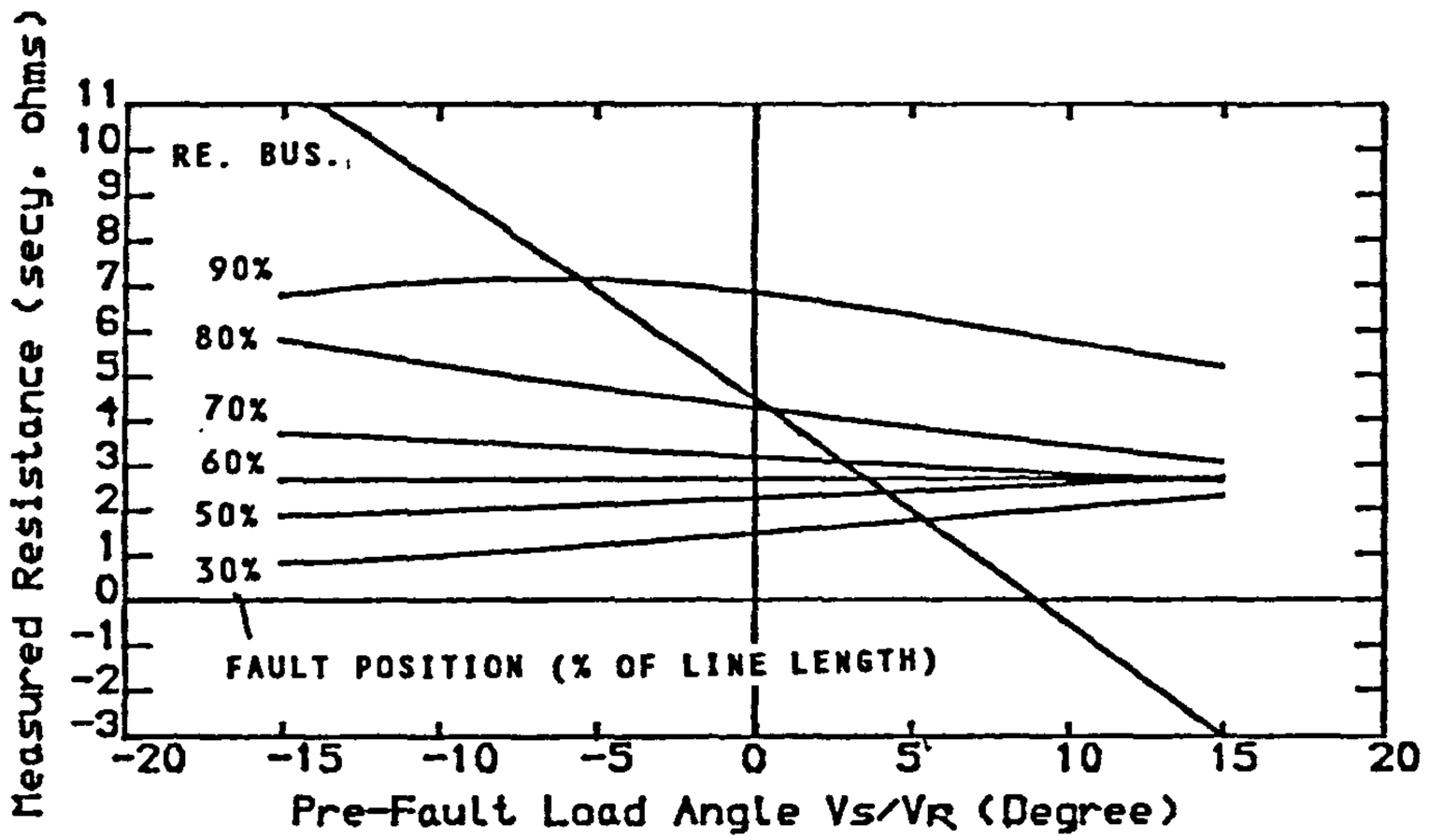

Fig 5.17.a- SE SCL=5 GVA, RE SCL=35 GVA

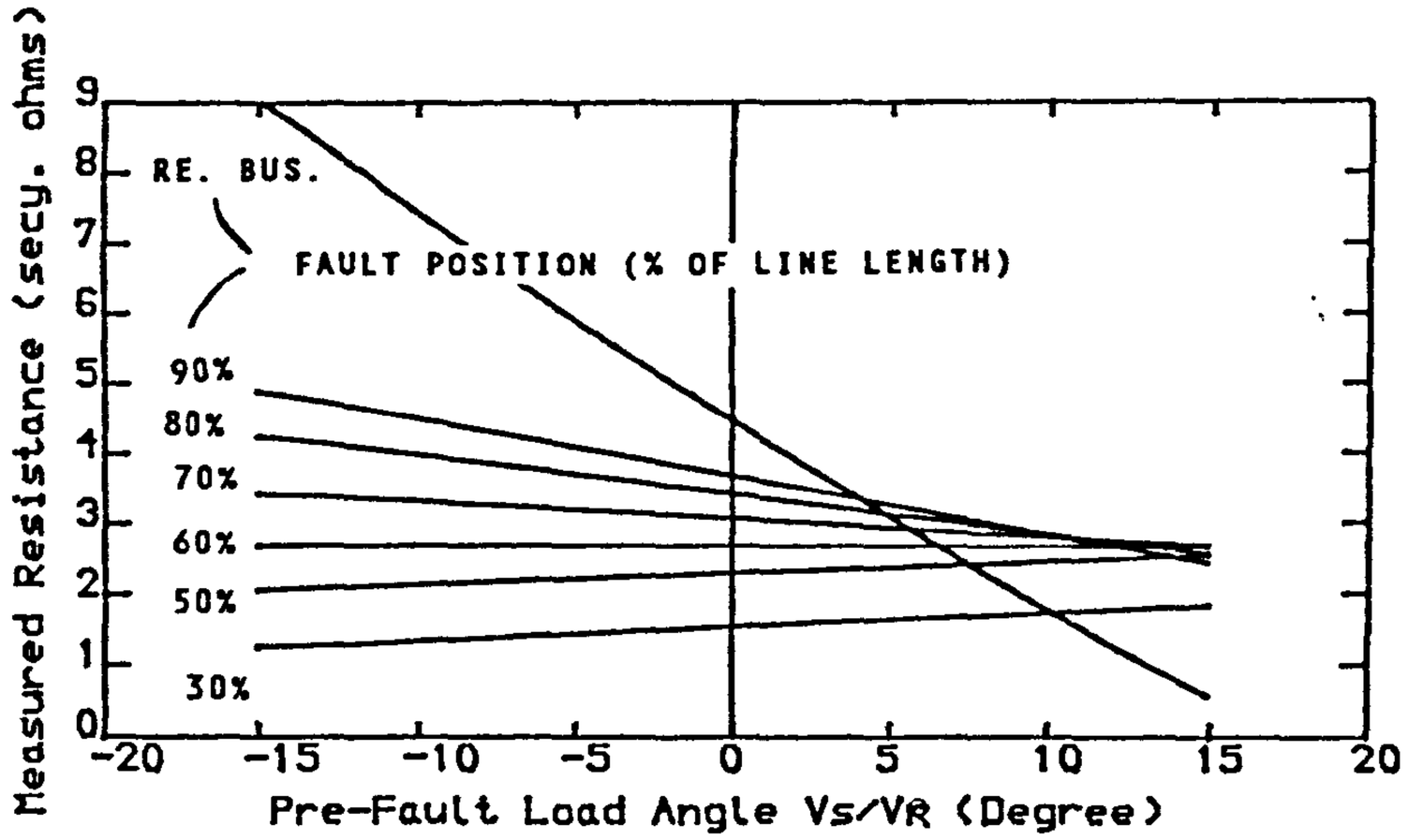

Fig 5.17.b- SE SCL=35 GVA, RE SCL=5 GVA

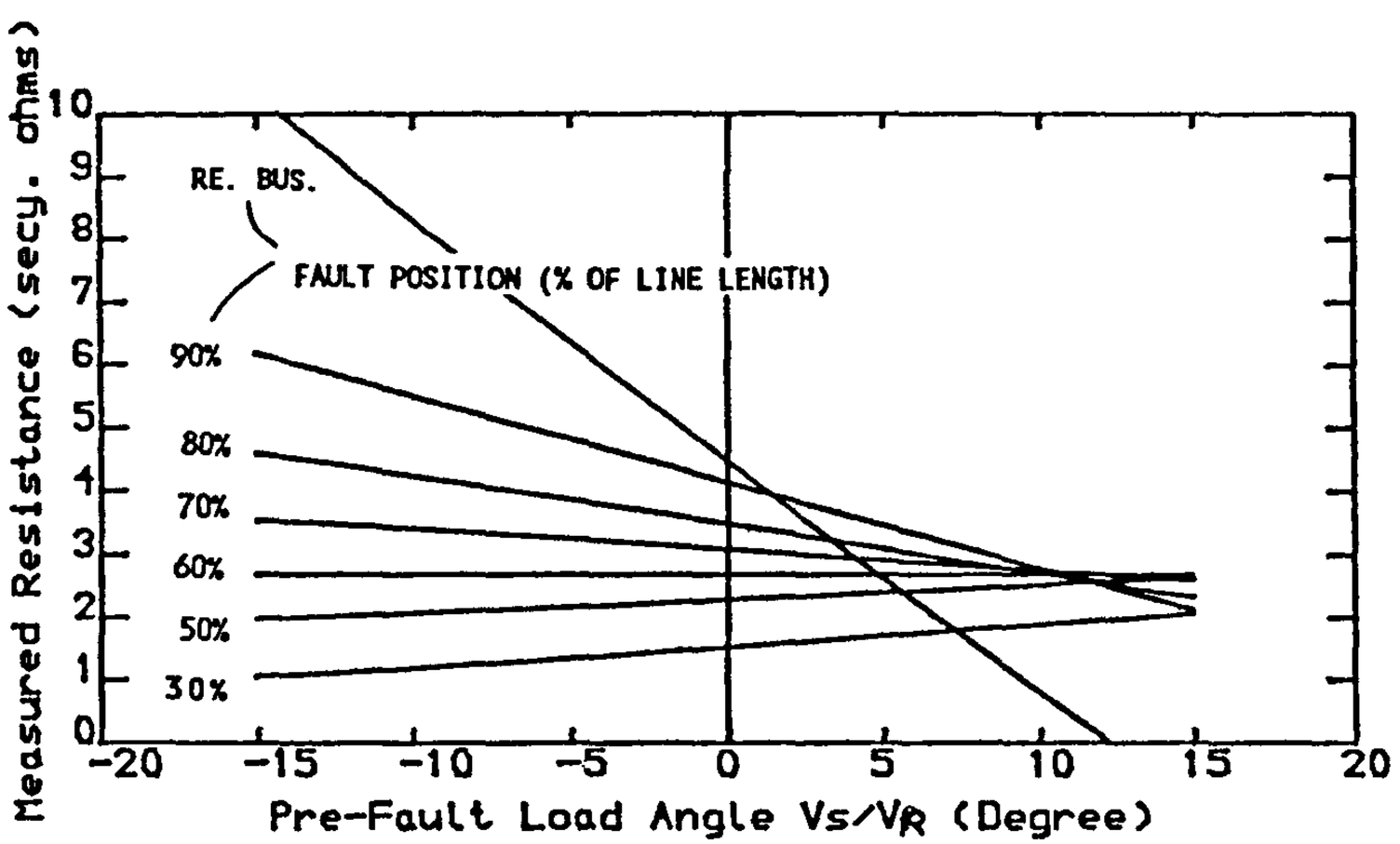

Fig 5.17.c- SE SCL=10 GVA, RE SCL=10 GVA

Fig 5.17-Measured Resistance VS Pre-fault Load, with the New Residual Compensation Factor, $K_{\alpha r}=1.82\angle -4.5°$, $\alpha r=0.6$ of line length.

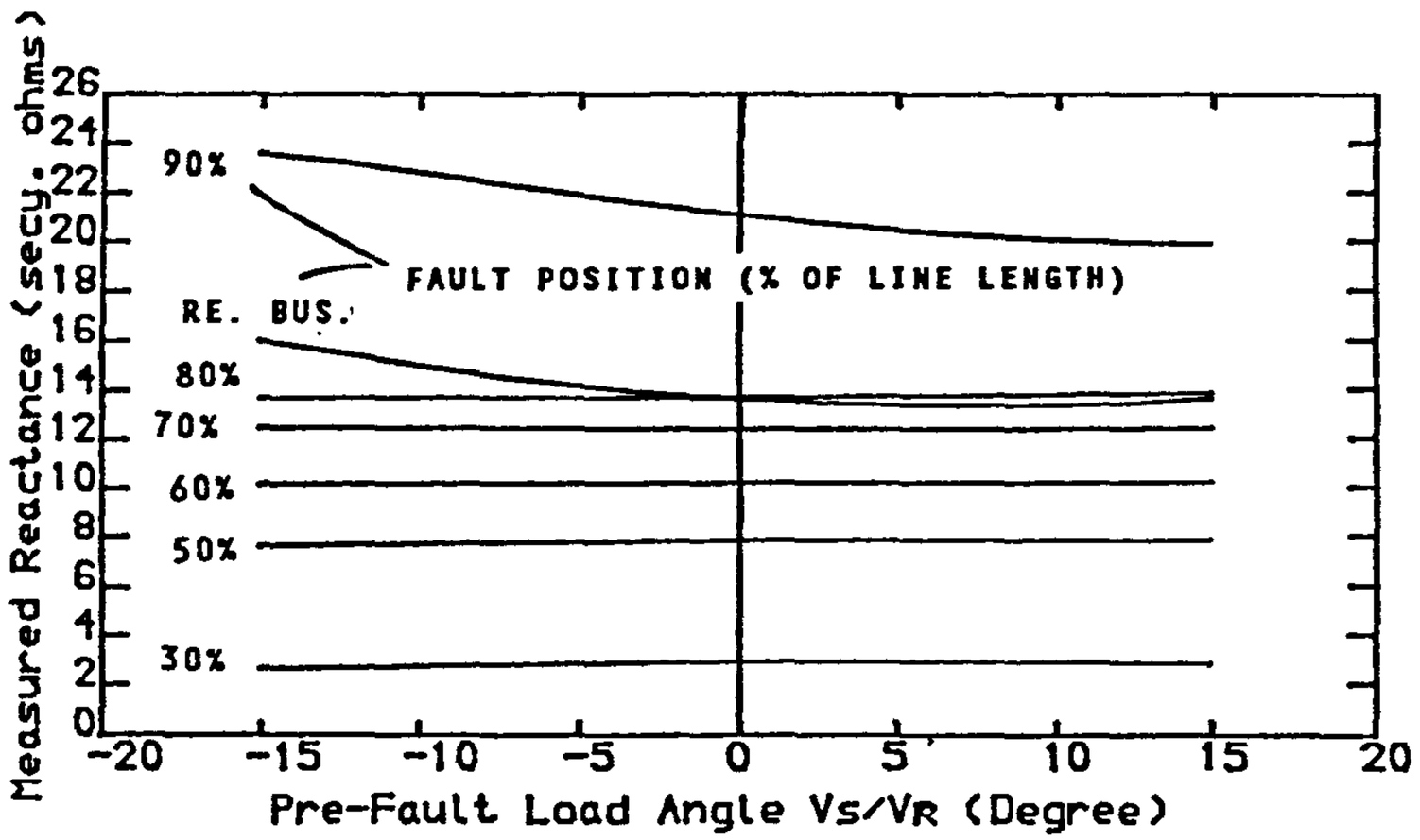

Fig 5.18.a- SE SCL=5 GVA, RE SCL=35 GVA

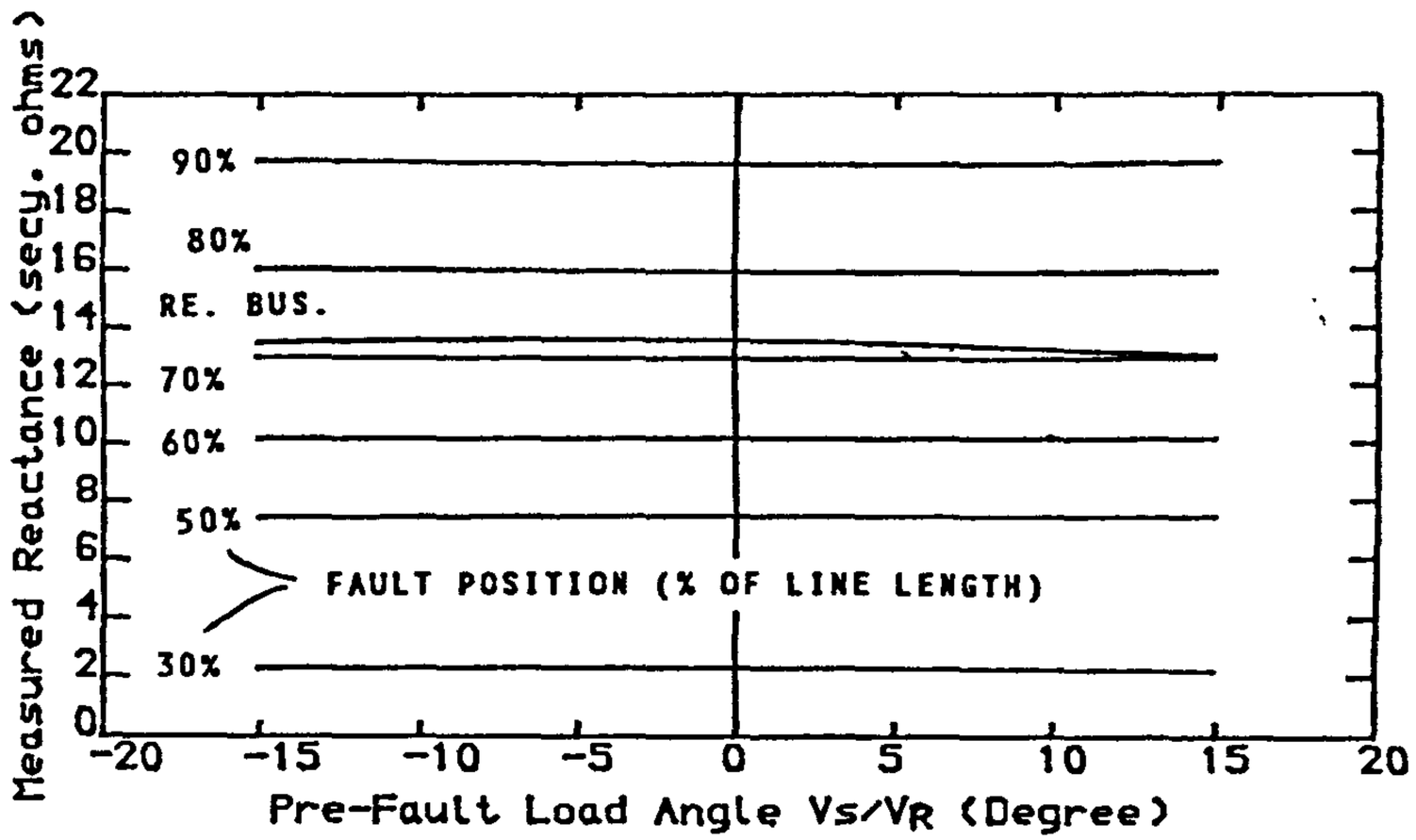

Fig 5.18.b- SE SCL=35 GVA, RE SCL=5 GVA

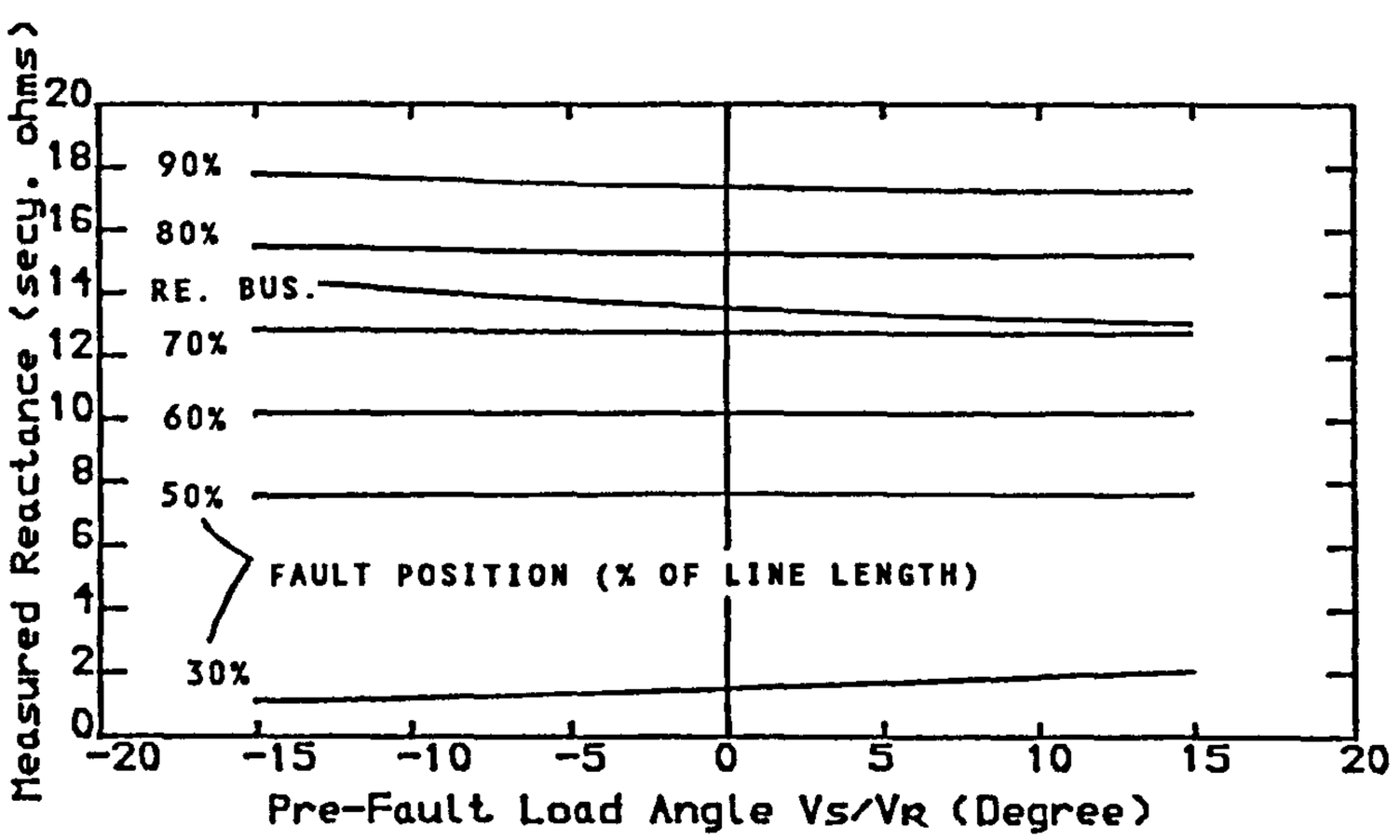

Fig 5.18.c- SE SCL=10 GVA, RE SCL=10 GVA

Fig 5.18-Measured Reactance VS Pre-fault Load, with the New Residual Compensation Factor, $K_{\alpha r}=1.82\angle -4.5°$, $\alpha r=0.6$ of line length.

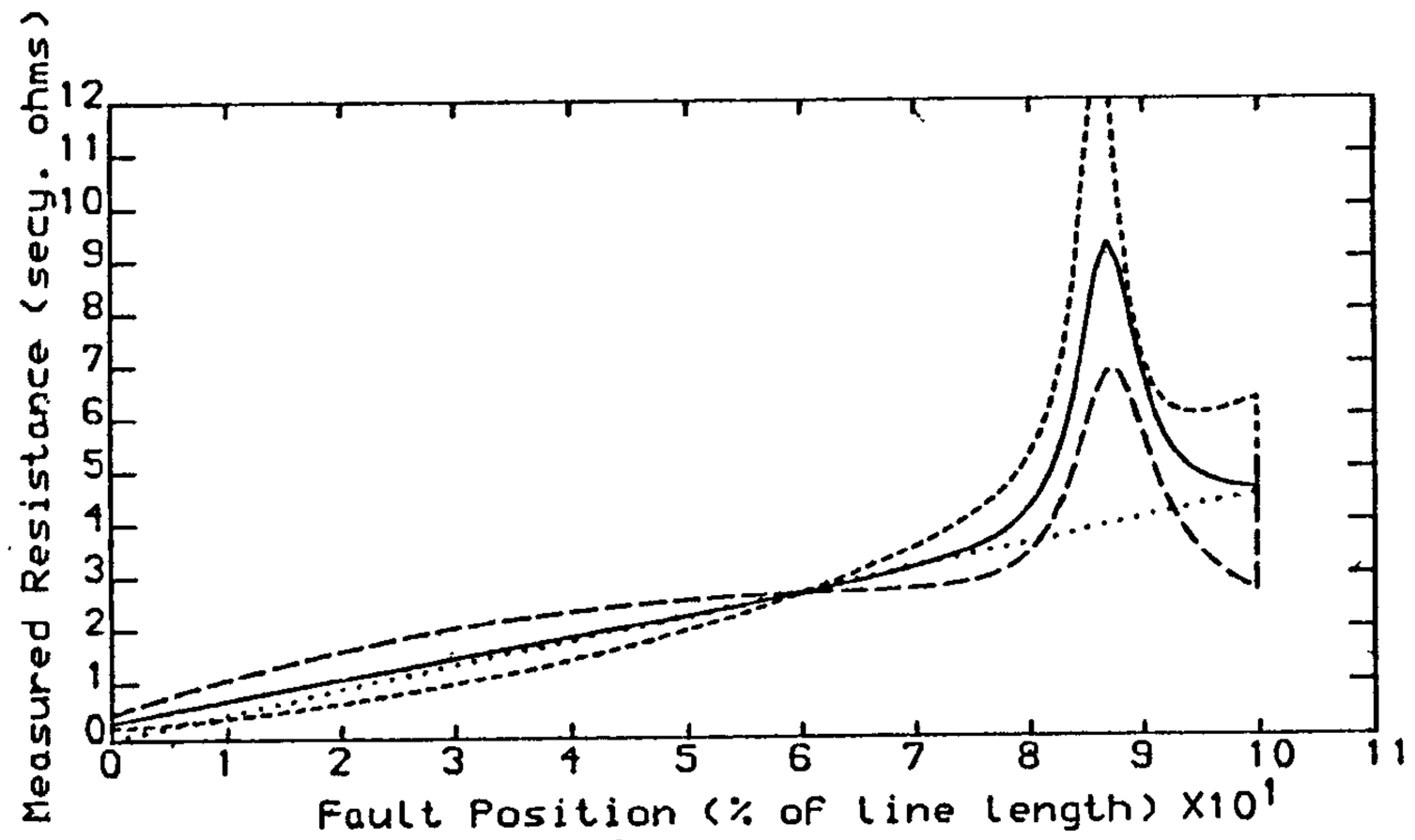

Fig 5.19.a- SE SCL=5 GVA, RE SCL=35 GVA

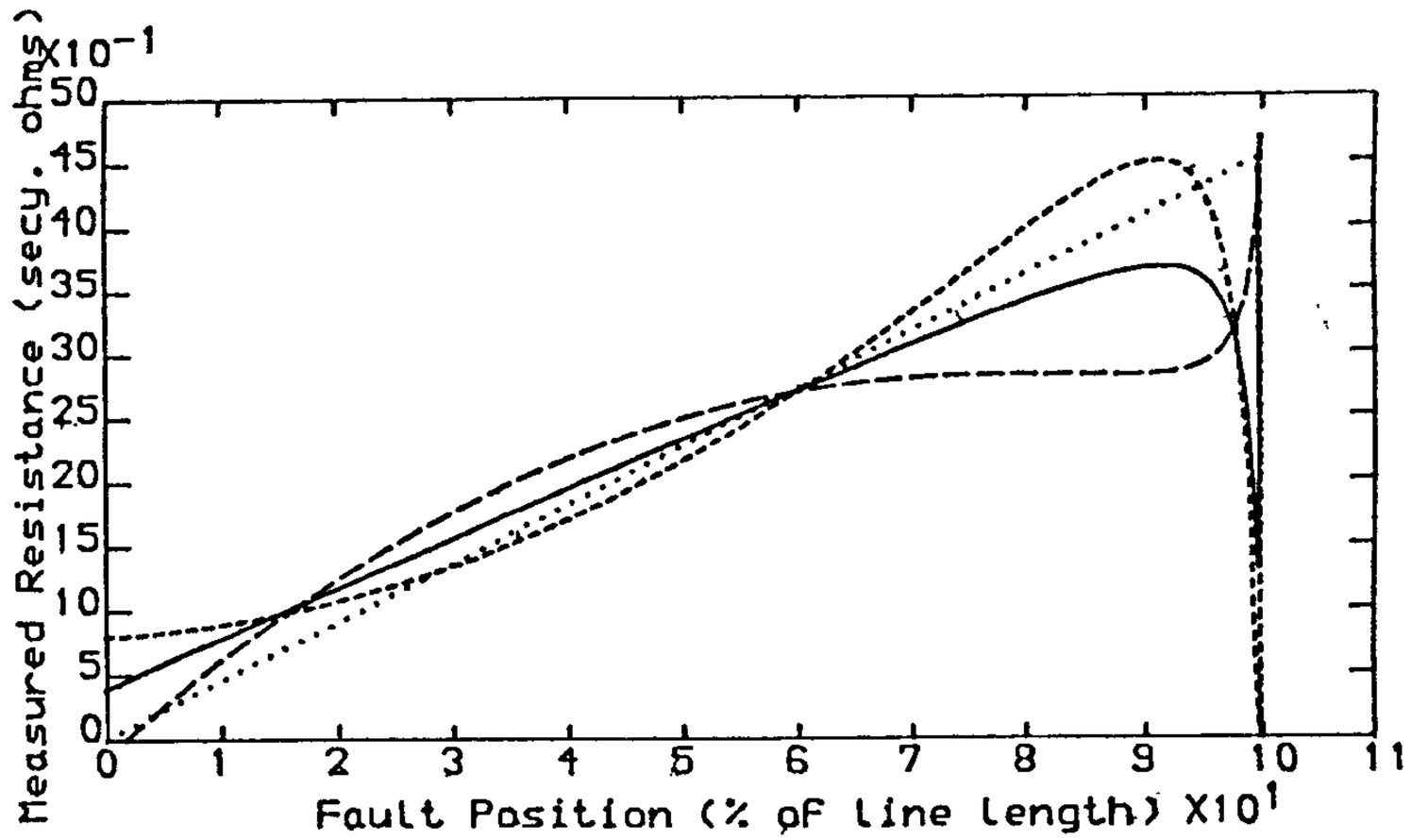

Fig 5.19.b- SE SCL=35 GVA, RE SCL=5 GVA

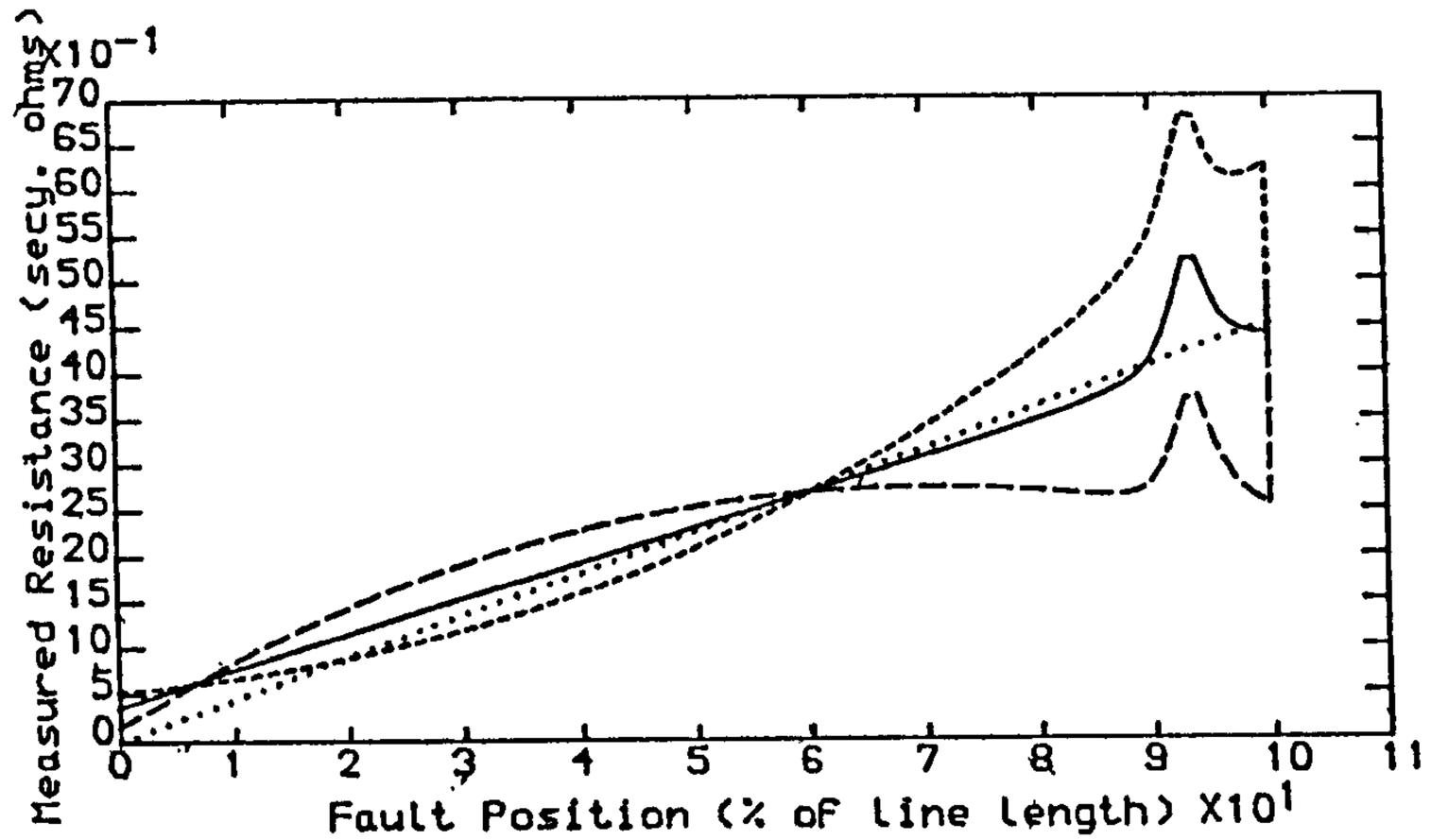

Fig 5.19.c- SE SCL=10 GVA, RE SCL=10 GVA

Fig 5.19-Measured Resistance VS Fault Position with the New Residual Compensation Factor, $K_{\alpha r}=1.82\angle -4.5°$, $\alpha r=0.6$ of line length.

.... Line Locus
---- Pre-Fault Load Angle=-10 deg.
——— Pre-Fault Load Angle=0 deg.
—— Pre-Fault Load Angle=+10 deg.
Line Length=300 km

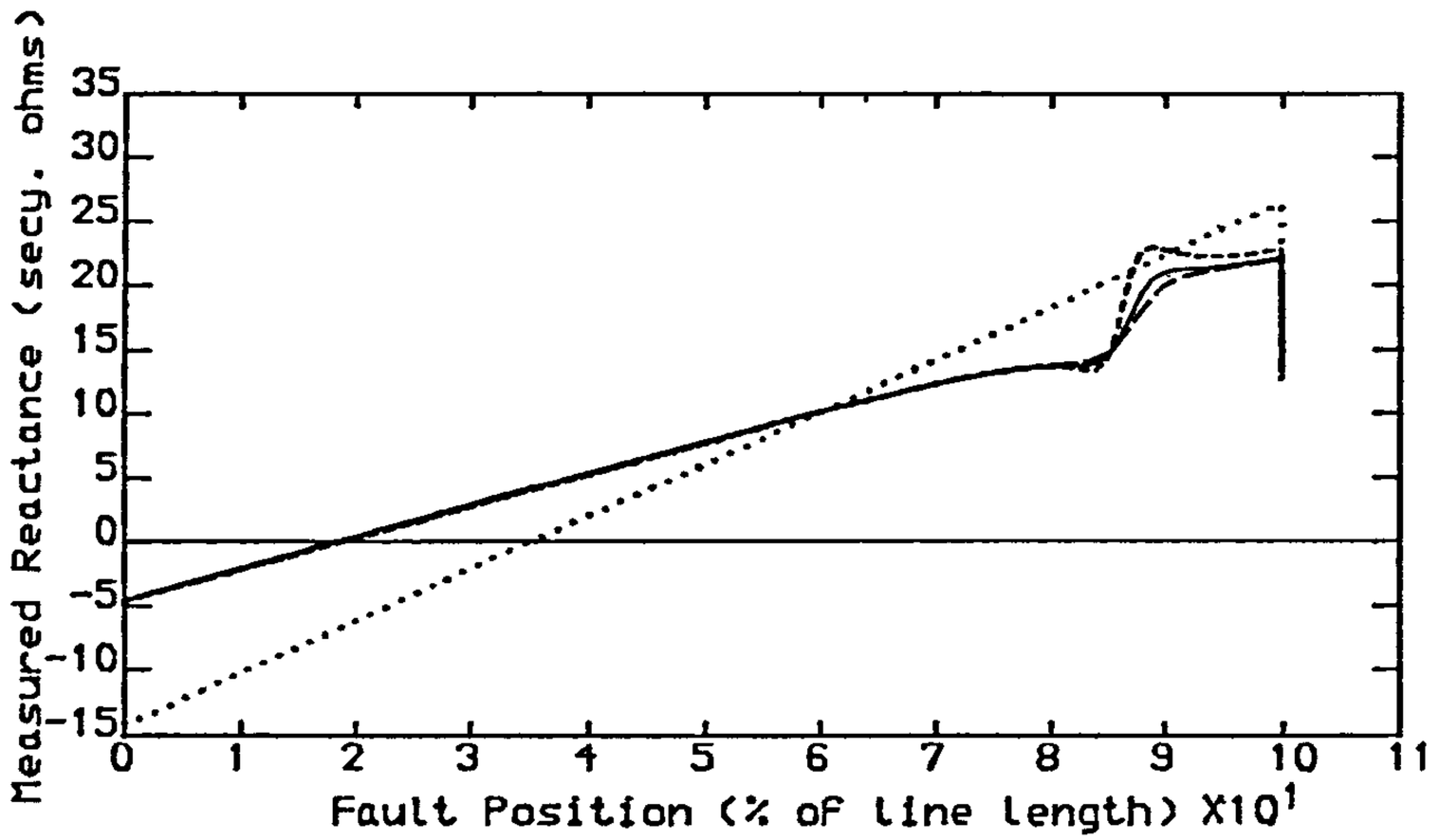

Fig 5.20.a- SE SCL=5 GVA, RE SCL=35 GVA

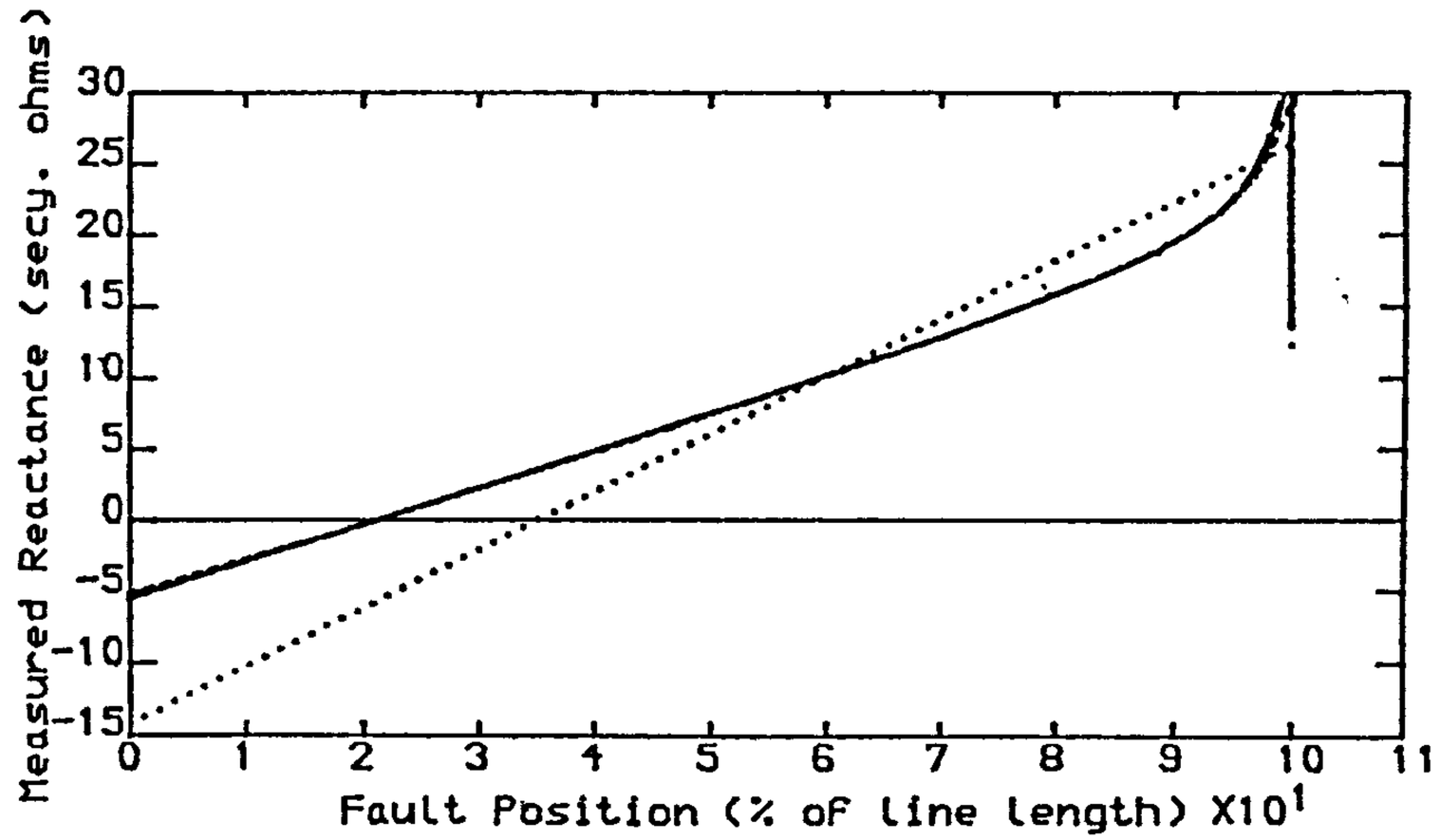

Fig 5.20.b- SE SCL=35 GVA, RE SCL=5 GVA

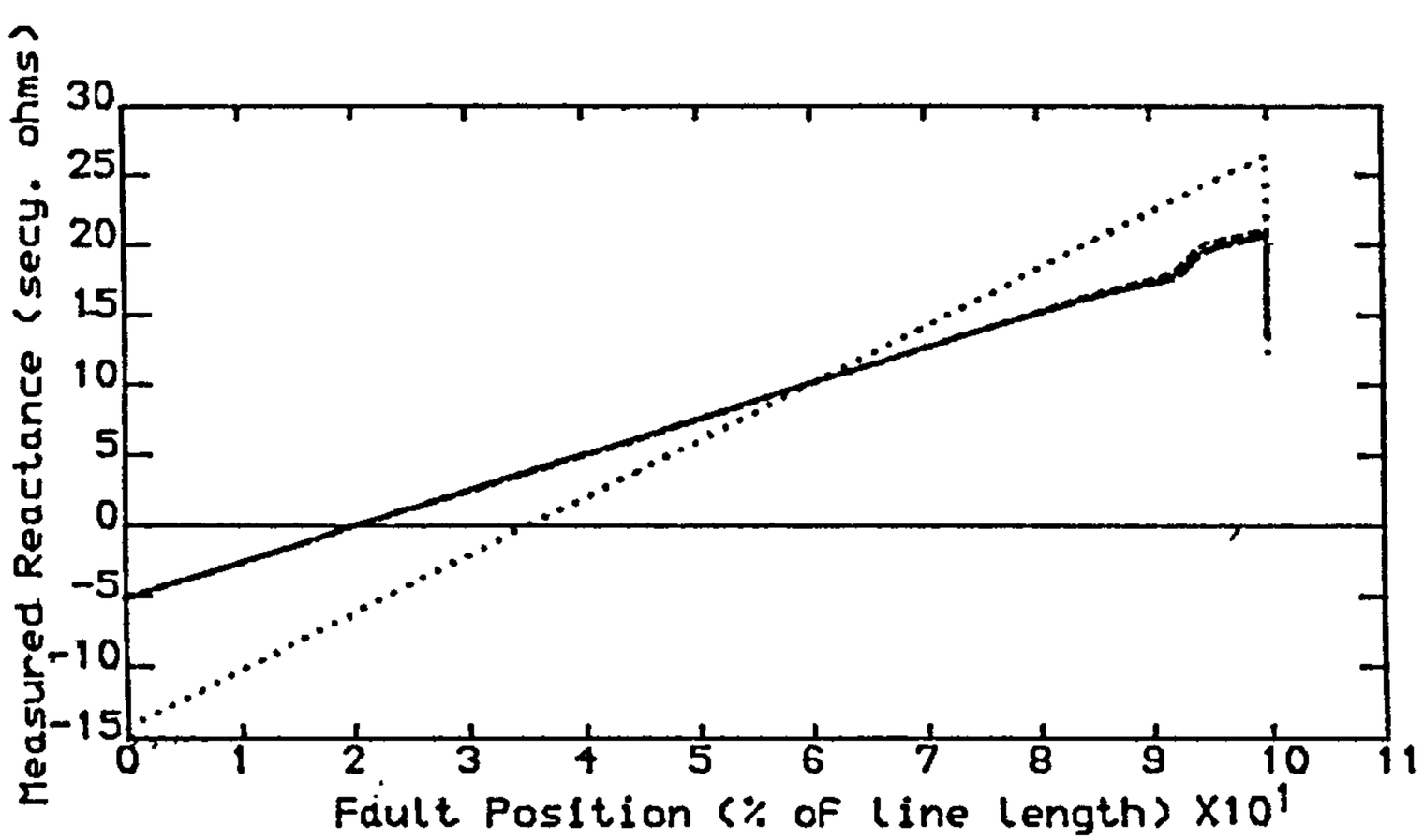

Fig 5.20.c- SE SCL=10 GVA, RE SCL=10 GVA

Fig 5.20-Measured Reactance VS Fault Position with the New Residual Compensation Factor, $K_{\alpha r}=1.82\angle -4.5°$, $\alpha r=0.6$ of line length.

.... Line Locus
---- Pre-Fault Load Angle=-10
——— Pre-Fault Load Angle=0
—— Pre-Fault Load Angle=+10
Line Length=300 km

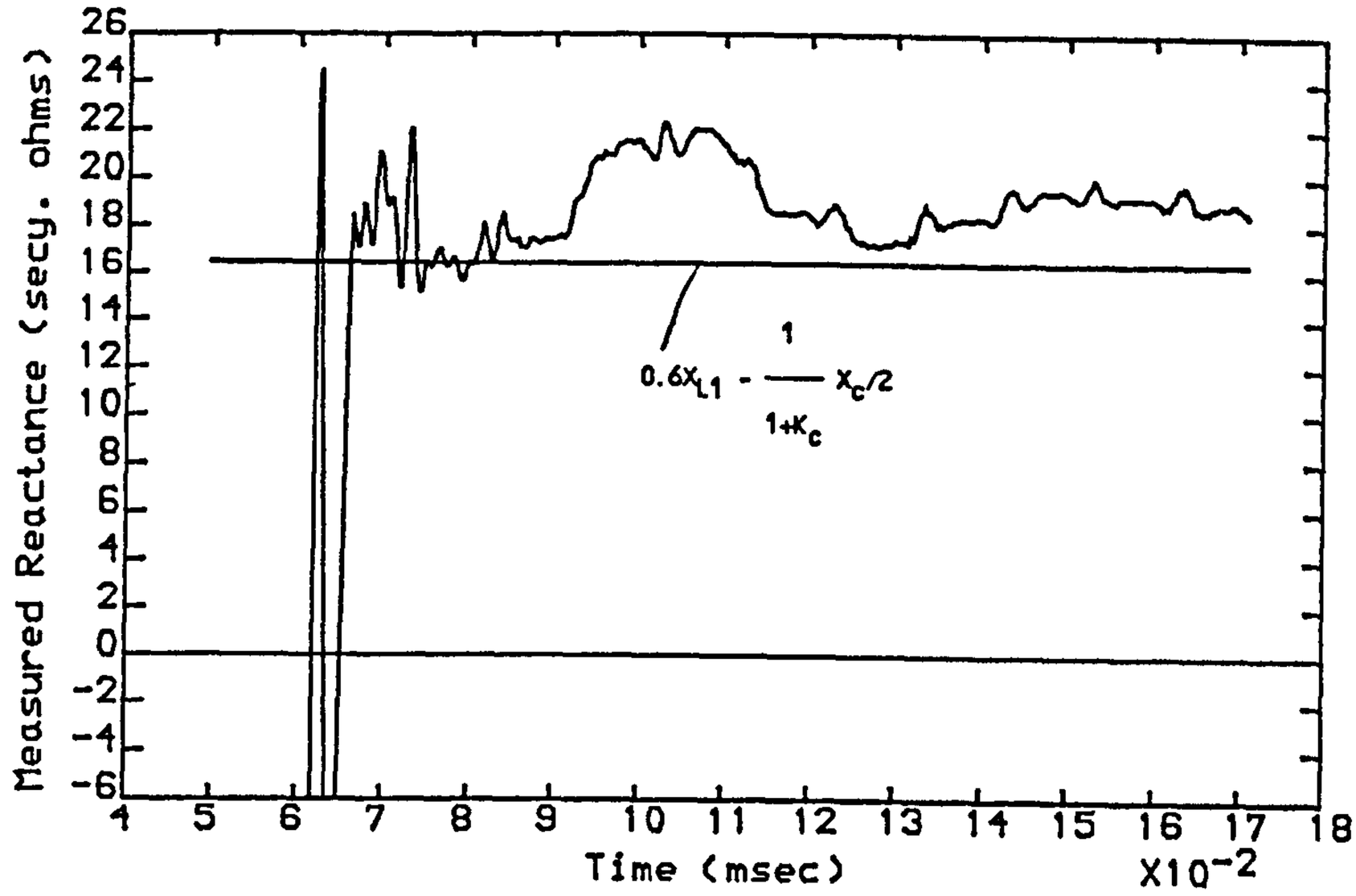

Fig 5.21.a-Measured Reactance vs Time with Complex Kc (CRCF)

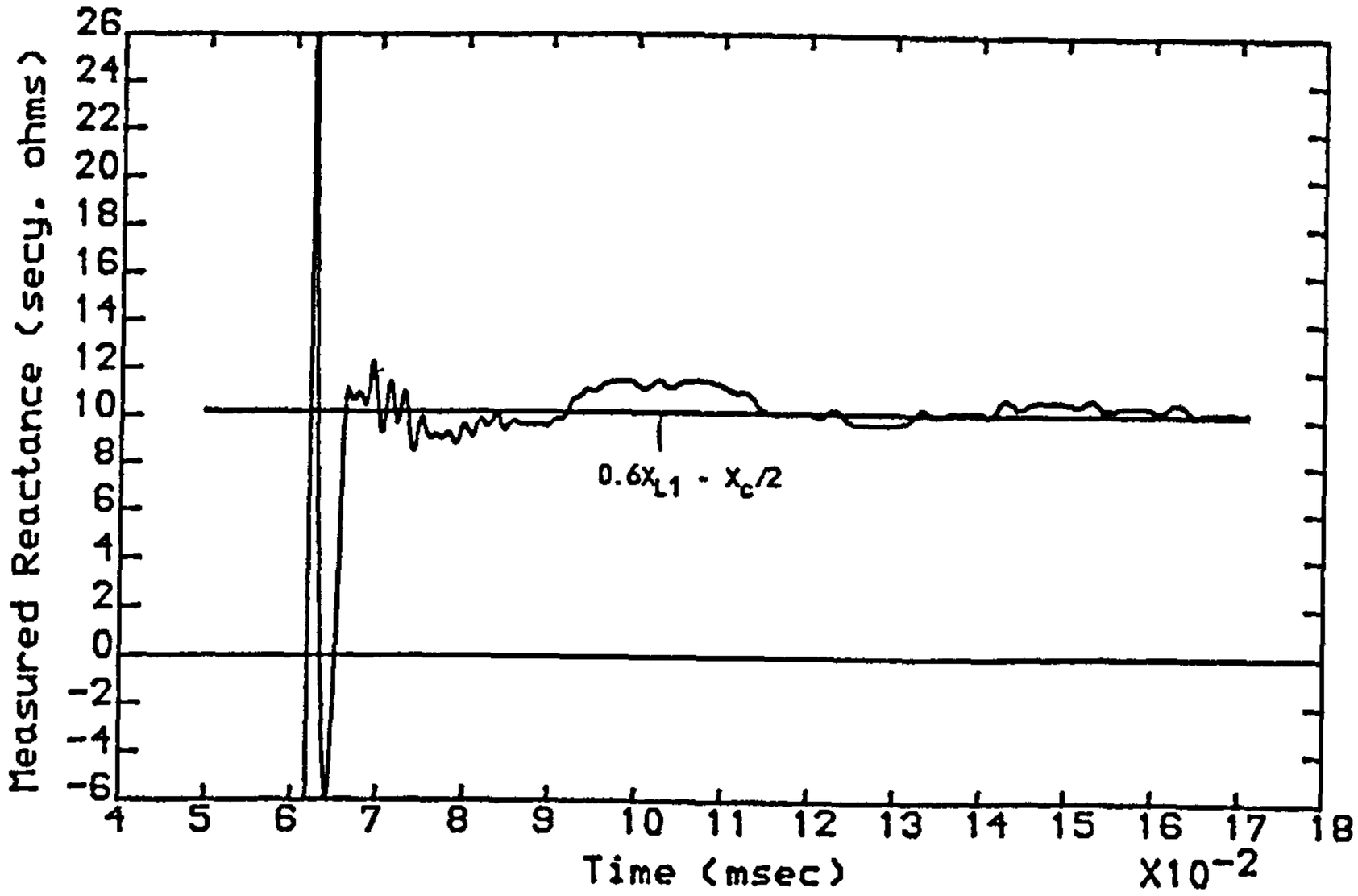

Fig 5.21.b-Measured Reactance vs Time with Kαr (NRCF)

SE SCL=5 GVA, RE SCL=35 GVA,
fault at 60% of line length
$K_c = 0.78 \angle -13.5°$
$K_{\alpha r} = 1.82 \angle -4.5°$

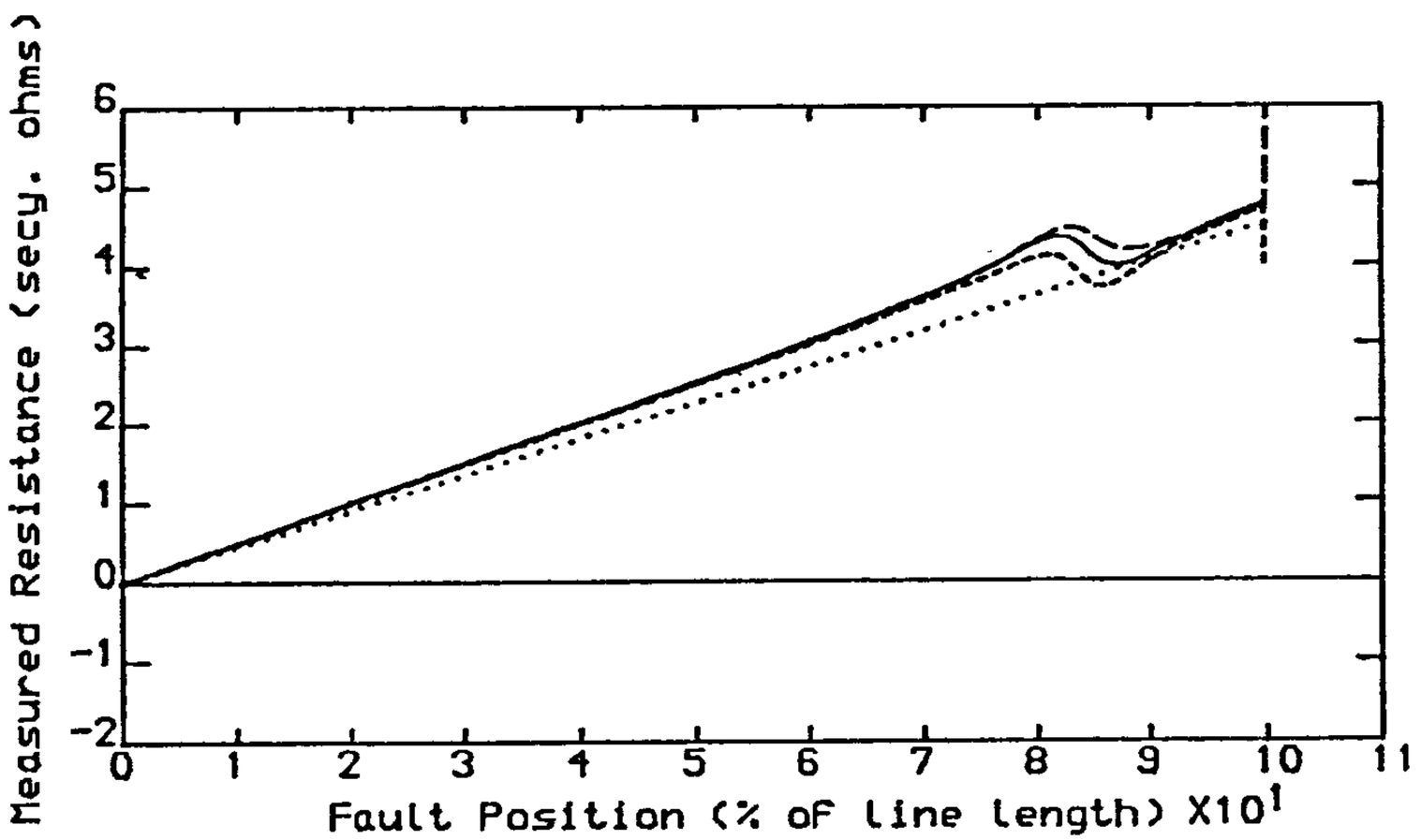

Fig 5.22.a- SE SCL=5 GVA, RE SCL=35 GVA

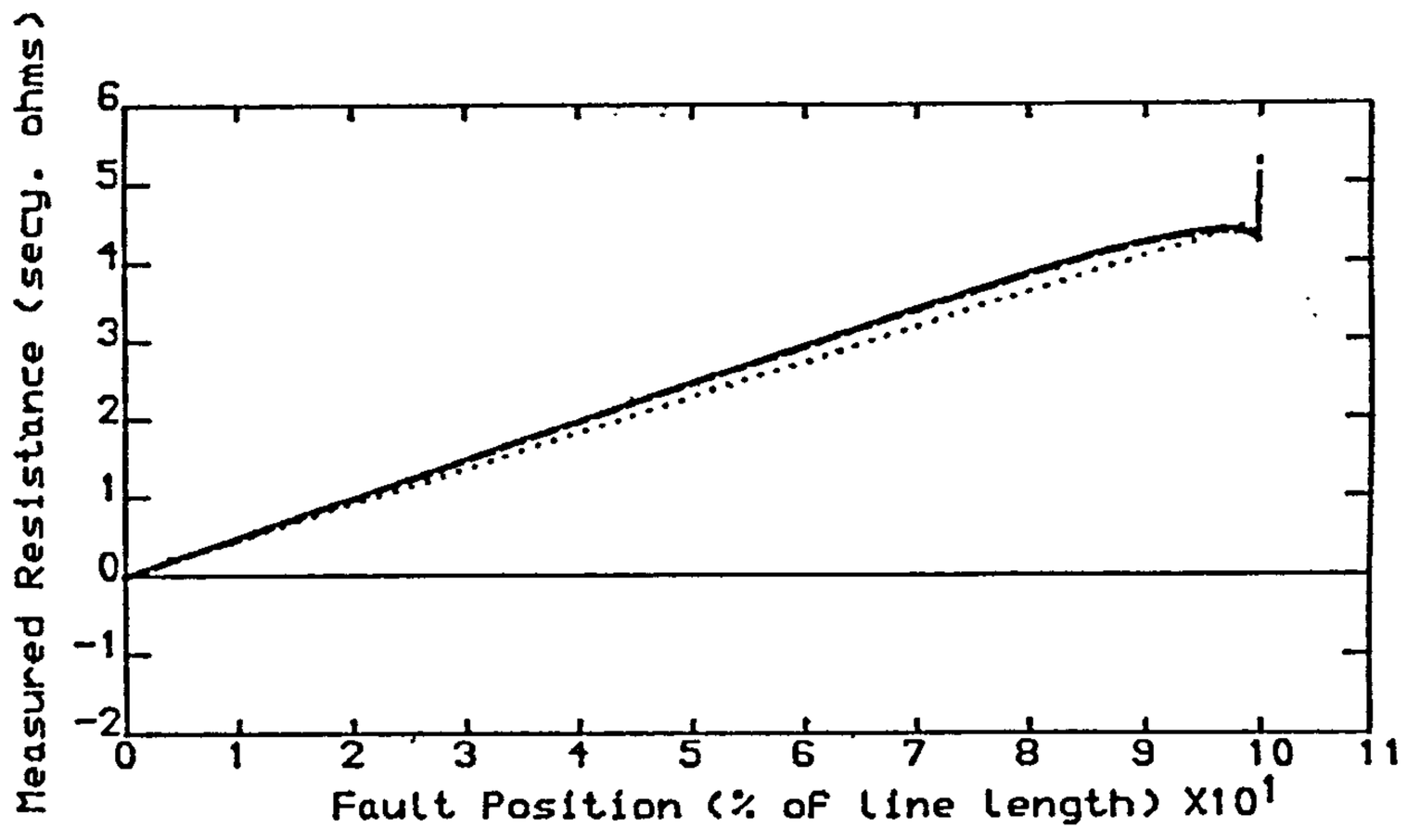

Fig 5.22.b- SE SCL=35 GVA, RE SCL=5 GVA

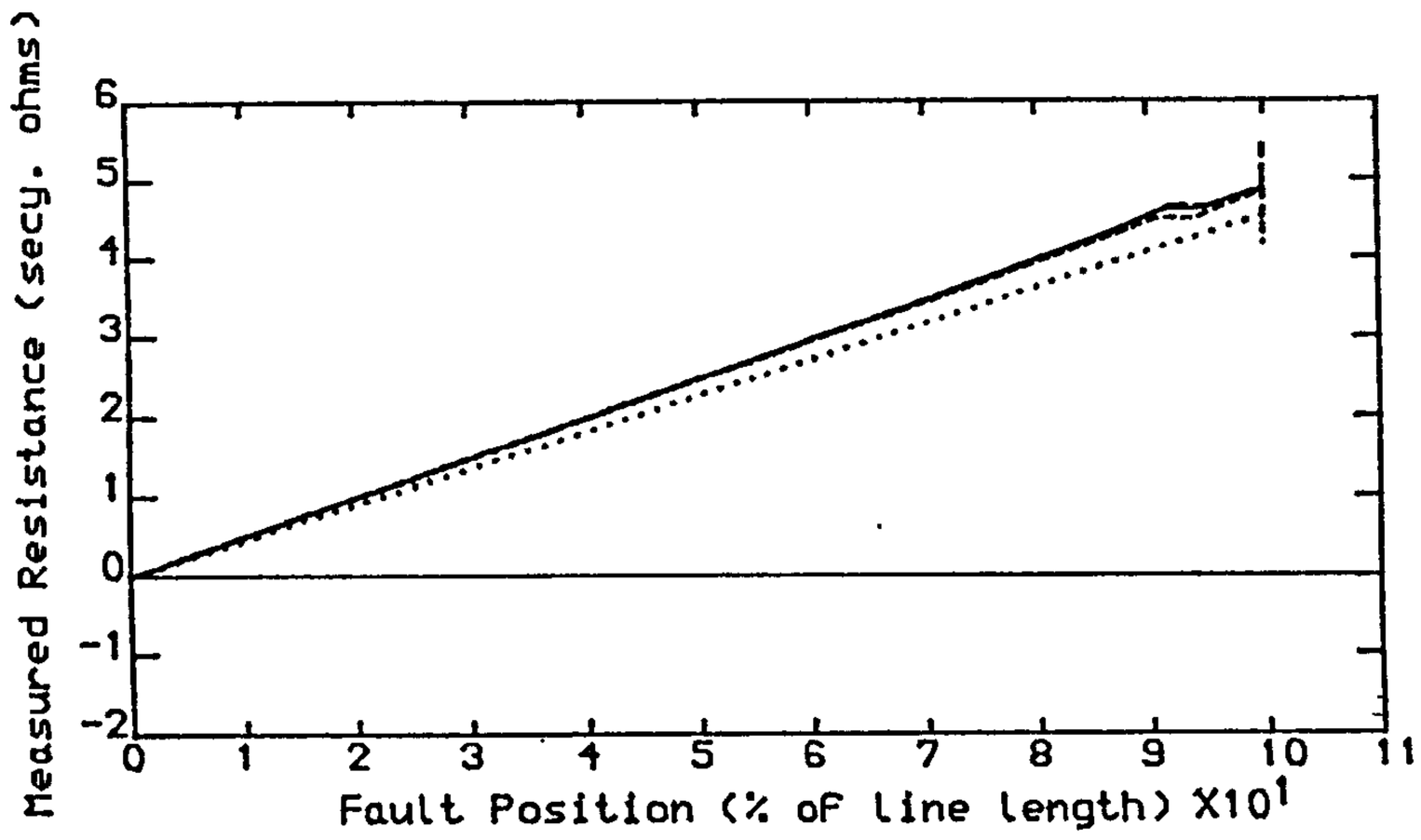

Fig 5.22.c- SE SCL=10 GVA, RE SCL=10 GVA

Fig 5.22-Measured Resistance VS Fault Position with the Complex Conventional Residual Compensation Factor, $K_c=0.78\angle-13.5°$, and Phase Voltage Compensation ($V_{sae}+jI_{sa}X_c/2$).

.... Line Locus
---- Pre-Fault Load Angle=-10 deg.
——— Pre-Fault Load Angle=0 deg.
—— Pre-Fault Load Angle=+10 deg.
Line Length=300 km

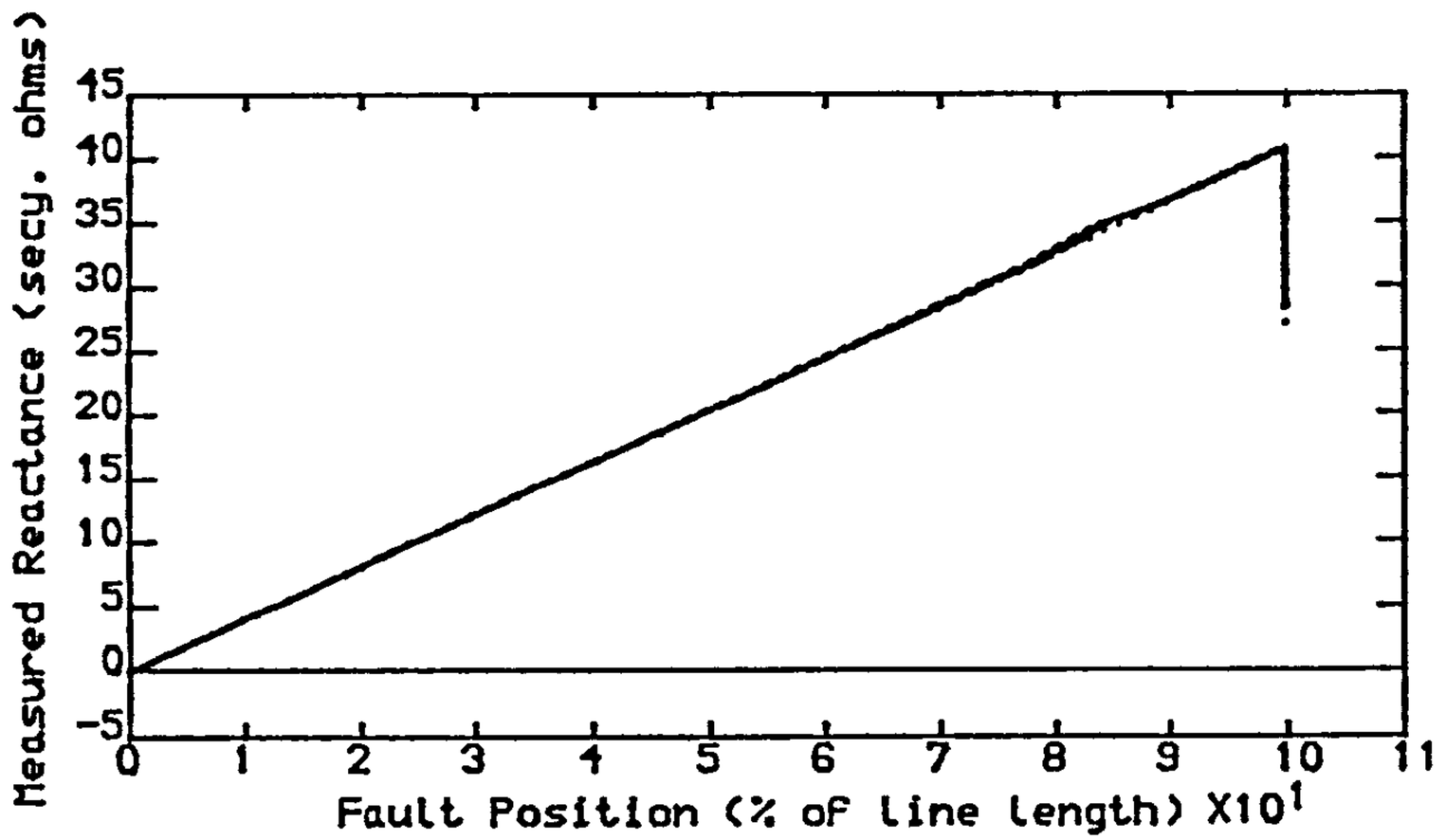

Fig 5.23.a- SE SCL=5 GVA. RE SCL=35 GVA

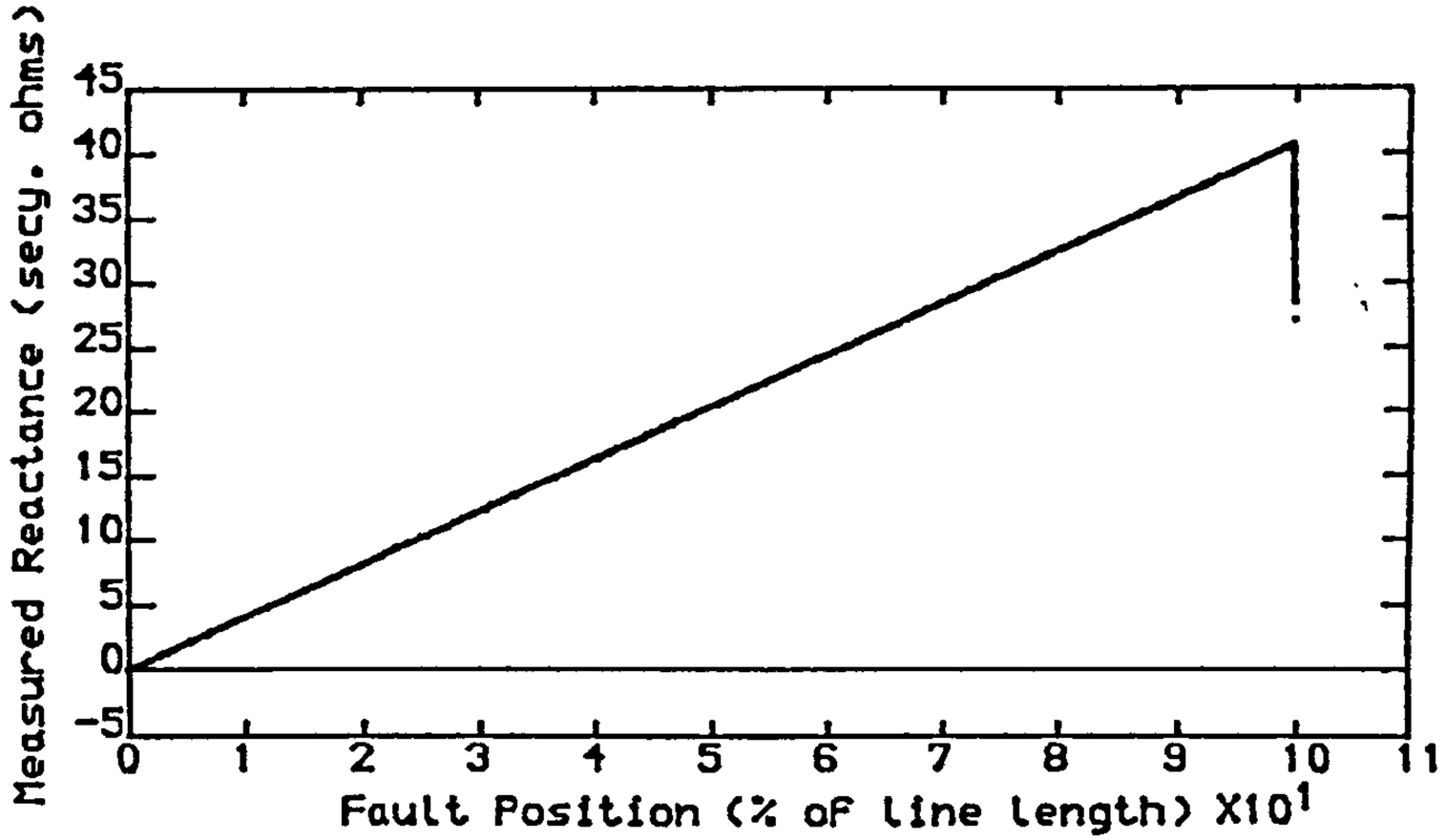

Fig 5.23.b- SE SCL=35 GVA. RE SCL=5 GVA

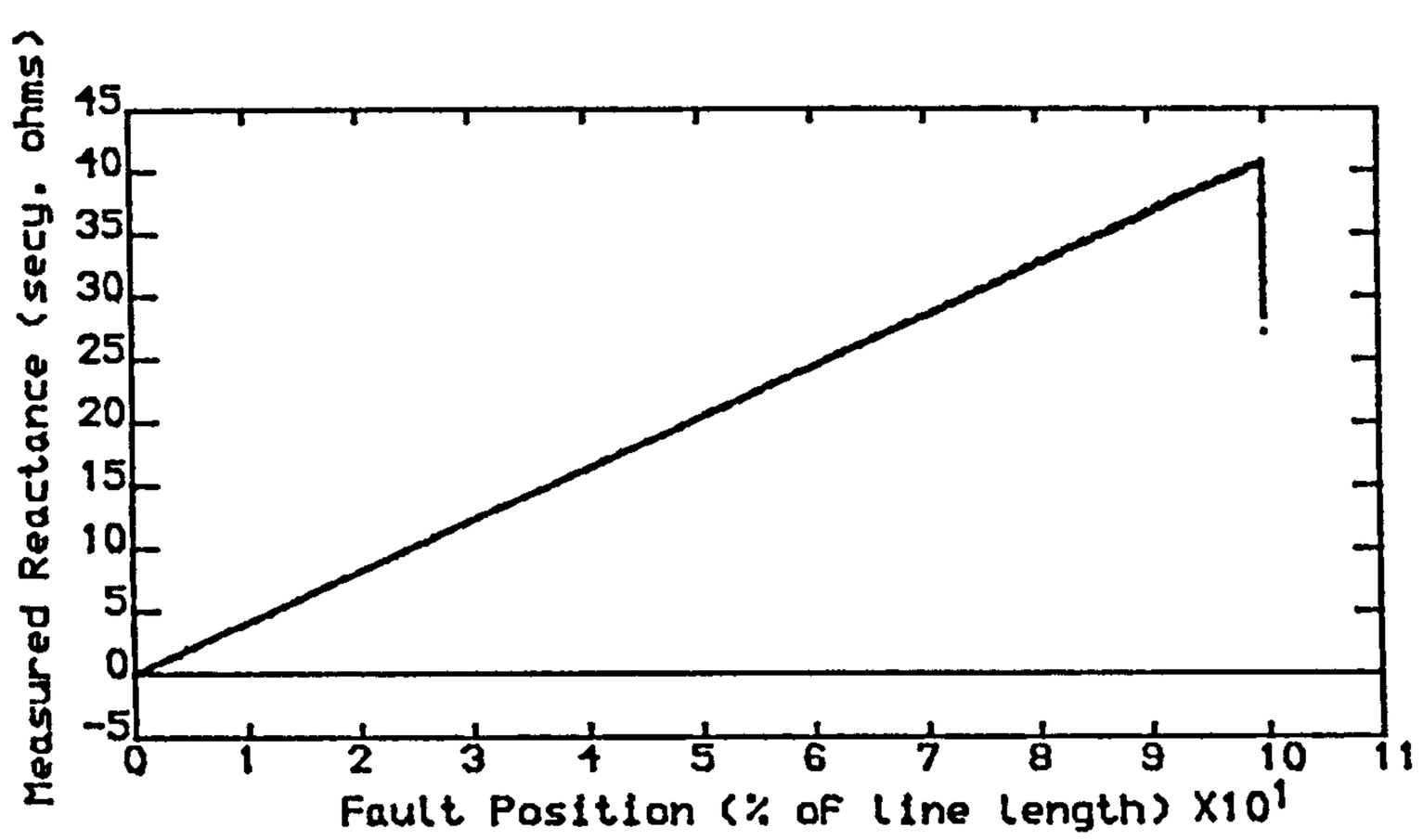

Fig 5.23.c- SE SCL=10 GVA. RE SCL=10 GVA

Fig 5.23-Measured Reactance VS Fault Position with the Complex Conventional Residual Compensation Factor, $K_c=0.78\angle -13.5°$, and Phase Voltage Compensation $(V_{sae}+jI_{sa}X_c/2)$.

.... Line Locus
---- Pre-Fault Load Angle=-10
——— Pre-Fault Load Angle=0
—— Pre-Fault Load Angle=+10
Line Length=300 km

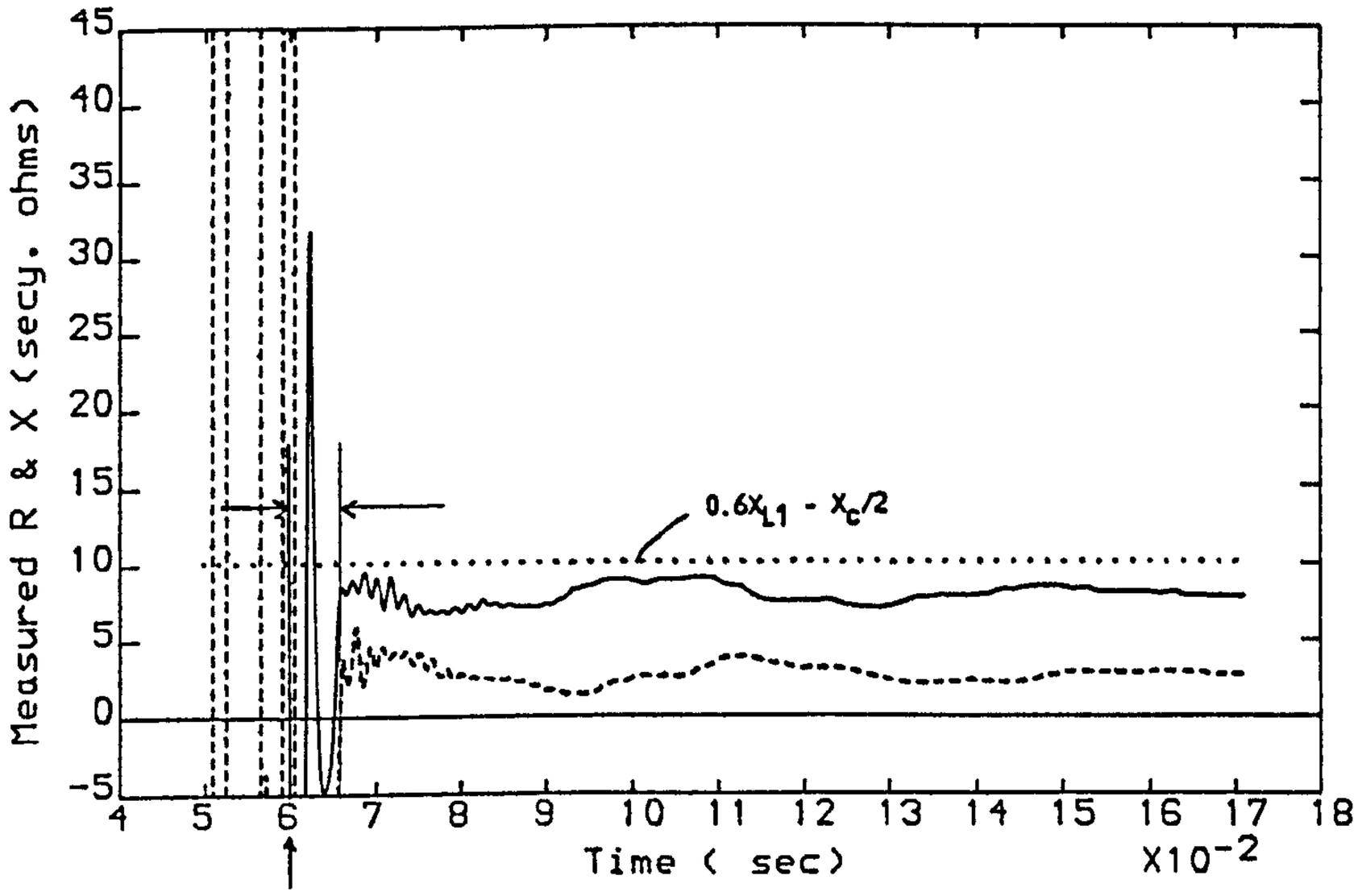

Fig 5.24.a-Measured Reactance vs Time with Kar (NRCF)

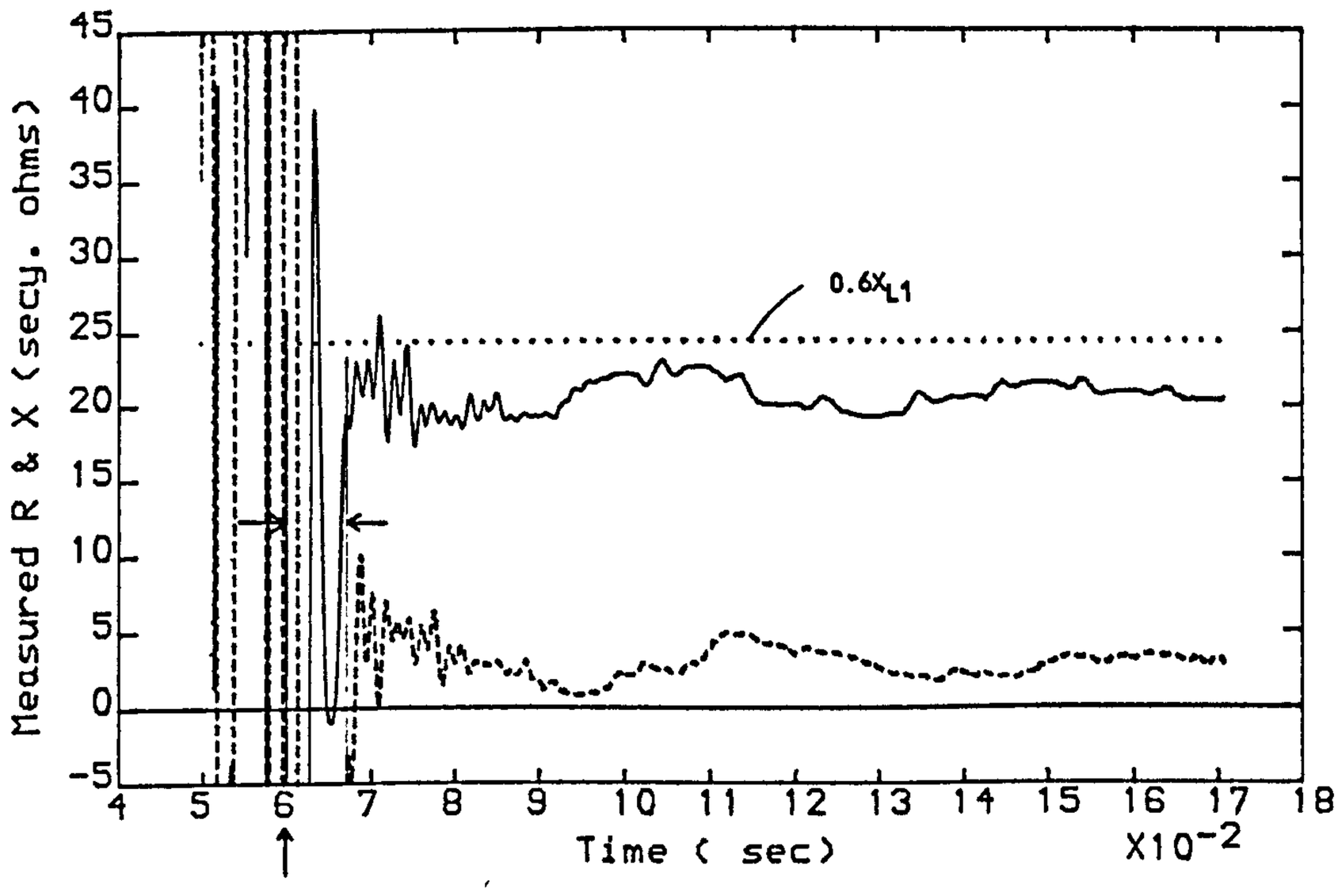

Fig 5.24.b-Measured Reactance vs Time with Complex Kc & Voltage Compensation

.... forward reactive reach
———— measured reactance
---- measured resistance
fault inception angle-90 degree
fault at 50% of line length
line length-300 km
SE SCL-5 GVA, RE SCL-35 GVA, NO LOAD

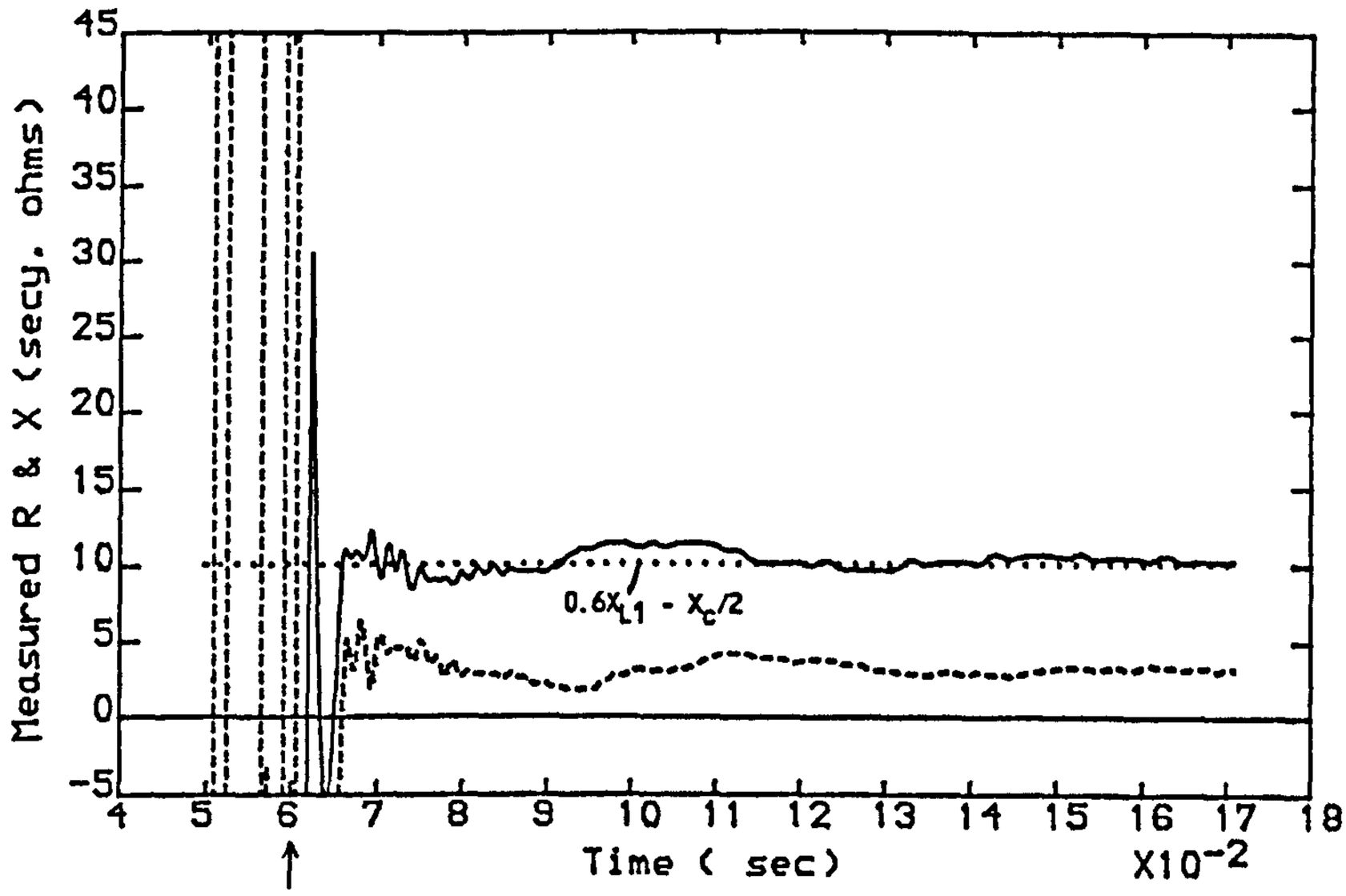

Fig 5.25.a-Measured Reactance vs Time with Kar (NRCF)

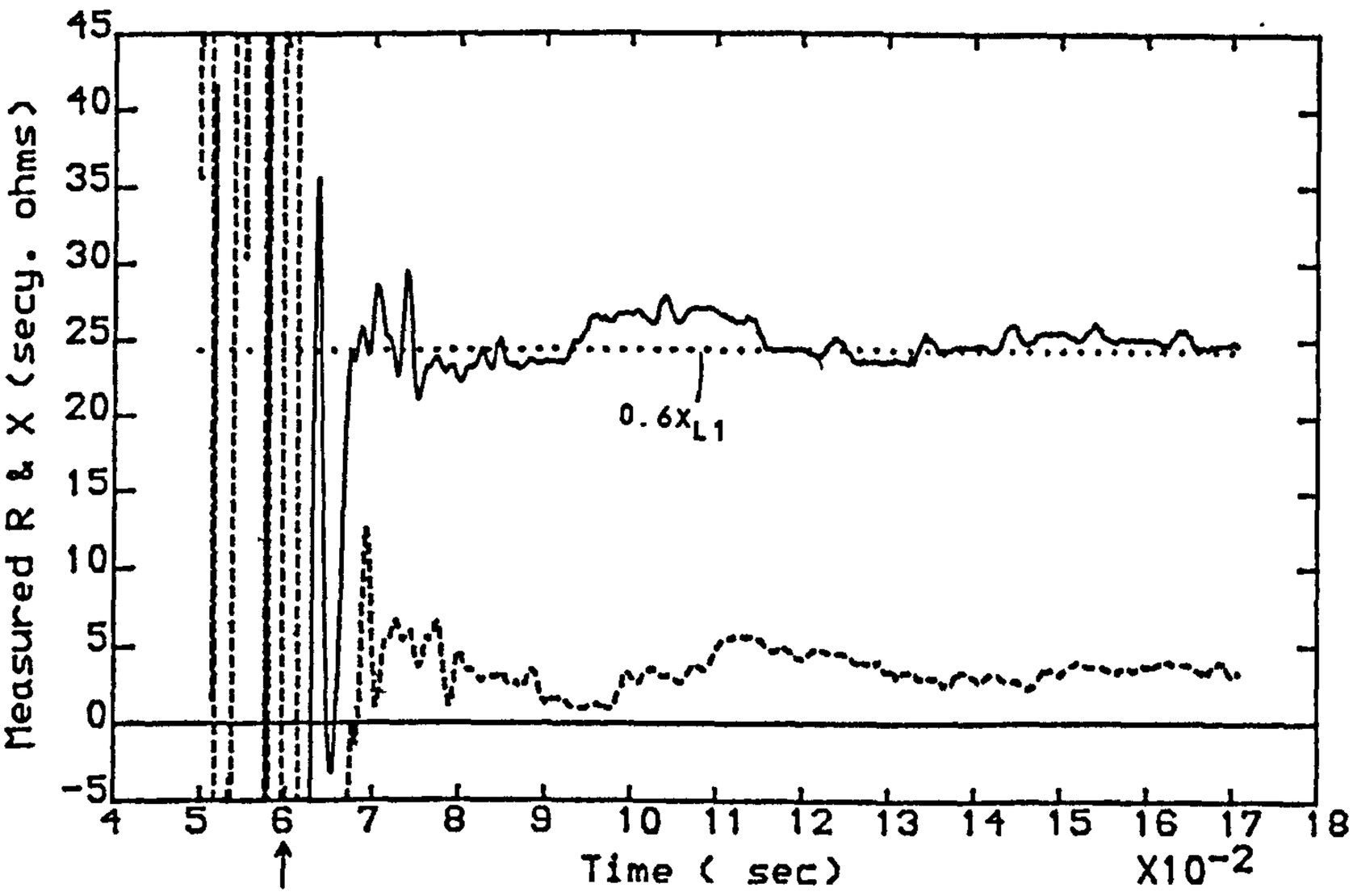

Fig 5.25.b-Measured Reactance vs Time with Complex Kc & Voltage Compensation

.... forward reactive reach
——— measured reactance
---- measured resistance
fault inception angle-90 degree
fault at 60% of line length
line length-300 km
SE SCL-5 GVA, RE SCL-35 GVA, NO LOAD

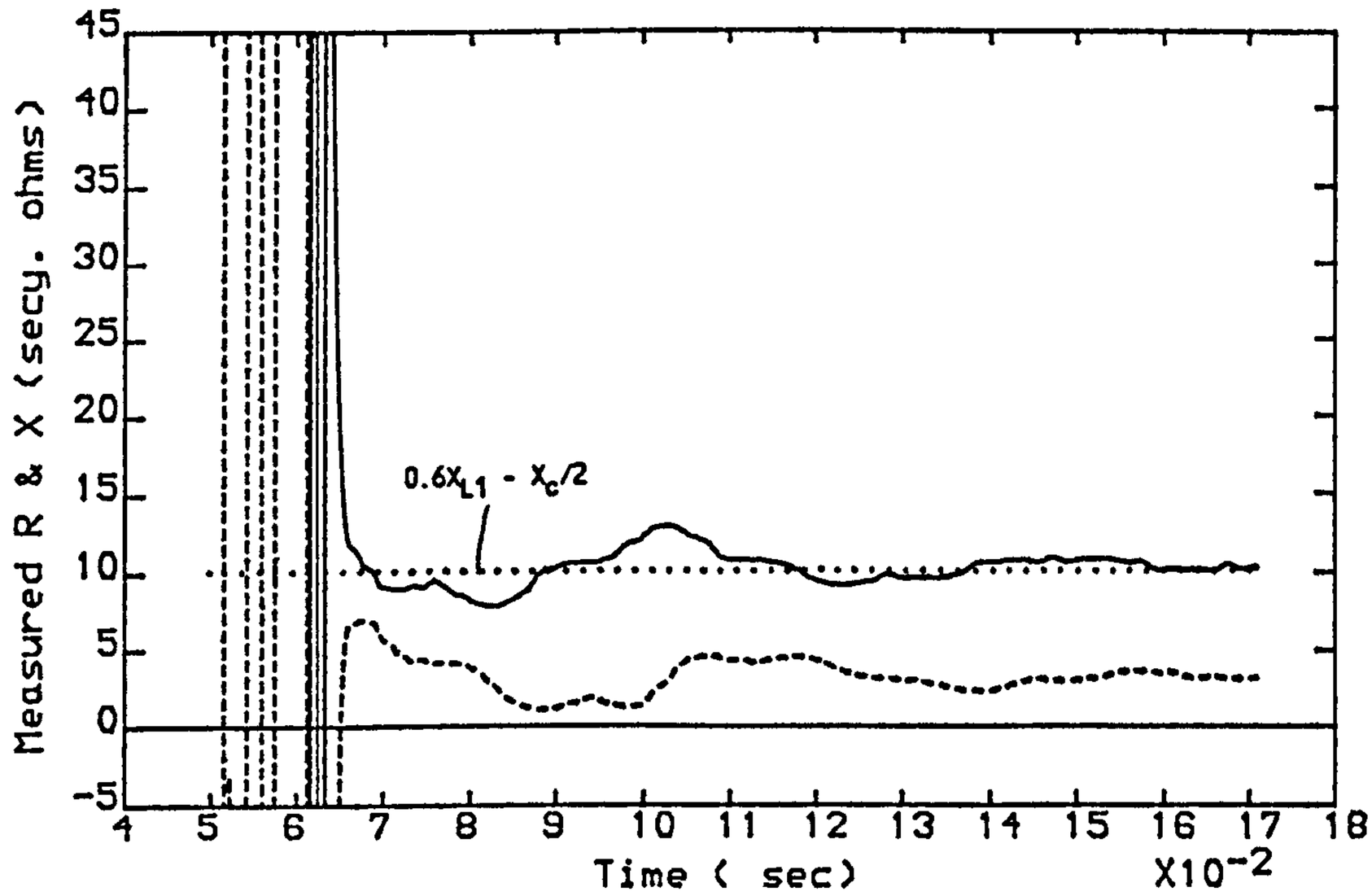

Fig 5.26.a-Measured Reactance vs Time with Kar (NRCF)

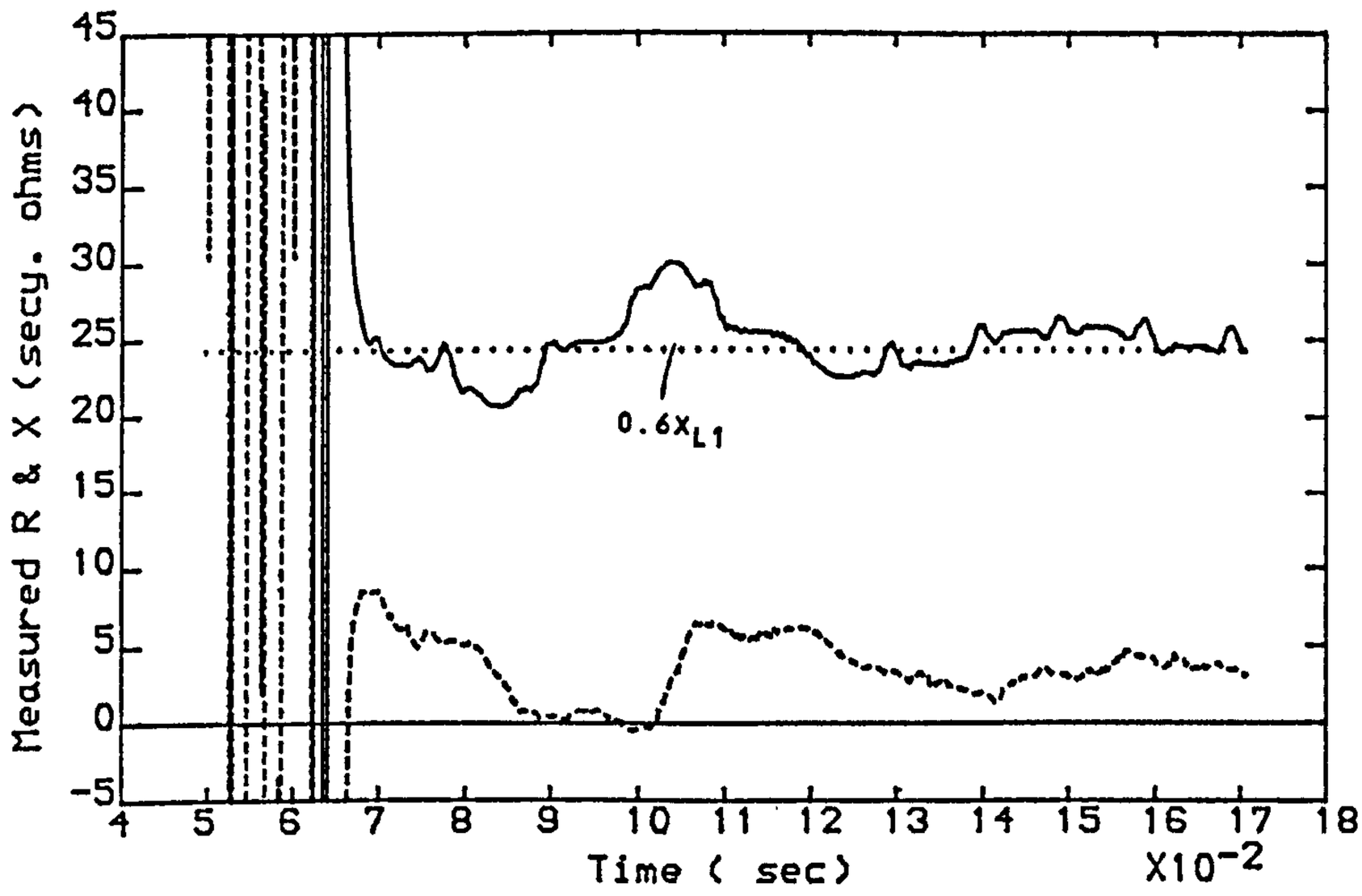

Fig 5.26.b-Measured Reactance vs Time with Complex Kc & Voltage Compensation

.... forward reactive reach
———— measured reactance
---- measured resistance
fault inception angle= 0 degree
fault at 60% of line length
line length=300 km
SE SCL=5 GVA. RE SCL=35 GVA. NO LOAD

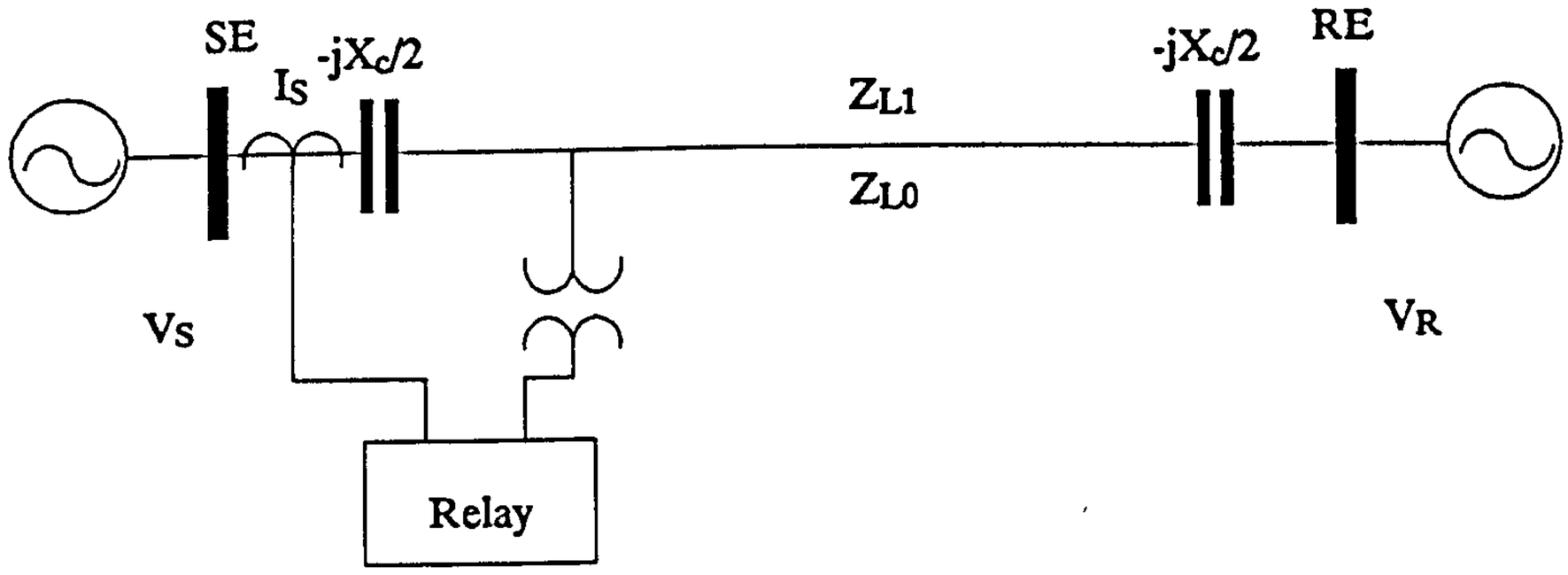

Fig 5.27-System Configuration with Line Side V.T.

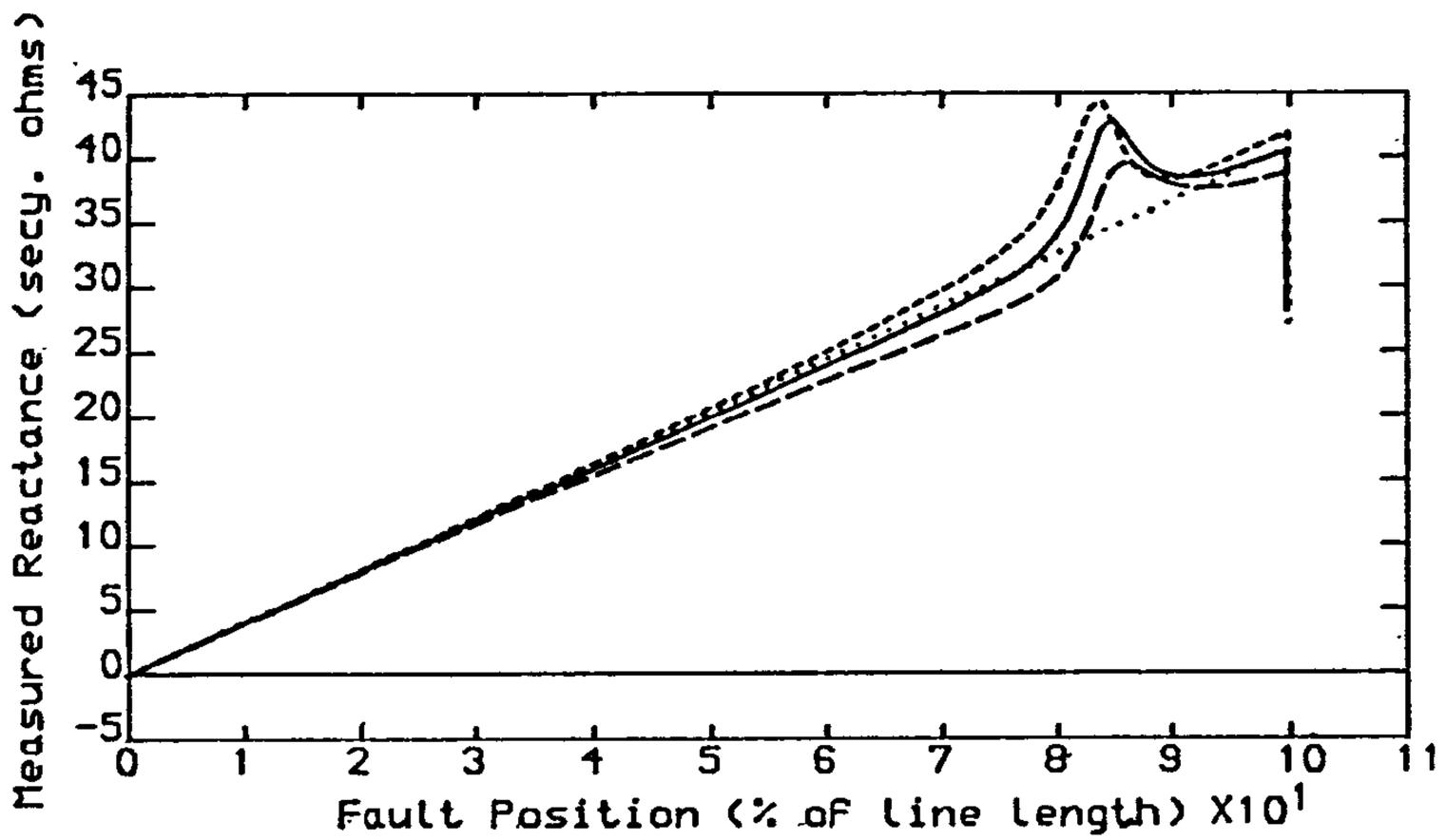

Fig 5.28.a- SE SCL=5 GVA, RE SCL=35 GVA

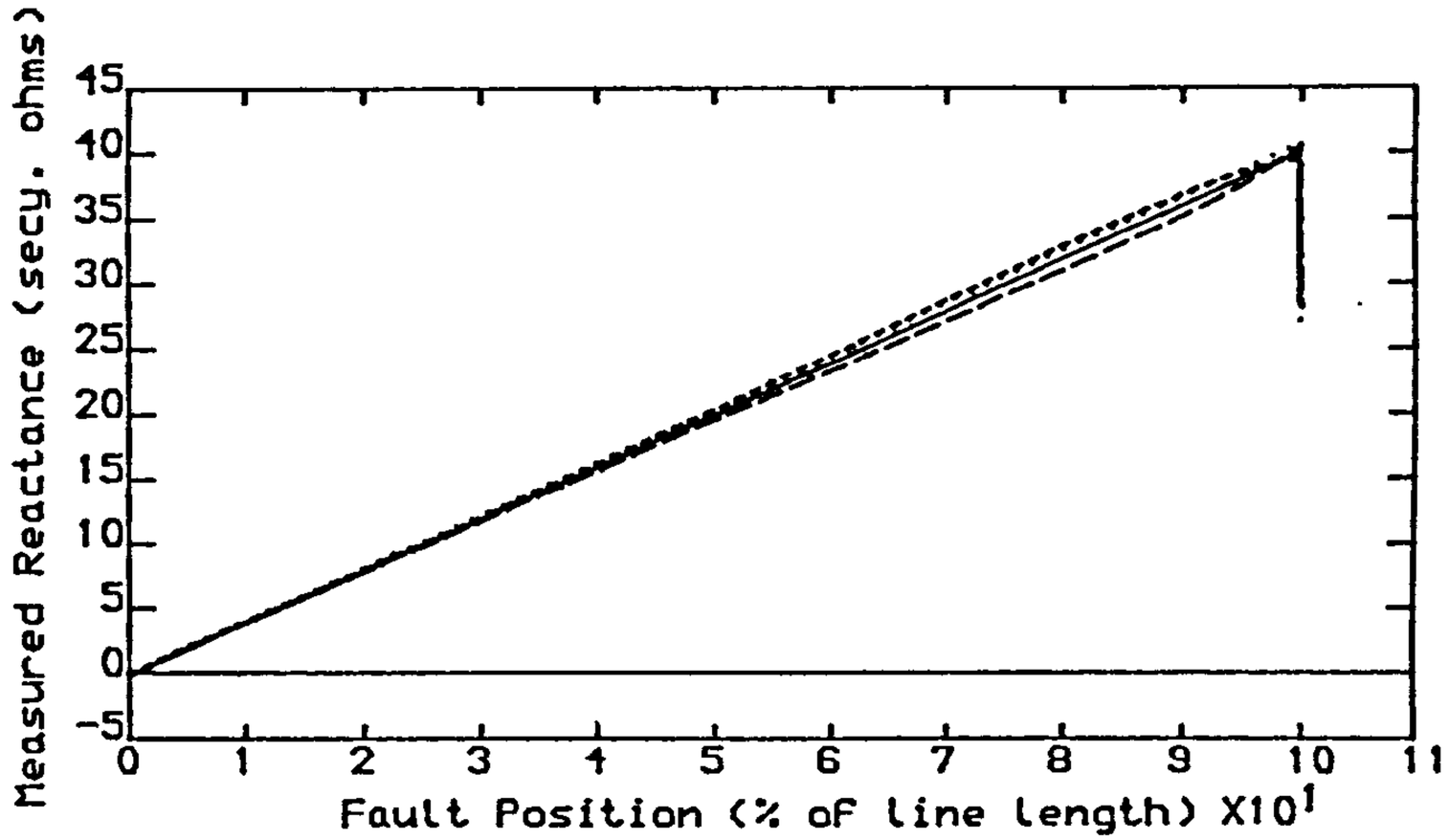

Fig 5.28.b- SE SCL=35 GVA, RE SCL=5 GVA

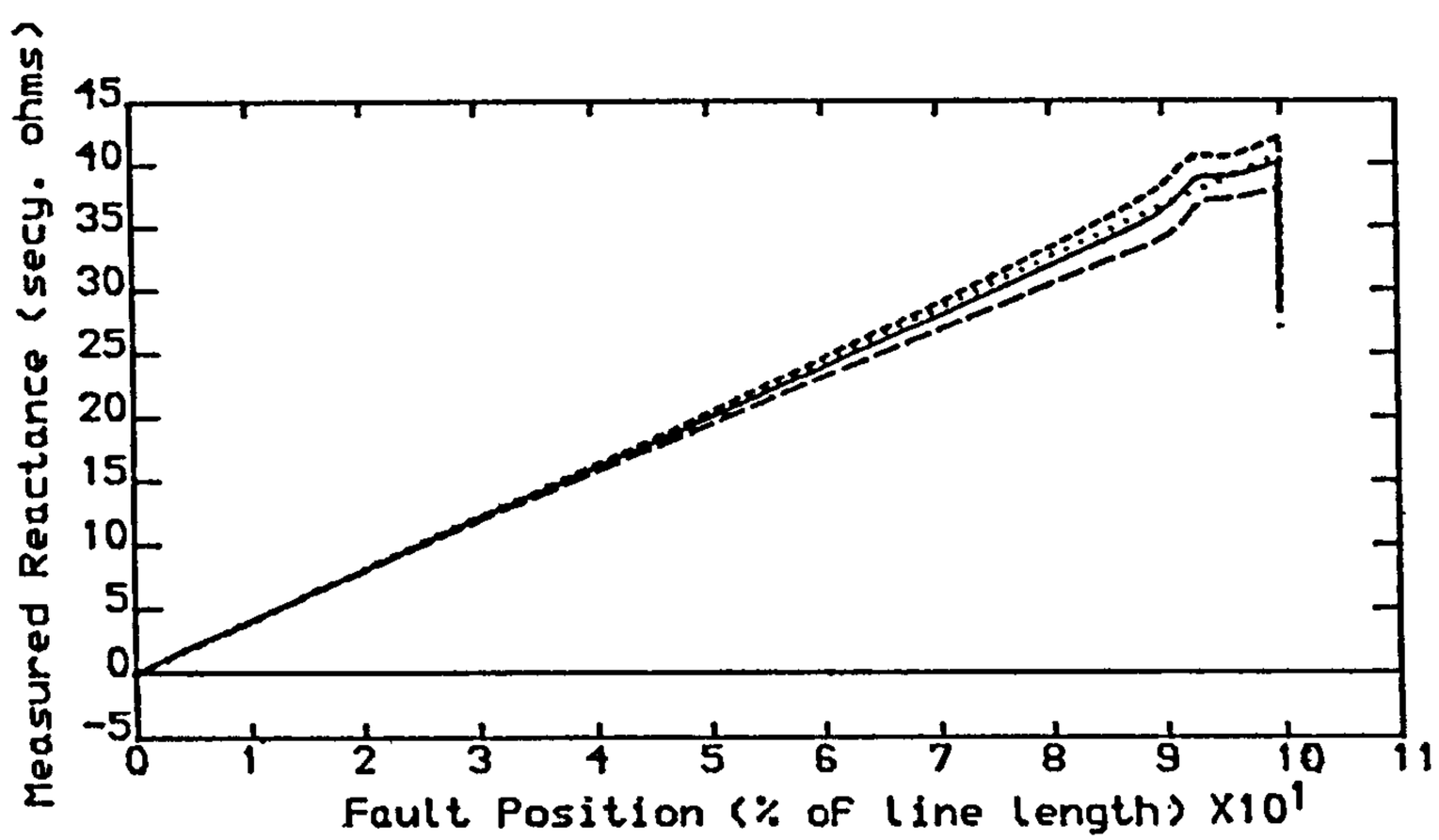

Fig 5.28.c- SE SCL=10 GVA, RE SCL=10 GVA

Fig 5.28-Measured Reactance VS Fault Position with the Conventional Residual Compensation Factor, K_C=0.774, with the Line Side C.V.T.

.... Line Locus
---- Pre-Fault Load Angle=-10
——— Pre-Fault Load Angle=0
—— Pre-Fault Load Angle=+10
Line Length=300 km

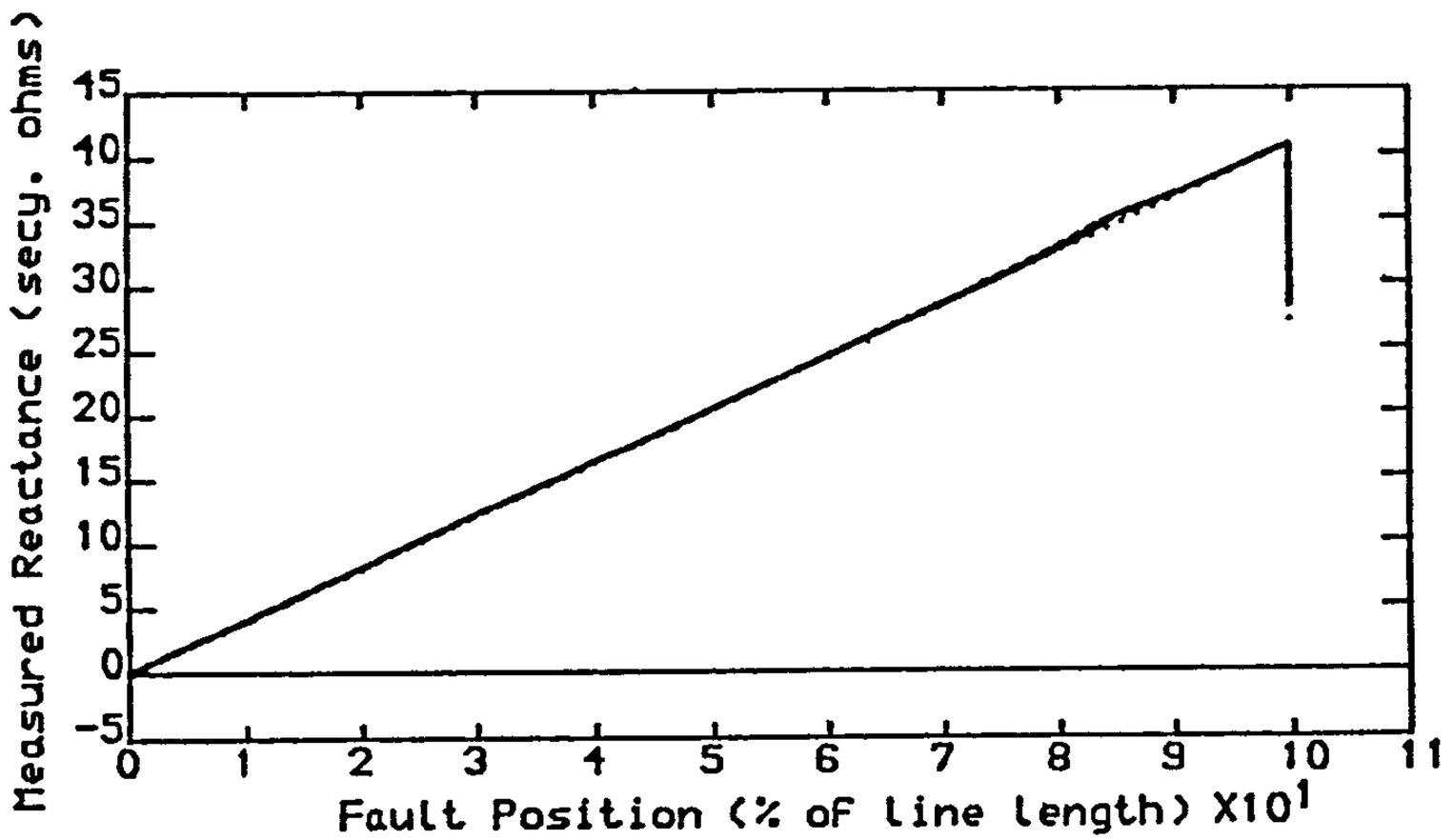

Fig 5.29.a- SE SCL=5 GVA, RE SCL=35 GVA

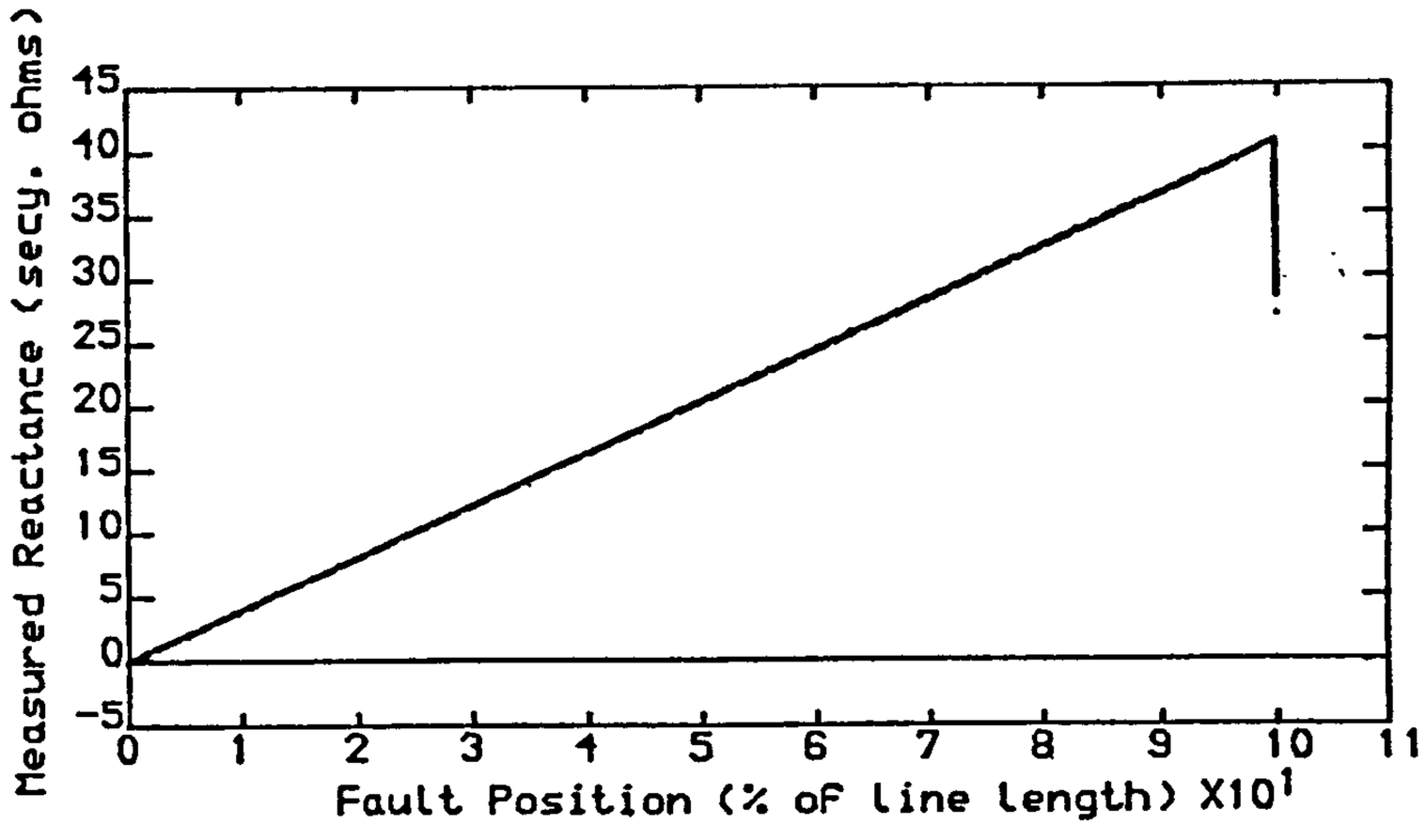

Fig 5.29.b- SE SCL=35 GVA, RE SCL=5 GVA

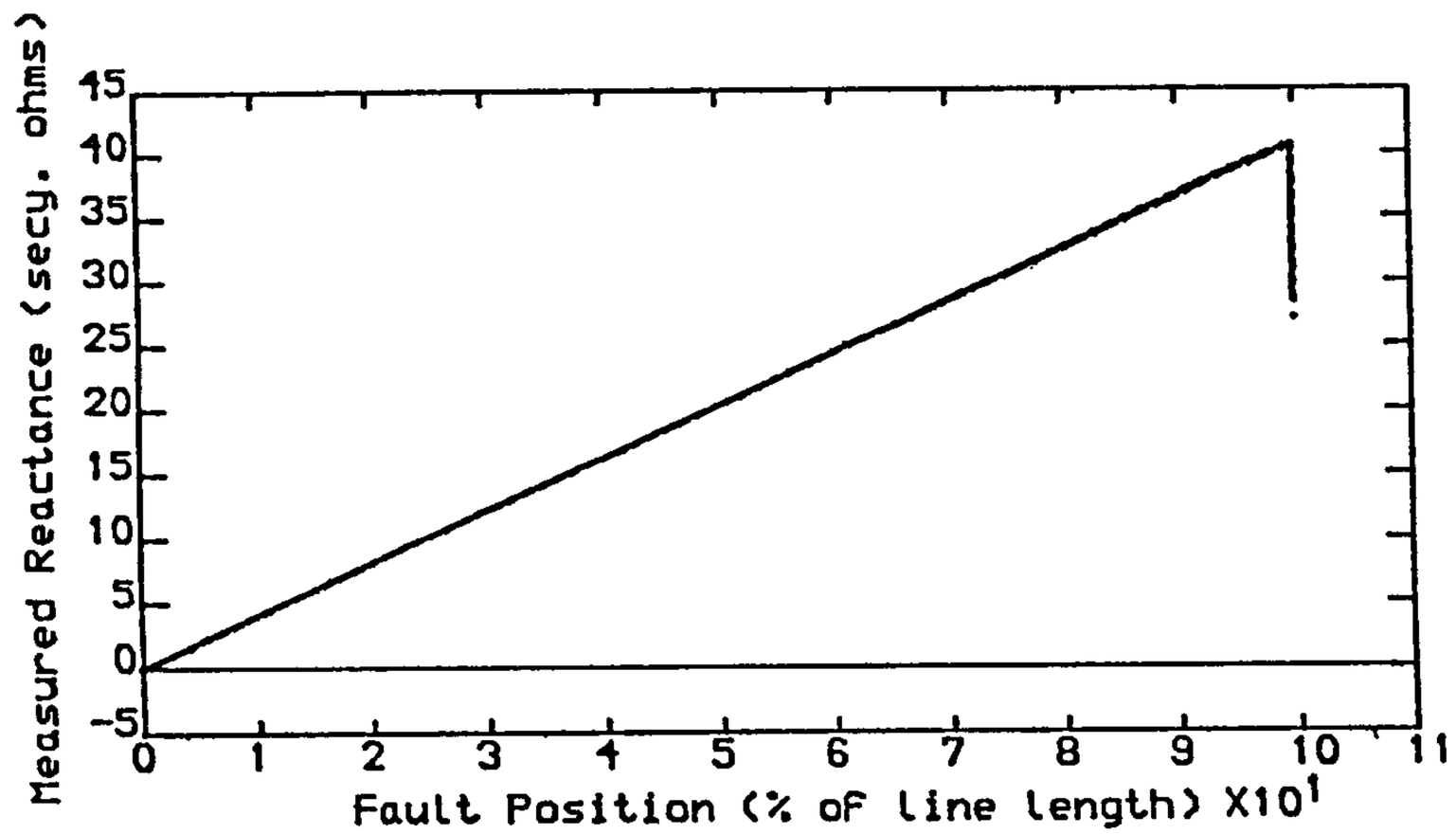

Fig 5.29.c- SE SCL=10 GVA, RE SCL=10 GVA

Fig 5.29-Measured Reactance VS Fault Position with the Complex Conventional Residual Compensation Factor, $K_C=0.78\angle -13.5°$, with the Line Side C.V.T.

.... Line Locus
---- Pre-Fault Load Angle=-10
——— Pre-Fault Load Angle=0
——— Pre-Fault Load Angle=+10
Line Length=300 km

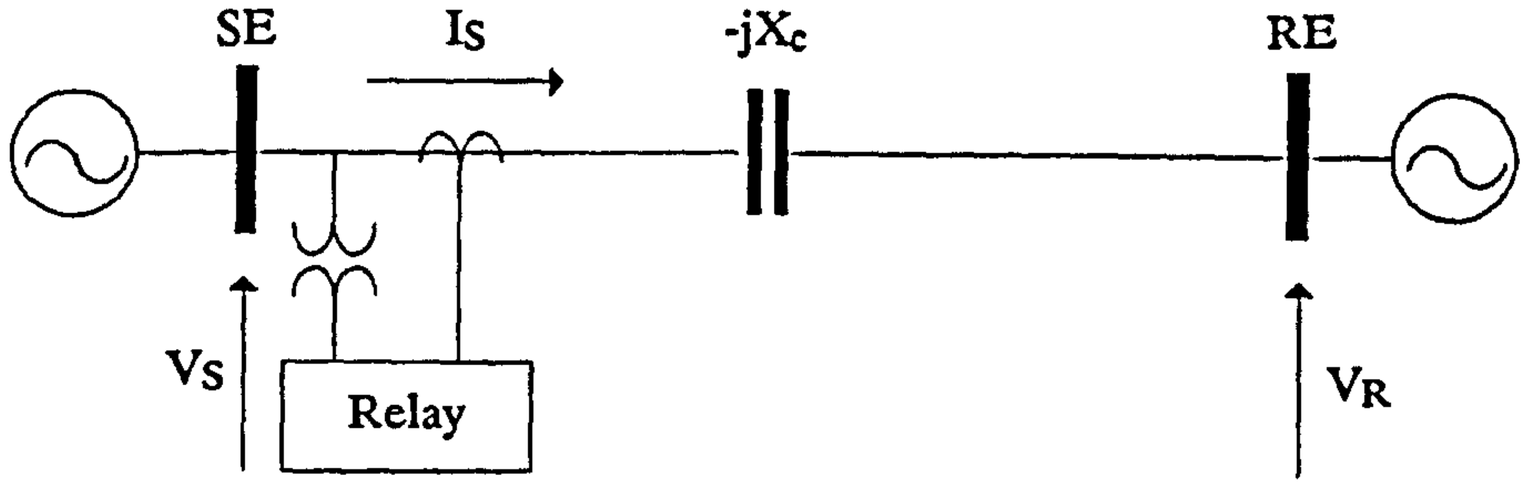

Fig 5.30-System Configuration with Compensation at the Mid-Point of Line.

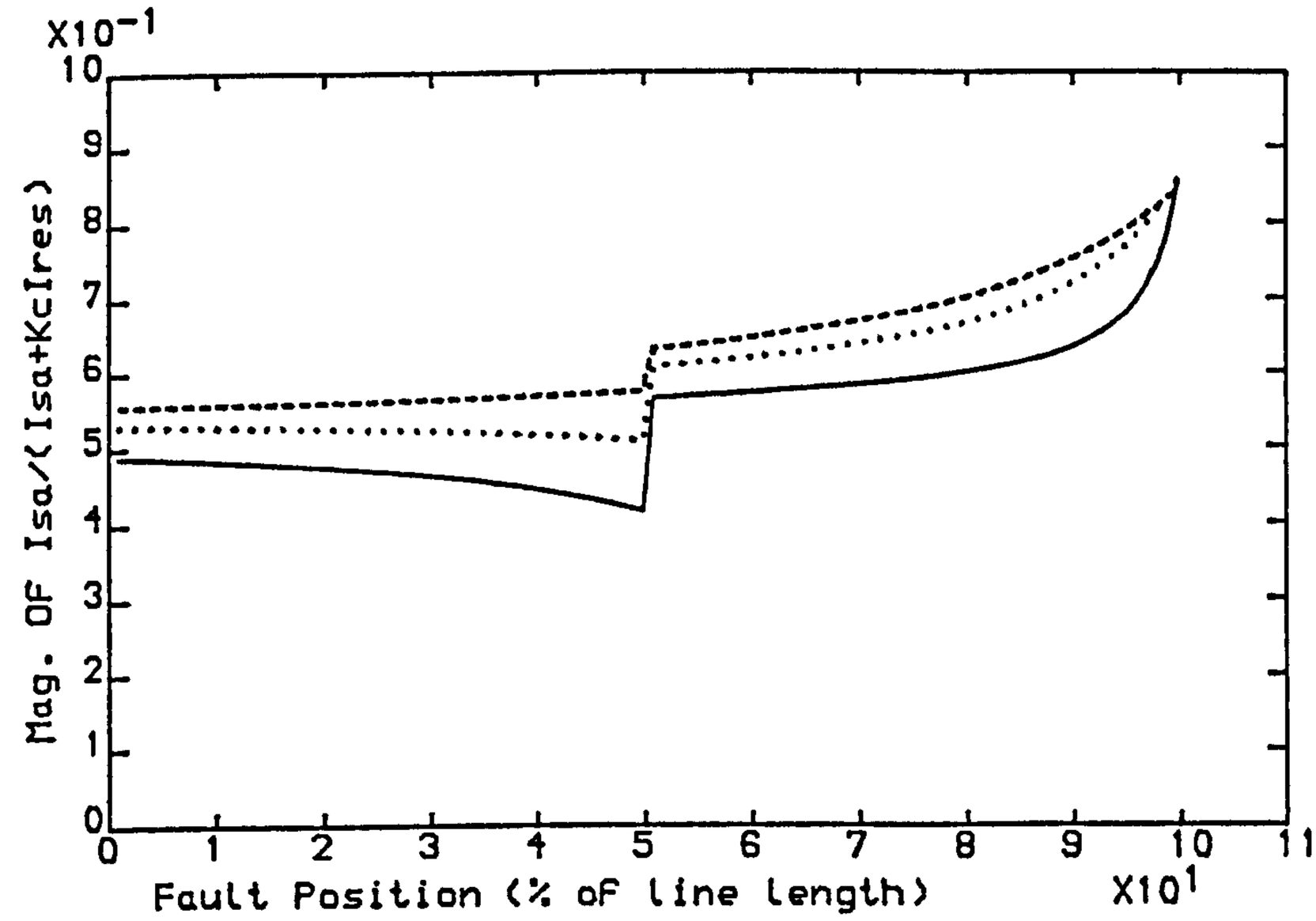

Fig 5.31.a-Variation in Mag. Of Isa/(Isa+KcIres) VS Fault Position For Pre-Fault Load Angle Of -10 Degrees (50% series comp.)

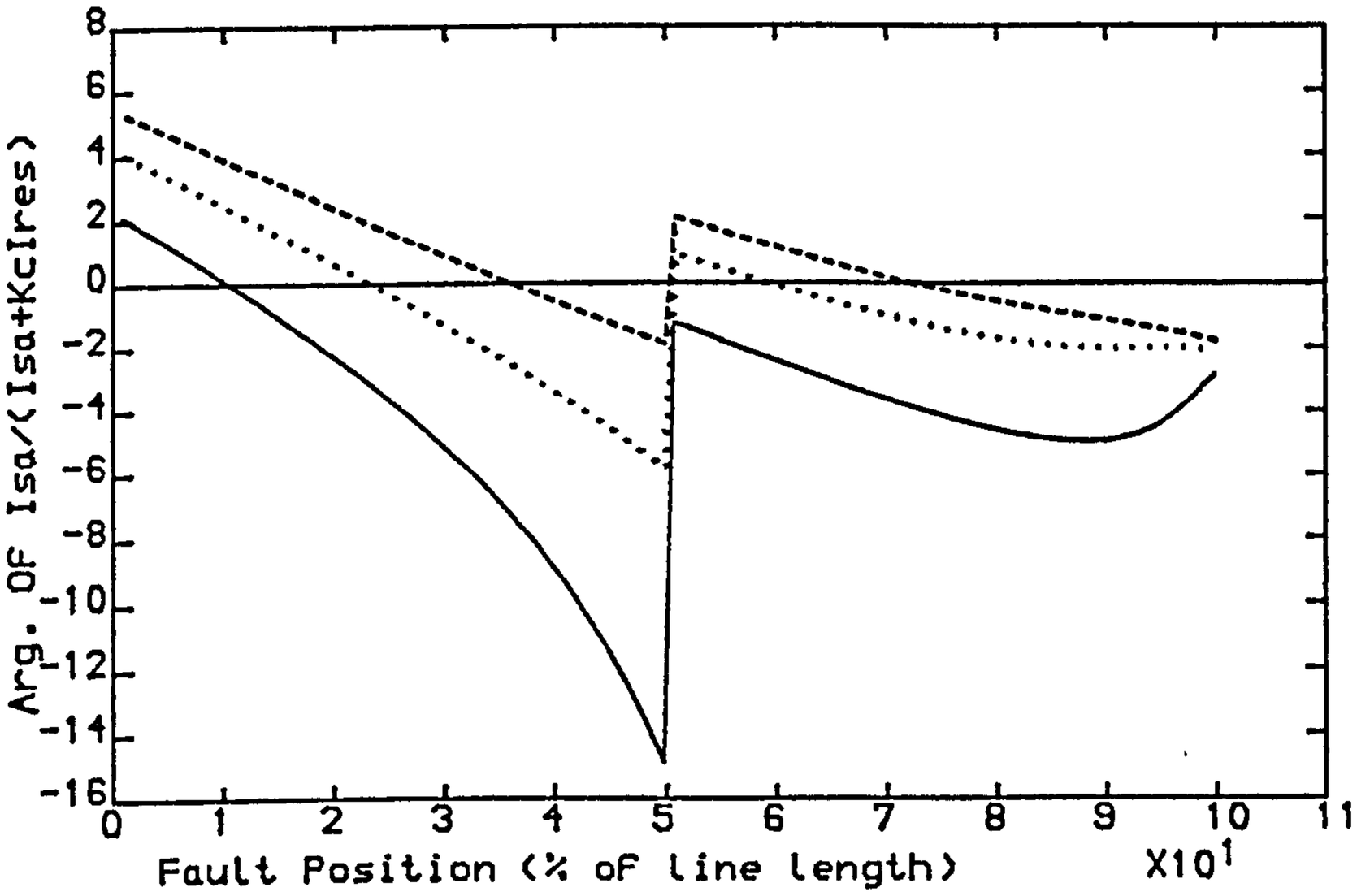

Fig 5.31.b-Variation in Arg. Of Isa/(Isa+KcIres) VS Fault Position For Pre-Fault Load Angle Of -10 Degrees (50% series comp.)

——— SE SCL=5 GVA, RE SCL=35 GVA
– – – SE SCL=35 GVA, RE SCL=5 GVA
.... SE SCL=10 GVA, RE SCL=10 GVA
Line Length =300 km

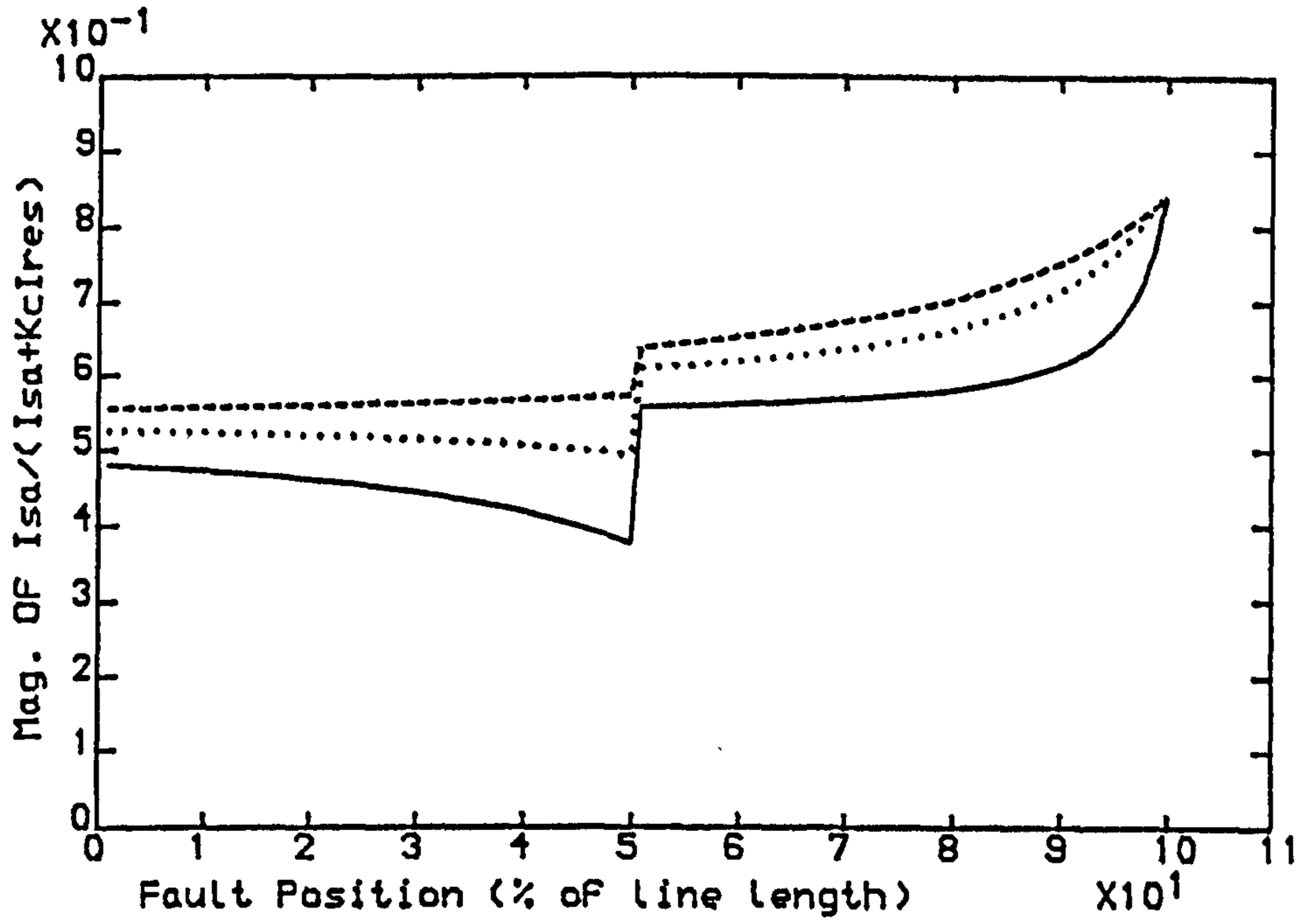

Fig 5.32.a-Variation in Mag. Of Isa/(Isa+KcIres) VS Fault Position For Pre-Fault Load Angle Of 0 Degrees (50% series comp.)

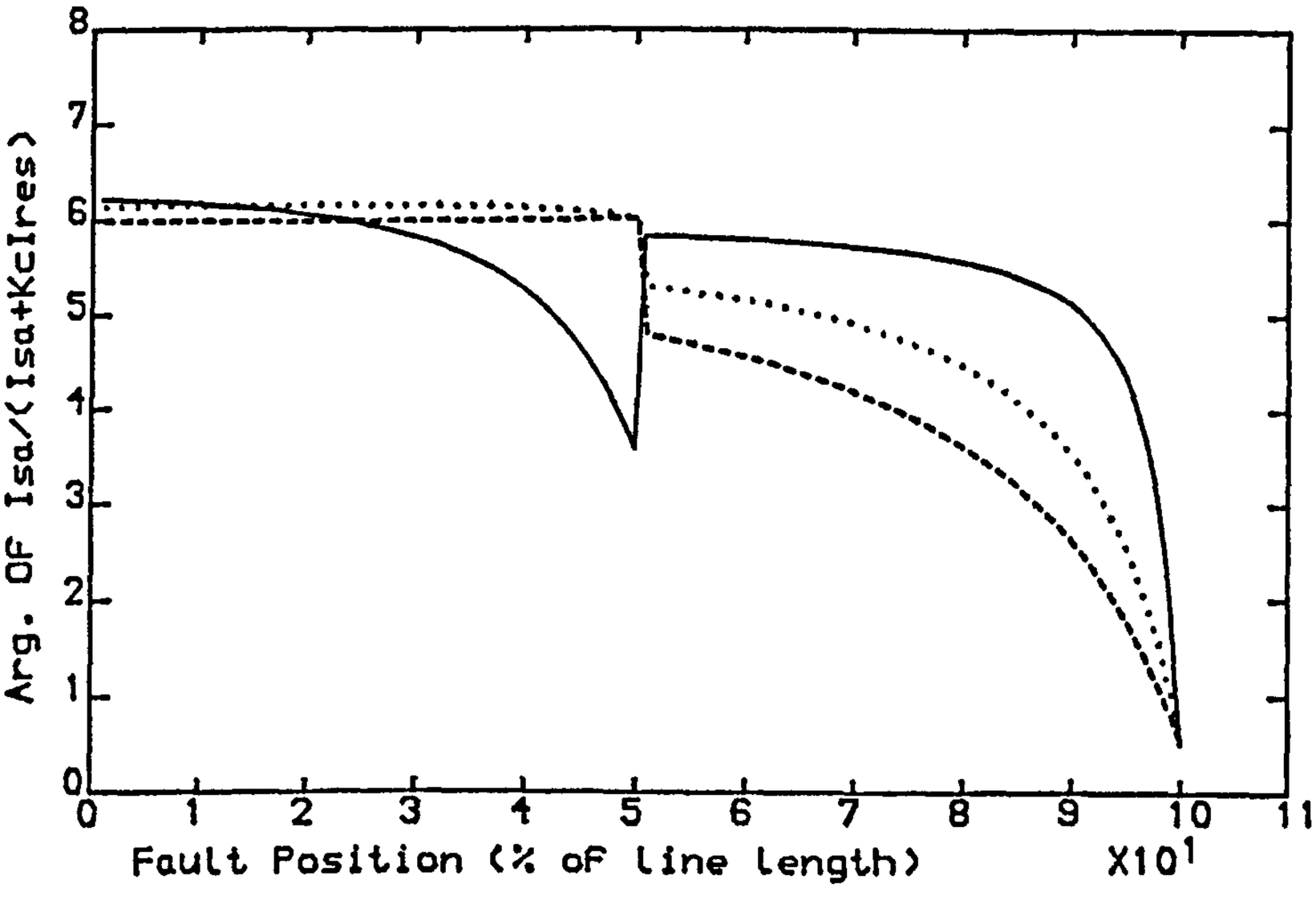

Fig 5.32.b-Variation in Arg. Of Isa/(Isa+KcIres) VS Fault Position For Pre-Fault Load Angle Of 0 Degrees (50% series comp.)

——— SE SCL-5 GVA, RE SCL-35 GVA
---- SE SCL-35 GVA, RE SCL-5 GVA
.... SE SCL-10 GVA, RE SCL-10 GVA
Line Length -300 km

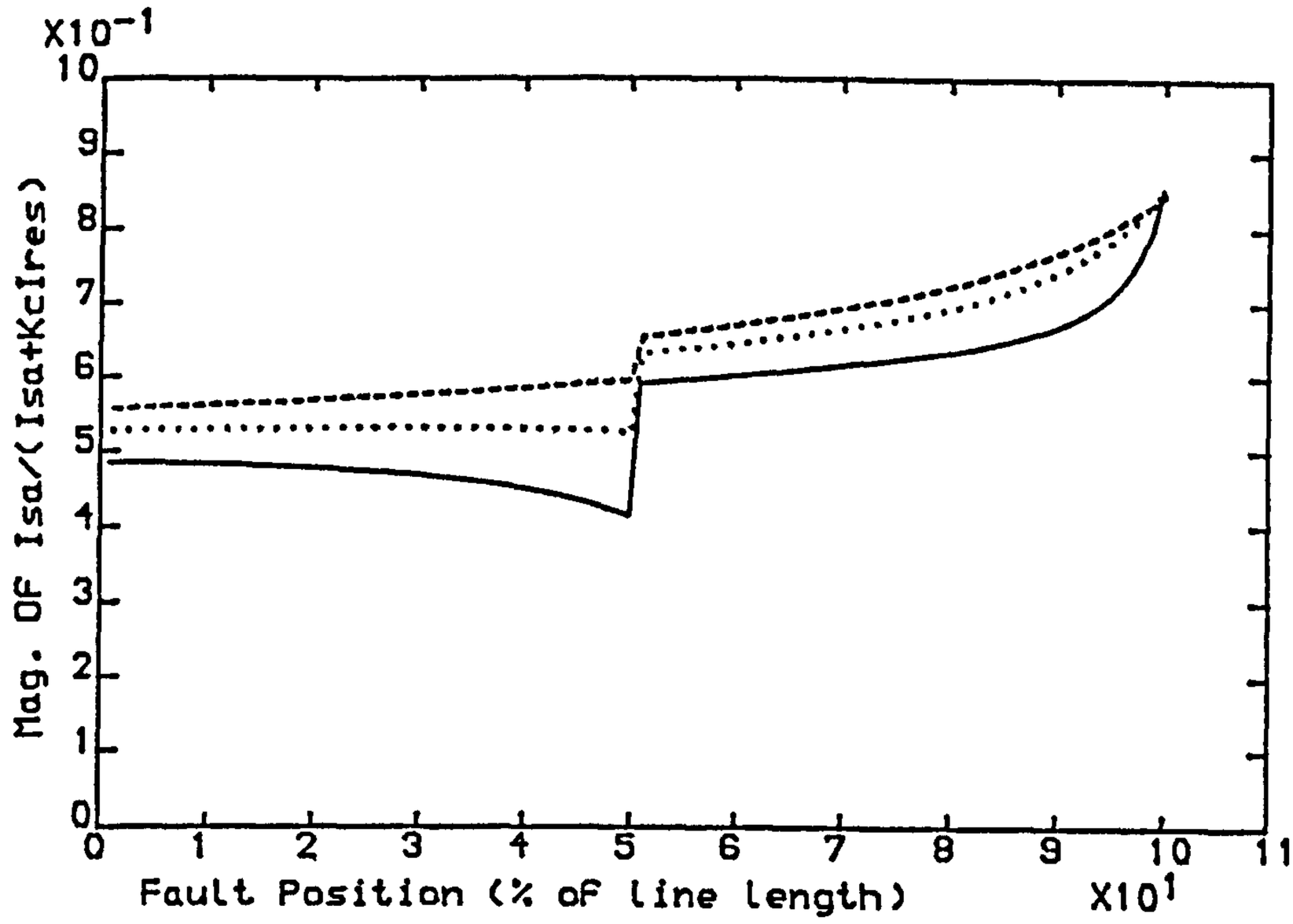

Fig 5.33.a-Variation in Mag. Of Isa/(Isa+KcIres) VS Fault Position For Pre-Fault Load Angle Of +10 Degrees (50% series comp.)

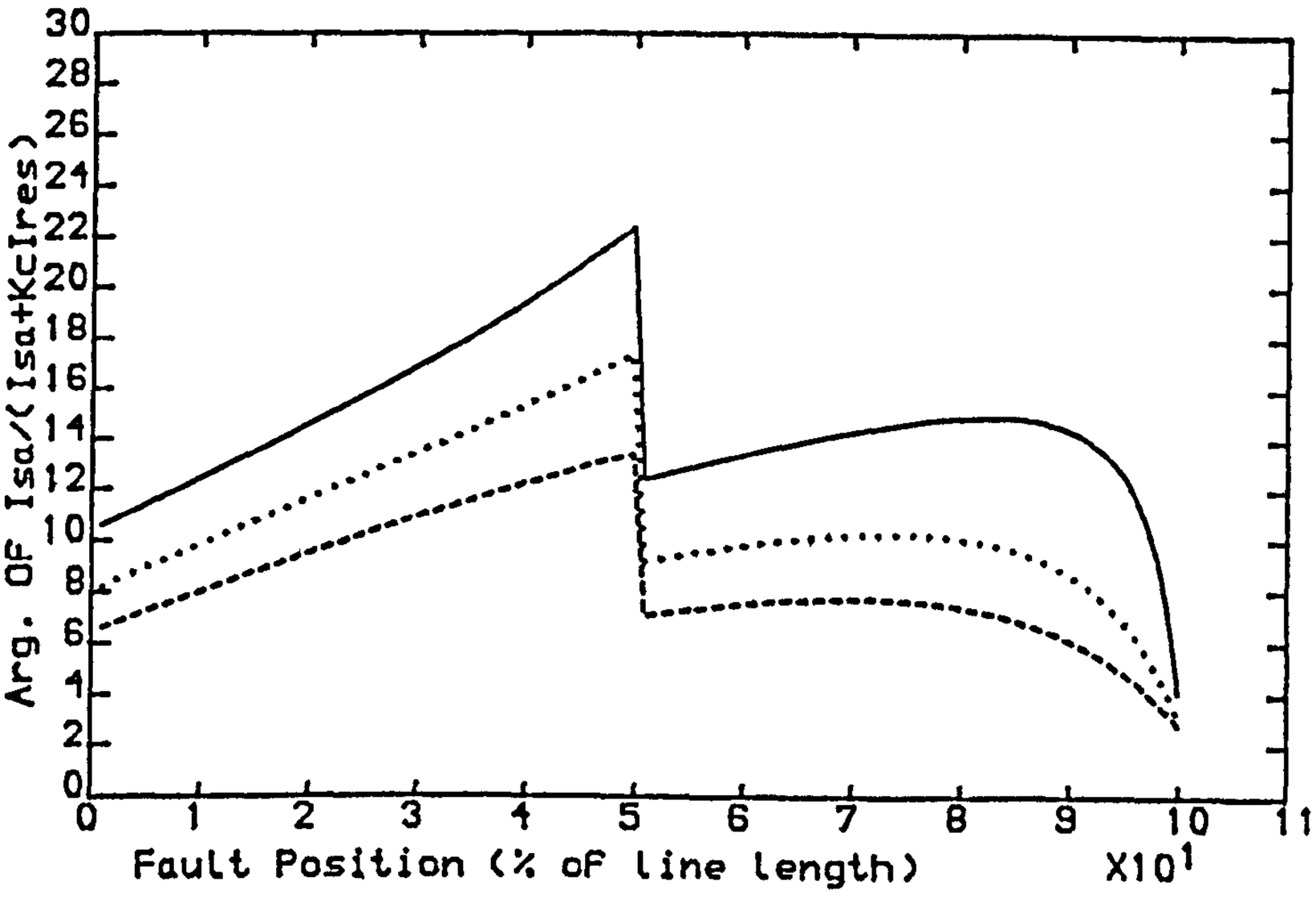

Fig 5.33.b-Variation in Arg. Of Isa/(Isa+KcIres) VS Fault Position For Pre-Fault Load Angle Of +10 Degrees (50% series comp.)

——— SE SCL=5 GVA, RE SCL=35 GVA
- - - - SE SCL=35 GVA, RE SCL=5 GVA
.... SE SCL=10 GVA, RE SCL=10 GVA
Line Length =300 km

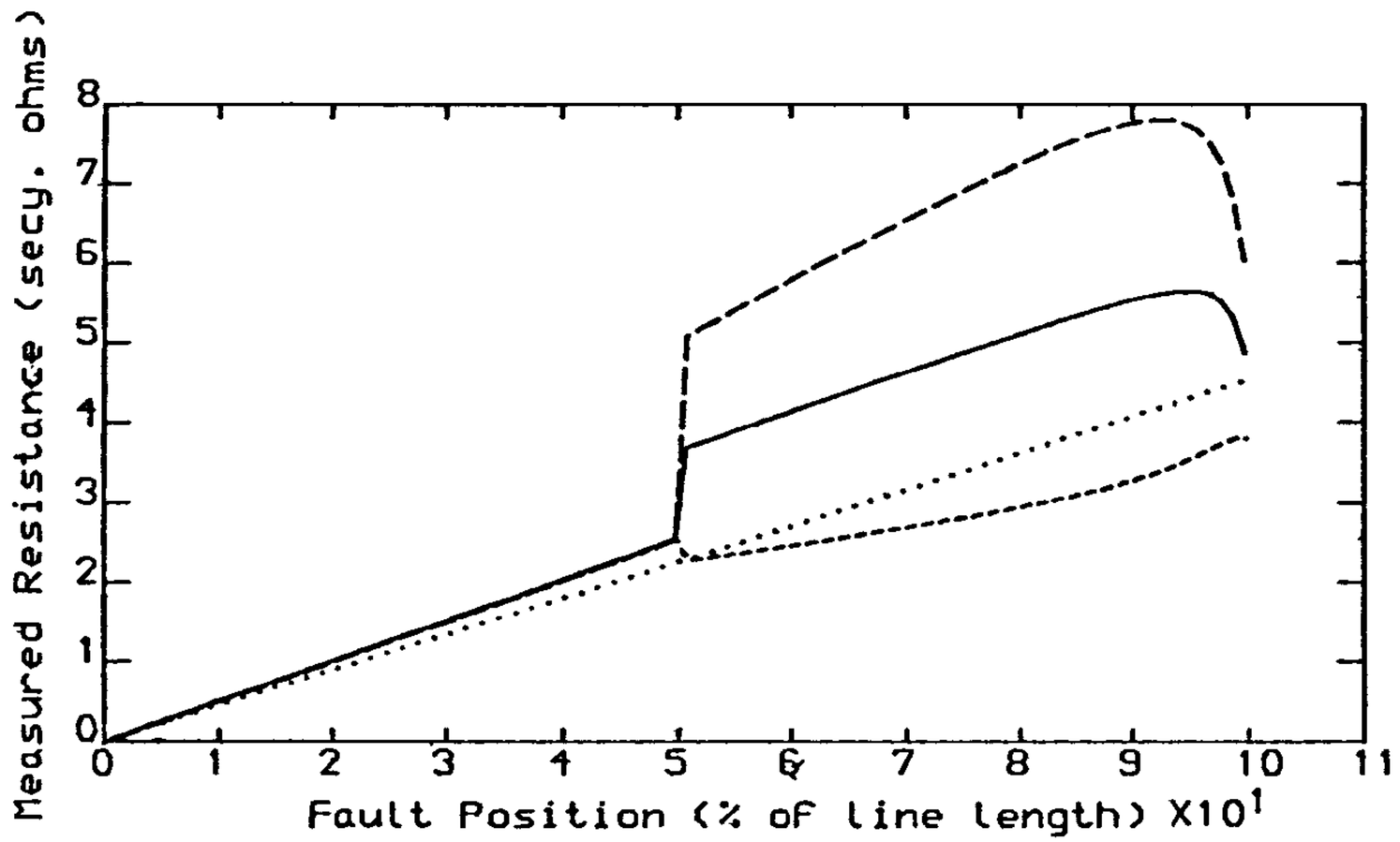

Fig 5.34.a- SE SCL=5 GVA. RE SCL=35 GVA

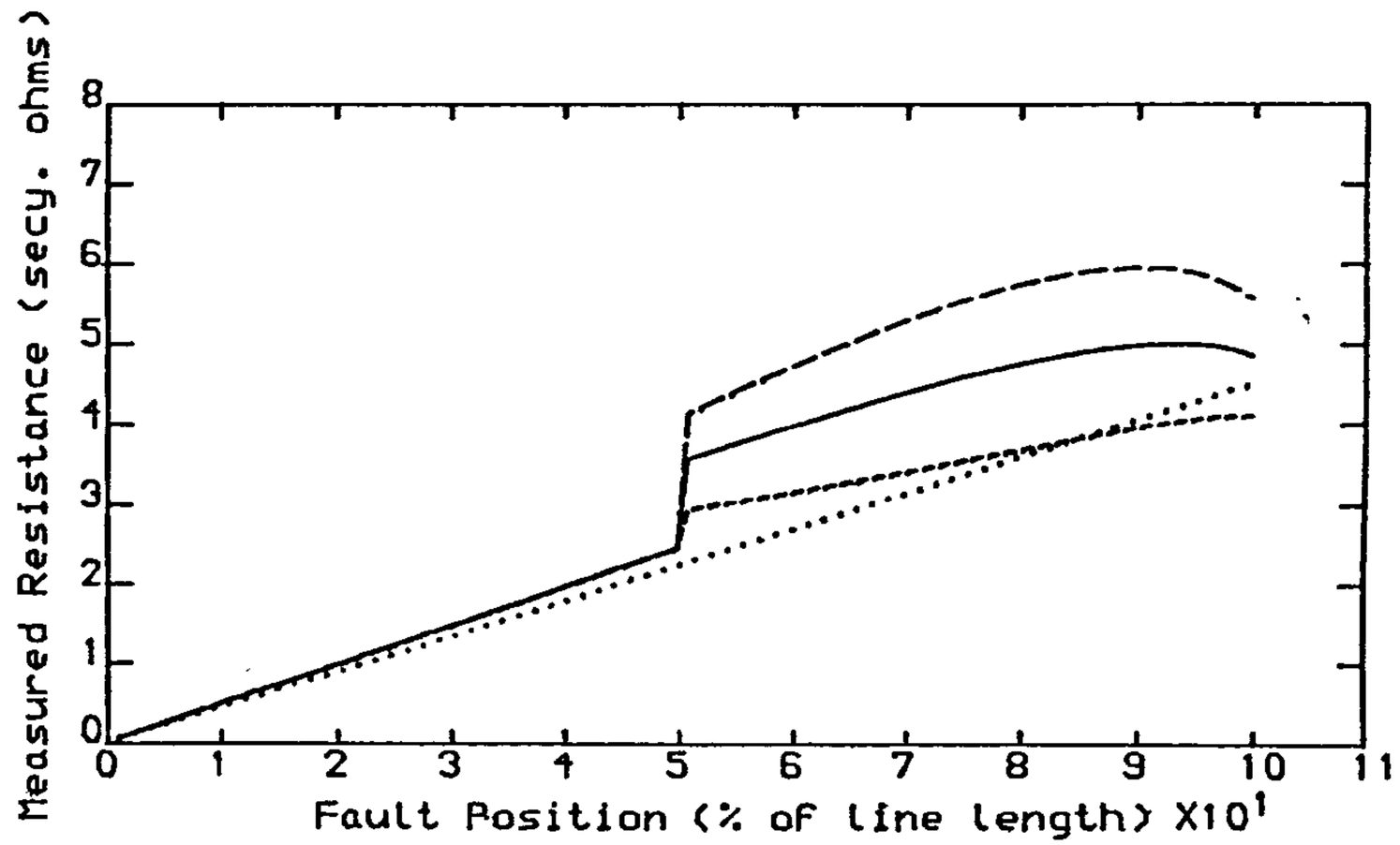

Fig 5.34.b- SE SCL=35 GVA. RE SCL=5 GVA

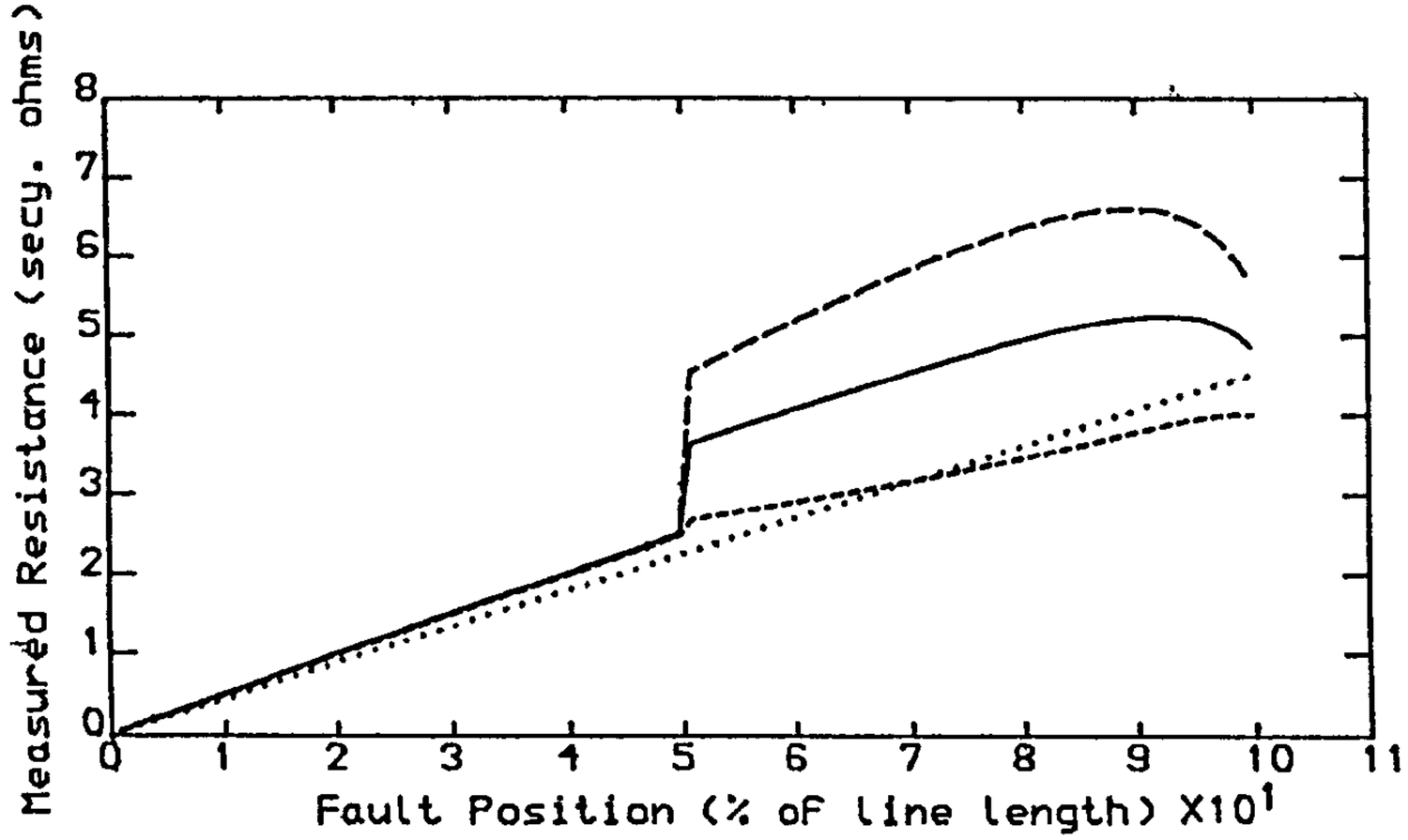

Fig 5.34.c- SE SCL=10 GVA. RE SCL=10 GVA

Fig 5.34-Measured Resistance VS Fault Position with the Complex Conventional Residual Compensation Factor, $K_C = 0.78 \angle -13.5°$ (50% Series Compensation at Mid-Point)

.... Line Locus
---- Pre-Fault Load Angle=-10 deg.
——— Pre-Fault Load Angle=0 deg.
—— Pre-Fault Load Angle=+10 deg.
Line Length=300 km

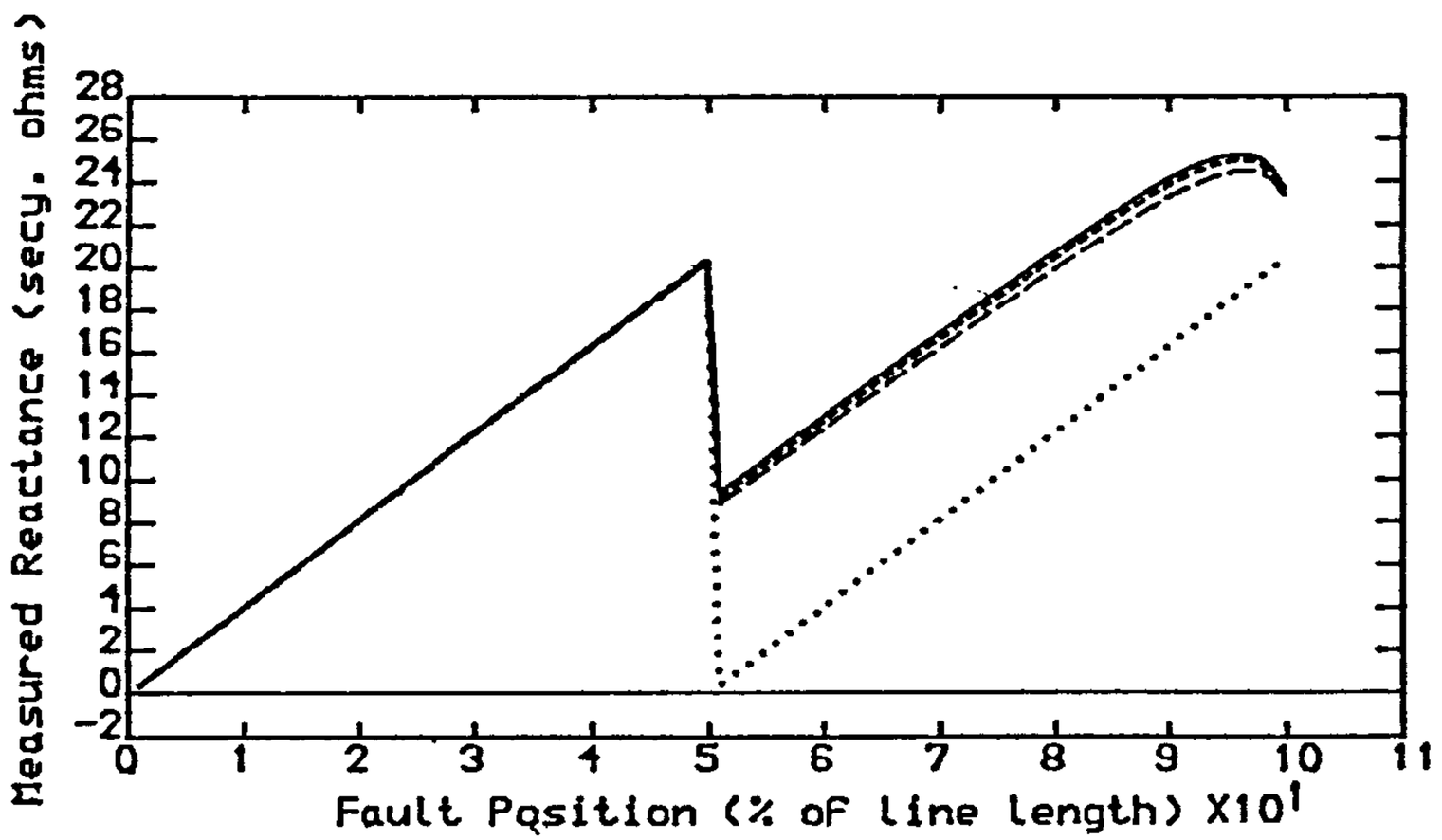

Fig 5.35.a- SE SCL=5 GVA, RE SCL=35 GVA

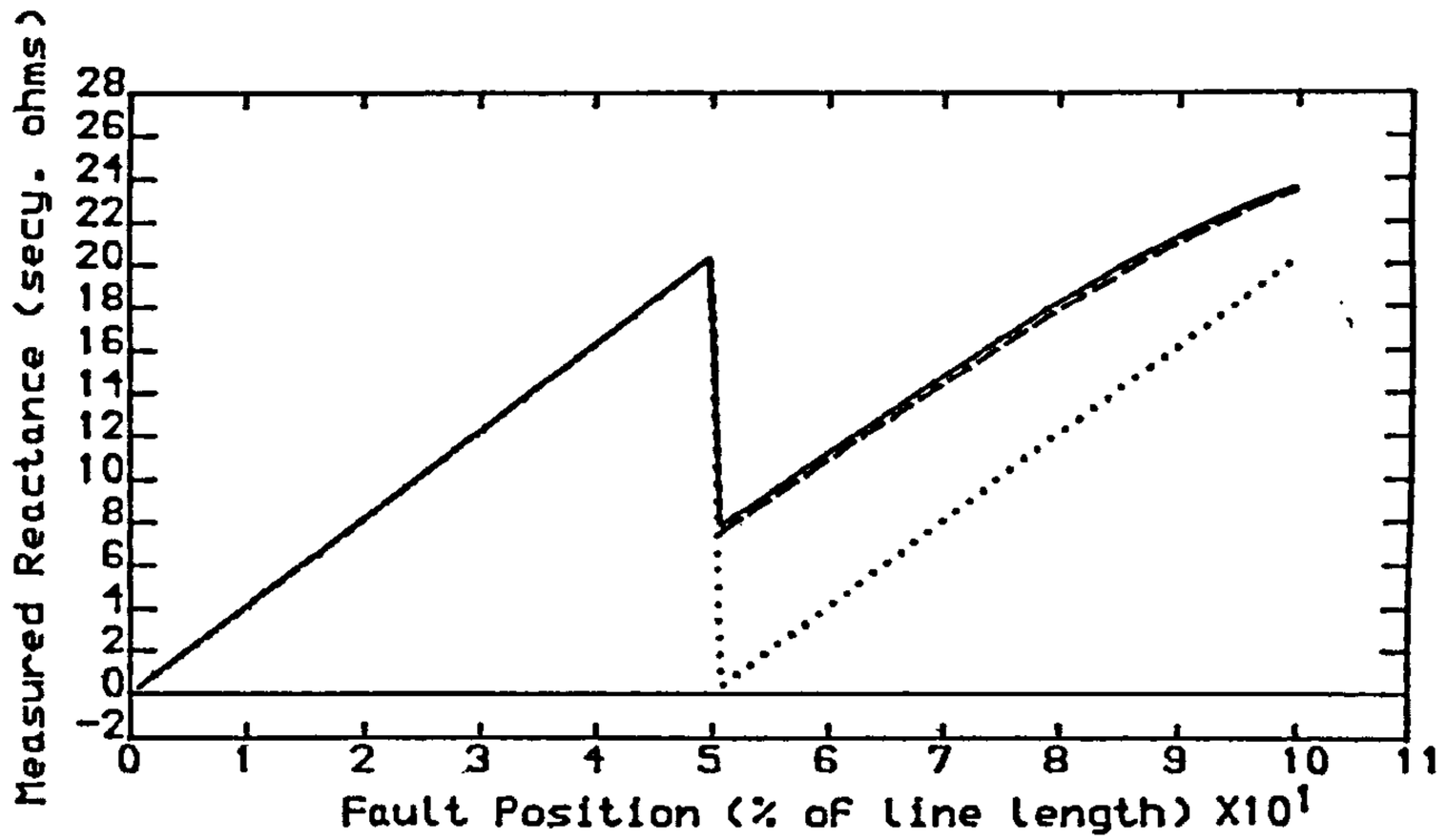

Fig 5.35.b- SE SCL=35 GVA, RE SCL=5 GVA

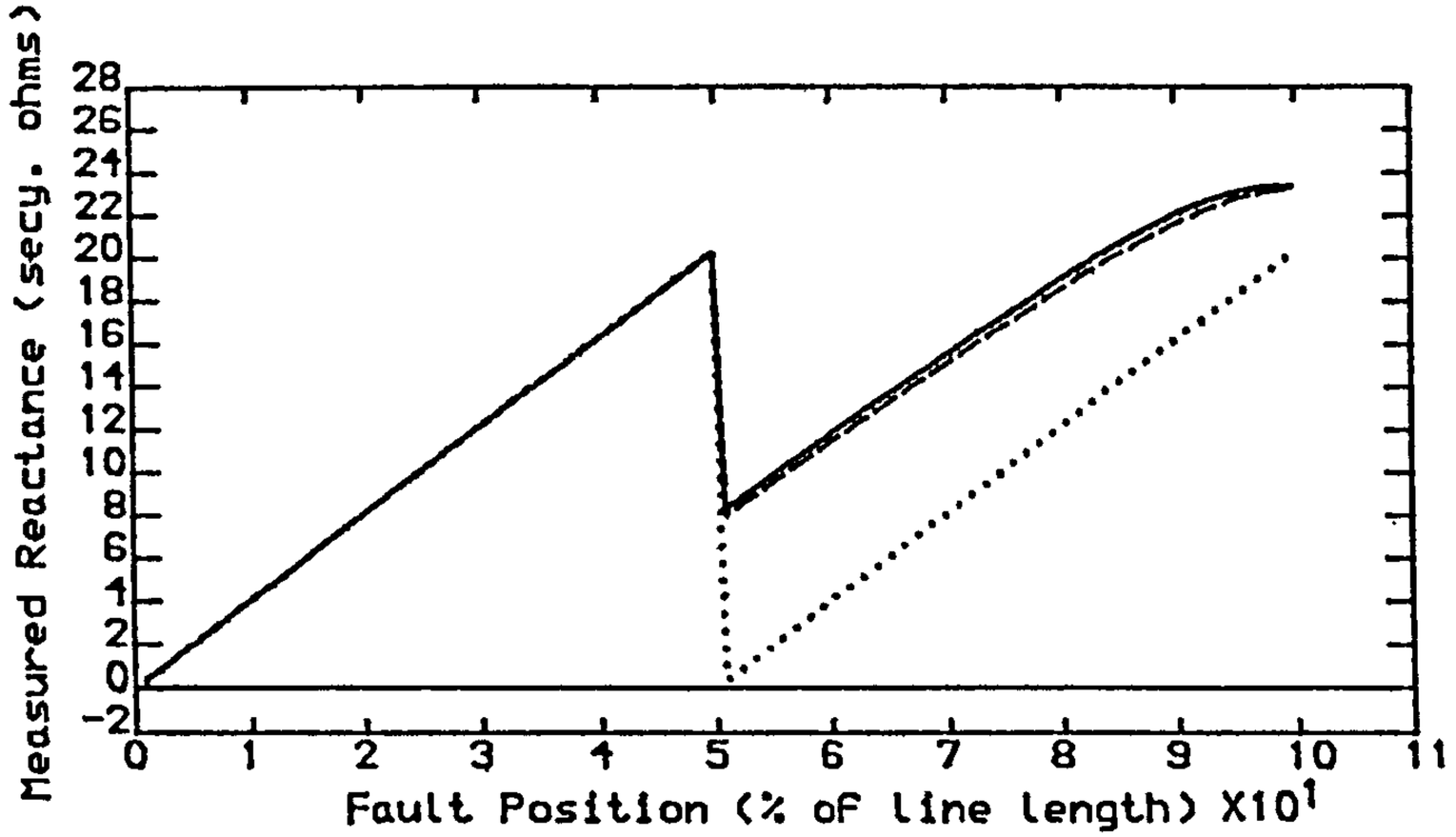

Fig 5.35.c- SE SCL=10 GVA, RE SCL=10 GVA

Fig 5.35-Measured Reactance VS Fault Position with the Complex Conventional Residual Compensation Factor, $K_C=0.78\angle -13.5°$ (50% Series Compensation at Mid-Point)

.... Line Locus
---- Pre-Fault Load Angle=-10
——— Pre-Fault Load Angle=0
—— Pre-Fault Load Angle=+10
Line Length=300 km

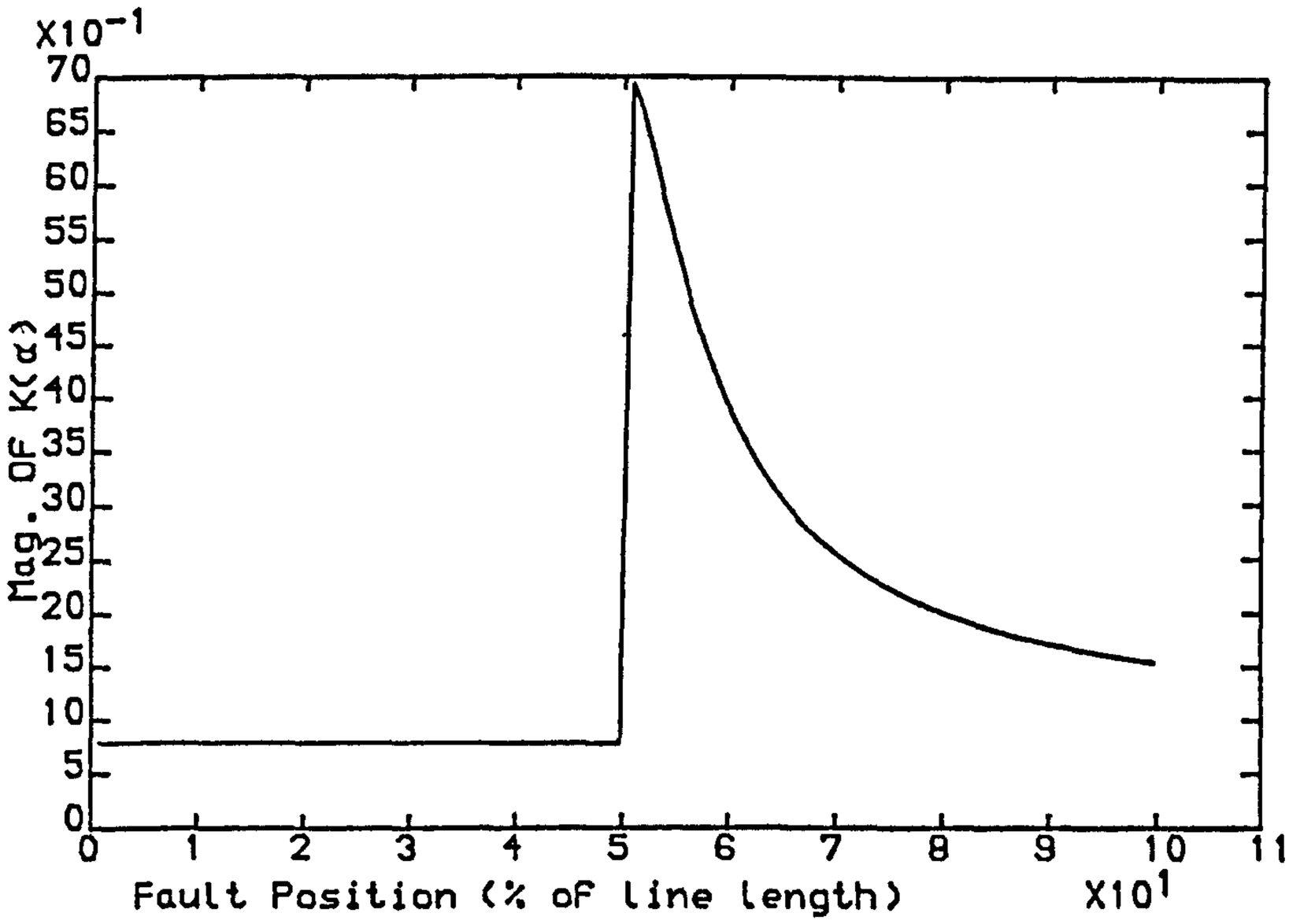

Fig 5.36.a-Variation in Mag. Of K(a) with Fault Position (50% series comp.)

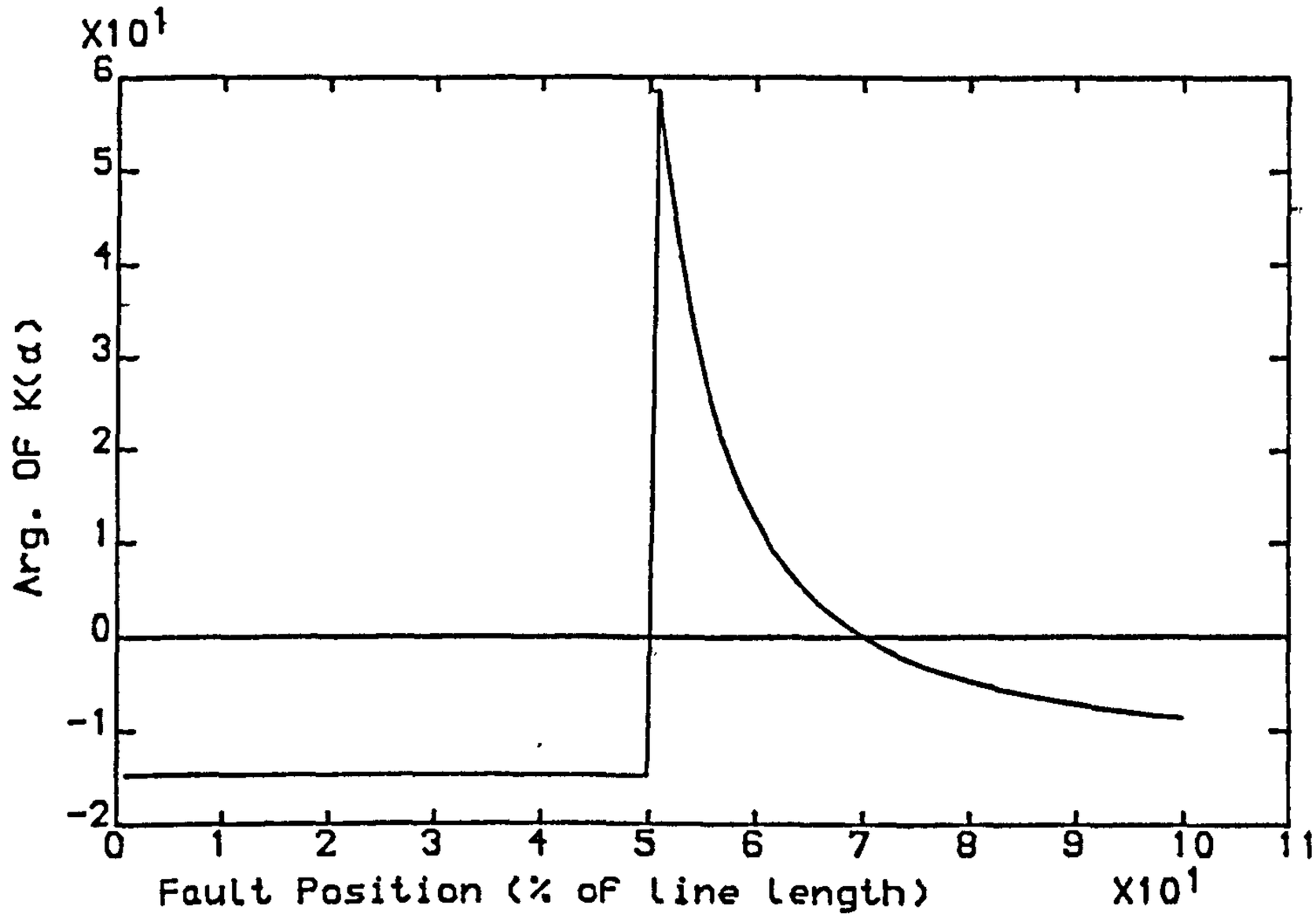

Fig 5.36.b-Variation in Arg. Of K(a) with Fault Position (50% series comp.)

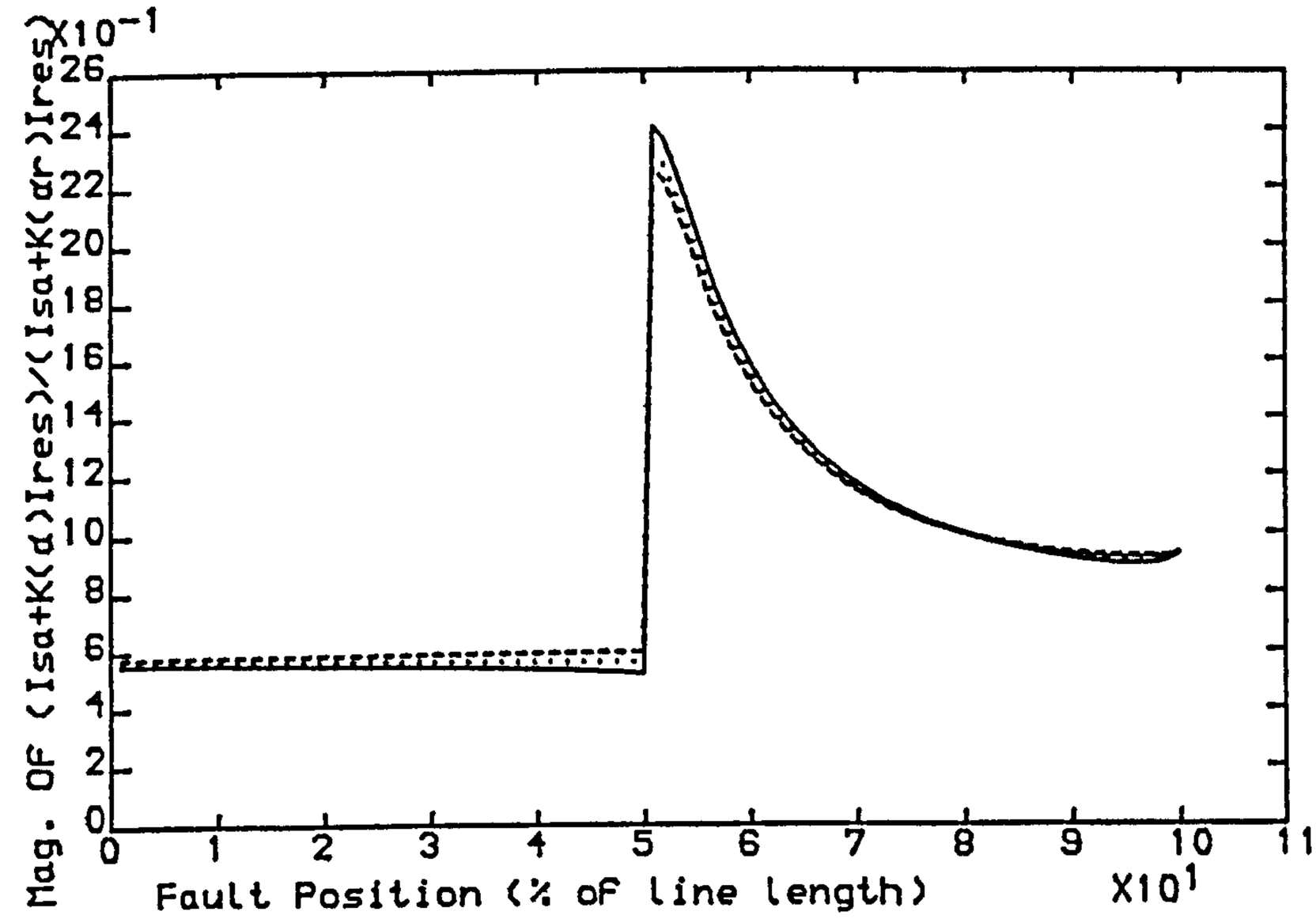

Fig 5.37.a-Variation in Mag. Of
(Isa+K(a) Ires) / (Isa+K(ar) Ires) with
Fault Position For Pre-Fault
Load Angle Of -10 Degrees

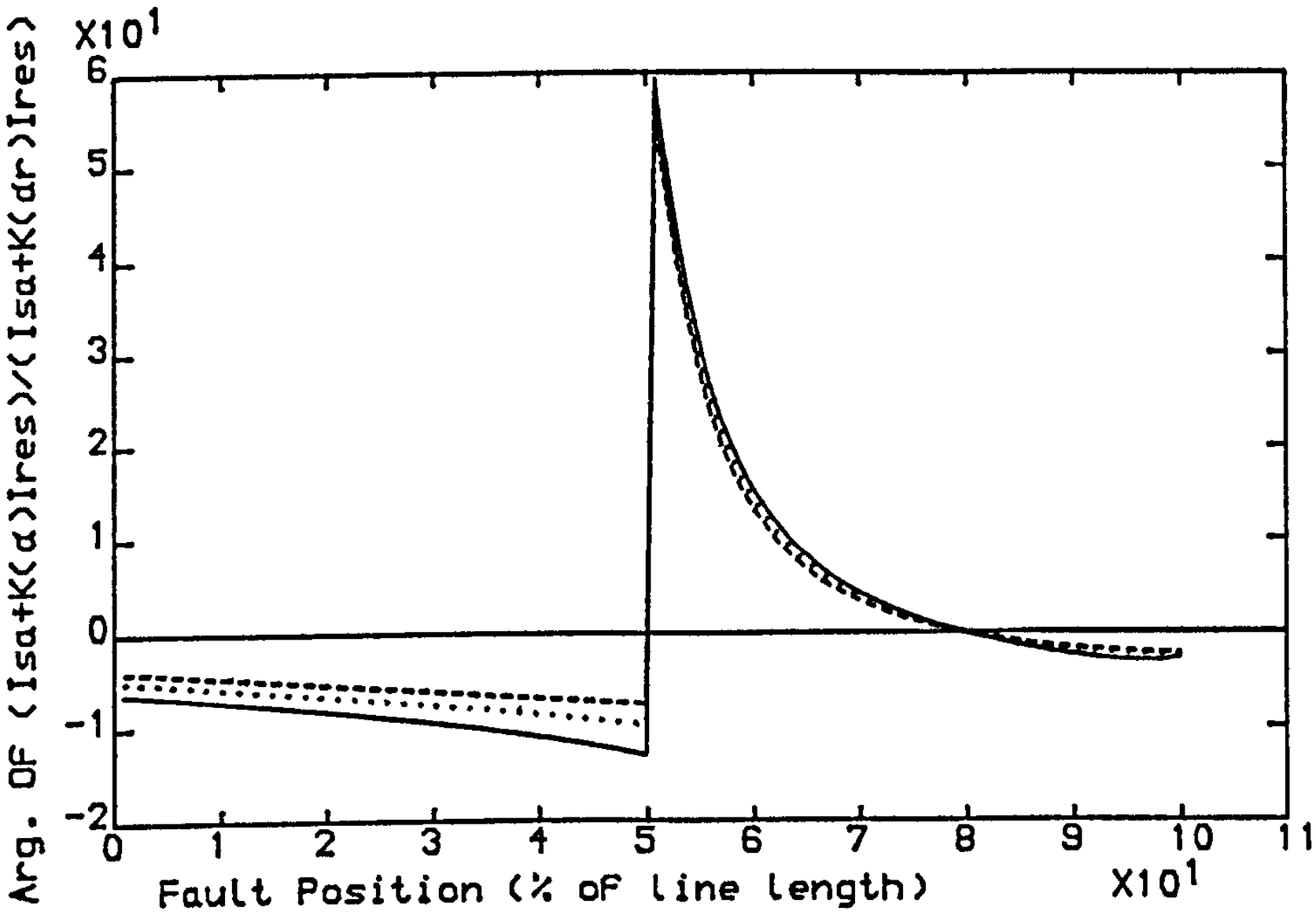

Fig 5.37.b-Variation in Arg. Of
(Isa+K(a) Ires) / (Isa+K(ar) Ires) with
Fault Position For Pre-Fault
Load Angle Of -10 Degrees

——— SE SCL=5 GVA, RE SCL=35 GVA
-·-·- SE SCL=35 GVA, RE SCL=5 GVA
···· SE SCL=10 GVA, RE SCL=10 GVA
Line Length =300 km

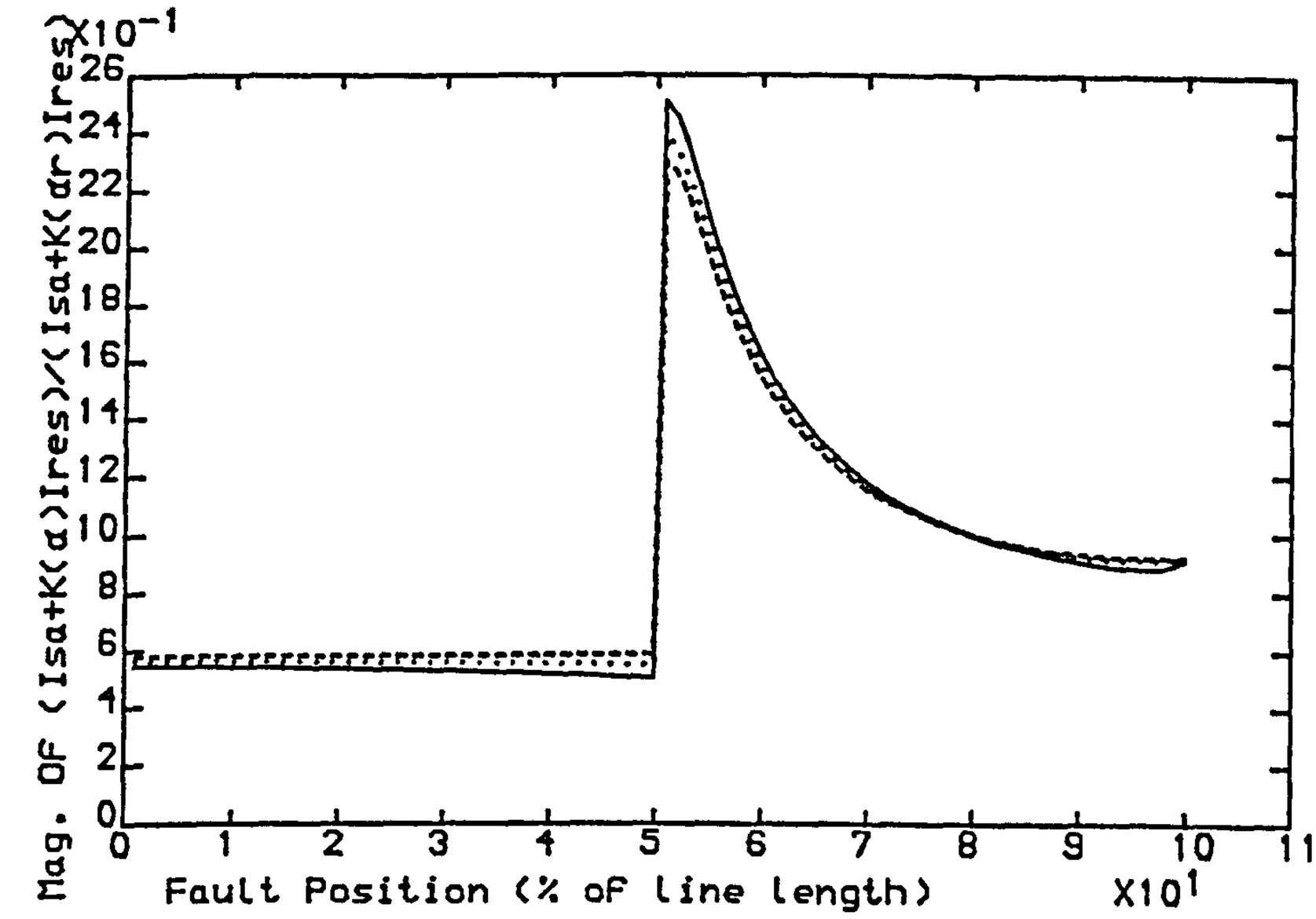

Fig 5.38.a-Variation in Mag. Of (Isa+K(a)Ires)/(Isa+K(ar)Ires) with Fault Position For Pre-Fault Load Angle Of 0 Degrees

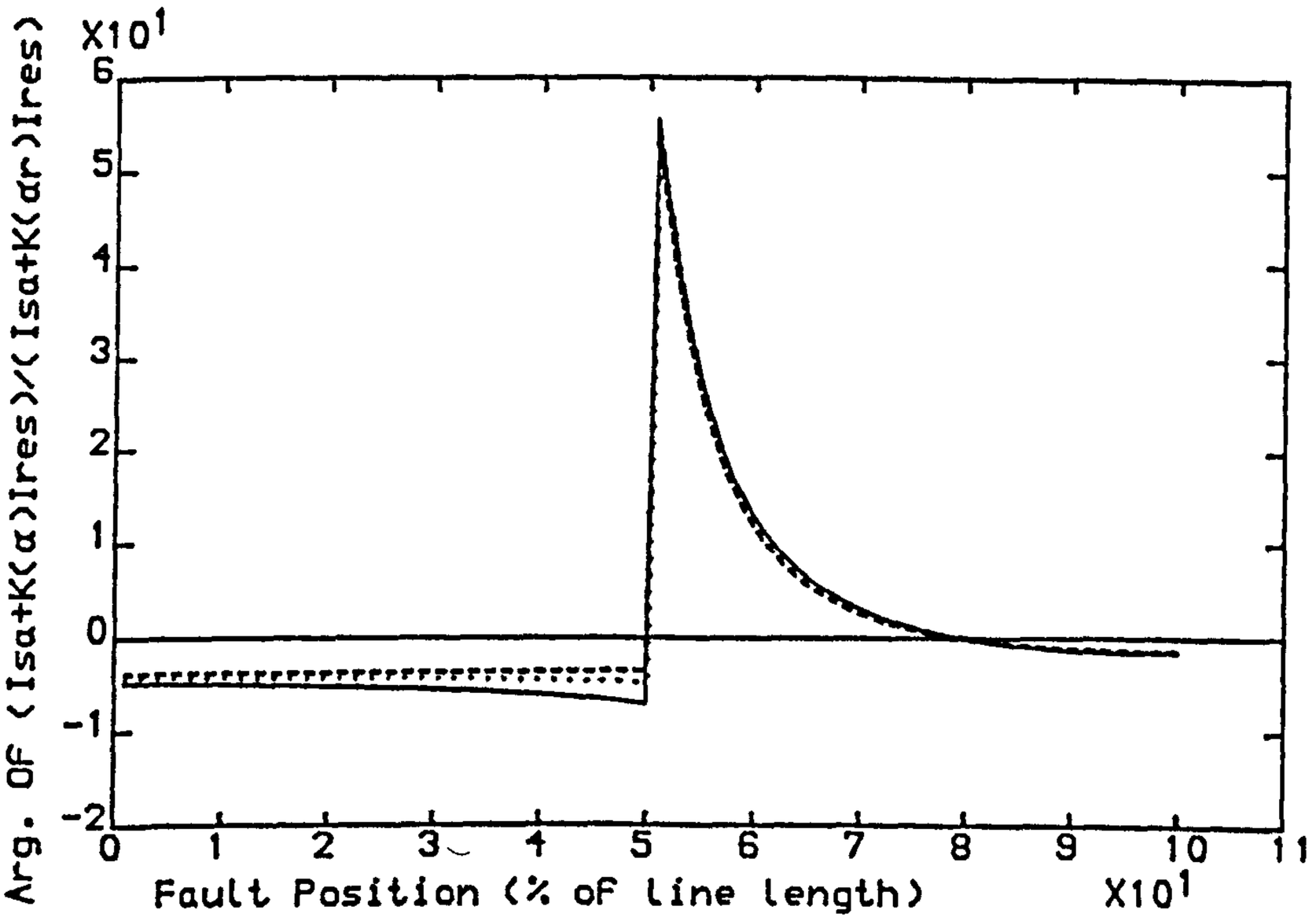

Fig 5.38.b-Variation in Arg. Of (Isa+K(a)Ires)/(Isa+K(ar)Ires) with Fault Position For Pre-Fault Load Angle Of 0 Degrees

——— SE SCL=5 GVA, RE SCL=35 GVA
---- SE SCL=35 GVA, RE SCL=5 GVA
.... SE SCL=10 GVA, RE SCL=10 GVA
Line Length =300 km

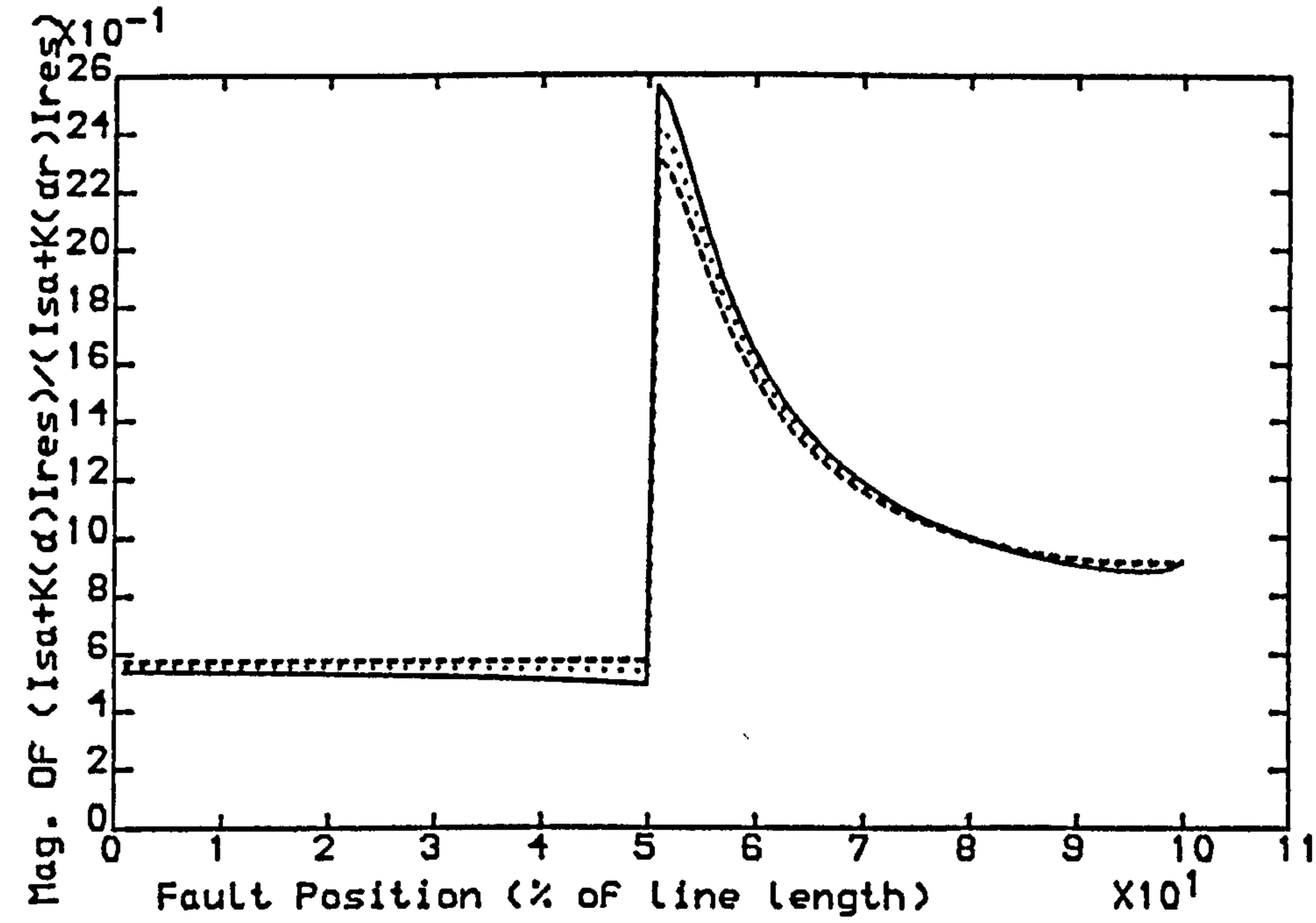

Fig 5.39.a-Variation in Mag. Of
(Isa+K(a) Ires) / (Isa+K(ar) Ires) with
Fault Position For Pre-Fault
Load Angle Of +10 Degrees

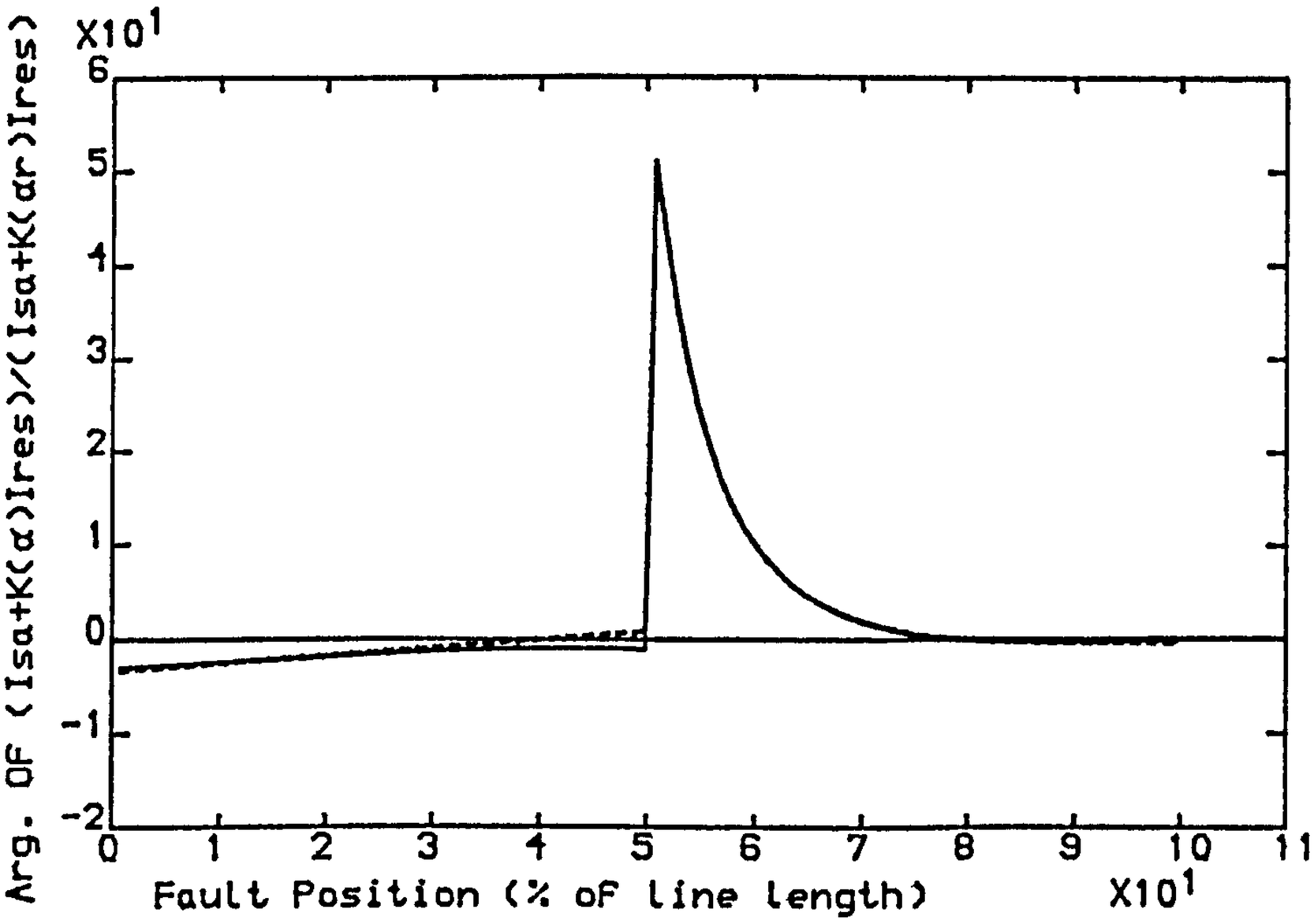

Fig 5.39.b-Variation in Arg. Of
(Isa+K(a) Ires) / (Isa+K(ar) Ires) with
Fault Position For Pre-Fault
Load Angle Of +10 Degrees

——— SE SCL=5 GVA, RE SCL=35 GVA
---- SE SCL=35 GVA, RE SCL=5 GVA
.... SE SCL=10 GVA, RE SCL=10 GVA
Line Length =300 km

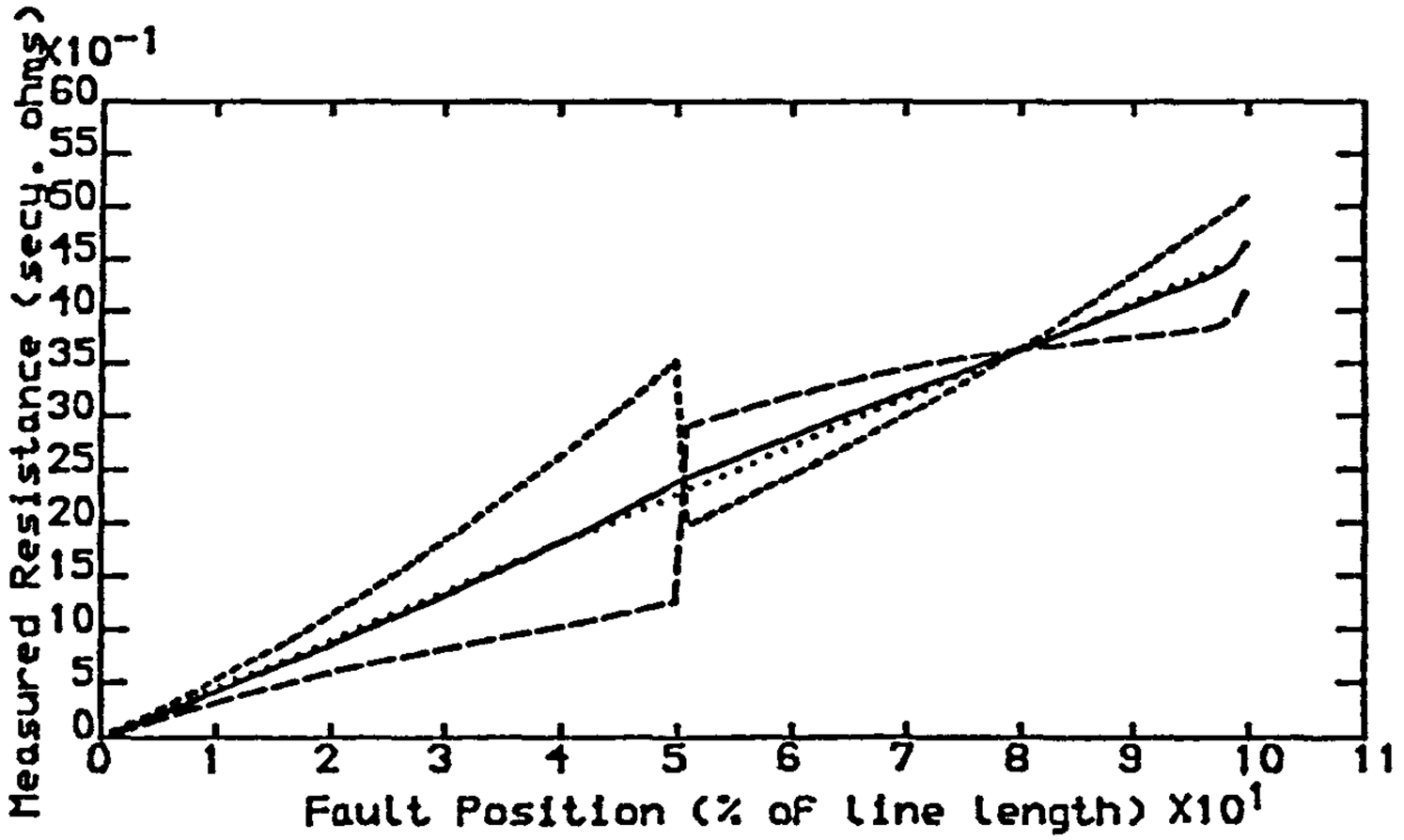

Fig 5.40.a- SE SCL=5 GVA, RE SCL=35 GVA

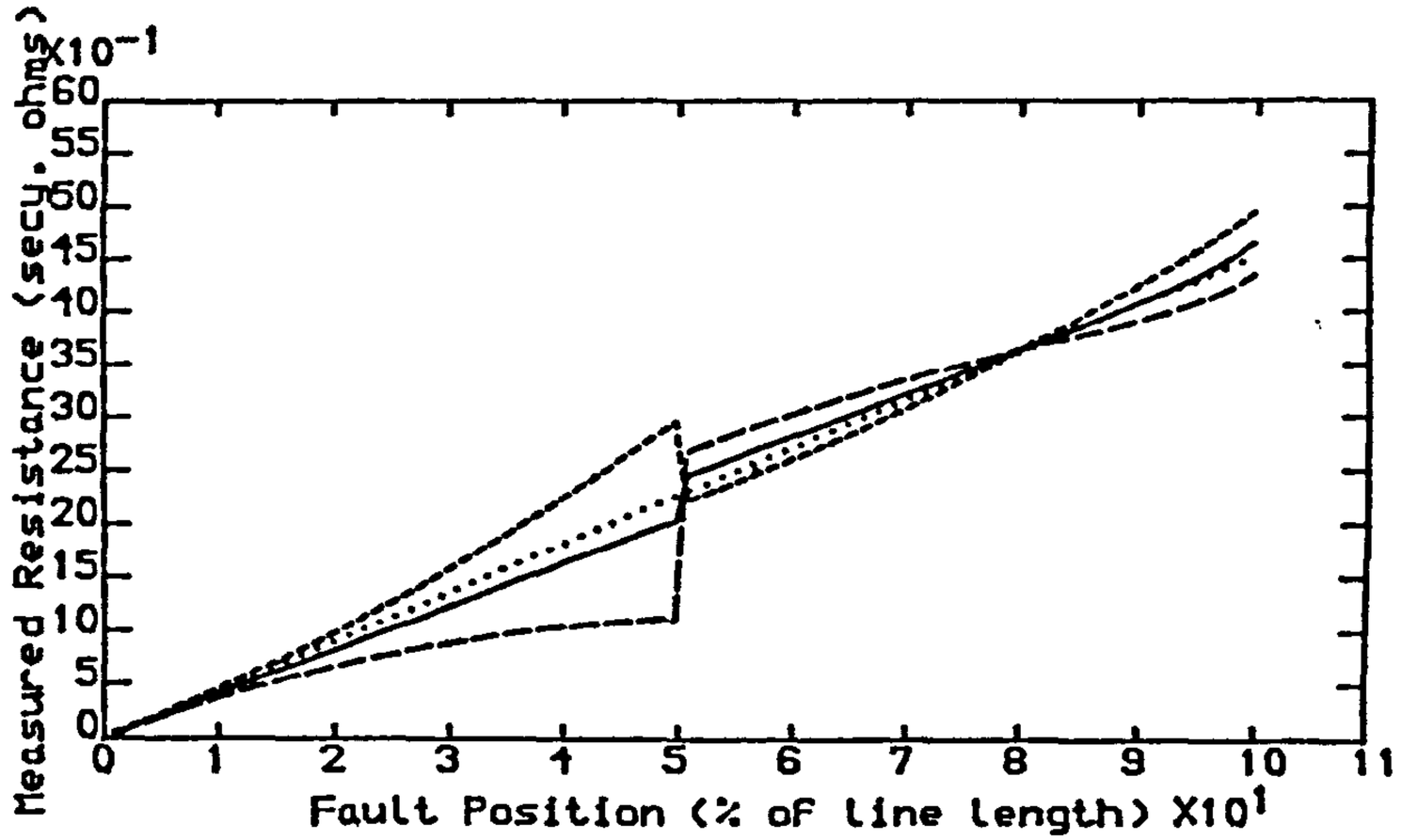

Fig 5.40.b- SE SCL=35 GVA, RE SCL=5 GVA

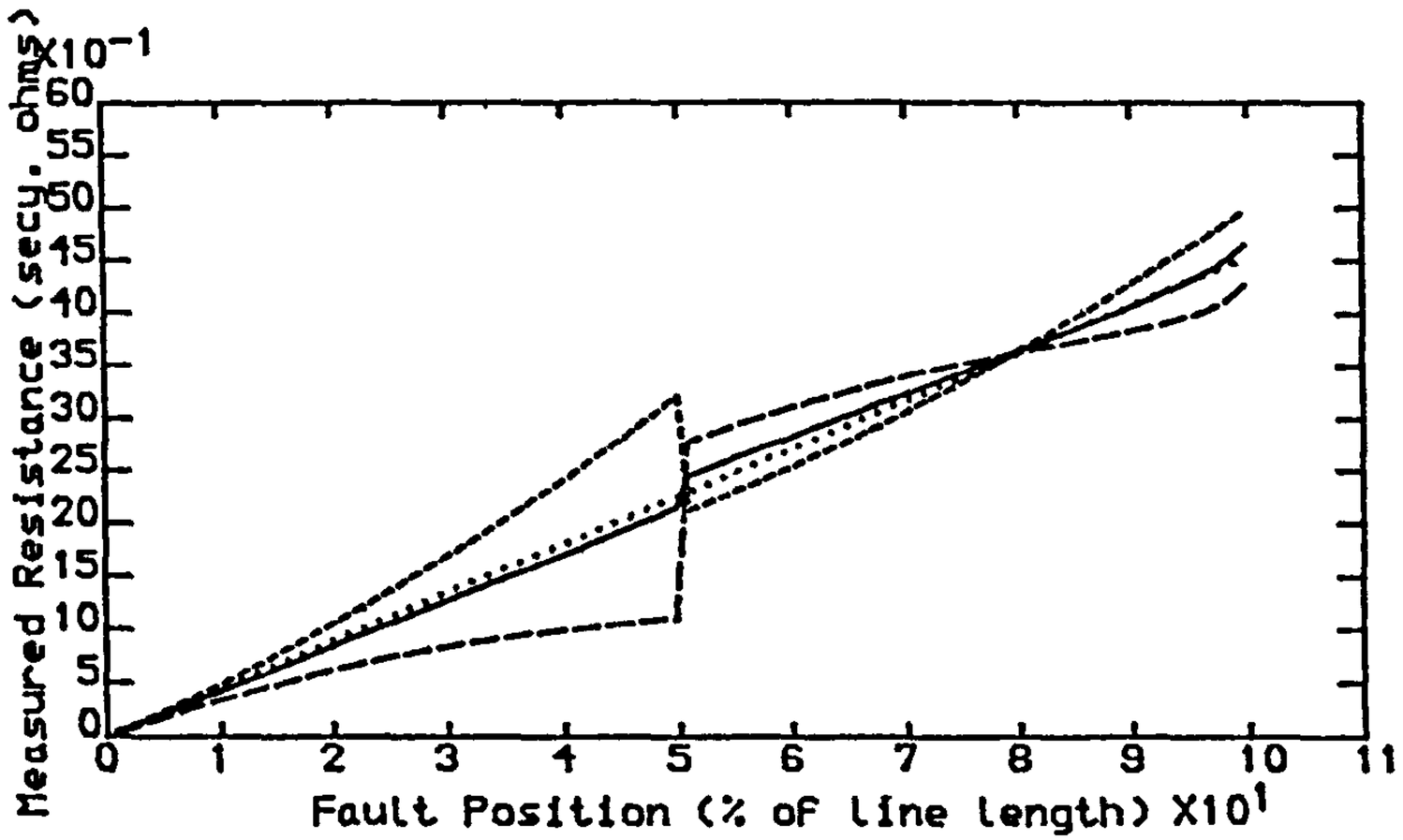

Fig 5.40.c- SE SCL=10 GVA, RE SCL=10 GVA

Fig 5.40-Measured Resistance VS Fault Position, with the New Residual Compensation Factor, $K_{\alpha r}=2.015\angle -4.5°$, $\alpha r=0.8$ of line length (50% Series Compensation at Mid-Point).

.... Line Locus
---- Pre-Fault Load Angle=-10 deg.
——— Pre-Fault Load Angle=0 deg.
——— Pre-Fault Load Angle=+10 deg.
Line Length=300 km

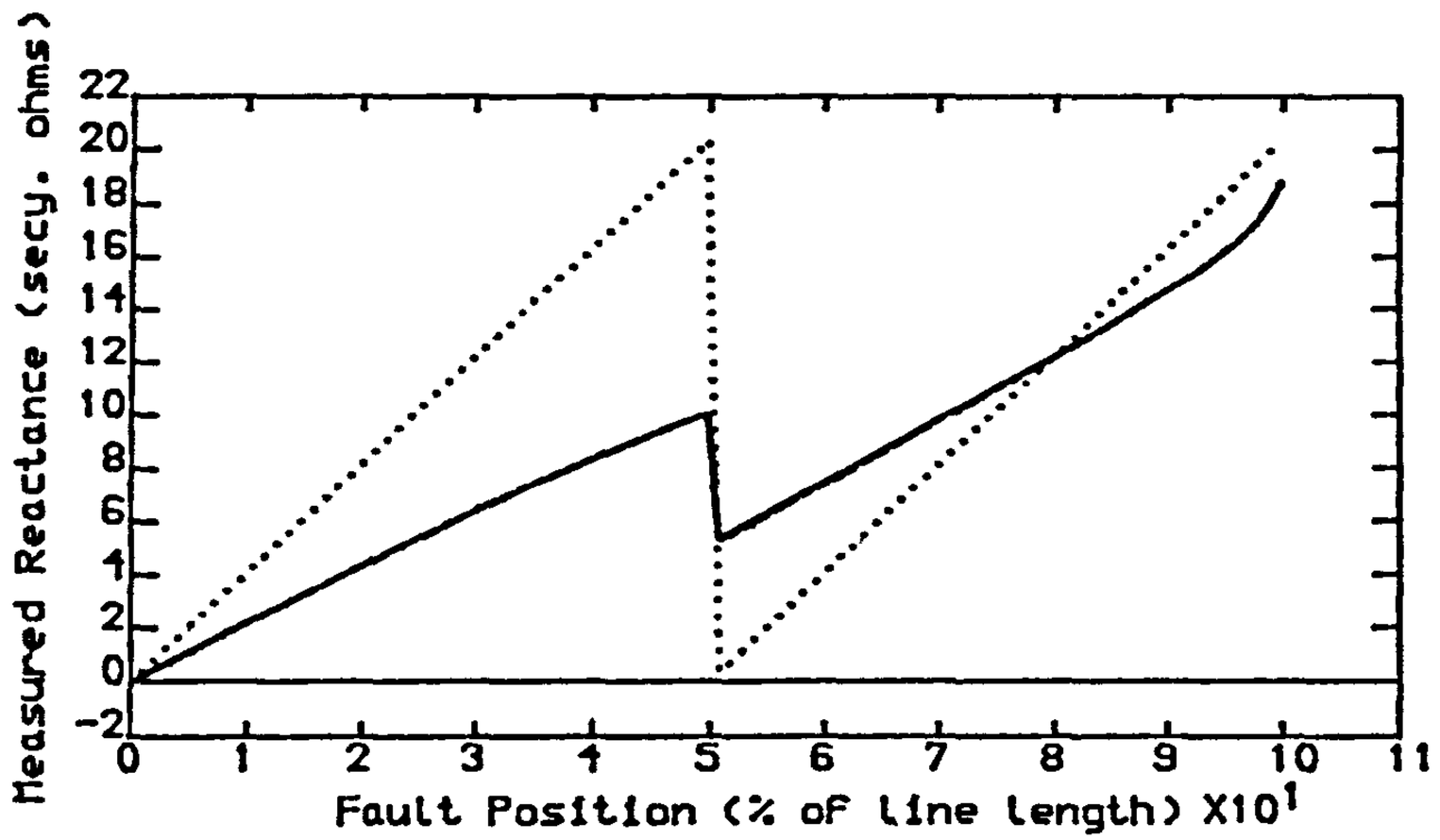

Fig 5.41.a- SE SCL=5 GVA, RE SCL=35 GVA

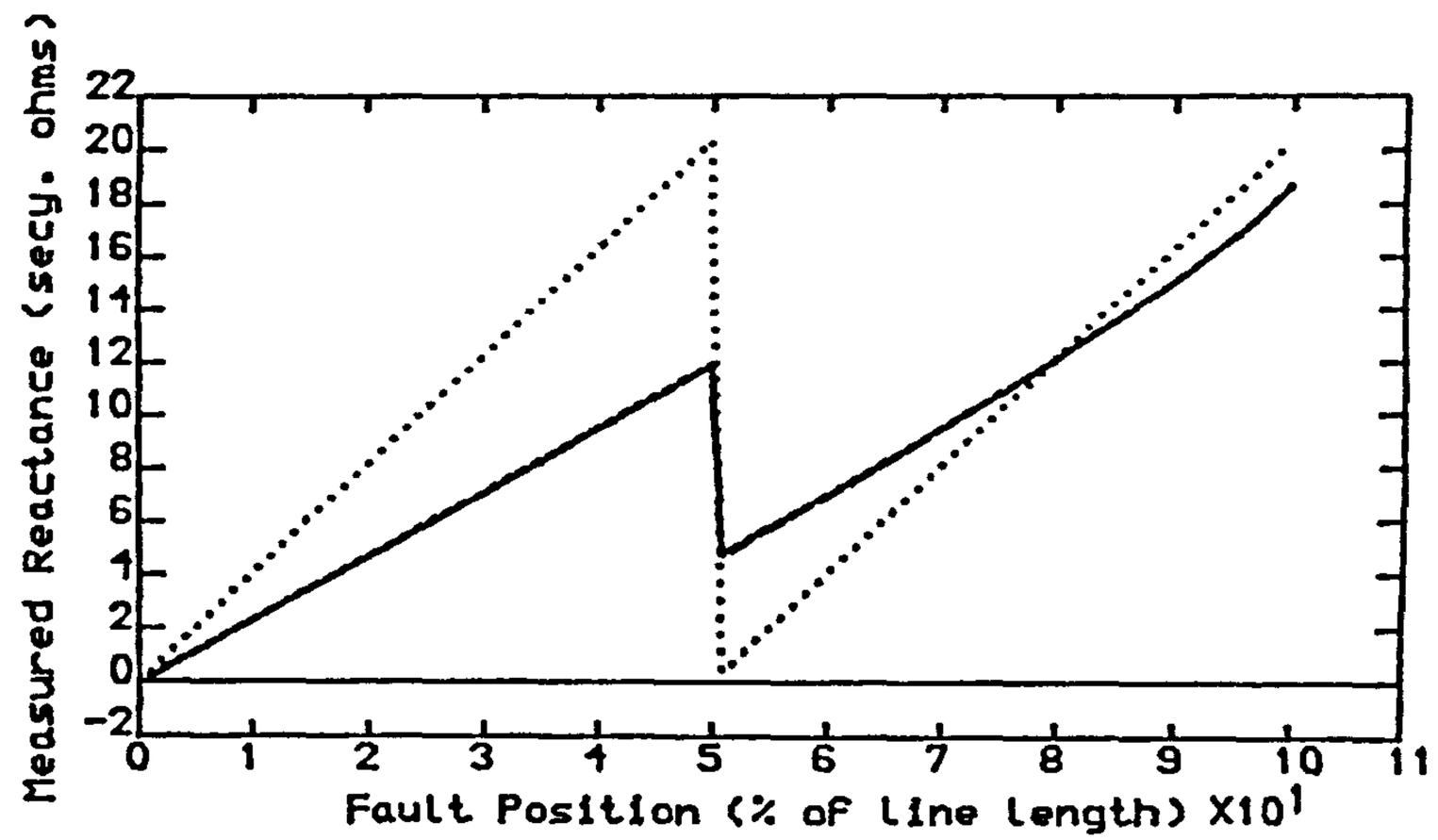

Fig 5.41.b- SE SCL=35 GVA, RE SCL=5 GVA

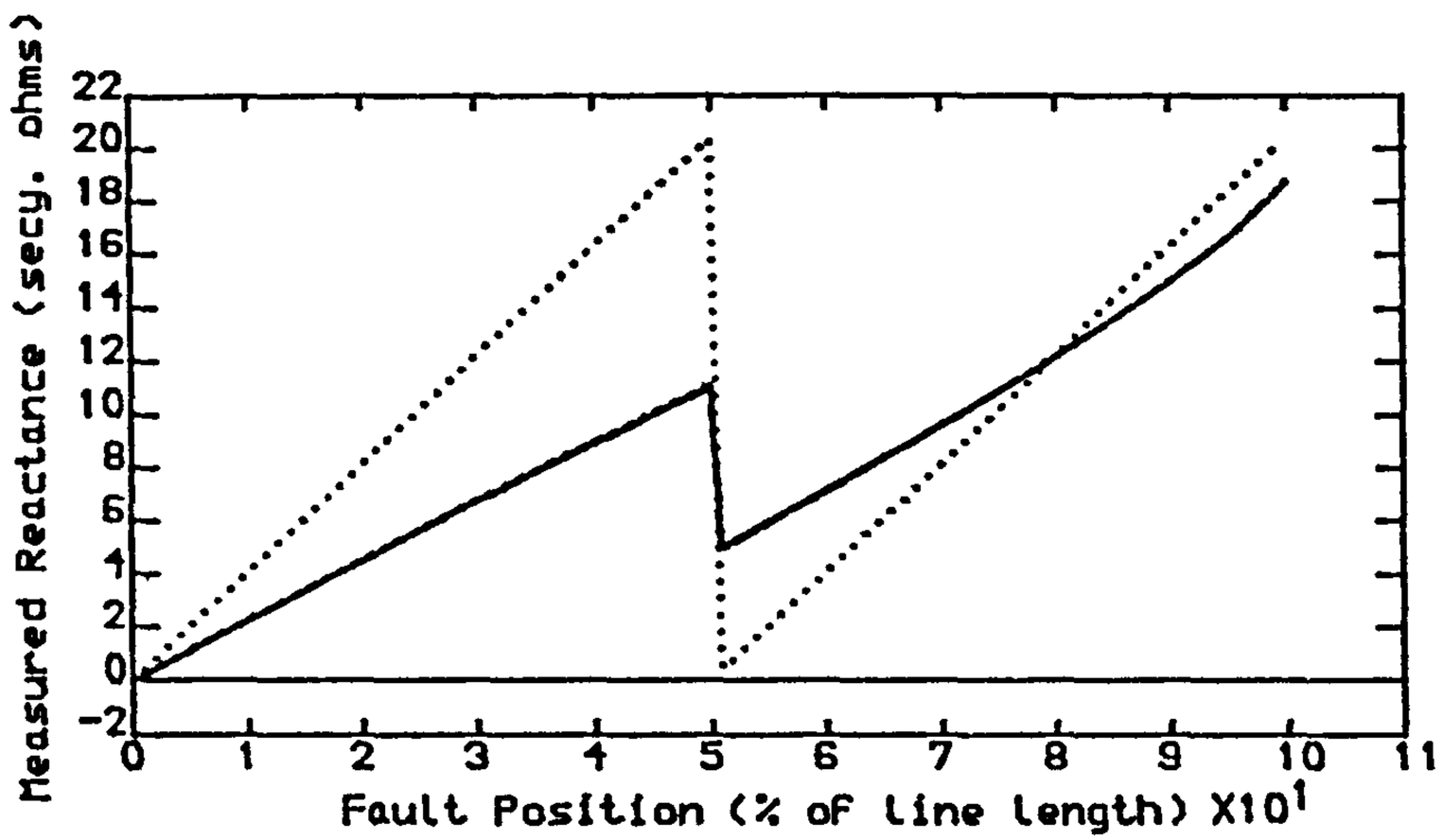

Fig 5.41.c- SE SCL=10 GVA, RE SCL=10 GVA

Fig 5.41-Measured Reactance VS Fault Position, with the New Residual Compensation Factor, $K_{\alpha r}=2.015\angle -4.5°$, $\alpha r=0.8$ of line length (50% Series Compensation at Mid-Point).

.... Line Locus
---- Pre-Fault Load Angle=-10
——— Pre-Fault Load Angle=0
——— Pre-Fault Load Angle=+10
Line Length=300 km

CHAPTER 6

RELAY RESPONSE FOR A LINE WITH 70% COMPENSATION

When a transmission line is designed with a series compensation of more than half of its series reactance, say 70%, it is common practice to install half of the series capacitance at each end of the line, e.g. 35% at each end.

To apply distance protection to series compensated lines demands a different setting philosophy than that adopted on plain feeders. Basically the presence of a capacitor in front of the relay will distort the reach of an impedance measuring element.

As the zone-1 of the distance scheme trips independantly of any additional information from the far end of the line, it is vital that the element does not over-reach. If there is a series capacitor in front of the relay at the remote end bus-bar, then the worst case assumption is to allow for that capacitor to be fully in circuit. For this reason it has been suggested that the zone-1 reach be set at 80% of the compensated impedance [13], although some utilities have considered this coverage as unsatisfactory and completely ignored distance schemes for the first independant zone [32].

However, as explained in Chapter 5, for an "a"-phase-ground fault, the measured reactance is bigger than the actual line reactance for faults beyond the remote end capacitor, if the new method of residual compensation (NRCF) is used. Therefore, it is possible to set the relay forward reactance reach at a value higher than 80%

of the compensated impedance, or 52% of line length. In this study the relay forward reach is set at 60% of the line length (or 92% of the compensated reactance).

6.1-Line With 70% Compensation And C.V.T. On The Source Side Of The Capacitor

Consider Figure 6.1 which shows a typical series compensated line with 35% of the compensation at each end.

Since the C.V.T. is on the source side of the series capacitor the line impedance locus will be in the fourth and first quadrant of the impedance plane, as shown in Figure 6.2.

6.1.1-relay trip characteristic

As previously mentioned, the relay forward reactance reach setting is determined by the remote end capacitor. Thus the forward zone-1 reactance reach is set at 60% of the line length in order to exclude faults at the receiving end bus-bar from the boundary.

The reverse reactance reach is, on the other hand, set considering the effect of the local capacitor bank. The relay trip characteristic may be arranged so that it excludes the local capacitor, as shown in Figure 6.3. This implies that some internal faults do not fall within the relay trip characteristic as long as the capacitor bank protection, namely the spark gap, does not flash-over (i.e. capacitor remains in the circuit).

However, if it is ensured that the relay directional ability is maintained for all reverse faults, irrespective of system conditions, it is possible to include all faults in front of the capacitor that are within the relay boundary, as shown in Figure 6.4.

It has already been explained in Chapter 4 that the directionality of the relay is maintained by the directional reactance XM. Simulation tests have revealed that the relay does not trip for reverse faults on the sending end bus-bar.

It is common practice in distance protection to expand the forward resistance reach to cater for the high fault resistance. In general, it is preferred to set the resistive reach as high as practicable and usually not less than half of the load resistance.

6.1.2-relay decision logic

The principle of the relay trip decision logic and count regime were explained in Chapter 4. The trip characteristic is divided into three different counting region, as shown in Figure 6.5. The incremental values INC1 and INC2 are initially set at 8 and 32. They will be changed twice after fault detection to 2 and 8 and then 1 and 4 respectively. Figure 6.6 shows the relay decision logic flow chart suitable for a system with 70% series compensation. Note that if a trip does not occur and CRL2 is greater than 60 and the Trip-Counter becomes zero for one msec (4 samples) the relay considers the fault as an out of zone fault and resets both Control-Counters, CRL1 a CRL2. INC1 and INC2 are also reset to their initial values of 8 and 32 respectively.

The counter is decremented by DEC1=8 or DEC2=32 (see Figure 6.5) after fault detection for any sample falling outside the trip characteristic.

6.1.3-the relay trip response

Since the main objective of the work presented here is

to improve the distance relay response when the capacitors are (or remain) in circuit, the operating time response of the digital distance relay, specifically designed for series compensated line applications is examined when it is assumed that the capacitors are permanently in the circuit. This is achieved by adjusting the capacitors' spark-gap threshold at a very high value.

Figures 6.7 to 6.16 illustrate the corresponding relay operating time response. Different system source, pre-fault load and line length have been considered.

It is clearly seen that the relay operating time is about 10 msec for fault positions of up to 65% of the relay reach, for all system condition considered. The relay, generally operates in less than 20 msec for faults between 65% and 80% of the relay reach. But operating times of up to 30 msec is observed for some faults in this region. These are associated with situations in which the local source is much stronger than the remote source and load is imported. In such situations the measured impedance takes a longer time to enter the relay characteristic, thus delaying initiation of count up. No relay over-reach was observed.

The relay was tested for faults at the receiving end bus-bar (behind the remote capacitor), which showed no maloperation.

A lumped parameter program has been used to simulate the primary system. This program has been used to test the relay for many different situations and fault inception angles (in excess of 2000 runs) when the capacitors' spark-gaps flash-over was prevented. The

lumped parameter program was used merely because it has a much faster excution time than a distributed parameter program. The relay performance is shown in Figures 6.7 to 6.16. No relay over-reach/under-reach was observed.

The distributed parameter simulation [9] was used to briefly examine the relay response when the capacitors' protective gaps operate.

Figures 6.17 and 6.18 show the typical relay operating time versus fault position when the capacitors' gap flash-over has been considered.

None of the capacitors in healthy phases were by-passed for all faults considered.

It can be seen that the relay operating times are generally less than 15 msec for faults up to 50% of the relay reach, and that the relay trip times for faults with the inception angle of 0 degree are longer than the faults with the inception angle of 90 degree.

This is caused by a high exponential component in the current signal (when the fault inception angle is around 0 degree) which in turn causes the voltage across the capacitor (or spark-gap) to build up much faster than the case when the current is not offset by exponential term (i.e. for inception angle of around 90 degree).

The flash-over, also introduces a transient in the measurement. Thus, depending upon the window of the algorithm, the measured reactance (and resistance) takes a finite time to reach its post flash-over values. Hence delaying the trip initiation.

Also, it can be seen that for faults with inception angle of 90 degree the relay has initiated trips for

faults up to the approximately 70% of the relay reach in about 10 to 12 msec. This is due to the fact that the relay trips before the capacitor spark-gap flashing over (see Tables 6.1 and 6.2).

Throughout the test the sources were considered to have X to R and zps to pps impedance ratio of 30 and 0.5 respectively. Also in all tests the C.V.T. response was included in the simulation.

The residual compensation factor considered in the relay was equal to $1.82\angle -4.5^{\circ}$.

6.2-Line With 70% Compensation And C.V.T. On The Line Side Of The Capacitor

In this section, the voltage supply for the relay is assumed to be taken from the line side of the capacitor bank (see Figure 6.19) and the relay behaviour is examined.

Since the capacitor bank, in the line side C.V.T. case, can be assumed to be part of the local source, the flash-over of the protective gap will not affect the relay impedance measurement. Furthermore, the line model equation which the relay algorithm solves return to the plain feeder model which consists of only the line resistance and inductive reactance. It follows that the capacitor has a very insignificant effect on the measurands with regard to the sub-synchronous oscillation.

6.2.1-relay characteristic for line side C.V.T

The relay characteristic for a line side voltage transducer is shown in Figure 6.20. Note that the local capacitor reactance exhibits a positive reactance to the relay and is inside the characteristic. The nearby

external faults are also within the protected zone and are therefore detected by the relay. For these (reverse) faults however, the directional reactance measurement, XM (see Chapter 4), prevents relay maloperation. Figure 6.20.a shows the measured X and XM for a reverse fault at the sending end bus-bar.

The forward reactance reach of the relay is, as mentioned in Section 6.1.1, determined by the remote end capacitor and, therefore set at 60% of the line length to exclude the faults at the receiving end bus-bar.

It was explained in Chapter 5 that in order to improve the measurement accuracy of the relay a complex residual compensation factor must be used in the relay, which is calculated to be equal to $0.78\angle -13.5^{\circ}$ (see Chapter 5, Section 5.2).

Figures 6.21 to 6.27 show the relay operating times versus the relay reach, for different system pre-fault load and source conditions.

It is evident that although the count regime and trip logic had originally been designed for the source side C.V.T. configuration with very much stronger sub-synchronous resonance, it coped very well with the line side C.V.T. situation.

The relay response is observed, from Figures 6.21 to 6.26 to be about 10 msec up to about 85% of the relay reach. No relay over-reach was observed. Moreover, the relay restrained for all faults on the receiving end bus-bar (behind the remote capacitor).

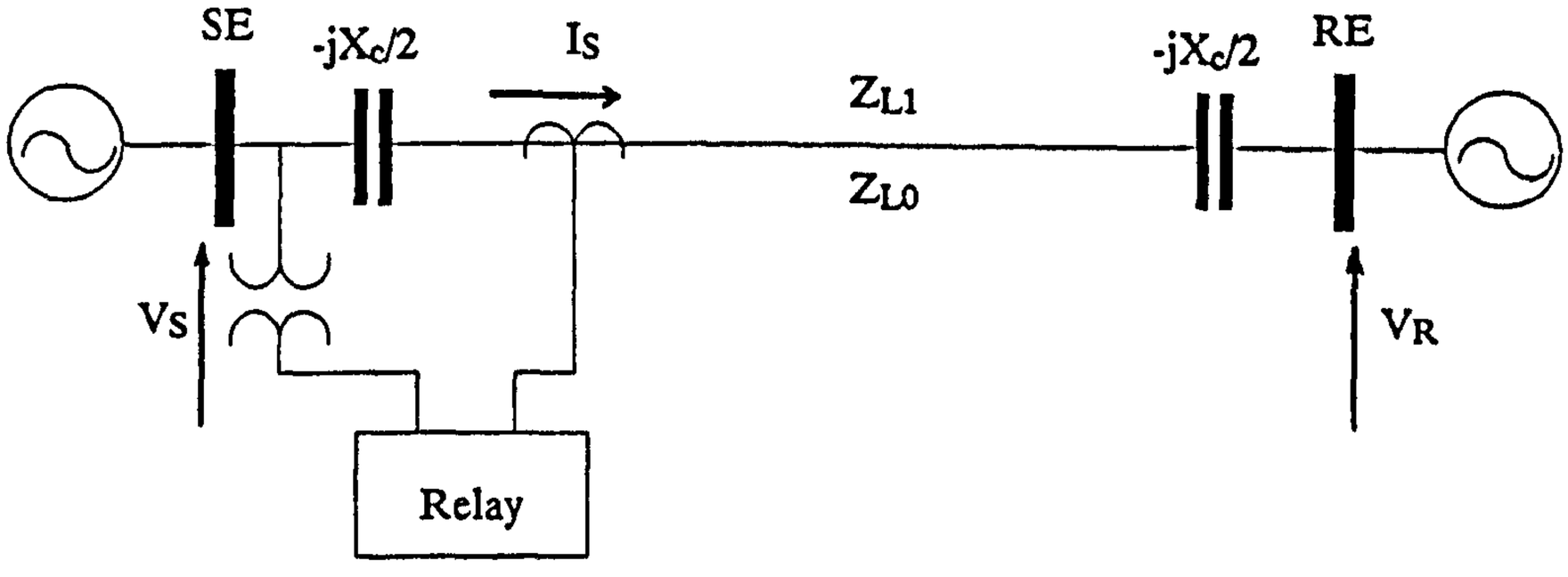

Fig 6.1-Line Configuration With Series Capacitors At The Line Ends And Source Side C.V.T.

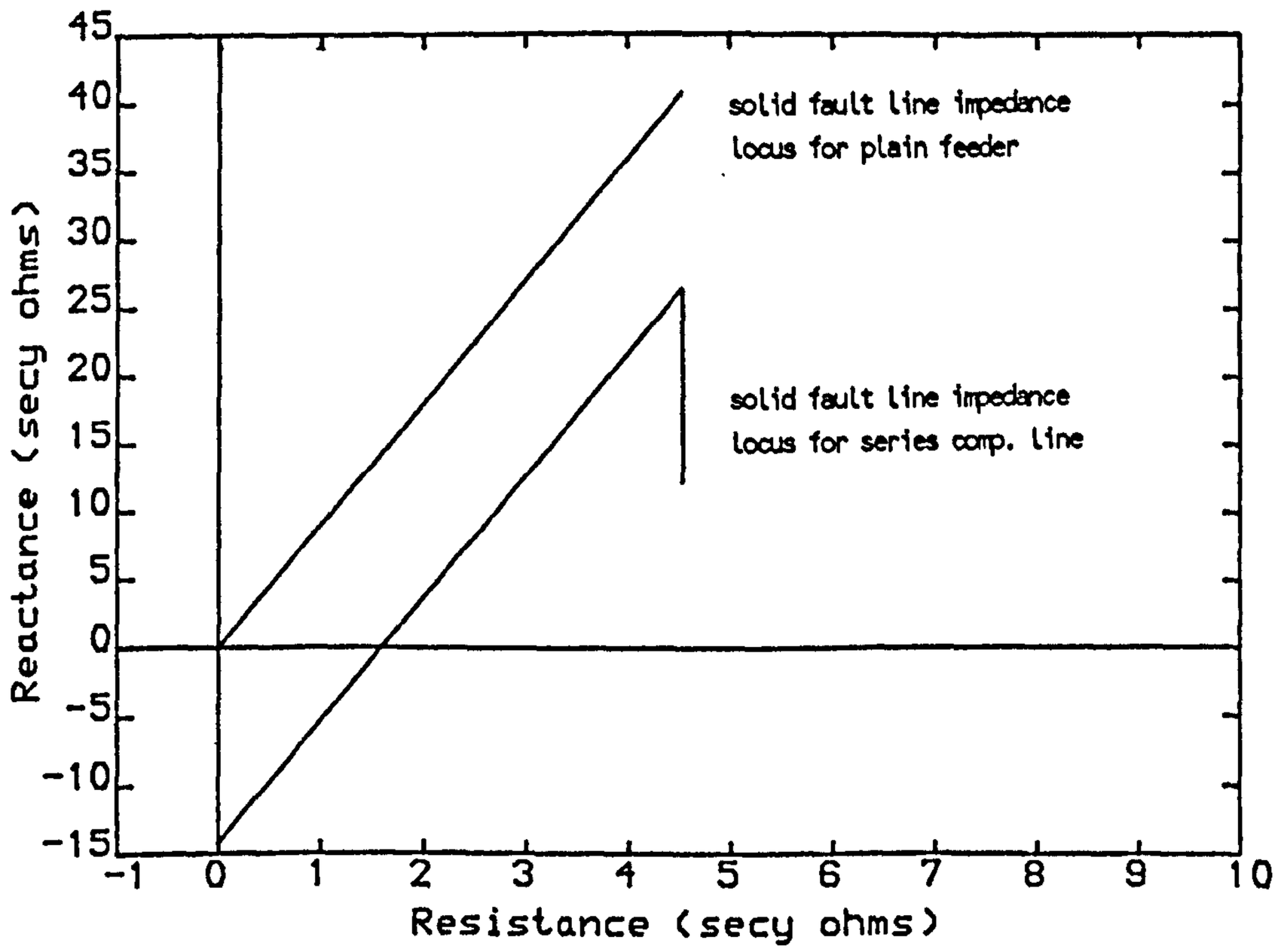

Fig 6.2-Impedance Locus For A Line With 70% Comp. And Source Side C.V.T.

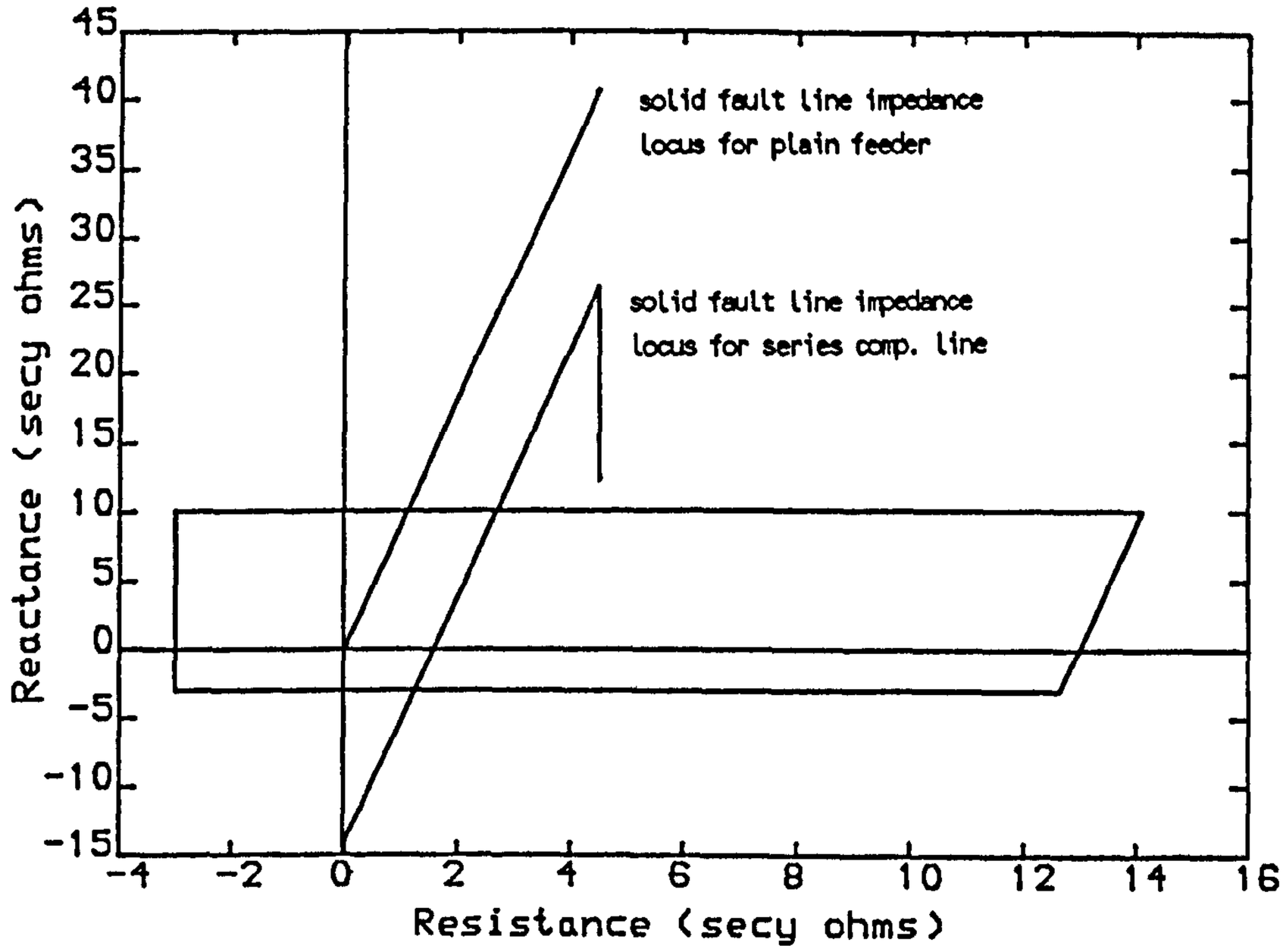

Fig 6.3-Impedance Locus And Relay Characteristic (the local cap. is NOT included in the boundary

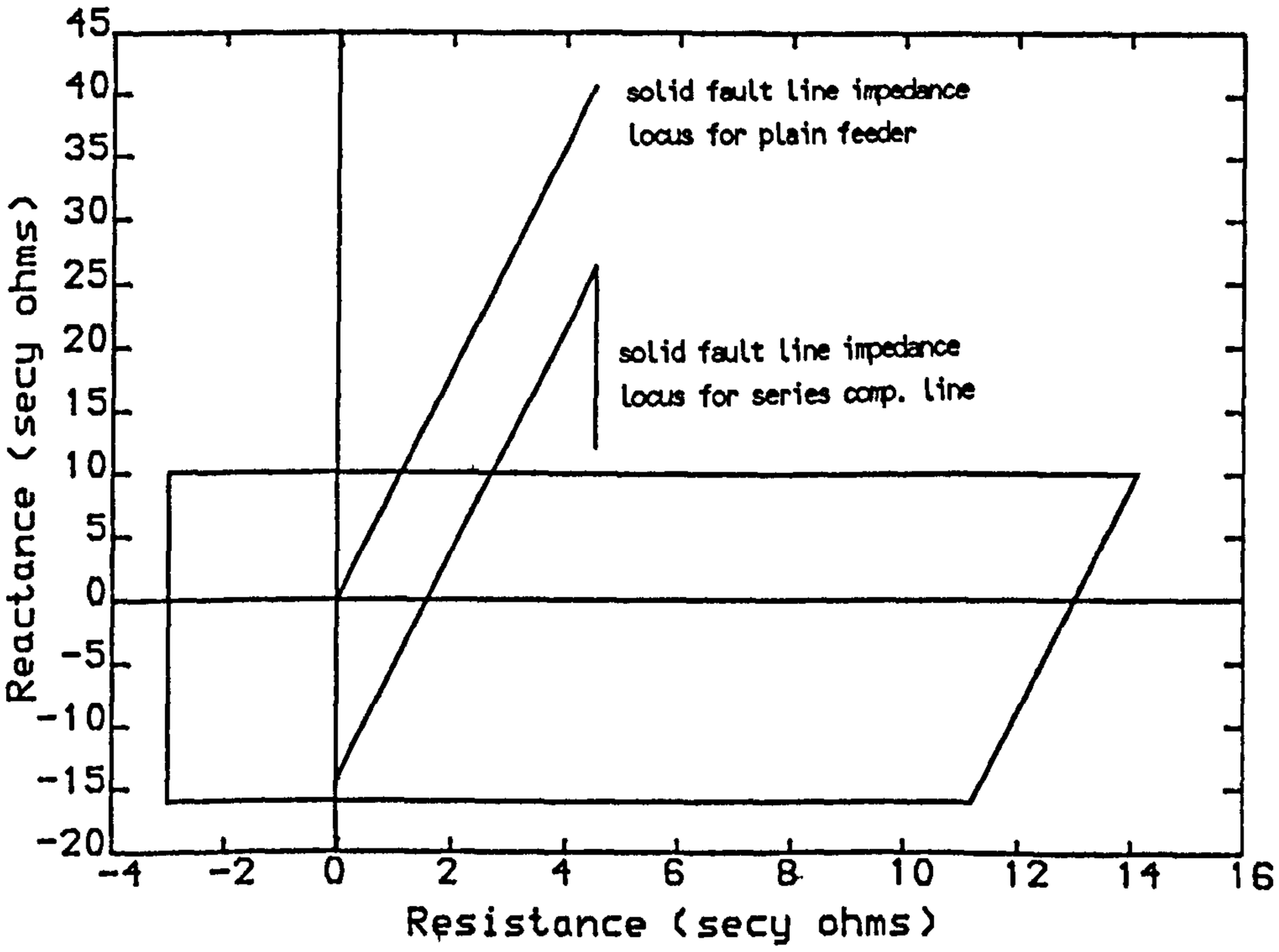

Fig 6.4-Impedance Locus And Relay Characteristic (the local cap. is included in the boundary

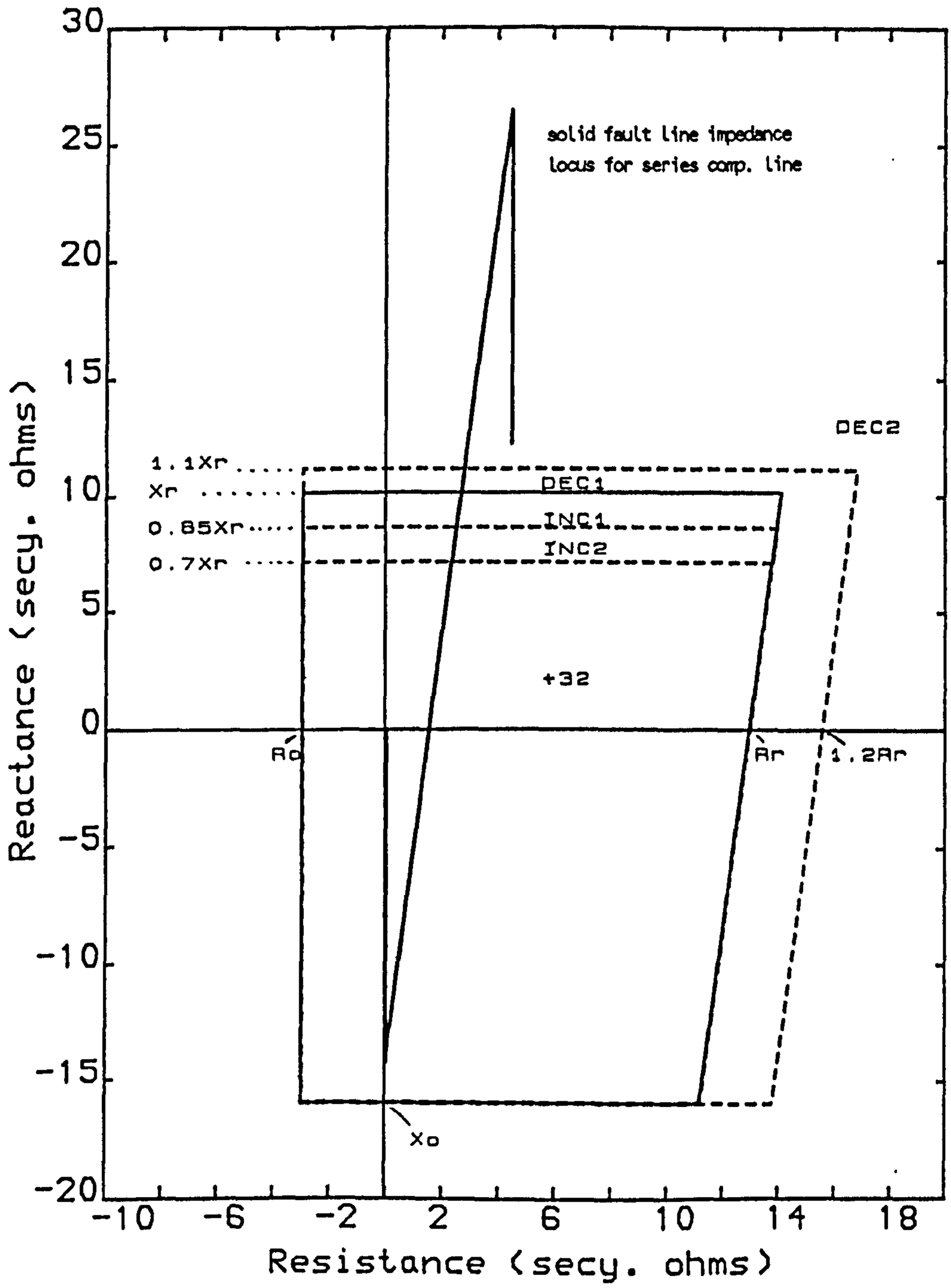

Fig 6.5-Relay Quadrilateral Characteristic And Count Regime For 70% Comp.

INC1
INC2
] see section 6.1.2

DEC1= -8
DEC2= -32

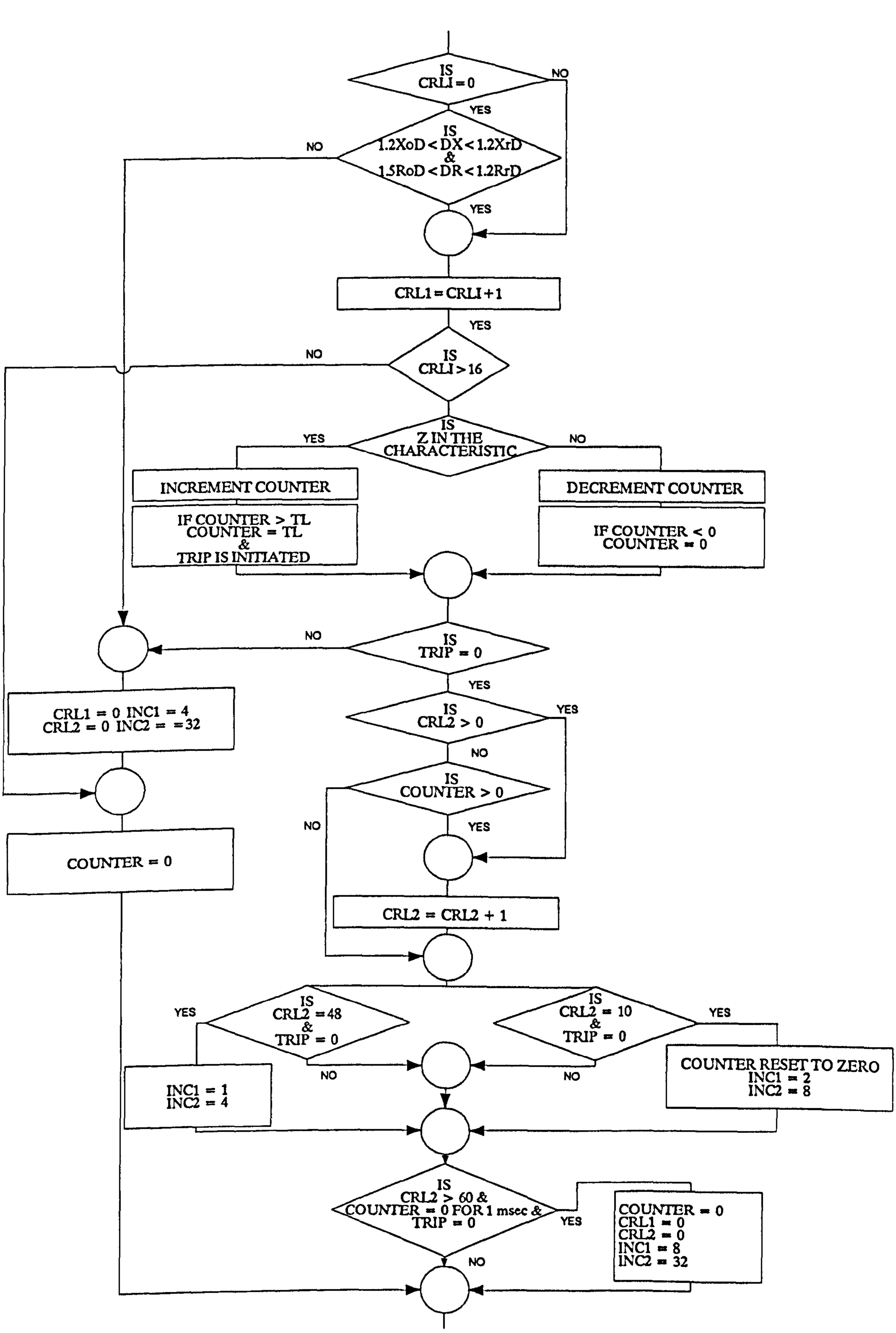

Fig 6.6-Flow Chart For The Relay Decision Logic

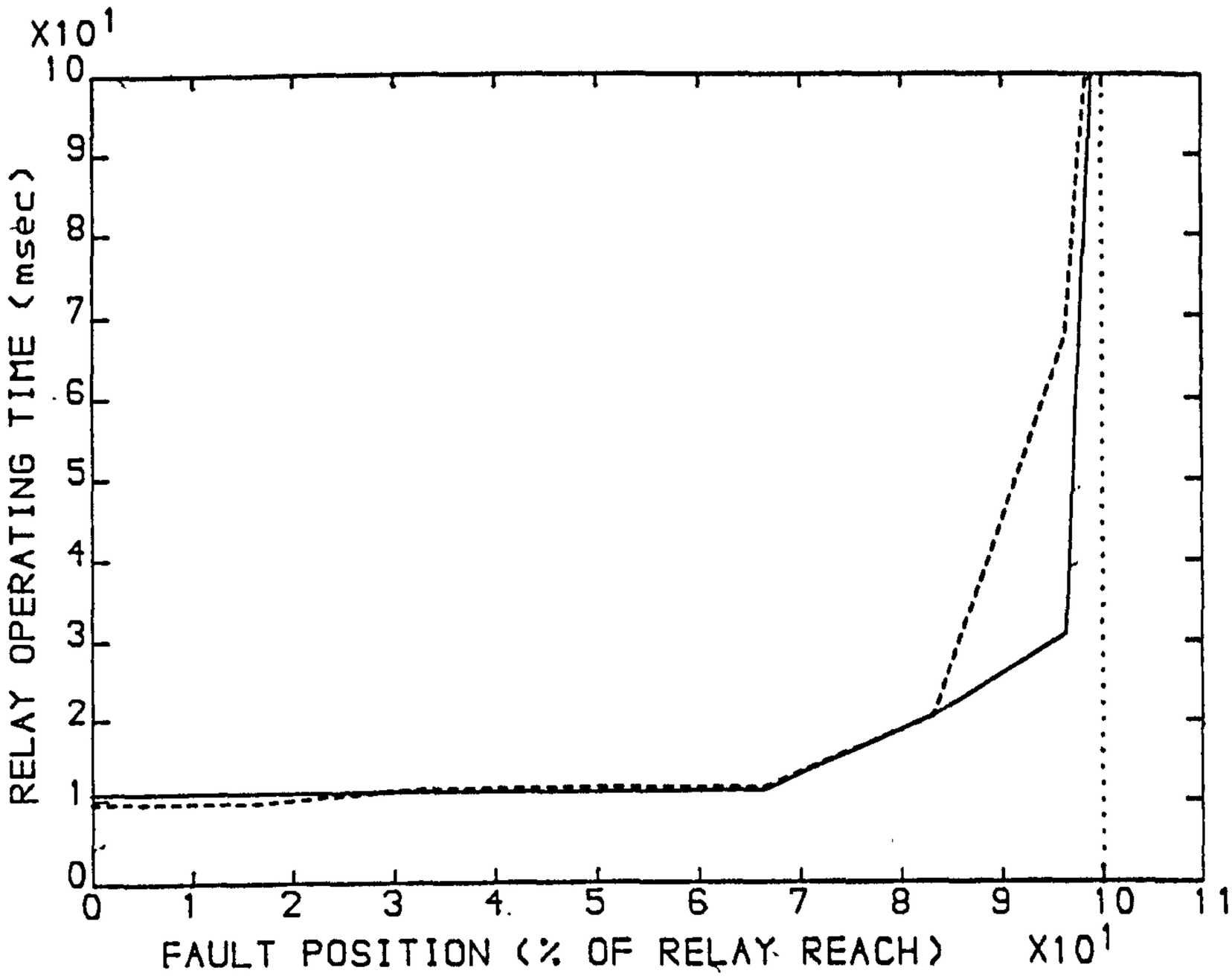

Fig 6.7-Relay Operating Time VS Fault Position For:

SÈ SCL=5, RE SCL=35
Load ang.=0 deg., LL=300 km
70% Series Compensation

Relay Set At 60% Of Line Length
Xr=10.1, Xo=-16.0 secy. ohms
Rr=13.0, Ro=-3.0 secy. ohms

——— Fault Incep. Ang.=0 deg
---- Fault Incep. Ang.=90 deg

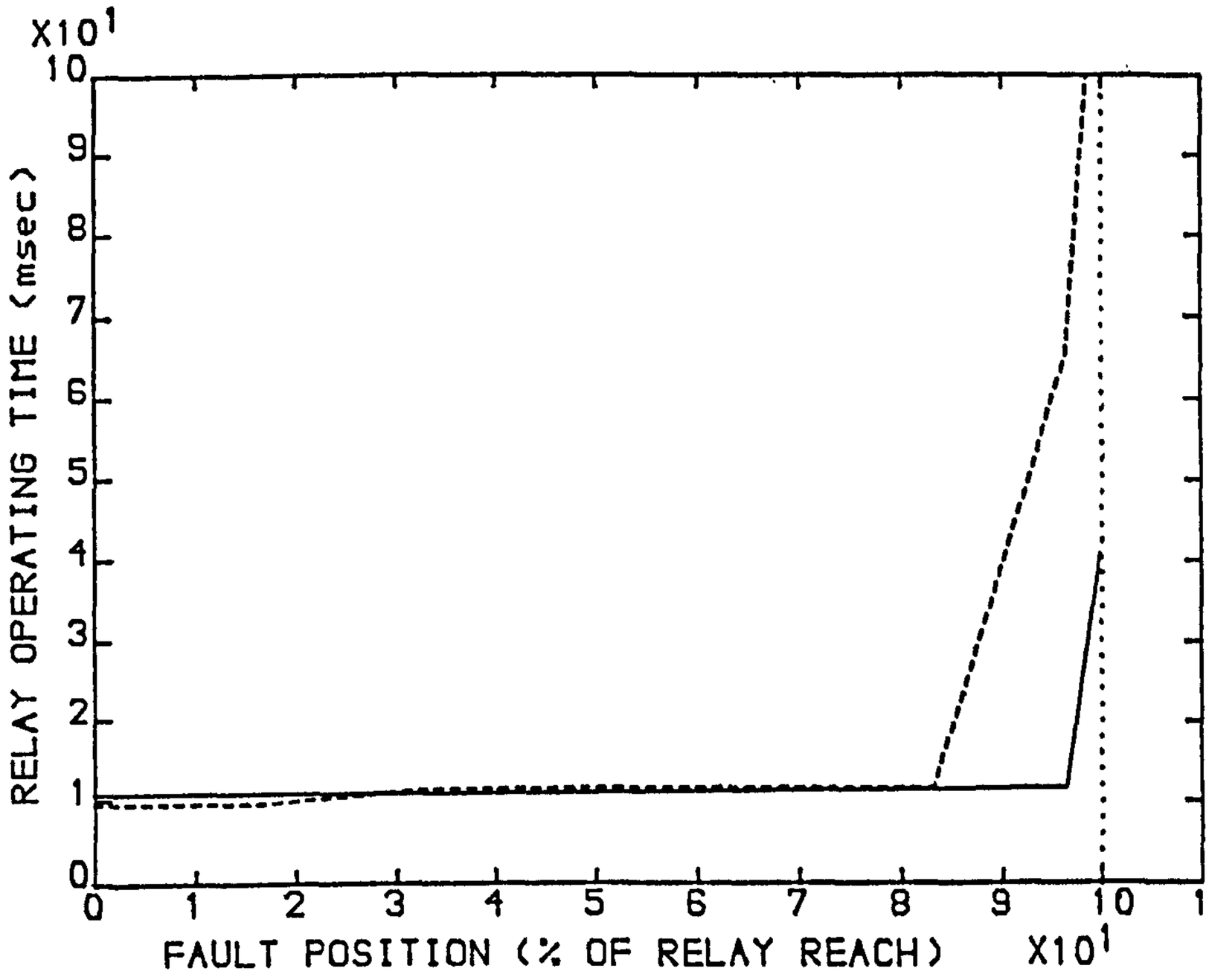

Fig 6.8-Relay Operating Time VS Fault Position For:

SE SCL=5, RE SCL=35
Load ang.=+10 deg., LL=300 km
70% Series Compensation

Relay Set At 60% Of Line Length
Xr=10.1, Xo=-16.0 secy. ohms
Rr=13.0, Ro=-3.0 secy. ohms

——— Fault Incep. Ang.=0 deg
---- Fault Incep. Ang.=90 deg

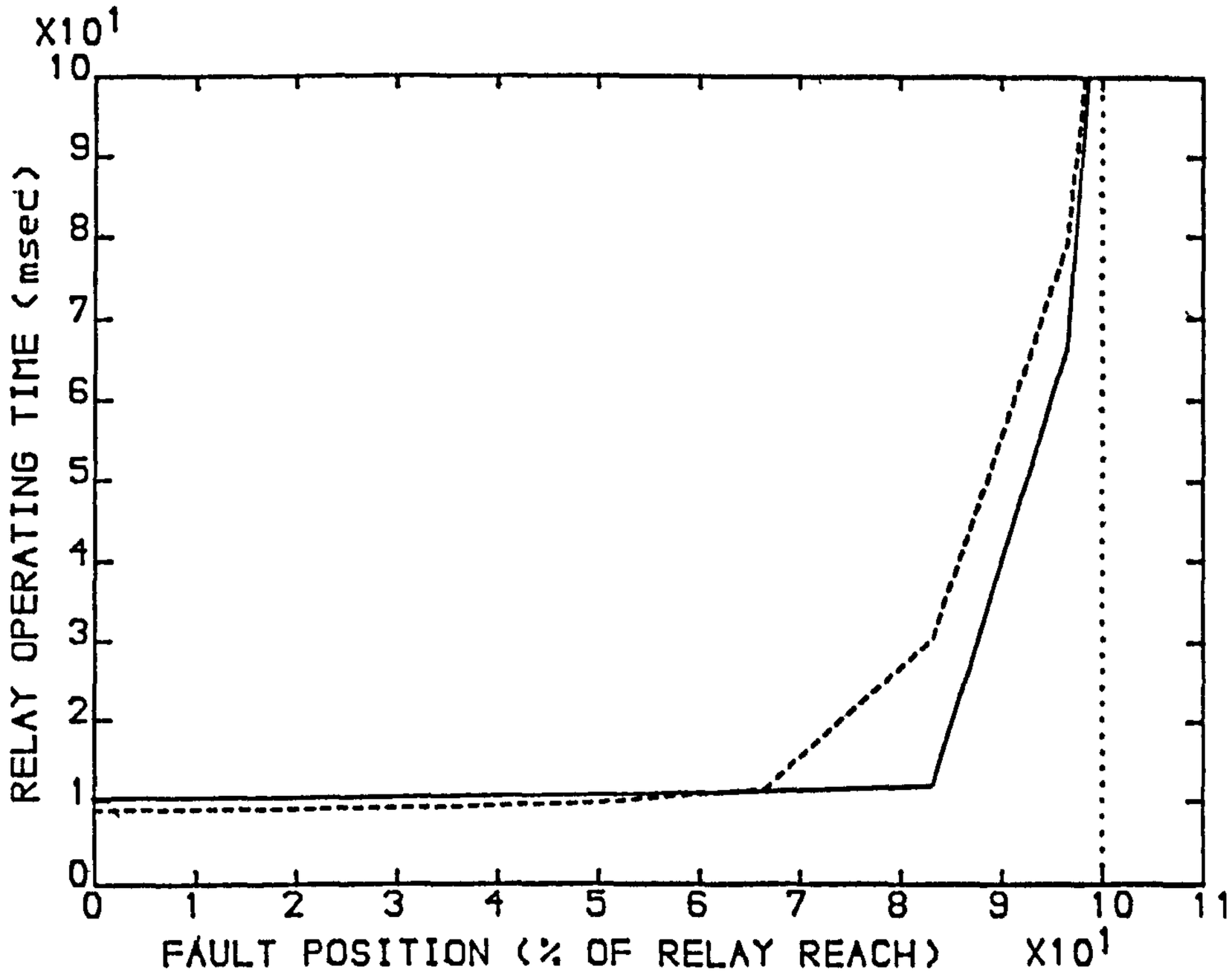

Fig 6.9-Relay Operating Time VS Fault Position For:

SE SCL-35, RE SCL-5
Load ang.-0 deg., LL-300 km
70% Series Compensation

Relay Set At 60% Of Line Length
Xr-10.1, Xo--16.0 secy. ohms
Rr-13.0, Ro--3.0 secy. ohms

——— Fault Incep. Ang.-0 deg
– – – Fault Incep. Ang.-90 deg

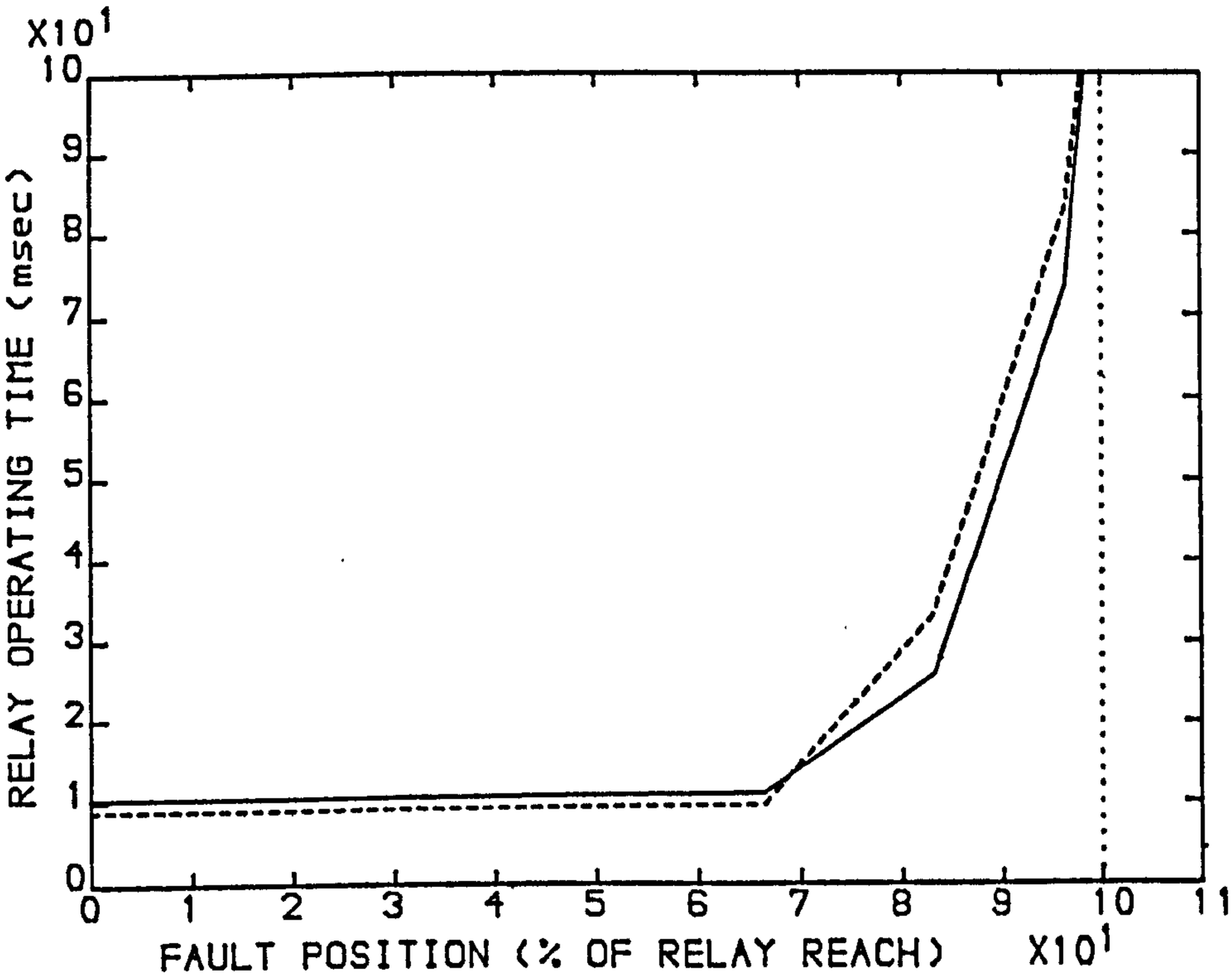

Fig 6.10-Relay Operating Time VS Fault Position For:

SE SCL=35, RE SCL=5
Load ang.=-10 deg., LL=300 km
70% Series Compensation

Relay Set At 60% Of Line Length
Xr=10.1, Xo=-16.0 secy. ohms
Rr=13.0, Ro=-3.0 secy. ohms

——— Fault Incep. Ang.=0 deg
---- Fault Incep. Ang.=90 deg

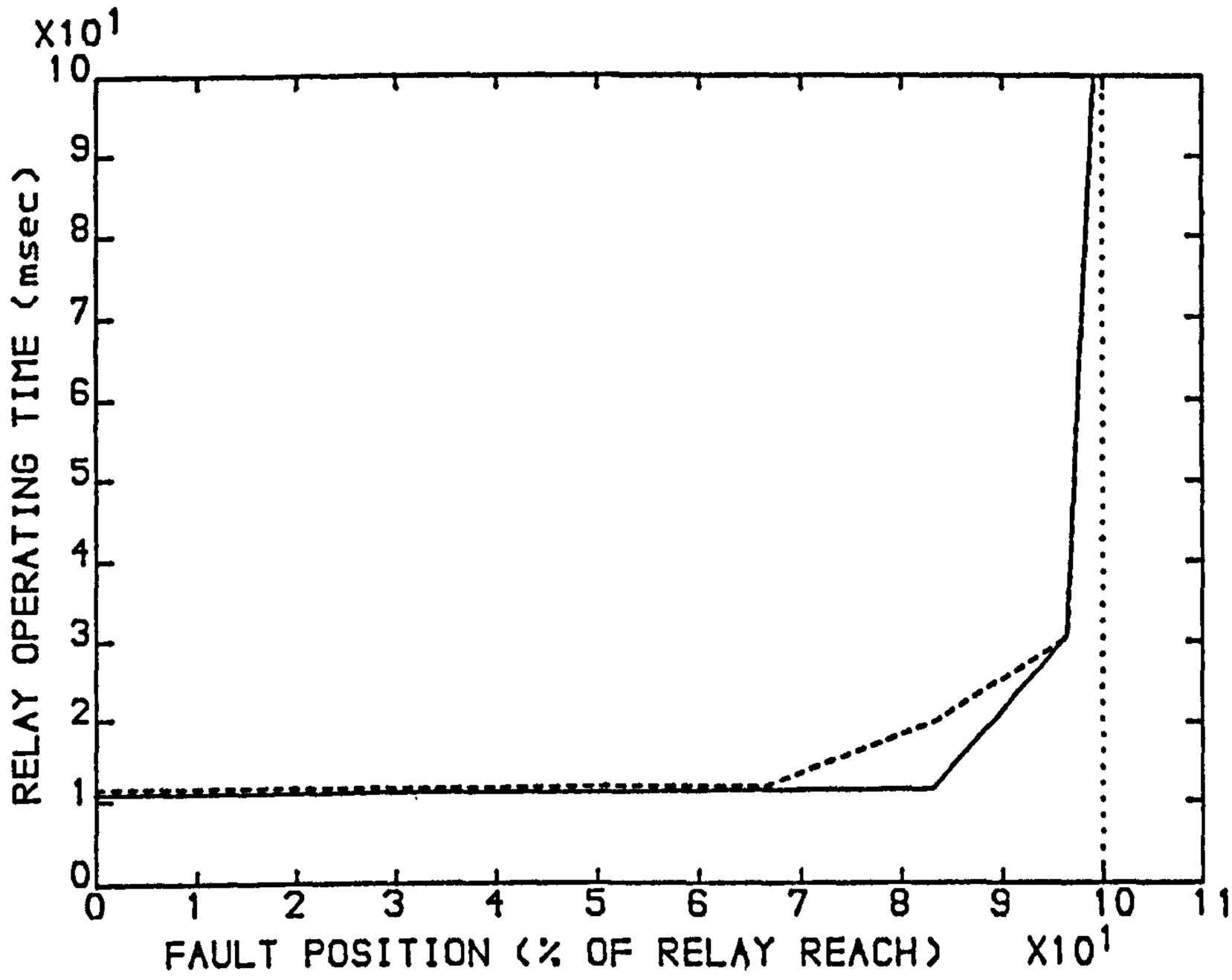

Fig 6.11—Relay Operating Time VS Fault Position For:

SE SCL=5, RE SCL=35
Load ang.=0 deg., LL=400 km
70% Series Compensation

Relay Set At 60% Of Line Length
Xr=13.6, Xo=-20.0 secy. ohms
Rr=14.0, Ro=-3.0 secy. ohms

——— Fault Incep. Ang.=0 deg
---- Fault Incep. Ang.=90 deg

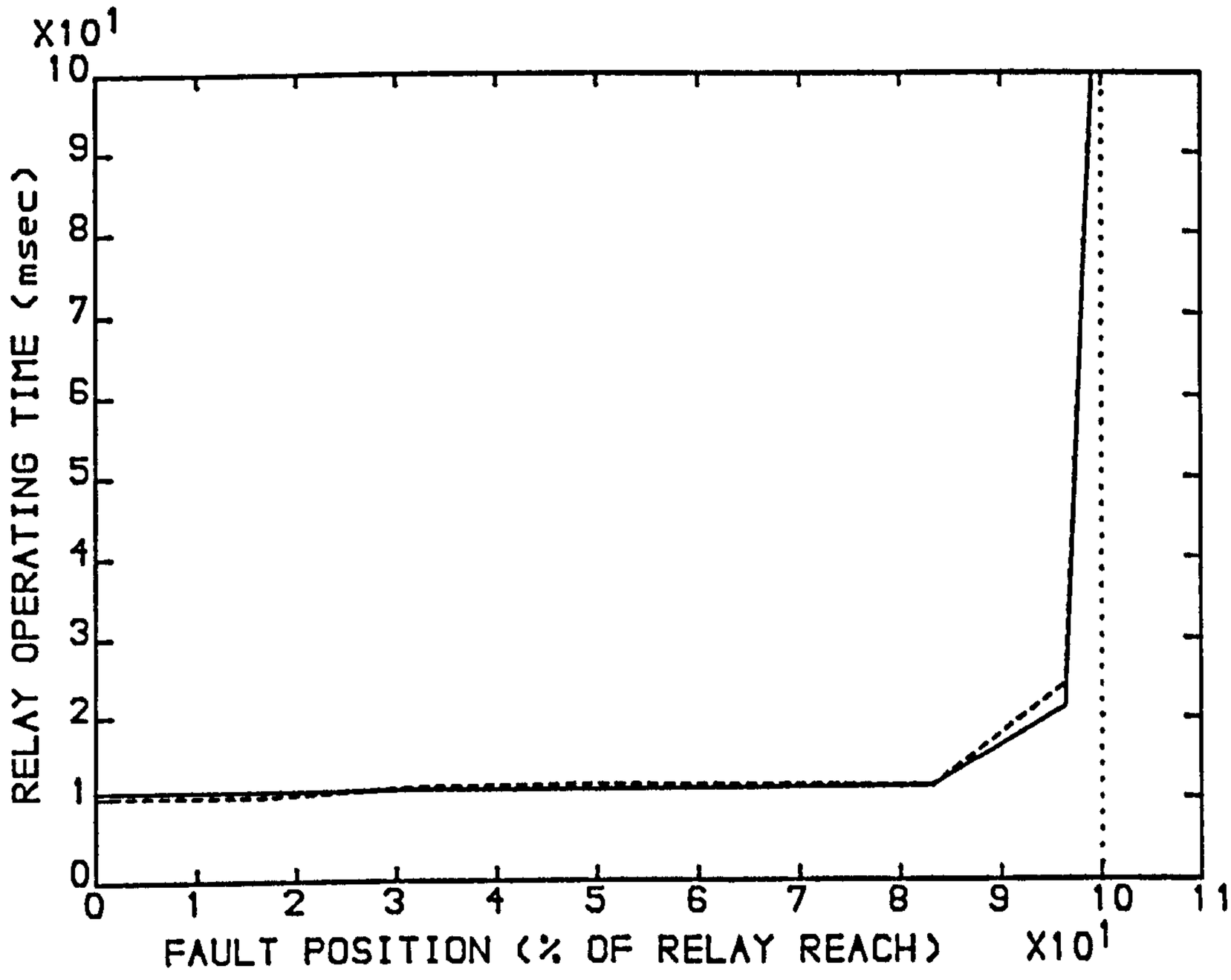

Fig 6.12-Relay Operating Time VS Fault Position For:

SE SCL=35, RE SCL=5
Load ang.=+5 deg., LL=400 km
70% Series Compensation

Relay Set At 60% Of Line Length
Xr=13.6, Xo=-20.0 secy. ohms
Rr=14.0, Ro=-3.0 secy. ohms

——— Fault Incep. Ang.=0 deg
---- Fault Incep. Ang.=90 deg

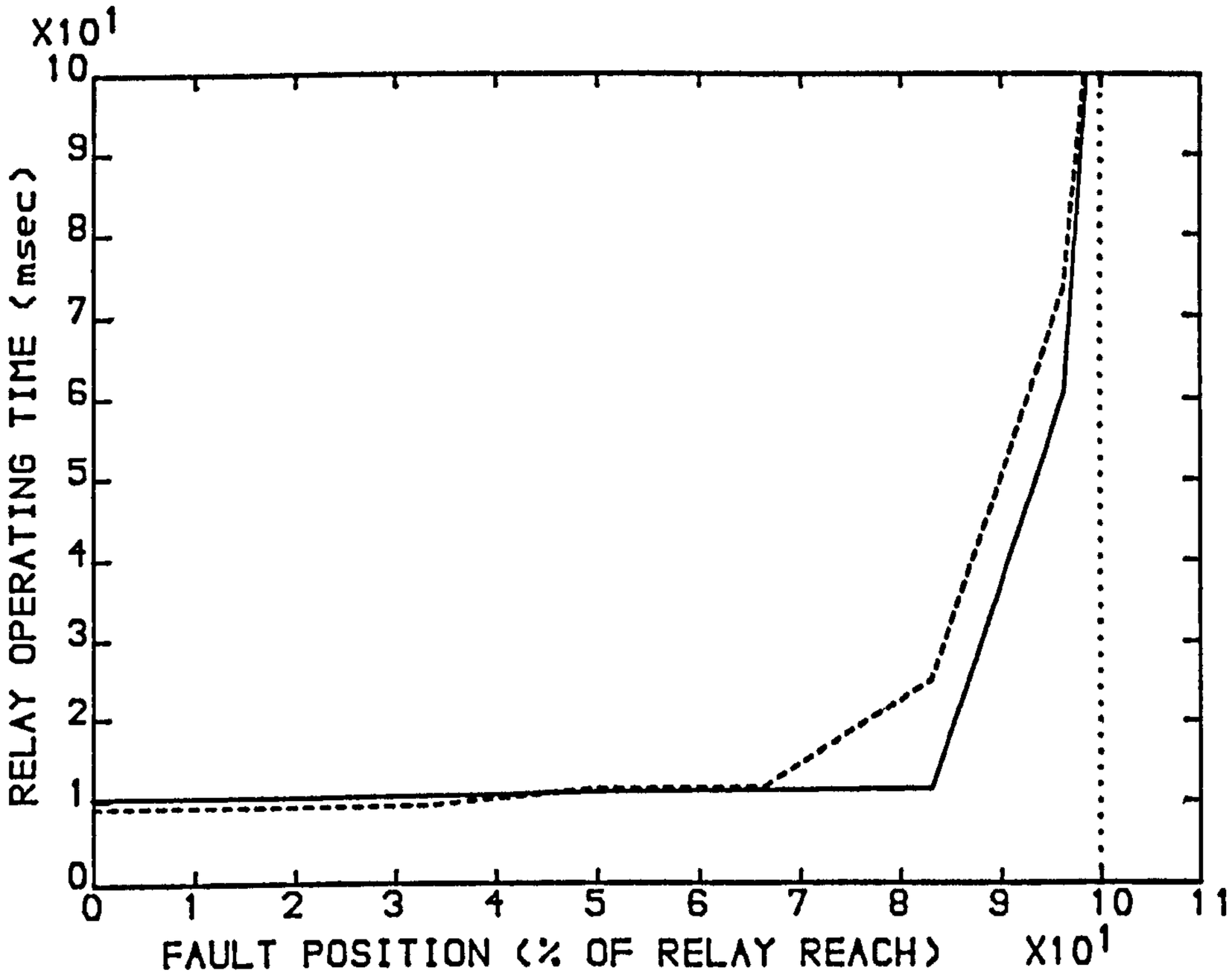

Fig 6.13-Relay Operating Time VS Fault Position For:

SE SCL=35, RE SCL=5
Load ang.=+10 deg., LL=400 km
70% Series Compensation

Relay Set At 60% Of Line Length
Xr=13.6, Xo=-20.0 secy. ohms
Rr=14.0, Ro=-3.0 secy. ohms

——— Fault Incep. Ang.=0 deg
---- Fault Incep. Ang.=90 deg

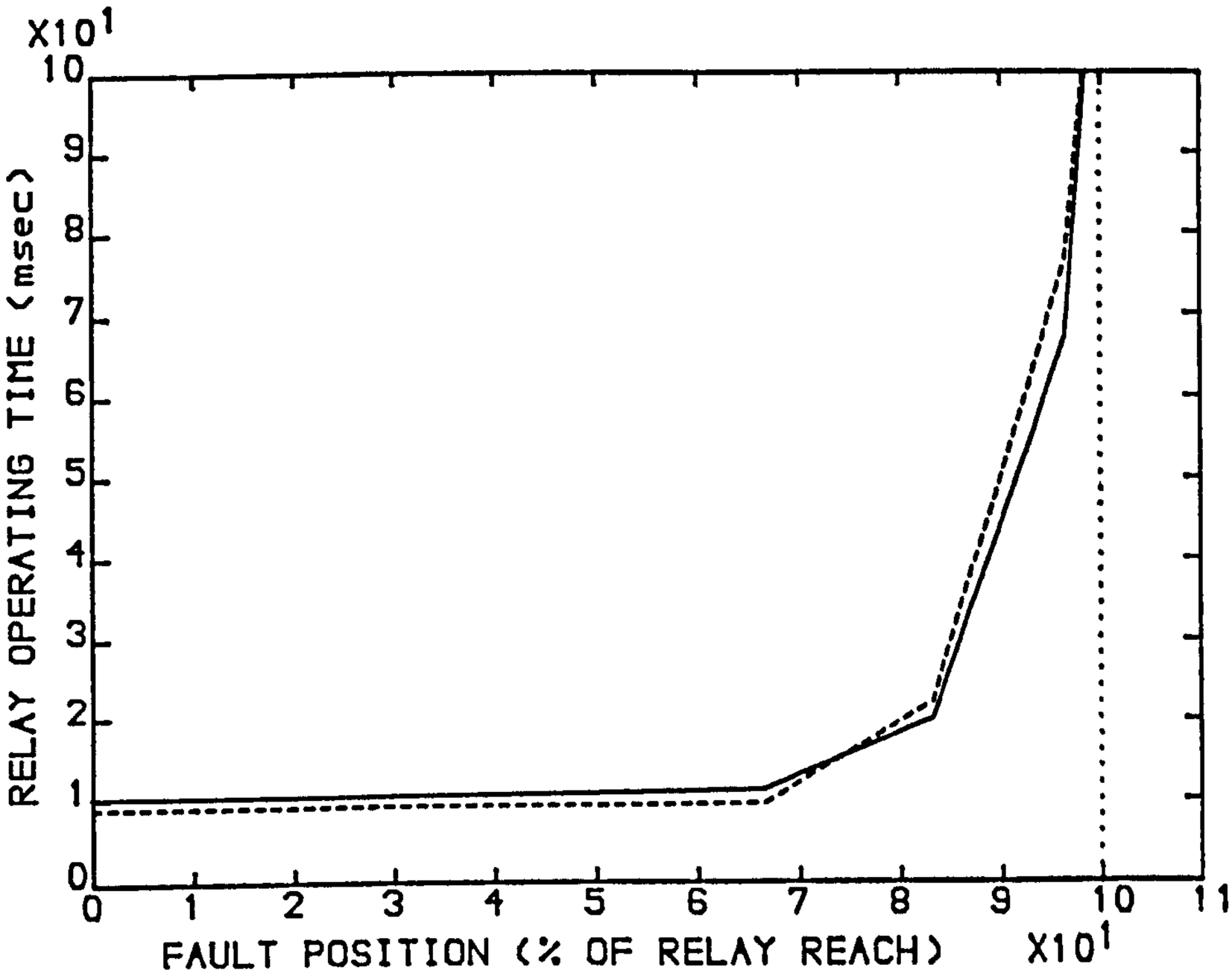

Fig 6.14-Relay Operating Time VS Fault Position For:

SE SCL=35, RE SCL=5
Load ang.=-5 deg., LL=200 km
70% Series Compensation

Relay Set At 60% Of Line Length
Xr=6.79, Xo=-9.5 secy. ohms
Rr=11.0, Ro=-3.0 secy. ohms

——— Fault Incep. Ang.=0 deg
- - - - Fault Incep. Ang.=90 deg

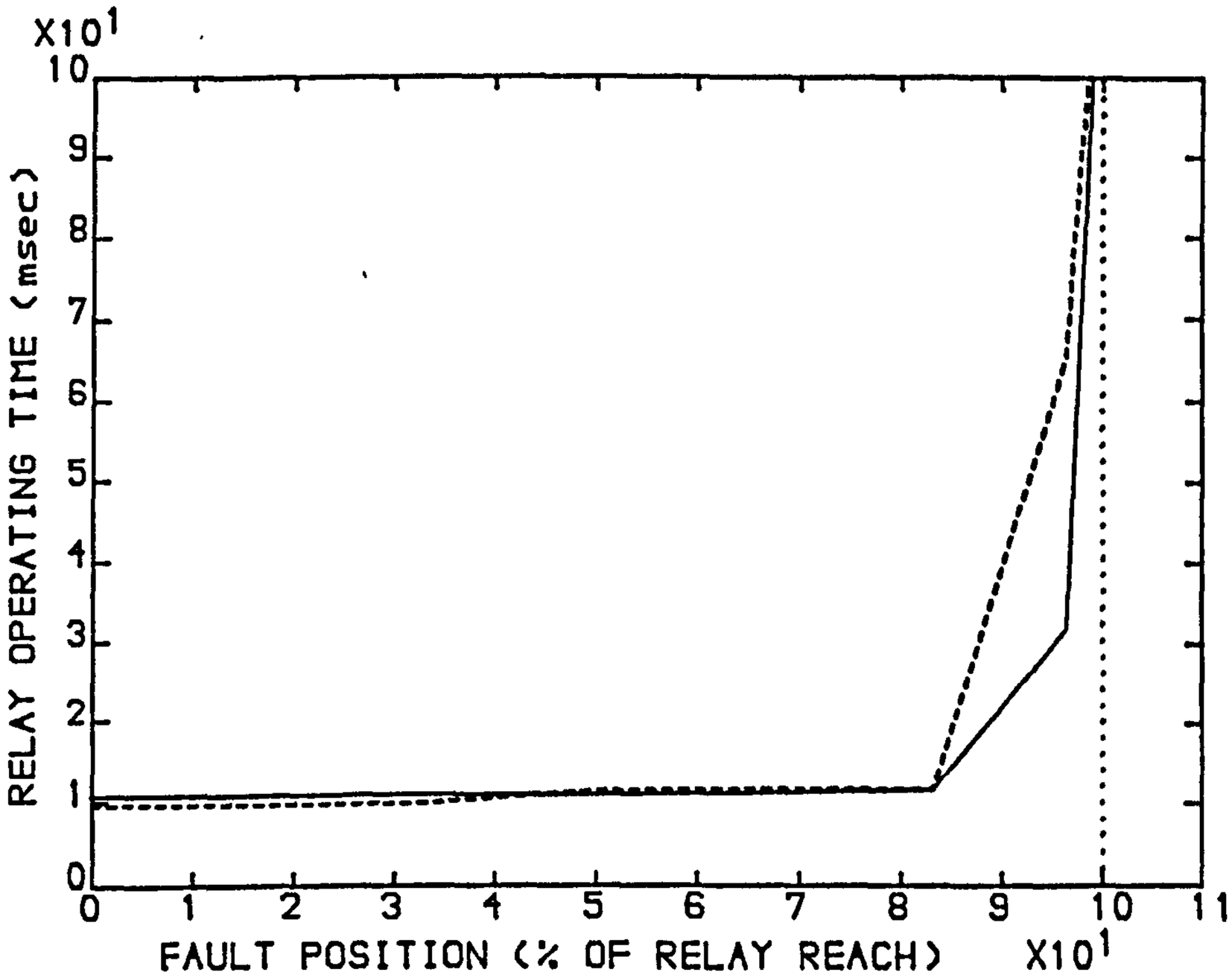

Fig 6.15-Relay Operating Time VS Fault Position For:

SE SCL=5, RE SCL=35
Load ang.=0 deg., LL=200 km
70% Series Compensation

Relay Set At 60% Of Line Length
Xr=6.79, Xo=-9.5 secy. ohms
Rr=11.0, Ro=-3.0 secy. ohms

——— Fault Incep. Ang.=0 deg
- - - - Fault Incep. Ang.=90 deg

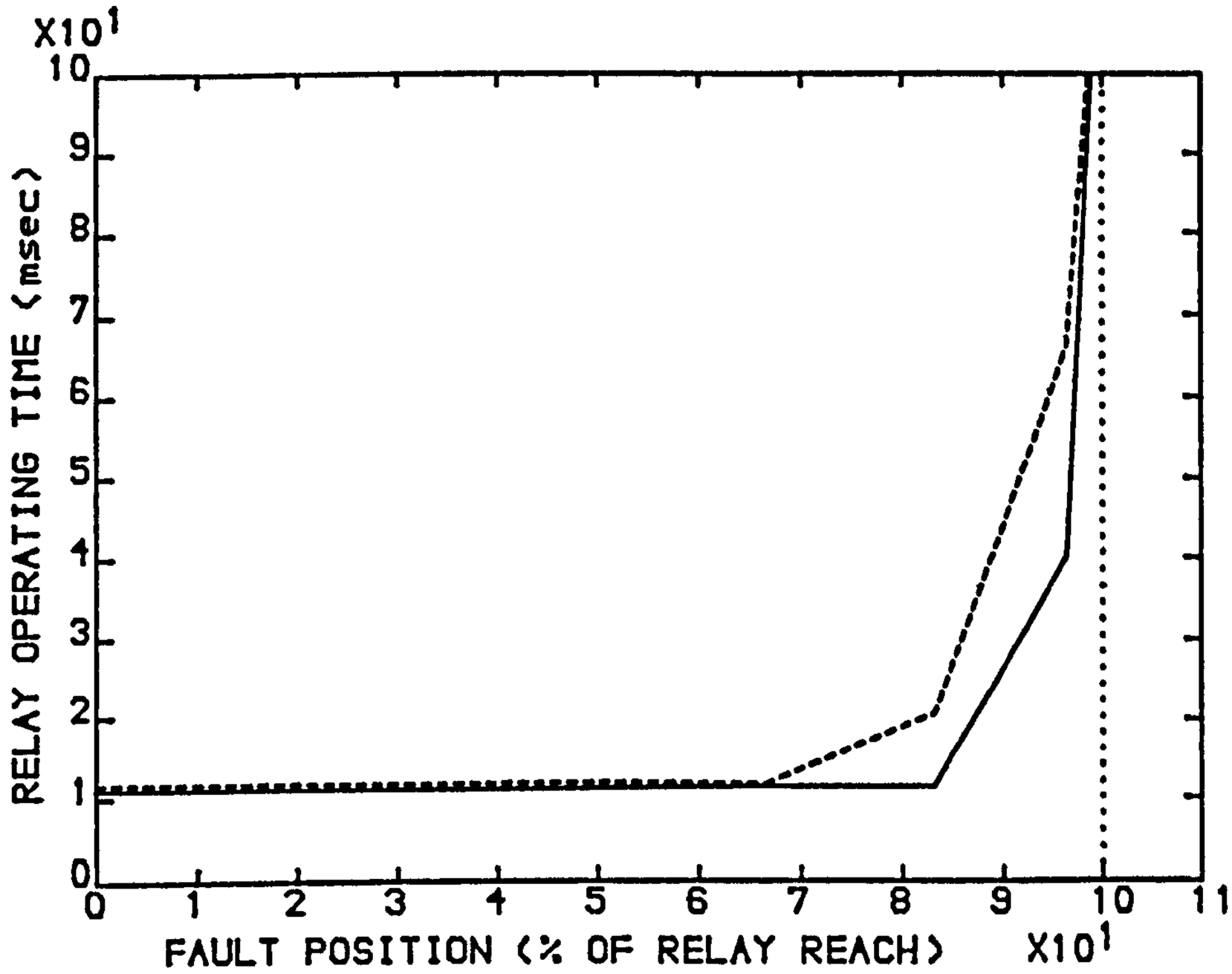

Fig 6.16-Relay Operating Time VS Fault Position For:

SE SCL=3, RE SCL=7
Load ang.=0 deg., LL=300 km
70% Series Compensation

Relay Set At 60% Of Line Length
Xr=10.1, Xo=-16 secy. ohms
Rr=13.0, Ro=-3.0 secy. ohms

——— Fault Incep. Ang.=0 deg
- - - - Fault Incep. Ang.=90 deg

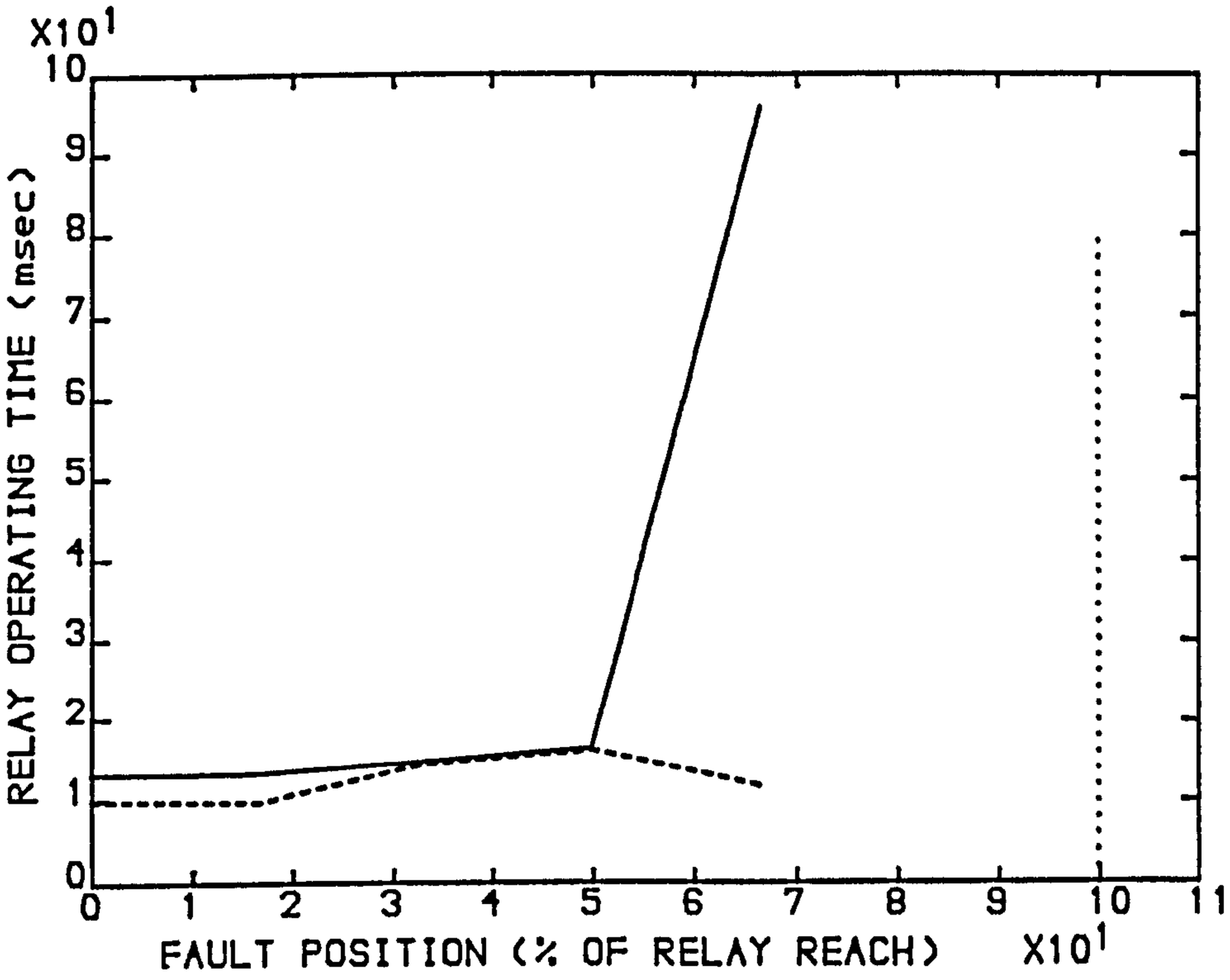

Fig 6.17-Relay Operating Time VS Fault Position With Cap. Flash-Over (SGS) For:

SE SCL=5, RE SCL=35
Load ang.=0 deg., LL=300 km
70% Series Compensation

Relay Set At 60% Of Line Length
Xr=10.1, Xo=-16 secy. ohms
Rr=13.0, Ro=-3.0 secy. ohms

——— Fault Incep. Ang.=0 deg
---- Fault Incep. Ang.=90 deg

fault position % ofline length	gap flash-over time, after fault (msec)			
	fault incep. ang. 0°		fault incep. ang. 90°	
	SE cap.	RE cap.	SE cap.	RE cap.
0	5.25	7.75	4.075	15.4
10	5.50	7.50	4.125	15.375
20	6.00	7.25	4.875	15.125
30	6.50	7.00	5.75	14.75
40	6.875	6.75	7.0	6.25
50	7.375	6.25	15.75	5.375
60	7.75	5.875	16.625	4.75

Table 6.1-Cap. Gap Flash-Over Time For Different Fault Position For:
SE SCL=5 GVA, RE SCL=35 GVA,
Load Angle=0, LL=300 km,
Single Gap Scheme (SGS),

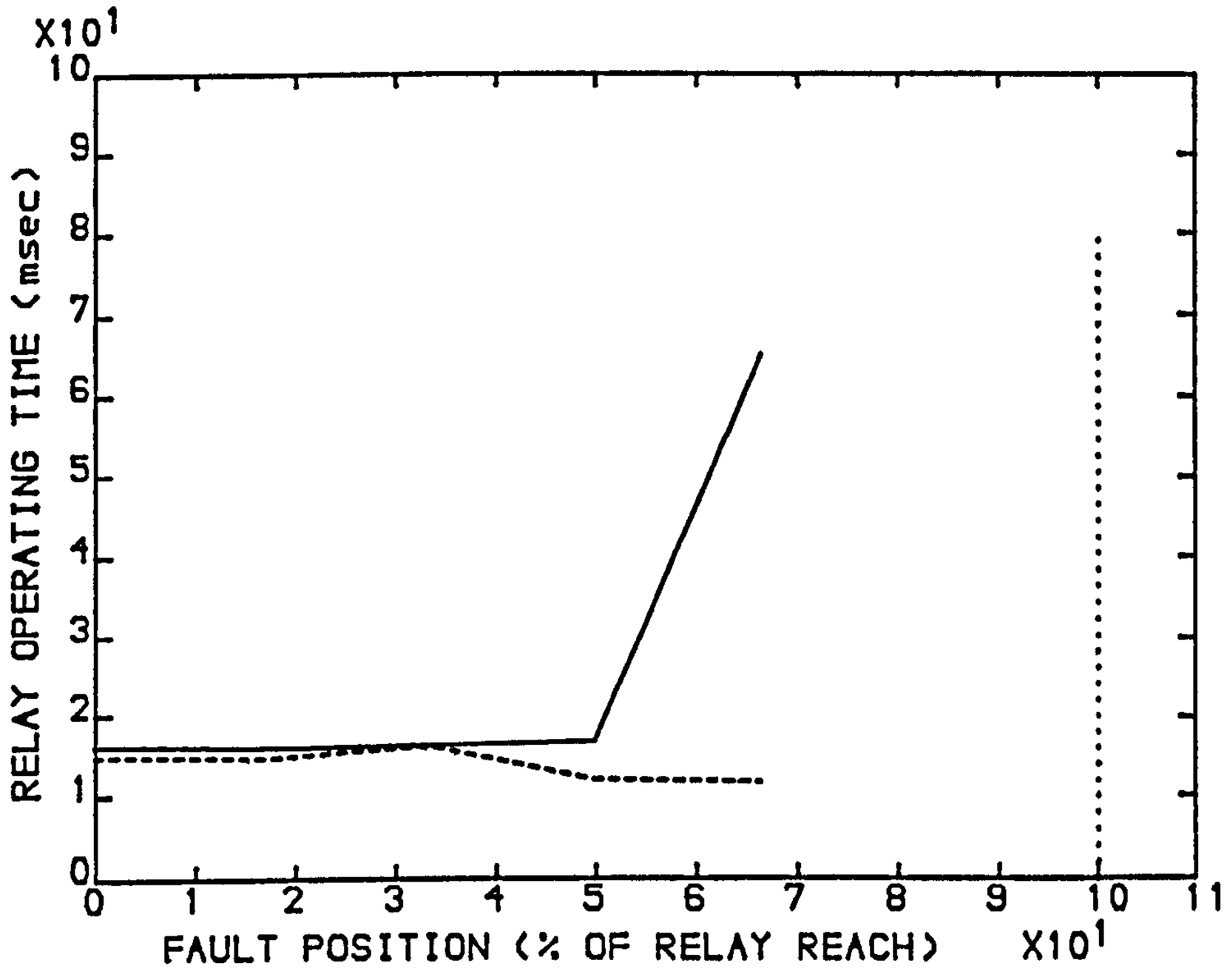

Fig 6.18-Relay Operating Time VS Fault Position With Cap. Flash-Over (SGS) For:

SE SCL=3, RE SCL=7
Load ang.=0 deg., LL=300 km
70% Series Compensation

Relay Set At 60% Of Line Length
Xr=10.1, Xo=-16 secy. ohms
Rr=13.0, Ro=-3.0 secy. ohms

——— Fault Incep. Ang.=0 deg
– – – – Fault Incep. Ang.=90 deg

fault position % ofline length	gap flash-over time, after fault (msec)			
	fault incep. ang. 0°		fault incep. ang. 90°	
	SE cap.	RE cap.	SE cap.	RE cap.
0	6.00	8.25	4.35	16.90
10	6.25	8.125	4.375	16.875
20	6.75	7.875	6.25	16.625
30	7.125	7.625	15.50	16.125
40	7.625	7.375	16.375	15.625
50	8.0	7.0	17.25	7.00
60	8.375	6.625	18.375	5.875

Table 6.2-Cap. Gap Flash-Over Time For Different Fault Position For:
SE SCL=3 GVA, RE SCL=7 GVA,
Load Angle=0, LL=300 km,
Single Gap Scheme (SGS),

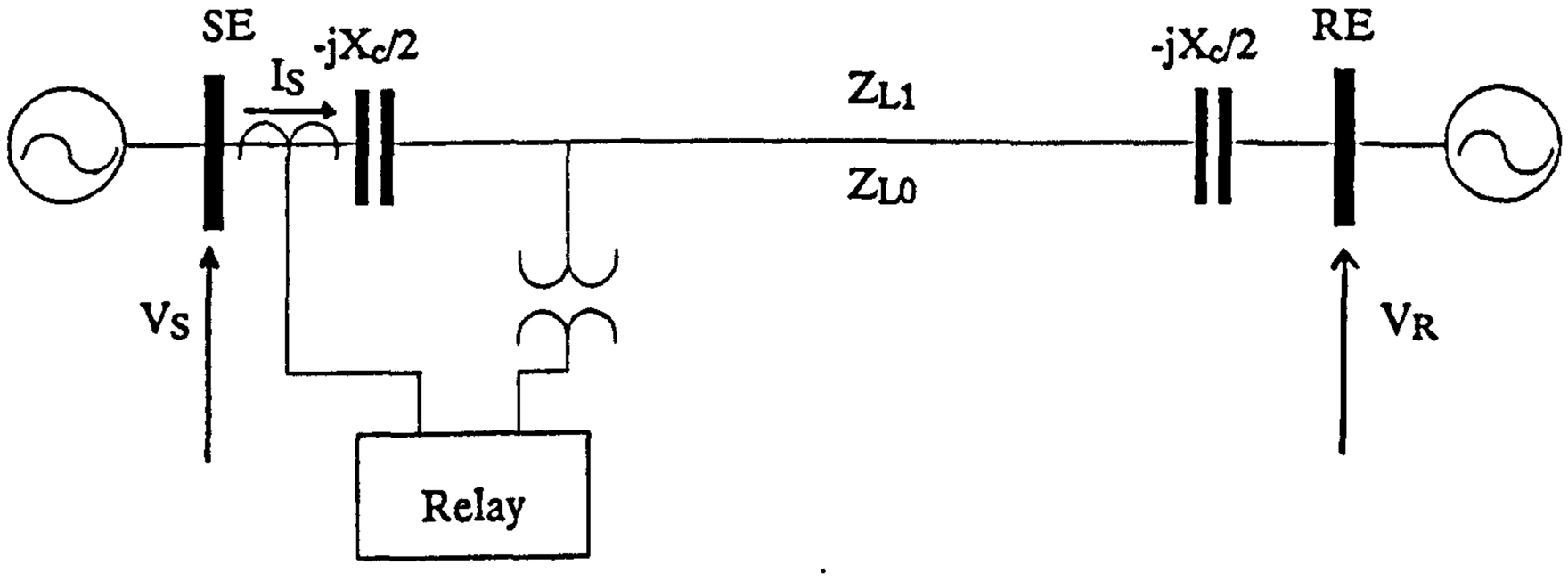

Fig 6.19-Line Configuration With Series Capacitors At The Line Ends And Line Side C.V.T.

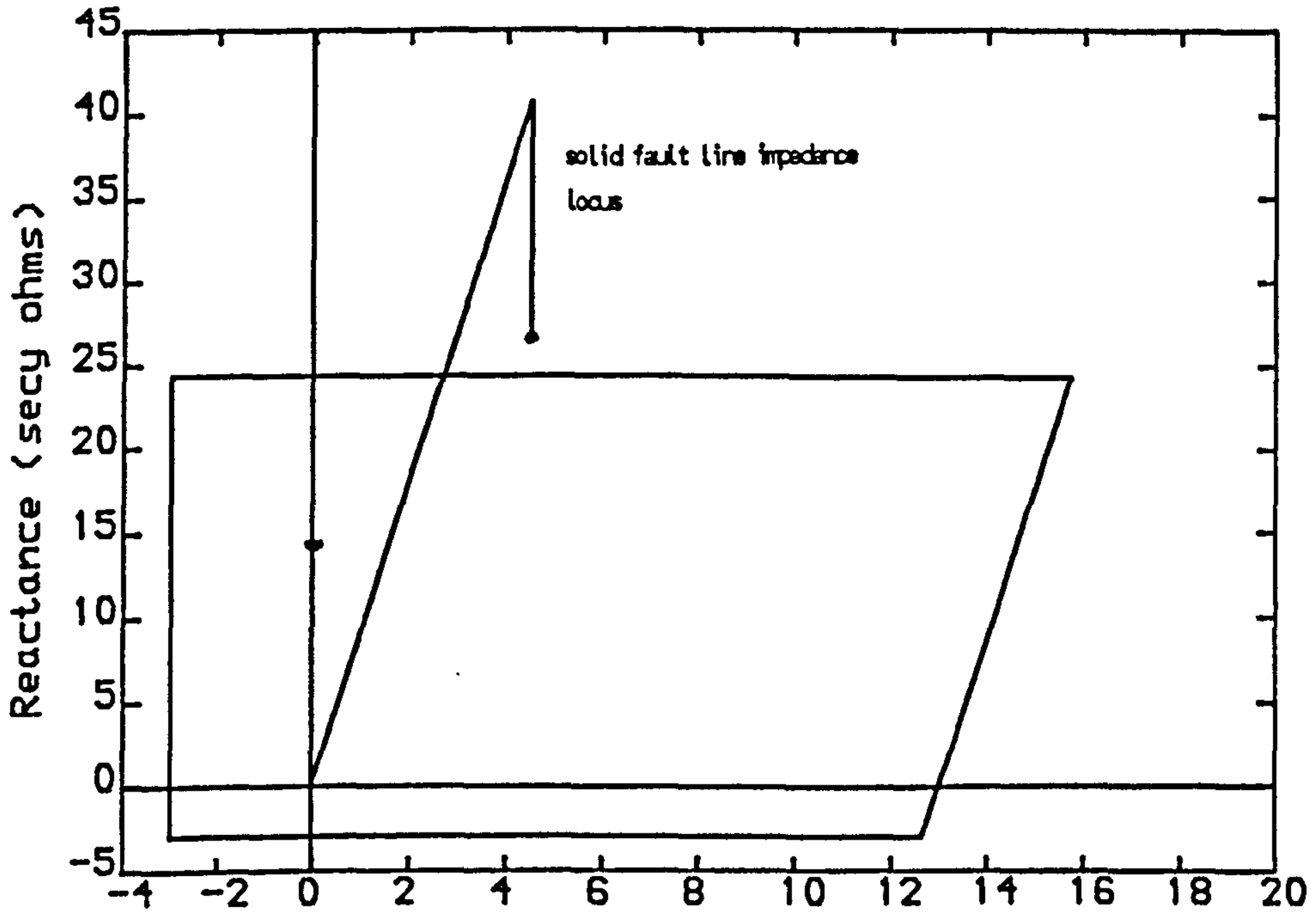

Fig 6.20-Impedance Locus And Relay Characteristic For 70% Comp. And Line Side C.V.T.

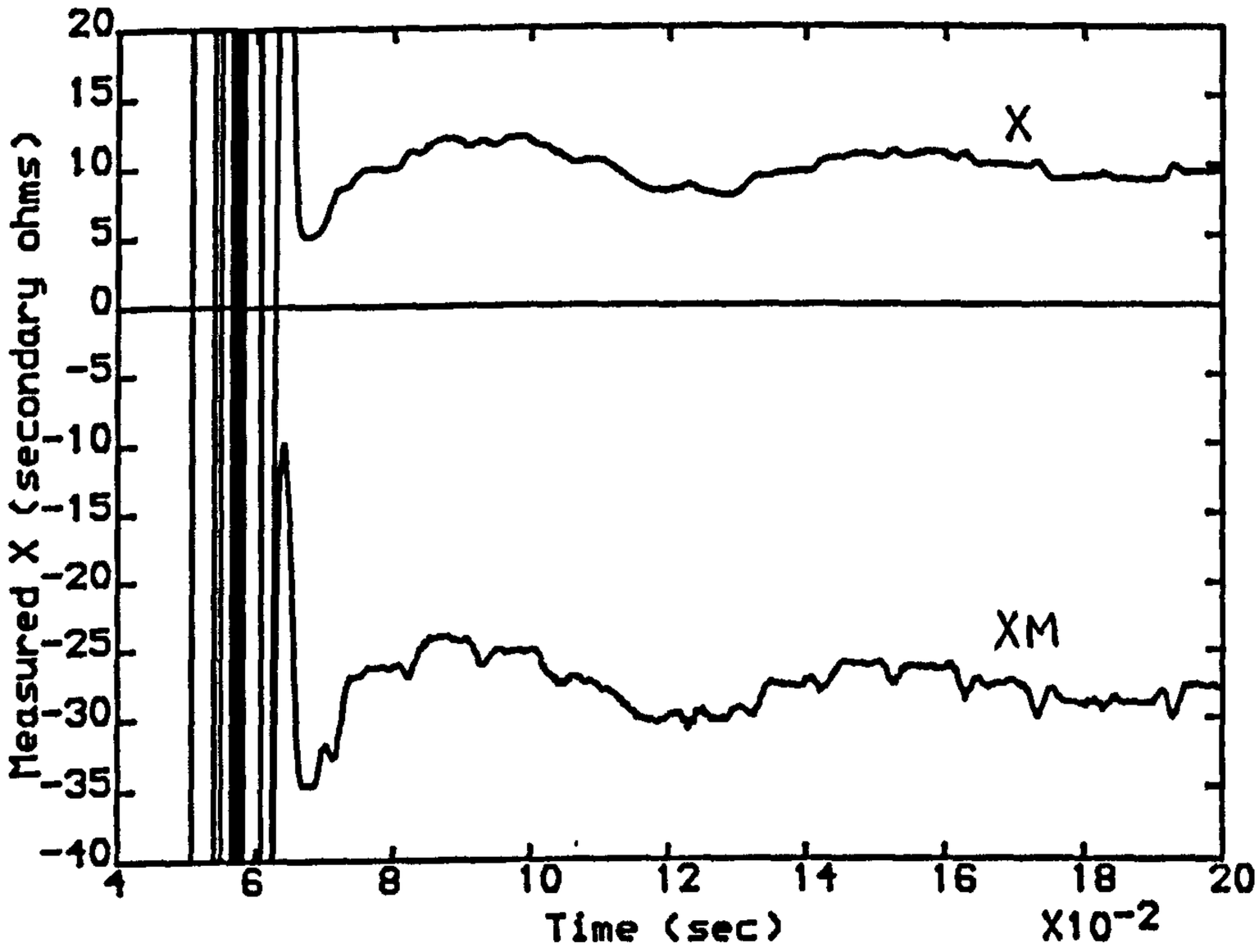

Fig 6.20.a-Measured Reactance VS Time For Reverse Fault At SE Bus-Bar

For 70% Series Compensation
(35% At Each End)
And Line Side C.V.T And With
SE SCL=35 GVA, RE SCL=5 GVA
Load ang.=0 deg., LL=300 km
Inception Ang.=90 Deg.
No Cap. Flash-Over

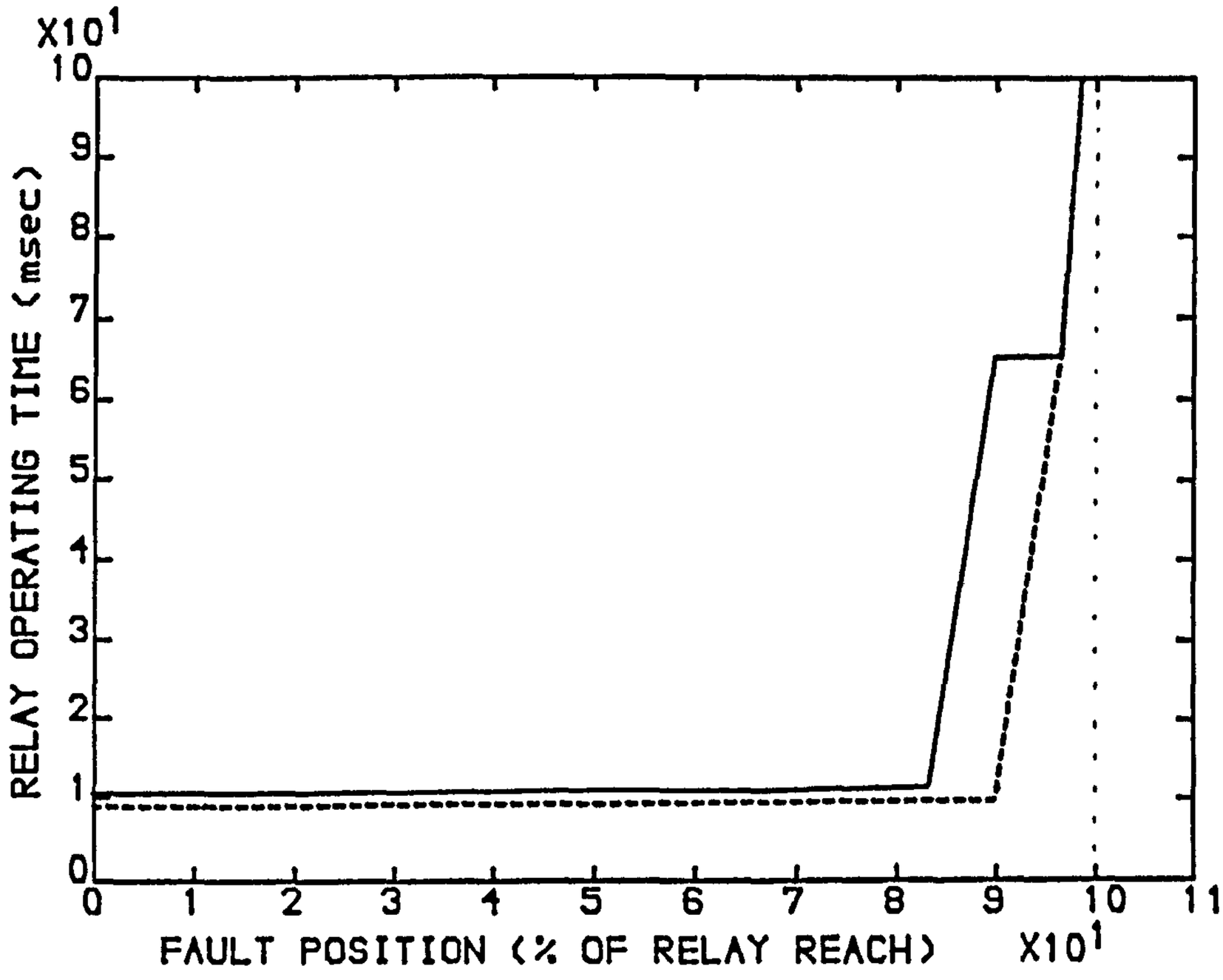

Fig 6.21-Relay Operating Time VS Fault Position For Line Side C.V.T.

SE SCL-12, RE SCL-27
Load ang.-0 deg., LL-300 km
70% Series Compensation

Relay Set At 60% Of Line Length
Xr-24.4, Xo--3 secy. ohms
Rr-13.0, Ro--3.0 secy. ohms

——— Fault Incep. Ang.-0 deg
---- Fault Incep. Ang.-90 deg

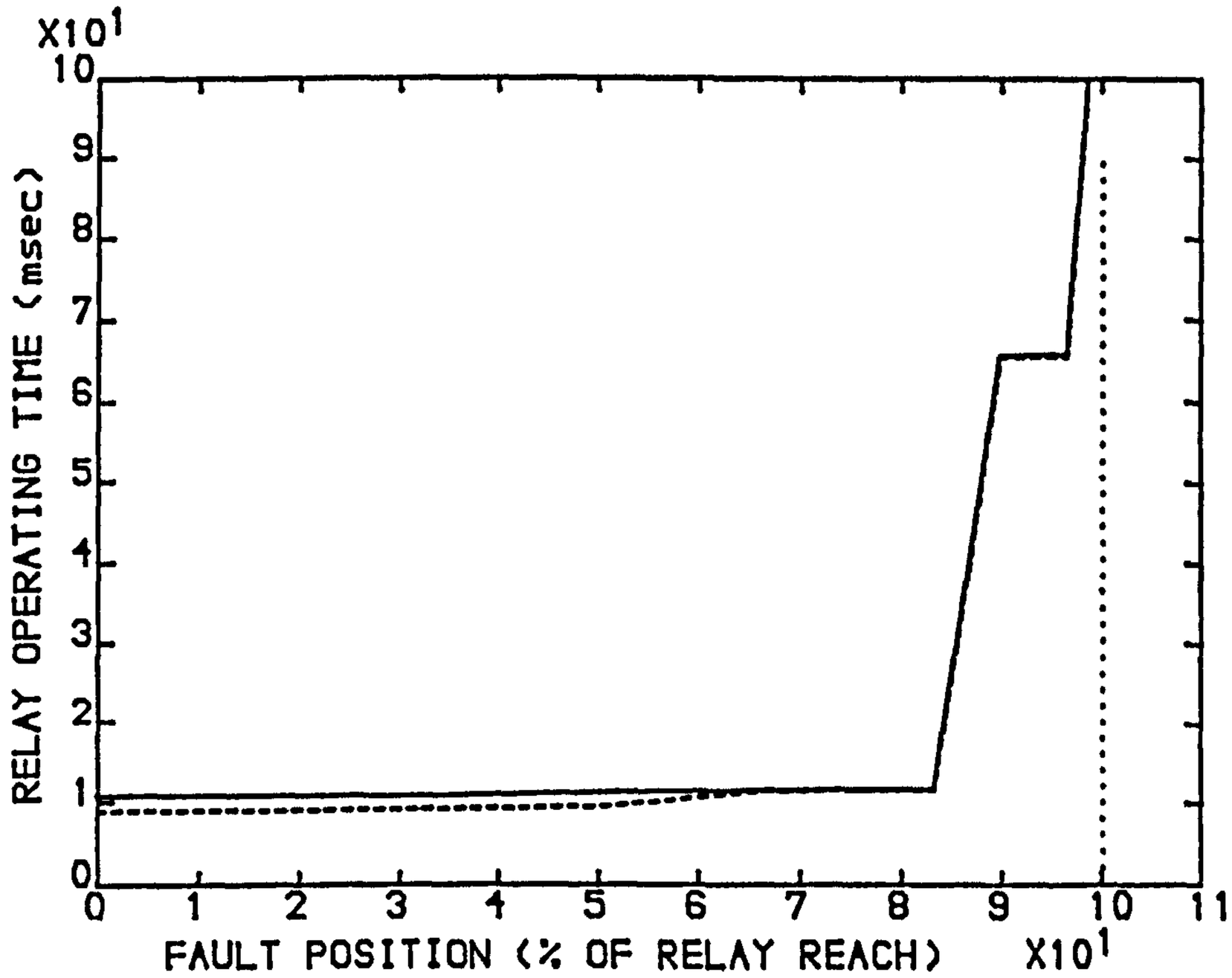

Fig 6.22-Relay Operating Time VS Fault Position For Line Side C.V.T.

SE SCL=35, RE SCL=5
Load ang.=+10 deg., LL=300 km
70% Series Compensation

Relay Set At 60% Of Line Length
Xr=24.4, Xo=-3 secy. ohms
Rr=13.0, Ro=-3.0 secy. ohms

——— Fault Incep. Ang.=0 deg
---- Fault Incep. Ang.=90 deg

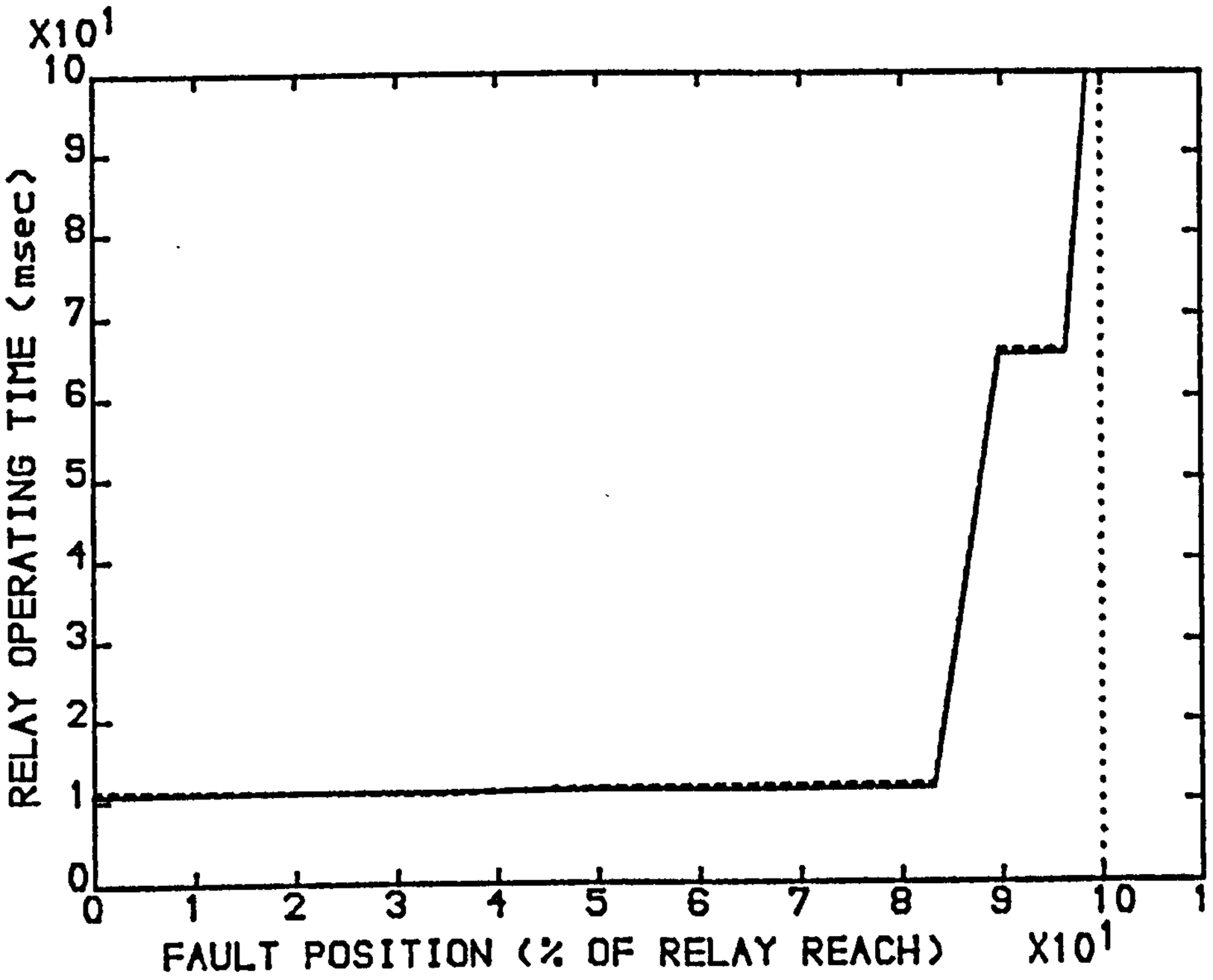

Fig 6.23-Relay Operating Time VS Fault Position For Line Side C.V.T.

SE SCL=5, RE SCL=35
Load ang.=0 deg., LL=400 km
70% Series Compensation

Relay Set At 60% Of Line Length
Xr=32.6, Xo=-3 secy. ohms
Rr=14.0, Ro=-3.0 secy. ohms

——— Fault Incep. Ang.=0 deg
---- Fault Incep. Ang.=90 deg

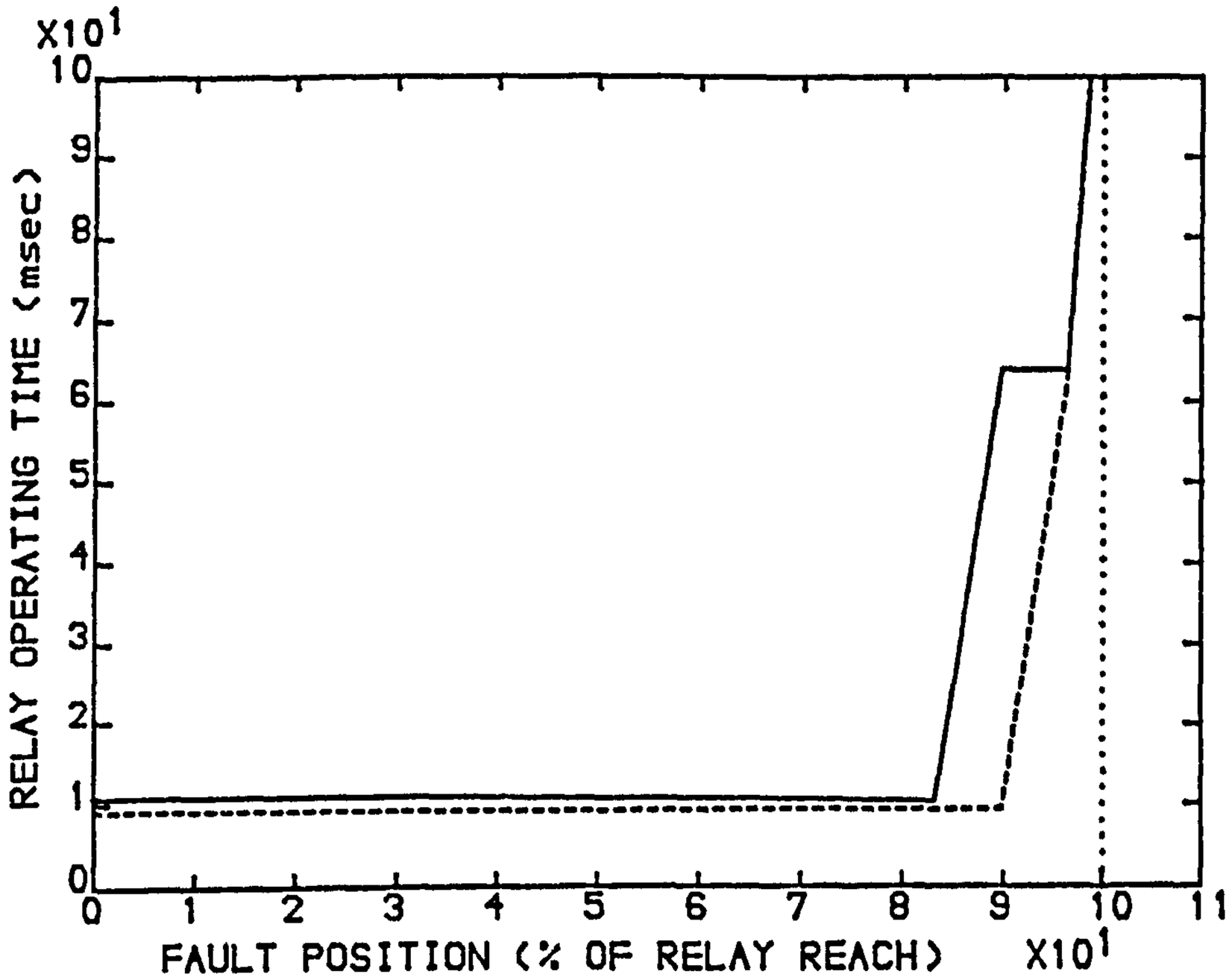

Fig 6.24-Relay Operating Time VS Fault Position For Line Side C.V.T.

SE SCL-5, RE SCL-35
Load ang.=-10 deg., LL=400 km
70% Series Compensation

Relay Set At 60% Of Line Length
Xr=32.6, Xo=-3 secy. ohms
Rr=14.0, Ro=-3.0 secy. ohms

——— Fault Incep. Ang.=0 deg
- - - - Fault Incep. Ang.=90 deg

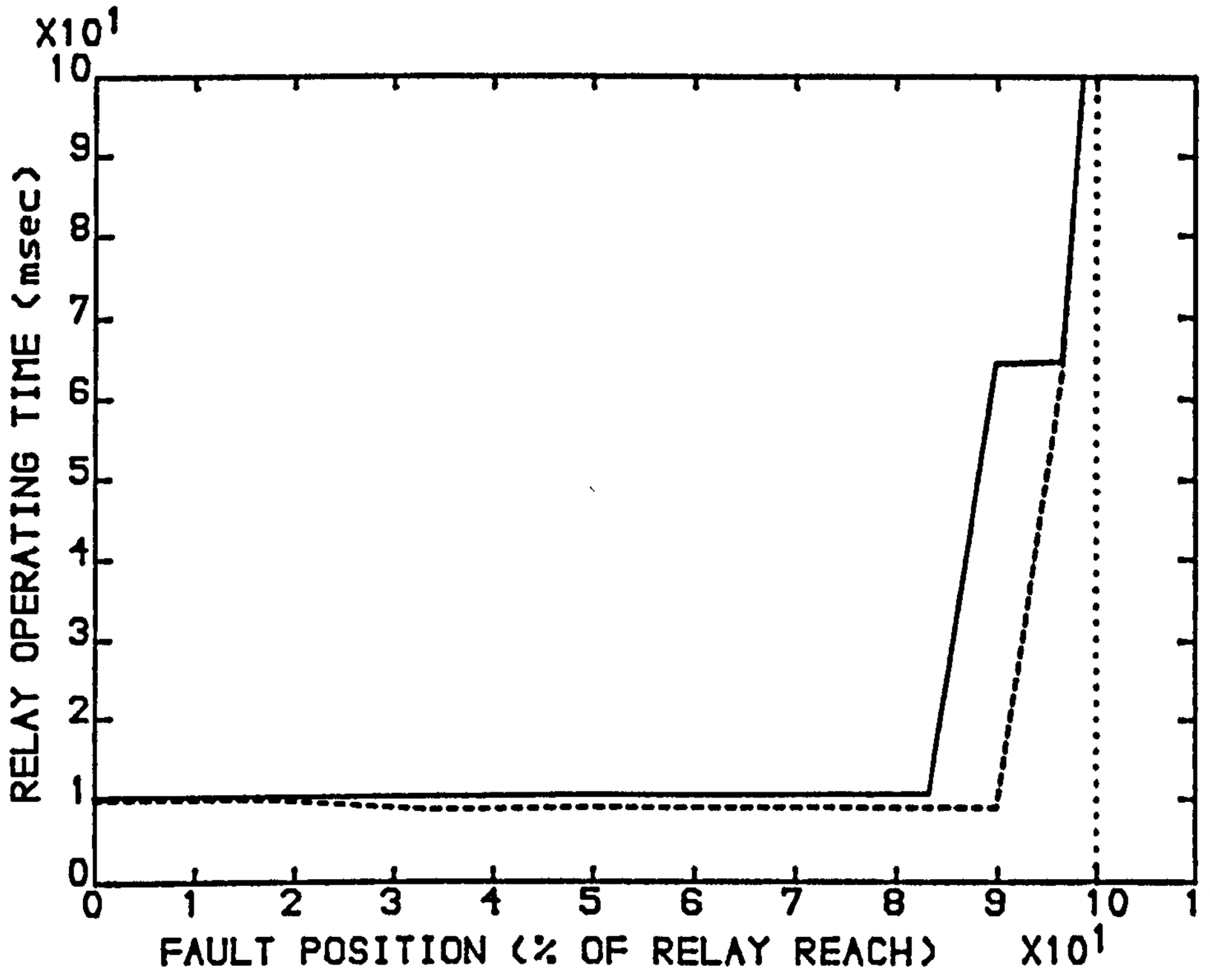

Fig 6.25-Relay Operating Time VS Fault Position For Line Side C.V.T.

SE SCL=35, RE SCL=5
Load ang.=-5 deg., LL=200 km
70% Series Compensation

Relay Set At 60% Of Line Length
Xr=16.3, Xo=-3 secy. ohms
Rr=12.0, Ro=-3.0 secy. ohms

——— Fault Incep. Ang.=0 deg
---- Fault Incep. Ang.=90 deg

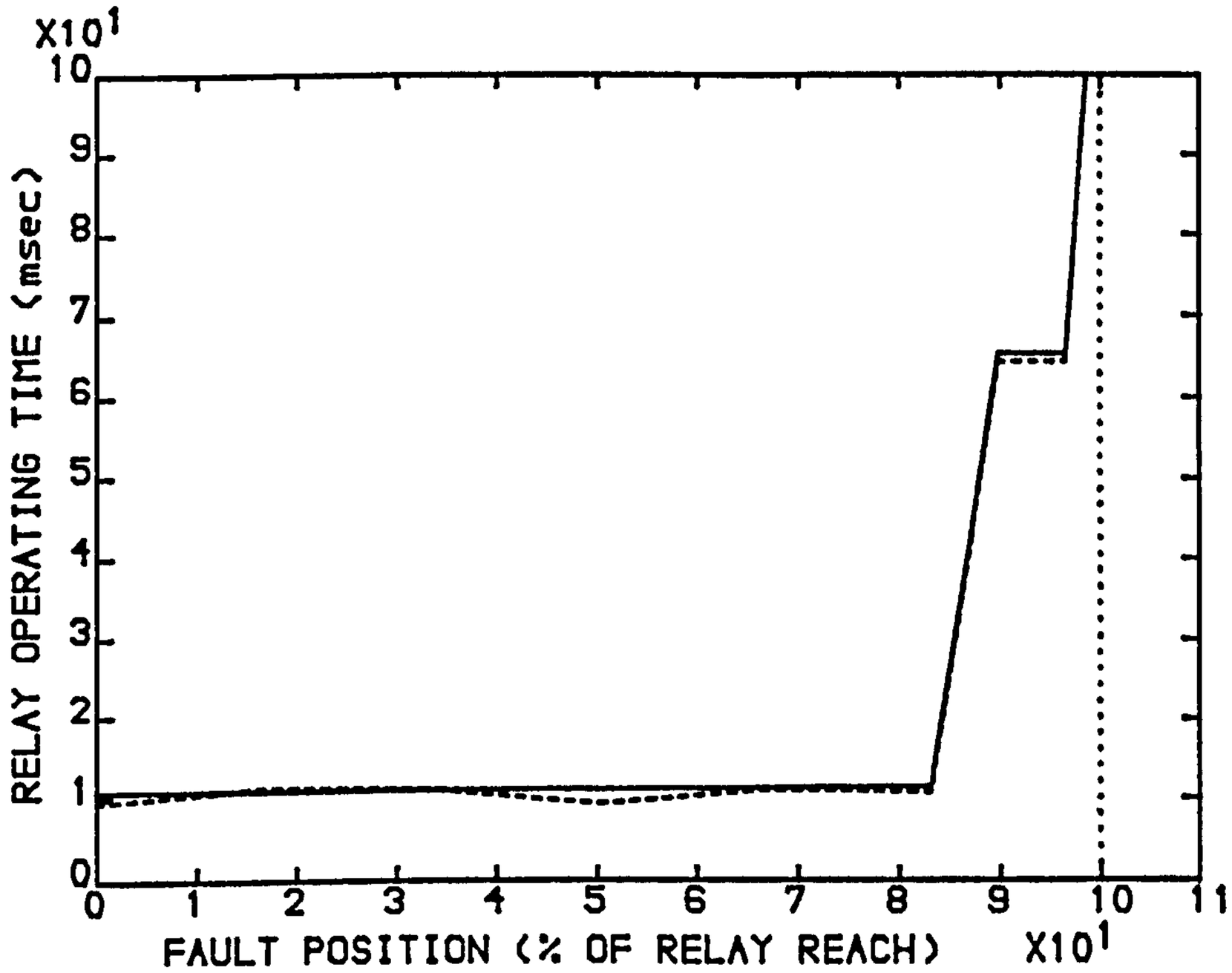

Fig 6.26-Relay Operating Time VS Fault Position For Line Side C.V.T.

SE SCL-5, RE SCL-35
Load ang.-0 deg., LL-200 km
70% Series Compensation

Relay Set At 60% Of Line Length
Xr-16.3, Xo--3 secy. ohms
Rr-12.0, Ro--3.0 secy. ohms

——— Fault Incep. Ang.-0 deg
----- Fault Incep. Ang.-90 deg

CHAPTER 7

RELAY RESPONSE FOR A LINE WITH THE SERIES CAPACITOR AT THE MID-POINT OF THE LINE

Consider Figure 7.1 which shows a series compensated line with the series capacitor situated at the mid-point of the line. In such systems the degree of series compensation is often less than 50%.

It has been explained in Chapter 5 that the new modified residual current compensation can be used for a line with the compensating capacitor installed at the mid-point of the line. Furthermore, it was explained that if the new modified residual compensation factor is used, the measured reactance for faults before the capacitor location is smaller than the actual line reactance.

If the relay independent zone-1 reach is considered to be before the series capacitor, say at 45% (αr=0.45 see Chapter 5) and a complex residual compensation factor (assuming $\angle Z_{L0} \neq \angle Z_{L1}$) is considered in the relay, the relay measures accurate impedance for all faults before the mid-point of the line. But for faults beyond the capacitor, the relay measurement will not be accurate.

However if it is required to set the relay reach at a value higher than 50%, then the relay measurement is accurate only at the reach point.

In this work it was decided to set the relay zone-1 reach at 80% of the line length, which is the common practice in plain uncompensated feeder distance protection schemes. The required residual compensation factor, for boundary setting of 80% (αr=0.8) is, from Figures 5.36.a

and b, found to be approximately equal to $2.015\angle -4.6°$.

Figure 7.2 shows the Quadrilateral characteristic of the relay. It can be seen that the line locus before the capacitor location is outside the characteristic. However as previously mentioned due to the new method of residual compensation, the measured impedance falls within the characteristic.

It has been explained in Chapter 4 that in order to improve discrimination ability of the relay around the forward reach, a longer time is allowed for the relay to reach a trip decision by dividing the relay characteristic into fast and slow counting regions. For the foregoing reasons, although the steady state locus of the measured impedance more likely fall within the relay characteristic, high speed operation may not be achieved for faults just before the capacitor bank. Relay operating time of up to 60 msec was observed for some system conditions, for a fault at 48% of the line length.

In order to improve the relay operating time response a new modified relay characteristic suitable for lines with mid-point compensation is proposed. The new relay boundary requires a new counting strategy in order to cope with the long line transient effects and the sub-synchronous resonance. Figure 7.3 illustrates the new relay characteristic with different counting regions.

The principle of fault detection and counting is similar to that explained in Chapter 4. INC1 and INC2 are initially set at 8 and 32 respectively and σ is also set to unity (see Figure 7.3). If trip is not initiated within 2.5 msec after the first upcount, INC1, INC2 and σ

are changed to 2, 8 and 0.7 respectively. The counter is also reset to zero. If the relay does not trip within 12 msec after the first upcount, INC1 is changed to 1 and INC2 to 4.

It is essential to use a time graded characteristic as explained to ensure that the relay maintains a fast operating time for faults before the series capacitor, and also does not over-reach for faults outside the characteristic if the spark-gap across the capacitor does not flash-over.

Figure 7.4 illustrates the characteristic and the locus of the measured impedance on a R-X plane for a fault at the relay reach. Although the measured impedance traverses the relay characteristic, no trip is initiated. This is due to the fact that the measured impedance remains in the slow-counting region of the boundary and then moves outside which results in the counter being decremented.

Figures 7.5 to 7.8 show the relay operating times versus fault position for a system with 50% series compensation at the middle of the line, when the capacitor flash-over was prevented by adjusting the spark-gap threshold at a high value.

Figure 7.9 shows the relay operating time response for a system with 40% series compensation at the mid-point.

It is clearly evident that the relay maintains a fast operating time for the majority of its reach.

Figure 7.10 illustrates the relay operating time versus fault position when the capacitor flash-over is considered. It can be seen that the relay operates in about 11 msec for faults up to the mid-point where the

capacitor is situated. For faults beyond the capacitor, the change in measured reactance following the gap flash-over, causes the relay to under-reach.

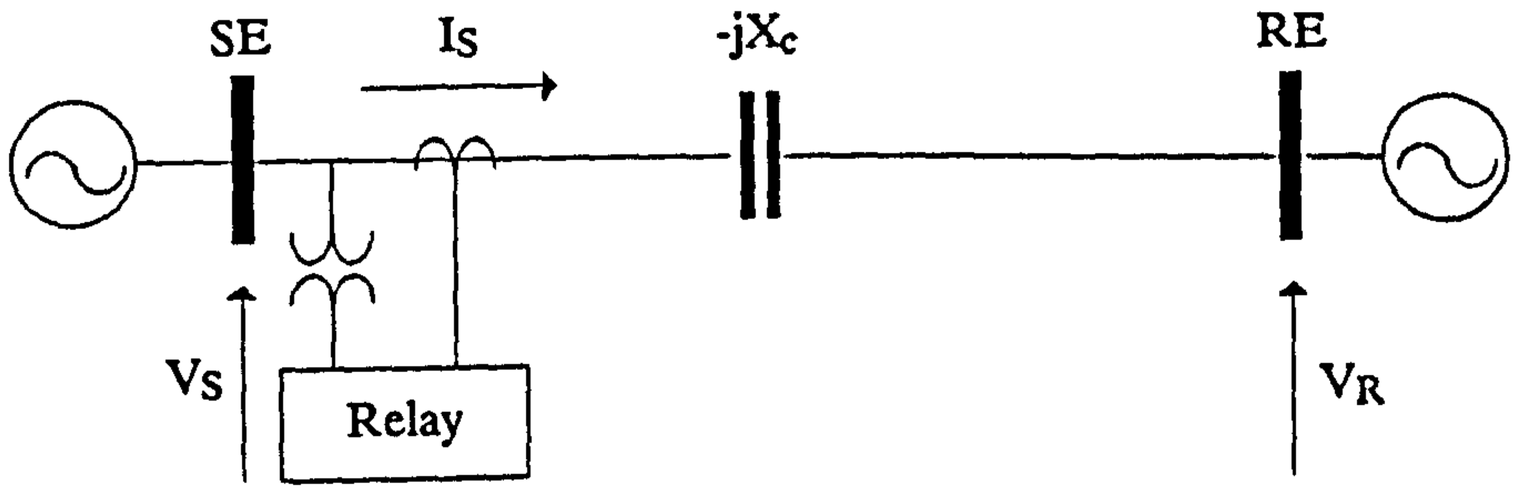

Fig 7.1-System Configuration For A Mid-Point Compensation.

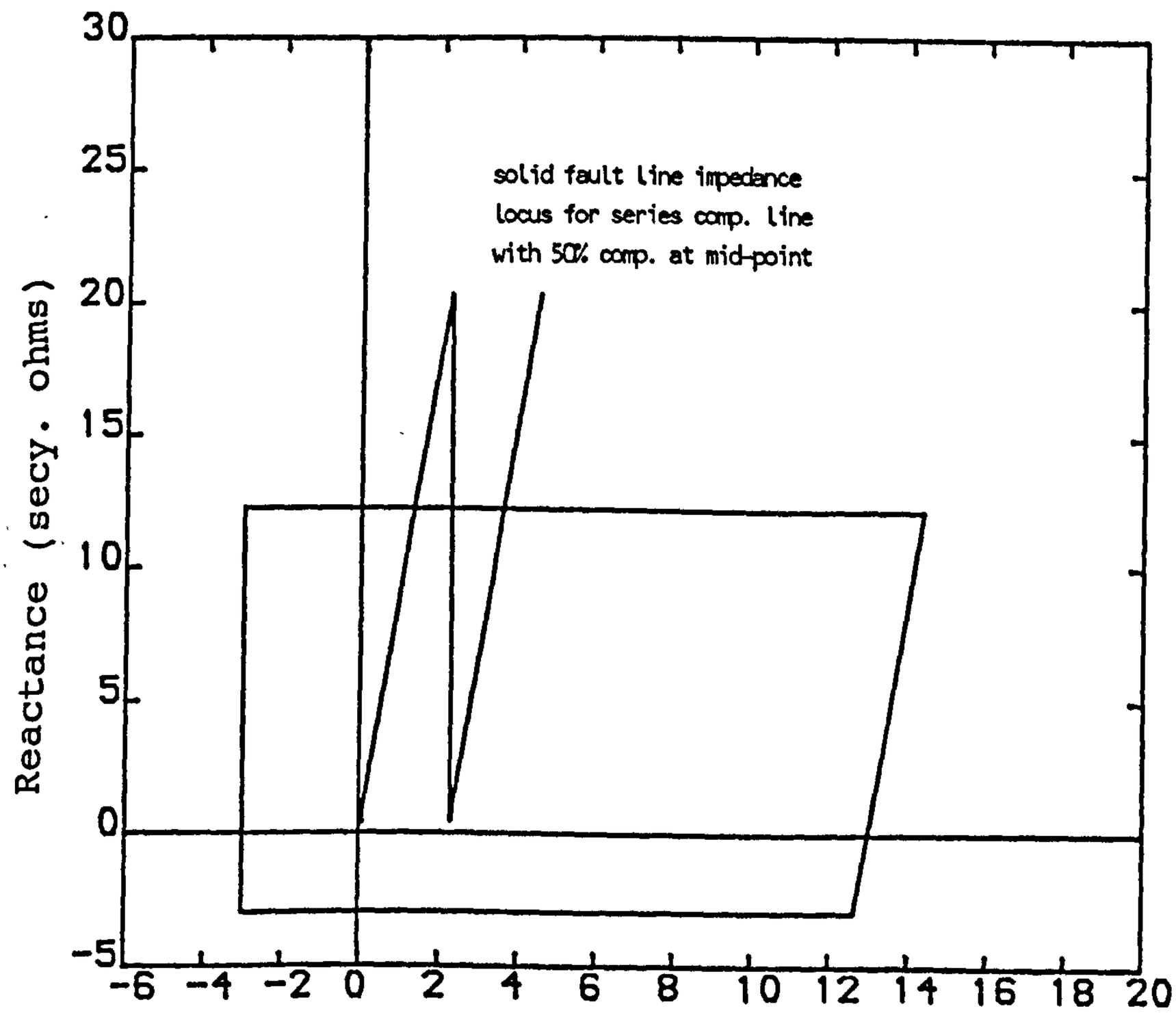

Fig 7.2-The Trip Characteristic And The Line Locus For Mid-Point Compensation.

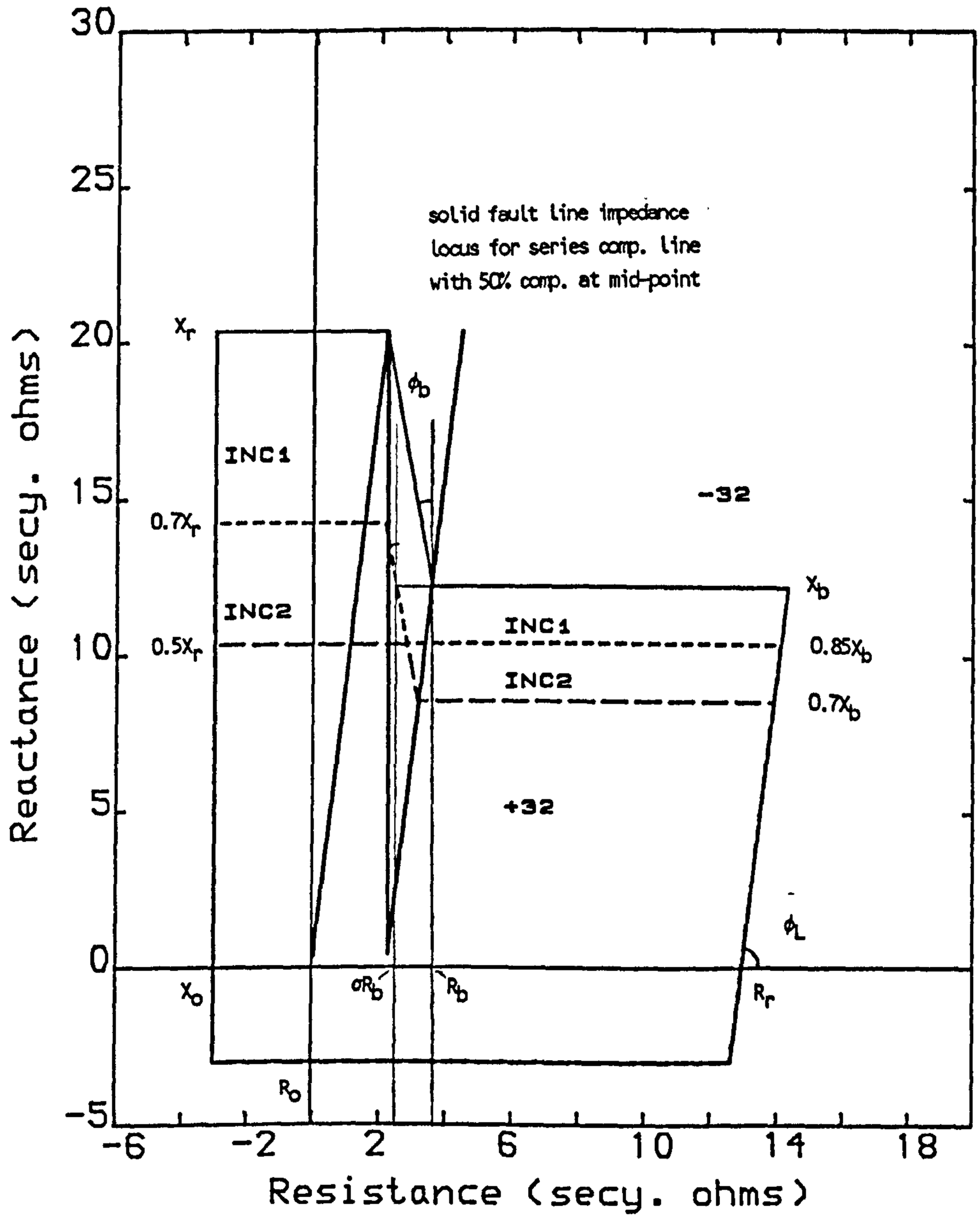

Fig 7.3-The New Relay Trip Characteristic
For Mid-Point Series Compensation

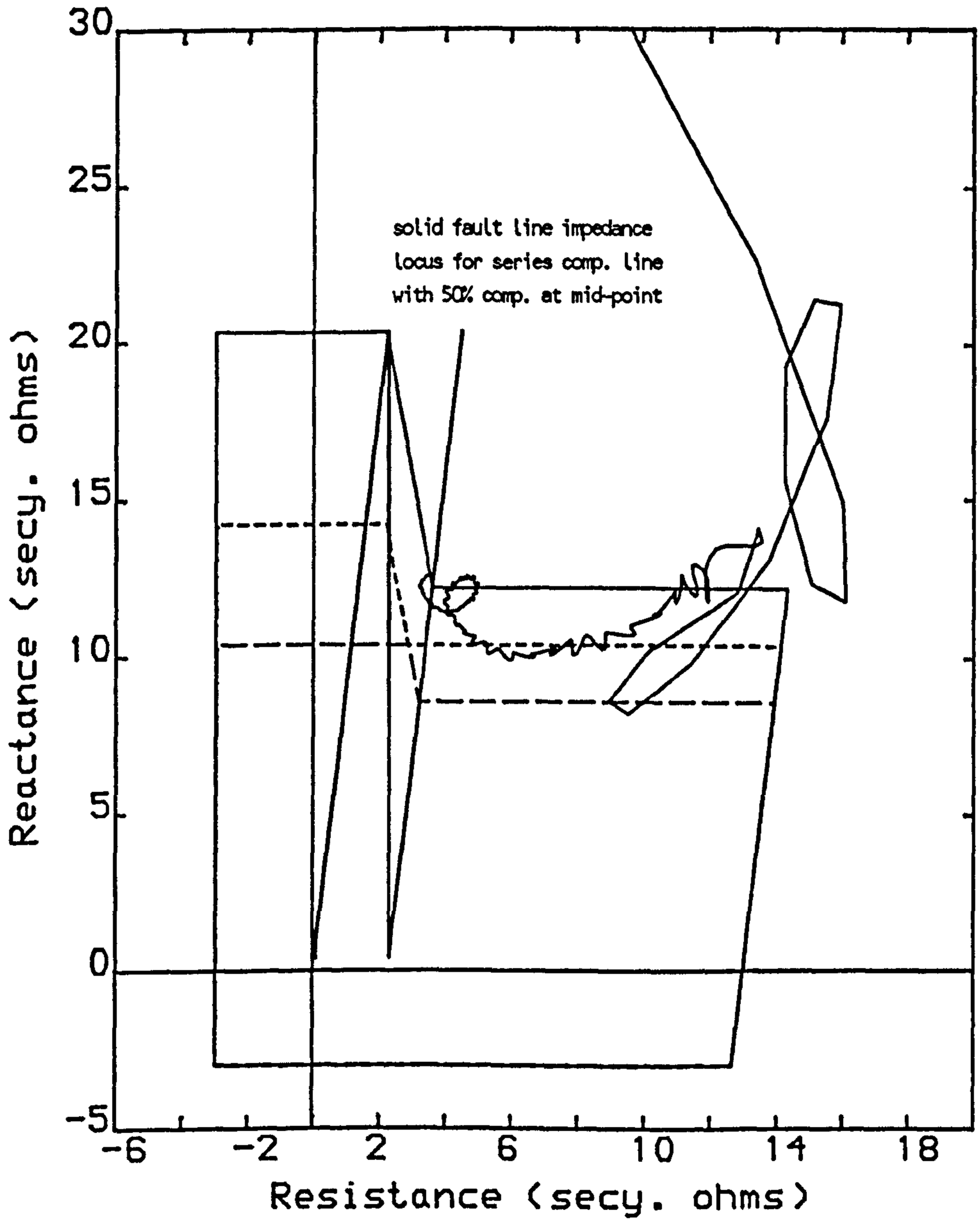

Fig 7.4-The New Trip Characteristic, Measured Impedance And Line Loci For A Fault At The Relay Reach (80% Of The Line Length).

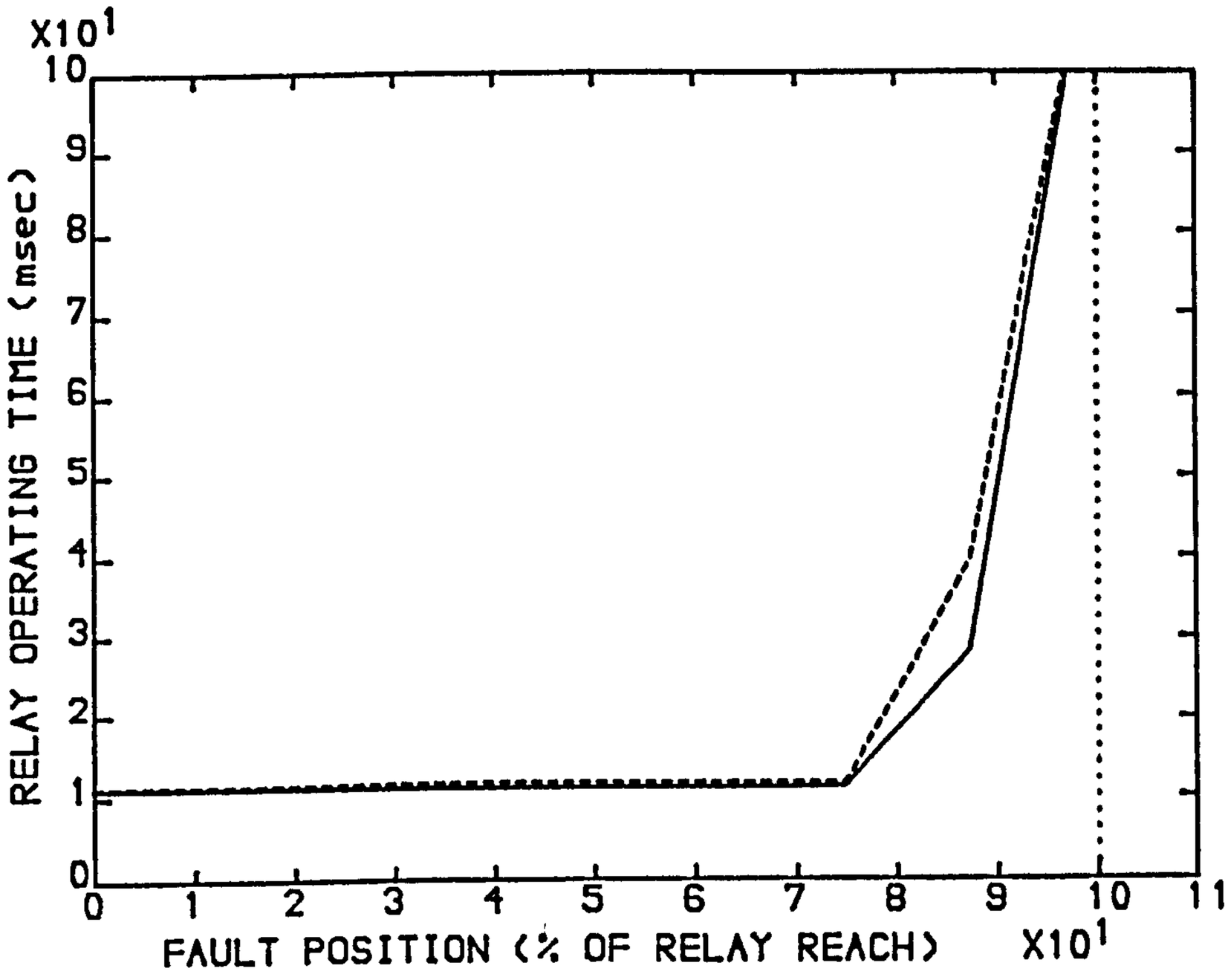

Fig 7.5-Relay Operating Time VS Fault Position With The Mid-Point comp. For:

SE SCL=5 GVA, RE SCL=35 GVA
Load ang.=0 deg., LL=300 km

50% Series Compensation

Relay Set At 80% Of Line Length
Xr=20.4, Xo=-3 secy. ohms
Rr=13.0, Ro=-3.0 secy. ohms
Rb=12.2, Ro=3.6 secy. ohms. and -10

——— Fault Incep. Ang.=0 deg
---- Fault Incep. Ang.=90 deg

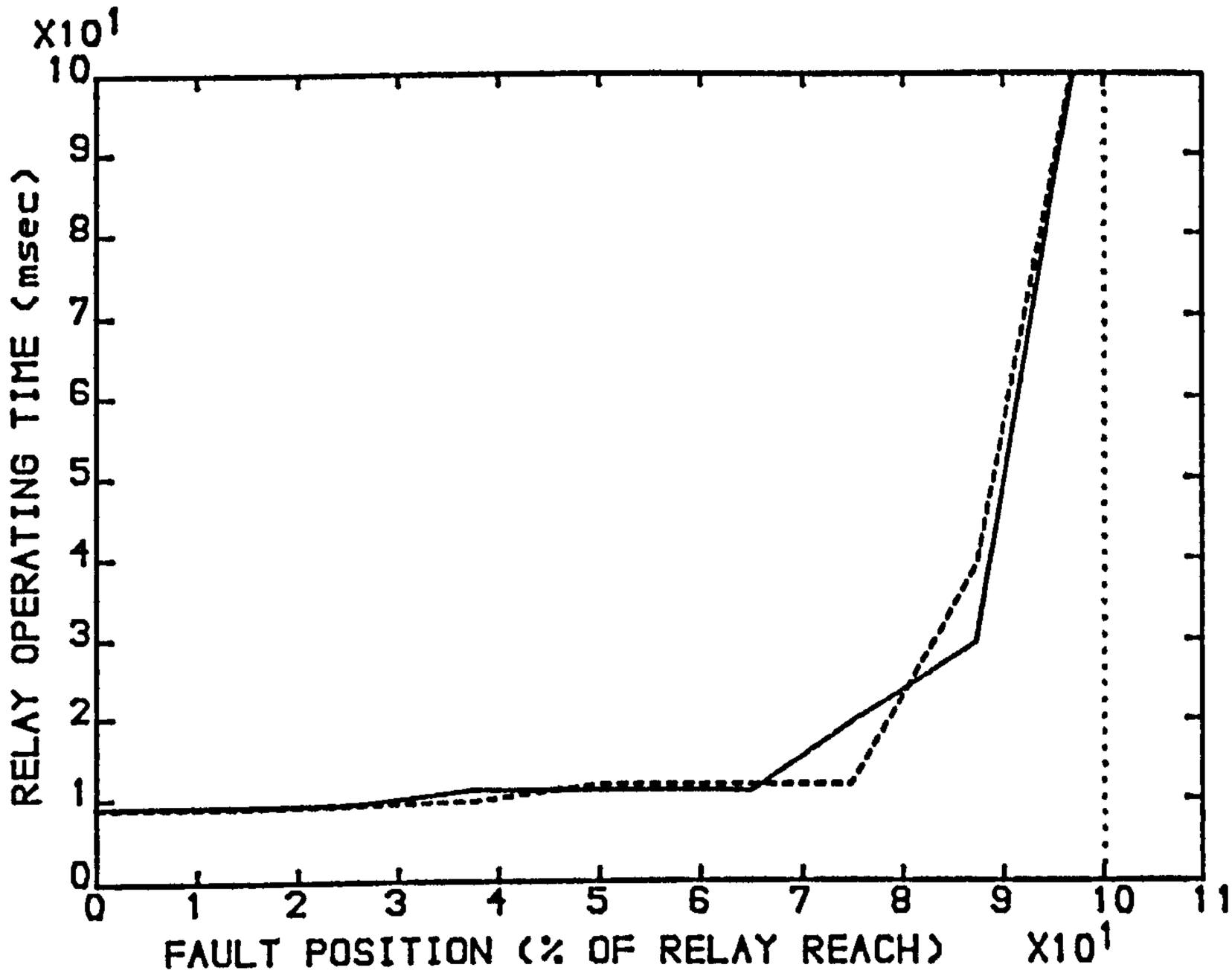

Fig 7.6-Relay Operating Time VS Fault Position With The Mid-Point comp. For:

SE SCL=35 GVA, RE SCL=5 GVA
Load ang.=0 deg., LL=300 km

50% Series Compensation

Relay Set At 80% Of Line Length
Xr=20.4, Xo=-3 secy. ohms
Rr=13.0, Ro=-3.0 secy. ohms
Rb=12.2, Ro=3.6 secy. ohms. and =10

——— Fault Incep. Ang.=0 deg
----- Fault Incep. Ang.=90 deg

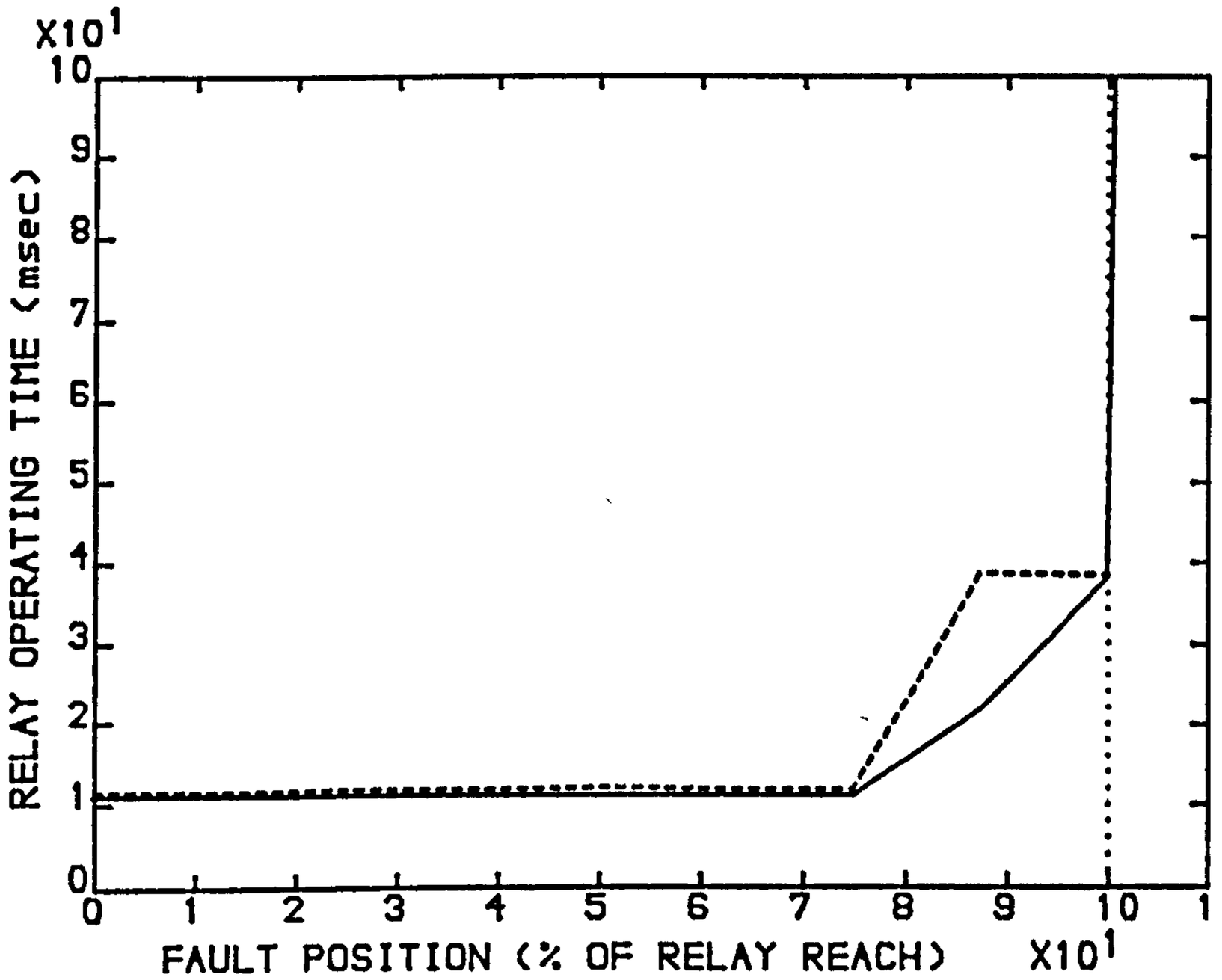

Fig 7.7-Relay Operating Time VS Fault Position With The Mid-Point comp. For:

SE SCL=5 GVA, RE SCL=35 GVA
Load ang.=+10 deg., LL=300 km

50% Series Compensation

Relay Set At 80% Of Line Length
Xr=20.4, Xo=-3 secy. ohms
Rr=13.0, Ro=-3.0 secy. ohms
Rb=12.2, Ro=3.6 secy. ohms. and =10

——— Fault Incep. Ang.=0 deg
---- Fault Incep. Ang.=90 deg

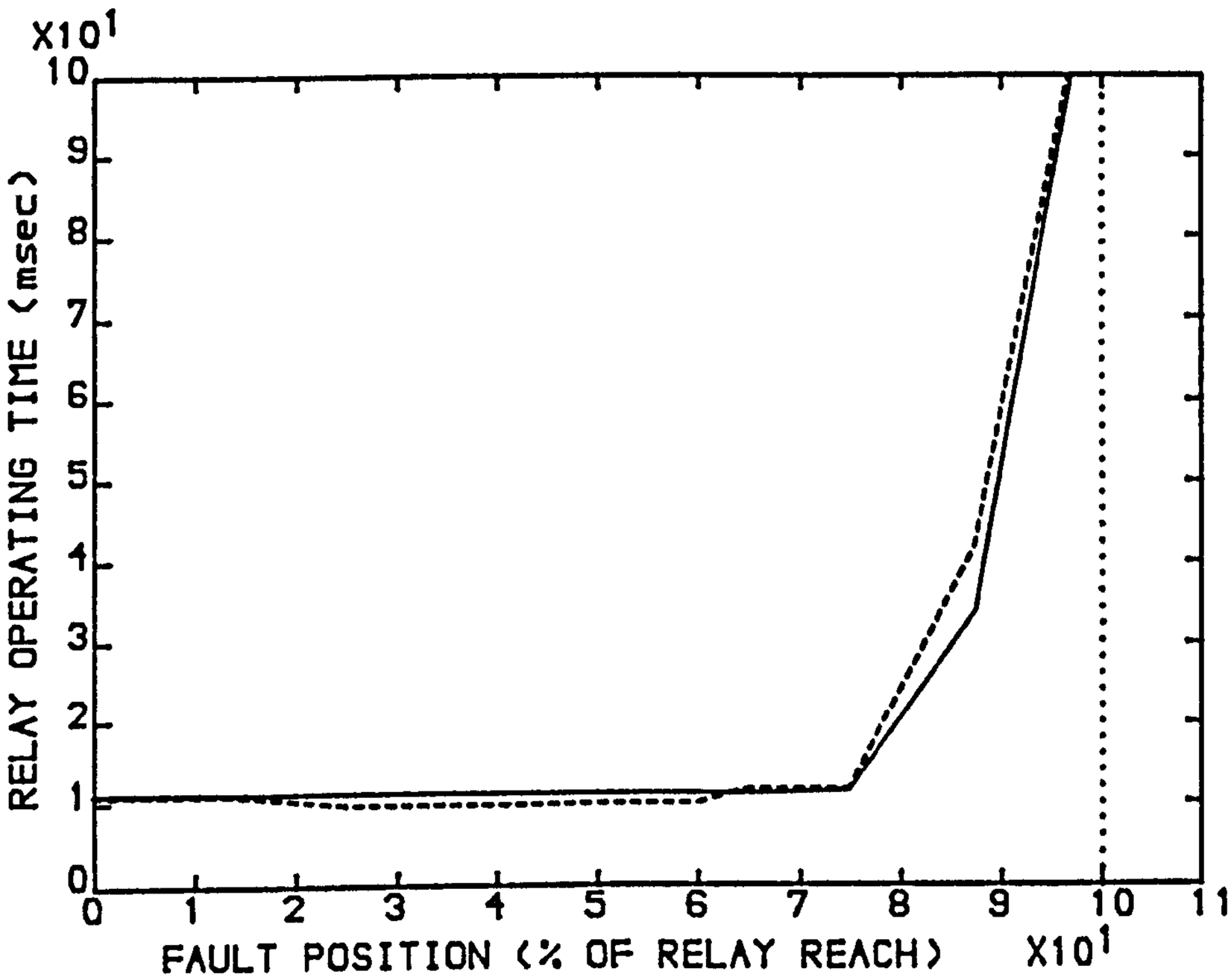

Fig 7.8—Relay Operating Time VS Fault Position With The Mid-Point comp. For:

SE SCL=5 GVA, RE SCL=35 GVA
Load ang.=-10 deg., LL=300 km

50% Series Compensation

Relay Set At 80% Of Line Length
Xr=20.4, Xo=-3 secy. ohms
Rr=13.0, Ro=-3.0 secy. ohms
Rb=12.2, Ro=3.6 secy. ohms. and =10

——— Fault Incep. Ang.=0 deg
- - - - Fault Incep. Ang.=90 deg

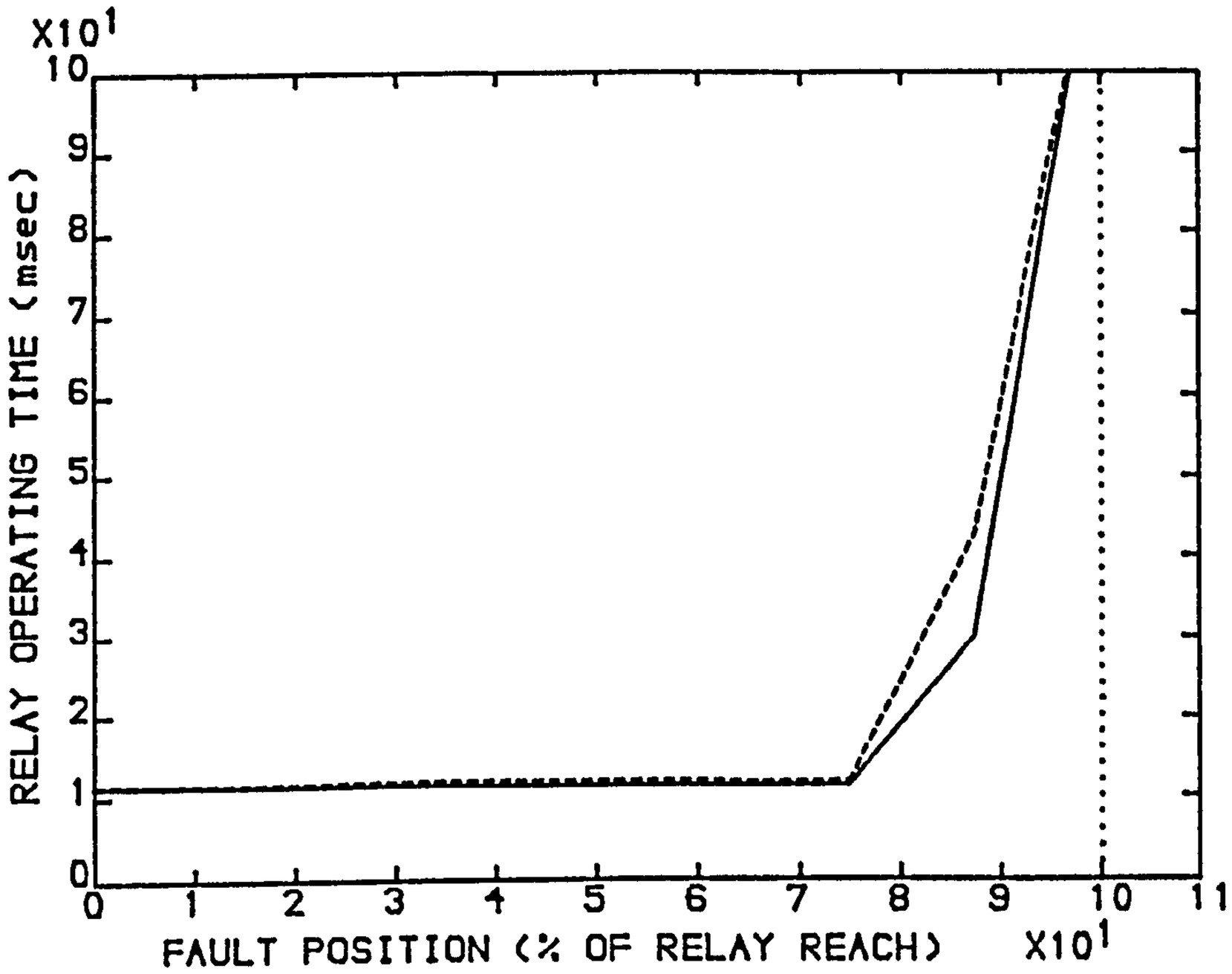

Fig 7.9-Relay Operating Time VS Fault Position With The Mid-Point Comp. For:

SE SCL=5 GVA, RE SCL=35 GVA
Load ang.=0 deg., LL=300 km

40% Series Compensation

Relay Set At 80% Of Line Length
Xr=20.4, Xo=-3 secy. ohms
Rr=13.0, Ro=-3.0 secy. ohms
Rb=16.3, Ro=3.6 secy. ohms. and =10

——— Fault Incep. Ang.=0 deg
---- Fault Incep. Ang.=90 deg

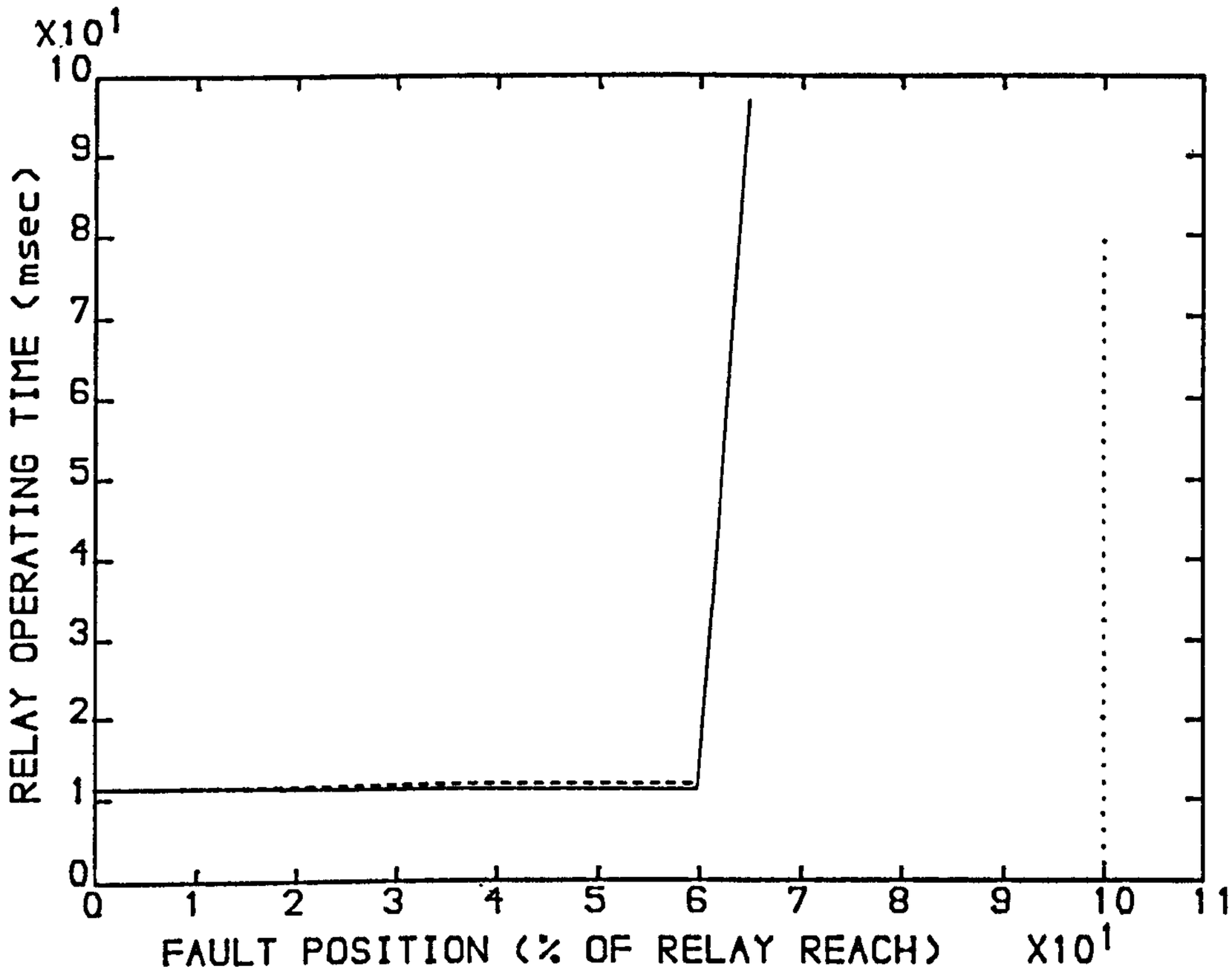

Fig 7.10-Relay Operating Time VS Fault Position
With The Mid-Point Comp. And
Gap Flash-Over (SGS) For:

SE SCL=5 GVA, RE SCL=35 GVA
Load ang.=0 deg., LL=300 km

50% Series Compensation

Relay Set At 80% Of Line Length
Xr=20.4, Xo=-3 secy. ohms
Rr=13.0, Ro=-3.0 secy. ohms
Rb=12.2, Ro=3.6 secy. ohms. and =10
——— Fault Incep. Ang.=0 deg
---- Fault Incep. Ang.=90 deg

CHAPTER 8

CONCLUSIONS AND FUTURE WORK

8.1-General Conclusions

The work presented in this thesis describes the design and performance of a new digital distance relay suitable for series compensated line applications. Based upon impedance measuring techniques, it provides a satisfactory response for lines with capacitors installed at the line ends or mid-point.

The problems associated with the case when the capacitors' protective gaps do not operate, i.e. the capacitors remain in the circuit, or when flash-over times are longer than the relay minimum operating times (which as a result causes the relaying signals to be distorted) were discussed.

It was explained that, since series compensated lines are usually long, a special filtering process is required to eliminate high frequency oscillations, caused by travelling waves, from the relaying signals. A digital band-pass filter with 14 points in its impulse response was employed which attenuates the dc exponential and frequencies above 500 Hz. However, for faults far from the relay , the frequency of the travelling waves are so low that they fall within the pass band of the filter, hence affecting the final algorithm output.

Also, the interaction between the line inductance and the series capacitor, as long as the capacitors remain in the circuit, imposes a sub-harmonic oscillation on the relaying signals. The bandwidth of this oscillation was

shown to be approximately between dc and 80 Hz, depending on system source condition and fault position for a typical series compensated line.

It was explained that the filtering of this frequency from the system signals is very difficult to achieve. Thus, it was found more appropriate to attenuate the resonance oscillation on the final algorithm output, i.e. measured reactance and resistance.

In order to attenuate any oscillation on the measured reactance and resistance, an adaptive feature, using a new recursive averaging filter was incorporated in the relay. This is a low-pass filter with a very low cut-off frequency, which attenuates any frequency component but the dc. The filter is applied when the dominant oscillation on the measurands is the sub-synchronous oscillation. If the travelling wave effect is stronger than the sub-harmonic oscillation, then the filter acts as a non-recursive averager, with a finite impulse response, and together with the relay count regime and decision logic any relay maloperation is prevented.

The errors in the measurement when a single-phase to earth fault occurs were discussed. It was shown that when the capacitors are placed at the line ends, and the voltage transformers are located at the source side of the capacitors, the conventional current compensation (residual current and sound phase current) methods do not provide an accurate measurement.

Two new methods were presented and examined in detail. One utilises the conventional residual compensation factor, but it requires modification of the

relaying voltage signal in order to enable the relay to measure the positive phase sequence impedance of the line from the relaying to fault point. This method provides an accurate measurement for all faults between the two capacitors, i.e. on the line.

The other method uses a new residual compensation factor which is calculated assuming the fault is always at the relay zone-1 forward reach; hence it implies that the measurement is accurate only if a fault occurs at that point. In this method a complex residual compensation factor is considered, which was explained in considerable detail.

The latter method proved to have the advantage of reducing the high frequency oscillation, caused by travelling waves, and sub-synchronous frequency effect by providing a better replica of the primary system. Thus it was decided to use the new residual compensation factor in the relay.

When the capacitors are situated at the line ends, a new setting philosophy must be adopted. The presence of a capacitor in front of the relay affects the reach of the distance relay. In order to avoid relay operation for faults at the receiving end bus-bar (or beyond), the relay zone-1 forward reach must be set at a value less than the conventional distance schemes for plain feeders. It was shown that, with the improved relay performance (as a result of using the new residual compensation factor and the recursive averager which deals with low frequency oscillations) the relay can be set at 60% of the line length for 70% total series compensation (35% at each

end). Thus, theoretically a margin of 8% exists between faults at the relay zone-1 forward reach and faults at the receiving end bus-bar. However, due to the fact that the measurement is not accurate for faults at any other points but the boundary, the actual measurement for a fault at the receiving end bus-bar is bigger than the actual line locus. Therefore the margin between the measured impedance for a fault at the zone-1 forward reach and a fault at the receiving end bus-bar is even larger.

It was explained that, when the voltage transformers are located on the line side of the capacitor banks, the conventional residual compensation factor must be used. However, a complex residual compensation factor provides a better relay measurement and response. As mentioned earlier, the forward reach setting is restricted to 60% of line length.

It was shown that when the capacitors are situated at the middle of the line and the residual compensation factor is used, the relay measures correct impedance only if a fault occurs before the series capacitor. For faults beyond the capacitor location the relay measurement is not accurate. However, if the new residual compensation factor is used the relay forward reach can be extended to include the series capacitor. In this study the relay was set at 80% of the line length. In order to improve the relay operating time response, a new characteristic was proposed which greatly improved the relay operating time.

In order to maintain the discrimination ability of the relay, a time graded characteristic with different counting regions was used. The sub-synchronous phenomena

imposes a very difficult task on the trip decision logic. The process of counting, following a fault, is initiated by detecting the disturbance. The incremental values of the characteristic are changed to a lower values after a pre-set time has elapsed following the fault detection, to allow more time to the relay to reach a decision. In this way, a more stable performance was observed from the relay.

A directional element was incorporated in the relay in order to maintain the directionality of the relay. The directional reactance element utilises the memory voltage polarisation.

A double end fed, single circuit system was simulated using a distributed parameter model of transmission lines. The sources were represented by their impedances. In order to examine the relay behaviour when the capacitors remain in the circuit, the gap flash-over was prevented by setting the gap threshold level at a very high value.

It was shown that the relay operating times were about 10 msec for the majority of the relay reach and independent of fault inception angles. However, for faults near the boundary, the relay operating time appears to be dependent upon the fault inception angle.

The relay was also tested for faults at the receiving end bus-bar, where a severe sub-synchronous oscillation was superimposed on the measurands. No relay over-reach was observed for these cases.

The relay restrained for all reverse fault tests at the sending end bus-bar, for both source side and line side C.V.T. This is particularly important for line side

C.V.T, where for a reverse fault the capacitor reactance (or any other impedance behind it) looks positive to the relay and hence falls inside the relay characteristic.

A few tests were carried out when the capacitor protective gap flash-over is considered. A fixed relay characteristic was assumed. The relay characteristic was set assuming the capacitors are in the circuit.

With the capacitors situated at the line ends, the relay operating time was about 15 msec for faults up to 30% of the line length, irrespective of the fault inception angle. Also, the relay did trip for faults up to 40% of the line length with the fault inception angle of 90 degree. This is due to the fact that the gap flash-over time was longer than the relay operating time and the relay tripped before the capacitor is by-passed.

The gap flash-over was also considered for the situation where the capacitors are placed at the mid-point of the line. The relay operating time was, as expected, about 10 msec for faults before the capacitor location, since the capacitor gap flash-over has no significant effect on the measured impedance. However, the relay under-reaches for faults beyond the capacitor location when the gap flashes.

8.2-Future Work

As mentioned earlier, when the capacitor banks are situated at the line ends and the C.V.Ts are connected to the source side of the capacitors, or in the cases where they are placed at the mid-point of the line, they become part of the line impedance, which is measured by the relay. Thus, when the capacitor protective gaps flash

over, there is an increase in the measured reactance. This causes the relay under-reach, if the relay characteristic has been set assuming the capacitor to be in circuit. Therefore, it is highly desirable to detect the gap flash-over in order to dynamically change the relay characteristic.

Different approaches may be adopted to overcome the aforementioned problems. Since in a digital distance relay the locus of the measured impedance is available at any instant of time, it seems possible to detect the change in the measured reactance following a gap flash-over. However, it is known that when a gap flashes, as a result of change in voltage and current, a travelling wave phenomena is established in the system. This high frequency oscillation is superimposed on the measured resistance and reactance which in turn makes it difficult ,in most cases, to detect the change in the measured reactance due to the capacitor by-passing. Figure 8.1 shows the measured reactance for a typical single phase to earth fault, far from the relay. It is clearly evident that the change in the measured reactance cannot be determined. Therefore, it is necessary to design a suitable filter to cope with such effects and also does not impose any significant time delay to the process.

It must also noted that, when a phase to earth fault occurs and the new residual compensation factor is used in the relay, the measured impedance is only accurate for a fault at the relay forward reach, as long as the capacitors remain in the circuit. Following a gap flash-over, the measurement is not accurate. Thus, the change

in the measured reactance is not equivalent to the capacitor reactance, and therefore a comparison of the measured reactance, before and after the gap flash over is very difficult.

The other approach is to detect any low frequency oscillation on the measured impedance. As previously mentioned, as long as the capacitors remain in the circuit a sub-synchronous oscillation is superimposed on the measured resistance and reactance. When the capacitor is by-passed, the magnitude of this oscillation is greatly reduced (as some sub-synchronous effect still appears on the system signals via the mutual coupling to the other phases). In order to detect any low frequency component, between 5 to 60 Hz (note that the algorithm produces an oscillation on the measured impedance which has a frequency equal to the difference of the system frequency and the main sub-synchronous oscillation on the system signals), an especial filtering process is required to extract the low frequency components.

To design such a filter is extremely difficult, bearing in mind that the relay must detect the flash over in a relatively short time.

The other method which can be considered is the effect of capacitor gap flash-over on the magnitude of the voltage and current signals and the phase angle between them. Algorithms are available which calculate the magnitude of any sinusoidal signal in real time. The phase angle between them can also be estimated.

When capacitor bank is by-passed as a result of the gap flashing, the magnitude of the current decreases and

as a result the voltage at the relaying point increases. Of course, the degree of the change depends on the source impedance. The phase angle between the voltage and current also changes and becomes approximately the line angle.

If the signals were pure sine waves, it would not be difficult to devise an algorithm to detect these changes. However, in practice, the signals are contaminated with travelling wave effects, making it extremely difficult to achieve a satisfactory result. Particularly, it is known that the algorithms available for calculating the signal magnitudes and phases often accentuate high frequencies. Also, if the source impedance is small the change in the voltage is not great, which in turn makes it difficult to detect the changes in the voltage magnitude in such cases.

As it appears in the thesis the relay has been thoroughly tested for single phase to earth faults, for different system conditions.

It is felt that, it is necessary to fully evaluate the relay response for other type of faults, particularly a double phase fault. In this situation if none of the gaps flashes, two capacitors are in the faulted path which in turn imposes a more severe sub-synchronous oscillation on the measurands.

Finally, the relay must be tested for a double circuit system, where there is another infeed route to the fault point. It is envisaged that the relay perform correctly in such systems.

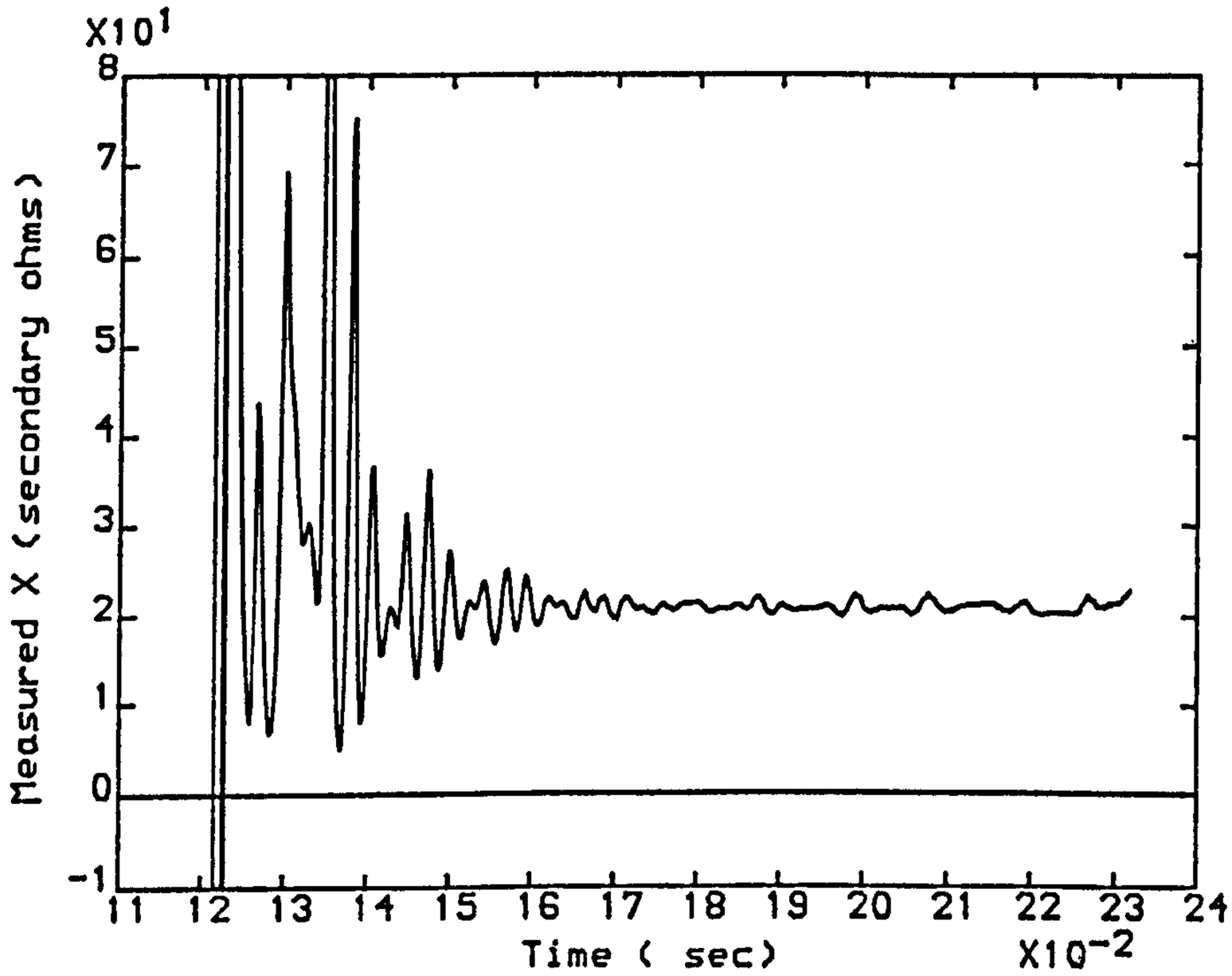

Fig 8.1-Measured Reactance VS Time
For 70% Series Compensation
(35% At Each End)
And Source Side C.V.T And With
Cap. Flash-Over (SGS) For:
SE SCL=3 GVA, RE SCL=7 GVA
Load ang.=0 deg., LL=300 km
Inception Ang.=0 Deg.
Flash-Over Time=9 msec After Fault

REFERENCES

1-G.Janke, L.Ahlgren, L.Hanning, T.Johansson,"15 years development and experience with series capacitors in transmission systems",CIGRE Report Nº 316, 1966.

2-D.A.Giliiies, E.W.Kimbark, F.G.Schaufelberger, R.M.Partington,"High voltage series coapacitors, experience and planning",CIGRE Report Nº 118, 1966.

3-J.Samuelsson,"Series compensation in A.C. transmission systems",Report from ASEA, 1973.

4-H.W.Anderl, S.M.Merry,"Lowering E.H.V. transmission costs with series capacitors",Indian Journal Power and River, Vol. Dev, Jan. 1975.

5-J.P.Bickford,"Electrical power transmission",M.sc. course studying notes, UMIST, UK, 1984.

6-L.Ahlgrn, N.Fahlen, K.E.Johansson,"EHV series capacitors with dual gaps and non-linear resistors provide technical and economic advantages",IEEE PES winter meeting, New York, Feb. 1979.

7-A.L.Courts, N.G.Hingorani, G.E.Stemler,"A new series capacitor protection scheme using non-linear resistors",IEEE PES summer meeting, Mexico City, Jul. 1977.

8-J.R.Hamann, S.A.Miske, I.B.Johnson, A.L.Courts,"A zinc oxide varistor protective system for series capacitors",IEEE PES summer meeting, Minneapolis, 1980.

9-R.K.Aggarwal, A.T.Johns, A.Kalam,"Computer modelling of series compensated E.H.V transmission systems", IEE Proc. Vol. 131, Pt.C, Nº 5, September 1984.

10-F.Iliceto, M.Cinieri, M.Cazzani, G.Santagostino,"Transient voltage and current in series

compensated E.H.V lines",IEE Proc., Vol. 123, Nº 8, Aug 1976, pp. 811-817.

11-W.J.Cheetham, A.Newbould, G.Stranne,"Series compensated line protection: System modelling and test result", 15th annual western protective relay conference, Washington State University, Spokane, Washington, 25-27 October 1988.

12-C.A.Mathews, S.B.Wilkinson,"Series compensated line protection with a directional comparison relay scheme",2nd IEE Conference on developments in power system protection, Nº 185, Jun. 1980, pp. 215-220.

13-A.Newbould, I.A.Taylor,"Series compensated line protection: system modelling and relay testing",4th IEE Conference on developments in power system protection, Edinburgh, Apr. 1989, pp. 182-186.

14-R.K.Aggarwal, A.T.Johns,"Modelling of capacitor compensated power systems and associated protection",19th UPEC, Aberdeen, Apr. 1984.

15-M.M.El-Kateb, W.J.Cheetham,"Problems in the protection of series compensated lines", 2nd IEE Conference on developments in power system protection, Nº 185, Jun. 1980.

16-J.Berdy,"Protection of circuits with series capacitors",AIEE Trans., Feb 1963, pp. 926-935.

17-W.L.Hinman, R.W.Gonnam,"A new relaying system to protect series compensated lines,"Presented to Georgia Institute of technology protective relaying conference, May 1973.

18-IEEE Power System Relaying Committee Report,"EHV Protection Problems",IEEE Trans. on PAS, PAS-100, Nº5,

May 1981, pp. 2399-2406.

19-M.M.El-Kateb, W.J.Cheetham,"A new approach to high speed phase selection", 2nd IEE Conference on developments in power system protection, Nº 185, Jun. 1980.

20-D.Tripp, R.K.Aggarwal, A.T.Johns,"The application of a new directional comparison protection scheme to capacitor compensated E.H.V. transmission systems",20th UPEC, Apr. 1985.

21-A.T.Johns,"New ultra-high-speed directional comparison technique for the protection of ehv transmission lines",IEE Proc., Vol.127, Pt. C, 1980, pp. 228-239.

22-J.W.Ballance, S.Goldberg,"Sub-synchronous resonance in series compensated transmission lines",IEEE Trans. PAS, Dec 1972, pp. 1649-1658.

23-A.T.Johns, R.K.Aggarwal, "Digital simulation of faulted E.H.V transmission lines with particular reference to Very-High-Speed protection", IEE Proc., Vol. 123, No 4, April 1976.

24-G.E.Gilerest, G.D.Rockefeller, E.A.Udren,"High speed distance relaying using digital computer", IEEE Trans. PAS, May 1971, pp.1235-1243.

25-B.E.McInnes, I.F.Morrison, "Real time calculation of resistance and reactance for transmission line protection by digital computer", Institute of Eng. (Australia), March 1971, pp. 16-24.

26-A.G.Phadke, T.Hlibka, M.Ibrahim,"A digital computer system for EHV substations: Analysis and field test",IEEE Trans. on PAS, Vol. PAS-95, Nº 1, Jan/Feb. 1976, pp. 291-301.

27-B.J.Mann, I.F.Morrison,"Digital calculation of impedance of transmission line protection",IEEE Trans. on PAS, Vol. PAS-90, Nº 1, Jan/Feb 1971, pp. 270-279.

28-A.T.Johns, M.A.Martin, "New Ultra-High-Speed distance protection using Finite-Transform techniques", IEE Proc., Vol. 130, Pt. C, Nº 3, May 1983, pp. 127-138.

29-P.J.Moore, A.T.Johns, "Impedance measurement techniques for digital EHV line protection", Universities Power Eng. Conf., September 1988.

30-D.Tripp,"The design & application of a new directional comparison line protection scheme to series compensated systems",Ph.D. Thesis, University Of Bath, 1986.

31-Y.Mansour, T.G.Martinich, J.E.Drakos,"B.C. hydro series capacitors bank staged fault test",IEEE Trans. on PAS, Vol. PAS-102, Nº 7, pp. 1960-1969.

32-R.G.Coney, G.H.Topham, M.G.Fawkes,"Experience and problems with the protection of series compensated lines",IEE Conference on developments in power system protection, Edinburgh, April 1989.

33-A.G.Phadke, J.S.Thorp, "Computer relaying for power systems", John Wiley & Sons Inc., 1988.

34-A.M.Ranjbar, B.J.Cory, "Filters for digital protection of long transmission lines", IEEE Trans. PAS, Vol. PAS-94, May 1975,pp. 544-547.

35-IEEE Tutorial Course on Computer Relaying. PB 33390, 79EH0145-7-PWR, May 1980.

36-J.V.Sanderson, W.S.Kwong, C.C.Wong, "Microprocessor based distance protection-Some design considerations", IEE Conf. Publ. 185, 1980, pp. 127-131.

37-A.Savitzky, M.J.E.Golay, "Smoothing and differentiation

of data by simplified least squares procedures", Analytical chemistry, Vol. 36, Nº 8, July 1964.

38-P.J.Moore, "Adaptive digital distance relay", PhD Thesis, City University, London, 1989.

39-Electro-magnetic Transient Program (EMTP) Handbook.

40-A.Kalam,"Simulation of series compensated lines and their associated protection",Ph.D Thesis, University of Bath, 1981.

41-A.Stalewski, G.C.Weller,"Novel capacitor-divider voltage sensor for high voltage transmission systems",IEE Proc. Vol. 126, No 11, November 1979.

42-K.F.Al-janabi,"Finite Fourier transform distance protection for E.H.V transmission systems",Ph.D Thesis, University of Bath, 1985.

43-Bewley,"Travelling waves on transmission systems",wiley 1951.

44-L.N.Walker, A.D.Ogden, G.E.Ott, J.R.Tudor,"Special purpose digital computer requirements for power system substation needs",IEEE winter power meeting, NY, January 25-30, 1970.

45-G.W.Swift,"The spectra of fault-induced transients",IEEE Trans. on PAS, Vol. PAS-98, No3, 940-947.

46-P.J.Moore, A.T.Johns,"The performance of new Ultra-High-Speed distance protection",24th Universities Power Eng. Conf., Sunderland, April 1986.

47-IEEE Tutorial Course,"Microprocessor relays and protection systems",No 88EH0269-1-PWR, 1988.

48-P.Müller,"Progress in the protection of series compensated lines and in the determination of very high

earth fault resistance",Brown Boveri Review, Feb. 1981.

49-M.Shafik, F.Ghassemi, A.T.Johns,"Performance of digital distance protection for series compensated systems",24th Universities Power Eng. Conf., Sunderland, April 1986.

50-A.Newbould, P.Hindle,"Series compensated lines: Application of distance protection",14th Annual western protection relay conference, Washington State University, Spokane, Washington, 20-22 Oct. 1987.

51-M.A.Martin, A.T.Johns,"New approach to digital distance protection using time graded impedance characteristic",paper A 5.5.11, Proc. 16th UPEC 1981.

52-Power system protection, Electricity council publication, Vol. 2.

53-W.A.Lewis, S.L.Tippett,"Fundamental basis for distance relaying on three-phase system", AIEE Trans., 1947, pp. 694-709.

54-A.R.Van C. Warrington,"Graphical method for estimating the performance of distance relays during faults and power swings", AIEE Trans., 1949, pp. 608-621.

55-C.Adamson, A.Tureli,"Errors of sound-phase-compensation and residual compensation systems in earth-fault distance relaying",IEE Proc. Vol. 112, No 7, July 1965, pp. 1369-1382.

56-E.B.Davison, A.Wright,"Some factors affecting the accuracy of disrance-type protective equipment under earth-fault conditions",IEE Proc. Vol. 110, No 9, Sep. 1963, pp. 1678-1688.

APPENDIX 3A

Let the voltage and current signals be expressed as pure sinusoidal waveforms:

$$v_{(t)}=V\cdot\sin(w_o t) \qquad 3A1$$

$$i_{(t)}=I\cdot\sin(w_o t-\phi) \qquad 3A2$$

where: w_o=power system frequency.

ϕ=phase angle between the fundamental voltage and current.

The relaying signals can be expressed as:

$$v_{1(t)}=V\cdot\sin(w_o t) \qquad 3A3$$

$$i_{1(t)}=I\cdot\sin(w_o t-\phi) \qquad 3A4$$

$$v_{2(t)}=V\cdot\sin(w_o t-\Theta) \qquad 3A5$$

$$i_{2(t)}=I\cdot\sin(w_o t-\phi-\Theta) \qquad 3A6$$

Where Θ is the delay angle which is used to produce the second equation.

D, R and L are calculated using the following equations.

$$D=i_{1(t)}i'_{2(t)} - i'_{1(t)}i_{2(t)} \qquad 3A7$$

$$R=\frac{1}{D}[v_{1(t)}i'_{2(t)} - v_{2(t)}i'_{1(t)}] \qquad 3A8$$

$$L=\frac{1}{D}[v_{2(t)}i_{1(t)} - v_{1(t)}i_{2(t)}] \qquad 3A9$$

The current derivatives are calculated as:

$$i'_{1(t)}=I\cdot w_o\cdot\cos(w_o-\phi) \qquad 3A10$$

$$i'_{2(t)}=I\cdot w_o\cdot\cos(w_o-\phi-\Theta) \qquad 3A11$$

Substituting for voltages and currents in Equation 3A7 D term can be calculated.

$$D=I\cdot\sin(w_o t-\phi)\ \cdot\ I\cdot w_o\cdot\cos(w_o t-\phi-\Theta)$$
$$-I\cdot w_o\cdot\cos(w_o t-\phi)\ \cdot\ I\cdot\sin(w_o t-\phi-\Theta) \qquad 3A12$$

Taking $I^2\cdot w_o$ common Equation 3A12 can be written as:

$$D=I^2\cdot w_o\cdot[\sin(w_o t-\phi)\cdot\cos(w_o t-\phi-\Theta)$$
$$-\cos(w_o t-\phi)\cdot\sin(w_o t-\phi-\Theta)] \qquad 3A13$$

Equation 3A13 can be expressed as:

$$D=I^2\cdot w_o\cdot\{1/2[\sin(w_o t-\phi-w_o t+\phi+\Theta)+\sin(w_o t-\phi+w_o t-\phi-\Theta)]$$
$$-1/2[\sin(w_o t-\phi+w_o t-\phi-\Theta)-\sin(w_o t-\phi-w_o t+\phi+\Theta)]\} \qquad 3A14$$

or

$$D=I^2\cdot w_o\cdot\{1/2[\sin(\Theta)+\sin(2w_o t-2\phi-\Theta)]$$
$$-1/2[\sin(2w_o t-2\phi-\Theta)-\sin(\Theta)]\} \qquad 3A15$$

Note that the double frequency components are eliminated from the expression. Equation 3A15 can be written as:

$$D=I^2\cdot w_o\cdot\sin(\Theta) \qquad 3A16$$

The measured resistance is given by Equation 3A8. Substituting for voltages and currents yields:

$$R=\frac{1}{D}[V\cdot\sin(w_o t)\ \cdot\ I\cdot w_o\cos(w_o t-\phi-\Theta)$$
$$-V\cdot\sin(w_o t-\Theta)\ \cdot\ I\cdot w_o\cdot\cos(w_o t-\phi)] \qquad 3A17$$

Taking $V\cdot I\cdot w_o$ common and use similar method as above, Equation 3A17 can be written as:

$$R=\frac{V\cdot I\cdot w_o}{D}\{1/2[\sin(\phi+\Theta) + \sin(2w_ot-\phi-\Theta)] - 1/2[\sin(\phi-\Theta) + \sin(2w_ot-\phi-\Theta)]\} \quad 3A18$$

Note the double power system frequency oscillation which are cancelled from the expression. Rewriting equation 3A18 yields:

$$R=\frac{V\cdot I\cdot w_o}{D}[\sin(\phi+\Theta) - \sin(\phi-\Theta)] \quad 3A19$$

Substituting for D and expanding Equation 3A19 gives:

$$R=\frac{V}{I}\cdot\cos(\phi) \quad 3A20$$

The line model inductance is calculated by:

$$L=\frac{1}{D}[V\cdot\sin(w_ot-\Theta)\cdot I\cdot\sin(w_ot-\phi) - V\cdot\sin(w_ot)\cdot I\cdot\sin(w_ot-\phi-\Theta)] \quad 3A21$$

Equation 3A21 can be written as:

$$L=\frac{V\cdot I}{D}\{1/2[\cos(\phi-\Theta) - \cos(2w_ot-\phi-\Theta)] - 1/2[\cos(\phi+\Theta) - \cos(2w_ot-\phi-\Theta)]\} \quad 3A22$$

Note the double power system frequency oscillations which are eliminated from the expression. Rewriting equation 3A15 gives:

$$L=\frac{V\cdot I}{D}[\cos(\phi-\Theta) - \cos(\phi+\Theta)] \quad 3A23$$

Substituting for D and expanding Equation 3A23 gives:

$$L=\frac{V}{I\cdot w_o}\sin(\phi) \quad 3A24$$

APPENDIX 3B

Consider input signals of the form:

$$v_{(t)}=V_o \cdot \sin(w_o t) + V_{su} \cdot \sin(w_{su} t+\beta) \quad \text{3B1}$$

and

$$i_{(t)}=I_o \cdot \sin(w_o t-\phi_o) + I_{su} \cdot \sin(w_{su} t+\beta-\phi_{su}) \quad \text{3B2}$$

where:

w_o, w_{su} =power system and sub-synchronous frequency respectively.

V_o, I_o =voltage and current magnitude of fundamental components respectively.

V_{su}, I_{su} =voltage and current magnitude of sub-synchronous components respectively.

β =phase angle between the fundamental & sub-synchronus components.

ϕ_o =phase angle between the power system fundamental voltage and current.

ϕ_{su} =phase angle between the sub-synchronous voltage and current.

The relaying components $v_{1(t)}$, $v2_{(t)}$, $i_{1(t)}$ and $i_{2(t)}$ can thus be written as:

$$v_{1(t)}=V_o \cdot \sin(w_o t) + V_{su} \cdot \sin(w_{su} t+\beta) \quad \text{3B3}$$

$$i_{1(t)}=I_o \cdot \sin(w_o t-\phi_o) + I_{su} \cdot \sin(w_{su} t+\beta-\phi_{su}) \quad \text{3B4}$$

$$v_{2(t)}=V_o \cdot \sin(w_o t-\Theta) + V_{su} \cdot \sin(w_{su} t+\beta-\Theta) \quad \text{3B5}$$

$$i_{2(t)}=I_o \cdot \sin(w_o t-\phi_o) + I_{su} \cdot \sin(w_{su} t+\beta-\phi_{su}-\Theta) \quad \text{3B6}$$

Where Θ is the delay angle which is used to produce the second equation.

D, R and L' are calculated using the following

equations.

$$D=i_{1(t)}i'_{2(t)} - i'_{1(t)}i_{2(t)} \qquad 3B7$$

$$R=\frac{1}{D}[v_{1(t)}i'_{2(t)} - v_{2(t)}i'_{1(t)}] \qquad 3B8$$

$$L'=\frac{1}{D}[v_{2(t)}i_{1(t)} - v_{1(t)}i_{2(t)}] \qquad 3B9$$

The current derivatives are calculated as:

$$i'_{1(t)}=w_o \cdot I_o \cdot \cos(w_o t-\phi_o) + w_{su} \cdot I_{su} \cdot \cos(w_{su} t+\beta-\phi_{su}) \qquad 3B10$$

$$i'_{2(t)}=w_o \cdot I_o \cdot \cos(w_o t-\phi_o-\Theta) + w_{su} \cdot I_{su} \cdot \cos(w_{su} t+\beta-\phi_{su}-\Theta) \qquad 3B11$$

Substituting for voltages and currents in Equation 3B7 D term can be calculated.

$$i_{1(t)} \cdot i'_{2(t)}=[I_o \cdot \sin(w_o t-\phi_o) + I_{su} \cdot \sin(w_{su} t+\beta-\phi_{su}] \cdot [w_o \cdot I_o \cdot \cos(w_o t-\phi_o-\Theta) + w_{su} \cdot I_{su} \cdot \cos(w_{su} t+\beta-\phi_{su}-\Theta)] \qquad 3B12$$

$$i'_{1(t)} \cdot i_{2(t)}=[w_o \cdot I_o \cdot \cos(w_o t-\phi_o) + w_{su} \cdot I_{su} \cdot \cos(w_{su} t+\beta-\phi_{su}) \cdot [I_o \cdot \sin(w_o t-\phi_o-\Theta) + I_{su} \cdot \sin(w_{su} t+\beta-\phi_{su}-\Theta)] \qquad 3B13$$

Rearranging Equations 3B12 and 3B13 yield:

$$\begin{aligned} i_{1(t)} \cdot i'_{2(t)}=& w_o \cdot I_o^2 \cdot \sin(w_o t-\phi_o) \cdot \cos(w_o t-\phi_o-\Theta) \\ &+ w_{su} \cdot I_{su} \cdot I_o \cdot \sin(w_o t-\phi_o) \cdot \cos(w_{su} t+\beta-\phi_{su}-\Theta) \\ &+ w_o \cdot I_{su} \cdot I_o \cdot \sin(w_o t+\Theta-\phi_{su}) \cdot \cos(w_o t-\phi_o-\Theta) \\ &+ w_{su} \cdot I_{su}^2 \cdot \sin(w_{su} t+\beta-\phi_{su}) \cdot \cos(w_{su} t+\beta-\phi_{su}-\Theta) \end{aligned} \qquad 3B14$$

$$\begin{aligned} i'_{1(t)} \cdot i_{2(t)}=& w_o \cdot I_o^2 \cdot \cos(w_o t-\phi_o) \cdot \sin(w_o t-\phi_o-\Theta) \\ &+ w_o \cdot I_o \cdot I_{su} \cdot \cos(w_o t-\phi_o) \cdot \sin(w_{su} t+\beta-\phi_{su}-\Theta) \\ &+ w_{su} \cdot I_o \cdot I_{su} \cdot \cos(w_{su} t+\beta-\phi_{su}) \cdot \sin(w_o t-\phi_o-\Theta) \\ &+ w_{su} \cdot I_{su}^2 \cdot \cos(w_{su} t+\beta-\phi_{su}) \cdot \sin(w_{su} t+\beta-\phi_{su}-\Theta) \end{aligned} \qquad 3B15$$

Equation 3B14 and 3B15 can be expressed as:

$$i_{1(t)} \cdot i'_{2(t)} = \frac{w_o \cdot I_o^2}{2}[\sin(\Theta)+\sin(2w_o t-2\phi_o-\Theta)]$$

$$+ \frac{w_{su} \cdot I_{su} \cdot I_o}{2}\{\sin[(w_o-w_{su})t-\beta-(\phi_o-\phi_{su})+\Theta]$$

$$+ \sin[(w_o+w_{su})t+\beta-(\phi_o+\phi_{su})-\Theta]\}$$

$$+ \frac{w_o \cdot I_{su} \cdot I_o}{2}\{-\sin[(w_o-w_{su})t-\beta-(\phi_o-\phi_{su})-\Theta]$$

$$+ \sin[(w_o+w_{su})t+\beta-(\phi_o+\phi_{su})-\Theta]\}$$

$$+ \frac{w_{su} \cdot I_{su}^2}{2}[\sin(\Theta)+\sin(2w_{su}t+2\beta-2\phi_{su}-\Theta)] \qquad 3B16$$

$$i'_{1(t)} \cdot i_{2(t)} = \frac{w_o \cdot I_o^2}{2}[-\sin(\Theta)+\sin(2w_o t-2\phi_o-\Theta)]$$

$$+ \frac{w_{su} \cdot I_{su} \cdot I_o}{2}\{\sin[(w_o-w_{su})t-\beta-(\phi_o-\phi_{su})-\Theta]$$

$$+ \sin[(w_o+w_{su})t+\beta-(\phi_o+\phi_{su})-\Theta]\}$$

$$+ \frac{w_o \cdot I_{su} \cdot I_o}{2}\{-\sin[(w_o-w_{su})t-\beta-(\phi_o-\phi_{su})+\Theta]$$

$$+ \sin[(w_o+w_{su})t+\beta-(\phi_o+\phi_{su})-\Theta]\}$$

$$+ \frac{w_{su} \cdot I_{su}^2}{2}[-\sin(\Theta)+\sin(2w_{su}t+2\beta-2\phi_{su}-\Theta)] \qquad 3B17$$

Note that there are four frequency components in $i_{1(t)} \cdot i'_{2(t)}$ and $i'_{1(t)} \cdot i_{2(t)}$ which are given by, $2w_o$, $2w_{su}$, w_o-w_{su} and w_o+w_{su}. The determinant term D, is given by Equation 3B7. Thus:

$$D = i_{1(t)} \cdot i'_{2(t)} - i'_{1(t)} \cdot i_{2(t)}$$

$$D = w_o \cdot I_o^2 \cdot \sin(\Theta) + w_{su} \cdot I_{su}^2 \cdot \sin(\Theta)$$

$$+ \frac{w_{su} \cdot I_o \cdot I_{su}}{2}\{\sin[(w_o-w_{su})t-\beta-(\phi_o-\phi_{su})+\Theta]$$

$$- \sin[(w_o-w_{su})t-\beta-(\phi_o-\phi_{su})-\Theta]\}$$

$$- \frac{w_o \cdot I_{su} \cdot I_o}{2}\{\sin[(w_o-w_{su})t-\beta-(\phi_o-\phi_{su})-\Theta] - \sin[(w_o-w_{su})t-\beta-(\phi_o-\phi_{su})+\Theta]\} \quad 3B18$$

Note that frequency components of $2w_o$, $2w_{su}$ and w_o+w_{su} have been eliminated from the D term. Expanding and taking sin(Θ) common Equation 3B18 can be expressed as:

$$D=\sin(\Theta)\cdot\{w_o\cdot I_o^2 + w_{su}\cdot I_{su}^2 + I_o\cdot I_{su}\cdot(w_o+w_{su})\cdot\cos[(w_o-w_{su})t-\beta-(\phi_o-\phi_{su})]\} \quad 3B19$$

It is evident from Equation 3B19 that, the D term oscillates about a dc level given by $w_o\cdot I_o^2 + w_{su}\cdot I_{su}^2$,with a frequency of w_o-w_{su}.

Measured R is given by Equation 3B8. Cross multiply D Equation 3B8 can be written as:

$$D\cdot R=v_{1(t)}\cdot i'_{2(t)} - v_{2(t)}\cdot i'_{1(t)} \quad 3B20$$

Substituting Equations 3B3 to 3B6 into Equation 3B20 gives:

$$v_{1(t)}\cdot i'_{2(t)}=[V_o\cdot\sin(w_ot) + V_{su}\cdot\sin(w_{su}t+\beta)]\cdot [w_o\cdot I_o\cdot\cos(w_ot-\phi_o-\Theta) + w_{su}\cdot I_{su}\cdot\cos(w_{su}t+\beta-\phi_{su}-\Theta)] \quad 3B21$$

and

$$v_{2(t)}\cdot i'_{1(t)}=[V_o\cdot\sin(w_ot-\Theta) + V_{su}\cdot\sin(w_{su}t+\beta-\Theta)]\cdot [w_o\cdot I_o\cdot\cos(w_ot-\phi_o) + w_{su}\cdot I_{su}\cdot\cos(w_{su}t+\beta-\phi_{su})] \quad 3B22$$

Equations 3B21 and 3B22 can be expanded and written in the following form:

$$v_{1(t)}\cdot i'_{2(t)}=w_o\cdot V_o\cdot I_o\cdot\sin(w_ot)\cdot\cos(w_ot-\phi_o-\Theta) + w_{su}\cdot V_o\cdot I_{su}\cdot\sin(w_ot)\cdot\cos(w_{su}t+\beta-\phi_{su}-\Theta) + w_o\cdot V_{su}\cdot I_o\cdot\sin(w_{su}t+\beta)\cdot\cos(w_ot-\phi_o-\Theta)$$

$$+ w_{su} \cdot V_{su} \cdot I_{su} \cdot \sin(w_{su}t+\beta) \cdot \cos(w_{su}t+\beta-\phi_{su}-\Theta) \quad 3B23$$

$$v_{2(t)} \cdot i'_{1(t)} = w_o \cdot V_o \cdot I_o \cdot \sin(w_o t-\Theta) \cdot \cos(w_o t-\phi_o)$$
$$+ w_{su} \cdot V_o \cdot I_{su} \cdot \sin(w_o t-\Theta) \cdot \cos(w_{su}t+\beta-\phi_{su})$$
$$+ w_o \cdot V_{su} \cdot I_o \cdot \sin(w_{su}t+\beta-\Theta) \cdot \cos(w_o t-\phi_o)$$
$$+ w_{su} \cdot V_{su} \cdot I_{su} \cdot \sin(w_{su}t+\beta-\Theta) \cdot \cos(w_{su}t+\beta-\phi_{su}) \quad 3B24$$

Equation 3B23 and 3B24 can be written in the form of Equation 3B25 and 3B26.

$$v_{1(t)} \cdot i'_{2(t)} = \frac{w_o \cdot V_o \cdot I_o}{2}[\sin(\phi_o+\Theta) + \sin(2w_o t-\phi_o-\Theta)]$$
$$+ \frac{w_{su} \cdot V_{su} \cdot I_{su}}{2}[\sin(\phi_{su}+\Theta) + \sin(2w_{su}t+2\beta-\phi_{su}-\Theta)]$$
$$+ \frac{w_{su} \cdot V_o \cdot I_{su}}{2}\{\sin[(w_o-w_{su})t-\beta+\phi_{su}+\Theta]$$
$$+ \sin[(w_o+w_{su})t+\beta-\phi_{su}-\Theta)]\}$$
$$+ \frac{w_o \cdot V_{su} \cdot I_o}{2}\{-\sin[(w_o-w_{su})t-\beta-\phi_o-\Theta]$$
$$+ \sin[(w_o+w_{su})t+\beta-\phi_o-\Theta)]\} \quad 3B25$$

$$v_{2(t)} \cdot i'_{1(t)} = \frac{w_o \cdot V_o \cdot I_o}{2}[\sin(\phi_o-\Theta) + \sin(2w_o t-\phi_o-\Theta)]$$
$$+ \frac{w_{su} \cdot V_{su} \cdot I_{su}}{2}[\sin(\phi_{su}-\Theta) + \sin(2w_{su}t+2\beta-\phi_{su}-\Theta)]$$
$$+ \frac{w_{su} \cdot V_o \cdot I_{su}}{2}\{\sin[(w_o-w_{su})t-\beta+\phi_{su}-\Theta]$$
$$+ \sin[(w_o+w_{su})t+\beta-\phi_{su}-\Theta)]\}$$
$$+ \frac{w_o \cdot V_{su} \cdot I_o}{2}\{-\sin[(w_o-w_{su})t-\beta-\phi_o+\Theta]$$
$$+ \sin[(w_o+w_{su})t+\beta-\phi_o-\Theta)]\} \quad 3B26$$

Note that there are four frequency components in $v_{1(t)} \cdot i'_{2(t)}$ and $v_{2(t)} \cdot i'_{1(t)}$ which are given by, $2w_o$,

$2w_{su}$, w_o-w_{su} and w_o+w_{su}. Using Equation 3B20, $D\cdot R$ is calculated. Thus:

$$D\cdot R=\frac{w_o\cdot V_o\cdot I_o}{2}[\sin(\phi_o+\Theta) - \sin(\phi_o-\Theta)]$$

$$+ \frac{w_{su}\cdot V_{su}\cdot I_{su}}{2}[\sin(\phi_{su}+\Theta) + \sin(\phi_{su}-\Theta)]$$

$$+ \frac{w_{su}\cdot V_o\cdot I_{su}}{2}\{\sin[(w_o-w_{su})t-\beta+\phi_{su}+\Theta] - \sin[(w_o-w_{su})t-\beta-\phi_{su}-\Theta)]\}$$

$$+ \frac{w_o\cdot V_{su}\cdot I_o}{2}\{-\sin[(w_o-w_{su})t-\beta-\phi_o-\Theta] + \sin[(w_o-w_{su})t-\beta-\phi_o+\Theta)]\} \quad 3B27$$

It is clear from Equation 3B27 that the ac components whose frequencies are given by $2w_o$, $2w_{su}$ and w_o+w_{su} are eliminated. Expanding Equation 3B27 and taking $\sin(\Theta)$ common yields:

$$D\cdot R=\sin(\Theta)\cdot\{w_o\cdot V_o\cdot I_o\cdot\cos(\phi_o) + w_{su}\cdot V_{su}\cdot I_{su}\cdot\cos(\phi_{su}) + [w_{su}\cdot V_o\cdot I_{su}\cdot\cos(\phi_{su}) + w_o\cdot V_{su}\cdot I_o\cdot\cos(\phi_o)]\cdot\cos[(w_o-w_{su})t-\beta)] + [w_o\cdot V_{su}\cdot I_o\cdot\sin(\phi_o) + w_{su}\cdot V_o\cdot I_{su}\cdot\sin(\phi_{su})]\cdot\sin[(w_o-w_{su})t-\beta)]\} \quad 3B28$$

Equation 3B28 can be expressed as:

$$D\cdot R=\sin(\Theta)\cdot\{w_o\cdot V_o\cdot I_o\cdot\cos(\phi_o)+w_{su}\cdot V_{su}\cdot I_{su}\cdot\cos(\phi_{su}) +(A_R^2+B_R^2)^{\frac{1}{2}}\cdot\sin[(w_o-w_{su})t-\beta+\tan^{-1}(A_R/B_R)]\} \quad 3B29$$

where:

$$A_R=w_{su}\cdot V_o\cdot I_{su}\cdot\cos(\phi_{su}) + w_o\cdot V_{su}\cdot I_o\cdot\cos(\phi_o) \quad 3B30$$

$$B_R=w_o\cdot V_{su}\cdot I_o\cdot\cos(\phi_o) + w_{su}\cdot V_o\cdot I_{su}\cdot\cos(\phi_{su}) \quad 3B31$$

It is evident from Equation 3B29 that the measured $D\cdot R$

consists of dc and ac components and frequency of the ac part is given by w_o-w_{su}.

Measured L' is given by Equation 3B9. Cross multiply D Equation 3B9 can be written as:

$$D \cdot L' = v_{2(t)} \cdot i_{1(t)} - v_{1(t)} \cdot i_{2(t)} \qquad 3B32$$

Substituting Equations 3B3 to 3B6 into Equation 3B32 gives:

$$v_{2(t)} \cdot i_{1(t)} = [V_o \cdot \sin(w_o t - \Theta) + V_{su} \cdot \sin(w_{su} t + \beta - \Theta)] \cdot [I_o \cdot \sin(w_o t - \phi_o) + I_{su} \cdot \sin(w_{su} t + \beta - \phi_{su})] \qquad 3B33$$

and

$$v_{1(t)} \cdot i_{2(t)} = [V_o \cdot \sin(w_o t) + V_{su} \cdot \sin(w_{su} t + \beta)] \cdot [I_o \cdot \sin(w_o t - \phi_o - \Theta) + I_{su} \cdot \sin(w_{su} t + \beta - \phi_{su} - \Theta)] \qquad 3B34$$

Equations 3B33 and 3B34 can be expanded and written in the following form:

$$\begin{aligned} v_{2(t)} \cdot i_{1(t)} = {} & V_o \cdot I_o \cdot \sin(w_o t - \Theta) \cdot \sin(w_o t - \phi_o) \\ & + V_o \cdot I_{su} \cdot \sin(w_o t - \Theta) \cdot \sin(w_{su} t + \beta - \phi_{su}) \\ & + V_{su} \cdot I_o \cdot \sin(w_{su} t + \beta - \Theta) \cdot \sin(w_o t - \phi_o) \\ & + V_{su} \cdot I_{su} \cdot \sin(w_{su} t + \beta - \Theta) \cdot \sin(w_{su} t + \beta - \phi_{su}) \end{aligned} \qquad 3B35$$

$$\begin{aligned} v_{1(t)} \cdot i_{2(t)} = {} & V_o \cdot I_o \cdot \sin(w_o t) \cdot \sin(w_o t - \phi_o - \Theta) \\ & + V_o \cdot I_{su} \cdot \sin(w_o t) \cdot \sin(w_{su} t + \beta - \phi_{su} - \Theta) \\ & + V_{su} \cdot I_o \cdot \sin(w_{su} t + \beta) \cdot \sin(w_o t - \phi_o - \Theta) \\ & + V_{su} \cdot I_{su} \cdot \sin(w_{su} t + \beta) \cdot \sin(w_{su} t + \beta - \phi_{su} - \Theta) \end{aligned} \qquad 3B36$$

Equation 3B35 and 3B36 can be written in the form of Equation 3B37 and 3B38.

$$v_{2(t)} \cdot i_{1(t)} = \frac{V_o \cdot I_o}{2}[\cos(\phi_o - \Theta) - \cos(2w_o t - \phi_o - \Theta)]$$

$$+ \frac{V_{su} \cdot I_{su}}{2}[\cos(\phi_{su} - \Theta) - \cos(2w_{su} t + 2\beta - \phi_{su} - \Theta)]$$

$$+ \frac{V_o \cdot I_{su}}{2}\{\cos[(w_o - w_{su})t - \beta + \phi_{su} - \Theta]$$

$$- \cos[(w_o + w_{su})t + \beta - \phi_{su} - \Theta)]\}$$

$$+ \frac{V_{su} \cdot I_o}{2}\{\cos[(w_o - w_{su})t - \beta - \phi_o + \Theta]$$

$$- \cos[(w_o + w_{su})t + \beta - \phi_o - \Theta)]\} \qquad 3B37$$

$$v_{1(t)} \cdot i_{2(t)} = \frac{V_o \cdot I_o}{2}[\cos(\phi_o + \Theta) - \cos(2w_o t - \phi_o - \Theta)]$$

$$+ \frac{V_{su} \cdot I_{su}}{2}[\cos(\phi_{su} + \Theta) - \cos(2w_{su} t + 2\beta - \phi_{su} - \Theta)]$$

$$+ \frac{V_o \cdot I_{su}}{2}\{\cos[(w_o - w_{su})t - \beta + \phi_{su} + \Theta]$$

$$- \cos[(w_o + w_{su})t + \beta - \phi_{su} - \Theta)]\}$$

$$+ \frac{V_{su} \cdot I_o}{2}\{\cos[(w_o - w_{su})t - \beta - \phi_o - \Theta]$$

$$- \cos[(w_o + w_{su})t + \beta - \phi_o - \Theta)]\} \qquad 3B38$$

Note that there are four frequency components in $v_{2(t)} \cdot i_{1(t)}$ and $v_{1(t)} \cdot i_{2(t)}$ which are given by, $2w_o$, $2w_{su}$, $w_o - w_{su}$ and $w_o + w_{su}$. Using Equation 3B32, $D \cdot L'$ is calculated. Thus:

$$D \cdot L' = \frac{V_o \cdot I_o}{2}[\cos(\phi_o - \Theta) - \cos(\phi_o + \Theta)]$$

$$+ \frac{V_{su} \cdot I_{su}}{2}[\cos(\phi_{su} - \Theta) - \cos(\phi_{su} + \Theta)]$$

$$+ \frac{V_o \cdot I_{su}}{2}\{\cos[(w_o - w_{su})t - \beta + \phi_{su} - \Theta]$$

$$- \cos[(w_o - w_{su})t - \beta + \phi_{su} + \Theta)]\}$$

$$+ \frac{V_{su} \cdot I_o}{2}\{\cos[(w_o-w_{su})t-\beta-\phi_o+\Theta] - \cos[(w_o-w_{su})t-\beta-\phi_o-\Theta)]\} \quad 3B39$$

It is clear from Equation 3B39 that the ac components with the frequencies of $2w_o$, $2w_{su}$ and w_o+w_{su} are eliminated. Expanding Equation 3B39 and taking sin(Θ) common yields:

$$\begin{aligned} D \cdot L' = \sin(\Theta) \cdot \{ & V_o \cdot I_o \cdot \sin(\phi_o) + V_{su} \cdot I_{su} \cdot \sin(\phi_{su}) \\ & + [V_o \cdot I_{su} \cdot \cos(\phi_{su}) - V_{su} \cdot I_o \cdot \cos(\phi_o)] \\ & \cdot \sin[(w_o-w_{su})t-\beta)] \\ & + [V_{su} \cdot I_o \cdot \sin(\phi_o) + V_o \cdot I_{su} \cdot \sin(\phi_{su})] \\ & \cdot \sin[(w_o-w_{su})t-\beta)]\} \end{aligned} \quad 3B40$$

Equation 3B40 can be expressed as:

$$\begin{aligned} D \cdot L' = \sin(\Theta) \cdot \{ & V_o \cdot I_o \cdot \sin(\phi_o) + V_{su} \cdot I_{su} \cdot \sin(\phi_{su}) \\ & + (A_X^2+B_X^2)^{\frac{1}{2}} \cdot \sin[(w_o-w_{su})t-\beta+\tan^{-1}(A_X/B_X)]\} \end{aligned} \quad 3B41$$

where:

$$A_X = V_o \cdot I_{su} \cdot \sin(\phi_{su}) + V_{su} \cdot I_o \cdot \sin(\phi_o) \quad 3B42$$

$$B_X = V_o \cdot I_{su} \cdot \cos(\phi_{su}) - V_{su} \cdot I_o \cdot \cos(\phi_o) \quad 3B43$$

It is evident from Equation 3B41 that the measured $D \cdot L'$ consists of dc and ac components and frequency of the ac part is given by w_o-w_{su}.

APPENDIX 3C

Consider a_n to be the approximation to the differential i'.

$$a_n = \frac{i_{(k+n)} - i_{(k-n)}}{2nh} \qquad 3C1$$

Using Taylor expansion formula yeilds:

$$i_{(k+n)} = i_{(k)} + nhi'(k) + \frac{(nh)^2}{2!} i''(k) + \frac{(nh)^3}{3!} i'''(k) + ... \qquad 3C2$$

$$i_{(k-n)} = i_{(k)} - nhi'(k) + \frac{(nh)^2}{2!} i''(k) - \frac{(nh)^3}{3!} i'''(k) + ... \qquad 3C3$$

Subtracting 3 from 2 and ignoring the higher order of h gives:

$$i_{(k+n)} - i_{(k-n)} = 2nhi'(k) + \frac{2(nh)^3}{3!} i'''(k) \qquad 3C4$$

Substituting 3C4 into 3C1 gives:

$$a_{(n)} = i'(k) + \frac{(nh)^2}{3!} i'''(k) \qquad 3C5$$

Using one point on each side of sample k gives:

$$a_1 = i'(k) + \frac{h^2}{3!} i'''(k) \qquad 3C6$$

Using four points on each side gives:

$$a_4 = i'(k) + \frac{16h^2}{3!} i'''(k) \qquad 3C7$$

It can be seen that the error term is proportional to h^2, and is 16 times bigger when 4 points on each side is used.

APPENDIX 4A:Line data

The line is horizontally constructed and discretely transposed. An earth plane resistivity of 100 Ω·m is assumed and due to the horizental construction, the material of the earth wires is alumoweld, which is known to be approximately 25 times more resistive than ACSR phase conductors. The following power frequency (50 Hz) parameters are then applicable:

Phase conductor resistance = 0.0339 Ω/km

Phase conductor reactance = 0.0078 Ω/km

Phase conductor radius = 9.05 cm
(Two conductors per phase)

Earth wire resistance = 1.882 Ω/km

Earth wire reactance = 0.388 Ω/km

Earth wire radius = 1.8 cm

The above parameters, together with the tower arrangements and earth plane effects, produce the following parameters:

Self impedance	Z_{LS}=	0.1223 + j0.5358	Ω/km
Mutual impedance	Z_{LM}=	0.0878 + j0.2268	Ω/km
Self admittance	Y_{LS}=	$j0.354 \cdot 10^{-5}$	Ω^{-1}/km
Mutual admittance	Y_{LM}=	$j0.298 \cdot 10^{-6}$	Ω^{-1}/km

The positive and zero phase sequence impedances and admittances of the line are calculated by:

$Z_{L1}=Z_{LS}-Z_{LM}$

Z_{L1}= 0.0345 + j0.309 Ω/km

Z_{L1}= 0.3109 $\angle$+83.629° Ω/km

and

$Z_{L0}=Z_{LS}+2Z_{LM}$

Z_{L0}= 0.2979 + j0.9894 Ω/km

$$Z_{L0} = 1.033 \angle +73.243^{\circ} \quad \Omega/km$$

$$Y_{L1} = Y_{LS} + Y_{LM} \quad \Omega/km$$

$$Y_{L1} = j0.384 \cdot 10^{-5} \quad \Omega^{-1}/km$$

$$Y_{L0} = j0.294 \cdot 10^{-5} \quad \Omega^{-1}/km$$

APPENDIX 5A

Figure 5A.1 shows the symmetrical component network connection for an "a"-phase-ground fault. During a phase fault to ground, for the source side VT the phase potential V_{sae} at the relay location consists of the following drops in the sequence networks:

$$V_{sae}=I_{s1}(\alpha Z_{L1}-jX_{c1}/2)+I_{s2}(\alpha Z_{L2}-jX_{c2}/2)+I_{s0}(\alpha Z_{L0}-jX_{c0}/2) \quad 5A.1$$

But $Z_{L1}=Z_{L2}$ for lines and $X_{c1}=X_{c2}=X_{c0}=X_c$ for the capacitor banks. Therefore:

$$V_{sae}=(I_{s1}+I_{s2})(\alpha Z_{L1}-jX_c/2)+I_{s0}(\alpha Z_{L0}-jX_c/2) \quad 5A.2$$

The phase current is given by:

$$I_{sa}=I_{s1}+I_{s2}+I_{s0} \quad 5A.3$$

rearranging 5A.3 gives:

$$I_{s1}+I_{s2}=I_{sa}-I_{s0} \quad 5A.4$$

Substituting 5A.4 into 5A.2 yields:

$$V_{sae}=(\alpha Z_{L1}-jX_c/2)I_{sa}+[(\alpha Z_{L0}-jX_c/2)-(\alpha Z_{L1}-jX_c/2)]I_{s0} \quad 5A.5$$

The residual current can be calculated from:

$$I_{res}=I_{sa}+I_{sb}+I_{sc}=3I_{s0} \quad 5A.6$$

Therefore equation 5A.5 can be written as:

$$V_{sae}=(\alpha Z_{L1}-jX_c/2)I_{sa}+ 1/3[(\alpha Z_{L0}-jX_c/2)-(\alpha Z_{L1}-jX_c/2)]I_{res} \quad 5A.7$$

or

$$V_{sae}=\alpha Z_{L1}I_{sa}-jX_c/2I_{sa}+1/3\left(\frac{Z_{L0}}{Z_{L1}}-1\right)\alpha Z_{L1}I_{res} \quad 5A.8$$

The impedance measured by the relay, when conventional

residual compensation is used, is thus given by:

$$Z = \frac{V_{sae}}{I_{sa}+K_c I_{res}} = \alpha Z_{L1} - j \left(\frac{I_{sa}}{I_{sa}+K_c I_{res}}\right) X_c/2 \qquad 5A.9$$

where:

$$K_c = 1/3\left(\left|\frac{Z_{L0}}{Z_{L1}}\right| - 1\right) = 1/3\left(\frac{Z_{L0}}{Z_{L1}} - 1\right)$$

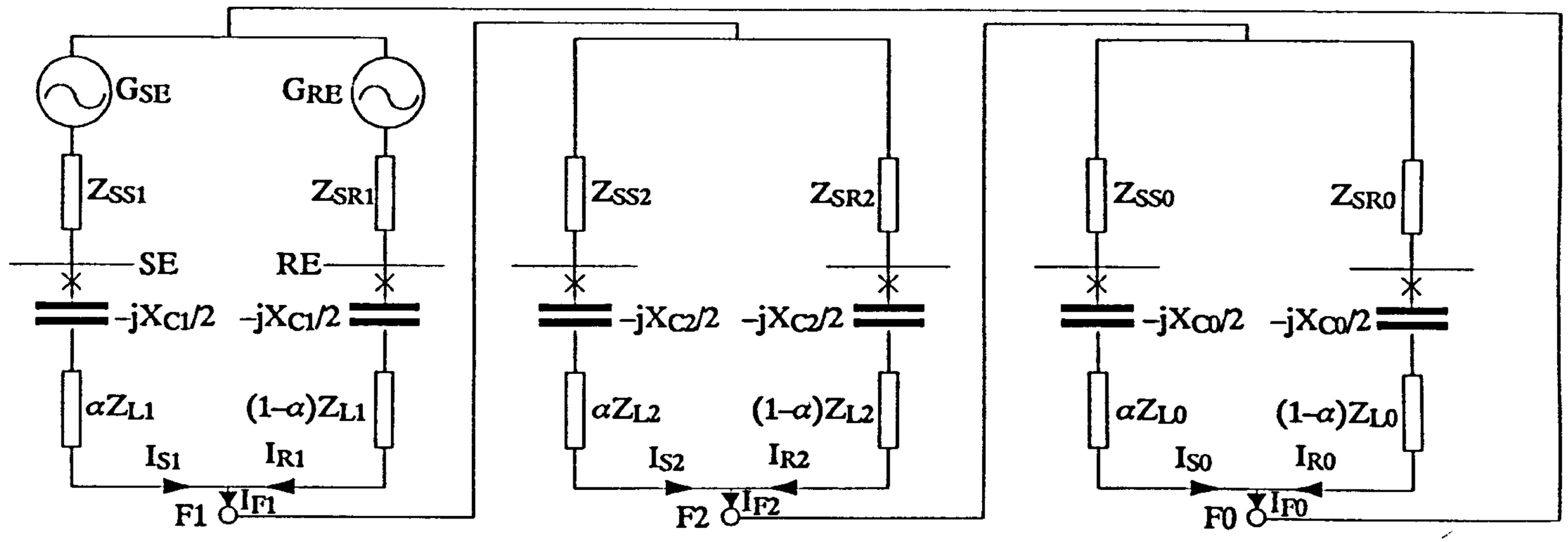

Fig 5A.1-Symmetrical Component Connection for "a"-Phase-Ground, with Source Side V.T.

APPENDIX 5B

Equation 5A.7 can be rewritten as:

$$V_{sae}=(\alpha Z_{L1}-jX_C/2)I_{sa}+ 1/3(\alpha Z_{L0} - \alpha Z_{L1})I_{res} \quad 5B.1$$

but the mutual impedance of the line is given by:

$$Z_{LM}=1/3(Z_{L0}-Z_{L1}) \quad 5B.2$$

Substituting Equations 5A.6 and 5B.2 into Equation 5B.1 gives:

$$V_{sae}=\alpha Z_{L1}I_{sa}-jX_C/2I_{sa}+\alpha Z_{LM}(I_{sa}+I_{sb}+I_{sc}) \quad 5B.3$$

or

$$V_{sae}=\alpha Z_{L1}I_{sa}-jX_C/2I_{sa}+\alpha Z_{LM}I_{sa}+\alpha Z_{LM}(I_{sb}+I_{sc}) \quad 5B.4$$

Equation 5B.4 can be written as:

$$V_{sae}=\alpha\ (Z_{L1}+Z_{LM})I_{sa}-jX_C/2I_{sa}+\alpha Z_{LM}(I_{sb}+I_{sc}) \quad 5B.5$$

but $Z_{L1}+Z_{LM}$ is equal to the self impedance of the line.

$$Z_{LS}=Z_{L1}+Z_{LM} \quad 5B.6$$

Substituting Equation 5B.6 into Equation 5B.5 gives:

$$V_{sae}=\alpha\ Z_{LS}I_{sa}-jX_C/2I_{sa}+\alpha Z_{LM}(I_{sb}+I_{sc}) \quad 5B.7$$

Equation 5B.7 can be written as:

$$V_{sae}=\alpha\ Z_{LS}[I_{sa}+\frac{\alpha Z_{LM}}{\alpha Z_{LS}}(I_{sb}+I_{sc})]-jI_{sa}X_C/2 \quad 5B.8$$

The measured impedance by the relay is given by:

$$Z=\frac{V_{sae}}{I_{sa}+K_s(I_{sb}+I_{sc})}=\alpha\ Z_{LS} - j\ \frac{I_{sa}}{I_{sa}+K_s(I_{sb}+I_{sc})}\ X_C/2 \quad 5B.9$$

where:
$$K_s=\frac{\alpha Z_{LM}}{\alpha Z_{LS}} = \frac{Z_{LM}}{Z_{LS}} \quad 5B.10$$

APPENDIX 5C

Equation 5A.7 can be rewritten as:

$$V_{sae}=(\alpha Z_{L1}-jX_C/2)I_{sa}+1/3\left(\frac{\alpha Z_{L0}-jX_C/2}{\alpha Z_{L1}-jX_C/2}-1\right)\cdot(\alpha Z_{L1}-jX_C/2)I_{res} \qquad 5C.1$$

or

$$V_{sae}=(I_{sa}+K_{(\alpha)}I_{res})(\alpha Z_{L1}-jX_C/2) \qquad 5C.2$$

where:

$$K_{(\alpha)}=1/3\left(\frac{\alpha Z_{L0}-jX_C/2}{\alpha Z_{L1}-jX_C/2}-1\right) \qquad 5C.3$$

Thus:

$$Z=\frac{V_{sae}}{I_{sa}+K_{(\alpha)}I_{res}}=\alpha Z_{L1}-jX_C/2 \qquad 5C.4$$

APPENDIX 5D

The voltage at the relaying point is given by equation 5C.2. Using the new method of residual compensation, the measured impedance for any fault along the line is given by:

$$Z = \frac{V_{sae}}{I_{sa}+K_{\alpha r}I_{res}} \qquad 5D.1$$

where:

$$K_{\alpha r}=1/3\left(\frac{\alpha r Z_{L0}- jX_C/2}{\alpha r Z_{L1}- jX_C/2} -1\right) \qquad 5D.2$$

αr=proportional fault position for a fault at the zone-1 reach point. Note that αr is constant (relay forward reach).

Substituting equation 5C.2 into equation 5D.1 gives:

$$Z=\frac{I_{sa}+K_{(\alpha)}I_{res}}{I_{sa}+K_{\alpha r}I_{res}} (\alpha Z_{L1}- jX_C/2) \qquad 5D.3$$

APPENDIX 5E

Figure 5E.1 shows the symmetrical component network connection for an "a"-phase-ground fault. During a phase fault to ground, for the line side VT the phase potential V_{sae} at the relay location consists of the following drops in the sequence networks:

$$V_{sae}=I_{s1}(\alpha Z_{L1})+I_{s2}(\alpha Z_{L2})+I_{s0}(\alpha Z_{L0}) \qquad 5E.1$$

but $Z_{L1}=Z_{L2}$ for lines Therefore:

$$V_{sae}=(I_{s1}+I_{s2})(\alpha Z_{L1})+I_{s0}(\alpha Z_{L0}) \qquad 5E.2$$

The phase current is given by:

$$I_{sa}=I_{s1}+I_{s2}+I_{s0} \qquad 5E.3$$

rearranging 5E.3 gives:

$$I_{s1}+I_{s2}=I_{sa}-I_{s0} \qquad 5E.4$$

Substituting 5E.4 into 5E.2 yields:

$$V_{sae}=(\alpha Z_{L1})I_{sa}+(\alpha Z_{L0}-\alpha Z_{L1})I_{s0} \qquad 5E.5$$

The residual current can be calculated from:

$$I_{res}=I_{sa}+I_{sb}+I_{sc}=3I_{s0} \qquad 5E.6$$

Therefore equation 5E.5 can be written as:

$$V_{sae}=(\alpha Z_{L1})I_{sa}+ 1/3(\alpha Z_{L0}-\alpha Z_{L1})I_{res} \qquad 5E.7$$

or

$$V_{sae}=\alpha Z_{L1}I_{sa}+1/3(\frac{Z_{L0}}{Z_{L1}} -1)\alpha Z_{L1}I_{res} \qquad 5E.8$$

The impedance measured by the relay, when the conventional residual compensation is used, is thus given

by:

$$Z = \frac{V_{sae}}{I_{sa}+K_C I_{res}} = \alpha Z_{L1} \qquad 5E.9$$

where:

$$K_C = 1/3\left(\frac{Z_{L0}}{Z_{L1}} - 1\right) \qquad 5E.10$$

PUBLISHED PAPERS

IEEE POWER ENGINEERING SOCIETY SUMMER MEETING

JULY 1989, LONG BEACH, USA

PAPER No 89SM 725-3 PWRD

INVESTIGATION OF ALTERNATIVE RESIDUAL CURRENT COMPENSATION FOR IMPROVING SERIES COMPENSATED LINE DISTANCE PROTECTION

F.GHASSEMI A.T.JOHNS Senior Member

The City University
London - UK

ABSTRACT

In this paper the results of investigations into methods of improving the measuring accuracy of distance protection applied to series compensated lines is given. It is shown that in order to compensate the error in impedance measurement under earth-fault conditions, an alternative to conventional residual current compensation must be used. The effect of load and source impedances on the measurands, when the conventional and alternative compensation factors are used, is given.

INTRODUCTION

Series capacitors have become an important component in economical long distance power transmission[1,2]. The economical location for any capacitor bank is generally in the vicinity of the line end and hence it may represent a part of the terminal substation. This paper concentrates on a transmission system with compensation at each end.

The series capacitors and their over-voltage protection introduce fairly well known difficulties in protecting series compensated lines. This is particularly so when distance schemes are applied[3,4]. It is known that, there are system conditions that do not result in capacitor protection gear operation after the occurrance of a fault[5]. Also with the new generation of Ultra-High-Speed protection, the fault may be cleared in considerably less than one cycle which can in turn be much shorter than capacitor gap flash-over times[6]. Therefore it is highly desirable that distance protection schemes perform the impedance measurements with the highest degree of accuracy with capacitor banks in circuit.

One of the problems which arises, when capacitors are in the circuit, is the effect of the residual compensation on the accuracy of the distance relay when an earth fault occurs. The authors reported some preliminary investigation into this effect in reference 7. In this paper, a more detailed investigation is presented and a proposed solution is given.

RESIDUAL CURRENT COMPENSATION TECHNIQUES

Consider the system shown in Figure 1 with typical series compensation of 70%. Line data is given in Appendix A.

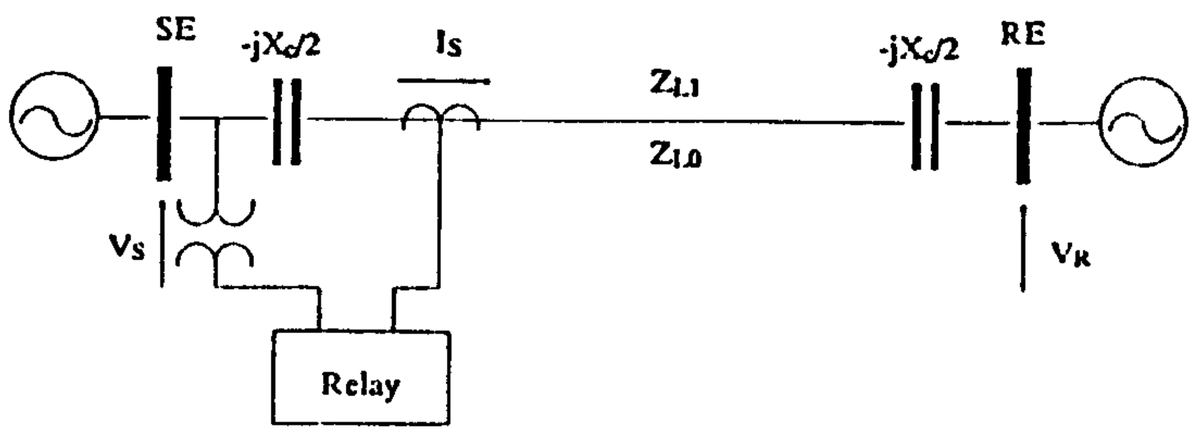

FIG 1 SYSTEM CONFIGURATION

It is well known that in distance protection, for phase to ground faults, compensation methods are used to allow the relay to measure the positive phase sequence (pps) impedance of the line from the relaying to fault point[8]. The most commonly used method employs residual current compensation, where a fraction of the residual current is added to the phase currents. It is shown in Appendix B that if the conventional residual compensation factor (CRCF) is used, the impedance seen by the distance relay is given by:

$$Z_r = \frac{V_{sae}}{I_{sa}+K_c I_{res}} \approx \alpha Z_{L1} - j\left(\frac{I_{sa}}{I_{sa}+K_c I_{res}}\right)X_c/2 \qquad (1)$$

where:

Z_r=measured impedance
V_{sae}=phase voltage at the relaying point
I_{sa}=faulted phase current at the relaying point
I_{res}=residual current
Z_{L1}=total pps impedance of line
X_c=total capacitor reactance/phase
α=proportional fault position
K_c=conventional residual compensation factor

$$= \frac{1}{3}\left(\left|\frac{Z_{L0}}{Z_{L1}}\right| - 1\right) \qquad (2)$$

From equation (1) it is clear that the impedance measured depends on and varies with the value of $I_{sa}/(I_{sa}+K_c I_{res})$. Figs 2.a and 2.b illustrate the variation in magnitude and argument of the ratio $I_{sa}/(I_{sa}+K_c I_{res})$ for different source capacities and pre-fault load. In the case where the source capacities at the line ends are equal(10 GVA symmetrical short-circuit level) and the system is pre-fault unloaded the ratio stays approximately at a constant value, for fault positions of up to 80%. However, note the large variation in the current ratio for situations where the

local source is much weaker than that at the remote end or when the system is loaded. This implies that the relay will measure different impedances for different source and load situations.

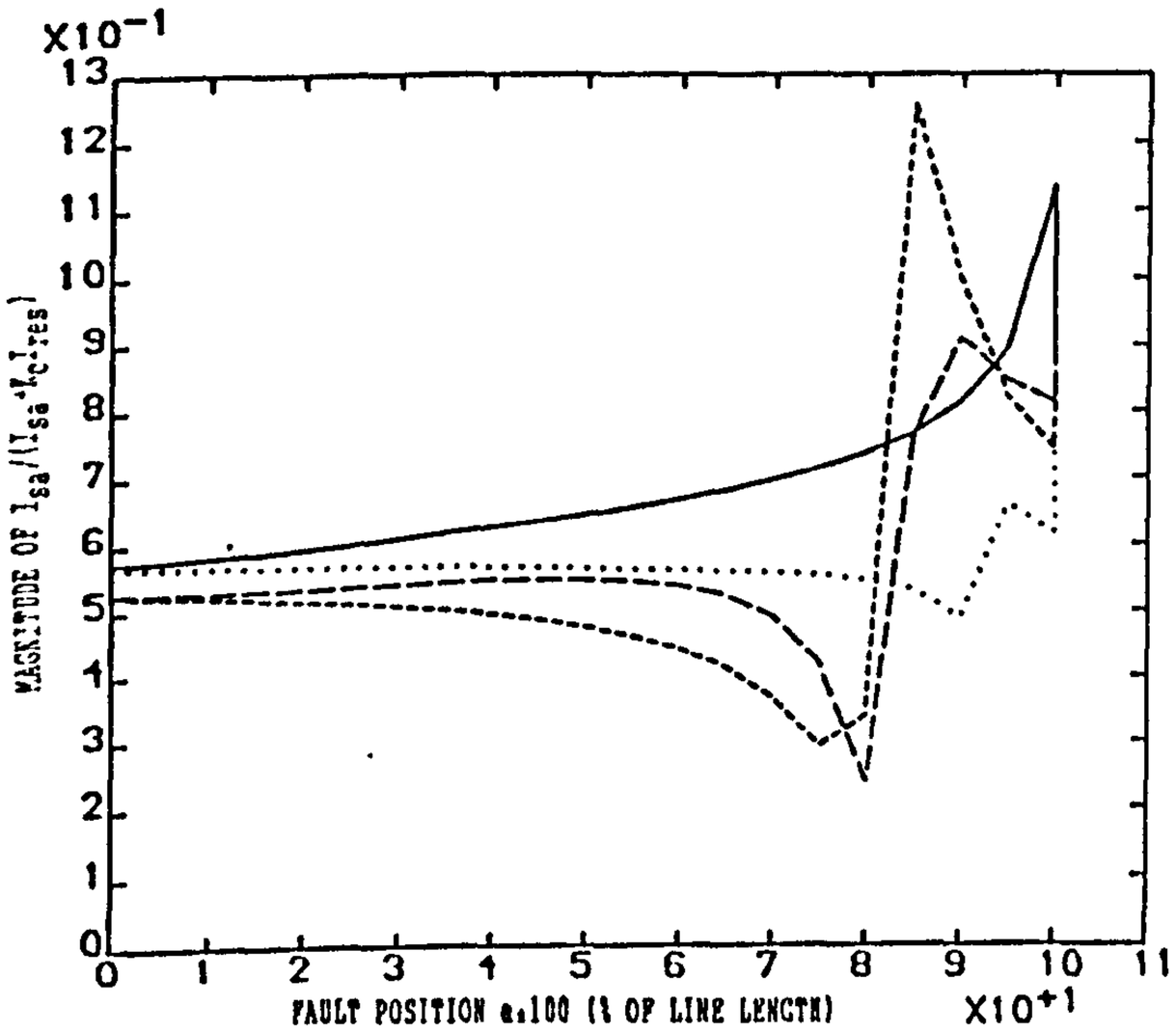

FIG 2.a VARIATION IN $|I_{sa}/(I_{sa}+K_c I_{res})|$ WITH FAULT POSITION

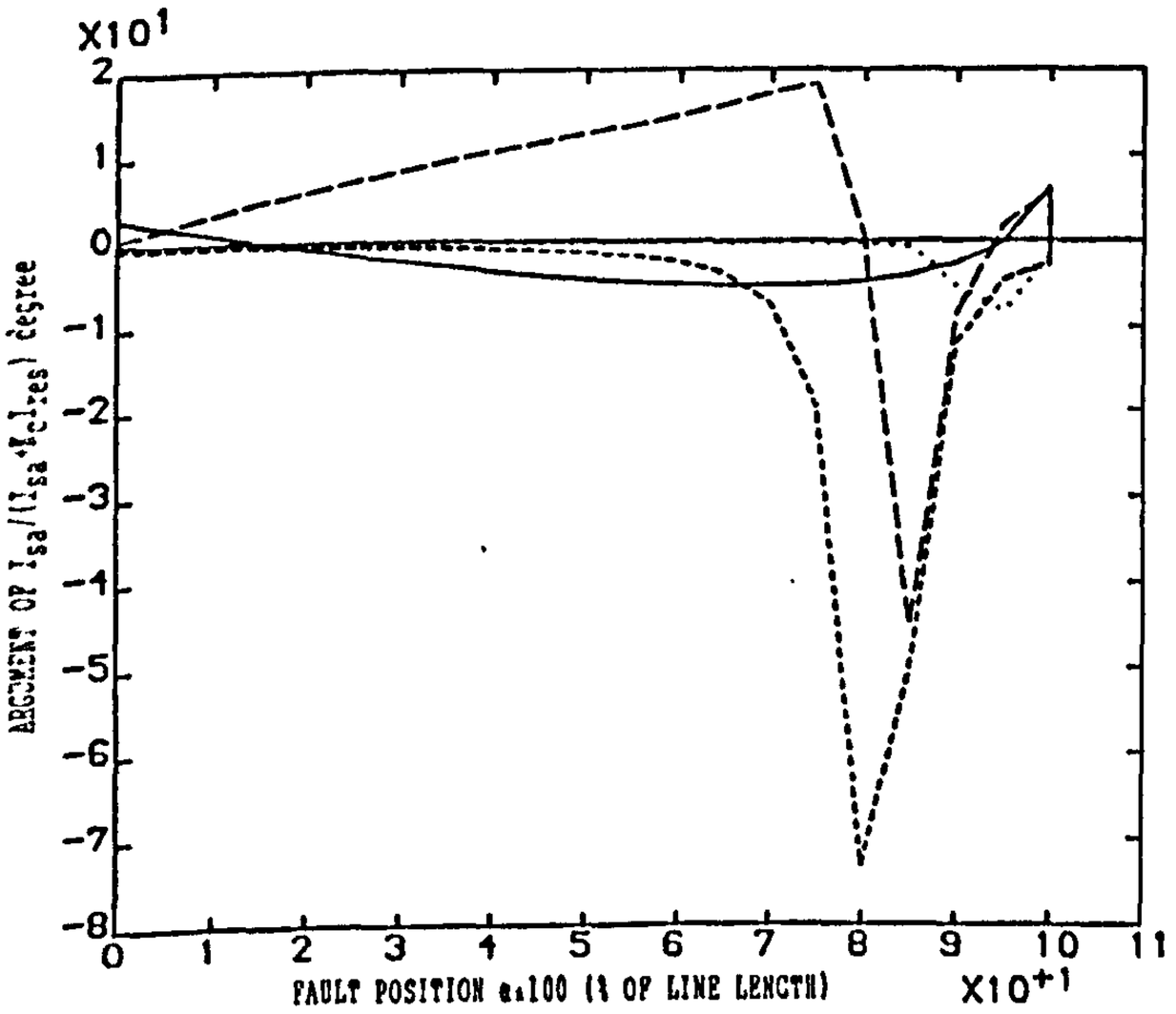

FIG 2.b VARIATION IN $\angle I_{sa}/(I_{sa}+K_c I_{res})$ WITH FAULT POSITION

——— SE SCL=35 GVA, RE SCL=5 GVA, LOAD ANG=-10 deg
..... SE SCL=10 GVA, RE SCL=10 GVA, LOAD ANG=0 deg
– – – – SE SCL=5 GVA, RE SCL=35 GVA, LOAD ANG=+10 deg
..... SE SCL=5 GVA, RE SCL=35 GVA, LOAD ANG=0 deg

In order to ensure that the relay measures the equivalent pps impedance of the line from the relay to fault point(for relay setting purposes) it is shown in Appendix C that the residual compensation factor must be set according to the proportional fault position α. The measured impedance is then given by:

$$Z_r = \frac{V_{sae}}{I_{sa}+K(\alpha)I_{res}} = \alpha Z_{L1} - j\ X_c/2 \qquad (3)$$

where: $$K_{(\alpha)} = \frac{1}{3}\left(\frac{\alpha Z_{L0} - j\ X_c/2}{\alpha Z_{L1} - j\ X_c/2} - 1\right) \qquad (4)$$

This means that only if the fault position is known to the relay will the measured value of impedance be independant of source and load current.

Figures 3.a and 3.b show the variation in magnitude and argument of $K_{(\alpha)}$ versus fault location for the line under study. It must, however, be noted that for a given fault location and degree of series compensation the residual compensation factor is the same as that shown irrespective of the actual line length.

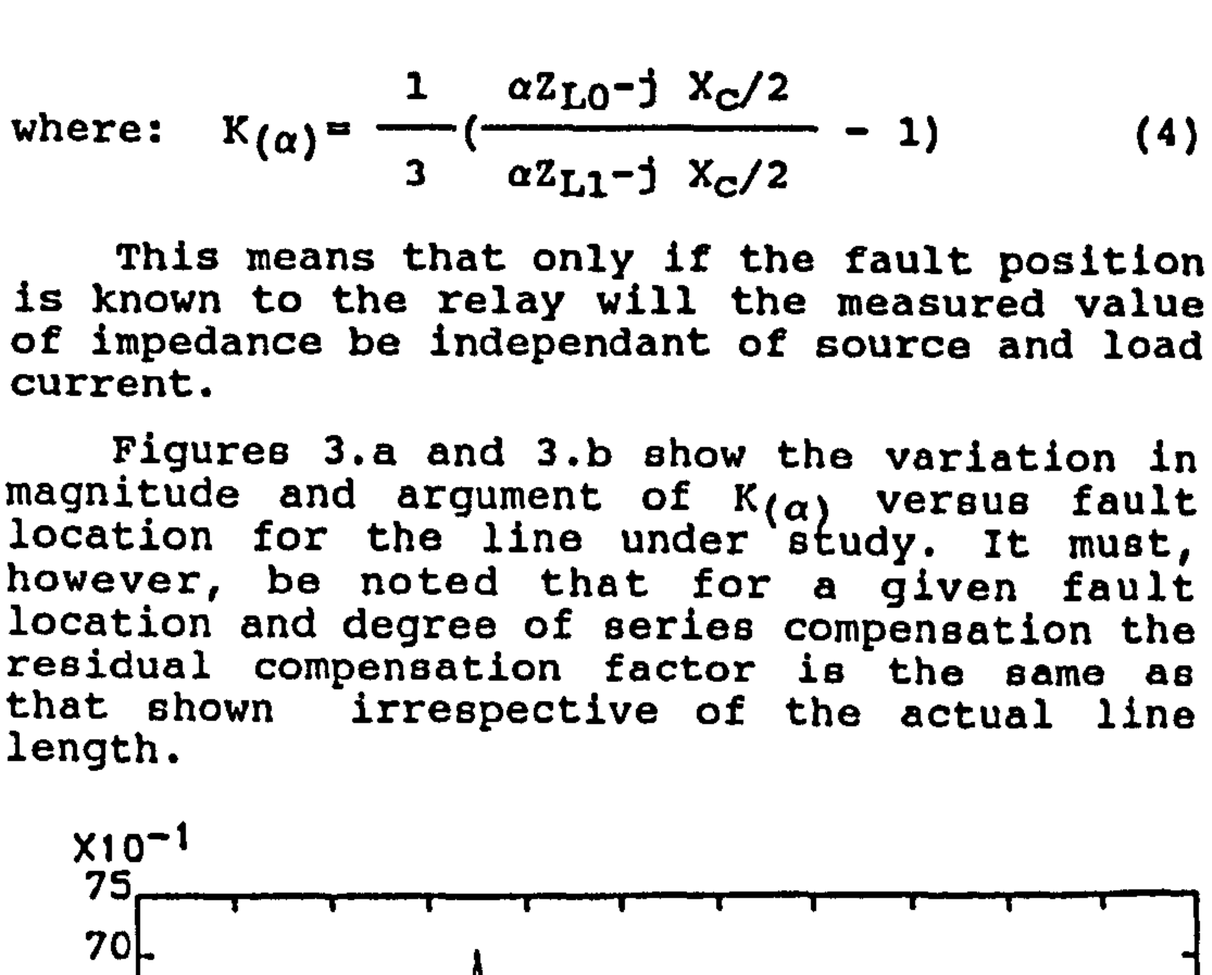

FIG 3.a VARIATION OF $|K_{(\alpha)}|$ WITH FAULT POSITION

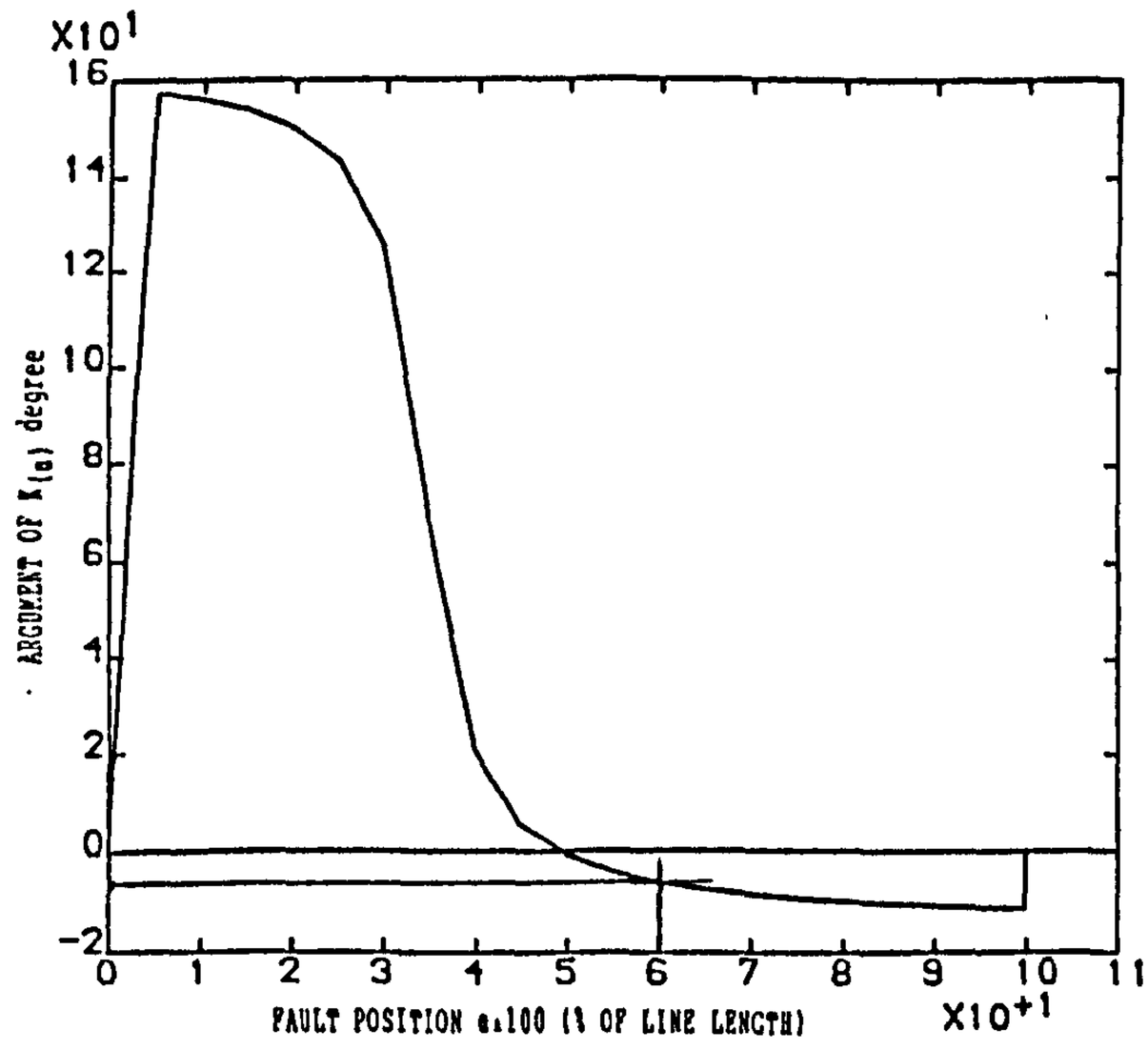

FIG 3.b VARIATION OF $\angle K_{(\alpha)}$ WITH FAULT POSITION

Modified Residual Compensation For Series Compensated Lines

Because the fault position is unknown, it is not possible to set the residual compensation factor according to the fault position, it is proposed that the residual compensation factor is set at a fixed value $K_{(\alpha r)}$, assuming the fault position to be at the relay zone-1 reach boundary. Appendix D shows that the impedance seen by the relay is then given by:

$$Z_r = \frac{I_{sa}+K_{(\alpha)}I_{res}}{I_{sa}+K_{(\alpha r)}I_{res}}(\alpha Z_{L1} - jX_C/2) \qquad (5)$$

$$\text{where: } K_{(\alpha r)} = \frac{1}{3}\left(\frac{\alpha r Z_{L0} - jX_C/2}{\alpha r Z_{L1} - jX_C/2} - 1\right) \qquad (6)$$

αr=proportional fault position for fault at the relay zone-1 reach point.

Figures 4.a and 4.b illustrate the variation in the expression $(I_{sa}+K_{(\alpha)}I_{res})/(I_{sa}+K_{(\alpha r)}I_{res})$ with fault position for an assumed zone-1 forward reach of 60% (αr=0.6) and different source and load situations. It is revealed that, at the forward reach, the expression has a magnitude of unity and angle of zero for all situations considered. With reference to equation 5, this means that the relay measures a unique and constant impedance for a fault at the zone-1 boundary (60% for the reach assumed).

It is evident from Figures 4.a, b that the source impedance affects the measurement of the fault location; this is primarily due to the fact that the residual current distribution is affected to a small degree by the remote source impedance.

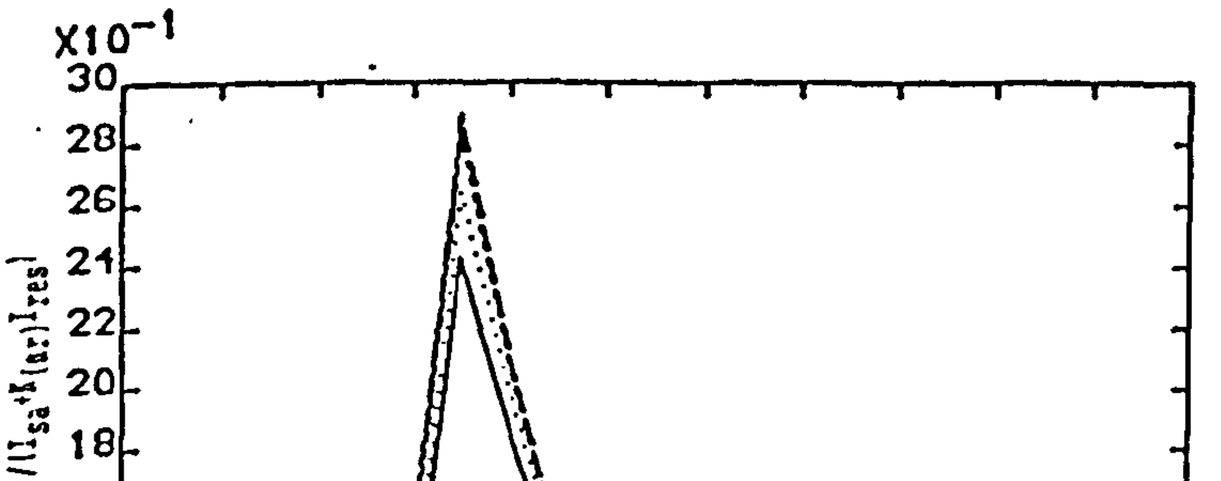

FIG 4.a VARIATION OF $|(I_{sa}+K_{(\alpha)}I_{res})/(I_{sa}+K_{(\alpha r)}I_{res})|$ WITH FAULT POSITION

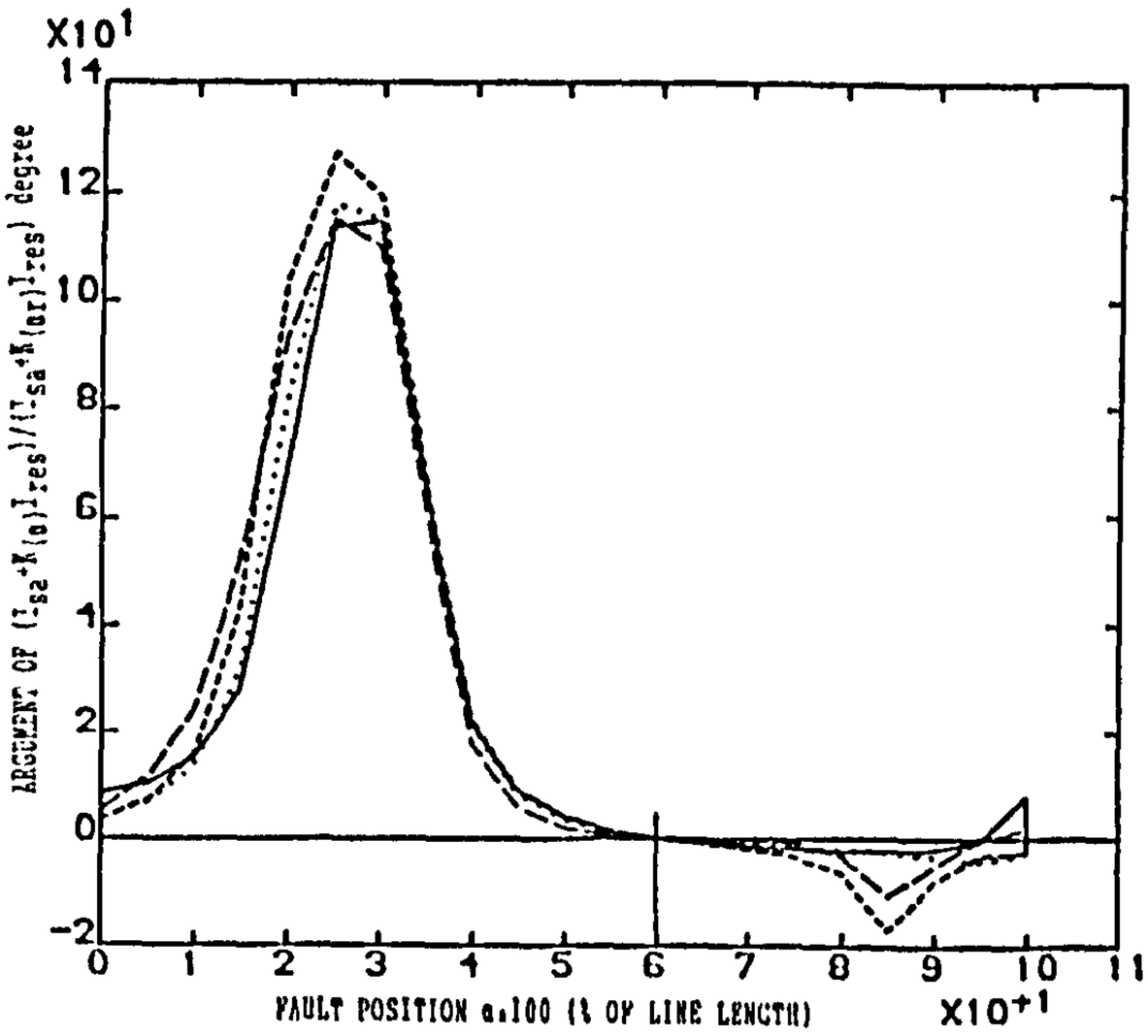

FIG 4.b VARIATION OF $\angle(I_{sa}+K_{(\alpha)}I_{res})/(I_{sa}+K_{(\alpha r)}I_{res})$ WITH FAULT POSITION

IMPLEMENTATION IN DIGITAL DISTANCE RELAYS

A large number of papers have described and investigated the performance of digital distance relays of which those given in reference 9, 10 and 11 are typical. These are particularly suited to the implementation of a complex, rather than real, modified residual current compensation factor of the type proposed in the previous section. Since samples of the residual current are available at discrete instants of time $\Delta T=1/f_s$ (where f_s is the digital sampling frequency) it is possible to effectively implement the phase shift associated with the modified residual compensating factor $\angle K_{(\alpha r)}$ by taking a sample n samples previous to any measuring sample instant. For example, it can be seen from Fig 3 that, for a relay set with a forward reach of 60%, which in turn eliminates the possibily of indiscrimination for faults beyond the remote capacitor, the modified compensating factor $K_{(\alpha r)}$ is equal to approximately $1.82\angle -6.2°$. Thus, in a digital relay operating at a sampling frequency say 4 kHz, on a power system having a nominal frequency of 60 Hz, one sample interval corresponds to a phase shift of approximately -5.4°. A constraint is thus imposed on choosing the value of n which, for the assumed sampling frequency (4kHz) and application illustrated, is equal to unity. For any particular relay and application, the value of n that gives the closest equivalent phase shift to the ideal value ($\angle K_{(\alpha r)}$) is used.

It will be evident from Fig 3.b that for all zone-1 setting above about 50% the argument of the modified residual compensation factor is small and it has been found that little error occurs if $K_{(\alpha r)}$ is assumed real. Since in most practical application the zone-1 reach exceeds 50% the need to implement an

effective phase-shift by the means described is often obviated. In the results that follow, which relate to an application with a nominal zone-1 reach setting of 60%, the value $K_{(\alpha r)}$ has thus been taken as real ($K_{(\alpha r)}=1.82\angle 0.0^{\circ}$).

EVALUATION OF IMPROVEMENT IN ACCURACY

A good illustration of the improvement in accuracy made possible by implementing the modified residual compensating factor developed can be obtained by considering a system with 5 GVA and 35 GVA symmetrical short-circuit level sources at the sending and receiving ends respectively. In all cases, the line is subjected to a single-phase to ground fault. The prefault load angle is defined by the argument of the ratio V_S/V_R (see Figure 1) so that a positive value of $\angle V_S/V_R$ is associated with pre-fault load exporting from the relay location and a negative value prefault load importing.

Figures 5.a and 5.b show the measured resistance and reactance versus load angle for different fault positions when the conventional residual compensation factor (CRCF) (given in equation 2) is used. The change in measured impedance for different load angles is clearly evident. The resistance measurement in particular is more affected by the load current than is the reactance. When Quadrilateral Distance relay characteristics are used, the variation of measured reactance, particularly for faults near the boundary of the zone-1 reach can be particularly troublesome because errors of measurement with pre-fault load can cause either overreaching or underreaching. Figures 6.a and 6.b, show the corresponding performance when the new modified residual compensation factor (NRCF) is used. In this case , the measurements at the boundary (60%) are unaffected by the pre-fault load. Furthermore variations in reactance measurements with load for other fault positions, especially those near the boundary, are minimal. This in turn enables measuring accuracy to be maximised and avoids both overreaching and underreaching in Quadrilateral relay applications.

Figures 7 and 8 illustrate the variation with fault position of the resistance and reactance measured for different load angles when CRCF and NRCF are used respectively. The pps resistance and reactance of the fault loop are also shown. Again the effect of NRCF on the measurement is clear. In particular, note the constant and load invariant measurement at the boundary (60%) for different load currents when NRCF is used. Note also that, when CRCF is used, a relay with a Quadrilateral characteristic will significantly underreach if the reactance reach is set at a value corresponding to the fault loop reactance for a fault at the zone-1 reach boundary. It is also evident from Fig 7.b in particular that some variation in measurement accuracy (and hence relay reach) occurs with pre-fault cicuit loading.

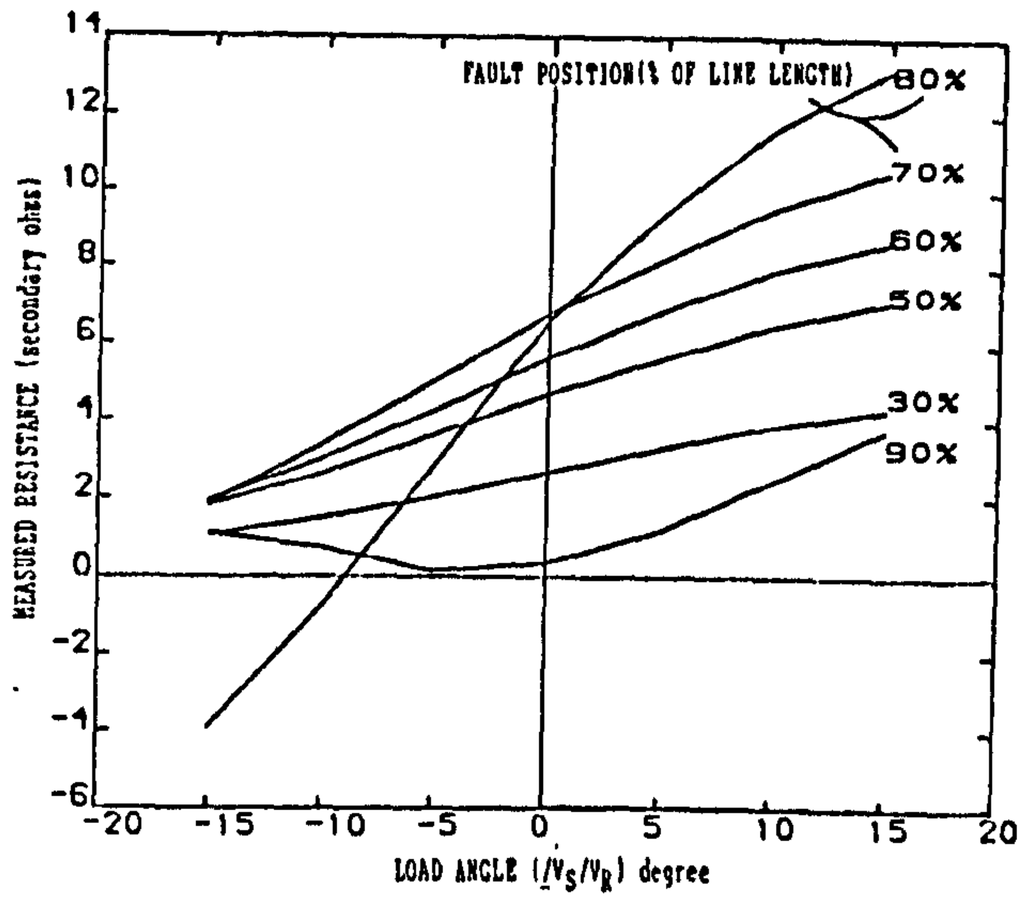

FIG 5.a VARIATION OF MEASURED RESISTANCE WITH PRE-FAULT LOAD ANGLE WITH CRCF

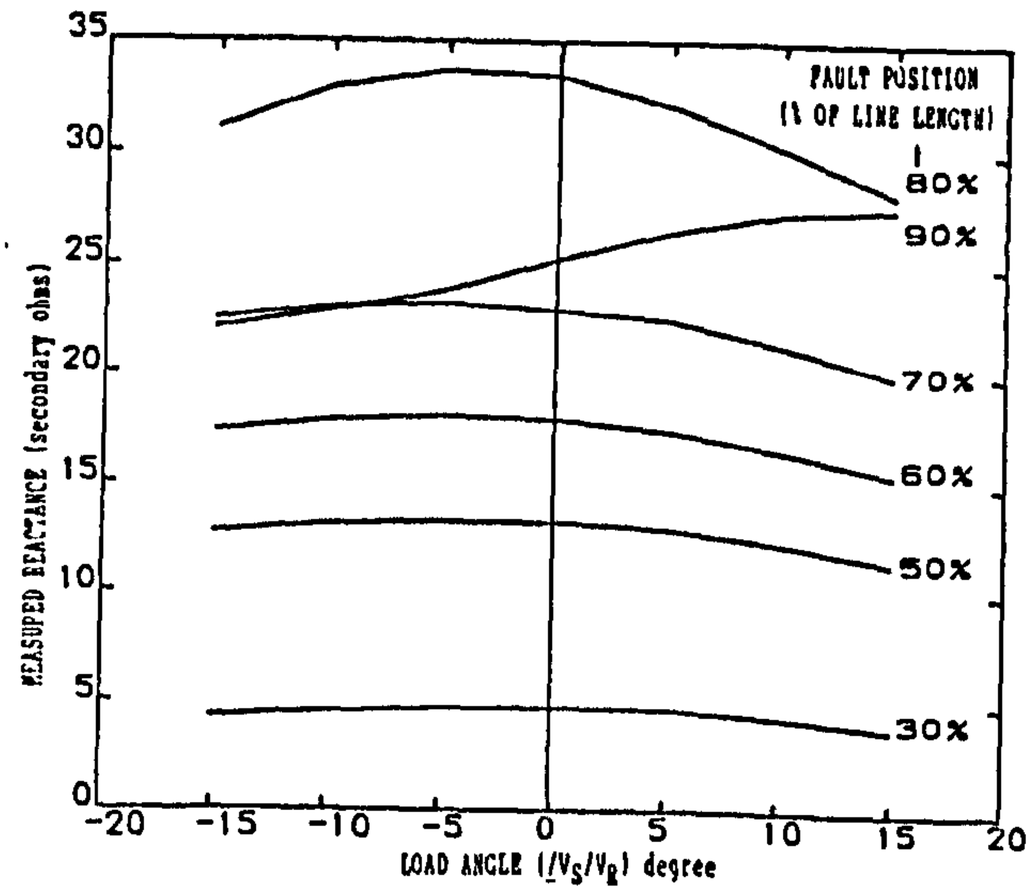

FIG 5.b VARIATION OF MEASURED REACTANCE WITH PRE-FAULT LOAD ANGLE WITH CRCF

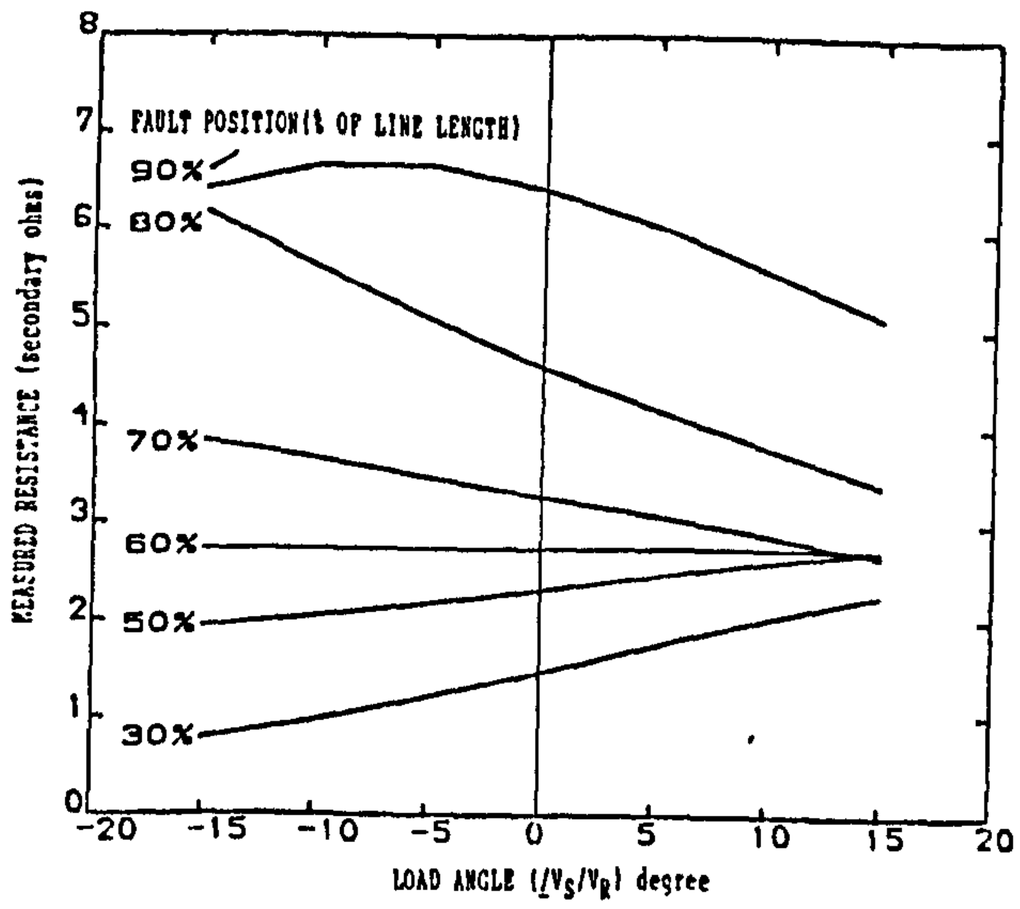

FIG 6.a VARIATION OF MEASURED RESISTANCE WITH PRE-FAULT LOAD ANGLE WITH NRCF

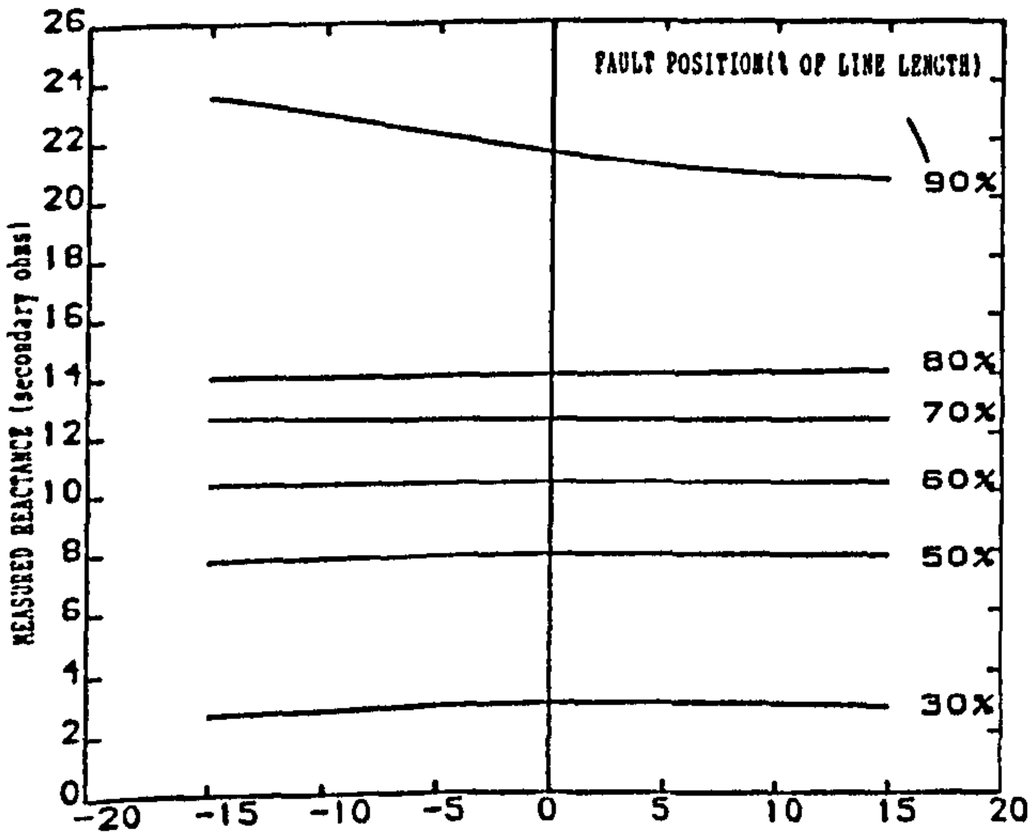

FIG 6.b VARIATION OF MEASURED REACTANCE WITH PRE-FAULT LOAD ANGLE WITH NRCF

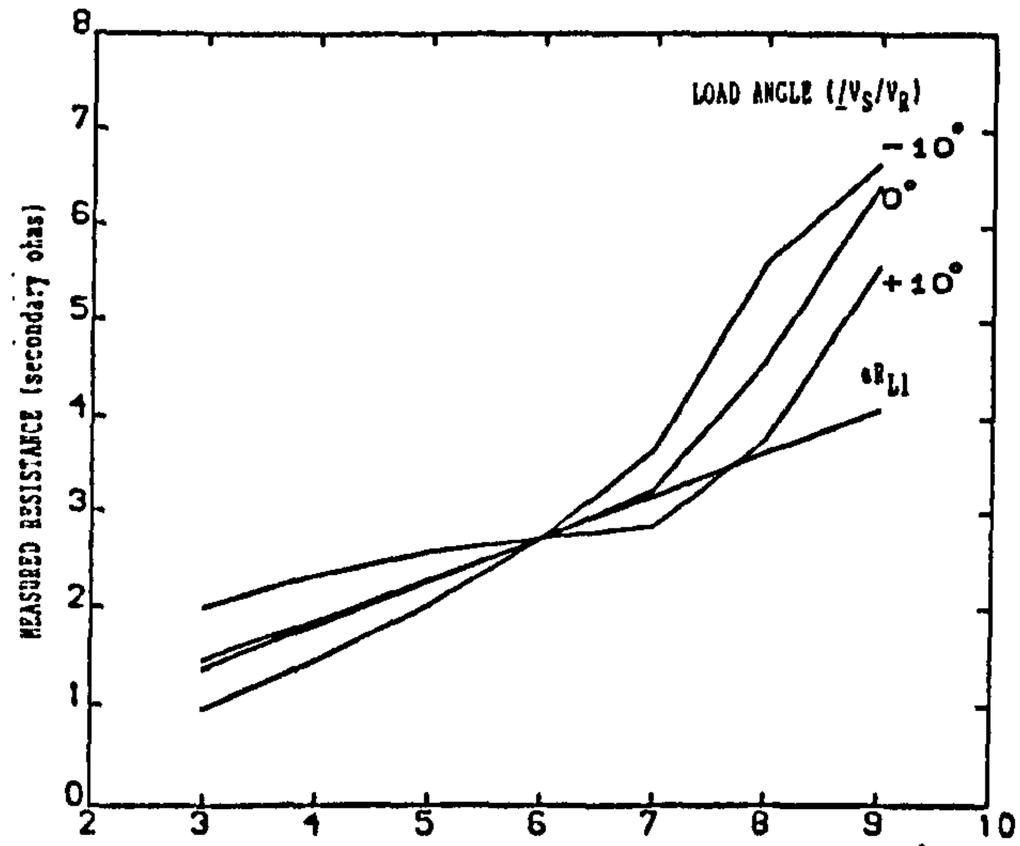

FIG 8.a VARIATION OF MEASURED RESISTANCE WITH FAULT POSITION WITH NRCF

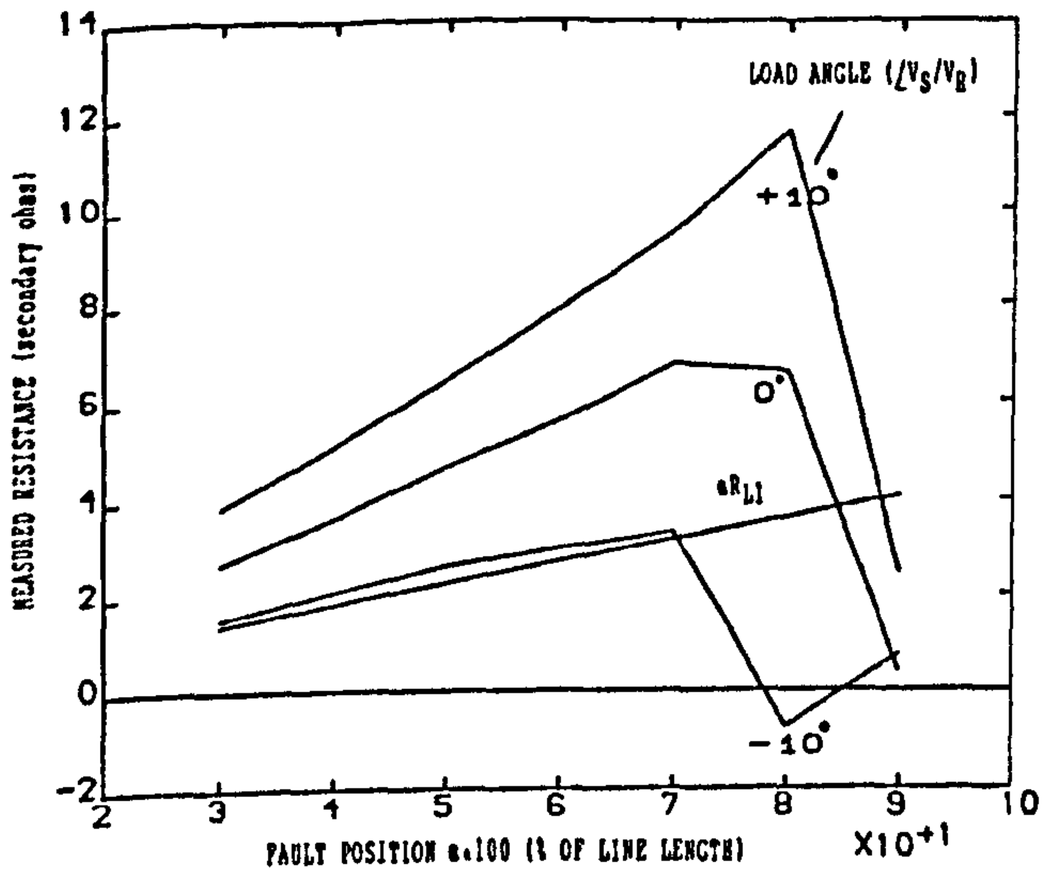

FIG 7.a VARIATION OF MEASURED RESISTANCE WITH FAULT POSITION WITH CRCF

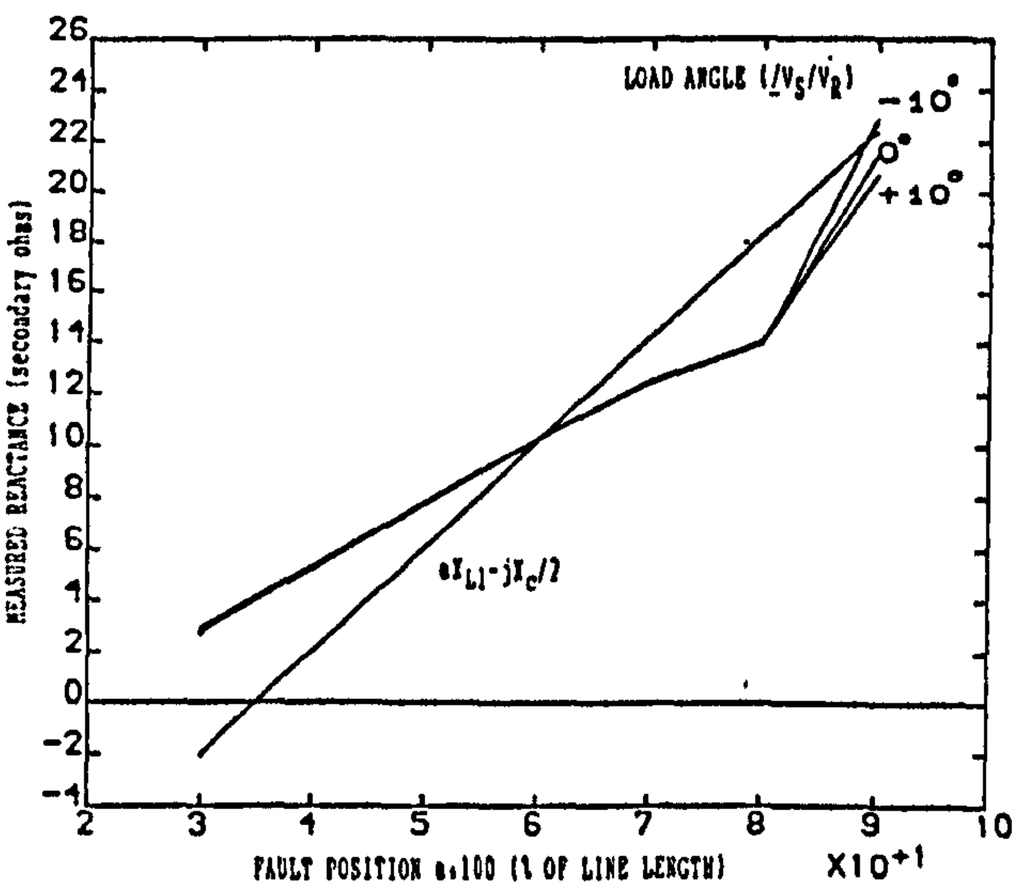

FIG 8.b VARIATION OF MEASURED REACTANCE WITH FAULT POSITION WITH NRCF

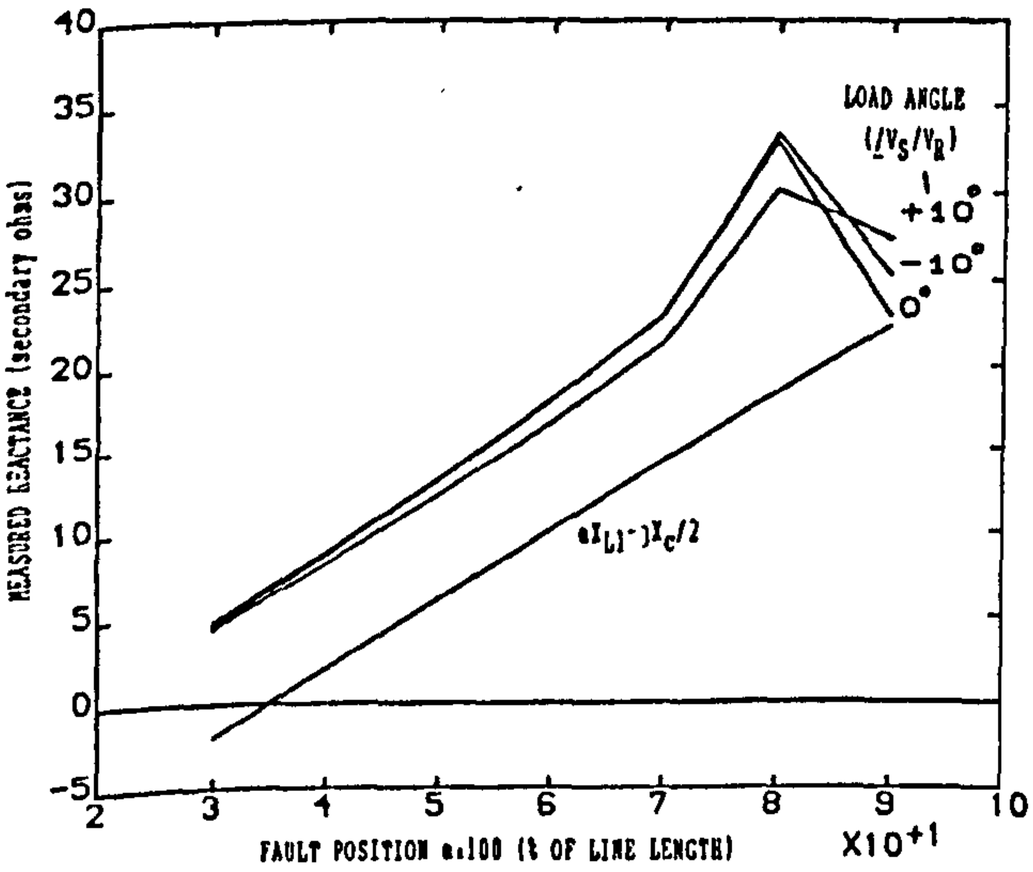

FIG 7.b VARIATION OF MEASURED REACTANCE WITH FAULT POSITION WITH CRCF

CONCLUSIONS

The effect of the residual compensation factor on the measuring accuracy of distance protection measurements when an earth fault occurs on a series compensated line has been investigated. It has been shown that when conventional residual compensation is used, there will be an error in impedance measurement which depends on the ratio $I_{sa}/(I_{sa}+K_C I_{res})$. It has also been shown that this expression depends on load current and source conditions at the line ends. In consequence, errors of measurement and concomitant overreaching/underreaching can occur when conventional residual compensation methods, as applied to plain feeders, is used in series compensated applications. An alternative method of compensation has therefore been developed. This has been found to improve accuracy of measurement at the boundary and also improves relay measurement integrity for other fault positions in series compensated line applications.

ACKNOWLEDGEMENT

The authors would like to thank The City University, London, UK, and the Science and Engineering Research Council UK for the provision of facilities and support for this research.

REFERENCES

[1] R.S.Seymour, E.C.Starr,"Economic aspect of series capacitors in high voltage transmission,"AIEE Trans, PAS, Vol 70, pp. 1660-1670, 1951.

[2] G.Jahnke, N.Fahlen, O.Nerf,"Series capacitors in power system,"IEEE Trans, PAS-94, No 3, pp. 915-925, May/June 1975.

[3] M.M.Elkateb, W.J.Cheetham,"Problems in the protection of series compensated lines," IEE Conference publication on power system protection, No 185, pp. 215-220, 1980.

[4] M.Shafik, F.Ghassemi, A.T.Johns,"Performance of digital distance protection for series compensated systems,"Universities Power Engineering Conference, SUNDERLAND-UK, April 1987.

[5] J.Berdy,"Protection of circuits with series capacitors,"AIEE Summer general meeting, DENVER-COLO, June 1962.

[6] Y.Mansour, T.G.Martinich, J.E.Drakos,"B.C. Hydro series capacitors bank staged fault test,"IEEE Trans, PAS-102, No7, pp. 1960-1969, July 1983.

[7] A.T.Johns, F.Ghassemi,"Analysis and compensation of errors in distance protection measurement for series compensated systems,"Universities Power Engineering Conference, NOTTINGHAM-UK, September 1988.

[8] W.A.Lewis, S.L.Tippett,"Fundamental basis for distance relaying on three-phase systems,"AIEE Trans, pp. 694-709, January 1947.

[9] B.J.Mann, I.F.Morrison,"Relaying a three phase transmission line with a digital computer,"IEEE Trans, PAS-90,No 2, pp. 742-749, March/April 1971.

[10] G.D.Rockefeller, E.A.Udren, G.Gilcrest, "High speed distance relaying using a digital computer," Parts 1 & 2, IEEE Trans. PAS-91,No 3, pp. 1235-1258,May/June 1972

[11] A.T.Johns, M.A.Martin,"New Ultra High Speed distance protection using finite transform techniques,"Proc. IEE, Vol 131, pt.C No 5, pp.188-196, May 1983.

APPENDIX A: SYSTEM DATA

The line is horizontally constructed and discretely transposed. System voltage is 500 kV. The pps and zps impedances of the line are:

Z_{L1}= 0.3109∠83.62° Ω/km primary
= 0.1367∠83.62° Ω/km secondary
Z_{L0}= 1.033∠73.24° Ω/km primary
= 0.4545∠73.24° Ω/km secondary

Reactance of capacitor/phase at each end= 32.44 Ω primary.
= 14.27 Ω secondary
Line Length=300 km

Appendix B

Figure B1 shows the symmetrical component network connection for an "a"-phase-ground fault. During a phase fault to ground, for the line side VT the phase potential V_{sae} at the relay location consists of the following drops in the sequence networks:

$$V_{sae}=I_{s1}(\alpha Z_{L1}-j\ X_{c1}/2)+I_{s2}(\alpha Z_{L2}-j\ X_{c2}/2)+ I_{s0}(\alpha Z_{L0}-j\ X_{c0}/2) \quad (B1)$$

But $Z_{L1}=Z_{L2}$ for lines and $X_{c1}=X_{c2}=X_{c0}=X_c$ for the capacitor banks. Therefore:

$$V_{sae}=(I_{s1}+I_{s2})(\alpha Z_{L1}-j\ X_c/2)+I_{s0}(\alpha Z_{L0}-j\ X_c/2) \quad (B2)$$

The phase current is given by:

$$I_{sa}=I_{s1}+I_{s2}+I_{s0} \quad (B3)$$

Rewriting B3 gives:

$$I_{s1}+I_{s2}=I_{sa}-I_{s0} \quad (B4)$$

Substituting B4 into B2 yields:

$$V_{sae}=(\alpha Z_{L1}-j\ X_c/2)I_{sa}+[(\alpha Z_{L0}-j\ X_c/2)-(\alpha Z_{L1}-j\ X_c/2)]I_{s0} \quad (B5)$$

The residual current can be calculated:

$$I_{res}=I_{sa}+I_{sb}+I_{sc}=3I_{s0} \quad (B6)$$

Therefore equation B5 can be written as:

$$V_{sae}=(\alpha Z_{L1}-j\ X_c/2)I_{sa}+ 1/3[(\alpha Z_{L0}-j\ X_c/2)-(\alpha Z_{L1}-j\ X_c/2)]I_{res} \quad (B7)$$

or

$$V_{sae}=\alpha Z_{L1}I_{sa}-j\ X_c/2 I_{sa}+1/3\left(\frac{Z_{L0}}{Z_{L1}}-1\right)\alpha Z_{L1}I_{res} \quad (B8)$$

The impedance measured by the relay, when conventional residual compensation is used, is thus given by:

$$Z_r=\frac{V_{sae}}{I_{sa}+K_cI_{res}} \approx \alpha Z_{L1}-j\left(\frac{I_{sa}}{I_{sa}+K_cI_{res}}\right) X_c/2 \quad (B9)$$

where:

$$K_c= 1/3\left(\left|\frac{Z_{L0}}{Z_{L1}}\right| -1\right) \approx 1/3\left(\frac{Z_{L0}}{Z_{L1}} -1\right)$$

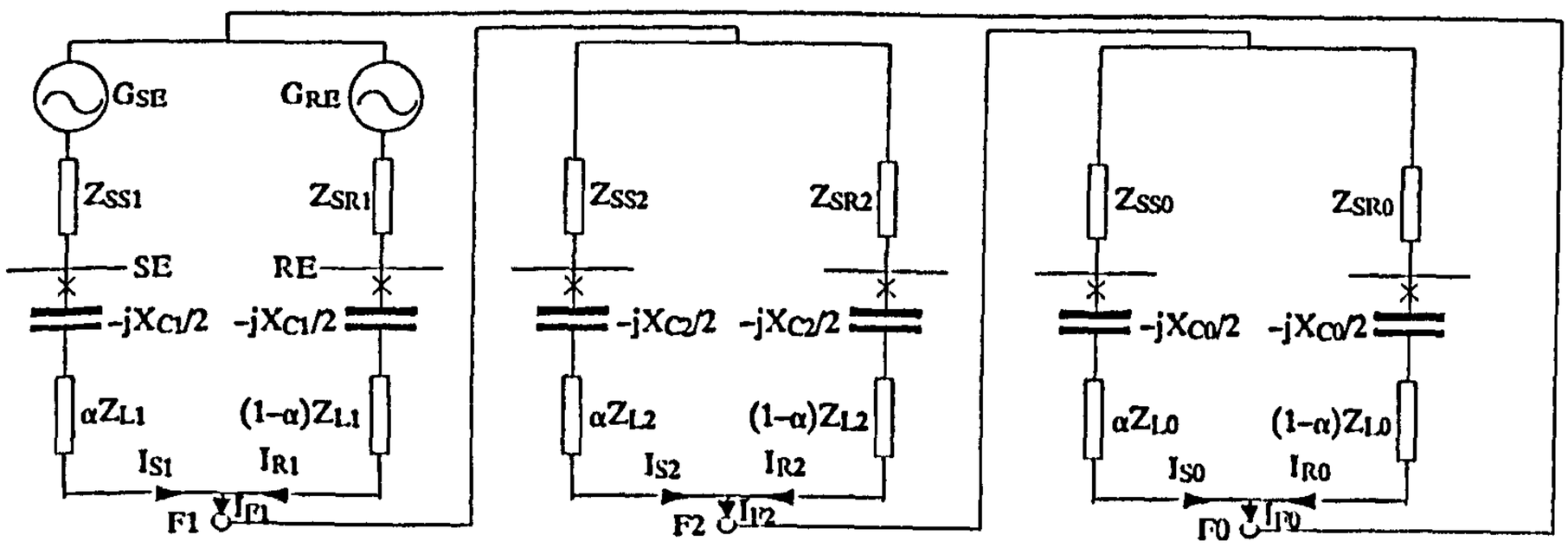

FIG B1 SYMMETRICAL COMPONENT CONNECTION FOR AN "a"-PHASE-GROUND FAULT

APPENDIX C

Equation B7 can be rewritten as:

$$V_{sae}=(\alpha Z_{L1}-j\ X_C/2)I_{sa}+1/3\left(\frac{\alpha Z_{L0}-j\ X_C/2}{\alpha Z_{L1}-j\ X_C/2}-1\right)*(\alpha Z_{L1}-j\ X_C/2)I_{res} \quad (C1)$$

or

$$V_{sae}=(I_{sa}+K(\alpha)I_{res})(\alpha Z_{L1}-j\ X_C/2) \quad (C2)$$

where:

$$K_{(\alpha)}=1/3\left(\frac{\alpha Z_{L0}-j\ X_C/2}{\alpha Z_{L1}-j\ X_C/2}-1\right) \quad (C3)$$

Thus:

$$Z_r=\frac{V_{sae}}{I_{sa}+K(\alpha)I_{res}}=\alpha Z_{L1}-j\ X_C/2 \quad (C4)$$

APPENDIX D

The voltage at the relaying point is given by equation C2. Using the new method of residual compensation, the measured impedance for any fault along the line is given by:

$$Z_r=\frac{V_{sae}}{I_{sa}+K(\alpha r)I_{res}} \quad (D1)$$

where:

$$K_{(\alpha r)}=1/3\left(\frac{\alpha r Z_{L0}-\ j\ X_C/2}{\alpha r Z_{L1}-\ j\ X_C/2}-1\right) \quad (D2)$$

and

αr=proportional fault position for a fault at the zone-1 reach point.

Substituting equation C2 into equation D1 gives:

$$Z_r=\frac{I_{sa}+K(\alpha)I_{res}}{I_{sa}+K(\alpha r)I_{res}}(\alpha Z_{L1}-\ j\ X_C/2) \quad (D3)$$

Foroozan Ghassemi was born in Abadan, Iran in September 1958. He obtained his Master of Science degree in Power Systems Technology from University of Bradford, Bradford, UK. in November 1985. He joined the Power System Protection Research Group at City University, London, UK. in January 1986 and is working towards his PhD degree. His main area of interest is the reactive power compensation and protection of transmission lines.

Allan Thomas Johns (SMIEEE, 1988) is Head of the Department of Electrical, Electronic and Information Engineering, and Professor of Electrical and Electronic Engineering at City University, London, England, UK. Professor Johns is best known for his work on the protection, simulation and control of Power Systems and he is the author of over 100 papers on these topics. He is a fellow of the Institution of Electrical Engineers and in 1982 was awarded the degree of Doctor of Science by the University of Bath, UK. for an original and substantial contribution to knowledge of Electrical Engineering.

UPEC 1987, SUNDERLAND, UK

PERFORMANCE OF DIGITAL DISTANCE PROTECTION FOR SERIES COMPENSATED SYSTEMS.

M. Shafik F. Ghassemi A.T. Johns

The City University, London.

ABSTRACT

Research is being performed into the use of modern digital signal processing technology in the design and engineering of next generation digital distance protection for application to series compensated systems. This paper reviews the work being performed and in particular details the performance which is obtained under practical fault operating conditions in typical compensated feeder systems. The effect of series capacitor gap flashover on the performance is investigated together with investigations into the effect of subsynchronous resonance phenomena. The paper concludes with a discussion of the prospective performance benefit in relation to present day equipment.

INTRODUCTION

The use of series capacitors to compensate long transmission lines has became an increasingly common practice during the last decade. This is mainly to:-

(a) Increase the carrying capacity of transmission lines.

(b) Reduce the losses associated with transmission lines.

(c) Improve both the transient and steady state stability of transmission systems.

(d) Control the load flow between parallel circuits.

(e) Obtain a desired voltage profile.

Series capacitors are either located in the middle of the line for less than 50% compensation or at both its ends for compensation greater than that limit. Capacitors are usually protected against over-voltage by means of spark gaps across the terminals and by-pass breakers. Different techniques are now in use to operate capacitor protection schemes, each having different operational advantages [Jancke (1) and Ahlgren (2)].

On the other hand, the use of capacitors and their over-voltage protection has introduced some difficulties in protecting long series compensated lines. The object of this paper is to investigate these difficulties especially, with the introduction of digital relays and outline the facilities they can provide to this practice.

Operational Problems with Series Compensated Lines

During the last few years, a number of publications tackled the common protection problems of long series compensated lines [Berdy (3), El-Kateb (4) and Ballance (5)]. These can be summarised as follows:-

(a) Transient Stability - The operation of the capacitor protection gear (namely the spark gap) results in the loss of the capacitor when it is most needed, thus jeopardizing the systems stability. To compensate for that, by-passed capacitors are reinserted back into the system as soon as the fault is cleared. The process of by-passing the capacitor and reinserting it again in the circuit often results in system disturbances that can cause line protection schemes (especially distance relays) to maloperate.

(b) Subsynchronous Resonance - The existence of series capacitors in the transmission circuit gives rise to a resonance phenomenon with a frequency between 0 and 60 Hz. When combined with the characteristics of a synchronous machine, it can create the possibility of sustained or poorly damped subsynchronous oscillations. These can result in an oscillating torque and torsional vibrations in the turbo-generator shaft. To a protection scheme, such as distance protection, these oscillations can again result in maloperation.

(c) Loss of Directionality of Relays - When conventional distance relays are used with series capacitor compensated lines, the leading fault current may cause the relay to lose its directional discrimination abilty and, as a result, the relay may block instead of tripping or vice versa.

Digital Relays

Recent advances in the field of microprocessors have resulted in a great improvement in their reliability, increase in their speed and reduction of their cost. Current research clearly shows that the next generation of protection relays is likely to be implemented using microprocessors. The following advantages are clear:-

(a) Flexibility of implementation is provided through the use of software to implement the relaying functions. This leads to the use of standard hardware to achieve an economical design.

(b) The use of modern high speed microprocessors capable of addressing large high speed memory facilitates the implementation of very complex relaying functions which can substantially improve the performance (e.g. intelligent relays). This can be easily done using currently available high level languages (e.g. C).

(c) Ease of communication between different equipment through the use of standardised, high speed communication links.

(d) The use of high capacity storage devices allows data logging for off-line analysis and performance evaluation.

In the study outlined below, a digital distance relay based on the 'Phase Modified Fourier Transform Principle' is considered for evaluation with a capacitor compensated long transmission line. The theory and development of that relay is outlined in several recent publications [e.g. Johns (6)]. The relaying process is based on solving the plain feeder circuit equation:-

$$v(t) = R_\alpha i(t) + L_\alpha \frac{d}{dt} i(t) \qquad 1$$

where R_α and L_α are the line resistance and inductance up to the fault point while v(t) and i(t) are the voltage and current at the relaying point. For series compensated lines the equation to be solved by the relay is:-

$$v(t) = R_\alpha i(t) + L_\alpha \frac{d}{dt} i(t) + \frac{1}{C} \int i(t)dt \qquad 2$$

The relay algorithm contains a number of digital filters and signal processing operations for signal conditioning and mathematical manipulations.

RELAY PERFORMANCE EVALUATION

The study is performed using a digital computer simulation which is divided into primary and secondary stages as follows:-

Primary System Simulation

Highly accurate digital simulations for faulted, series compensated lines were used to produce voltage and current waveforms for different types of faults on a given line configuration. These programs were developed within the Power Systems Measurement and Protection Group and are described in ref. [Aggarwal (7)]. Due to the length and memory requirement, primary system simulation was performed on a main frame computer and the resulting wave forms data files were down-line loaded to a PDP 11/23 microcomputer where the relay simulation was performed. It should be noted that both the current transformer and the capacitor voltage transformer simulations are included with the primary system.

Secondary System Simulation

The digital relay used for the study was simulated according to the block diagram of Fig. 1 where:-

(a) Linear current and voltage interfaces are considered.

(b) The low pass antialiasing filter is realised by the impulse response of a second order Butterworth with 1 kHz bandwidth.

(c) A 12-bit A/D converter is considered with ± 10 V input limits. Both the current and voltage interface gains are adjusted according to that limit.

(d) A 16-bit microprocessor was considered during the simulation for the relay realization.

(e) The characteristics of the preconditioning filter stage used is shown in Fig. 2 where it is required to block both the dc offset and the travelling wave components from the measured signals.

(f) The two orthogonal components of each current and voltage waveforms are obtained using the two orthogonal filters with the impulse responses shown in Fig. 3.

(g) The quadrilateral relay characteristics for the line represented by the parameters of Appendix [A] are shown in Fig. 4. From the figure it is clear that in order that the relay would not respond to faults occuring at the receiving end busbar, the protected zone has to be reduced to 58% of the line length. In order to protect this reduced zone (including the sending end capacitor), the reverse reach is extended to -40% of the line length, as shown.

The relay operation is based on determining an estimate of the line impedance up to the fault from the waveforms of the line voltages and current at the

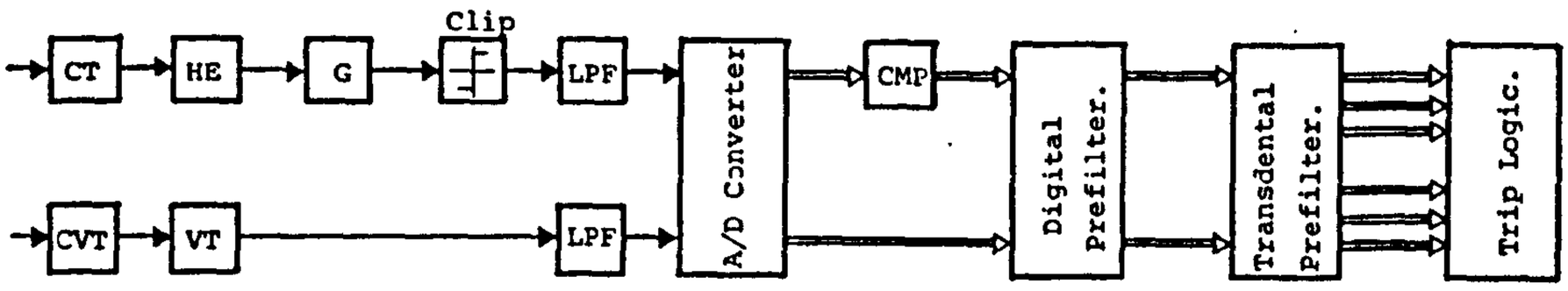

Fig. 1 Block Diagram For the Digital Distance Relay

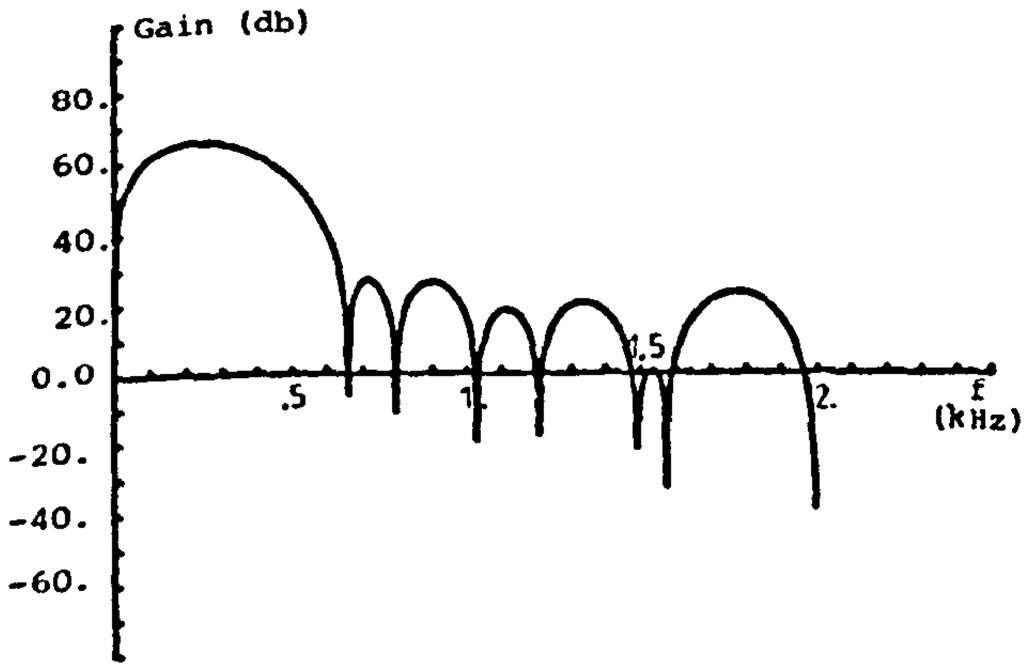

Fig 2 Frequency Responce of the Digital Prefilter.

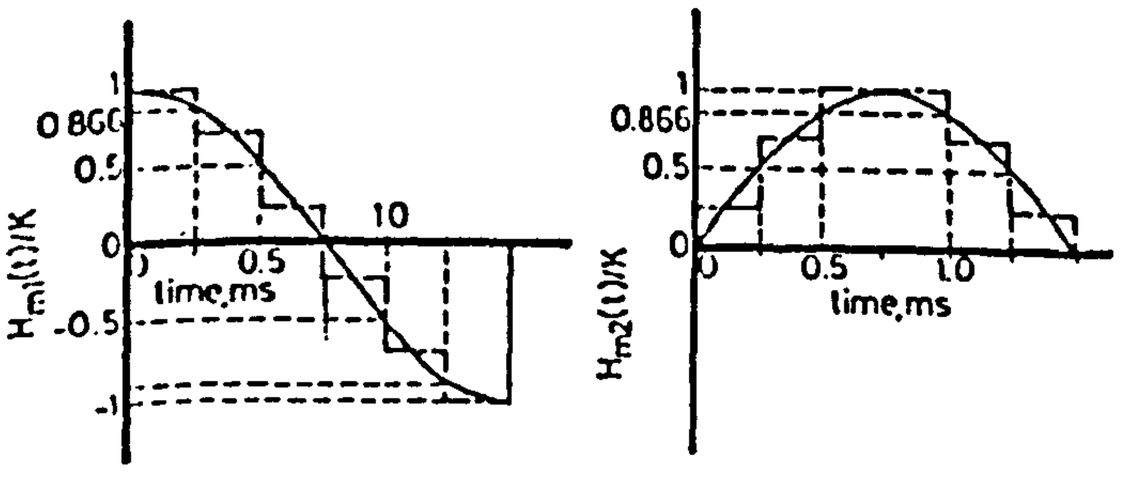

Fig 3 Impulse Responce for the SIN and COS Orthogonal Filters.

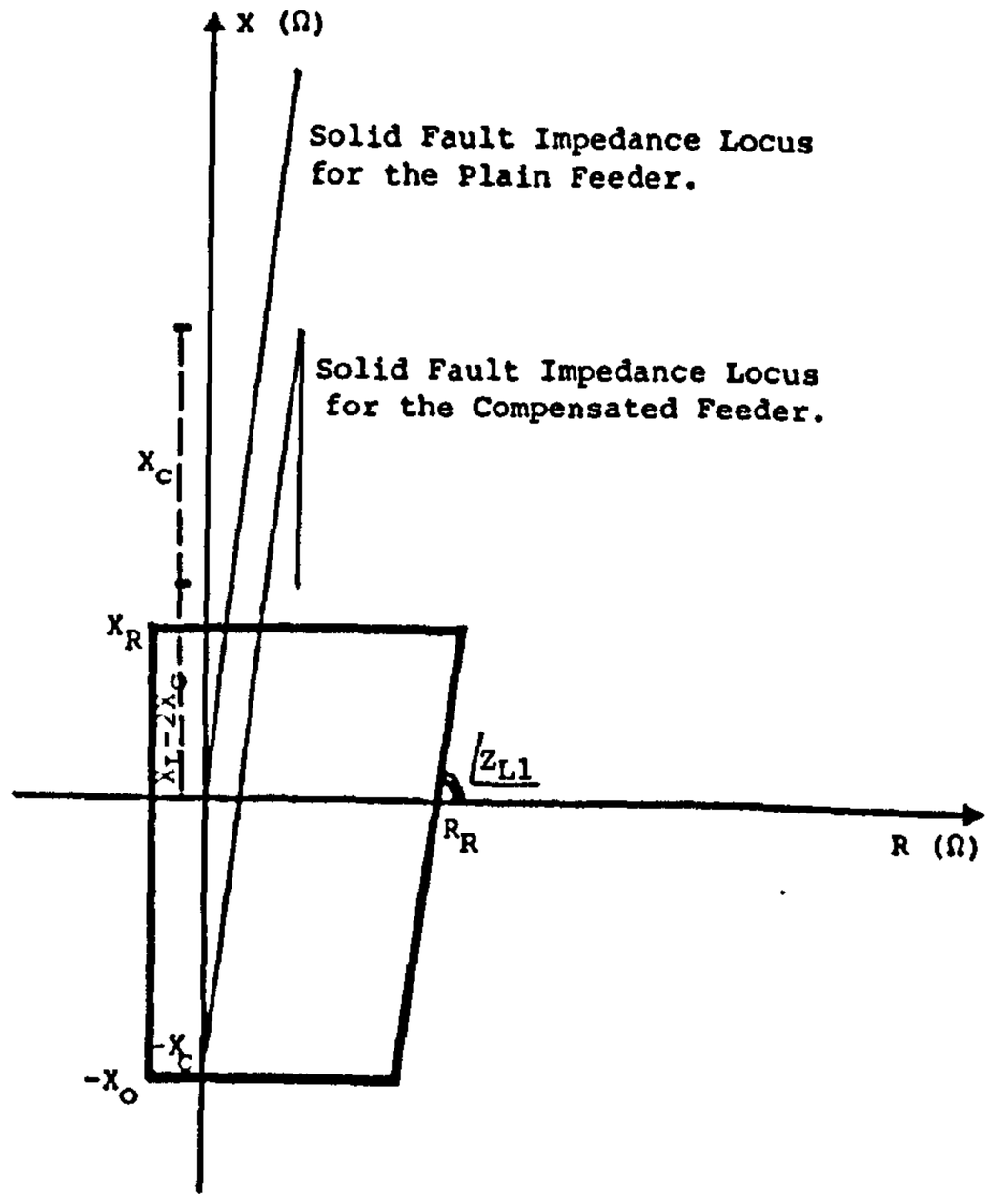

Fig 4 Quadrilateral Tripping Characteristics.

relaying point. These values are compared with the boundaries of the protected zone. A counter, which is implemented in the relay software is incremented every time the impedance is found to be inside the protected zone and decremented if found outside. A trip signal is issued when the trip counter reaches a certain prespecified level.

Simulation Results

In the following part some examples are given for the performance of the digital distance relay using the test transmission line outlined in Appendix [A]:-

(a) Plain Feeder Applications - Fig. 5 shows the relay performance when connected to the test line with no compensation (i.e. plain feeder) following voltage maximum, solid "a"-earth faults at different locations on the line. The figure clearly shows how the measured resistance and reactance converge inside the protected zone and the corresponding trip counter behaviour.

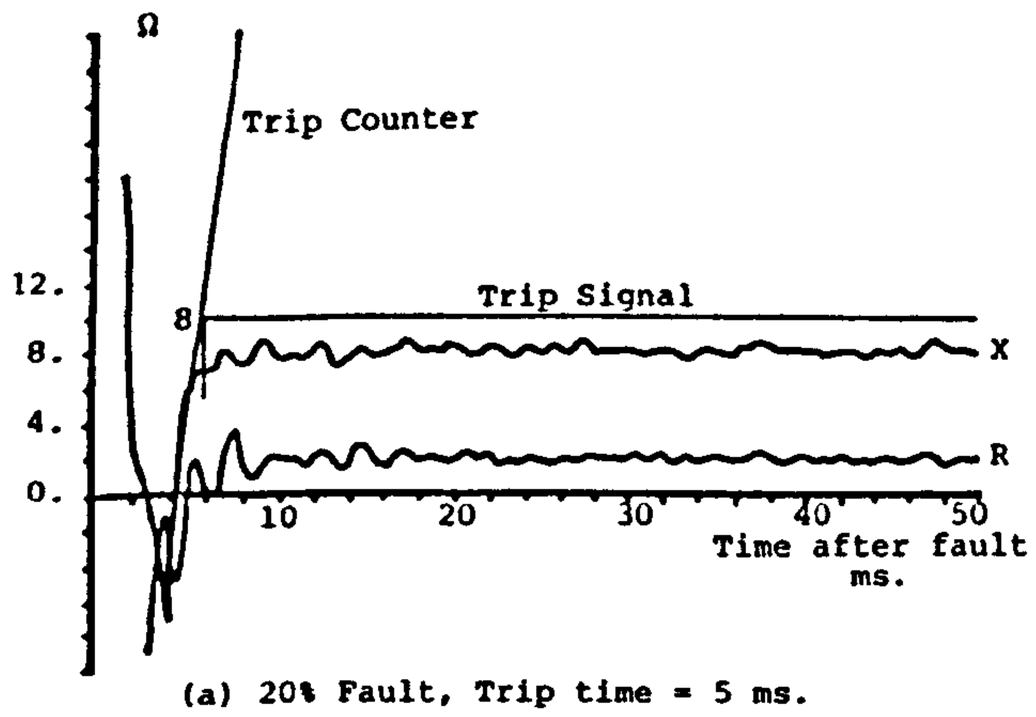

(a) 20% Fault, Trip time = 5 ms.

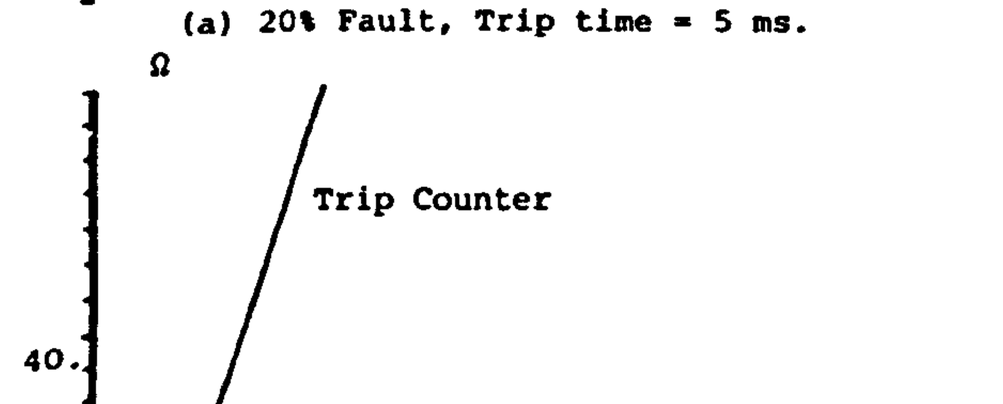

(b) 40% Fault, Trip Time = 5 ms.

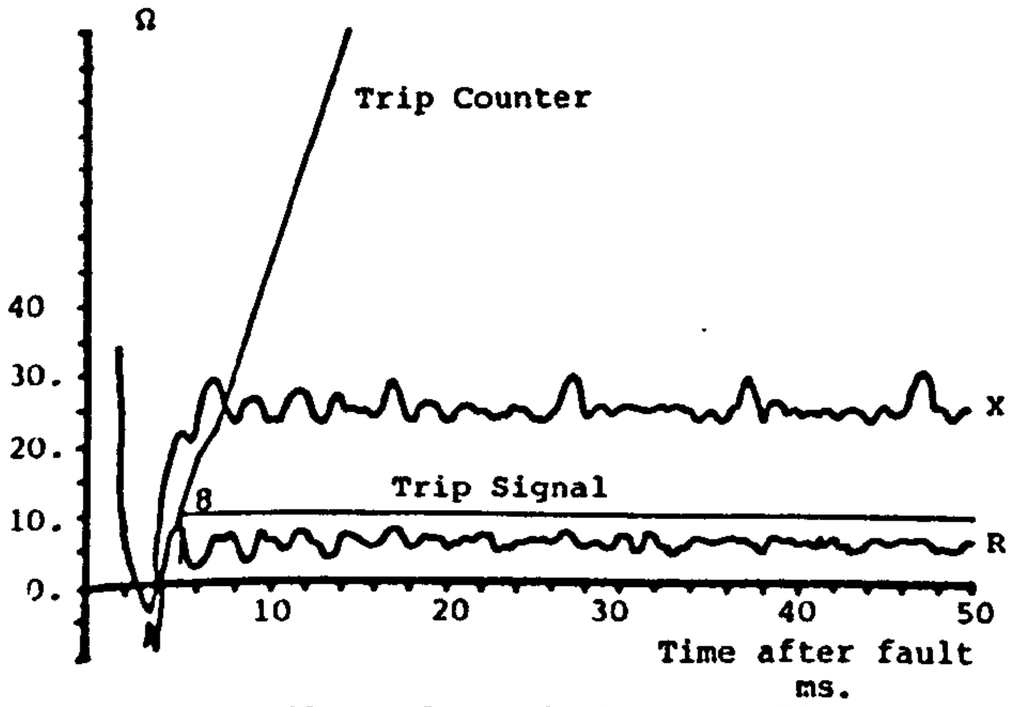

(c) 60% Fault, Trip Time = 4.75 ms.

Fig 5 Relay Performance for Plain Feeder.

(b) Series Compensated Line Application - When the same line was compensated using two capacitors at both ends, each with 35% of the total line reactance, the following performance was obtained:-

(i) Effect of Subsynchronous Resonance - When the protective gaps were prevented from flashing over (by setting their sparking level to a very high value), the effect of subsynchronous resonance on the measured line impedance to the fault can be clearly seen from Fig. 6. It is clear that the relay performance can be greatly affected by this phenomenon especially for faults close to zone boundaries. In such cases, the relay logic may experience difficulty in deciding whether a fault is more likely to be inside or outside the protected zone (and thus maloperate).

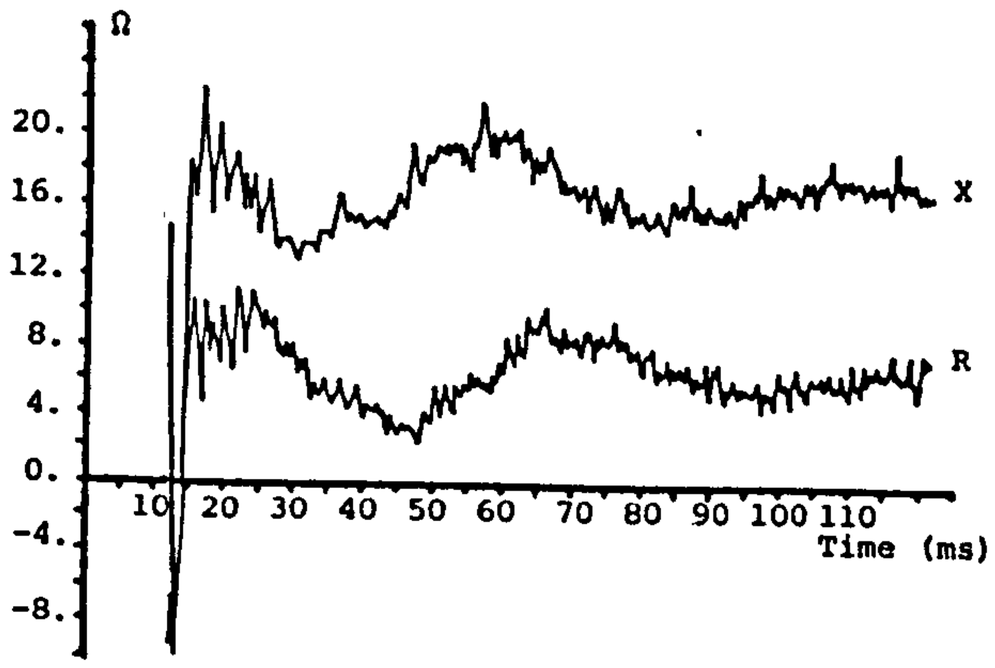

Fig 6 Effect of Subsynchronous Resonance.

(ii) Effect of Protective Gap Flashover - When the flashover level was set at 2.5 p.u. of the rated capacitor voltage and the relay was tested with the test line subject to a maximum voltage fault on the "a"-phase, at 10% of the line length, the performance shown in Fig. 7 was obtained. (The figure shows the behaviour of the measured reactance when the flashover occurs as compared to the case with no flashover). It is clear that the measured reactance changes as soon as the capacitor is bypassed by the flashover gap, and the relay can under-reach in this case.

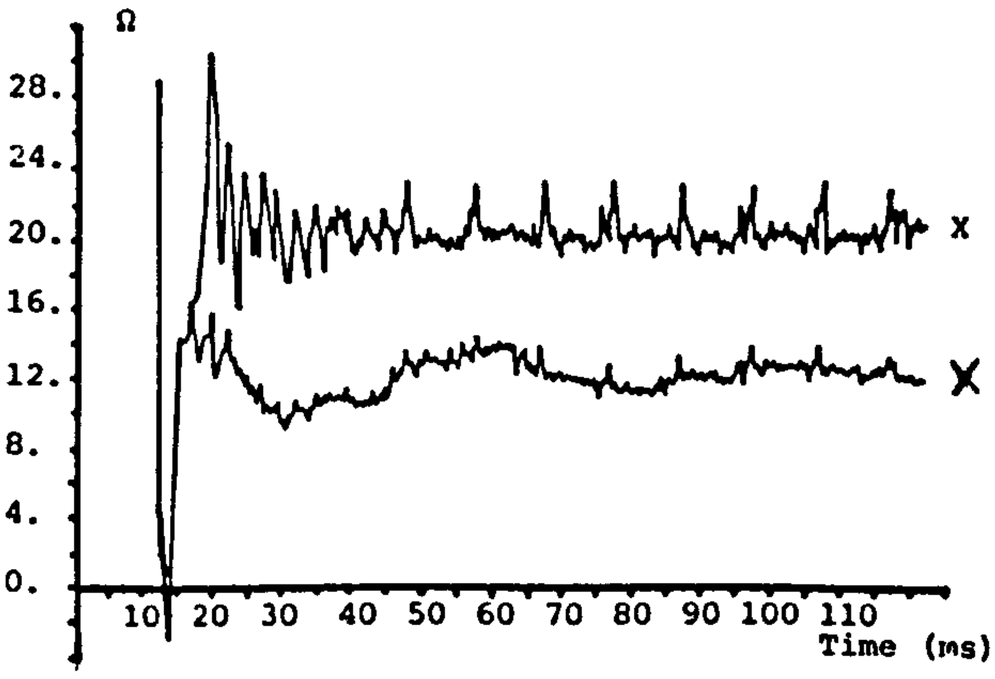

Fig 7 Effect of Capacitor Gap Flashover.

General Discussion

In order that the digital relay can operate correctly with series compensated lines, the following recommendations are to be considered:-

(a) The relay should be capable of detecting protective gap flashover and take necessary action to compensate for any under-reach.

(b) The relay logic has to be modified to cater for the effect of subsynchronous frequency

components in the measured line impedance. It is clear that filtering out such low frequencies in the vicinity of the power frequency is not practical given the requirement of ultra high speed operation of the relay. When an averaging process was employed before the trip counter, a great improvement in the relay performance was achieved. Fig. 8 shows the inverse relay characteristics with the simple counter regime while Fig. 9 shows the same characteristics with the averaging process.

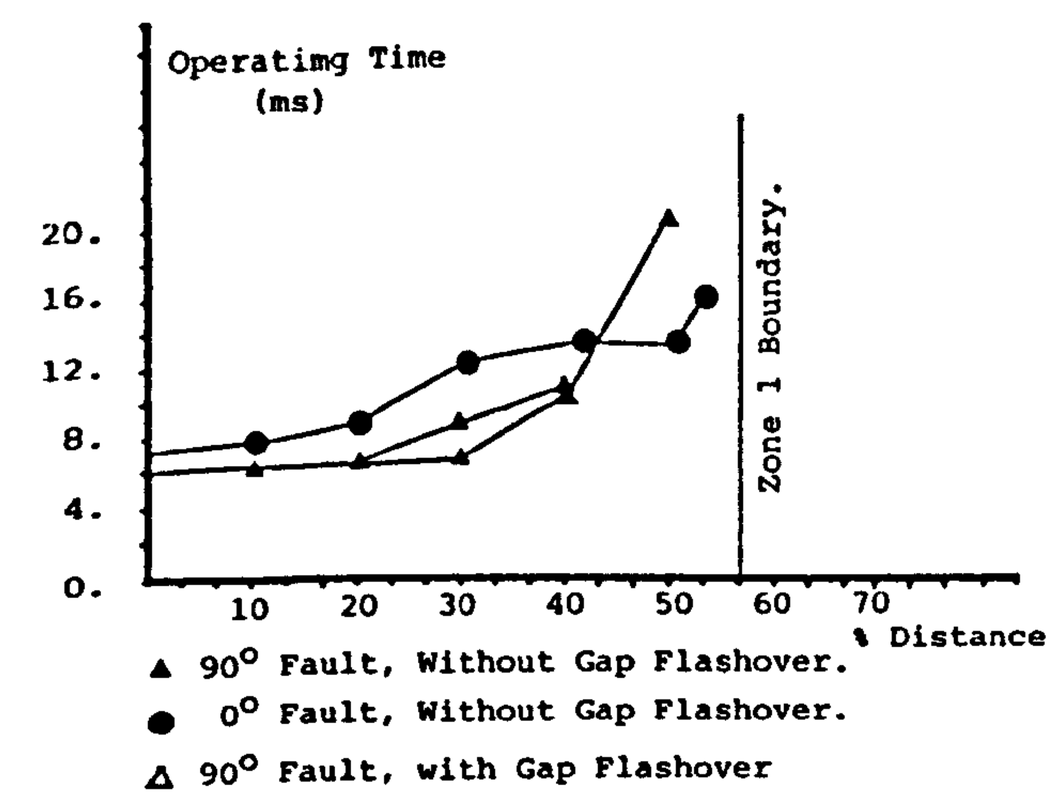

Fig 8 Relay Responce With the Simple Count Regime.

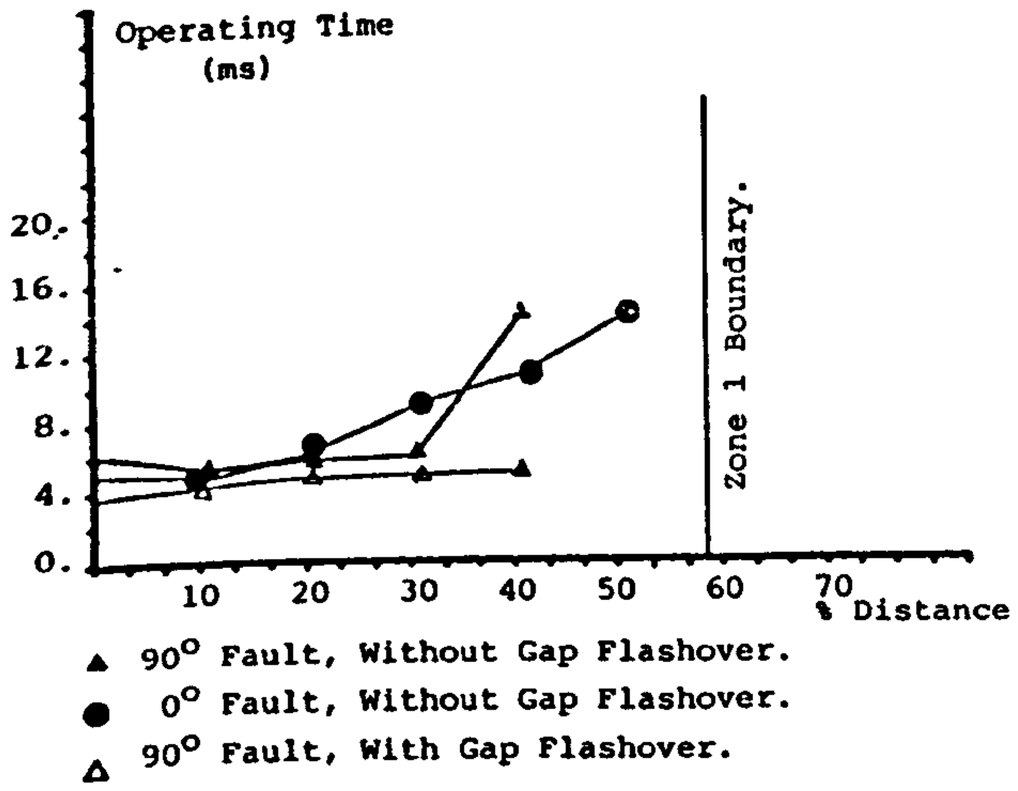

Fig 9 Relay Responce With The Averaging Count Regime.

CONCLUSIONS

In this paper, some aspects of the performance of a digital distance relay are studied when operated with series compensated lines. Major operational problems are outlined to investigate the possible research directives to improve the performance.

The study showed the potential of digital distance relays in the field of series compensated lines. Research is currently in progress to overcome the problems outlined and to develop a modified version of the relay suitable for these difficult applications.

ACKNOWLEDGEMENTS

The authors are grateful for the provision of facilities at The City University, London and G.E.C. Measurements Ltd., Stafford. Especial thanks are due to engineers at G.E.C. Measurements Ltd. for helpful discussions. The support of the U.K. Science and Engineering Research Council and G.E.C. Measurements Ltd. are greatly acknowledged.

APPENDIX A

Main line length is 300 km, the line is horizontally constructed and discretely transposed. The line can have 70% compensation using two capacitor banks at its ends. The line self and mutual impedances are given below:-

$$Z_s = 0.1223 + j0.5358 \quad \Omega/km$$
$$Z_m = 0.0878 + j0.2268 \quad \Omega/km$$

The positive and zero phase sequence impedances of the line were calculated:-

$$Z_1 = Z_s - Z_m$$
$$\therefore Z_1 = 0.0345 + j0.309 \quad \Omega/km$$
$$Z_1 = 0.3109\underline{/83.629}$$
$$\text{and } Z_0 = Z_s + 2Zm$$
$$Z_0 = 0.2979 + j0.9894 \quad \Omega/km$$
$$Z_0 = 1.033\underline{/73.243}$$

The relay's quadrilateral characteristics can be defined by the following parameters:-

$X_c = 32.445\ \Omega$
$X_r = 21.321\ \Omega$
$X_0 = -37.08\ \Omega$
$R_r = 13.0\ \Omega$
$R_0 = -3.0\ \Omega$
Line angle $\Psi = 83.622$

Faults were single phase to earth fault (phase 'a') and applied at phase 'a' peak voltage.

REFERENCES

1. G. Jancke, N. Fahlin, O. Nerf, July 15-20 1973, 'Series Capacitors in Power Systems', IEEE/PES Summer Meeting and EHV/UHV Conference, Vancouver, B.C., Canada, 915-925.

2. L. Ahlgren, N. Fahlen, K.E. Johanson, February 4-9 1979, 'EHV Series Capacitors With Dual Gaps and Nonlinear Resistors Provide Technical and Economical Advantages', IEEE/PES Winter Meeting, New York, NY.

3. J. Berdy, June 17-22 1962, 'Protection of Circuits With Series Capacitors', AIEE Summer General Meeting, Denver, Colorado, 929-935.

4. M.M. El-Kateb, W.J. Cheetham, 1980, 'Problems in the Protection of Series Compensated Lines', IEE Conference Publication on Power System Protection No. 185, 215-220.

5. J.W. Ballance, S. Goldberg, January 28 - February 2 1973, 'Subsynchronous Resonance in Series Compensated Transmission Lines', IEEE/PES Winter Meeting, New York, N.Y., 1649-1658.

6. A.T. Johns, M.A. Martin, May 1983, 'New Ultra High Speed Distance Protection Using Finite Transform Techniques', IEE Proc., Vol. 130, Pt. C, No. 3, May, 127-138.

7. R.K. Aggarwal, A.T. Johns, A. Kalam, September 1984, 'Computer Modelling of Series Compensated EHV Transmission Systems', Proc. IEE, Vol. 131, Pt. C, No. 5, 188-196.

UPEC 1988, NOTTINGHAM, UK

ANALYSIS AND COMPENSATION OF ERRORS IN DISTANCE PROTECTION MEASUREMENT FOR SERIES COMPENSATED SYSTEMS

A.T. Johns and F. Ghassemi

City University, London, UK

ABSTRACT

This paper investigates the operation and accuracy of a digital distance relay when used on series compensated systems. Residual compensation factor was found to be one source of error in measurement for phase to earth faults. New method of residual compensation is proposed and relay performance is investigated.

INTRODUCTION

Series capacitors have proven to be an important component in economical long distance power transmission [1, 2, 3]. The capacitor banks are either located at line ends or in the middle, each scheme has its own merits and disadvantages. From a protection point of view the former proves to be more difficult to deal with. For this reason this paper considers a transmission line with 70% compensation (35% at each end). Series capacitors introduce some difficulties in protecting such lines especially in distance schemes [4, 5, 6]. One of the difficulties which arises is the effect of residual compensation on accuracy of the distance relay for earth faults. The object of this paper is to investigate this effect and propose a method to enhance the digital distance relay accuracy.

RESIDUAL COMPENSATION

It is well known that in distance protection, for phase to earth faults, compensation methods are used to allow the relay to measure the positive sequence impedance of the line from relaying to fault points [7]. One of these methods is residual compensation, where a fraction of the residual current is added to the phase currents as shown by equation 1:-

$$Z_r = \frac{V_{ae}}{I_a + KI_{res}} = \alpha Z_{L1} \qquad (1)$$

Where: Z_r measured impedance
K residual compensation factor =

$$\frac{1}{3}\left(1\frac{Z_{L0}}{Z_{L1}}1 - 1\right)$$

V_{ae} faulted phase voltage at relay
I_a phase current
I_{res} residual current
Z_{L1}, Z_{L0} positive and zero sequence impedance of line
α fault position

Appendix [A] shows that if the same residual compensation factor is used, when protecting series compensated lines, the relay would not measure the positive sequence impedance of the line to the fault point and an error will exist in the measurement. This error depends on the expression

$$\frac{I_a}{I_a + KI_{res}} .$$

If the relay is required to measure the positive sequence impedance of the line (for relay setting purposes) a modification to residual compensation factor is needed.

As shown in appendix [B], if the residual compensation factor is set according to fault position, the relay will measure:-

$$Z_r = \frac{V_{ae}}{I_a + K(\alpha)I_{res}} = \alpha Z_{L1} - j\frac{X_C}{2}$$

This means that only if the fault position is known to the relay will the measured value be very close to the positive sequence value of the line.

Proposed Method for Residual Compensation

Clearly, knowing the fault position to carry out the measurement is neither realistic nor practical. Since the relay is required to be most accurate at and around the boundary, it is proposed that the fault position (α) in equation B3 is set at a fixed value assuming the fault is at the boundary of the relay. Thus accuracy of the relay will be max for faults at and around the forward reach. It is clear that when capacitor flashover occurs the residual compensation factor must be modified to the plain feeder value.

RELAY PERFORMANCE EVALUATION

The study is performed using a digital computer simulation which is divided into primary and seccondary stages as follows:-

Primary System Simulation

A horizontal configuration, single circuit line was simulated, using highly accurate computer program. The program is described in reference [8]. The line data is given in appendix [C].

To observe the effect of the capacitor, the action of the capacitor protection gear was prevented by adjusting the gap threshold setting to a high value.

Digital Relay

The digital distance relay used in the study is based on the work which was originally carried out by Johns and Martin [9]. A number of papers have since described and investigated the performance of this relay for both series compensated and plain lines [6, 10]. The relay has a quadrilateral characteristic which is set according to positive sequence impedance of the line.

Unlike plain feeder distance protection schemes, where the forward reach of the relay is set at 80%, in series compensated lines the forward reach of the first independent zone is set at a lower value to exclude the remote end busbar and to allow for errors in discrimination. Fig. 1 shows the relay characteristic and the line locus. The forward reach was set at 60% of the line to exclude the receiving end busbar. The relay protects the local capacitor bank.

ANALYSIS OF THE RELAY PERFORMANCE

In distance relaying the accuracy of the resistance measurement is not important to the decision making logic. Accordingly, only reactance measurements are illustrated here.

Using conventional methods, the residual compensation factor was calculated to be 0.77. When the new method was used it was calculated to be 1.82 by putting $\alpha = 0.6$ in equation B3 (assuming the fault position to be at the boundary). Fig. 2 illustrates the variation of measured reactance versus magnitude of K, for different fault positions. No load was considered on the system. The marked values on the reactance axis are the actual line reactances for the shown fault positions.

The error in measurement is clear when K = 0.77. However, for faults at the boundary (60% of line length), the measurement is very close to the line reactance when K = 1.82. Fig. 3 illustrates the variation of measured reactance versus fault position and the line reactance locus. If K = 0.77 there is an error in measurement and the relay under-reaches. But if K is calculated according to the new method, the measurement is very accurate at the boundary.

Simulation Results

Fig. 4 shows the measured reactance by the relay for a fault at 50% of the line length. It is clear that when K is calculated conventionally, the relay has under-reached and did not trip. However, setting K = 1.82, the measured value is inside the boundary and the relay responded correctly.

Fig. 5 illustrates that the accuracy of the relay has greatly increased for a fault at the boundary. The strong subsynchronous oscillation was dealt with by filtering and suitable decision logic. A number of tests were carried out to evaluate the relay response for different load and fault inception angle situation. No maloperation was observed and the relay responded correctly for faults close to the reach point.

Fig. 6a and 6b show operating time versus the relay reach for 2 load situation.

CONCLUSION

In series compensated lines, the presence of the series capacitor causes inaccuracy in distance protection scheme. One source of inaccuracy in earth fault measurements is the residual compensation factor. A new method of residual compensation was proposed. The results presented, show that the accuracy and hence descrimination ability of the relay has improved. In the new method the capacitor flash over must be detected to modify the compensation factor to maintain the accuracy in measurement.

ACKNOWLEDGEMENTS

The authors would like to thank City University, London, GEC Measurements, Stafford and the Science and Engineering Research Council for the provision of facilities and support for this research.

APPENDIX A

During a phase fault to ground the phase potential V_{ae} at the relay consists of the following drops in the sequence networks.

$$V_{ae} = I_1(\alpha Z_{L1} - j\frac{X_{C1}}{2}) + I_2(\alpha Z_{L2} - j\frac{X_{C2}}{2}) + I_0(\alpha Z_{L0} - j\frac{X_{C0}}{2}) \quad (A1)$$

But $Z_{L1} = Z_{L2}$ for lines and $Z_{C1} = X_{C2} = X_{C0}$ for capacitor banks

therefore $$V_{ae} = (I_1 + I_2)(\alpha Z_{L1} - j\frac{X_{C1}}{2}) + I_0(\alpha Z_{L0} - j\frac{X_{C1}}{2}) \quad (A2)$$

The phase current is given by

$$I_a = I_1 + I_2 + I_0 \quad (A3)$$

Rewriting A3 gives

$$I_1 + I_2 = I_a - I_0 \quad (A4)$$

Substituting A4 into A2 yields

$$V_{ae} = (\alpha Z_{L1} - j\frac{X_{C1}}{2})I_a + [(\alpha Z_{L0} - j\frac{X_{C1}}{2}) - (\alpha Z_{L1} - j\frac{X_{C1}}{2})]I_0 \quad (A5)$$

The residual current can be calculated as follows

$$I_{res} = I_a + I_b + I_c = 3I_0 \quad (A6)$$

therefore equation A5 can be written as

$$V_{ae} = (\alpha Z_{L1} - j\frac{X_{C1}}{2})I_a + \frac{1}{3}[(\alpha Z_{L0} - j\frac{X_{C1}}{2}) - (\alpha Z_{L1} - j\frac{X_{C1}}{2})]I_{res} \quad (A7)$$

or

$$V_{ae} = \alpha Z_{L1} I_a - j\frac{X_{C1}}{2} I_a + \frac{1}{3}(\frac{Z_{L0}}{Z_{L1}} - 1)\alpha Z_{L1} I_{res} \quad (A8)$$

The measured impedance by the relay is given by equation A9

$$Z_r = \frac{V_{ae}}{I_a + KI_{res}} = \alpha Z_{L1} - j\frac{X_C}{2}\frac{I_a}{I_a + KI_{res}} \quad (A9)$$

where $K = \frac{1}{3}(|\frac{Z_{L0}}{Z_{L1}}| - 1)$

APPENDIX B

Equation A7 can be rewritten as

$$V_{ae} = (\alpha Z_{L1} - j\frac{X_{C1}}{2})I_a + \frac{1}{3}(\frac{\alpha Z_{L0} - j\frac{X_{C1}}{2}}{\alpha Z_{L1} - j\frac{X_{C1}}{2}} - 1)(\alpha Z_{L1} - j\frac{X_{C1}}{2})I_{res} \quad (B1)$$

or

$$V_{ae} = (I_a + K(\alpha)I_{res})(\alpha Z_{L1} - j\frac{X_{C1}}{2}) \quad (B2)$$

where $$K(\alpha) = \frac{1}{3}(\frac{\alpha Z_{L0} - j\frac{X_{C1}}{2}}{\alpha Z_{L1} - j\frac{X_{C1}}{2}} - 1) \quad (B3)$$

Thus $$Z_r = \frac{V_{ae}}{I_a + K(\alpha)I_{res}} = \alpha Z_{L1} - j\frac{X_{C1}}{2} \quad (B4)$$

APPENDIX C

Main line length is 300 km, the line is horizontally constructed and discretely transposed. System voltage is 500 kV. Local and remote sources capacities are 5 and 35 GVA respectively.

The positive and zero phase sequence impedances of the line are:-

Z_1 = 0.0345 + j0.309 Ω/km

or

Z_1 = 0.3109/83.629 Ω/km

Z_0 = 0.2979 + j0.9894 Ω/km

or

Z_0 = 1.033/73.243 Ω/km

The relay's quadrilateral characteristics in terms of secondary values can be defined by the following parameters:-

X_r = 10.19 Ω
X_0 = -16.0 Ω
R_r = 13.0 Ω
R_0 = -3.0 Ω
Line angle 4 = 83.629°

Reactance of capacitor at each end:-
32.445 Ω primary
14.275 Ω secondary

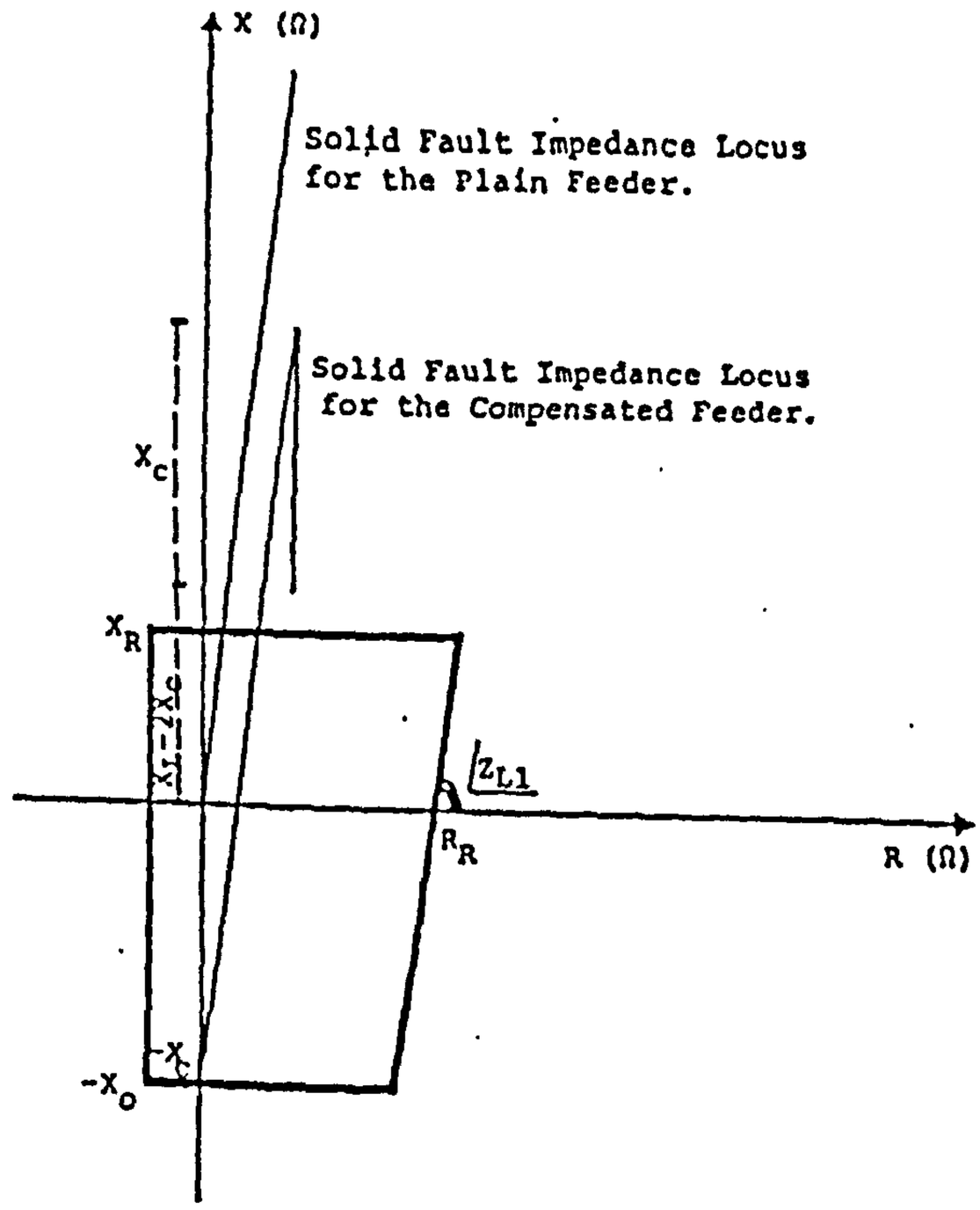

Figure 1 Quadrilateral Tripping Characteristics.

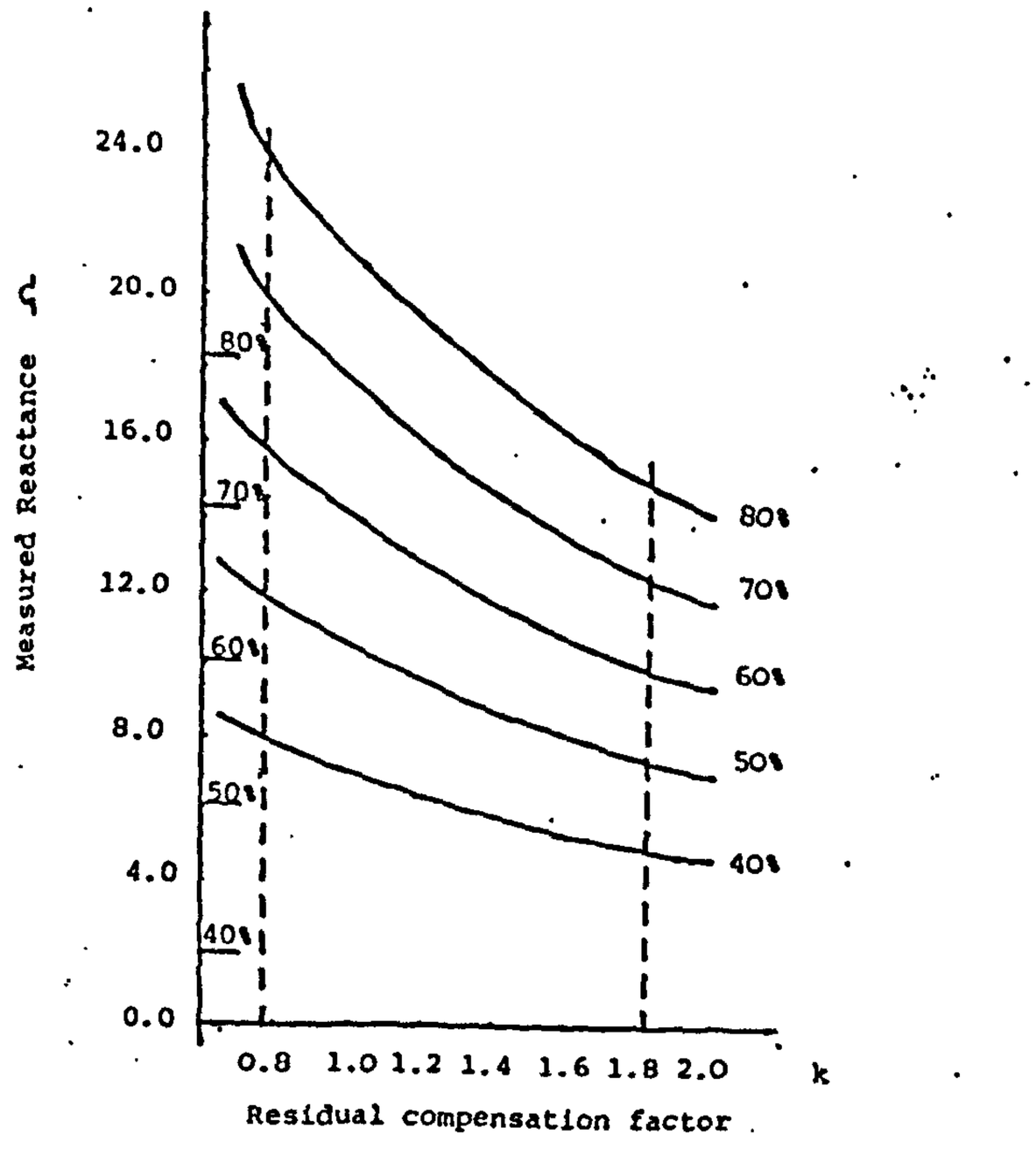

Figure 2 Measured Reactance Vs Residual Compensation Factor

REFERENCES

1. Seymour, R.S. and Starr, E.C., 1951, "Economic aspect of series capacitors in high voltage transmission", AIEE Trans, Power Apparatus and Systems, 70, 1660-1670.

2. Maneatis, J.A., Hubacher, E.J., Rothenbuhler, W.N. and Sabath, J., 1971, "500 kV series capacitor installations in California", IEEE Trans PAS, PAS90, 1138-1149.

3. Jahnke, G., Fahlen, N. and Nerf, O., 1975, "Series capacitors in power system", IEEE Trans PAS, PAS94, 915-925.

4. Berdy, J., 1962, "Protection of circuits with series capacitors", AIEE Summer General Meeting, Denver, Colorado, 929-935.

5. El-Kateb, M.M. and Cheetham, W.J., 1980, "Problems in the protection of series compensated lines", IEE Conference Publication on Power System Protection, NO.185, 215-220.

6. Shafik, M., Ghassemi, F. and Johns, A.T., 1987, "Performance of digital distance protection for series compensated systems", UPEC, Sunderland.

7. Lewis, W.A. and Tippett, S.L., 1947, "Fundamental basis for distance relaying on three-phase system", AIEE Trans., 694-709.

8. Aggarwal, R.K., Johns, A.T. and Kalam, A., 1984, "Computer modelling of series compensated EHV transmission systems", Proc IEE, 131, PtC, No5, 188-196.

9. Johns, A.T. and Martin, M.A., 1983, "New ultra-high-speed distance protection using finite-transform techniques", Proc IEE, 130, PtC, No3, 127-138.

10. Moore, P.J. and Johns, A.T., 1987, "The performance of new ultra-high-speed distance protection", UPEC, Sunderland.

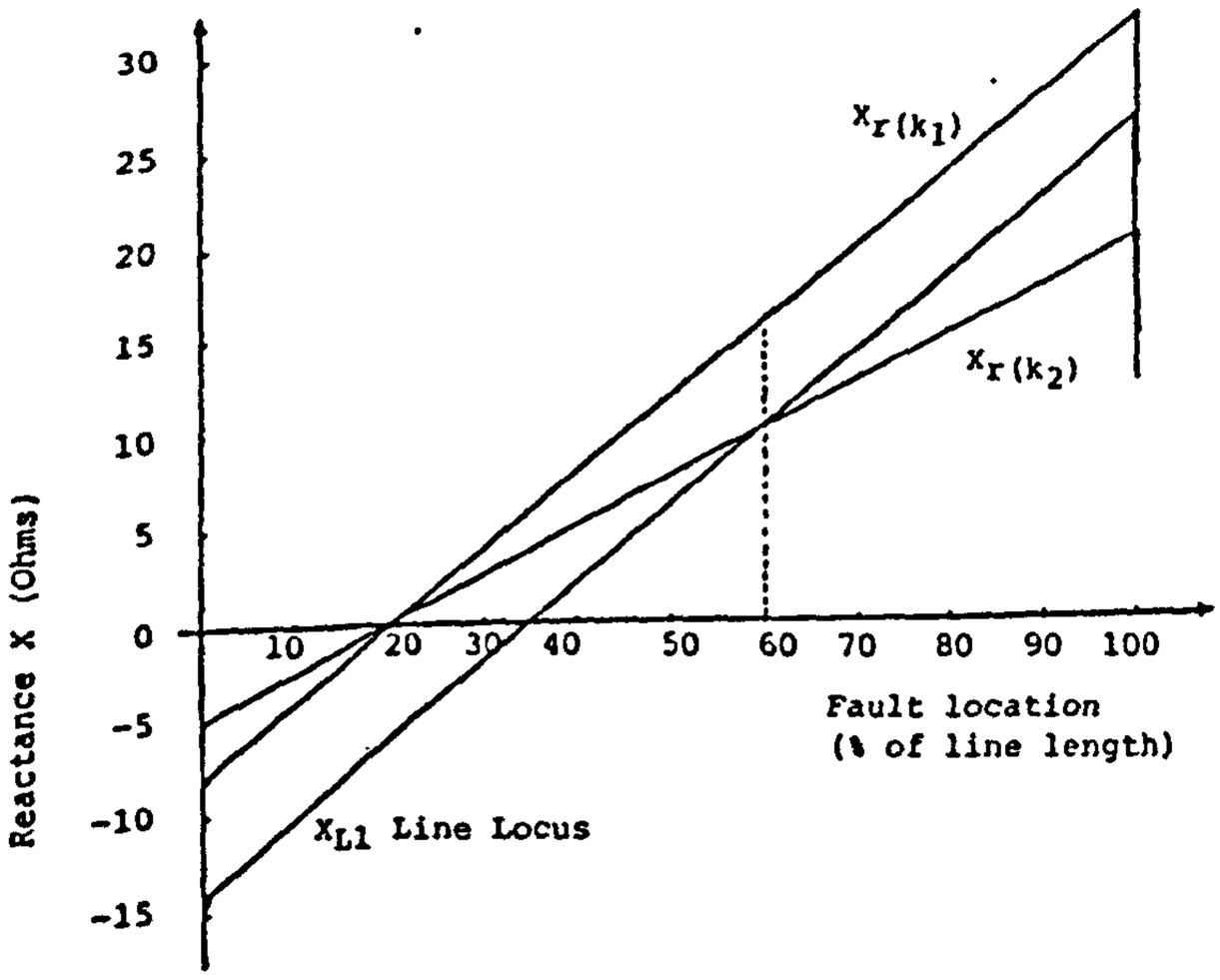

Fig 3. Variation of reactance vs fault position

$$k_1 = \frac{1}{3}\left(\left|\frac{Z_{L0}}{Z_{L1}}\right| - 1\right)$$

$$k_2 = \frac{1}{3}\left(\frac{\alpha_r . Z_{L0} - jX_c}{\alpha_r . Z_{L1} - jX_c} - 1\right)$$

where $\alpha_r = 0.6$

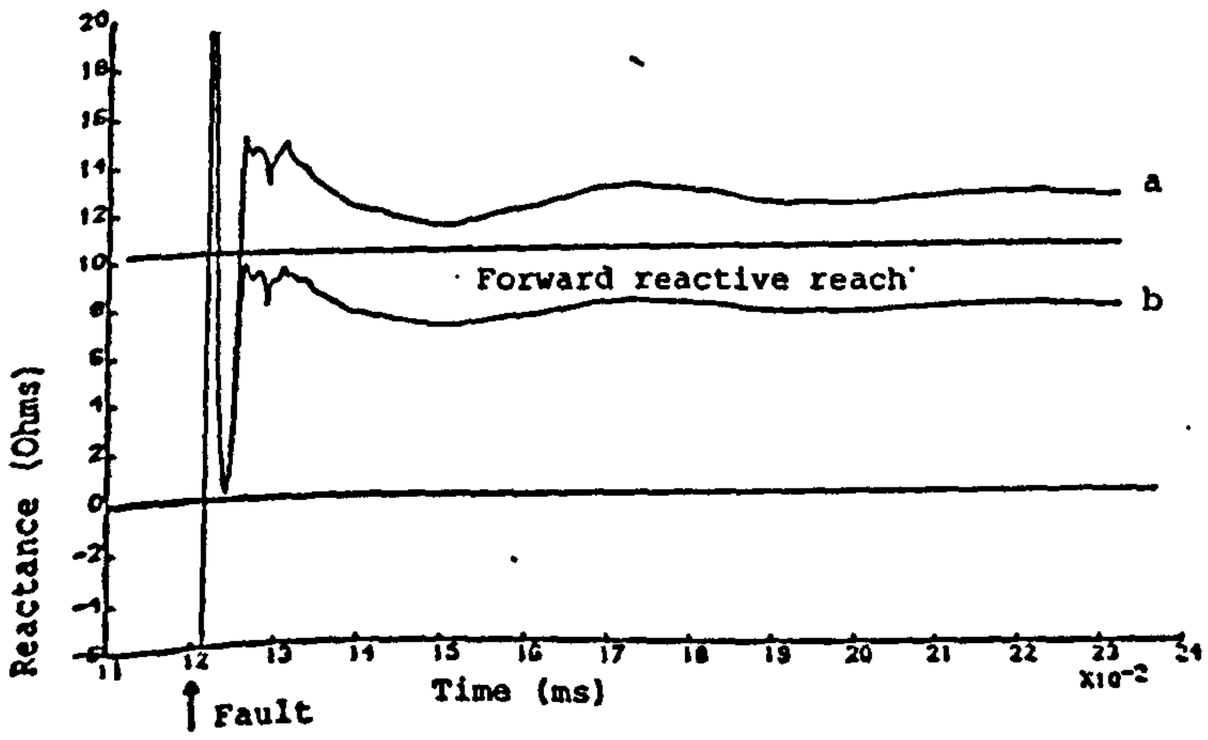

Fig 4. Measured reactance vs time

a) Measured reactance when k=0.77

b) Measured reactance when k=1.82

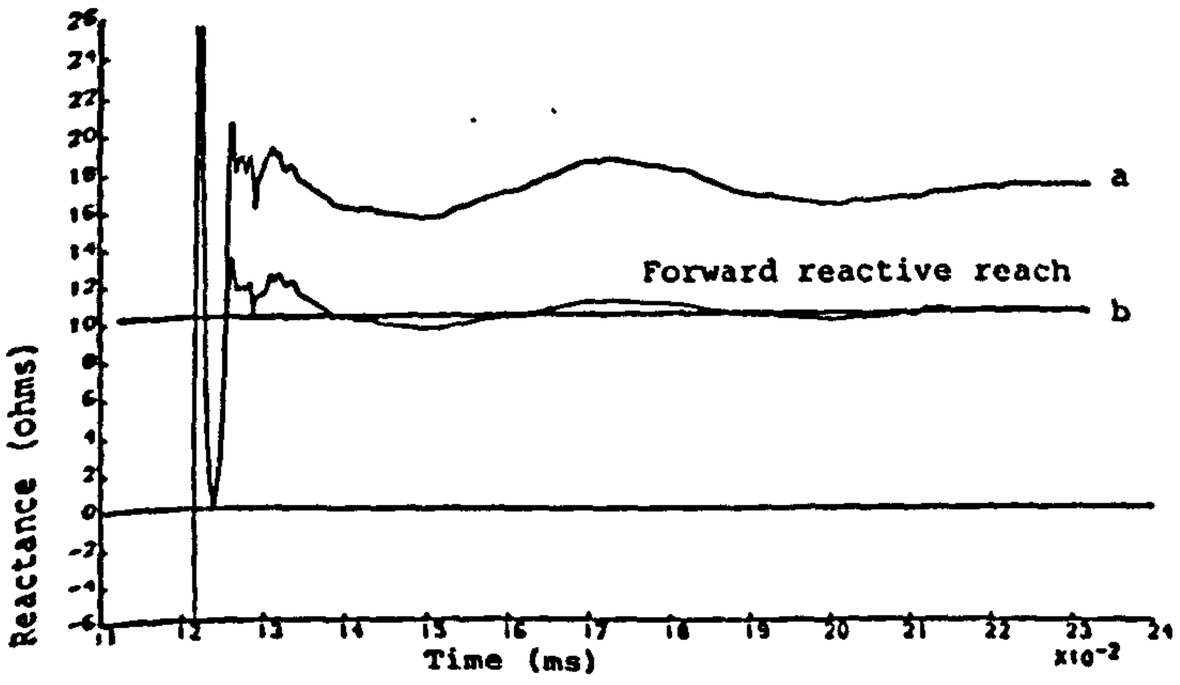

Fig 5. Measured reactance vs time

a) Measured reactance when k=0.77

b) Measured reactance when k=1.82

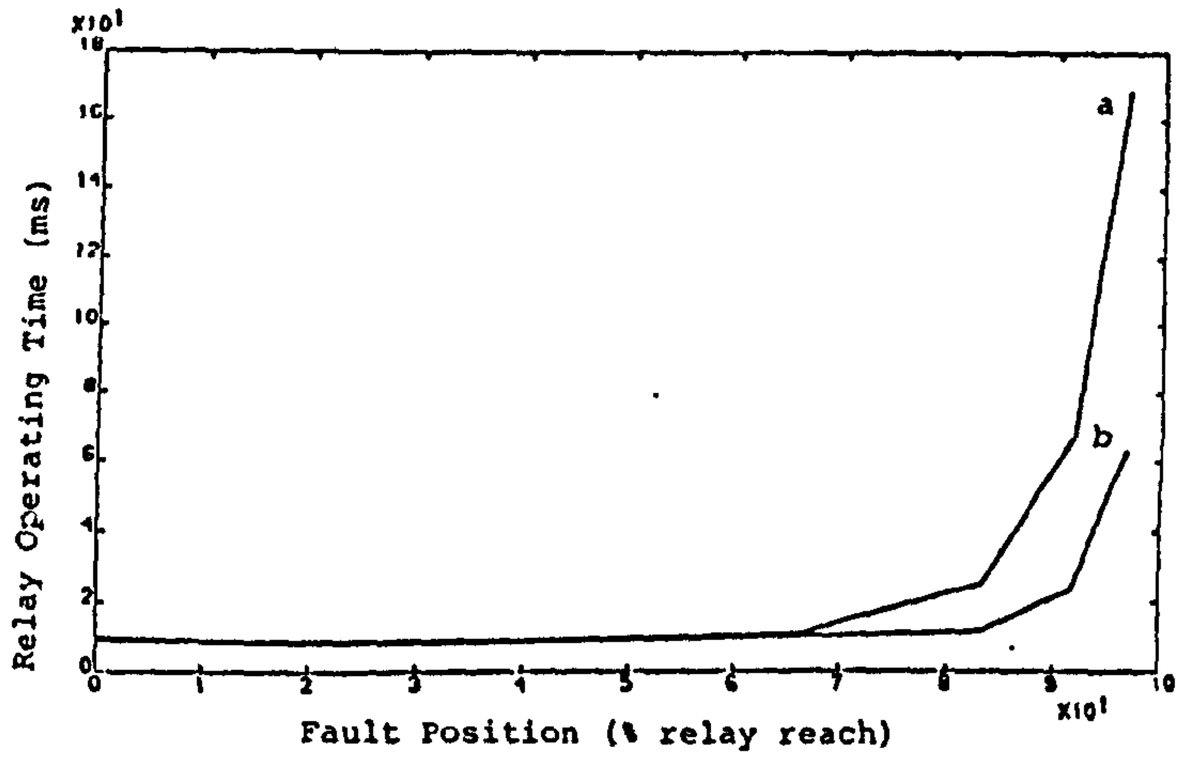

Fig 6a. Relay response for no load condition

a) Fault inception angle 90

b) Fault inception angle 0

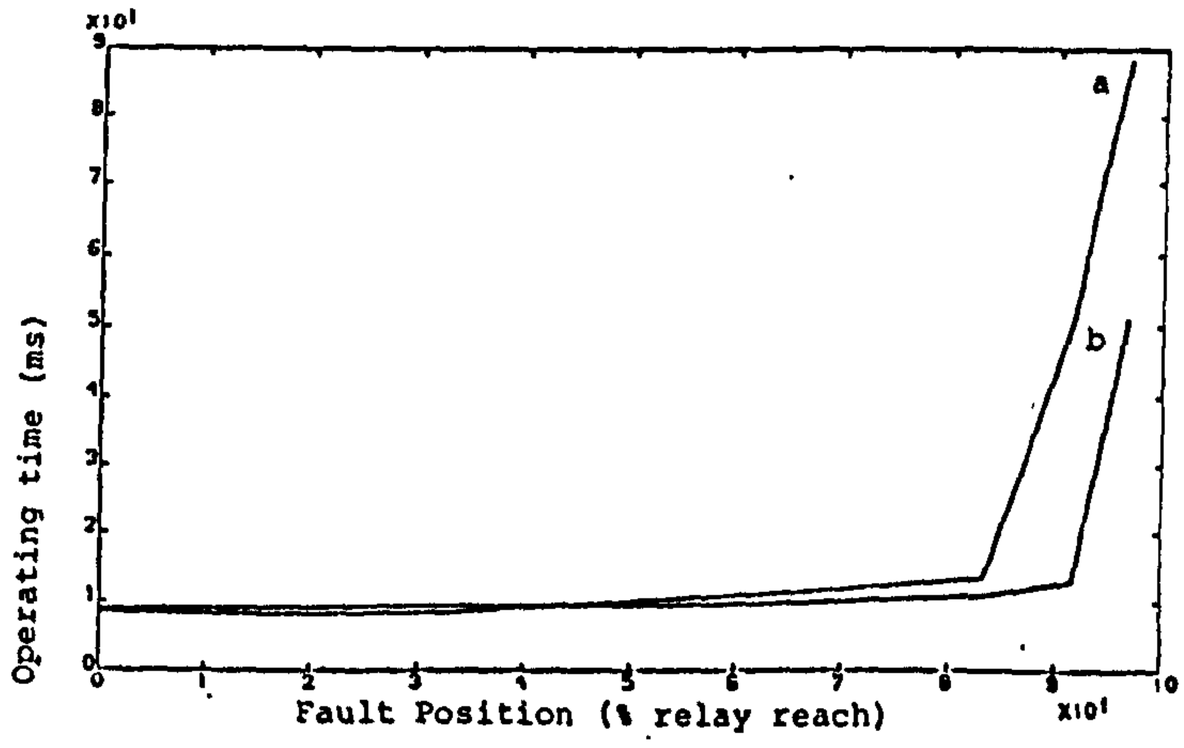

Fig 6b. Relay response for +10 load angle

a) Fault inception angle 90

b) Fault inception angle 0

UPEC 1989, BELFAST, UK

PERFORMANCE OF EARTH FAULT ELEMENTS OF DIGITAL DISTANCE RELAYS APPLIED TO SERIES COMPENSATED LINES

F.GHASSEMI AND A.T.JOHNS

THE CITY UNIVERSITY, LONDON

ABSTRACT

This paper investigates the operation and accuracy of distance relay when applied to series compensated systems with 50% compensation at the mid-point of the line. The new modified residual compensation factor proposed by the authors in earlier papers is implemented in a distance relay. It is shown that, to modify the response of the distance relay a new relay characteristic may be employed.

INTRODUCTION

Series capacitors are well known for improving the cost and operation of the EHV transmission lines. Series compensated lines have always been considered to require special protective relays and schemes. The performance of the relays, especially distance relays, depends on capacitor location and its percentage compensation with respect to the associated transmission line.

It is known that, there are system conditions that do not result in capacitor protection gear operation after the occurance of a fault [1]. Also, with the new generation of the Ultra-High-Speed protection, the fault may be cleared in considerably less than one cycle which may be much shorter than capacitor gap flash-over times [2]. Therefore it is highly desirable that distance protection schemes perform the impedance measurements with the highest degree of accuracy with capacitor banks in circuit. Several papers have investigated the difficulties associated with protection of series compensated lines [3,4,5,6]. One of these problems is the effect of the residual compensation factor when an earth fault occurs. Reference 5 and 6 have investigated this effect for systems with 70% compensation and proposed a new method to improve the distance relays performance when capacitors are assumed in the circuit. In this paper the application of the new modified residual compensation factor to series compensated lines with 50% series compensation at the mid-point of the line is investigated.

RESIDUAL CURRENT COMPENSATION FACTOR

Consider the system shown in Fig. 1 with series capacitor situated at the mid-point (line data is given in Appendix A).

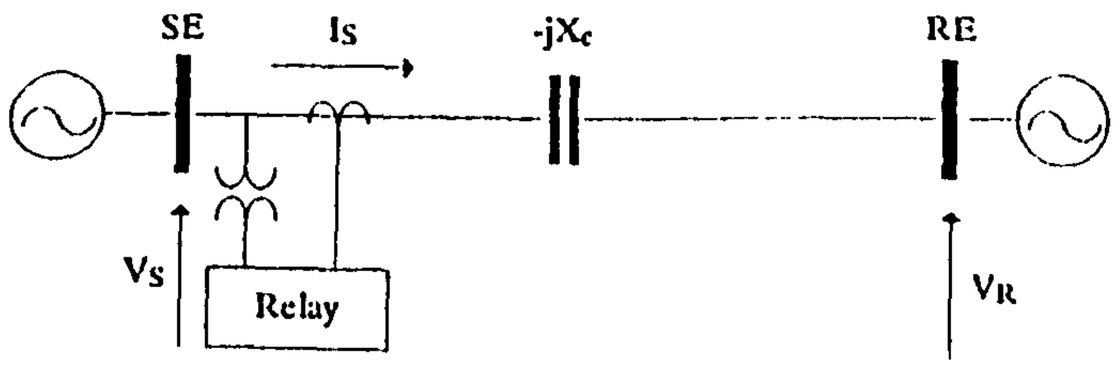

Fig 1:SYSTEM CONFIGURATION

It is well known that in distance protection, for phase to earth faults, compensation methods are used to allow the relay to measure the positive phase sequence (pps) impedance of the line from the relaying to fault point [7]. The most commenly used method employs residual current compensation, where a fraction of the residual current is added to the phase currents. It has been revealed in reference 5 and 6 that, if the conventional residual compensation factor (CRCF) is used, the impedance measurement by the distance relay is not accurate. When the series capacitor bank is located at the middle of the line and using similar analysis as reference 6, it can be shown that the impedance seen by the distance relay for faults before and after the series capacitor are given by Eqn. 1 and 2 respectively:

$$Z_r=\frac{V_{sae}}{I_{sa}+K_cI_{res}} \approx \alpha Z_{L1} \qquad \text{for } \alpha<0.5 \qquad 1$$

$$Z_r=\frac{V_{sae}}{I_{sa}+K_cI_{res}} \approx \alpha Z_{L1}-j\left(\frac{I_{sa}}{I_{sa}+K_cI_{res}}\right)X_c \qquad \text{for } \alpha>0.5 \qquad 2$$

Where:

Z_r=measured impedance
V_{sae}=phase voltage at the relaying point
I_{sa}=faulted phase current at the relaying point
I_{res}=residual current=$I_{sa}+I_{sb}+I_{sc}$
Z_{L1}=total pps impedance of the line
X_c=total capacitor reactance/phase
α=proportional fault position
K_c=conventional residual compensation factor

$$=\frac{1}{3}\left(\left|\frac{Z_{L0}}{Z_{L1}}\right| - 1\right) \qquad 3$$

Figs 2 and 3 show the measured impedance by distance relay on impedance (R-X) plain for different source and pre-fault load. Note that the relay measurements are not accurate, even for faults before the capacitor bank. This is due to the fact that the angle of the line zero phase sequence (zps) and pps impedances in Eqn. 3 are assumed to be the same. However, it can be seen that the measured resistance is more affected than the reactance. Fig 4 shows the measured reactance versus fault position which confirms that for faults before the capacitor location the discrepancy in the measured reactance and the actual line reactance is minimal if the impedance ratio Z_{L0}/Z_{L1} is taken as real.

In order to ensure that the relay measures the correct value of pps impedance of the line from the relay to fault point (for relay setting purposes) it has been shown that in series compensated lines, the residual compensation factor must be set according to the fault position α [6]. Considering series compensated line with 50% compensation at the middle of the line it can be shown that the measured impedance by the relay is given by:

$$Z_r = \frac{V_{sae}}{I_{sa}+K_{(\alpha)}I_{res}} \approx \alpha Z_{L1} - j\,X_{ce} \qquad 4$$

where:

$$K_{(\alpha)} = \frac{1}{3}\left(\frac{\alpha Z_{L0} - j\,X_{ce}}{\alpha Z_{L1} - j\,X_{ce}} - 1\right) \qquad 5$$

$X_{ce} = 0$ for $\alpha < 0.5$
$X_{ce} = X_c$ for $\alpha > 0.5$

Figs 5.a and 5.b shows the magnitude and argument of $K_{(\alpha)}$ versus fault position. It is evident that $K_{(\alpha)}$ stays at a constant value for fault positions of less than 50% of the line length (capacitor location). However note the variation in magnitude and argument of $K_{(\alpha)}$ with fault position, α, for faults beyond the series capacitor.

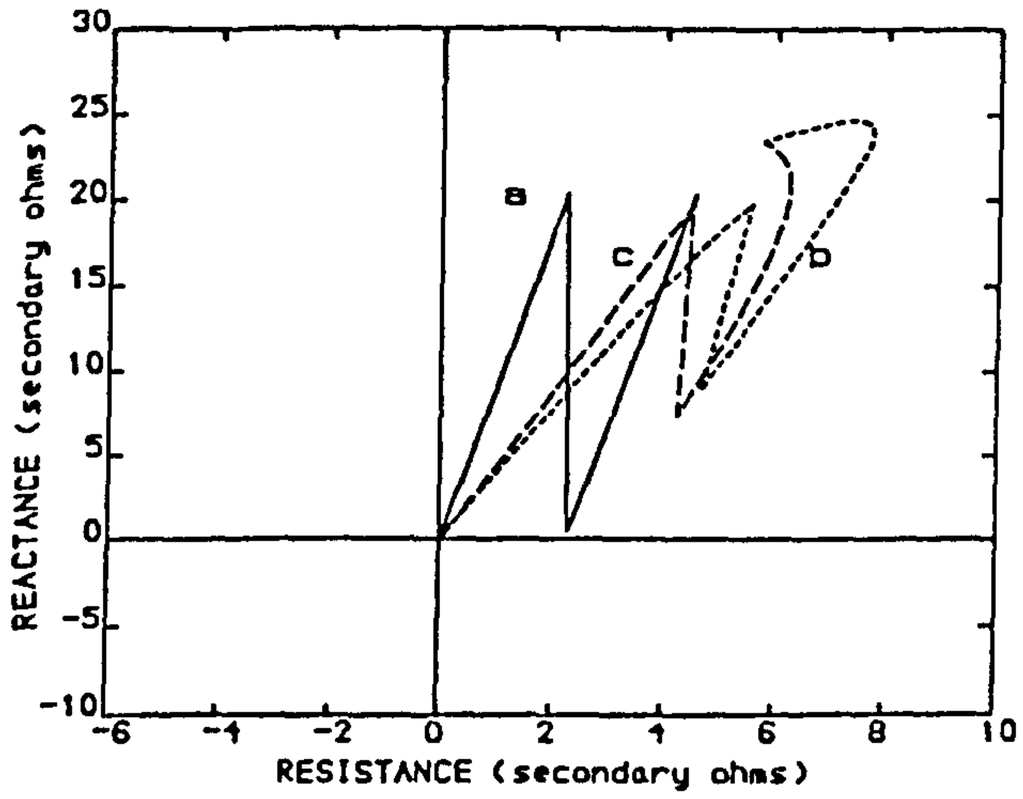

Fig 2:Measured Impedance For Different System Sources With CRCF ($K_C = 0.774\angle 0^\circ$)

a: Line Locus
b: SE SCL=5 GVA, RE SCL=35 GVA, Load Angle=0°
c: SE SCL=35 GVA, RE SCL=5 GVA, Load Angle=0°

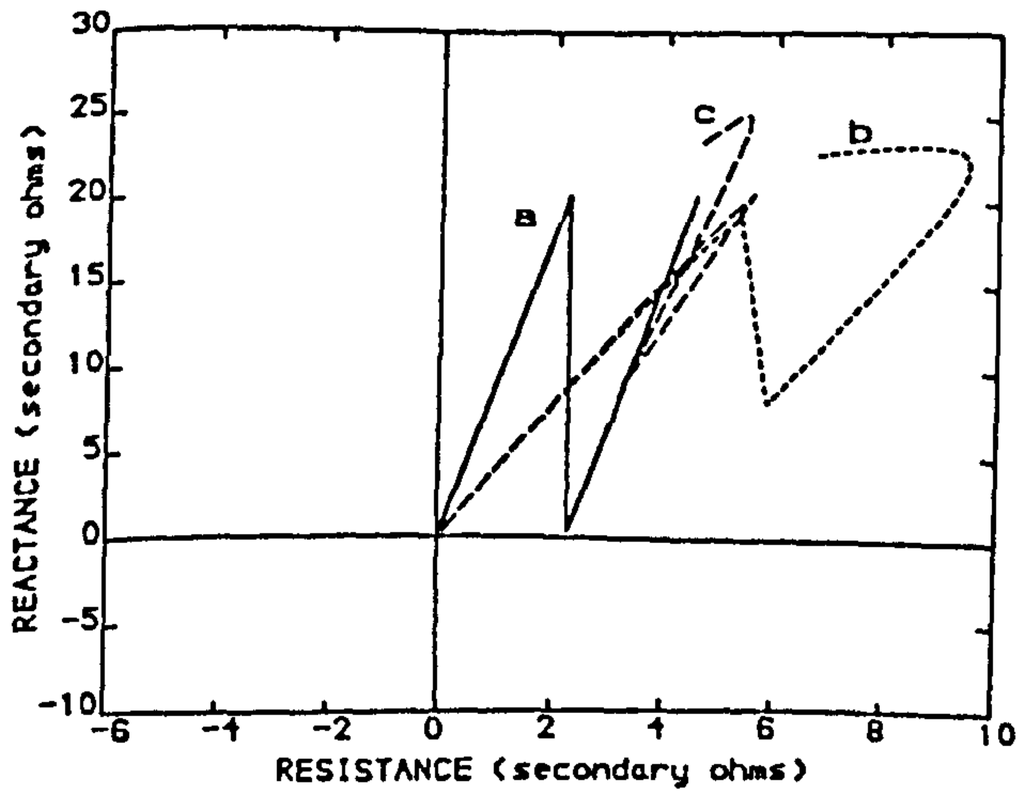

Fig 3:Measured Impedance For Different System Load With CRCF ($K_C = 0.774\angle 0^\circ$)

a: Line Locus
b: SE SCL=5 GVA, RE SCL=35 GVA, Load Angle=+10°
c: SE SCL=5 GVA, RE SCL=35 GVA, Load Angle=-10°

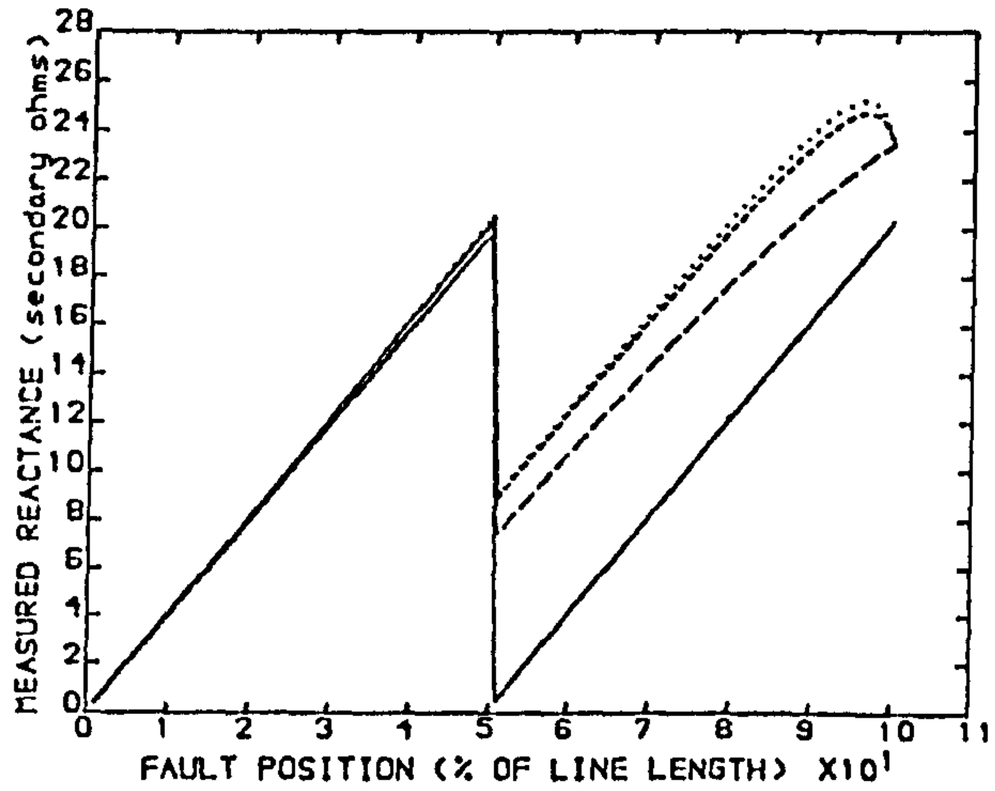

Fig 4:Measured Reactance With CRCF ($K_C = 0.774\angle 0^\circ$)

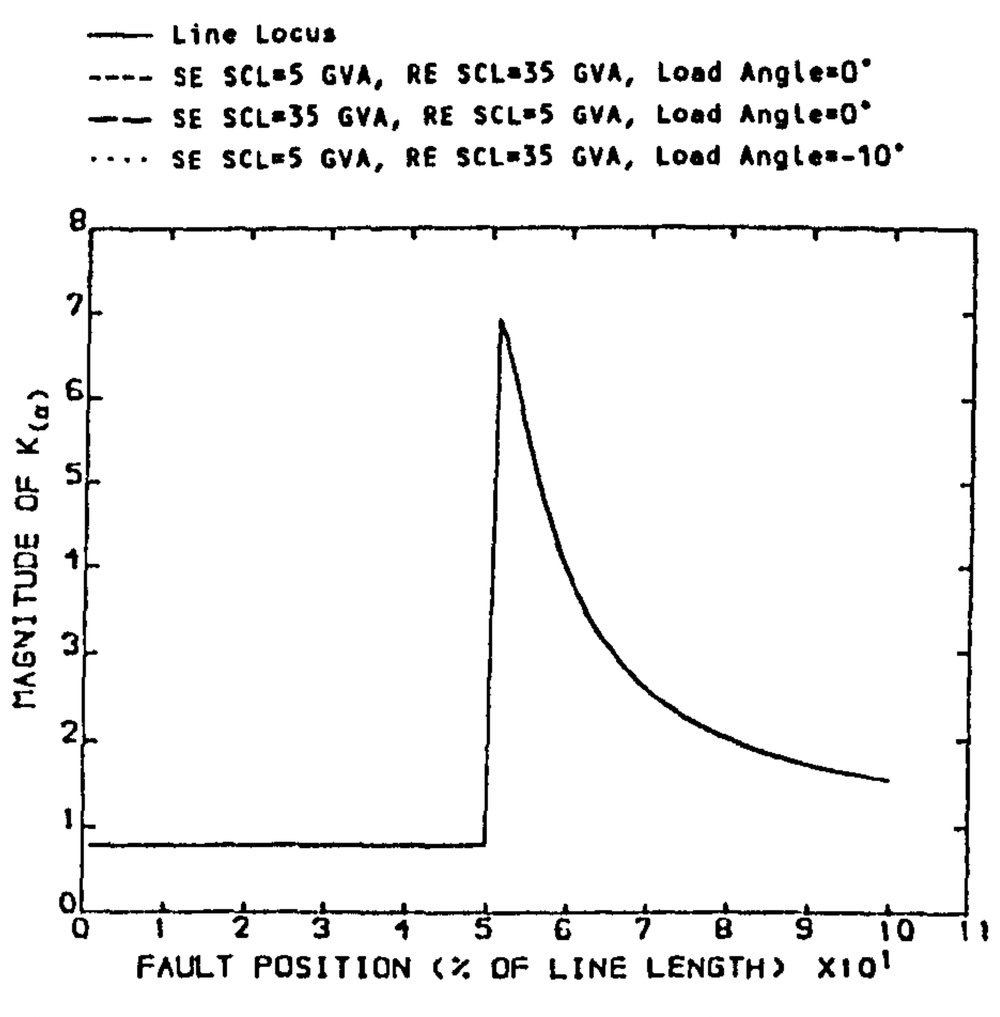

Fig 5.a:VARIATION OF $|K_{(\alpha)}|$ WITH FAULT POSITION

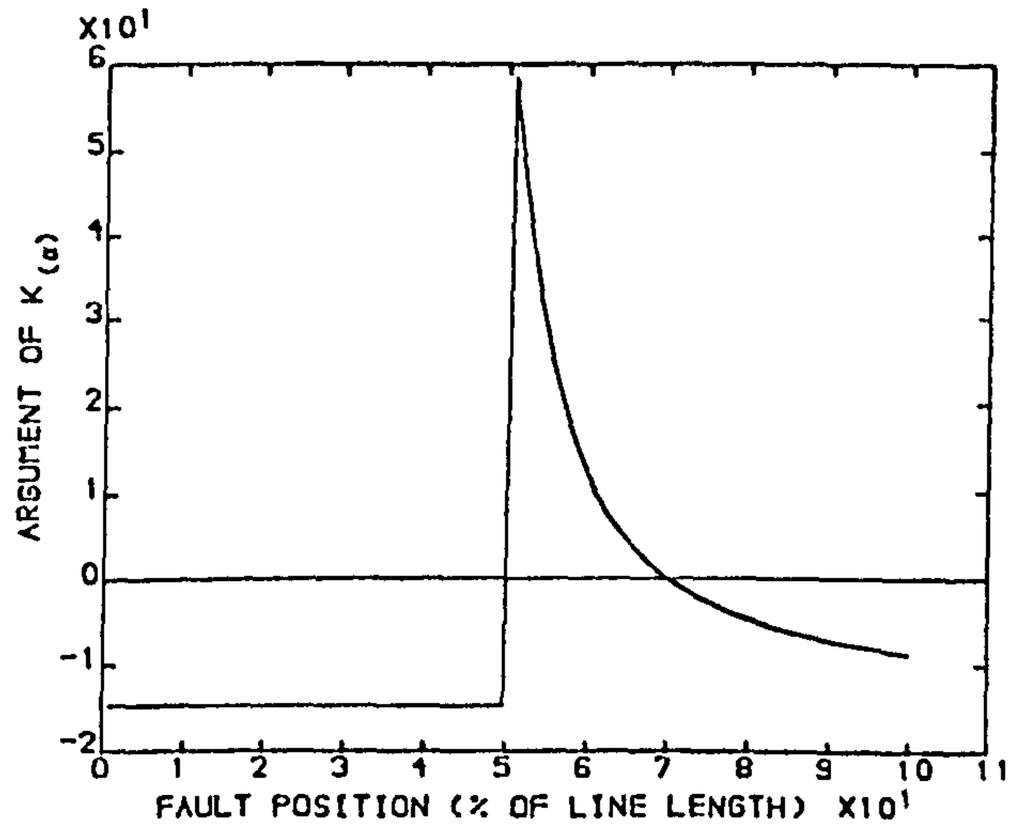

Fig 5.b:VARIATION OF $\angle K_{(\alpha)}$ WITH FAULT POSITION

Modified Residual Compensation Factor For Series Compensated Line

It has been suggested that, since the relay is required to be the most accurate at and arround the boundary, the residual compensation factor is set at a fixed value $K_{(\alpha r)}$, assuming the fault position to be at the relay zone-1 reach boundary [5,6]. If the relay independant zone-1 reach is considered

to be before series capacitor, say at 45% (αr=0.45) and a complex residual compensation factor (assuming $\angle Z_{L0} \neq \angle Z_{L1}$) is considered in the relay, the relay measures accurate impedances for all faults before the mid-point of the line. But for faults beyond the capacitor, the relay measurement will not be accurate.

If it is required to set the relay reach at a value higher than 50%, then the relay measurement is accurate only at the reach point [5,6]. In this work it was decided to set the relay zone-1 reach at 80% of the line length, which is the common practice in plain uncompensated feeder distance protection schemes. The required residual compensation factor, for boundary setting of 80% (αr=0.8) is, from Fig 5.a and b, found to be approximately equal to $2.015\angle -4.6^{\circ}$.

Figs 6 and 7 illustrate the measured impedance on an impedance plain for different source and load condition when the new residual compensation factor (NRCF) is used. It can be clearly seen that the measured impedance at the boundary is independant of source and pre-fault load. Also, due to over-compensation of the residual current in the relay ($2.015\angle -4.6^{\circ}$ instead of $0.782\angle -14.82^{\circ}$) for faults before the capacitor bank, the measured reactance is smaller than the actual line reactance.

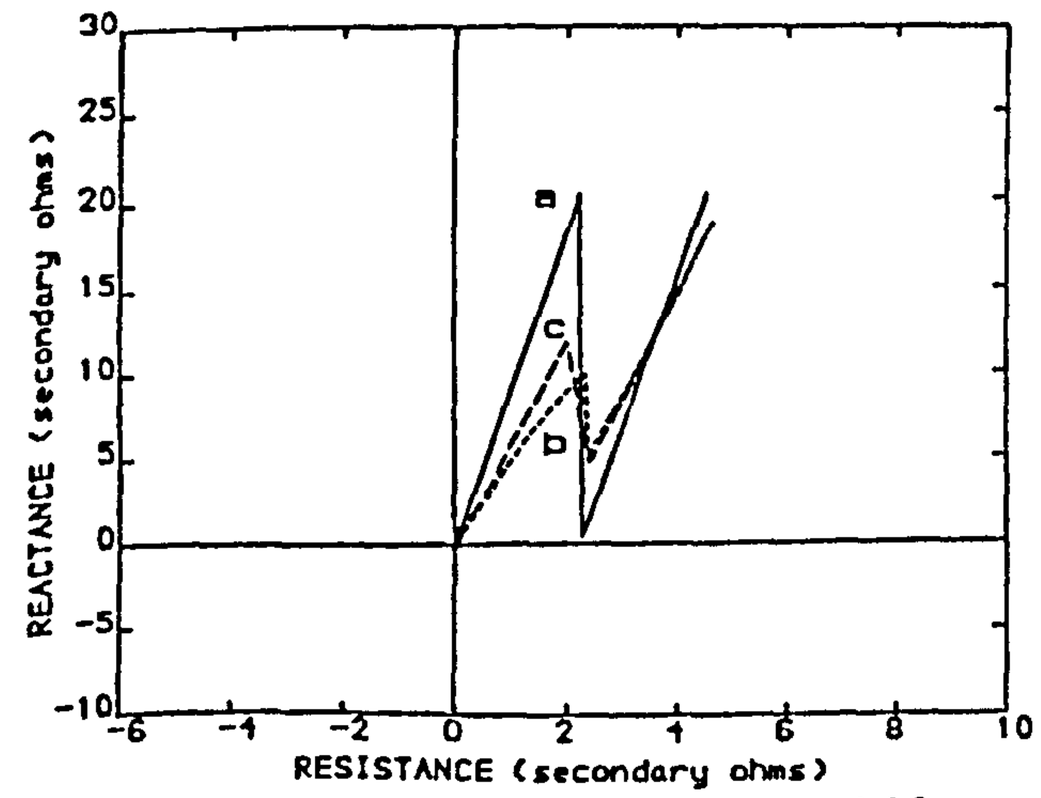

Fig 6:Measured Impedance For Different System Sources With NRCF ($K_{(\alpha r)}=2.015\angle 4.6^{\circ}$)

a: Line Locus
b: SE SCL=5 GVA, RE SCL=35 GVA, Load Angle=0°
c: SE SCL=35 GVA, RE SCL=5 GVA, Load Angle=0°

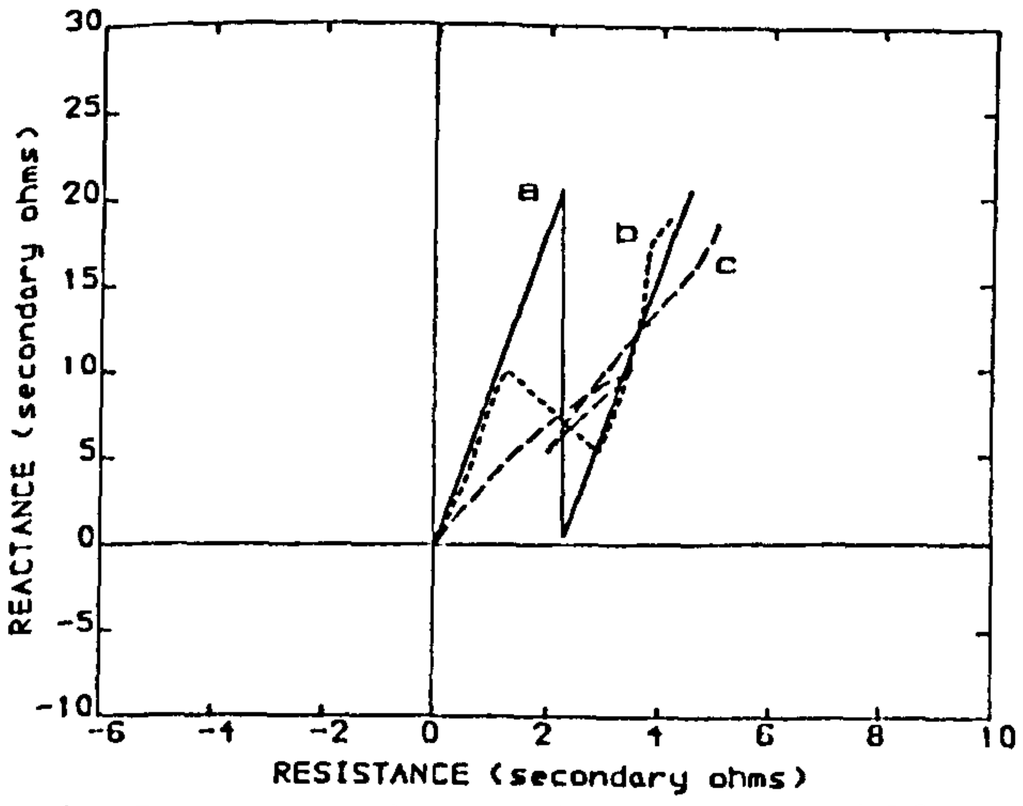

Fig 7:Measured Impedance For Different System Load With NRCF ($K_{(\alpha r)}=2.015\angle 4.6^{\circ}$)

a: Line Locus
b: SE SCL=5 GVA, RE SCL=35 GVA, Load Angle=+10°
c: SE SCL=5 GVA, RE SCL=35 GVA, Load Angle=-10°

RELAY CHARACTERISTIC

The new residual compensation factor was implemented on a digital distance relay described by reference 8 and 9. The relay forward reactance reach was set at 80% of the line length. Reference 6 has described how a complex residual compensation factor can be implemented in a digital relay. At the relay sampling frequency of 4 kHz, the first previous sample of the residual current is added to the phase current which corresponds to an angle of -4.5°.

The relay characteristic which was initially adopted in this work, the line actual impedance and the measured impedances for different source and pre-fault load are shown in Fig 8. It must be said that, in order to improve discrimination ability of the relay around the forward reach longer time is allowed for the relay to reach a trip decision by dividing the relay characteristic into fast and slow counting regions [10]. For the foregoing reasons, although the steady state locus of the measured impedances fall within the relay characteristic, high speed operation may not be achieved for faults just before the capacitor bank. Relay operating time of up to 60 msec was observed for some system conditions, for a fault at 48% of the line length.

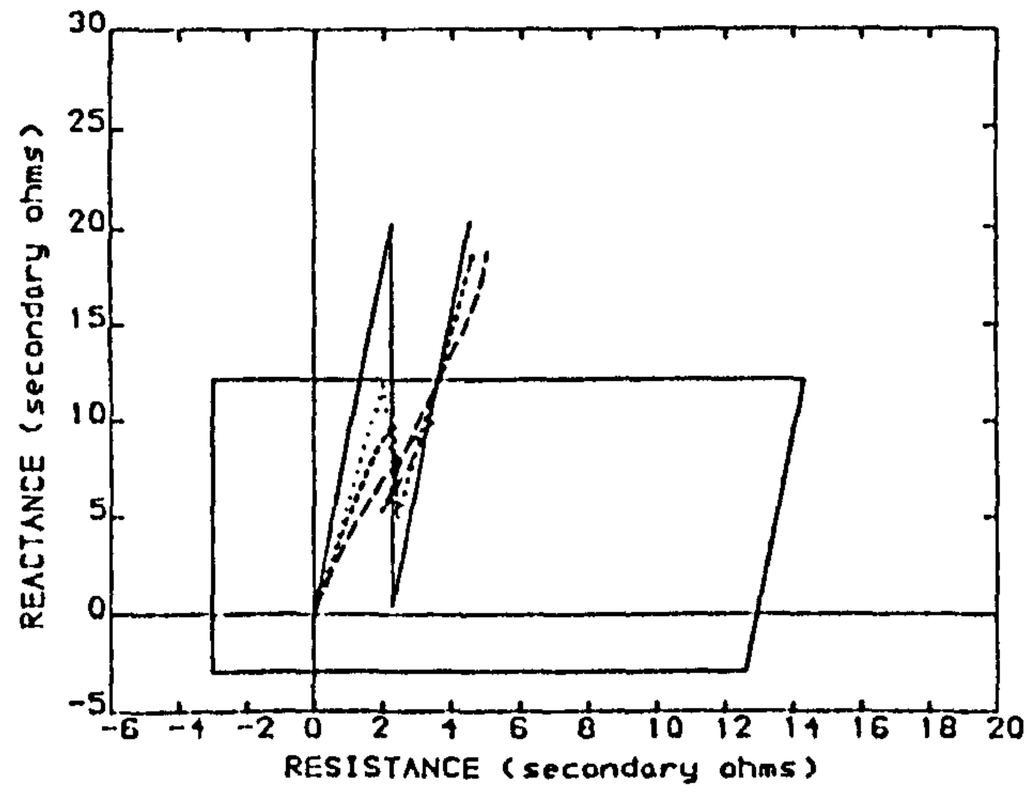

Fig 8:Quadrilateral Trip Characteristic And Measured Impedances With NRCF ($K_{(\alpha r)}=2.015\angle 4.5^{\circ}$)

—— Line Locus
---- SE SCL=5 GVA, RE SCL=35 GVA, Load Angle=0°
—— SE SCL=5 GVA, RE SCL=35 GVA, Load Angle=-10°
.... SE SCL=35 GVA, RE SCL=5 GVA, Load Angle=0°

To improve the relay operating time response the relay characteristic was modified to Fig 9. The new characteristic has the advantages of improving transient as well as steady state, and operating time responses of the relay. Figs 10 and 11 illustrate typical relay operating time for different source and load conditions. The primary system simulation is described in Reference 11.

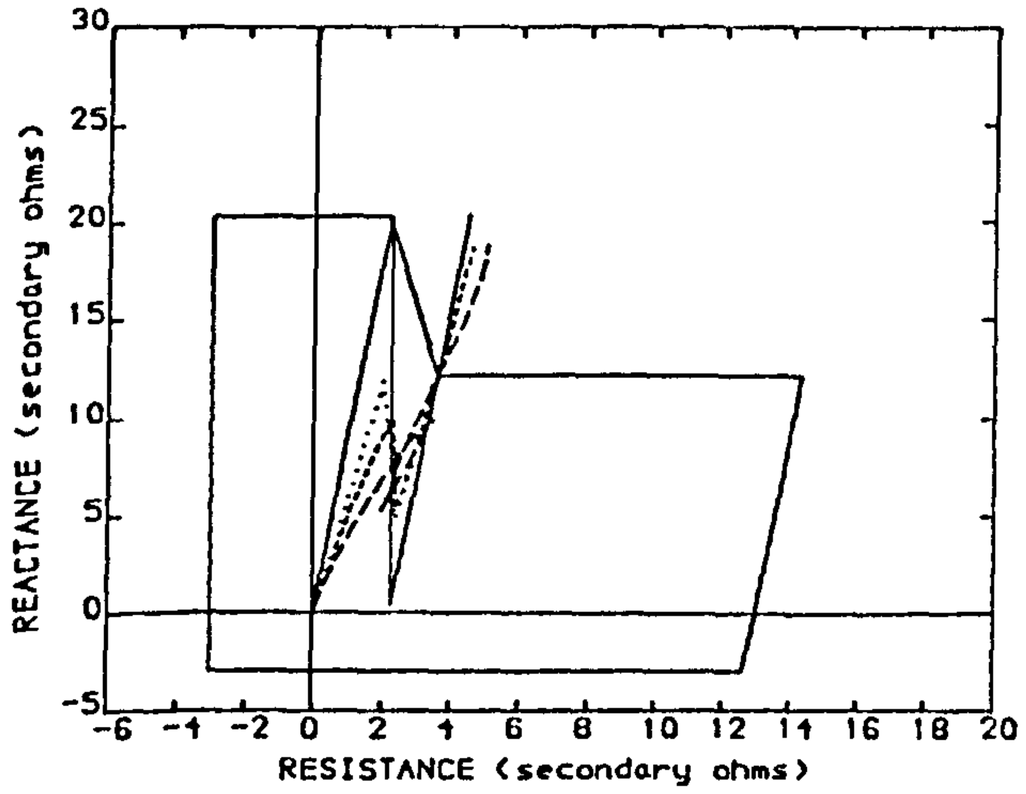

Fig 9:New Relay Trip Characteristic And Measured Impedances With NRCF ($K_{(\alpha r)}=2.015\angle 4.5^{\circ}$)

—— Line Locus
---- SE SCL=5 GVA, RE SCL=35 GVA, Load Angle=0°
—— SE SCL=5 GVA, RE SCL=35 GVA, Load Angle=-10°
.... SE SCL=35 GVA, RE SCL=5 GVA, Load Angle=0°

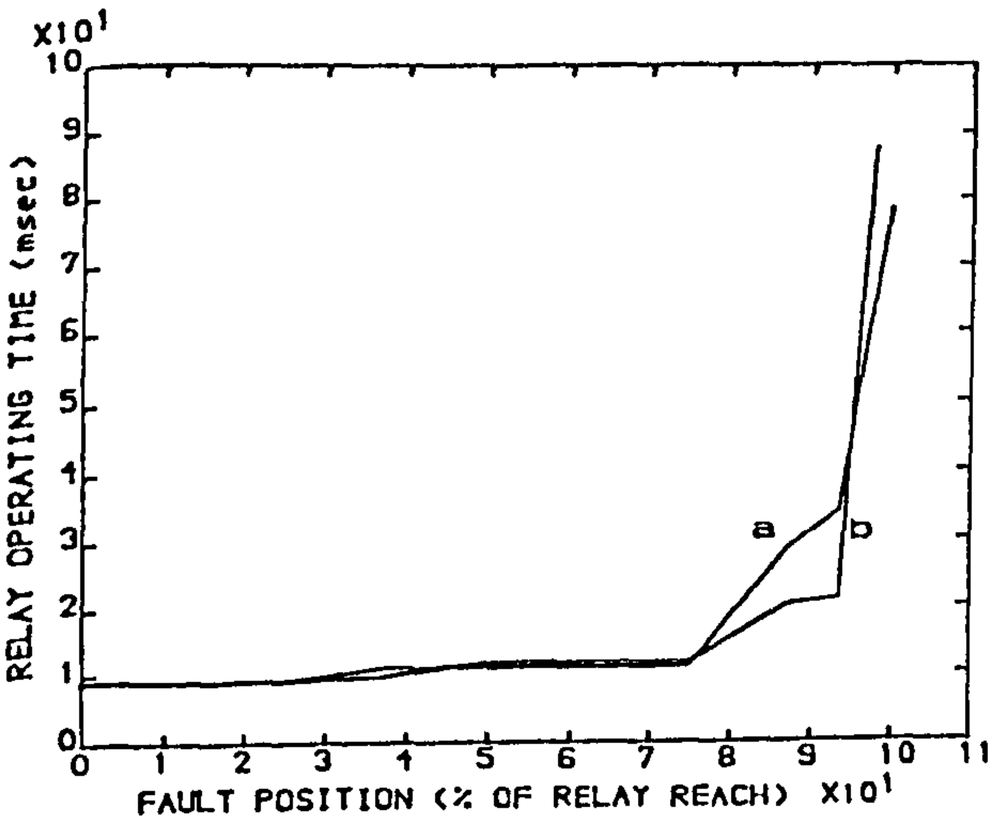

Fig 10:Relay Operating Time vs Relay Reach

SE SCL=35 GVA, RE SCL=5 GVA, Load Angle=0°
a:Fault Inception Angle=0°
b:Fault Inception Angle=90°

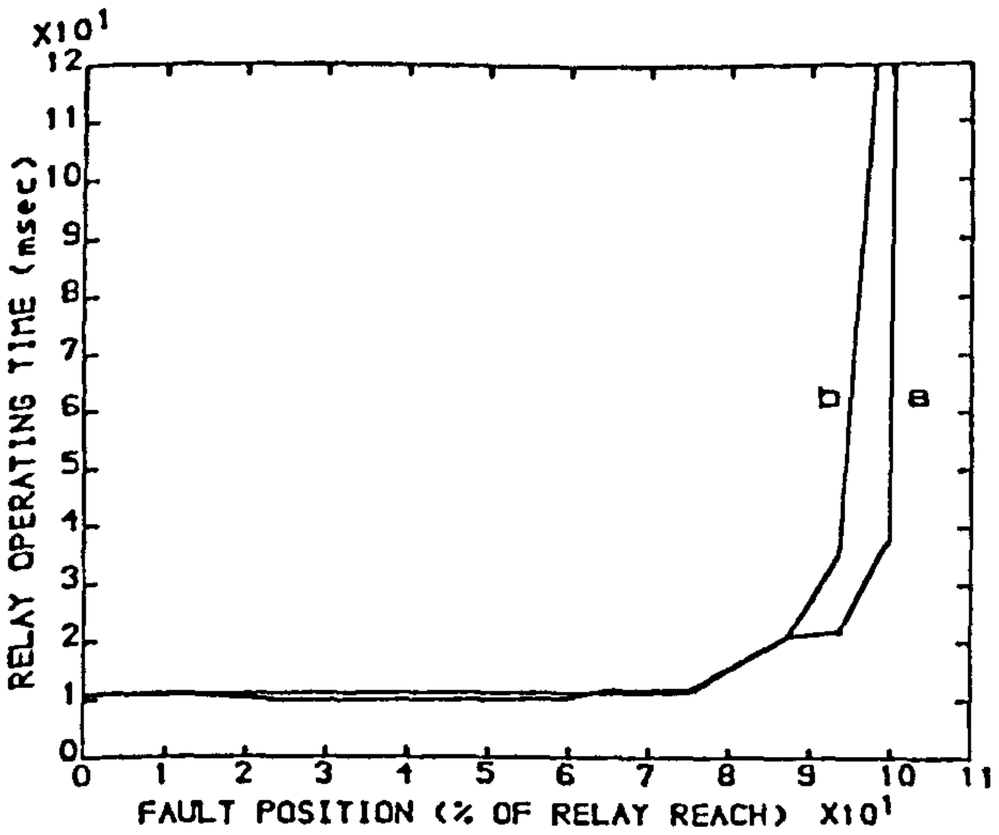

Fig 11:Relay Operating Time vs Relay Reach

SE SCL=5 GVA, RE SCL=35 GVA, Load Angle=-10°
a:Fault Inception Angle=0°
b:Fault Inception Angle=90°

CONCLUSIONS

The new method of the residual current compensation proposed in references 5,6 was investigated for a series compensated line with 50% compensation at the mid-point of the line. It was shown that the relay reach can be set at 80% of the line length with the highest degree of accuracy in impedance measurement at the reach point. The new method was implemented in a digital distance relay and it was shown that to improve the relay operating time, a modified relay characteristic may be used.

ACKNOWLEDGEMENT

The authors would like to thank The City University, London, GEC Measurements, Stafford-UK, and the Science and Engineering Research Council UK for the provision of facilities and support for this research.

APPENDIX A: SYSTEM DATA

The line is horizontally constructed and discretely transposed. System voltage is 500 kV. The pps and zps impedances of the line are:

Z_{L1}= $0.3109\angle 83.62^{\circ}$ Ω/km primary
= $0.1367\angle 83.62^{\circ}$ Ω/km secondary
Z_{L0}= $1.033\angle 73.24^{\circ}$ Ω/km primary
= $0.4545\angle 73.24^{\circ}$ Ω/km secondary
X_C/phase = 46.353 Ω primary.
= 20.390 Ω secondary
Line Length=300 km

REFERENCES

[1] J.Berdy,"Protection of circuits with series capacitor,"AIEE Summer general meeting, DENVER-COLO, June 1962.
[2] Y.Mansour, T.G.Martinich, J.E.Drakos,"B.C. Hydro series capacitors bank staged fault test,"IEEE Trans, PAS-102, NO7, PP. 1960-1969, July 1983.
[3] M.M.Elkateb, W.J.Cheetham,"Problems in the protection of series compensated lines," IEE Conference publication on power system protection, NO 185, PP. 215-220, 1980.
[4] M.Shafik, F.Ghassemi, A.T.Johns,"Performance of digital distance protection for series compensated systems,"UPEC, 1987.
[5] A.T.Johns, F.Ghassemi,"Analysis and compensation of errors in distance protection measurement for series compensated systems,"UPEC, 1988.
[6] F.Ghassemi, A.T.Johns,"Investigation of alternative residual current compensation for improving series compensated line distance protection,"Accepted for presentation in the IEEE summer meeting, California, July 1989.
[7] W.A.Lewis, S.L.Tippett,"Fundamental basis for distance relaying on three-phase system,"AIEE Trans, PP. 694-709, 1947.
[8] A.T.Johns, M.A.Martin,"New Ultra High Speed distance protection using finite transform techniques,"Proc. IEE, Vol 131, ptc No 5, PP.188-196, 1983.
[9] P.J.Moore,A.T.Johns,"Impedance measurement techniques for digital EHV line protection",UPEC, 1988.
[10] P.J.Moore, A.T.Johns,"Adaptive digital distance protection,"Forth international conference on developments in power system protection. Edinburgh, April 1989.
[11] R.K.Aggarwal, A.T.Johns, A.Kalam,"Computer modelling of series compensated EHV transmission systems",Proc. IEE, Vol. 131, PtC, No3, pp. 127-138.